Louisiana State University
LSU Digital Commons

LSU Historical Dissertations and Theses | Graduate School

1969

Fluid Dynamics and Flow Patterns in Stirred Tanks With a Turbine Impeller.

Abel Desouza
Louisiana State University and Agricultural & Mechanical College

Follow this and additional works at: https://digitalcommons.lsu.edu/gradschool_disstheses

Recommended Citation
Desouza, Abel, "Fluid Dynamics and Flow Patterns in Stirred Tanks With a Turbine Impeller." (1969). *LSU Historical Dissertations and Theses*. 1650.
https://digitalcommons.lsu.edu/gradschool_disstheses/1650

This Dissertation is brought to you for free and open access by the Graduate School at LSU Digital Commons. It has been accepted for inclusion in LSU Historical Dissertations and Theses by an authorized administrator of LSU Digital Commons. For more information, please contact gradetd@lsu.edu.

This dissertation has been
microfilmed exactly as received

70-9050

DeSOUZA, Abel, 1936-
FLUID DYNAMICS AND FLOW PATTERNS IN STIRRED TANKS WITH A TURBINE IMPELLER.

The Louisiana State University and Agricultural and Mechanical College, Ph.D., 1969
Engineering, chemical

University Microfilms, Inc., Ann Arbor, Michigan

FLUID DYNAMICS AND FLOW PATTERNS IN STIRRED TANKS WITH A TURBINE IMPELLER

A Dissertation

Submitted to the Graduate Faculty of the
Louisiana State University and
Agricultural and Mechanical College
in partial fulfillment of the
requirements for the degree of
Doctor of Philosophy

in

The Department of Chemical Engineering

by

Abel DeSouza
B.S., University of Bombay, 1959
M.S., Louisiana State University, 1966
August, 1969

ACKNOWLEDGEMENTS

This work was performed under the direction of Dr. Ralph W. Pike. His encouragement, counsel and guidance is gratefully acknowledged.

The author would like to express his thanks to the Chemical Engineering Department for financial support during his years in Graduate School and the LSU Computer Research Center for unlimited use of their facilities. The author would also like to thank Dr. P. M. Arnold, Vice-President of Research and Development, The Phillips Petroleum Company, for his keen interest and encouragement in this project, and the following companies who have supported this project: The Dow Chemical Company, Esso Research and Engineering Company, and The Phillips Petroleum Company.

The publication and typing costs of this dissertation was partially provided by the Charles E. Coates Memorial Fund of the LSU Foundation, donated by George H. Coates.

Special thanks are due to L. E. Veilleux for help in building the necessary apparatus of this project; to Miss Suzanne Hackler for typing the first drafts, Miss Madeline Jewell and Miss Debbie Kleinpeter for typing the manuscript and to my many friends whose advice and help is greatly appreciated.

TABLE OF CONTENTS

LIST OF TABLES

LIST OF FIGURES

LIST OF COMPUTER LISTINGS

ABSTRACT

Velocity measurements were made in a stirred tank with a turbine impeller. Two sizes of vertical cylinderical tanks were used (11.5 and 12.25 inches in diameter) and a simgle 3.0 inch diameter six flat-blade turbine impeller. The velocity measurements were made with a three dimensional pitot tube probe. A tangential jet model was found to adequately describe the flow in the region of the impeller. The velocity profile in the region of the impeller exhibits an angle profile which is not predicted by the tangential jet model. The model is, however, relatively insensitive to the angle profile and a weighted average angle was found to give satisfactory results.

The significant velocity in the neighborhood of the impeller centerline was shown to be $\vec{q}$ the resultant of $\bar{v}_r$ and $\bar{v}_\theta$. It was also shown that the three dimensional pitot tube is not sensitive enough to measure velocities below 0.5 ft/sec, the lower limit of probe response. $\vec{q}$ was found to fall rapidly beyond $\frac{1}{2}\bar{q}_{max}$, and this point was close to the limit of the probe response. However the tangential jet model shows that the half width of the jet is more than twice the limit of probe response.

The tangential jet model was successfully used to predict velocity profiles of the impeller streams reported in the literature.

The results of the combined data includes measurements made in air and water and spans varying impeller diameter, tank diameter and impeller speeds. For geometrically similar impellers it was found that the jet width was independent of the physical properties of the fluid, impeller diameter and tank diameter.

The tangential jet model is a three parameter model and correlations are presented for these parameters. The impeller discharge Q was found to be a function of ND^3 and the dimensionless pumping capacity Q/ND^3 was found to be a constant with a value of 0.93 ± 0.28 for the combined data in the literature and in this study.

In the region away from the jet flow, from the impeller it was shown that a three dimensional, low velocity, flow field exists. At 500 RPM for the 3.0 inch diameter impeller the resultant velocity was found to vary from 30 to 70 ft/min. The center of circulation is not a true stagnation point but appears to be so for streamlines plotted in the r-z plane. The flow at this point is predominantly tangential.

Two-dimensional potential flow was used to model this flow away from the impeller region, and the tank was divided into five regions. The intersection of these regions were adjusted to have smooth streamlines that closed and thus satisfied continuity. Due to the three-dimensional nature of the actual flow it was found that this model was not satisfacory to predict the velocities in these regions. A Calcomp plotter was used to draw streamlines from the model. It was demonstrated that this is a useful tool for

drawing flow patterns.

It was observed that the branching flow form the impeller was found to be restricted to the periphery of the tank in a narrow region about a baffle width thick. The 10% baffle is thus not only correctly placed but its width effectively controls the flow in the tank.

CHAPTER I

INTRODUCTION AND BACKGROUND

1. Introduction

The stirred tank is extensively used in fluid processing plants because of its simple mechanical construction and reliability. In addition it performs a variety of functions in liquids whose viscosity ranges from water to corn syrup or molasses. This range of viscosity is roughly 1:1,000,000 centipoises.

In Table 1 the use of a stirred tank, is divided into five broad classifications. These classifications may be further subdivided. For example, solid suspension might be easy or difficult depending on whether the solid material is a finely divided precipitate or a heavy mineral of varying particle size. Similarly, emulsification might be stable (permanent) or unstable as in the case of liquid-liquid extraction.

In the stirred tank these functions are performed with an impeller. The rotating impeller in typical industrial applications causes turbulent flow. For a particlar fluid and impeller the degree of turbulence and flow is in general a function of impeller diameter, tank diameter, and impeller speed. A wide variety of impellers are available. All these impellers can be

Table I-1: Classification of Stirred Tanks According to Functions Performed in the Tank (23)

Physical Criteria	Application Class	Mass Transfer Criteria
Suspension	Liquid-Solid	Dissolving
Dispersion	Liquid-Gas	Absorption
Emulsification	Immiscible Liquids	Extraction
Blending	Miscible Liquids	Reaction
Pumping	Fluid Motion	Heat Transfer

classified into three types depending on the three types of flow patterns observed in stirred tanks. (27) These patterns are observed in fully baffled tanks and are,

1. Axial flow; typical impeller that causes this type of flow is the three-blade marine propeller.
2. Radial flow; typical impeller is the flat blade turbine.
3. Mixed flow, which can be obtained by a pitch blade turbine.

Presently the design of stirred tanks, to meet the process conditions of Table I-1 is still an art in spite of the voluminous body of literature on the subject. This is because the mixing flow pattern required for a variety of processes are not only different, but mixing in the stirred tank is poorly understood. For example, suspension of solids and blending of miscible liquids required relatively larger bulk fluid motion rather than regions of intense turbulence. On the other hand, dispersion of gases in liquids and emulsification requires regions of intense turbulence and shear and relative less bulk fluid motion in the tank. In general each process situation demands its own optimum flow pattern. Thus what is good mixing in a stirred tank reduces to arriving at the right design so as to obtain the desired flow patterns.

The present approach used in the design of stirred tanks is through scale-up, using the principles of dynamic similarity. This requires previous knowledge either from an existing plant, or through experimental data obtained from careful laboratory measurements. It is thus desirable to make a thorough study of the flow patterns in a stirred tank to permit design of such units without the need of specific experimental data; which data in many cases is

usually expensive and difficult to obtain.

The purpose of this research work is to characterize the flow regions in a stirred tank and to arrive at a model which will describe the flow patterns generated in the vessel. As previously mentioned there are three basic types of flow patterns, and it was decided to study the radial flow pattern as generated by a turbine impeller. The turbine was selected as the impeller since it is more often used in industrial applications. Also an extension of this work to the other two types of flow patterns should not be overly difficult. The turbine used in this work was the Mixing Equipment Company's, 6-flat blade, turbine impeller since this unit is most frequently used in process applications, and considerable data is available in the literature for comparison.

2. Statement of the Problem

In unbaffled tanks, a turbine impeller (or any other symmetrically located impeller) produces mere swirl in liquids of relatively low viscosity such as water. The introduction of baffles produces the characteristic radial flow pattern. The fluid emerges as a radial jet with a tangential component which is significant near the impeller, but decreasing as it approaches the wall. The jet as it emerges from the impeller has a high velocity and hence entrains a considerable amount of fluid which tends to diminish its velocity as it approaches the wall. At the wall the jet divides into two streams one above the impeller and one below. These streams loop and return to the impeller. The loops form a center of circulation one above and one below the impeller as is seen in Figure I-1.

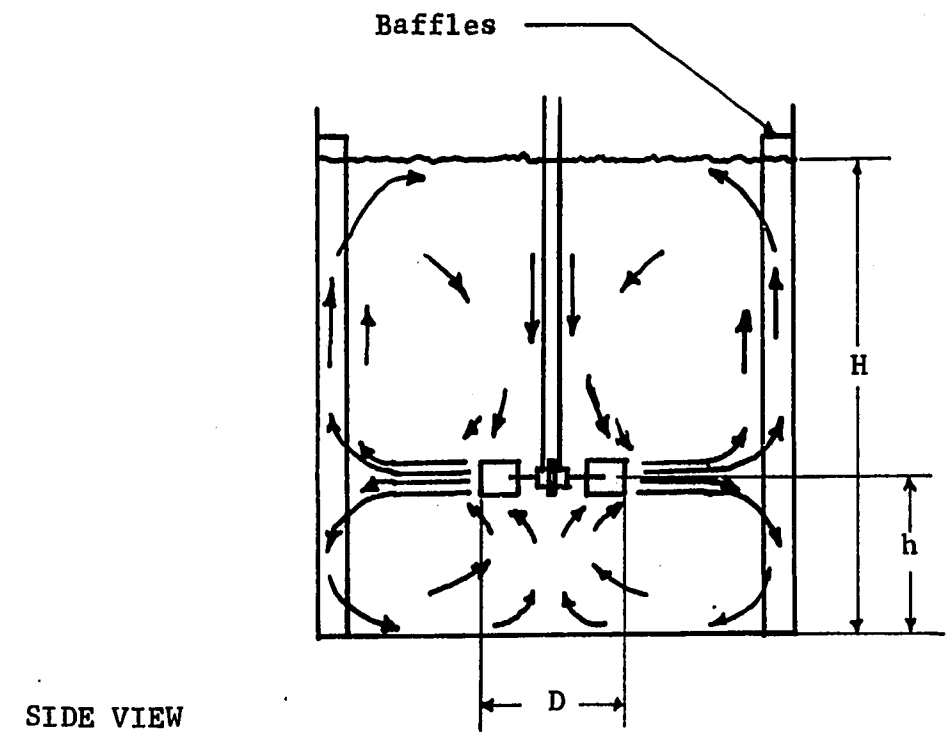

SIDE VIEW

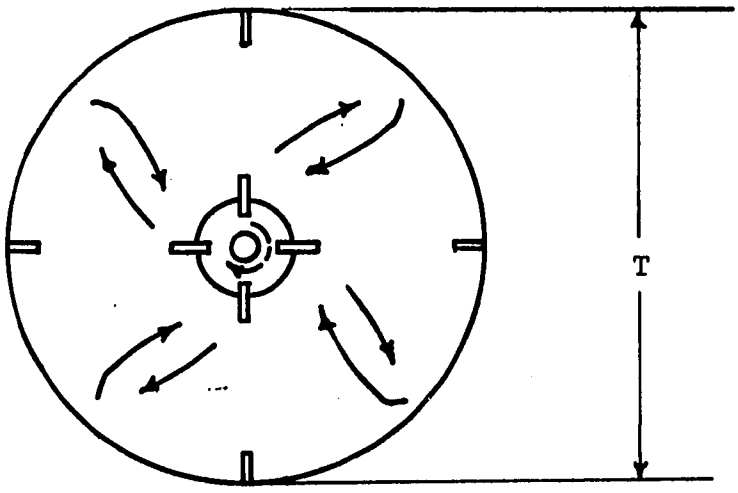

BOTTOM VIEW

Figure I-1. Flow Patterns in a Baffled Tank with a Turbine Impeller after Rushton (27).

The flow in a stirred tank is not a simple phenomena, and it is decided to restrict this work to a Newtonian fluid. Specifically distilled water was selected as the fluid, since it is easily handled and has a low viscosity typical of process fluids commonly used in stirred tanks. Furthermore, since stirred tanks are most frequently used in fully turbulent flow, this work will be restricted to a tank Reynolds number $N_{Re} = \rho ND^2/\mu$ greater than 10,000.

After surveying the literature, a summary of which will be presented in the next section, it was apparent that the flow in stirred tank was far from simple. There are approximately two regions of flow in the tank. One is the flow near the impeller, and this has received considerable attention. The other region is the rest of the tank. After considerable thought it was decided to divide the tank into several additional regions and model each separately.

The objectives of this research can now be clearly defined as:

1. To study the flow patterns in a tank stirred with a standard turbine impeller and to arrive at a suitable mathematical model to describe the flow in the tank.
2. To experimentally measure the actual velocities in the vessel with a three-dimensional pitot tube.
3. To obtain streamlines of the flow in the tank so as to have a visual picture of the flow, and to compare the experimental and theoretical velocity profiles in various regions of the tank for a 3.0 inch diameter impeller.
4. To correlate the parameters in the flow model so that quantities such as pumping capacity and eddy viscosity

in the region of the impeller can be predicted.

5. Compare the experimental and theoretical results of this work with that reported in the literature.

3. Literature Review

This section will be concerned with a review of the literature pertinent to flow patterns in a stirred tank. The stirred tank as a mixing device has been described in a considerable body of literature because of its extensive application, and the ingenuity of various investigators who have tried to describe and analyse the phenomena. Frequently the term mixing and stirred tank are synonymous as demonstrated by large sections devoted to the stirred tank in three books (12,33,34) published on mixing. There have been three dissertations and numerous articles on flow patterns. It is our opinion that the last word has not been said on the fluid dynamics of the stirred tank.

The description of the dynamics of the stirred tank has been approached by two methods.

1. The direct approach is used in which flow patterns and pumping capacities of impellers have been measured. Typical papers describing this approach are by Nagata (18,19,20) and Cooper (8).
2. Stirred Tanks are frequently used as perfect mixers or devices that will smooth out instantaneously any inhomogenuity in fluid property present in the tank. Actual stirred tanks seldom conform to this ideal but behave as perfect mixers in the region near the impeller

where high shear and turbulence exist and have very little mixing taking place in the rest of the tank. To obtain an idea of the extent of perfect mixing two methods of approach are used.

(i) Terminal blending time, or the time required to smooth out an impulse change in fluid property, for example, the concentration of a chemical species. An excellent review of work in this area is presented by Grey (40).

(ii) In the alternate approach, the tank is divided into four arbitrary elements or regions. These are plug flow, perfectly mixed, short circuit and dead water. The various fraction of the fluid residing in these regions is determined by measuring the residence time distribution. The residence time distribution is the response obtained from injection of pulse of a tracer material. A summary of the various linear models that can be built through combinations of the above four elements is given by Camps (7) and Uhl (34). The fact that only linear combination of elements is used restricts this method to linear systems. For example, in the study of chemical reactions in stirred tanks only first order reactions can be considered by this method. For second and higher order reactions additional information such as the flow pattern is needed.

Terminal blending time and residence time distributions, although useful in specific instances, give no insight into the

fundamental phenomena which is responsible for the observed behavior of the system. An accurate model of the fluid dynamics could be used to obtain these functions, if desired through theoretical analysis and without the need for additional experimental data.

In presenting a review of the literature it was found convenient to divide the material under various subheadings such as Power Consumption, Flow Patterns, etc. This approach was considered better than reviewing each individual work in its entirety, as it prevented undue repetition and put each topic in proper perspective. The reader will therefore find references to the same worker in one or more subheadings.

3.1. The Turbine Impeller

In the study of turbine impellers a variety of designs have been proposed and tested. Not all of these designs are of industrial importance. However the literature abounds with studies on different kinds of turbine impellers. In order to form a uniform basis for comparison and reference, five different basic designs of turbine impellers are shown in Figure I-2.

Type A is the flat blade, disk type turbine. Type B is the full flat blade turbine, and Type C is the curve blade turbine. Types B and C can have an additional parameter by raising the blades a distance h_1, above the plane of the impeller. This is shown by dotted lines for Type B in Figure I-2. Type D is the hammer headed turbine and Type E is the full blade turbine with a disk. Type A with six blades is the most frequently used turbine and is considered a standard design.

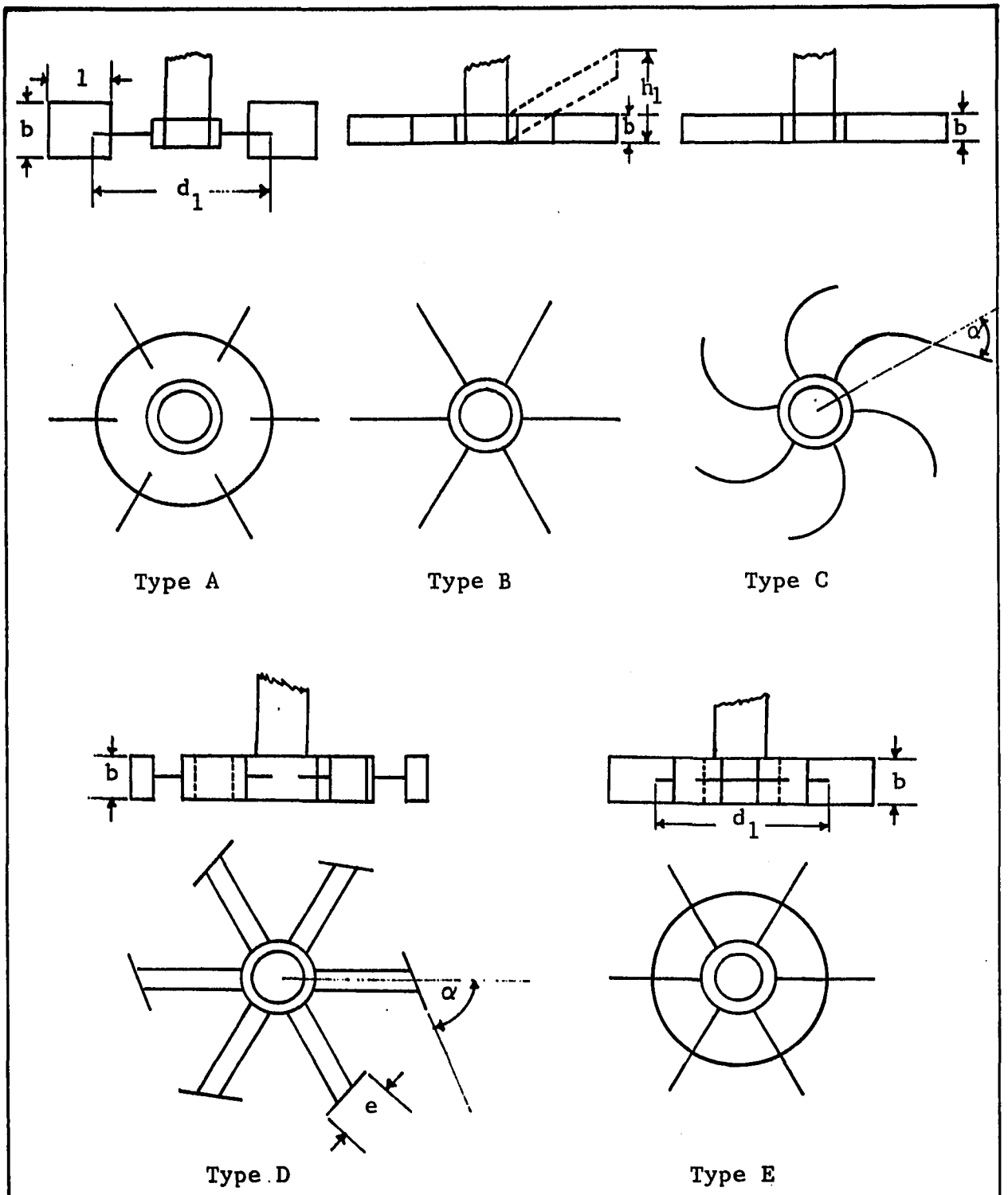

Figure I-2. Types of Turbine Impellers.

The parameters that can be varied are the breadth of the blade b, blade length l, disk diameter d_1, height of blade above impeller plane h_1, and in case of types C and D the angle α. In addition, the number of blades on the impeller can also be varied.

3.2. Power Consumption in Stirred Tanks

Power consumption was the first variable to be studied and reliable correlations of power input has been know for more than a decade. The most recent work is that of Bates and associates (3)

The correlation of power consumption using dimensional analysis is well known (26). For geometrically similar systems in baffled tanks (i.e. absence of swirl), dimensional analysis gives the following relationship,

$$N_p = k(N_{Re})^a \qquad \text{(I-1)}$$

where $N_p = \frac{Pg_c}{\rho N^3 D^5}$, is the Power Number and $N_{Re} = \frac{\rho ND^2}{\mu}$, is the Reynolds Number. As pointed out by Bates, when comparing or using power correlations of the form of equation I-1 care should be taken to ascertain if the systems considered are geometrically similar. This is frequently not the case, and is the reason why data reported in the literature often cannot be compared.

For the Type A turbine (see Figure 1-2) used in this work, the log-log plot of N_p versus N_{Re} as reported by Bates is not in agreement with the earlier and well known work of Rushton (26). The curves have the same general shape, and they reach a constant value of Power Number for Reynolds Number greater than 10,000. This limiting value of N_p is reported by Rushton to be 6.3 while that

reported by Bates is 5.0. The higher value of Rushton is said to be due to frictional errors. Lower values of N_p have been reported by other workers (35). Cutter (9) reported a limiting value of N_p to be 5.95. For a comprehensive review of power consumption the reader is referred to Grey (34). Bates (3) also claims that N_p is affected somewhat by number of baffles, baffle width and height of impeller above the bottom of the tank. These should therefore have some effect on the flow patterns and thus the power consumption.

3.3. Flow Patterns with Turbine Impellers

The word flow pattern by itself can and has been misconstrued. It can refer to:

1. Streamlines: These streamlines may be qualitative studies as in the work of Metzner (16) and Schumm (32), or the actual drawing of streamlines in a particular region as done by Nagata (19).
2. Velocity profiles: The velocity profile is the distribution of mean velocity across any plane. These planes are typically a cylinder surrounding the impeller or horizontal planes perpendicular to the axis of the impeller.

In addition flow patterns involve other factors or aspects. These are:

1. Whether the tank is baffled or unbaffled.
2. Kind of measuring device used. As there are a variety of devices employed, these will be reviewed separately in Section 3-5.
3. Frequently a theoretical analysis for the flow in a region

or the entire tank is attempted, and these will also be reviewed.

Comparison of Turbine Impellers by Nagata and Associates (18,19)

Any reference to flow patterns in stirred tanks is not complete without reviewing the extensive work of Nagata and associates. Their work is presented in three papers, and the object is to compare the performance of different types of impellers in unbaffled and baffled tanks. In order to make this comparison possible, the impeller diameter to tank diameter (D/T ratio) and the Reynolds number was kept approximately constant. In all but a few cases D/T = 0.513.

On the basis of kinds of impellers employed, in their first paper thirty impellers were investigated in unbaffled tanks. The impellers included types A, B, C and D of Figure I-2. All the impellers had eight or more blades. On the basis of the number of blades, there were eight different kinds of impellers. The thirty impellers were obtained by varying b, d_1 and l, the impeller parameter parameters shown in Figure I-2. In the second paper (19) the number of impellers was reduced to six. These six impellers were run in baffled tanks. In the third and last paper (20) the number of impellers were reduced to three, types A, B and C. All impellers had eight blades. The purpose of this study was to investigate the laminar and transitional regions in unbaffled tanks. Five runs were made using each impeller at approximately the same N_{Re}. The range of N_{Re} studied was approximately 6.7 to 10^5.

In all the work done by Nagata the impeller was centerally located. By centrally located it is meant that the impeller is placed at half the depth of the fluid in the tank. At high N_{Re} a specially designed pitot tube was used to measure velocities in the tank. At low N_{Re}, velocity measurements were made using the photographic method of Sachs (28)

Nagata presents his results as velocity profiles across a number of planes in the tank for one impeller, a sixteen blade type B impeller. It is implied that profiles for other impellers investigated are similar in form. For the purpose of quantative comparison Nagata defines a coefficient of discharge $N_{Q_1} = Q_1/ND^3$ and a coefficient of circulation $N_{Q_2} = \frac{Q_2}{ND_3}$. The quantity Q_1 is defined as the volumetric flow discharged by the impeller, To evaluate Q_1 consider Figure I-3, in which is shown a schematic velocity distribution in the upper quadrant of the tank. The dotted lines B′B′′ and C′C′′ are the streamlines that pass through the corners of the impeller, and thus enclosed the fluid discharged through the impeller. Nagata defines Q_1 to be this quantity fluid that is enclosed by the streamline B′B′′ and C′C′′. In the tank there will be some flow in the vicinity of the impeller blades. Hence the quantity Q_1, as defined by Nagata, will be lower than the value obtained if the discharge from the impeller is considered to be the flow across a cylinderical plane of diameter D, the impeller diameter. The latter definition of Q_1 is more often used.

The flow rate, Q_2, is obtained by integrating $\bar{v}_z$ in the plane that passes through the center of circulation and is from the

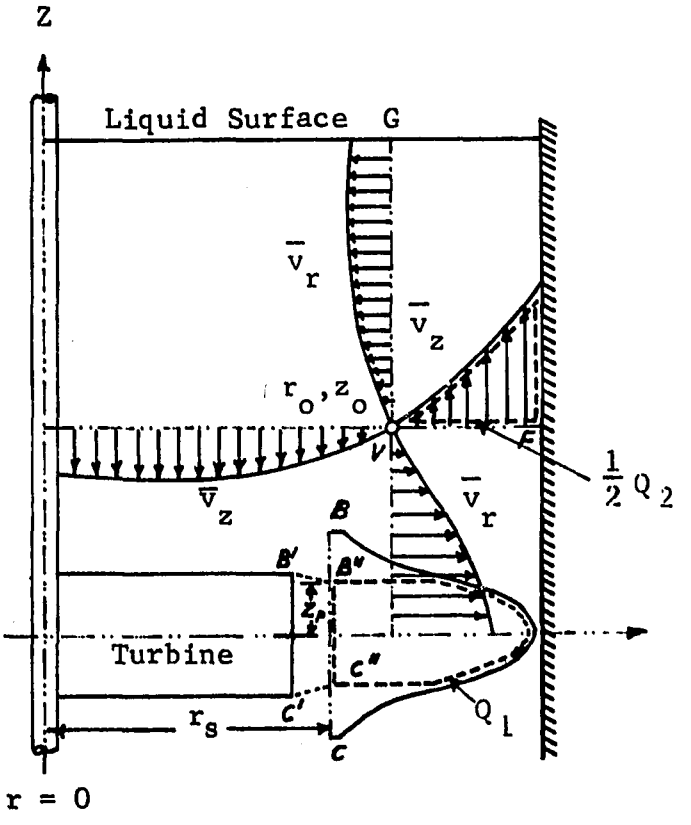

Figure I-3. Schematic Representation of Velocity Profiles in Baffled Tanks, after Nagata (19).

point V to F in Figure I-3. Thus,

$$Q_1 = 4\pi r \int_o^{z_p} v_r dz \qquad \text{(I-2)}$$

$$Q_2 = 4\pi \int_{r_o}^{T/2} v_z dr \qquad \text{(I-3)}$$

In equation I-2, z_p is the height at which the streamline B'C' intersects the cylinderical plane BC of radius r_s. In equation I-2 and I-3 it is assumed that the velocity profiles $\bar{v}_z$ and $\bar{v}_r$ are independent of θ, i.e. axial symmetry exists.

In unbaffled tanks Nagata (18) observed that the flow can be considered as two zones. An inner zone of radius r_c in which the tangential velocity $\bar{v}_\theta$ is approximately proportional to the radius r, and an outer zone in which the flow is quasi-potential flow. The radius r_c is about 80% of the impeller radius. There is a small circulatory flow which is caused by a small radial component, emerging from the impeller. Nagata called this a secondary circulation since the bulk of the flow is due to the tangential velocity $\bar{v}_\theta$

The secondary circulation is caused by the centrifugal forces due to the rotating impeller. At low N_{Re} the radial velocity profile at the impeller has a broad width. This width narrows considerably as N_{Re} increases. Nagata observed that the secondary circulation reaches a maximum in the transistion flow region being small in laminar or fully turbulent flow

In baffled tanks, the introduction of baffle plates was found to increase the width of the discharge from the impeller and also the velocity. The secondary circulation becomes the main flow and is well defined. The value of N_{Q_1} was found to range from 0.23 to 0.59 for most impellers in unbaffled tanks. In baffled tanks N_{Q_1} ranged from 0.78 to 1.34 indicating an increase in the discharge flow from the impeller by a factor of 2-4 on introducing baffles into the tank.

In baffled tanks Nagata (19) observed that the flow pattern repeats itself on an average, changing continuously with time in a complicated manner. These conclusions were based on observing the flow in five radial planes in a tank with four baffles as shown in Figure I-4(a). Progressing from Sections I to IV of Figure I-4(a), it was seen that the upper and lower centers of circulation in Section I were located very close to the impeller as shown in Figure I-4(d). In Section II the center of circulation moved further apart as shown in Figure I-4(e). In Sections III and IV the center of circulation becomes unstable and sometimes breaks into two eddies, as shown in Figure I-4(f). It was also observed that the baffles give rise to the eddy A shown in Figure I-4(b). The eddy A was found to break down into two eddies B and C, the eddy C being weak is easily dissipated. The eddy B is much stronger and is reinforced by similar eddies from other baffles and appears as a hollow vortex on the surface of the tank that rotates slowly in the same direction as the impeller. This surface vortex often sucks air into the system. Frequently it was found that all the eddies A, B and C completely disappear.

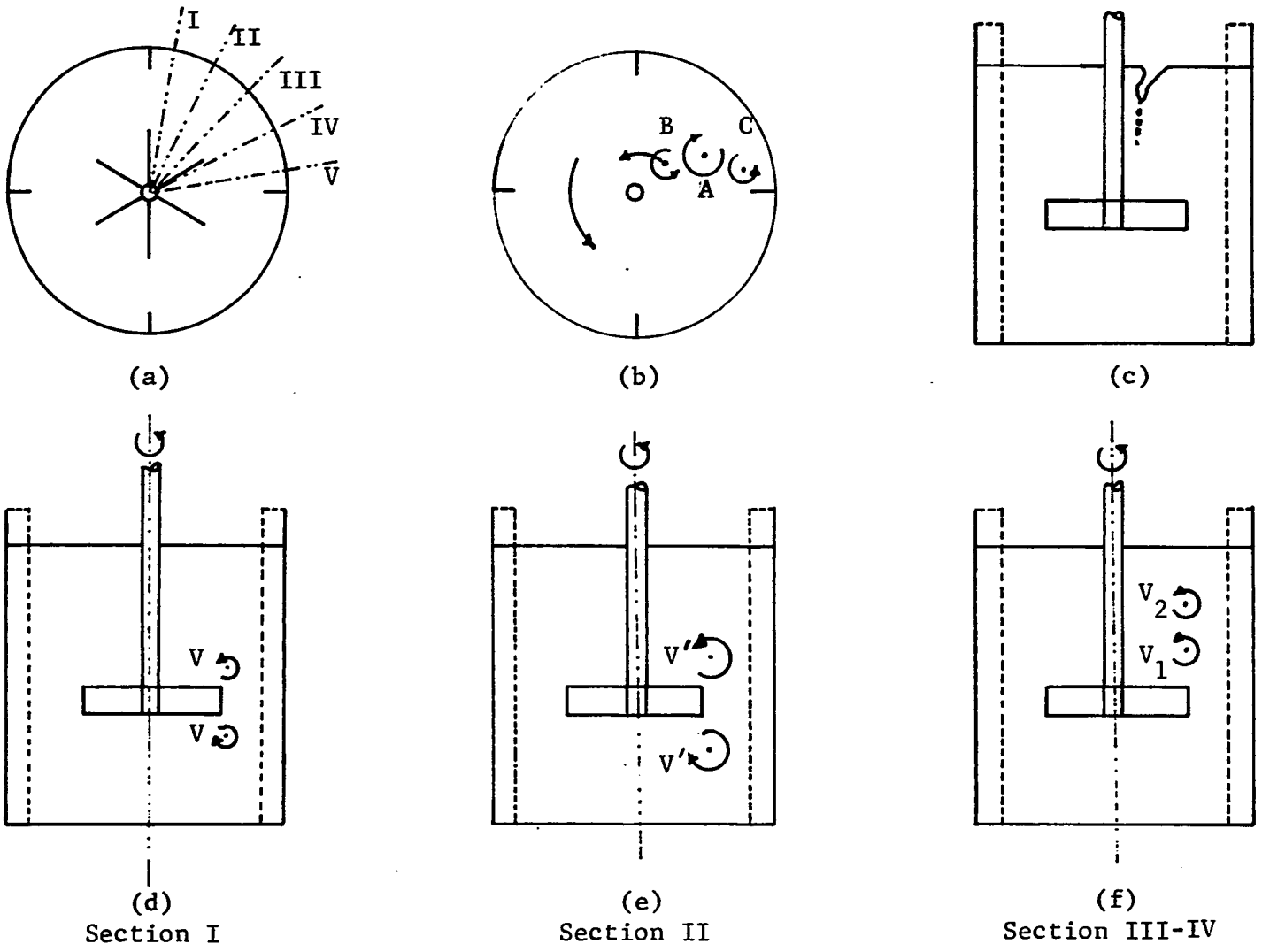

Figure I-4. Schematic Diagram of Vortex Formation in Baffled Tanks from Nagata (19).

In Figure I-5 the streamlines are shown in a radial plane which is typical of streamlines for all impellers in baffled tank. The center of circulation is continually fluctuating as noted in the preceding paragraph. For details of flow profiles in various planes the reader is referred to original papers or an excellent summary of them presented by Grey (38).

In calculating Q_1, the volumetric discharge from the impeller, Nagata found that there was a small variation in Q_1 depending on which radial plane the velocity profile was measured. This indicated that the velocity profile is not perfectly axially symmetrical. However, as the differences were not very large, Q_1 was reported as the average of measurements made in four different radial planes. Since Q_2 is the circulating flow hence Q_2/Q_1 will be the fractional entrainment. The value of Q_2/Q_1 ranges between 1.7 to 1.85 with an average value of 1.8. As pointed out earlier Q_1 has been defined differently by other authors such as Sachs (28), and the figure of 1.8 as the amount of entrainment cannot be directly compared.

The conclusions arrived at by Nagata for baffled vessels were that even though baffles increased the circulation the power efficiency was lowered. This meant that considerably more power was required to get the increased circulation. He also concluded that impellers having excellant performance in unbaffled conditions also perform better under baffled conditions.

Measurement of Velocity Profiles Near the Impeller by Sachs (28)

The first quantative measurements of velocities in the region

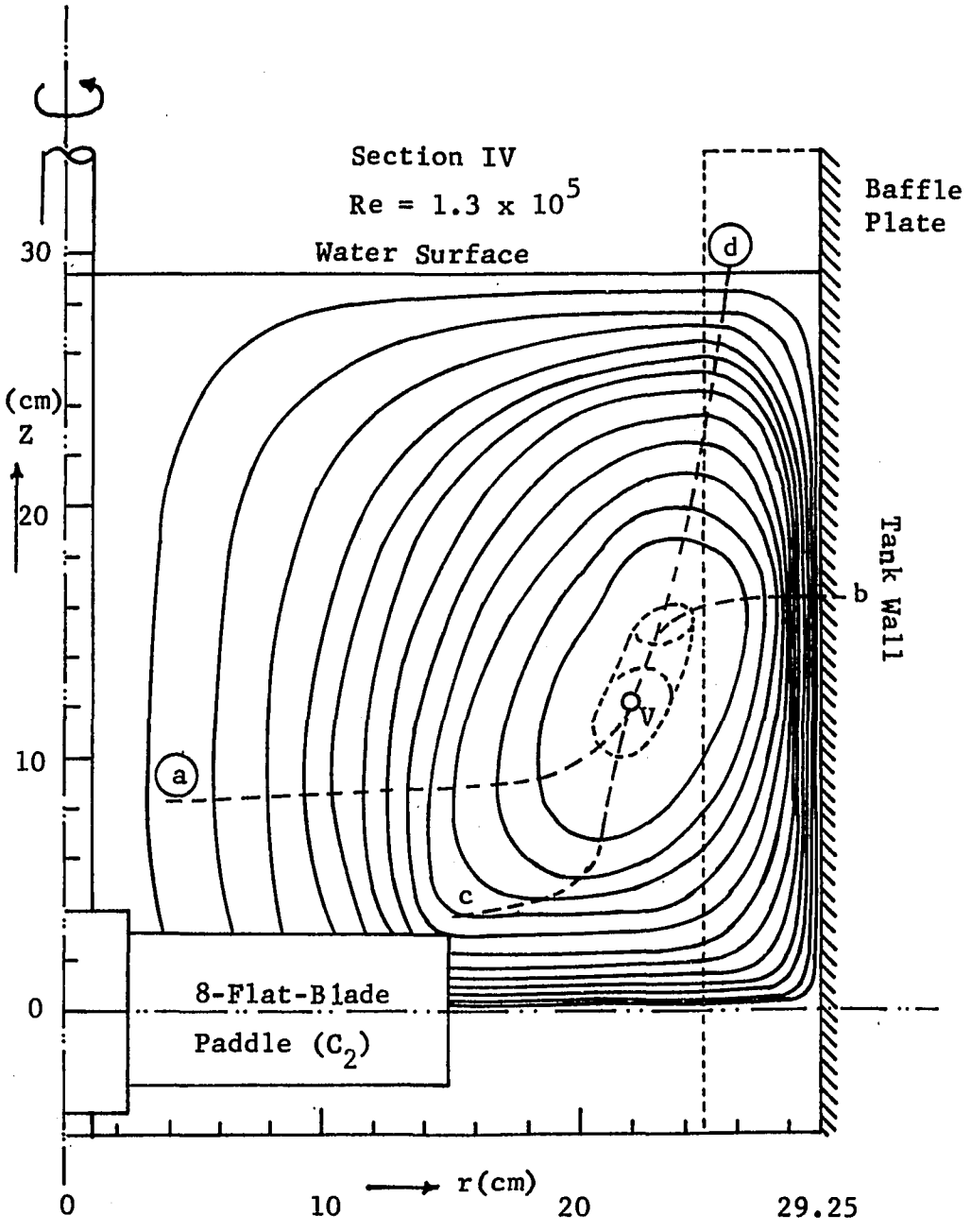

Figure I-5: Typical Streamlines in a Baffled Tank, From Nagata (19).

of the impeller was made by Sachs and Rushton (28). A 4.0 in. four blade type A impeller was used. Velocities were measured by the photographic method. Measurements were made at three impeller speeds and five radial positions. The velocity profiles were found to be bell-shaped and tended to flatten as the radial distance from the impeller increased. The ratio of the average velocity to maximum velocity ($\bar{v}/\bar{v}_{max.}$) was found to be independent of impeller speed but to increase with radial distance. The volumetric flow from the impeller increased with increasing r because of entrainment, and it reaches a maximum at r = 4.0 inches. The amount of entrainment was reported as 1.96 with practically no variation for the three observations reported. This value of entrainment cannot be compared with Nagata as the discharge flow is defined as all the liquid emerging from the impeller.

Sachs observed that the radial velocity in between impeller blades was not uniform but reached a maximum at about 50° ahead of the rotating blade. At this point the radial velocity was found to be 38% higher than the average and was an instantaneous value that should not be confused with average values of $\bar{v}_r$ at a point. This effect indicates that axial symmetry is only approximate, and depends upon the position of the impeller blade. This pulsating velocity distribution was found to persist as the radial distance was increased to about two-thirds of the distance to the wall. After this point the flow appeared uniform or axially symmetrical.

Sachs reported that the fluid leaves the impeller at an angle of 53° indicating a considerable tangential component at the periphery of the impeller. This tangential component decreased to 22° at r = 5.0 inches indicating that the tangential component decreases to a small but finite value at the wall.

Sachs and Rushton made no attempt to postulate a model for the flow from the impeller. They conclude that the volumetric flow is directly proportional to the impeller speed and that the flow from the impeller entrains a considerable quantity of fluid as it moves to the walls of the tank.

Nielson's Tangential Jet Model (21)

The fluid that emerges from the impeller is a narrow, high speed jet with a considerable tangential component. Nielson proposed a model of this tangential jet which replaced the impeller by a ring source of radius a, which is smaller than the radius of the impeller. The fluid emerges from this ring with a bell shaped velocity distribution, and the velocity vector $\vec{V}$ is tangent to the ring source at all points in the jet. This model not only accounts for an appreciable tangential velocity at the impeller periphery, but also the observation that the tangential component of $\vec{V}$ decreases as the tank wall is approached. A schematic drawing of the tangential jet is shown in Figure I-6.

Nielson time averaged the equations of motion, and simplified them using the boundary layer assumption to obtain the following equation for the tangential jet.

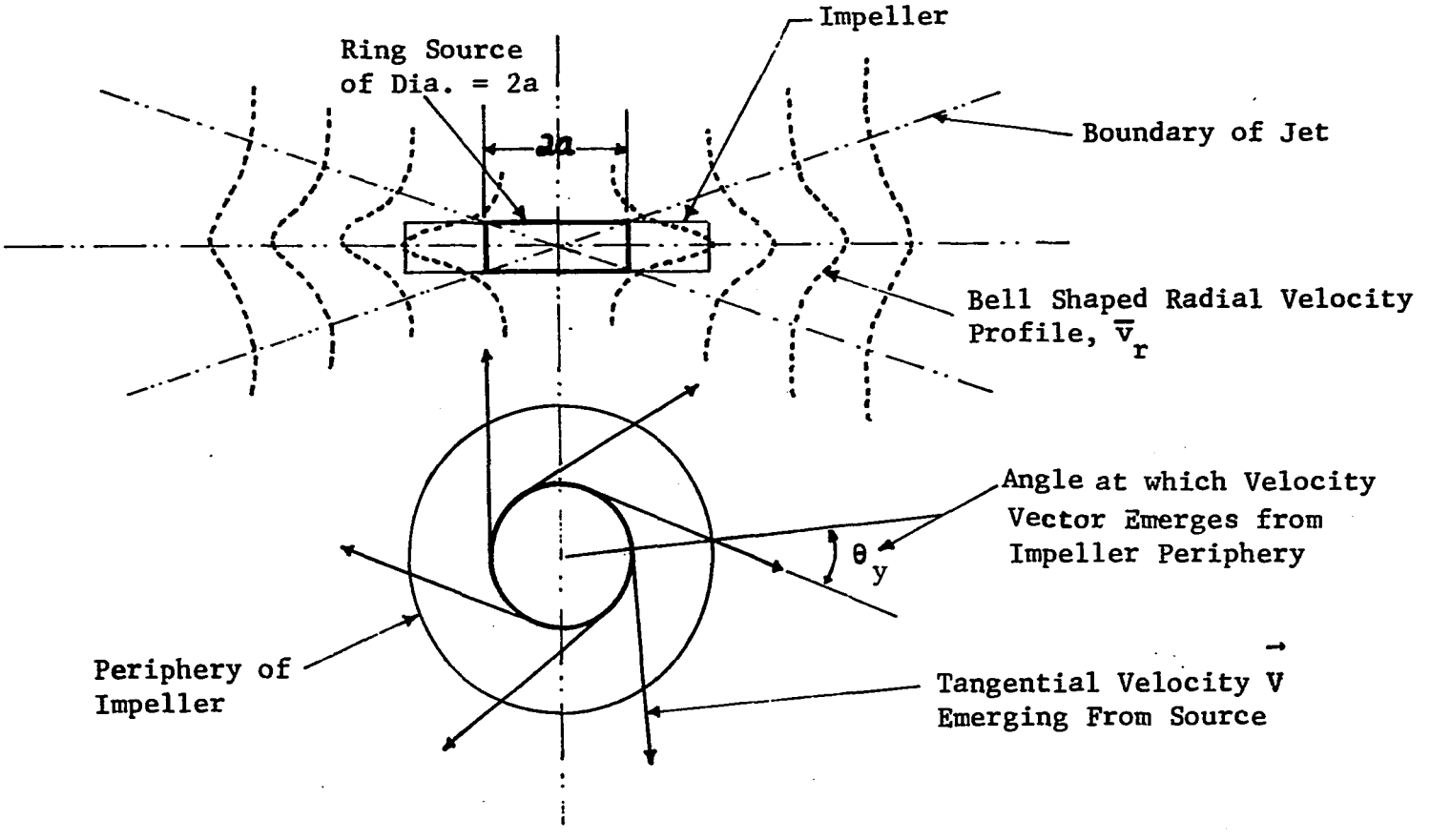

Figure I-6. Tangential Jet.

$$\bar{v}_r \frac{\partial \bar{v}_r}{\partial r} + \bar{v}_z \frac{\partial \bar{v}_r}{\partial z} - \frac{a^2}{r(r^2-a^2)} \bar{v}_r^2 = - \frac{1}{\rho} \frac{\sqrt{r^2-a^2}}{r} \frac{\partial |\vec{\tau}|}{\partial z} \qquad \text{(I-4)}$$

Equation I-4 has been derived in Appendix A, since Nielson's model of the tangential jet is the best available model to describe the flow in the region of the impeller. In Equation I-4, a is the radius of the ring source and $\vec{\tau}$ is the turbulent shear stress due to gradient of the velocity vector, $\vec{V}$, and is equivalent to considering $\vec{V}$ as one-dimensional boundary layer flow.

Nielson used Prandtl's Mixing-length Theory to evaluate $|\vec{\tau}|$. The velocity profiles were assumed similar which means $\bar{v}_r/(\bar{v}_r)_{max}$ is not a function of r. A similarity transformation of equation I-4 results in the ordinary differential equation

$$\frac{d^2F}{ds^2} = \frac{d}{2c^2} F \frac{dF}{ds} \qquad \text{(I-5)}$$

where d is a constant and c is the mixing-length constant. Other quantities are given by,

$$s = z/b \qquad \text{(I-6)}$$

$$\bar{v}_r/(\bar{v}_r)_{max} = f(s) \qquad \text{(I-7)}$$

$$F(s) = \int_0^s f(s)\,ds \qquad \text{(I-8)}$$

In the above equation f(s) is a dimensionless velocity profile, and states the condition of similarity. The variable s is a dimensionless z coordinate given by equation I-6, in which b is the width of the jet. It should be noted that b is a function of r and is shown to be equal to,

$$b = \frac{d}{2} \sqrt{r^2 - a^2} \qquad \text{(I-9)}$$

The velocity profile is given by the following equation

$$\bar{v}_r = \frac{A}{r\sqrt{b}} (r^2 - a^2)^{1/4} \frac{dF}{ds} \qquad \text{(I-10)}$$

In equation I-10, A is an arbitrary constant. It is evident that in order to obtain the velocity profile the function F(s) has to be evaluated. This is done by solving the differential equation I-5 with appropriate boundary condition. Nielson obtained an implicit solution in parametric form for the differential equation I-5, and this is

$$s = \frac{\sqrt{3}}{4\pi} \frac{(1-H+H^2)}{(1+H)} + \frac{3}{2\pi} \tan^{-1} \frac{(2H-1)}{\sqrt{3}} + \frac{1}{4} \qquad \text{(I-11)}$$

where the parameter H is given by

$$H = \left(\frac{M^{3/2}}{1-M^{3/2}} \right)^{1/3} \qquad \text{(I-12)}$$

and M is given by the following relationship

$$\frac{\bar{v}_r}{(\bar{v}_r)_{max}} = \frac{dF}{ds} = \frac{dM}{dt} = (1-M^{3/2})^{2/3} \qquad \text{(I-13)}$$

A numerical method can be used to evaluate $\bar{v}_r$ as a function of s. This is done as follows; for a series of values of M, H is calculated from I-12 which then enables the calculation of s. A table of M versus s is thus obtained. From I-13 this table can be converted to a table of s versus $\frac{dF}{ds}$. Then if the parameters A,

d and a are known, $\bar{v}_r$ can be evaluated as a function of z for a fixed value of r from I-9. Nielson solution is a three parameter model the parameters being A, a and d.

By a trial and error method, Nielson was able to fit his velocity profile data to the model given by equations I-10 to I-13. From Table I-2 it can be observed that three impellers were studied at four different speeds. Since all other conditions in the tank are constant, this constitutes four different flow patterns. Nielson uses these four points to evaluate some of the constants from the experimental plots of different equations. The value of d was found to be 0.782. The constant a, was assumed to be proportional to the impeller diameter D and obtained as

$$a^2 = 0.157D^2 \qquad \text{(I-14)}$$

The parameter A was not evaluated as such since it was not used directly.

Nielson presented equations for predicting $(\bar{v}_r)_{max}$, the velocity at the impeller center line, as a function of r and also the volumetric discharge Q as a function of r. Both these quantities were found to be dependent on D/T, the impeller diameter ratio. These prediction equations for $(\bar{v}_r)_{max}$ and Q are not entirely conclusive since they are based on only four data points.

From Prandt's mixing length theory, and the velocity profiles Nielson obtained the following equation for the shear stress

$$\tau_{zr} = \left(\frac{3}{4\pi}\right)^3 \frac{r\rho Q(\bar{v}_r)_{max}}{(r^2-a^2)^{3/2}} \left|\frac{d^2F}{ds^2}\right| \frac{d^2F}{ds^2}$$

Table I-2: Summary of Neilson's Investigation of Turbine Impellers

Impeller Diametric Inches	Radial Distance r Inches	Fluid Used	Fluid Temp. °F	Impeller Speed RPM
2.0	1.0	water	83	600
2.0	3.0	water	83	600
2.0	4.0	water	83	600
4.0	2.0	water	77	200
4.0	2.0	water	77	200
4.0	2.0	corn-syrup	--	100
7.0	3.5	water	83	75

Figure I-7 shows Nielson's comparison of theoretical shear stress calculated from equation I-15 and the experimental value obtained from the turbulent components of the velocity $\bar{v}_r$ and $\bar{v}_z$. The corresponding turbulent fluctuating components will be denoted by v_r' v_z' and the experimental shear stress $(\tau_{rz})_{exp}$ is given by

$$(\tau_{rz})_{exp} = -\rho \overline{v_r' v_z'} \qquad \text{(I-16)}$$

The bar over the v_r' and v_z' in equation I-16 signifies averaging. In Figure I-7 it is seen that the experimental values do not show any particular trend but might be interpreted as giving a maximum value of $(\tau_{rz})_{exp}$ smaller than the calculated τ_{rz} and at a distance z, closer to the impeller center line. The discrepancies in Figure I-7 may be because Nielson's photographic method of evaluating turbulent components v_r' and v_z' is not sufficiently accurate.

Velocity Profiles in Baffled and Unbaffled Tanks by Aiba (1)

Aiba measured flow profiles using three different impellers in unbaffled and baffled tanks. The measuring device was a radioactive ball and a miniature Geiger-Muller counter. Both laminar and turbulent flow regions were investigated. The impellers used were: paddle (similar to type B with two blades), a turbine (six blades type A) and a three blade marine propeller.

Aiba found that the flow in a stirred tank was symmetrical with no variations existing in radial planes in between baffles. This observation was contrary to that of Nagata (19) and Sachs (28) both of whom report small variations in these velocity profiles to exist. Aiba presented his results as a plot of dimensionless

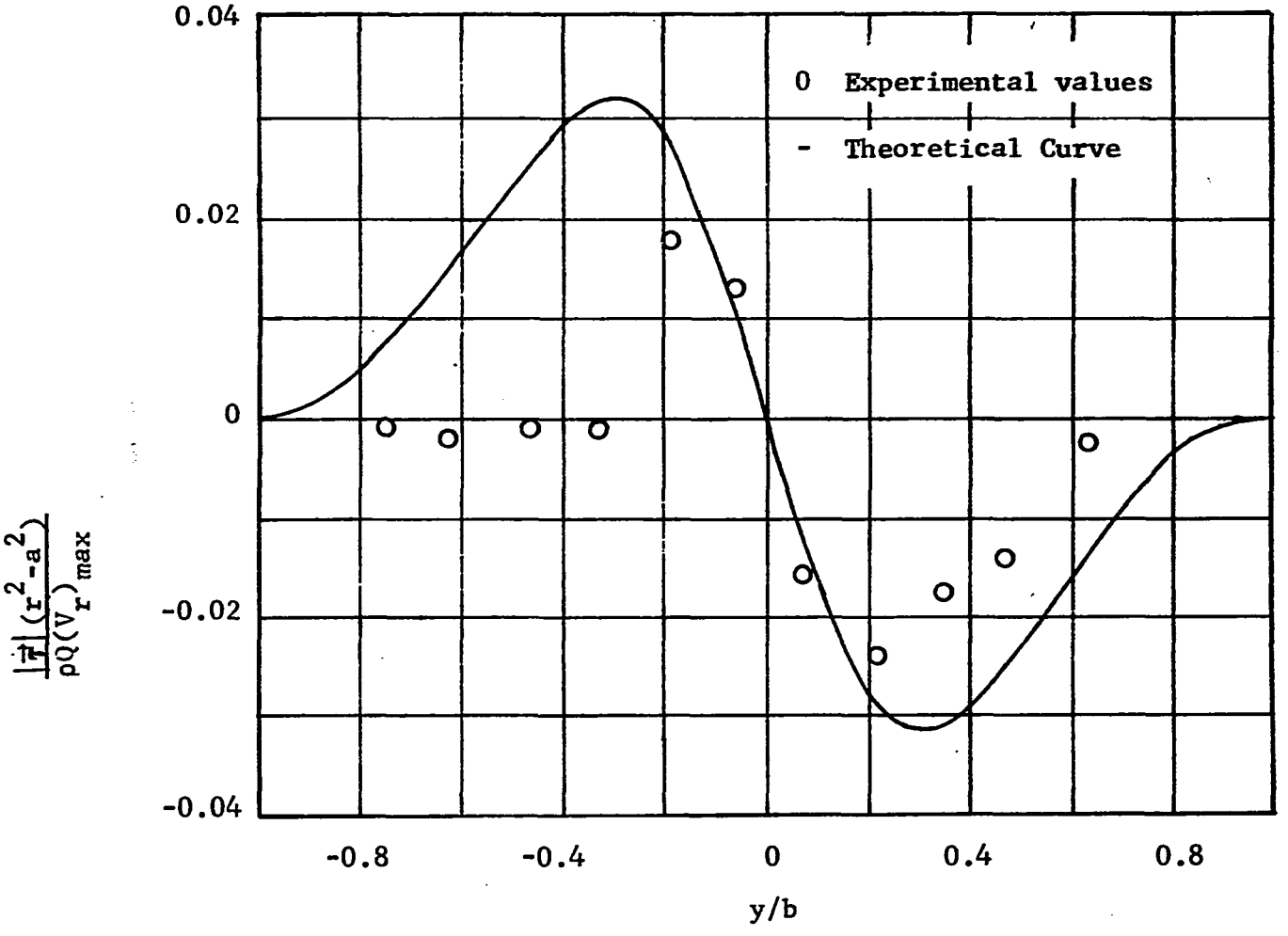

Figure I-7. Nielson's Comparison of Experimental and Theoretical Shear Stress at r is equal to 4.0 inches (21).

velocity, v/v^* against a dimensionless radius 2r/T. The liquid velocity is v, and v^* is the impeller tip velocity. Aiba observed that the dimensionless plots were independent of the depth within the tank and the speed of the impeller. However, different plots were obtained for different impellers and for baffled and unbaffled tanks. In unbaffled tanks with glycerine solution of vicosity 108 centipoises it was observed that v/v^* was dependent on speed. This indicated that viscosity has an effect on the flow patterns in unbaffled tanks although from a consideration of Reynolds number it would seem to have no effect. A representative plot at a depth of 7.0 inches was presented for the paddle impeller. The observation of dimensionless velocity being independent of impeller speed was in agreement with the findings of Sachs (28). No measurements were made in the vicinity of the impeller.

Aiba characterizes the flow in unbaffled tanks as a solid cylinderical core of fluid rotating at the center of the tank. The radius of the core is smaller than the impeller diameter. This observation is in agreement with Nagata for unbaffled tanks. In baffled tanks the radius of the core is said to be larger. The flow outside the core is similar to a free vortex. This description is very close to that of an ideal circular vortex (15). It is not very clear what velocity Aiba refers to, since a vortex has flow in a tangential direction only. The dimensionless plot of velocity, v looks very much like that for the resultant of v_θ and v_r. This is confirmed somewhat when Aiba's measuring device is

examined (see Section 3.5 for details).

Measurement of Flow Profiles at the Impeller by Cutter (9)

Cutter measured flow profiles in the neighborhood of the impeller using an improved photographic method. The object of his work was to study energy dissipation in a stirred tank. A 11.5 inch diameter tank was used with covers on both the top and bottom of the tank, in other words no free surface was maintained. The distance between the top and bottom covers was 12.0 inches. The impeller used was 4.0 inch diameter type A impeller, placed 6.0 inches from the bottom of the tank. Velocity measurements were made at 200, 400 and 600 rpm in water. Both the mean velocity and the turbulent fluctuating components were measured. The ratio of fluid velocity to impeller tip velocity was found to be independent of impeller speed, as observed by Sachs (28) and Aiba (1). Cutter also reports that the ratio of the turbulent fluctuating velocity component to impeller tip speed was independent of the impeller speed.

The fluctuating velocity components were measured at the impeller center line only. Hence turbulent parameters such as the correlation coefficient and scale of turbulence could be calculated only at the impeller center line. The radial scale of turbulence was observed to be larger than the tangential scale. The tangential scale had a maximum, while the radial scale increased as the tank wall was approached.

The integral form of the equation of motion and energy were used to determine the energy destribution in the region of the

impeller. The equations of motion and energy were time averaged and were simplified using the boundary layer approximation. The turbulent velocity components were simplified on the assumption that the turbulence behavior was approximately similar to turbulence in pipes. Observation from Laufer's well known study in pipes were then used to effect this simplification.

A torque table was used to obtain the input torque and also the energy input to the system. The momentum equation confirmed that all the angular momentum put into the tank could be accounted for in the impeller stream. This did not hold at the wall indicating that the flow regime had changed. The flow was then no longer free turbulence with high shear but in stagnation flow. The assumption used to simplify the equation of motion for the jet hence no longer applies. The integral form of the energy equation was used to calculate the energy in the fluid stream at various radial distances from the impeller. It was estimated that 20% of the energy was dissipated in the impeller itself, 50% in the impeller stream and 30% in the rest of the tank. These values were in close agreement with that obtained by using Batchelor's emperical relationship for energy dissipation in turbulent flow.

Potential Flow Solution by Larson (14)

Larson (14) investigated flow patterns and flow profiles using the photographic method. He used a 12.0 inch diameter tank with four baffles 1.0 inch wide and 1/4 inch thick. The impeller was a Type A with four blades and was made of lucite. The diameter of the disk was 2-5/8 inches and the impeller blades had a dimension of 1.0

by 1.0 inch. Fluids used were four different mixtures of corn syrup and water. This enabled studies to be made in the Reynolds number range of 31. to 25,800. The height of liquid in the tank was 12.0 inches and the impeller was placed 6.0 inches from the bottom of the tank.

Larson considered the flow in the entire tank to be irrotational flow. He admited that this was a weak assumption in the neighborhood of the impeller. The assumption of irrotational flow is equivalent to using inviscid flow theory. Irrotationality implies

$$\nabla \times \vec{V} = 0 \qquad \text{(I-17)}$$

In cylinderical coordinated 1-7 reduces to (43)

$$\frac{\partial \bar{v}_r}{\partial z} - \frac{\partial \bar{v}_z}{\partial r} = 0 \qquad \text{(I-18)}$$

provided $\bar{v}_\theta = 0$. This is probably true except in the vicinity of the impeller. Since the stream function Ψ satisfies the continuity equation, it was introduced in appropriate form into I-18. The resulting equation is

$$\frac{\partial^2 \Psi}{\partial r^2} - \frac{1}{r}\frac{\partial \Psi}{\partial r} + \frac{\partial^2 \Psi}{\partial z^2} = 0 \qquad \text{(I-19)}$$

Larson solved equation I-19 using the following boundary conditions

$$\bar{v}_r(0,z) = \bar{v}_r(R,z) = \bar{v}_z(r,z_1) = 0 \qquad \text{(I-20)}$$

$$\bar{v}_z(r,z_2) = f(r) \qquad \text{(I-21)}$$

Equation I-20 specifies the velocity components normal to the tank wall and normal to the tank surface to be zero. From the last statement it follows that z_1, is the height of the surface from the impeller centerline which is z = 0. The boundary condition I-21 is a velocity profile in a plane of height z_2, and it was obtained experimentally. The plane z_2 was chosen at z = 1 inch, as this was considered sufficiently far from the impeller centerline so that the flow could be considered as more nearly potential flow. The solution of I-19 with boundary conditions I-20 and I-21 had the form of an infinite series in terms of Bessels and Hyperbolic functions. Larson presents his data as velocity profiles of $\bar{v}_r$ and $\bar{v}_z$ at various points in the tank. The velocity data obtained in regions above and below the impeller are indistinguishable and was to be expected since the impeller was centrally located.

In laminar flow (N_{Re} = 62), $\bar{v}_z$ is presented as a function of r in several z planes at an interval of 0.5 inch appart. The $\bar{v}_z$ are negative, for r smaller than 4.0 inches and positive for r larger than 4.0 inches in all the plots. The velocities are presented scaled to 1 inch. On this scale for r less than 4.0 inch, $\bar{v}_z$ theoretical is approximately 0.25 inch lower than experimental values in all plots shown. Beyond r = 4.0 inch, which is the region near the wall, the theoretical equation does not hold at all and there were marked discrepancies.

Similarly $\bar{v}_r$ is presented as flow profiles in radial planes 0.5 inches a part. The velocities again reported on a scale of 1.0 inch and on this basis the theoretical $\bar{v}_r$ is lower by about 0.25

inch from the experimental values. For z ranging between zero and 2.0 inches, the region of the impeller, the correlation breaks down.

In turbulent flow the experimental data show considerable scatter. On the basis of a full scale for the velocities of 1.0 inch the experimental data scatters in a region of 0.5 inch or 50% of scale. The theoretical predicted profile is again consistently lower than experimental data points, and the model breaks down in the region of the wall and the impeller. Larson admits that under turbulent conditions there was no agreement between theory and experiment.

Flow Pattern Studies by Schumm (32).

Schumm made qualitative studies of flow patterns with five different impellers. These impellers were Types A and B with variations such as perforated blades or alternated blades unperforated, etc. All impellers were 4.0 inches in diameter and mounted in a 12.0 inch diameter tank, 1.25 diameters off the tank bottom.

Motion pictures of dye filiments and still pictures with ion-exchange beads were made that follow the flow patterns. All impellers gave the characteristic radial flow pattern. Type B impeller when placed close to the bottom of the tank gave a predominant flow above the impeller as shown in Figure 1-8.

Schumm goes through an involved mathematical analysis to calculate a theoretical shear stress in the region of the impeller. This calculated shear stress was later used to obtain an empirical correlation of the half time of the reaction of oleic acid with sodium hydroxide.

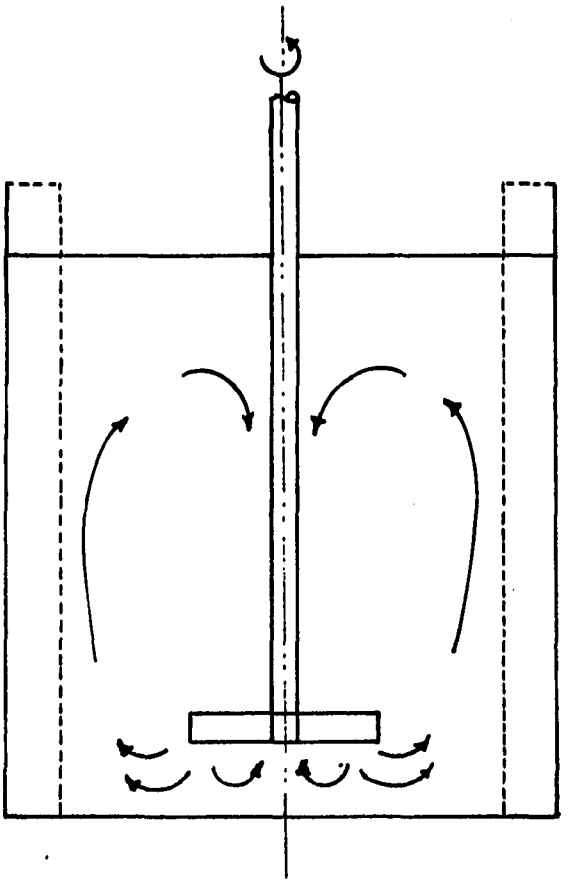

Figure I-8. Anamolous Flow Pattern Observed by Schumm (32) With Type B Turbine, with the Turbine Located Close to Tank Bottom.

Velocity Measurements in the Region of the Impeller by Cooper (8)

Cooper measured velocity profiles in a stirred tank with geometrically similar Type A impellers of varying diameter. With water as the fluid, a directional pitot tube was used, and with air as the fluid, a hot wire arenometer was used. The object of Cooper's work was to measure the flow profiles in the region of the impeller and determine pumping capacities. Measurements were made in a 15.0 inch diameter tank with four baffles. The impeller appeared to be centrally located. The height of fluid in the tank is not mentioned, but it was implied that it was the same as the diameter of the tank. Four geometrically similar Type A turbine impellers were used having diameters of 3.0, 4.0, 5.0 and 6.0 inches. The effect of varying the blade width for the 4.0 inch diameter turbine was also studied. In addition measurements were made for an 8.0 inch diameter, three blade marine propeller.

Cooper made velocity profile measurements at the impeller preiphrey and also at three other values of the radial distance from the impeller axis. The effect of entrainement was thus measured quantatively. The profiles were bell shaped as observed by Sachs (28) and others ([4,20,21]). Cooper also observed an angle profiles which was independent of impeller diameter and speed. The angle profile can best be understood by referring to Figure I-6 which shows a schematic diagram of the tangential jet. The velocity vector $\vec{V}$ has a bell shaped, however the vector $\vec{V}$ does not emerge at the same angle θ_y at the impeller periphrey for different z planes. The angle θ_y is thus a function of z and is the angle

profile referred to above. The value of θ_y was reported as 50° at the impeller centerline and increased to a maximum of 70° for both positive and negative values of increasing z. In other words if the flow from the impeller is considered a jet, then at the edge of the jet θ_y is 70°. The reason why this angle profile was not observed by the photographic method of Sachs (28) is because in the photogrphic method $\vec{V}$ is not measured but $\bar{v}_r$ and $\bar{v}_\theta$, the components of $\vec{V}$. Hence, in reconstructing $\vec{V}$, the angular dependence with z could very well be lost.

Cooper developed a theoretical equation to predict the velocity profile. The model assumed a stagnant core of radius kR, where R is the impeller radius. In the region (1-k)R the velocity $\bar{v}_z$ was assumed to have a finite value $\bar{v}_z$ and elsewhere $\bar{v}_z = 0$. This is shown in Figure I-9. Taking a material balance at a point z for an element of width ΔZ gives

$$- \rho\bar{v}_z\pi\,(R^2-k^2R^2)\Big|_{z+\Delta z} + \rho\bar{v}_z\pi\,(R^2-k^2R^2)\Big|_{z} - 2\pi R\,\Delta z\rho\bar{v}_r = 0 \qquad \text{(I-22)}$$

Taking the limit, as $\Delta z \to 0$, we get

$$\frac{d\bar{v}_z}{dz} = \frac{-2\bar{v}_r}{(1-k^2)R} \qquad \text{(I-23)}$$

Neglecting viscous forces, and taking a momentum balance on the element gives

$$-\rho\bar{v}_z^{\,2}\pi(R^2-k^2R^2)\Big|_{z} + \rho\bar{v}_z^{2}\pi(R^2-k^2R^2)\Big|_{z+\Delta z} + 2\rho\pi R\bar{v}_r^{2}\Delta z \qquad \text{(I-24)}$$

$$= \rho\pi^2w^2R^3(1-k^2)\,\Delta z$$

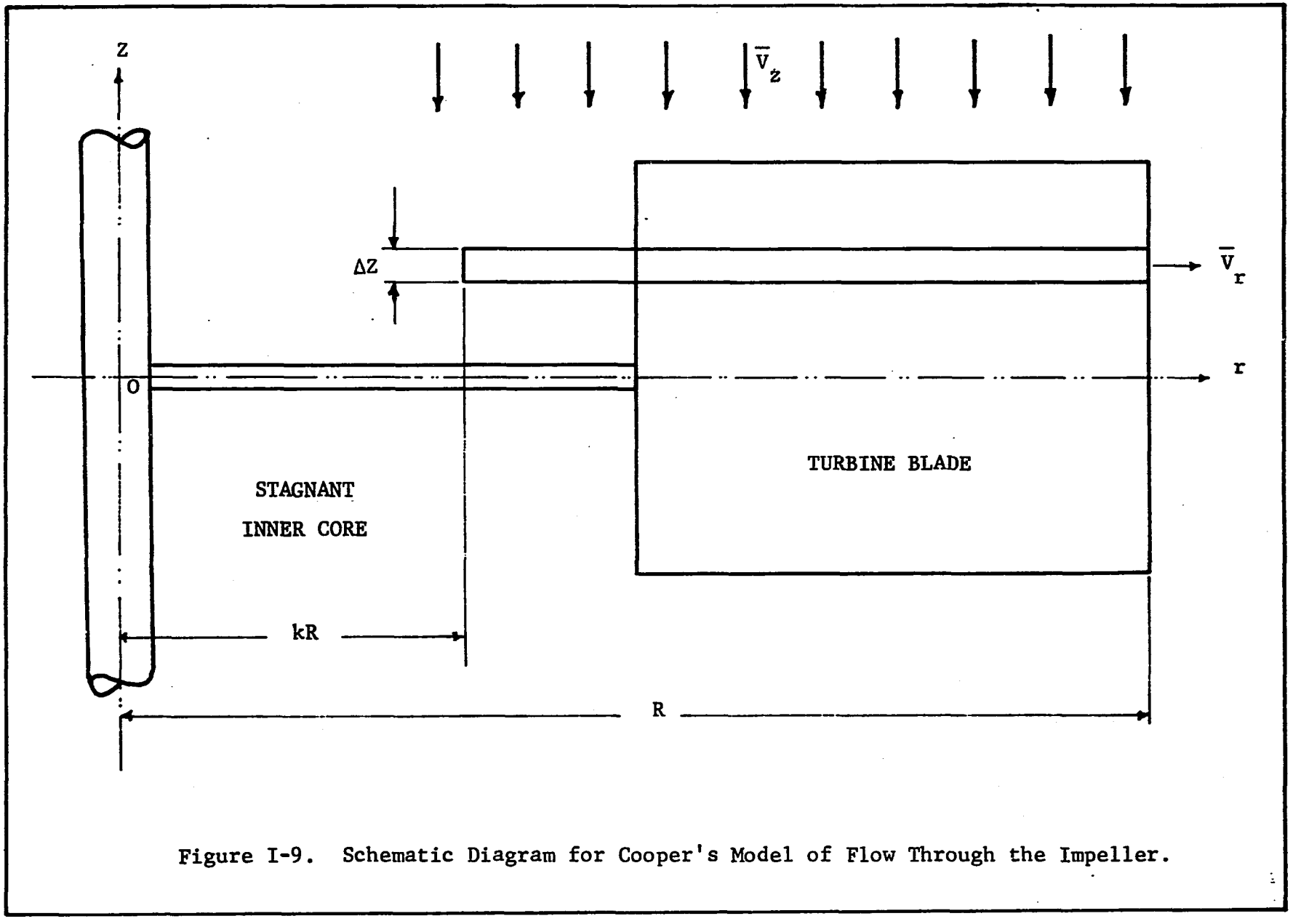

Figure I-9. Schematic Diagram for Cooper's Model of Flow Through the Impeller.

where w is the angular velocity of the impeller. Equation I-24 as given by Cooper is in error since the rate of momentum is a vector. The momentum in the z direction has been added to the rate of momentum in the r direction and the centrifugal force which also acts in the r direction. Cooper takes the limit on Δz in Equation I-24, then eliminates $\bar{v}_z$ using I-23 and solves the resulting second order differential equation for $\bar{v}_r$ with appropriate boundary conditions.

It is therefore not surprising that the experimental and theoretical values show no agreement. Cooper tries to salvage his theoretical equation for $\bar{v}_r$ by introducing a correction factor which improves the fit somewhat, but it has no theoretical basis. From the above analysis, Cooper obtains the following equation for the angle θ_y

$$\tan \theta_y = \frac{1}{C_1} \tan \frac{z}{2C_1^2 R} + \frac{\pi}{4} \qquad \text{(I-25)}$$

In equation I-25 C_1 is a constant to be evaluated from experimental data. Equation I-25 shows that θ_y is a function of z only and predicts α to range between 55° and 71°, very close to the experimental values observed. This is a surprising result considering that the theory is incorrect.

Another surprising result observed by Cooper is that the velocity profiles for water and air in the region of the impeller is remarkably close. This indicates that in this region of the tank the flow is governed by turbulence, and the effect of viscosity is negligible.

Flow Patterns in Newtonian and Non-Newtonian Fluids by Metzner (16)

Metzner investigated flow patterns using the photographic method in baffled stirred tanks for Newtonian and non-Newtonia fluids. The laminar and transistion regions were investigated using geometrically similar impellers (Type A, diameter ranges from 2.0 to 6.0 in.) and two fluids: Karo syrup which is Newtonian and CMC, sodium carboxymethyl cellulose which is non-Newtonian. Several photographs show streak lines of tracer particles describing qualitatively the transistion of flow from laminar to turbulent flow. The velocity data obtained by the photographic method was differentiated to obtain the local shear rates. Power dissipation was calculated from a knowledge of the behavior of shear rates to shear stress from viscometric studies. The following conclusions were noted:

1. In both Newtonian and non-Newtonian fluids the shear rates and power dissipation was directly proportional to impeller speeds under all conditions studied. The Reynolds number ranged from 2.1 to 450.
2. Shear rates and power dissipation are high in the region of the impeller. In laminar flow the power dissipation is proportionately larger elsewhere in the vessel than it is in the region of the impeller. As the impeller speed is increased and turbulent flow results, the reverse becomes true: more power is dissipated in the region of the impeller.

3. In laminar flow little mixing takes place with the circulation being confined close to the impeller.
4. At the start of the transistion range $\bar{v}_r$ increases rapidly with increasing impeller speed. The mixing is by transport and blending rather than turbulence in this range of N_{Re}.
5. At the middle of the transistion range (N_{Re} = 100) turbulence begins to appear and is first noticeable near or between the blades of the impellers. In pseudoplastics such as CMC local turbulence is rapidly damped out.
6. At the impeller centerline velocities increase slightly more than linearly with increasing impeller speed for Newtonian fluids. In non-Newtonian fluids this increase is more nearly exponential. The apparent viscosity of pseudoplastics decreases with increasing shear rate. Hence under conditions of high shear rates for the same apparent viscosity pseudoplastics will give a higher overall flow at a lower total power input than Newtonian fluids. The reverse was found to be true under conditions of low shear rates.

Turbulence Measurement in Stirred Tanks by Bowers (4) and Mujumdar (17)

Bowers measured average values and the turbulent quanties intensity and scale for Type B impellers, with two blades (paddles). Four blade and six blade turbines were also used. Design details were not specified. The measuring device was a hot wire anemometer

and the tank was unbaffled. General profiles for the paddle impeller were presented as dimensionless velocities (ratio of average velocity to impeller tip speed) and were found to be independent of impeller speed.

Mujumdar also investigated turbulent parameters in stirred tanks. A single hot wire anemometer was used, and measurements were made in the plane of the impeller center line for the radial velocity component. A 6.0 inch diameter Type A impeller was used in a 15.0 inch diameter tank. The hot-wire signal shows a definite periodicity superimposed on the random velocity fluctuation, even at a distance from the impeller. He made no attempt to correlate the data. The data for average value of radial velocity is generally in agreement with the findings of Cutter (9).

Summary

In Table I-3 a summary of the investigations of the turbine impellers reviewed in this section is presented. The work of Schumm and Metzner is not included as they were qualitative studies. The results of Mujumdar and Bowers were also not included since these articles predominantly deal with the study of turbulence in the impeller region of a stirred tank.

The symbols T, D, etc. in Table I-3 have the same meaning as shown in Figure I-1. All dimensions are in inches. Blanks in the table mean that the information was not reported. The column of impeller types gives the type of impeller used as shown in Figure I-2, and the number in brackets is the number of different

Table I-3: Comparison of Impellers and Conditions Under Which Flow Patterns Were Examined. All Measurements reported are in inches.

T	D	H/T	h	D/T	h/D	Impeller Type and Number	Baffle No. and Size	Flow ++ Type	Fluid + Used	Re No.	RPM	Distinct Flow Patterns	Comments	Ref.
23.0	11.8	1	11.5	0.513	1.05	A,B,C,D (30)		L	W	$1x10^5$		1	*	Nagata (18)
23.0	11.8	1	11.5	0.513	1.05	A,B,C,D (6)	8x1.77	T	W	$1.3x10^5$		1	*	Nagata (19)
11.8	5.9	1	5.9	0.5	1.	A_8,B_8,C_8 (3)		L	W&O	$6.7\text{-}1x10^5$		16	**	Nagata (20)
11.5	4.0	1.042	4.0	0.348	1.	A_4 (1)	4x1.	T	W		100 150 200	3	***	Sachs (28)
11.25	2.0 4.0 7.0		3.75			A_6(1)	4x1	T	W W&O W		600 200 75	4	***	Neilson (21)
11.5	4-46/64 3-15/12 2-61/64	0.957	1-13/64			Paddle A_4(1) Propeller	4x1-13/64	L&T	W	$1.47x10^4$ $-4.2x10^4$			****	Aiba (1)
11.5	4.	1.042	6.	0.348	1.5	A_6(1)	4x1.2	T	W	200 400 600		3	***	Cutter (9)
12.0	4.0	1.0	6.	0.333	1.5	A_4(1)	4x1	L&T	0	31. 25,800		+++	****	Larson (14)
15.0	3.-6.					A_6(9) Marine Propeller(1)	4x1.5	T	W		100 600	+++	***	Cooper (8)

\+ W = Water
0 = Corn Syrup-Water Mixture

+++ at least more than 10 distinct flow patterns

++L = Laminar Flow
T = Turbulent Flow

* Compares impeller performance
** Transistion range studies
*** Flow Measurements in the region of the Impeller

**** Flow Measurement over most of the Tank

impellers studied. The column listing distinct flow patterns indicates the number of distinct or separated flow conditions studied. For a given impeller, tank and fluid, specifying the impeller speed will determine the flow pattern. For a given flow pattern quantities such as pumping capacity, eddy viscosity, and intensity of turbulence are thus constant in a particular region of a tank.

Frequently in a review of the literature it appears that a large amount of effort has been expended to obtain a lot of data. However, if all conditions are kept fixed, such as in case of Nagata, this constitute only one flow pattern. In order to make predictions on flow patterns, a range of flow situations need to be studied. As seen in Table I-3 the only such studies are that of Cooper who used a Type A standard turbine and Larson who used a Type A four blade turbine.

3.4. Pumping Capacities of Turbine Impellers

Flow patterns and pumping capacities are invariably investigated together. The pumping capacity is a measure of the volumetric flow rate at a particular point, for example leaving the impeller. However the flow pattern indicates how the flow is distributed throughout the tank. From the work of Sachs (28), Nielson (21) and Nagata (19), it is clear that the flow from the impeller entrains considerable fluid as it approaches the wall. The entrainment is a function of radial distance from the impeller axis, and it increases as the radial distance increases. It reaches a maximum as shown in Figure I-3, at approximately r_o, the

center of circulation of the upper and lower flow loops. Beyond r_o, the stream is in stagnation flow. The radial component progressively decreases reaching zero at the walls and the vertical component increases. The radial pumping capacities thus decreases in this region. Hence in reporting pumping capacities it is necessary to indicate the point at which such measurements were made. The most logical point is the impeller periphery, since this gives the flow resulting from the impeller motion alone, and is independent of entrained fluid. There are two approaches to correlating pumping capacities. These are:

1. Centrifugal pump approach first used by Van de Vusse (41)
2. Dimensionless pumping capacity $N_Q = \frac{Q}{ND^3}$ introduced by Nagata (18). Q is the volumetric flow from the impeller.

It will be shown that both these methods are related under centain conditions. Grey (37) derives the equation for pumping capacity based on the flow from a curved blade impeller of a centrifugal pump. In this derivation it is assumed that the fluid entering the impeller has a zero momentum, friction losses are negligible, and the fluid leaving the impeller has a flat velocity profile. The last assumption is most questionable since a bell shaped profile has been observed by many investigators (20,21,28) From the centrifugal pump approach, Grey obtained a relationship between N_Q and the power number N_p to be

$$N_Q = N_p/\pi^2 q \qquad \text{(I-26)}$$

In equation I-26, q is the ratio of the angular fluid velocity at the blade tip to the angular velocity of the impeller. It can be considered as the relative slip between the impeller and the fluid.

Norwood (22) used this model to correlate the pumping capacity for a Type A turbine. The conditions under which the data were taken are: Impeller diameter ranging from 2.0 - 6.0 inches, impeller centrally located, and viscosity of fluid ranging from 0.3624 to 7,780 centipoises (obtained with corn-syrup water mixture). A correlation was made of the total flow actoss the impeller stream, from the center of vortex above the impeller to the center of the vortex below the impeller. The correlation thus includes all the entrainment, a fact which is not sufficiently emphasized. Norwood's equation is

$$Q = 9.0 \times 10^{-6} \, ND^2 b \left(\frac{D^{0.4} \rho}{\mu}\right)^{1/2} (1-q^2)^{1/2} \qquad \text{(I-27)}$$

where

Q is in $ft^3/sec.$

N is in rev/sec.

D is impeller diameter, ft.

ρ is density, lb-mass/$ft.^3$

b is impeller blade width, ft.

In equation I-27 the only unknown quantity is q, the relative slip between the fluid and the impeller at the impeller periphery. Norwood recommended deleting this quantity as q is experimentally observed to be a small value. Grey recommended that equation I-26 be used to estimate q.

Equation I-27 can be rearranged to read as

$$\frac{Q}{ND^3} = 9 \times 10^{-6} \left(\frac{b}{D}\right) T^{0.2} \left(\left(\frac{D}{T}\right)^{0.4} \frac{\rho}{\mu}\right)^{1/2} (1-q^2)^{1/2} \qquad \text{(I-28)}$$

For geometrically similar impellers the ratio of blade width to impeller diameter (b/D) is a constant. For a given tank, the tank diameter T is also constant. In practice the ratio, D/T, ranges from 0.2 to 0.6. If Norwood's observation is accepted, that the factor q can be deleted, then the quantity on the left hand side is approximately constant. Hence, the important result is that in given tank N_Q is approximately constant for geometrically similar impellers.

This result can also be obtained, if the velocity profiles are considered similar. This condition can be mathematically stated as

$$\frac{\bar{v}_r}{(\bar{v}_r)_{max}} = f(\eta) \qquad \text{(I-29)}$$

Where $f(\eta)$ is the similar velocity profile and η is a dimensionless variable which relates r and z. In general there are many ways of specifying η. In Nielson's similarity solution it is specified by equation I-6. In our similarity solution η is specified differently and is given by Equation B-2 of Appendix B, which gives η as

$$\eta = \sigma \frac{z}{r} \qquad \text{(I-30)}$$

where σ is a constant. In Appendix B, the relation for pumping capacity Q has been calculated and is given by equation B-26. This equation for Q is

$$Q = 4\pi r \int_o^\infty \bar{v}_r dz \qquad \text{(I-31)}$$

For a constant value of r, combining I-29, I-30, and I-31 results in

$$\int f(\eta) d\eta$$

$$Q = \frac{4\pi r^2}{\sigma} (\bar{v}_r)_{max} \int_o^\infty f(\eta) d\eta \qquad \text{(I-32)}$$

The integral is a definite integral and hence has a finite and constant value which for convience is represented by k. From the observations of Sachs (28), Aiba (1), and Cutter (9) it is known that $(\bar{v}_r)_{max}$ is proportional to the impeller tip speed, or

$$(\bar{v}_r)_{max} = k' \pi DN \qquad \text{(I-33)}$$

where k′ is the constant of proportionality. Since pumping capacity is defined as the volumetric flow at the impeller periphery where r = D/2, we have from I-32, I-33 and, that the integral is a constant k that

$$N_Q = \frac{Q}{ND^3} = \frac{\pi^2}{\sigma} kk' \qquad \text{(I-34)}$$

N_Q has thus been proved to be a constant when the velocity profiles are similar.

The condition of similarity would be expected to hold when operating in a given fluid. It will be shown later that for geometrically similar impellers this is indeed the case. Cooper reported $\frac{Q}{ND^3}$ to range between 0.726 to 0.89, showing a slight

dependence on impeller diameter for geometrically similar turbines in water. Holmes (13) reported N_Q to be 1.3 for water with Type A turbine. How the radial velocities were measured and a value of $N_Q = 1.3$ arrived at is not reported. Grey (39) summarizes values of N_Q for a variety of turbines reported in the literature. The value of N_Q ranges from 0.5 to 2.9. This wide range reflects the variation in number of blades and blade geometry of the turbines used.

Larson (14) in his review of Aiba's work, indicated that Aiba also gave an equation for pumping capacity and it was $Q = \frac{N_p}{q\pi^2} ND^3$, where q has the same meaning as in I-26. This will be recognized as equation I-26. While, Grey (37) recommended this equation to estimate q, Aiba used this relationship to calculate Q. The value of q is estimated by trial and error from an emperical chart of C^* vs. Re^*. This correlation is given in Reference (1) and the interested reader is referred to it for further details. Thus Aiba's correlation is not basically different from the others reviewed here.

3.5. Velocity Measurements in Stirred Tanks

A variety of methods have been used to measure velocities in the stirred tank. These generally fall under the categories of photographic methods, pitot tubes, hot wire anemometers and laser doppler meters. None of the methods reported in the literature is entirely satisfactory. All methods allow measurement of average velocity and some give estimates of the turbulent components. A

satisfactory device for measuring velocities in a stirred tank is still to be developed, and this is one of the reasons why analysing the fluid mechanics in a stirred tank is so difficult.

The first measuring device to be developed was the photographic method of Sachs (28). This method introduced a small amount of immiscible liquid into the tank which immediately breaks up into fine droplets. A sheet of light about 3/16 inch thick and 5 inches wide was used to illuminate the tank in any desired vertical or horizontal plane. A photograph was taken of the sheet of light at right angles to the light beam. The droplets of immiscible liquid appeared as streaks. The length of the streak, its direction, and the time of exposure of the photographic plate was used to determine the velocity.

Nielson (21) improved the photographic method by introducing a slotted wheel in between the tank and the sheet of light. The slots were alternately large and small. The wheel was rotated at constant speed by a synchronous motor. The streaks now appeared as dotted lines of alternately small and large length corresponding to the length of the slots in the slotted wheel. This permitted more accurate determination of time interval of the streaks and the direction of motion of the tracer particle. The immiscible liquid was replaced by silver coated ion exchange bends. The ion-exchange beads used by Nielson were Dowex 50 in the size range of 100 mesh.

Cutter (9) used the photographic method with some more modifications. The tracer particle was Lycopodium powder of average size

30 microns. The light source was a flash tube of approximately 2 milliseconds duration. The film was exposed for 1/600 of a second. Hence the start of the tracer streak was brighter and together with the slotted wheel gave better indication of the direction of motion of the tracer particle. A micro switch timed the flash to occur when the impeller blade was in a predetermined position and the slot in the slotted wheel was about to open. The flashing light source permitted taking photographs of all the tracer particles at the same time thus permitting calculations of Eulerian correlation coefficient from which the turbulence parameters of intensity and scale can be calculated.

Larson (14) used the photographic method with furthur modifications. The tank was illuminated by a strobe light. Multiple exposure of the tracer particles were photographed in two perpendicular planes simultaneously. One plane was that of the camera, and the other was the plane perpendicular to this plane is seen in a mirror placed at 45° adjacent to the tank. The multiple exposure in two planes permitted reconstruction of the streamlines. The reconstructed stream lines in laminar flow were fairly regular and well defined. In turbulant flow the reconstructed streamlines move in irregular directions, and it was impossible to detect a definite pattern.

The method of Nielson and Cutter appeared to be the best design for the photographic method. Data from a number of photographs were averaged to yield an average velocity and a turbulent component.

Another devise used to measure the velocity in a stirred tank was the Kiel tube. This is a pitot tube with a cylinderical shield. The shield acts as a vane to straighten the flow and permits velocity measurement independent of flow angle. The maximum flow angle (the angle which the velocity vector makes with the normal of the pitot tube) over which Kiel tube gives consistent results is 40°.

Cutter also used a Kiel tube to compare the results of the photographic method. The Kiel tube gave values which appeared to be within 10% of the best fitting line drawn through the data obtained by the photographic method. The agreement can be considered fairly good considering that the photographic data had a larger spread about the best fitting line.

Nagata (18) used an elaborate pitot tube set-up that permited accurately evaluating the direction of the velocity vector at a point and then placing a Prandtl type pitot tube in the direction of the velocity vector. This is a true three dimensional set up for measuring velocities in three dimensional flow that occur in the stirred tank. The details of the design of the pitot tube is reported by Nagata in Reference (18). Nagata's data for velocities at actual points in the tank was not reported, and hence any furthur comment is conjecture. From the meager details presented this device seemed very suitable for measurement of velocities over most of the tank in the fully turbulent region.

Aiba (1) used an ingeneous device to measure velocities in a stirred tank. A ball containing radioactive cobalt was suspended

from a platinum wire. About an inch away from the ball a miniature Geiger-Muller counter was placed. The counter monitored the radiation from the radioactive source. A calibration curve was made that related the deflection of the ball to the monitored radiation. The Geiger-Muller counter was thus used to determine the position of the ball. A force balance between the gravitational forces and the drag forces on the ball due to the moving fluid was made and this gave a relationship between deflection of the ball and velocity of the fluid. Knowing the position of the ball, and the drag coefficient of the ball the velocity was determined. From the reported analysis it was not clear how the direction of the velocity was determined. Aiba reported measurements of the vertical, radial and tangential components of velocity using this method. For high velocities a steel ball was used, and for low velocities the ball was made of an acrylic resin.

Cooper (8) used a three dimensional pitot tube made by United Sensors Corportation, for velocity measurements in water. In air he used a hot wire anemometer. The details of equipment used by Cooper is in general brief and sketchy. The fact that the angle of flow is measured more accurately by the directional pitot tube than the hot wire anemometer indicated that a single wire probe was used.

The hot-wire anemometer has been used by Bowers (4) and Mujumdar (17) in water. Both workers used single wire probes. The principle of the hot-wire anemometer is, briefly, based on cooling

of long thin cylinders. If such a cylinder is placed in a moving fluid then the rate of cooling is a function of the velocity component in a direction perpendicular to the axis of the cylinder. The hot-wire anemometer is a probe with a wire strung across two prongs. Effective length of wire in typical probe is about 0.05 inch, and its diameter is 0.00015 inch. The wire is thus effectively a long thin cylinder. A current is passed through the wire to heat it, and as the fluid flows past the wire it will be cooled. The wire has a coefficient of resistence which is a function of temperature, hence the resistance will change as its temperature changes. By means of a wheatstone bridge and suitable electronics the temperature of the wire can be maintained constant. The varying current to maintain the temperature constant is a function of the velocity and this functional relationship is non-linear. As the wire is very thin the response to changes in temperature will be almost immediate; and hence, the varying current almost exactly follows the varying velocity flowing past the wire. Two wires placed very close and at right angles but not in electrical contact can be used as a probe to measure velocity in two dimensional flow systems and also for measuring turbulence parameters.

In water the hot-wire anemometer encounters several problems. The overheat ratio is the ratio of the wire temperature to fluid temperature. This ratio has to be low in water since the temperature of the wire cannot exceed the boiling point of water. Should this occur then steam bubbles or bubbles of dissolved gases will form

and the heat transfer will follow an entirely different functional relationship. High overheat ratios give better sensitivity and response and are hence desirable.

The water must be absolutely clean otherwise lint collects on the wire. Also dirt will adhere to it, and both of these will cause changes in the calibration of the system.

Water has a high inertia, and in high shear flows; it can and does break the delicate wire. This is a serious problem, and it has been reported by Bowers. This difficulty might be overcome by using a hot film anemometer. However hot film probes do not have directional properties, and hence cannot be used in two and three dimensional flow systems.

Finally ordinary water conducts electricity. Although the mechanism is not well understood, hot-wires coated with fused quartz have been used successfully in tap water by Dell'Osso (10) Coated probes are also called hot film probes and should not be confused with the film probes mentioned earlier. The film probe is a film of material deposited on a wedge shaped probe tip.

An ideal measuring instrument for velocities in a stirred tank is one that does not interfere with the flow field and permits not only velocity measurements at the walls of the tank but also the turbulent velocity components. Such a device may be the laser-doppler velocity meter. This device has been used by Goldstein (11) to measure laminar flow in a square duct (1.0cm sq.). This device is based on the principle that the light beam from a laser which

is scattered from a moving tracer particle undergoes a doppler shift. The tracer particle typically used is 0.5 micron polystyrene particles which is then diluted by one part solids to 50,000 parts by volume water. The scattered beam and original beam are brought together and optically hetrodyned. This gives rise to an alternate light and dark band that moves at the doppler frequency. The moving bands are monitored by a photomultipler and through suitable electronics a signal can be obtained of the doppler frequency. A functional relationship exists between the doppler frequency, the scattering angle and the velocity of the tracer particle. Thus the velocity of the particle can be computed and taken equal to the fluid velocity. Since the tracer particles are small the response of the device is expected to be high. The method requires precision components and an elaborate set up. It is still in the experimental stage. Rolfe and associates (25) have developed a three dimensional laser doppler velocity meter to measure gas velocities in a wind tunnel up to a velocity of Mach 2. Results obtained were in close agreement with that of a hot-wire anemometer. They presented an excellant summary of the capabilities of this measuring device.

4. Conclusions

In this Chapter justification for investigating the flow patterns in stirred tanks has been presented. Of the three basic flow patterns occurring in stirred tanks it is proposed to study the radial flow pattern generated by a turbine impeller. Several

impeller designs are available, however the Type A design is considered to be standard and will be used in this work.

None of the investigators have been entirely successful in describing the fluid dynamics of the tank. However, some success has been achieved in certain regions of the tank. It was therefore decided to model the fluid dynamics of the tank by considering it to be made up of several regions. Each region will be treated separately using the best model available.

For example, in the region of the impeller, Nielson's tangential jet model appears to describe all the observed phenomena except the angle profile discovered by Cooper. However Nielson's solution is too involved and cumbersome to be useful. This is because of his use of Prandtl's Mixing Length Theory. The flow in the impeller region is essentially free turbulence, and in such cases Schlichtling (29) has shown that the use of Prandtl's second hypothesis can give an equivalent solution which is not only easier to obtain but also simpler in form. This will be apparent when Nielson's solution is compared with ours which is presented in Appendix B. Both theories are phenomenological, and the parameters in the solution are obtained by fitting experimental data. For free turbulence, Prandtl's second hypothesis is a simpler approach and hence favored.

The work of Larson shows that elsewhere in the tank potential flow might be applicable. The poor results obtained by Larson may well be because he considered the entire tank as one region. If

potential flow is assumed, it seems easier to map streamline using the simpler approach of the aerodynamist: fit streamlines in a flow region using combination of sources, sinks and vortices. This approach will be used in Chapter II.

The flow from a turbine impeller is a narrow high velocity turbulent stream. This stream has been measured in a limited manner as indicated under the heading data points of Table I-3. The recent work of Cooper makes available considerable data on velocity profile measurements in this region. The data is not complete, and hence it will be necessary to make some more measurements. With the help of an adequate flow model it will be possible to characterize the flow in this region of the tank.

It is felt that before making turbulent studies a first step would be to define and predict the bulk flow. It is our objective to understand the flow rather than the detail mechanism of turbulence. The flow model will use a phenomenological theory, and this will permit calculating an eddy viscosity which will be of immediate practical use.

As a study of the turbulence in a stirred tank is not the objective of this work only average velocities need to be measured. From the literature review presented in Section 3.4 the directional pitot tube used by Cooper was selected for experimental measurements, The selection of this device was based on its simple construction and the remarkable consistency of the data obtained. It has its drawbacks in that velocities lower than 30 ft/min. cannot be measured.

CHAPTER II

THEORETICAL ANALYSIS OF THE FLUID DYNAMICS IN THE STIRRED TANK

1. Development of a Mathematical Model for the Stirred Tank

In this chapter, a mathematical model will be developed to describe the flow pattern in the stirred tank. From the work of several investigators reviewed in Chapter I, it appears that the stirred tank can be separated into two regions: one in the neighborhood of the impeller which has received considerable attention and the other the rest of the tank.

The flow in a baffled stirred tank with a turbine impeller can be described as follows. First a high speed, narrow, highly turbulent stream emerges from the impeller. This high speed stream entrains a considerable amount of fluid which causes it to broaden and slow down as it approaches the tank wall. On approaching the tank wall the radial component of the fluid velocity decreases rapidly reaching zero at the tank wall, while there is a corresponding increase in the axial component of the velocity. The flow near the tank wall can be approximated by stagnation flow. The stagnation point occurs roughly at the point where the plane of the impeller center line intersects the walls of the tank. The stagnation flow results in the stream dividing into two equal parts giving rise to the clover leaf flow pattern as shown in Figure I-1,

of Chapter I. The divided stream circulates in the rest the tank returning to the impeller region. Part of this stream enters the impeller the rest is the entrained by the impeller stream. In the upper and lower sections of the tank are two doughnut shaped regions. These regions form the centers of circulation for the circulating flow in the tank, mentioned above. The center of circulation is shown in Figure I-5. The above description of the flow field is based primarily on the work of Nagata (19).

In developing a mathematical model, the work of Larson (14) showed that an attempt to model the fluid dynamics of the stirred tank as entirely one flow region gave poor results. On the other hand Nielson (21) has had fair success in modeling the flow in the region of the impeller. This is not exactly surprising since the flow in the vicinity of the impeller has not only had the highest velocities but also most of the energy is dissipated in this part of the tank. This latter conclusion is based on the work of Cutter (9) and Bowers (4). They have shown that the neighborhood of the impeller is a zone of high mean and turbulent velocities, while the rest of the tank is relatively quiescent. Cutter estimates that 20% of the energy is dissipated in the impeller itself, 50% in the impeller stream and 30% in the rest of the tank. Considering the relative volume of the rest of the tank to the region in the vicinity of the impeller it would appear that energy dissipation per unit volume in the rest of the tank is unimportant. We can thus conclude that the region of the impeller is a high shear region while in the rest of the tank shear forces are unimportant and hence potential flow could be applied.

We thus have two regions to be modeled separately. The region in the vicinity of the impeller is modeled using Nielson's tangential jet model, and the flow in the rest of the tank is described by potential flow. In using potential flow, the method of the aerodynamists was adopted. This approach divided the rest of the tank into several regions, each region being fitted by a model that best appears to describe the flow pattern in that region. Nagata's flow pattern shown in Figure I-5 was used as a guide for modeling the regions in the rest of the tank.

In Figure II-1 a computer drawn solution is shown of the stream lines in a r - z plane passing through the impeller axis, a line of symmetry of the system. This is from the solution of the model of the flow described in this chapter. In the figure the flow in the tank is divided into six regions. These regions are

I. The flow from the impeller, modeled by a tangential jet.

II. Impeller stream impinging on tank wall, modeled by stagnation flow.

III. Upper and lower corners of the tank, modeled by potential flow in a corner.

IV. Flow at the top and bottom of the tank axis, also modeled by potential flow in a corner.

V. Flow at the center of the tank axis, modeled by a circular jet.

VI. Two doughnut shaped regions, which have been modeled as dead water regions.

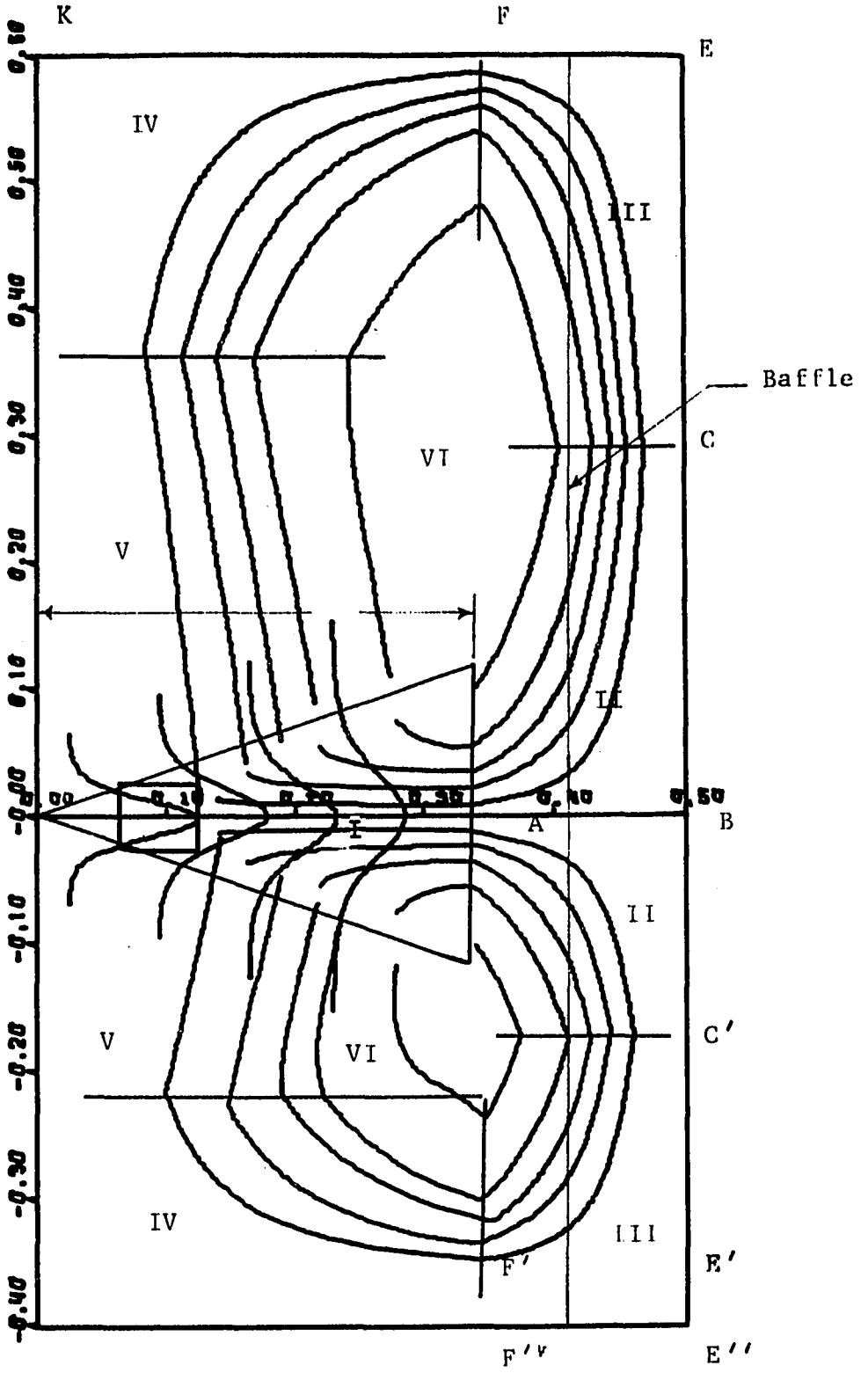

Figure II-1: Typical Computer Drawn Solution of Flow Patterns Showing the Regions into which the Tank is Divided

Regions shown in the figure have the same fluid dynamics model are given the same number. However, the parameters in the model of, region V, for example, shown above and below the impeller are not the same. Each of these regions will be examined in detail and the merits of the model chosen will be discussed.

1.1. Region I - Neighborhood of the Impeller

The Tangential Jet: This region is the area around the impeller. At a very early stage it was recognized that a free jet model would give a satisfactory description of flow in this region. The radial plane jet was first developed and tested on Nielson's data. The model seemed inadequate. The jet width was either too wide or too narrow and depended on where the origin of the jet was located. On examining Cooper's data (8) and in our own investigation of the problem it was apparent that a sizeable tangential velocity component existed near the impeller and should be taken into account. The tangential component decreases at increasing distances from the impeller and reached a small but non-zero value near the tank wall.

Nielson has accounted for this tangential component by considering a ring jet in which fluid emerged tangentially from the periphery of a cylinder of radius a and height 2b. A physical picture of the model consists in replacing the impeller by a cylinder of diameter 2a and height 2b. The fluid leaves this cylinder of diameter 2a on a tangent with an average velocity of $\vec{q}$. Consider a point, A, on the periphery of the source as shown in Figure II-2. The fluid leaves at a tangent to the source, and the yaw angle θ_y at A is 90°. The yaw angle θ_y is defined as the

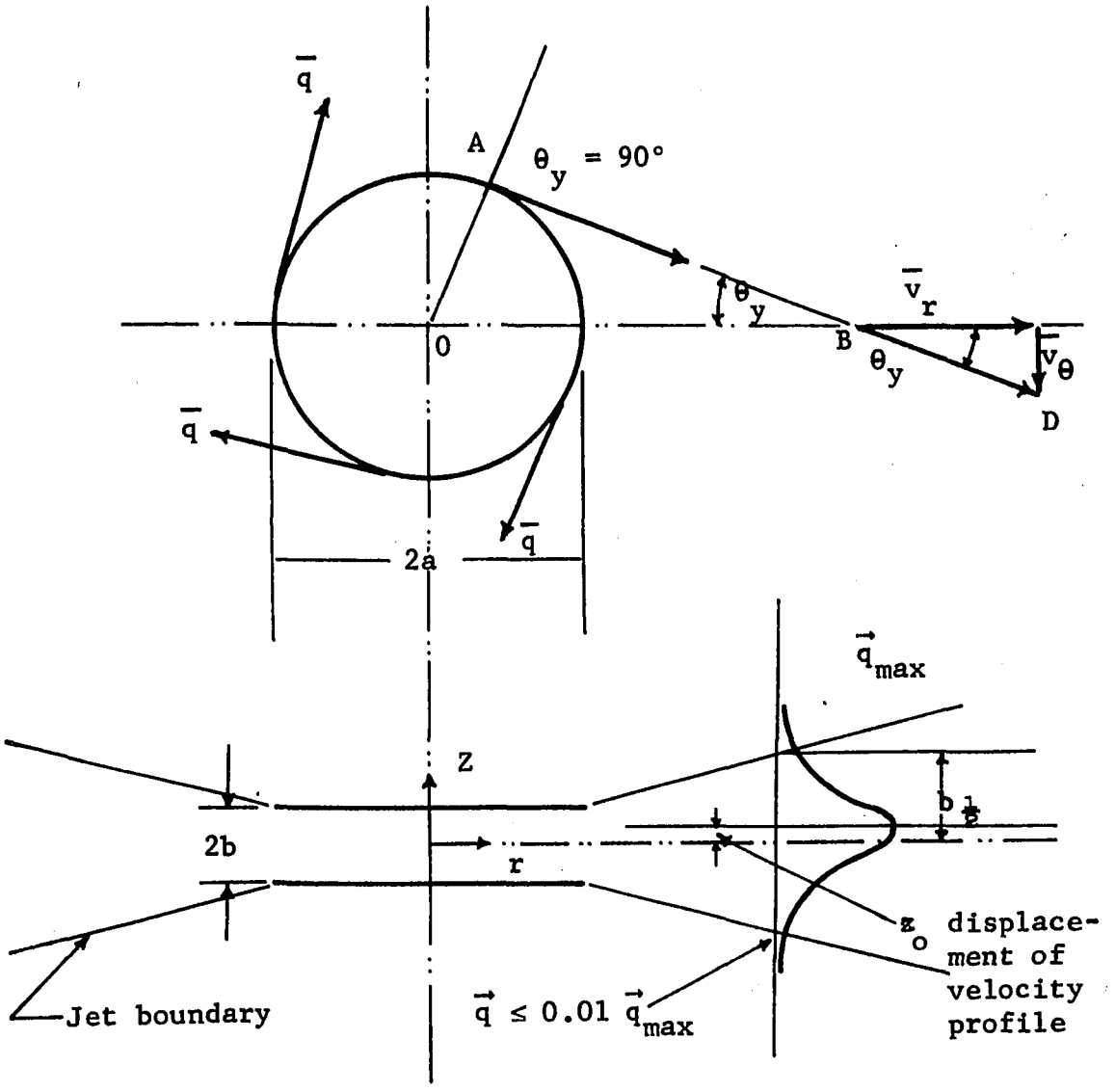

Figure II-2. The Tangential Jet.

angle between the velocity vector and the radius vector. Once the fluid leaves the cylinderical source, the baffles seem to freeze the flow, and fluid continues to move in the direction $\vec{q}$ it had as it left the ring source. Although the direction of $\vec{q}$ does not change, its magnitude decreases because of entrainment. At a point B far from the source the yaw angle θ_y has decreased and is less than 90°. It is thus clear that at r = a, the yaw angle $\theta_y = 90°$, decreasing to a small value near the tank wall. From the geometry of Figure II-2 it follows that $\bar{v}_r$ and $\bar{v}_\theta$ is given by,

$$\bar{v}_r = |\vec{q}|\cos\theta_y \qquad \text{(II-1)}$$

$$\bar{v}_\theta = |\vec{q}|\ \sin\theta_y \qquad \text{(II-2)}$$

In equation II-1 and II-2, the velocities, $\bar{v}_r$, $\bar{v}_\theta$ are time average values. A bar over a variable signifies a time average quantity. A vector is denoted by an arrow over the variable as for $\vec{q}$ in Equation II-1 and II-2.

The pumping capacity of the impeller depends on $\bar{v}_r$. From equation II-1, $\bar{v}_r$ has a limiting value of zero when $\theta_y = 90°$, and r = a. Hence, for $\bar{v}_r$ to be finite, θ_y must be less than 90°. As all impellers have a finite pumping capacity it follows then, that the radius of the ring source, a must be less than the impeller radius D/2.

Equations of Continuity and Momentum for the Tangential Jet: In Appendix A, the equations of motion for turbulent flow have been simplified for the assumptions of isothermal, incompressible flow and the boundary layer approximations. The resulting time

averaged equations that describe the flow in the turbulent tangential jet are

Continuity Equation:

$$\frac{\partial}{\partial r}(r\bar{v}_r) + \frac{\partial}{\partial z}(r\bar{v}_r) = 0 \qquad \text{(A-3)}$$

Equation of Motion:

$$\bar{v}_r \frac{\partial \bar{v}_r}{\partial r} + \bar{v}_z \frac{\partial \bar{v}_r}{\partial z} - \frac{a^2}{r(r^2-a^2)} \bar{v}_r^2 = -\frac{1}{\rho} \frac{\sqrt{r^2-a^2}}{r} \frac{\partial |\vec{\tau}|}{\partial z} \qquad \text{(A-22)}$$

These equations can be reduced to a single partial differential equation by introducing the stream function ψ, and into an ordinary differential equation by the similarity principle. The similarity principle assumes that the velocity profile to be similar in the direction of fluid motion.

In Appendix A, it was shown that the tangential jet is a one dimensional flow problem resulting in the single equation of motion A-22. As a result, the stress tensor $\bar{\bar{\tau}}$ was reduced to a vector $\vec{\tau}$. A phenomenological theory is used to define $\vec{\tau}$ since in this work; time average velocities are measured.

From the several theories available, Prandtl's Second Hypothesis (Schlichtling (29)) was selected as it was best suited to our problem. This is because the turbulence in the tangential jet is not due to a wall or boundary, and is hence essentially a case of free turbulence. It is a region of extreme velocity gradients, the velocity $\vec{q}$ is a maximum at the center and reaches zero at the boundaries of the jet which can be seen in Figure II-1.

Prandtl's Second Hypothesis (29) gives the value of $\vec{\tau}$ for flow in the $\vec{q}$direction as:

$$\vec{\tau} = \rho k b_{\frac{1}{2}} \left|(\vec{q}_{max} - \vec{q}_{min})\right| \frac{d\vec{q}}{dz} \qquad \text{(II-3)}$$

where ρ is the density, and k a constant, $b_{\frac{1}{2}}$ is the half width of the jet shown in Figure II-2 and is defined in Appendix B. Since $\vec{q}_{min}$, the velocity at the boundary of the jet is zero,

$$\vec{\tau} = \rho k b_{\frac{1}{2}} \left|\vec{q}_{max}\right| \frac{d\vec{q}}{dz} \qquad \text{(II-4)}$$

Defining ϵ as the virtual kinematic viscosity,

$$\epsilon = k b_{\frac{1}{2}} \left|\vec{q}_{max}\right| \qquad \text{(II-5)}$$

and hence

$$\vec{\tau} = \rho \epsilon \frac{d\vec{q}}{dz} \qquad \text{(II-6)}$$

Substituting for $\cos\theta_y$ from A-14 into II-1 gives

$$\left|\vec{q}\right| = \frac{r}{\sqrt{r^2 - a^2}} \bar{v}_r \qquad \text{(II-7)}$$

Introducing II-7 in II-6 and noting that $\bar{v}_r$ is not a function of r which will be emphasized by using partial derivatives we have

$$\left|\vec{\tau}\right| = \rho \epsilon \frac{r}{\sqrt{r^2 - a^2}} \frac{\partial \bar{v}_r}{\partial z} \qquad \text{(II-8)}$$

Substituting for $\left|\vec{\tau}\right|$ from II-8 into A-22 gives

$$v_r \frac{\partial v_r}{\partial r} + \bar{v}_z \frac{\partial \bar{v}_r}{\partial z} - \frac{a^2}{r(r^2 - a^2)} v_r^2 = - \epsilon \frac{\partial^2 \bar{v}_r}{\partial z^2} \qquad \text{(II-9)}$$

It should be noted the ϵ, the virtual kinematic viscosity is a function of $b_{\frac{1}{2}}$ and $\bar{q}_{max}$ which are functions of r and not z.

Solutions of the Tangential Jet Equations: A similarity solution of Equation II-9, subject to continuity Equation A-3 and boundary conditions A-28 and A-29, is detailed in Appendix B. The equations for the velocity profile are given by B-24 and B-26 which are reproduced below.

$$\bar{v}_r = (\bar{v}_r)_{max} [1 - \tanh^2(\eta/2)] \tag{B-24}$$

$$\bar{v}_z = - \frac{(\bar{v}_r)_{max}}{\sigma} \left[\frac{2r^2 - a^2}{r^2 - a^2} \tanh(\eta) - \eta(1 - \tanh^2(\eta/2)) \right] \tag{B-26}$$

where

$$(\bar{v}_r)_{max} = \frac{A}{2} \left(\frac{\sigma}{r^3} \right)^{\frac{1}{2}} (r^2 - a^2)^{\frac{1}{4}} \tag{B-25}$$

$$\eta = \sigma \frac{z}{r} \tag{B-2}$$

It should be noted that the above equations B-24 and B-26 are obtained from exactly the same basic analysis as presented by Nielson (21). The difference lies in the definition of $\vec{\tau}$ the shear stress. Nielson used Prandtl's mixing length theory which results in a cumbersome solution as described in Chapter I.

Both theories result in three parameter models and give an excellent fit of the velocity profile data. However the velocity profile as obtained by Nielson is not in explicit form but has to be evaluated from equations I-10 to I-13 and are thus harder to fit. In contrast, Equation B-24 is not only simpler to derive but gives the velocity profile directly. Another reason for selecting

Prandtl's Second Hypothesis is because it is a well tested approach to describing free turbulence, examples of which are jet and wakes; and these have been solved in Schlichtling (29).

Results of Tangential Jet Solution: In obtaining velocity profile data, as will be seen in Chapter III, neither $\bar{v}_r$, $\bar{v}_z$, or $\bar{v}_\theta$ is measured but the resultant of $\bar{v}_r$ and $\bar{v}_\theta$ which is $\vec{q}$. The velocity $\vec{q}$ is shown in Figure II-2, and its relation with $\bar{v}_r$ and $\bar{v}_\theta$ is given by Equations II-1 and II-2.

Substituting for $\bar{v}_r$ from B-24 and B-25 into II-7 gives,

$$\bar{q} = \frac{A}{2}\left(\frac{\sigma}{r}\right)^{\frac{1}{2}} \frac{1}{(r^2-a^2)^{\frac{1}{4}}} [1-\tanh^2(\eta/2)] \qquad \text{(II-10)}$$

Equation II-10 is non-linear, and as it has been explained earlier that a, should not exceed D/2.

It has been observed by Nielson (21) and from our analysis of Cooper's (8) data that $\vec{q}_{max}$ does not coincide with the impeller center line but is displaced by a small amount, z_o as shown in Figure II-2. Experimental data is made to fit equation II-10 using the least square criteria. An optimization technique known as Pattern Search has been found satisfactory to evaluate the four parameters σ, A, a, and z_o subject to constraint on a. An outline of the procedure and the computer program is presented in Appendix C.

The kinematic eddy viscosity ϵ has been evaluate in Appendix B, Equation B-15, and is

$$\epsilon = \frac{A}{2} \frac{1}{(\sigma^3 r)^{\frac{1}{2}}} \frac{2r^2-a^2}{(r^2-a^2)^{3/4}} \qquad \text{(B-15)}$$

Comparing B-15 and II-5 and substituting for q_{max} from II-10, the half width of the jet $b_{\frac{1}{2}}$ and the constant k can be calculated, a factor k′ is included in the calculations giving

$$b_{\frac{1}{2}} = \frac{(2r^2-a^2)}{(r^2-a^2)^{\frac{1}{2}}k'} \qquad \text{(II-12)}$$

$$k = \frac{k'}{\sigma^2} \qquad \text{(II-13)}$$

The factor k′, it is seen cancels out and thus has no effect on ϵ. It is included to make $b_{\frac{1}{2}}$ as defined in II-12 identical to that in B-34 and will be discussed in Chapter IV.

It will be observed that the velocity profile and expression for eddy viscosity contain three arbitrary parameters A, a, and σ. These were evaluated by a least square fit of experimentally obtained velocity profile data, as will be described in Chapter IV.

1.2. Regions II, III, and IV

Regions II, III, and IV will be modeled together. The reason why this is so will be apparent as we proceed. In these regions extreme velocity gradients do not exist, and the flow is considered to be in potential flow. This is confirmed somewhat by Larson's (14) work and also from the observation of Cutter (9) that energy dissipation in these regions are small. All of these regions are bounded by the walls except the surface.

Near the tank wall a turbulent boundary layer exists. This has been observed by Askew (2) who has investigated the flow profile close to the tank wall. The thickness of the boundary layer is of the order of 0.1 inch and does not exceed this value in all cases investigated. Askew's results were obtained using distilled

water with the following impellers: a 90° Turbine, a 45° Turbine (design details unknown) and a marine propeller. Impeller speed ranged from 0. to 18.75 revolutions per second (rps). For the 90° Turbine (presumably similar to the type used in this work) only one graph is presented at 9.0 rps for velocity profiles at various locations along the wall in regions II and III. From this work it appears that the boundary layer at the tank walls in regions II and III is very small, at least beyond the precision of the measuring instruments used in this work. The boundary layer effect can be accounted for by excluding the boundary layer region from the potential flow region. This follows from the definition of boundary layer which assumes that the region outside the boundary layer is in potential flow. From the discussion above it will be seen that 0.1 inch, the thickness of the boundary, is so small in comparison with the width of regions II and III that it can be neglected.

Regions II, III and IV are essentially two-dimensional flows, as the tangential component is assumed to have a small value in these regions and can thus be neglected. The flow is thus in the r - z plane and the velocities of interest are $\bar{v}_z$ and $\bar{v}_r$. Two dimensional flows are conveniently handled by using the stream function ψ which also makes the evaluation of streamlines easy. In Appendix D it was shown that the stream function given by Equation D-9 is a possible potential flow solution that satisfies the boundary conditions of Regions II, III and IV. Equation D-9 is given by

$$\psi = r^2 z \qquad \text{(D-9)}$$

and will be used to evaluate the streamlines.

In Figure II-3 (a) and (b) two solutions of equation D-9 are shown. It is noticed that Figure II-3 (b) is a part of Figure II-3 (a). This is a valid solution since by definition, a streamline is a line across which no flow occurs, and hence a streamline can be replaced by a boundary. The need for replacing a streamline by a boundary becomes clear on comparing Figure II-1 and II-3. It is seen that Figure II-3 (a) corresponds to Region II, while Figure II-3 (b) corresponds to regions III and IV. It is now apparent why regions II, III and IV are considered together. All these regions use the same equation, D-9, for the stream function; however, the origin 0 of Figure II-3 has a different location in different regions. In other words, each of the above regions uses that part of Figure II-3 (a), whose streamlines correspond to the experimentally observed streamlines.

The units on the stream function ψ is $ft^3/(min)(ft)$. It thus represents the volumetric flow between two streamlines. To give the streamlines a value, a zero streamline must be defined. In our problem, this is the streamline along which the velocity $\bar{v}_r$ is a maximum. From Figure II-2, this will correspond to a line parralled to the impeller centerline and displaced from it by an amount z_o. It thus follows that the equation of the streamline is obtained by giving ψ a suitable numerical value in Equation D-9. This will be more clear when the stream lines of Figure II-1 are developed in the Section 2.2.

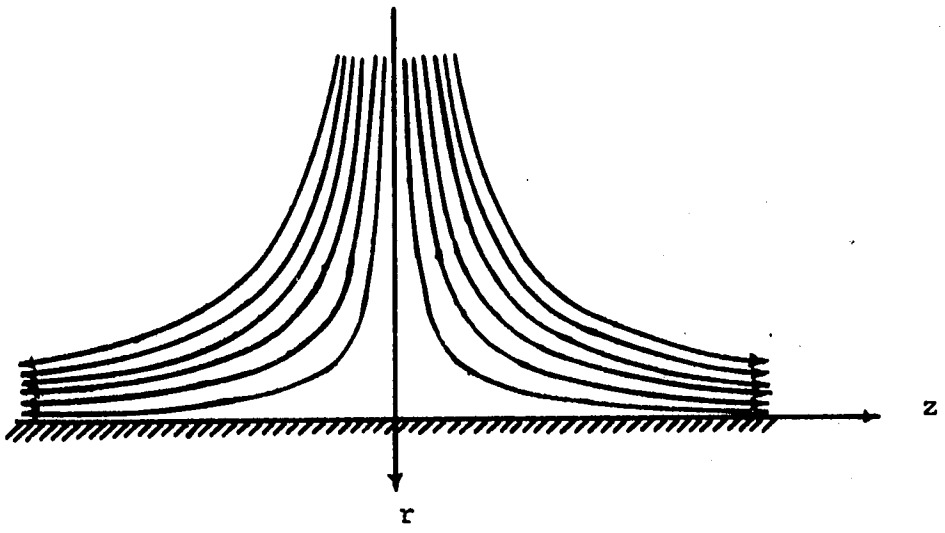

(a) Stagnation Flow

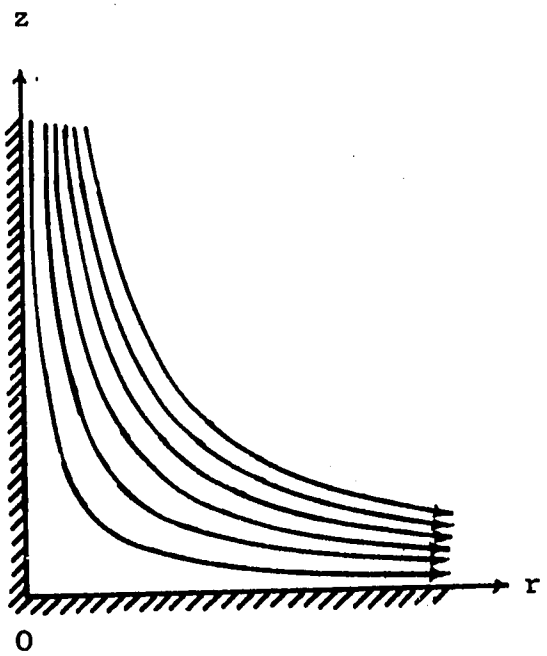

(b) Flow in a Corner

Figure II-3: Potential Flow Solution of Equation D-9

1.3. Region V

This region is modeled as a circular jet. In Figure II-4 is a sketch of a circular jet. The velocity profile and other quantities are shown in the figure. The fluid dynamics of the circular jet is well known. Schlichtling (31) gives a very good treatment of the circular jet using Prandtl's Second Hypothesis for the eddy viscosity. The equations as obtained by Schlichtling for the velo- profile and other pertinent data on the circular jet is summarized below.

The velocity in the z direction $\bar{v}_z$ is given by

$$\bar{v}_z = \frac{\epsilon_o}{(z+z_o)^\theta} \cdot \frac{2\gamma^2}{(1+\frac{1}{4}\xi^2)^2} \qquad \text{(II-14)}$$

The entrainment of fluid by the jet is due to the r-component, $\bar{v}_r$ and is given by

$$\bar{v}_r = \frac{\epsilon_o}{z+z_o} \gamma \frac{\xi-\frac{1}{4}\xi^3}{(1+\frac{1}{4}\xi^2)^2} \qquad \text{(II-15)}$$

where ξ is a dimensionless coordinate normal to the direction of flow and is given by

$$\xi = \gamma \frac{r}{z+z_o} \qquad \text{(II-16)}$$

where γ is the jet spreading parameter for circular jet defined above, and z_o is coordinate of origin of jet and is shown in Figure II-4. Other important quantities of the circular jet are the pumping capacity Q_c and momentum J_c and are

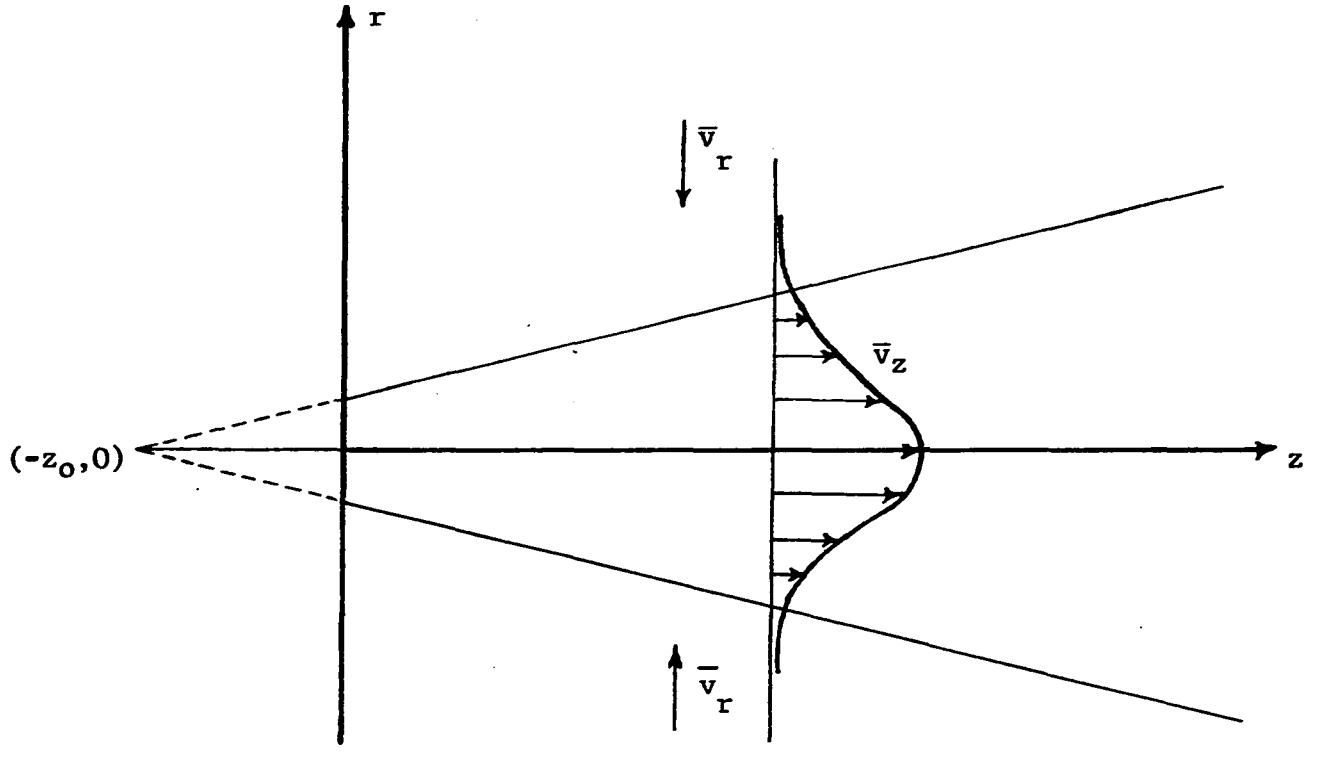

Figure II-4: The Circular Jet

$$Q_c = 8\pi\epsilon_o x \qquad \text{(II-17)}$$

$$J_c = \frac{16}{3}\pi\rho\gamma^2\epsilon_o^2 \qquad \text{(II-18)}$$

Equations II-14 to II-18 describe the circular jet and will be used in Section 2.4 to develop the streamlines in Region V.

1.4. Region VI

This region occupies two doughtnut shaped spaces, one above and one below the impeller as shown in Figure II-1. In the course of investigating several different models for fitting this region that of a pair of confined ring vortices appeared as a strong possibility. This was based on two observations from the literature (a) that a center of circulation existed as reported by Nagata (19), (b) that the tangential component of velocity $\bar{v}_\theta$ is small and can be neglected.

In order to obtain a more quantitative feel for the problem, velocity measurements were made in three horizontal planes that cuts across regions II, III, IV, V and VI. These measurements are discussed in Chapter IV. It was observed that velocity in general are extremely small in these regions and of the order of 0.5 ft/sec. It required a high impeller speed of 500 rpm in water (impeller diameter 3.0 in., and N_{Re} was 54,000) for the three dimensional probe used in this work to barely respond. This is because the lowest velocity to which the probe will respond is 0.5 ft/sec. The impeller speed is considered high because beyond 500 rpm, excessive entrainment of air occured. The air entrainment not

only adds another dimension to the problem, but is also not normal practice in the use of the stirred tank. It was observed that $\bar{v}_\theta$ was of the same order of magnitude as $\bar{v}_r$ and $\bar{v}_z$ and thus could not be neglected. The stagnation region described by Nagata (19) and shown in Figure I-5 is fictitious, existing only in the r - z plane when velocities components $\bar{v}_r$ and $\bar{v}_z$ are considered. The flow is three dimensional having a fairly constant value for the overall velocity $\vec{V}$. Thus, in the so called stagnation region the flow is predominantly tangential.

In order to arrive at a suitable model more adequate data on velocity profiles is needed. The fact that outside of the impeller we have a three dimensional flow field adds to the complexity of the problem. As a proposed model could not be adequately tested, and the flow is quiescent at low impeller speeds this region was modeled as a stagnation or deadwater region.

2. Development of Computer Program to Draw the Flow Pattern

In the previous section the stirred tank was divided into several regions and the fluid dynamics of each region was examined separately. In this section the models developed for each region will be tied together and the theoretical basis of the computer program for drawing the streamlines will be presented. The computer program itself is reproduced in Appendix E. It consists of two sections or subprograms called PLOTER and STREAM. The subprogram PLOTER is responsible for ploting the actual streamlines, the outline of the tank, the outline of the impeller and four velocity profiles in Region I. It reads in values of the parameters needed

for drawing the steamlines and prints out pertinent information on the plot. The program is designed to plot one quadrant at a time. Since the axis of the impeller is a line of symmetry only one half of the r - z plane need be plotted as shown in Figure II-1.

The plotting is done on a Calcomp Plotter Model 750 plotting unit made by California Computer Products, Inc. The device works as follows. The desired plot is scaled and all coordinate are converted into inches of plotter pen movements; the movement is from a reference zero on the plot which may or may not conincide with the zero of the coordinates on the plot. The Calcomp Plotter has a number of built in subroutines such as AXIS, PLOTS, PLOT, and LINE which permit calculating coordinates of the variables being plotted in proper form using any suitable computer. In the present case an IBM 360/65 and IBM 7040 were used. The output from the computer is obtained on tape which is then transferred to the Calcomp Plotter to make the desired plot.

The subroutine STREAM calculates the coordinates of one complete streamline as it passes through the various regions. Each streamline encloses a definite amount of fluid. In the sections that follow the equations used for evaluating the streamlines in subroutines STREAM will be detailed.

2.1. Equations for Streamlines in Region I

This region is modeled by a tangential jet. Combining Equations B-9 and B-21 gives the value of the stream function ψ as

$$\psi = A(r/\sigma)^{\frac{1}{2}} (r^2-a^2)^{\frac{1}{4}} \tanh(\eta/2) \qquad \text{(II-19)}$$

For a given streamline, ψ has a constant value expressed as $ft^3/(min)(ft)$ Equation II-19 does not have the proper units as will be seen by considering the equation for pumping capacity in the tangential jet Equation B-30, which is

$$Q = 4\pi A(r/\sigma)^{\frac{1}{2}} (r^2-a^2)^{\frac{1}{4}} \tanh(\eta/2) \qquad \text{(B-30)}$$

The numerical difference between Equation II-19 and B-30 is the factor 4π, while the dimensional difference is because II-19 represents a streamline in the r - z plane while B-30 is the fluid flowing out of an area of radius $2\pi r$ and width 2η. If axial symmetry is assumed, meaning that the streamlines are considered identical in all radial planes (and in particular in between baffles) then B-30 can be considered as a stream surface. It then follows that ψ is equal to Q with dimension of ft^3/min and is given by

$$\psi = 4\pi A(r/\sigma)^{\frac{1}{2}} (r^2-a^2)^{\frac{1}{4}} \tanh(\eta/2) \qquad \text{(II-20)}$$

In Equation II-20 ψ has the desired units of ft^3/min and represents the flow in Region I between two stream surfaces that are a distance η apart. Now for $\eta = 0$, $\tanh(\eta/2) = 0$ and the zero streamline occurs at $\eta = 0$. From Appendix B, η is given by

$$\eta = \sigma \frac{z}{r} \qquad \text{(B-2)}$$

However, it was observed in the previous section that the tangential jet is displaced in the axial direction by an amount z_o as shown in Figure II-2, hence η should be given by

$$\eta = \sigma \frac{z-z_o}{r} \qquad \text{(II-21)}$$

The value of z_o is in no case larger than 0.01 ft which is a very small quantity. This displacement is so small that it cannot be shown on Figure II-1. Hence for purpose of plotting z_o is neglected and η will be given by B-2.

We are now in a position to evaluate the equation of the streamline. Let Q_o be the incremental value of ψ between any two stream surfaces. Then in general ψ will be given by

$$\psi = kQ_o \qquad \text{(II-22)}$$

where k is some integral multiple of Q_o and represents the k^{th} stream surface. Combining II-20 and II-22

$$\tanh(\eta/2) = \frac{kQ_o}{4\pi A} \frac{(\sigma r)^{\frac{1}{2}}}{(r^2-a^2)^{\frac{1}{4}}} \cdot \frac{1}{r} \qquad \text{(II-23)}$$

From the property of hyperbolic tangents and Equation II-20 it can be shown that

$$z = \frac{r}{\sigma} \ln\left(\frac{r+kf}{r-kf}\right) \qquad \text{(II-24)}$$

where

$$f = \frac{Q_o(\sigma r)^{\frac{1}{2}}}{4\pi A(r^2-a^2)^{\frac{1}{4}}} \qquad \text{(II-25)}$$

Equation II-24 gives the streamline in terms of z as a function of r and k. The parameter k takes on values of 1, 2, 3, ..., and gives rise to pairs of stream surface on either side of the

impeller centerline that encloses fluid having a volumetric flow of kQ_o.

Figure IV-5 shows the streamline and velocity profiles for the tangential jet in Region I. Three streamlines are drawn, first with ψ having a value less than Q the impeller discharge. This streamline it is seen exists for r less than the impeller diameter. In drawing such a streamline it is started a little before r = D/2 as shown in Figure II-1. The second streamline has a value of ψ equal to Q, the impeller discharge. The streamline is asymptotic to ψ = D/2 and intersects the velocity profile at $b_{\frac{1}{2}}$ as shown in Figure IV-5. The third streamline has a value of ψ greater than Q. This streamline will be asymptotic to some radial distance r_c which is larger than D/2. To find r_c, we substitute kQ_o (greater than Q) for ψ in II-20 and solve for r_c. Since Equation II-23 is not explicit in r, r_c is evaluated by a Golden section search procedure (42). Once r_c is located subsequent points on the streamline is located for finite increments of r larger than r_c from Equation II-20 with ψ equals the appropriate value of kQ_o. A description of the Golden section section search procedure and a listing of the subroutine GOLD which performs the search, is given in Appendix E.

2.2. Region II, III, IV

In Region II the jet does divide, since the fluid is incompressible and assumed to be in potential flow it is reasonable to consider the width of the jet entering and leaving this region as the same. In other words the jet ceases to grow or expand but turns

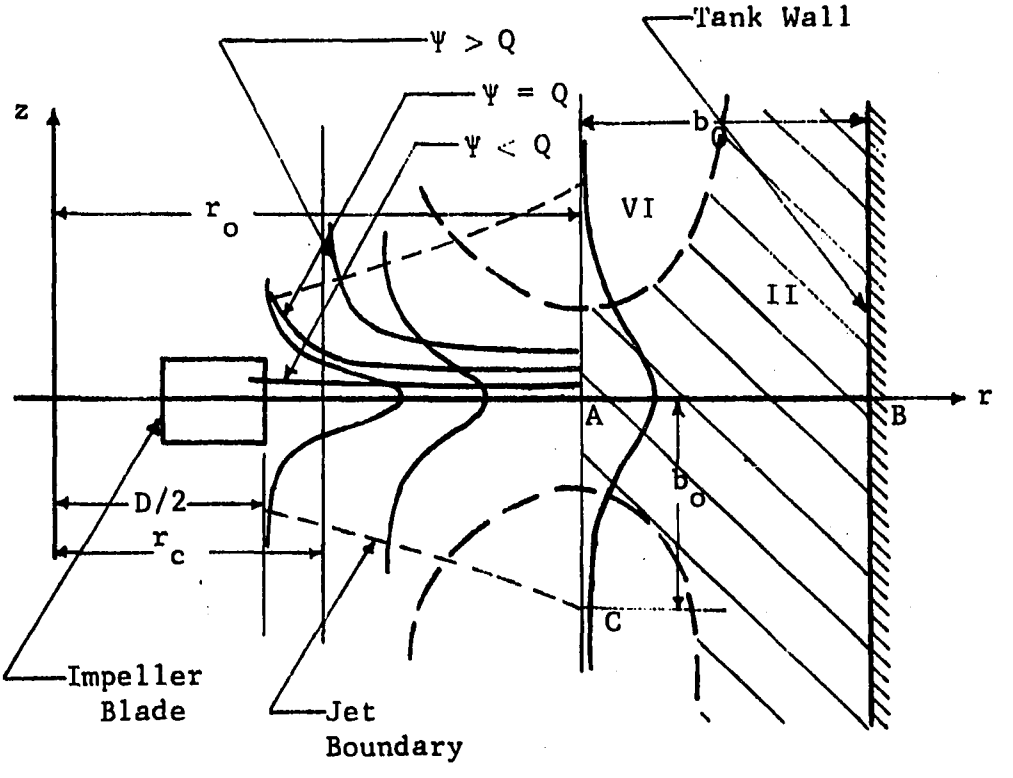

Figure II-5: Tangential Jet Model in Region I

around the corner intact. If r_o is the point at which this occurs, point A in Figure II-5, then from Equation B-34 of Appendix B, the half width of the jet $b_{\frac{1}{2}}$ at this point is

$$b_{\frac{1}{2}} = \frac{6r_o}{\sigma} \qquad \text{(II-26)}$$

From the above reasoning and Figure II-5 it follows that AB must equal b_o. From the geometry of Figure II-5, b_o equals $(T/2-r_o)$ hence,

$$\frac{T}{2} - r_o = \frac{6r_o}{\sigma} \qquad \text{(II-27)}$$

where, T in II-27 is the tank diameter. Simplifying

$$r_o = \frac{T\sigma}{12+2\sigma} \qquad \text{(II-28)}$$

Equation II-28 says that beyond r_o the jet no longer expands but is in stagnation flow. The radial component will decrease and the vertical component increases. Thus if the volumetric flow is measured in the jet with increasing r, then at r_o the volumetric flow should reach a maximum and this has been observed experimentally.

The stream function for Regions II, III, and IV is given by Equation D-9 of Appendix D and is

$$\psi = r^2 z \qquad \text{(D-9)}$$

Equation D-9 is strictly applicable for a uniform flow approaching a wall, or turning a corner. The jet at r_o, the start of Region II, has a flat bell shaped profile due to entrainment as seen in Figure II-5. For regions not far removed from the center of the jet the flow can be considered as approximately uniform and hence Equation D-9

can be used. The regions far removed from the center of the jet is essentially a part of Region VI and is thus modeled separately.

These remarks can be made clear by looking at Figure IV-5. Three velocity profile are shown. In the figure, the scale for $\bar{q}$ on the first profile is arbitrary. The other two profiles are drawn on the same scale as the first and hence correctly pictures the distortion of the flow profile due to entrainment. For the three streamlines shown, the flow enclosed by these streamlines is approximately uniform, beyond r_o. At the edges of the jet velocities get rapadily smaller and cannot be included in the analysis. To emphasize this point the extent of Region II has been cross-hatched in Figure IV-5.

Also shown in Figure IV-5 is an area where Region I and VI overlap. The velocities due to the jet in this region are small as can be seen in the jet profile that protrudes into this area. The boundary of the jet has been sketched in Figure IV-5 and is approximately linear as predicted by Equation II-12.

2.3. Mechanics of Plotting Streamlines in Regions I, II, III and IV

As mentioned earlier, to produce a trace of a line with the Calcomp Plotter the x and y coordinates are required at small increments Δx and Δy along the line. This is accomplished by subroutine STREAM which generates arrays PX and PY in which are stored the coordinates r and z or a complete streamline at small intervals Δr and Δz appart. The subroutine STREAM is called by the main program PLOTER each time a streamline is desired. The command to plot is executed by the program PLOTER.

From Section 2.1 it will be recalled that a streamline starts in Region I. Hence the number of streamlines plotted depends on the volumetric flow in the jet. Since extrainment stops at r_o, the extent of the jet, the maximum flow will occur at this point. The number of streamlines is thus, maximum flow divided by Q_o, the incremental flow rate on the streamline. It is observed in Figure IV-1 that there are five streamlines. It is also seen that the last streamline begins very near to r_o, hence the entrainment in the jet beyond this point is less than Q_o.

This section will detail the equations used and the steps involved in calculating a streamline as it proceeds from region to region and is the mathematical basis for the subroutine STREAM. FØRTRAN symbols will be used to denote all variables in this section as the discussion is closely related to the flow diagram and listing of program PLOTER given in Appendix E. The FØRTRAN symbols will be recognized as containing more than one upper case characters. To avoid confusion mathematical operations with these variables will also be written in FØRTRAN. For convenience the FØRTRAN symbols used in the text is listed separately in the section devoted to nomenclature.

Region I

As pointed in Section 2.1 and the illustration shown in Figure IV-5 two cases exists. The first case is when kQ_o is less than Q the impeller discharge. In this case the streamline is started at the impeller periphery and the coordinates of the streamline is calculated from Equation II-24 by incrementing r in increments of 0.005 ft. The calculated coordinates are stored in the

arrays of PX and PY. When kQ_o is larger than Q, then r_c is evaluated as outlined in Section 2.1 and the streamline started +0.01 ft from r. If the streamline is started at r_c the z coordinate obtained will be excessively large as the streamlines are asymptotic to r_c. When r equals r_o (calculated from Equation II-28), Region II is reached and the streamline is now given by Equation D-9.

Region II

In subroutine STREAM it will be noticed that in each region the calculations are based on a local X, Y axis which are then transformed into r, z corrdinates of the overall plot. Thus in Region II the origin of the local X, Y axis is point B in Figure II-1. Equation D-9 is then used in the local frame of axis giving rise to the stagnation flow pattern shown in Figure II-3 (a). In Equation D-9 a value of ψ is needed to evaluate the stream function. Since local coordinates are used a value for ψ in this frame of axis has to be calculated. This is possible since the entry point to Region II is a point on the streamline. Accordingly, if the last point in Region I is x_n, y_n, this is an entry point to Region II and thus a point on Equation D-9, hence

$$\psi = x_n^2 y_n \qquad \text{(II-29)}$$

The equation of the streamline with the point B of Figure II-1 as the origin is then obtained from D-9 and II-29 as

$$x = \left(\frac{x_n^2 y_n}{y}\right)^{\frac{1}{2}} \qquad \text{(II-30)}$$

The value of the streamlines in terms of the original r, z coordinates are from the geometry of Region II,

$$z = y \tag{II-31}$$

$$r = T/2 - \left(\frac{x_n^2 y_n}{y}\right)^{\frac{1}{2}} \tag{II-32}$$

The unanswered question is how far does Region II extend. This was determined by making a parameter study.

Scale Used for Plotting

In the process of making these plots it was found convenient to scale the entire plot in terms of T the tank diameter. A scale of unity was chosen for T equal 1.0 ft. Thus a 11.5 in. diameter tank will on this scale be represented as 0.96. All other dimensions of the tank are reported as fractions of T and are shown in Figure II-6 and defined in Table II-1. On the axis of the computer solution is printed a scale as seen in Figure II-1. The units on the scale is T equals 1.0 ft. The reason for choosing a scale of T equals 1.0 ft. is to permit generalization of solution to any size tank by use of a suitable scale factor. Thus for example the scale on the z axis shows the bottom most corner as -0.4 in Figure II-1. This means that the impeller is immersed to 60% of the depth of fluid H in the tank and it is also evident that H equals T.

Figure II-6 shows the boundary of the regions into which the tank is divided. AA is the boundary between Regions IV and V and has two possible locations 1 and 2. BB is the boundary between Regions III and IV and CC is the boundary between Regions II and III.

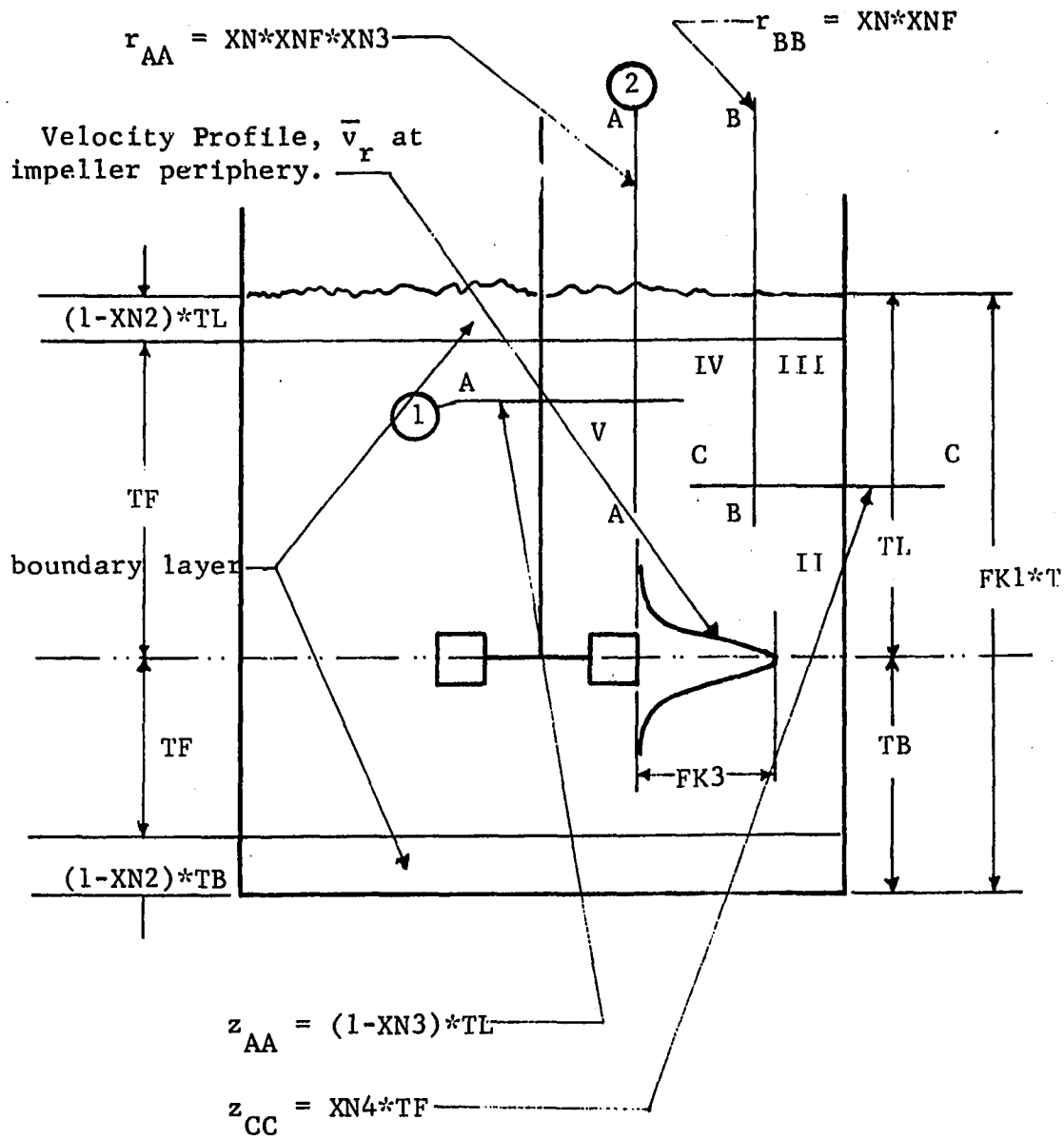

Figure II-6: Dimensionless Ratios Used for Obtaining the Theoretical Streamlines by Program PLOTER. Note all Symbols and Mathematical Operations are in FØRTRAN.

TABLE II-1

LIST AND DEFINITION OF SYMBOLS USED IN FIGURE II-6

Symbol	Defining Equation	Effect on the Theoretical Flow Patterns
FK1	FK1 = H/T	Controls depth of fluid
FK2	FK2 = h/T	Controls height of impeller above tank bottom
FK3		Scales $\bar{v}_r$, for velocity profile plot in Region I
TB	TB = FK2 * T	Depth of fluid below impeller
TL	TL = (FK1 - FK2) * T	Depth of fluid above impeller
TF	(1) TF = XN2 * TB (2) TF = XN2 * TL	Effective depth of fluid above or below the impeller considered in potential flow solution
XN	XN = r_o	Extent of tangential jet
XNF	r_{BB} = XN * XNF	Controls r_{BB}, r coordinate of boundary BB between regions III and IV
XN2	(1) t = (1 - XN2) * TL (2) t = (1 - XN2) * TB	Controls t, thickness of boundary layer
XN3	(1) z_{AA} = (1 - XN3) * TL	Controls z_{AA}, z coordinate of boundary AA between Regions IV and V
	(2) r_{AA} = XN * XNF * XN3	Controls r_{AA}, r coordinate of boundary AA between Regions IV and V
XN4	z_{CC} = XN4 * TF	Controls z_{CC}, z coordinate of boundary between Regions I and II

The dimensions of the tank, the coordinates of the boundary between the regions and their defining equations are given in Table II-1. The symbols and mathematical operations in Table II-1 and Figure II-6 are in FØRTRAN as noted above.

Provisions for a boundary layer exist and is the thickness of fluid removed from the potential flow solution. Since the subroutine STREAM calculates one complete streamline it makes no difference whether this streamline is above or below the impeller. Hence the boundary layer is shown at the top and bottom of the tank in Figure II-6. The boundary layer at the sides of the tank is small and hence neglected as seen from the work of Askew (2) which was discussed earlier. Physically a boundary layer is conceivable only at the bottom of the tank and this boundary layer is implemented in Figure II-1. The thickness of the boundary layer is controlled by XN2 which is a fraction of TL or TB the depth of fluid above and below the impeller. The variable TF is the depth of fluid after removing the boundary layer if any, and thus constitutes the effective depth of fluid in the potential flow solution. FK3 is a scale factor on the velocity profile $\bar{v}_r$, which is drawn at four equally spaced points between the impeller periphery and r_o.

The boundaries of the various regions are controlled by the parameters XN4, SNF and XN3. Thus the extent of Region II is fixed by XN4 which is in terms of a fraction of TF the effective depth of the potential flow region above or below the impeller centerline.

Region III and IV

The streamline in Regions III and IV are evaluated in a similar

manner as Region II. The local origin for Region III is point E while that of Region IV is point K of Figure II-1. As for Region II, x_n, y_n is the coordinates of the entry point to these regions and the streamline in the local frame of reference is given by II-30.

The extent of Region IV is given by T/2-XNF*XN, where XN is the program symbol for r_o. The boundary between Region III and IV can thus be varied by varying the parameter XNF.

Region IV can be terminated in two ways: either by a line parallel to the axis or a line parallel to the r axis. Both these limits are shown in Figure IV-6 and marked 1 and 2 respectively. The extent of Region IV is in the first case given by XN*XNF*XN3 and in the second case by TL*XN3. Region IV can thus be varied by varying the parameter XN3. This point will be discussed in more detail in Section 3.1.

2.4. Region V

In Appendix B, the equation for the stream function ψ is given for cylinderical coordinates. As z is the direction of flow, ψ is evaluated from Equation B-7, and not B-6 as in the case of the tangential jet. Integrating B-7 gives ψ as

$$\psi = 2\pi\int_o^r \bar{v}_r r dr \qquad \text{(II-33)}$$

where the additional 2π is necessary since ψ is a stream surface. The sign in Equation B-7 is taken as positive since $\bar{v}_z$ is positive and $\bar{v}_r$ is negative for the circular jet as can be seen in Figure II-3. Substituting for $\bar{v}_z$ and r from Equation II-14 and II-16 and simplifying

$$\psi = 2\pi\epsilon_o(z+z_o)\int_o^\xi \frac{2\xi d\xi}{(1+\frac{1}{4}\xi^2)^2} \qquad \text{(II-34)}$$

Integrating Equation II-34 results in

$$\psi = \frac{2\pi\epsilon_o(z+z_o)\xi^2}{1+\frac{1}{4}\xi^2} \qquad \text{(II-35)}$$

Equation II-35 is the desired equation of the streamline for a circulate jet. Ordinarily there are a number of parameters to be evaluated in II-35. However, these have been reduced to two parameters γ the jet width and z_o, the displacement of jet origin.

As before, let r_n, z_n be the end points of the previous region and the starting points for Region V. Then from Equation II-16.

$$\xi_o = \gamma \frac{r_n}{z_n + z_o} \qquad \text{(II-36)}$$

ψ can now be calculated at the point r_n, z_n from II-36 and II-35. This calculated value of ψ is called CK in the program PLOTER, thus

$$CK = \frac{2\pi\epsilon_o(z_n+z_o)\xi_o^2}{1+\frac{1}{4}\xi_o^2} \qquad \text{(II-37)}$$

Since ψ has a value CK, Equation II-35 is solved for ξ. On substituting for ξ from Equation II-16 results in

$$r = \frac{z + z_o}{r}\left(\frac{1}{\frac{2\pi\epsilon_o(z+z_o)}{CK} - \frac{1}{4}}\right)^{\frac{1}{2}} \qquad \text{(II-38)}$$

Substituting for CK from II-37 gives

$$r = \frac{z+z_o}{\gamma} \left(\frac{1}{(z+z_o)\left(\frac{1+\frac{1}{4}\xi_o^2}{(z_n+z_o)\xi_o^2} - \frac{1}{4} \right)} \right)^{\frac{1}{2}} \qquad \text{(II-39)}$$

Equation II-39 gives the streamlines for the circular jet in terms of r as a function of z. There are two parameters to be determined: z_o the displacement of the jet origin from the base of the potential flow region (see Figure II-4) and γ the jet width parameter. The best value of z_o is determined by making a parameter study, and this will be discussed in Section 3.

The jet width parameter, γ, controls the slope of the streamlines. In Figure II-1, the ends of the streamlines do not meet and are joined by dotted lines. γ is chosen such that the lengths of the dotted lines is minimized. This is done by calculating a γ that makes the lengths of the dotted lines zero for each individual streamline. Obviously a circular jet cannot have a different γ for each streamline, hence an average value of γ, for the individual streamline is selected for the final plot. This makes the ends of the streamlines in Region V, under shoot the start of the streamlines in Region I in some cases, and overshoot in others. This can be seen in Figure II-1. A sample calculation of the above procedure for evaluating γ is given in Appendix E.

3. Theoretical Flow Patterns

In the previous sections the theoretical basis of the computer program to draw the flow patterns were discussed. This section is devoted to a discussion of what the program can and cannot do. The program requires a number of parameters to be specified and this section will indicate how some of these parameters can be determined.

The main parameters are that of the tangential jet model: σ the jet width parameter, A the volumetric flow parameter and, a, the radius of source parameters. These will be obtained from experimental correlations which will be treated in Chapter IV. The values of σ, A and a used in the flow patterns of Figures II-5 through II-9 are from Cooper's (8) data (Profile 5 Table G-16 of Appendix G). The pertinent tank parameters are given in Table II-2 and are common to all the flow patterns. The value of Q, the impeller discharge, and ϵ the eddy viscosity are calculated from Equations B-30 and B-15. Table II-2 gives the angle θ_y at which the velocity vector $\vec{q}$ leaves the impeller periphery. This angle is calculated from Equation A-14. Finally the value of the incremental flow rate on the streamline Q_o is also given in Table II-2.

The parameters to be determined are the relative sizes of the six regions into which the stirred tank has been divided. There are five parameters which determine the relative extent of these regions. A large number of profiles were studied, with varying values of these parameters. From these studies, twelve different combinations of parameters were selected. These combinations illustrate the effect of varying the parameters on the solution and

TABLE II-2

OPERATING CONDITIONS AND PERTINENT DATA ON THE STIRRED TANK WHOSE THEORETICAL PROFILES ARE DRAWN IN FIGURES II-5 TO II-9

Tank Diameter T*	=	1.0	ft.
Depth of Fluid H*	=	1.0	ft.
Impeller Diameter D*	=	3.0	in.
Height of Impeller of Tank Bottom h	=	0.4	ft.
Impeller Speed	=	600	RPM
N_{Re}	=	64,780	
Eddy Viscosity at Impeller Periphery	=	0.79	$ft^2/min.$
Impeller Discharge Q	=	7.42	ft/sec.
Increment on Streamline	=	5.0	ft^3/min
Jet Width Parameter σ	=	12.62	
Volumetric Flow Parameter A	=	22.5	ft^3/min
Radius of Source, a	=	0.1038	ft.
Yaw Angle at Impeller Periphery θ_y	=	56.1°	
Extent of Tangential Jet r_o	=	0.339	ft.

* Nominal values used in Figures II-5 through II-9

the basis for selecting the best combination of these parameters. The parameters are varied one at a time and their effect on the flow patterns is discussed in the following sections.

The flow patterns in Figures II-7 through II-11 are drawn with the impeller immersed to 60% of the fluid depth. This is to illustrate the distortion that results by reducing the potential flow area below the impeller centerline. Also shown in these flow patterns is a boundary layer at the bottom of the tank. The thickness of this layer is 10% of the depth of fluid below the impeller centerline. The inclusion of the boundary layer in these flow patterns reduces the depth of the potential flow region adding to distortion of the flow patterns located below the impeller.

The scale shown in Figures II-7 through II-11 is based on T equal 1.0 ft. All other dimensions are in terms of fractions of T as shown in Figure II-8.

3.1. Extent of Region IV

The factor XN3 is used to control the effect of Region IV in two different ways. It can be limited in a horizontal plane as shown by the lines AA in Figure II-7, or in a cylinderical plane as shown by the lines AA in Figure II-8. The program PLOTER is operated in two different modes depending on whether Figures II-7 or II-8 is desired.

In the first mode of operation shown in Figure II-7, the boundary between Regions IV and V is fixed by the z coordinate of the line AA is given by TL*XN3. TL is the depth of fluid above the impeller

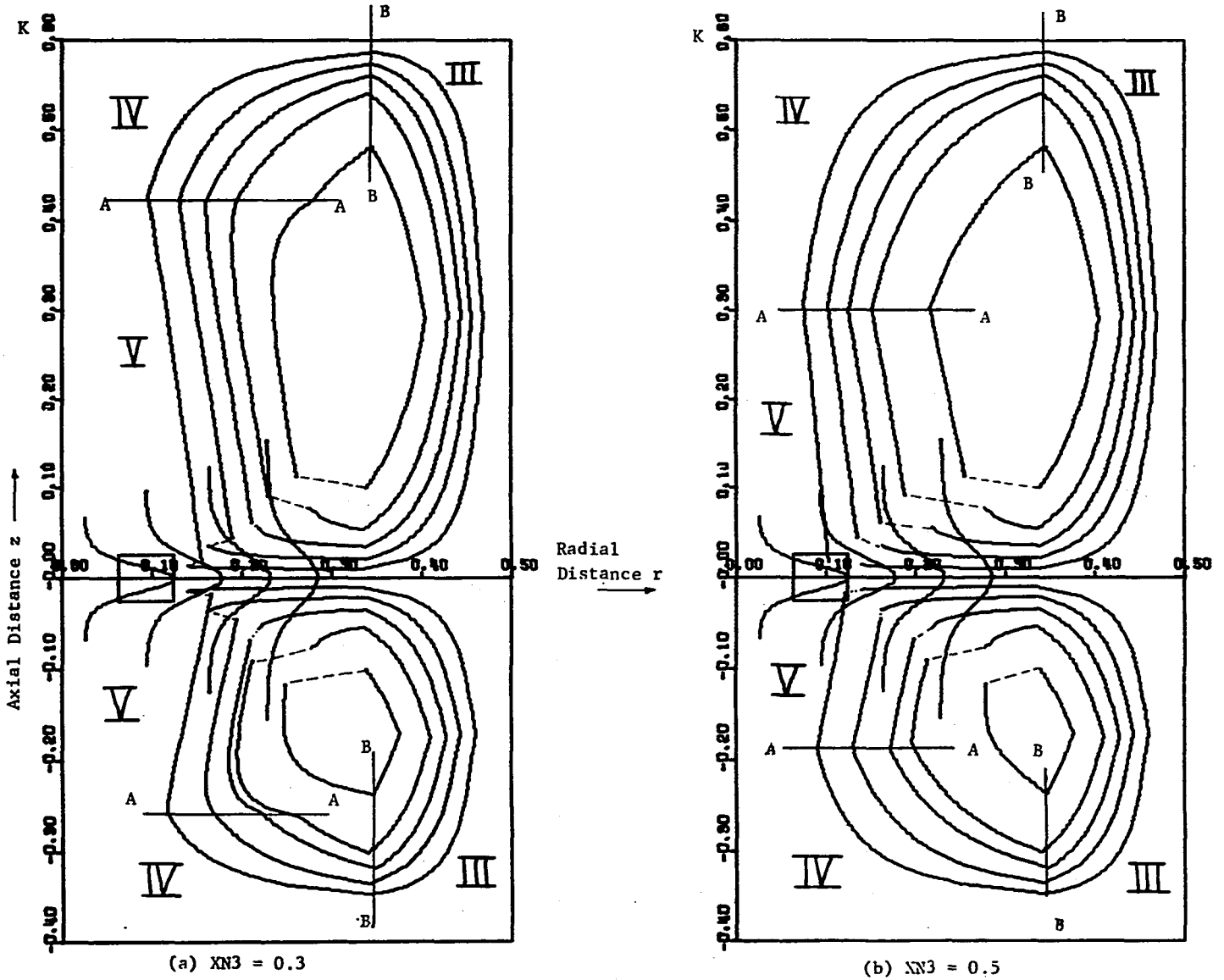

(a) XN3 = 0.3

(b) XN3 = 0.5

Scale: 1.0 = 1.0 ft.

Parameter settings: XN2 = 0.9, XNF = 1.0, XN4 = 0.5, F?O = 0.

Figure II-7: Effect of Varying the Boundary Between Regions IV and V in a Horizontal Plane on the Theoretical Flow Patterns.

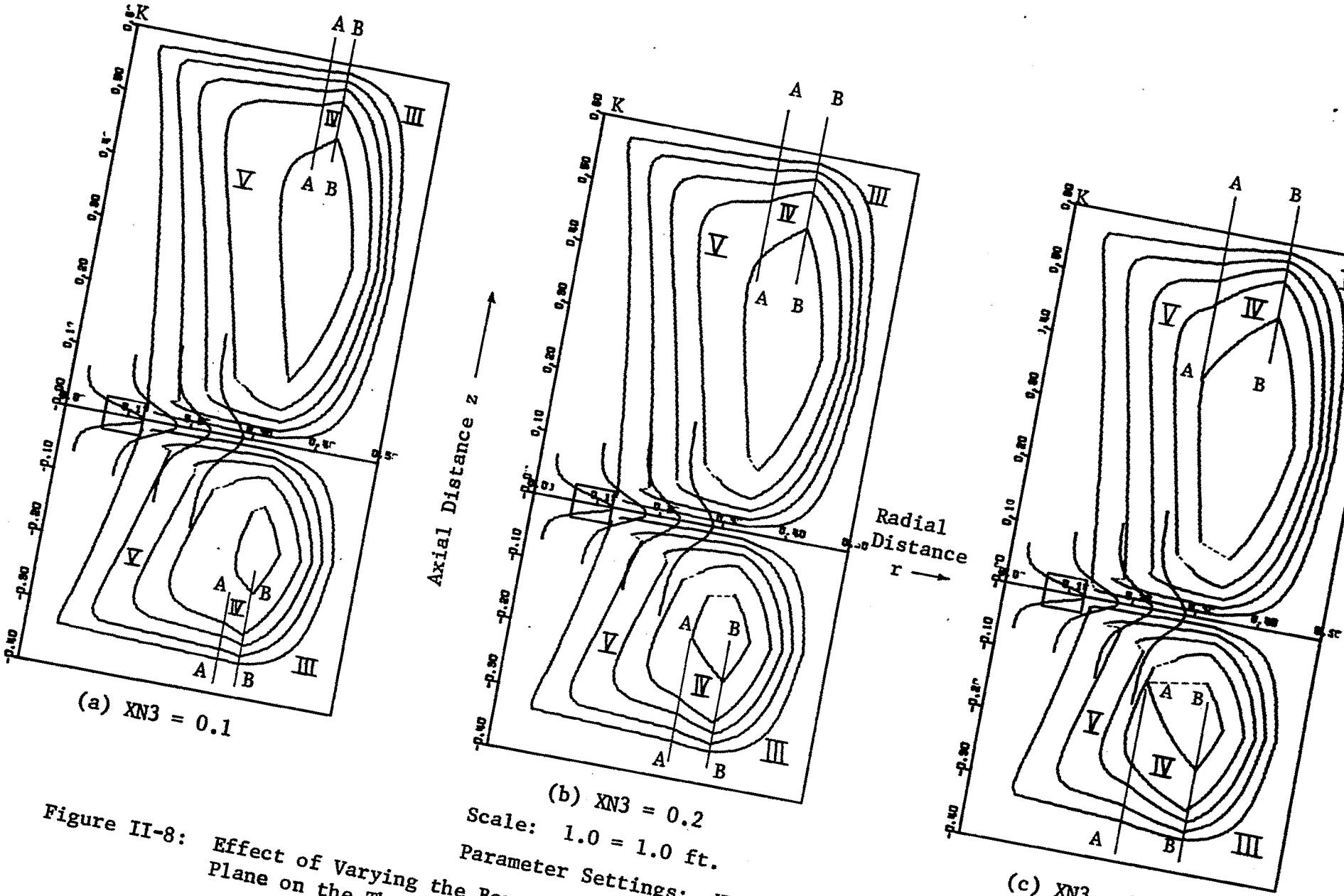

(a) XN3 = 0.1

(b) XN3 = 0.2

(c) XN3 = 0.3

Scale: 1.0 = 1.0 ft.

Figure II-8: Effect of Varying the Boundary Between Regions IV and V in a Cylinderical Parameter Settings: XN2 = 0.9, XNF = 1.0, XN4 = 0.5, FZO = 0. Plane on the Theoretical Flow Patterns.

centerline. Similarly below the impeller centerline the z coordinate of AA is given by TB*XN3. Two values of XN3; 0.3, 0.5 are used, resulting in the flow patterns of Figure II-7 (a) and II-7 (b). These plots show that the ends of the streamlines do not meet, also for large values of XN3 the boundary between Regions IV and V show a discontinuity. It is noticed that the reduction of the potential flow region causes distortion of the streamline. The maximum distortion occurs for the fifth streamline below the impeller.

In Figure II-8 is shown the other mode of operation in which Region IV is restricted by a line parallel to the z axis. The extent of Region IV in this case is controlled by the coordinate of the line AA, which is given by XN*XNF*XN3. By varying XN3 the position of the line AA can be changed. The coordinates of AA also depends on XNF which controls the coordinates of the line BB that marks the boundary between Regions III and IV. The coordinates of BB is given by XN*XNF.

In Figure II-8 the coordinates of the line BB is kept constant and three values of XN3 are examined. These are 0.1, 0.2 and 0.3. Increasing XN3 pushes the line AA to the left. In Figure II-8 (c) it is seen that if XN3 is increased beyond 0.3 then the last streamline will be deleted from the solution in Region V. This occurs in Figure II-7 (b) for the fifth streamline, below the impeller. Thus 0.3 is an upper limit for XN3.

Since point K in Figure II-8 is the origin for the local frame of reference in Region IV it would appear that the truncated Region IV of Figure II-8 is unnecessary. However on comparing Figures II-7

and II-8 it is seen that by locating AA as in Figure II-8 causes the ends of the streamline to more nearly approach each other. Hence truncating Region IV as in Figure II-8 is better than extending Region IV as in Figure II-7. In future plots AA is located as in Figure II-8.

3.2. Boundary Between Regions III and IV

The boundary between Regions III and IV is marked by the line BB in Figure II-8. The r coordinate of BB is given by XN*XNF, where XN is the computer symbol for r_o. In Figure II-9 (a), XNF = 0.9 while in Figure II-9 (b), XNF = 1.1. It is seen that increasing the value of XNF pushes BB to the right. This causes a discontinuous transistion of the streamlines from Region III to Region IV, particularly in the inner streamlines. Large values of XNF causes the streamlines in Region IV to move appart as seen in Figure II-9 (b).

In Figure II-9 (c) is shown a proper combination of XN3 and XNF. It is seen that the ends of the streamlines approach each other and the streamlines are fairly smooth at the boundaries of the various regions. The distortion of the streamlines below the impeller is also smaller than in Figures II-9 (a) or II-9 (b).

3.3. Locating the Origin of the Circular Jet

The origin of the circular jet is varied by the parameter z_o of Equation II-35. The computer symbol for z_o is FZO. In Figures II-7 to II-10, FZO equals zero. In these Figures the origin of the circular jet is at the point K, the intersection of the impeller axis with, the surface of the fluid above the impeller and the bottom surface of the tank below the impeller. In Figure II-11(a) and II-11(b) is shown the effect of varying FZO. Two values of FZO

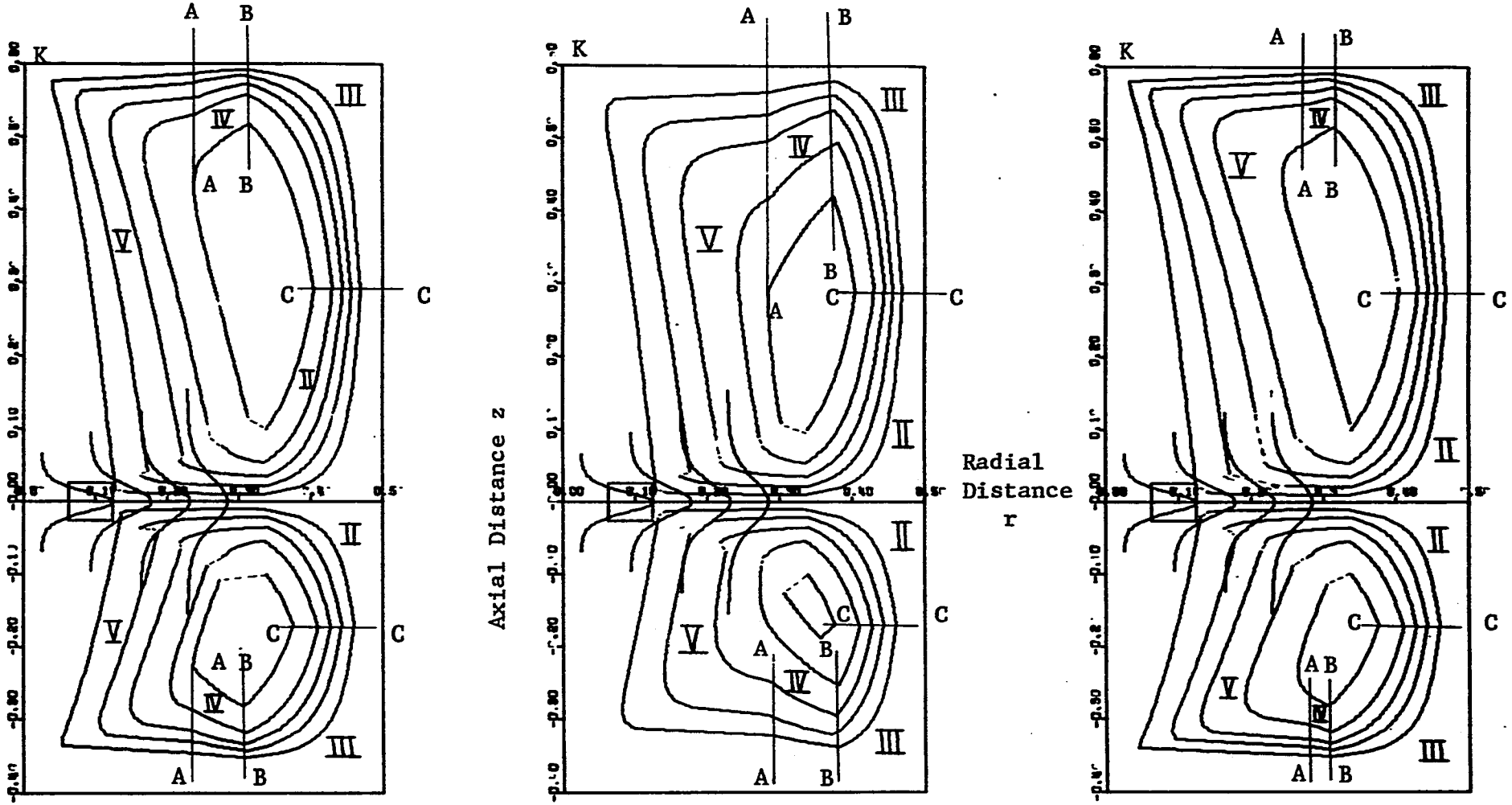

(a) XNF = 0.9

(b) XNF = 1.1

(c) XN3 = 0.1, XNF = 0.9

Scale: 1.0 = 1 ft.

Parameter Settings: XN2 = 0.9, XN3 = 0.25, XN4 = 0.5, FZO = 0

Figure II-9: Effect of Varying the Boundary Between Regions III and IV on the Theoretical Flow Patterns.

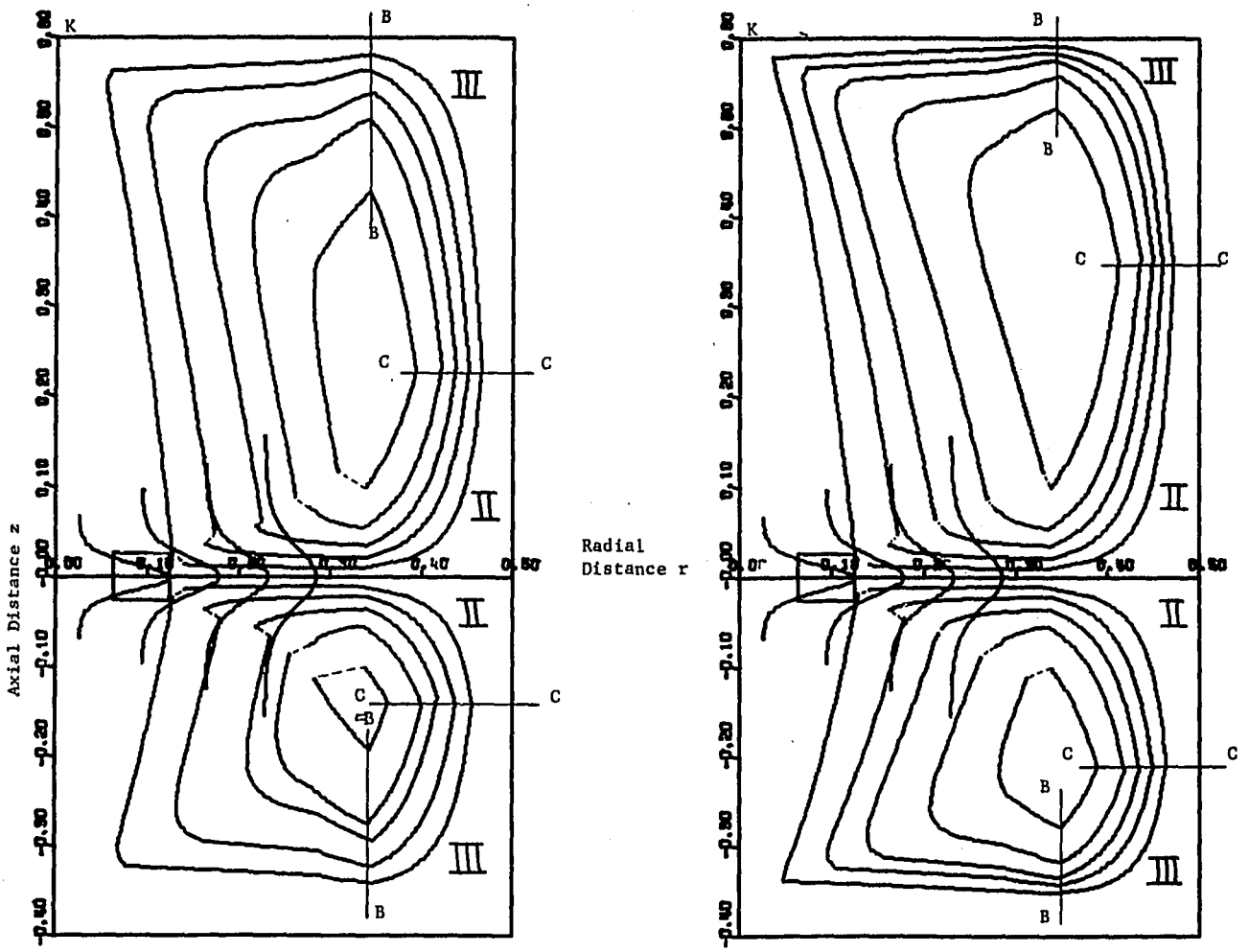

(a) XN4 = 0.4

(b) XN4 = 0.6

Scale: 1.0 = 1.0 ft.

Parameter Settings: XN2 = 0.9, XN3 = 0.2, XNF = 1.0, FZO = 0

Figure II-10. Effect of Varying the Boundary Between Regions II and III on the Theoretical Flow Patterns.

are chosen: 0.1 and 0.2. These values displace the point K away from the impeller centerline by the amount FZO. Negative values of FZO would bring the point K towards the impeller centerline. A large negative FZO will cause the knee or bend in the stream lines of the circular jet to be pushed towards the impeller resulting in an abrupt discontinuity. This effect is visible in the fourth streamline below the impeller in Figure II-7 (a). The exact location of K is shown for the potential flow solution above the impeller in Figure II-11.

Figure II-11 shows that increasing FZO tends to pull the flow patterns closer together, and away from the impeller axis. As it is more desirable to have the flow pattern fill the entire field, the best value of FZO is zero.

3.4. Desirable Values of Boundary Parameters

From examining more than thirty theoretical flow patterns, illustrative examples of which are given in Figures II-7 through II-10, it is concluded that Figure II-8 (c) is the best. In this figure the streamlines are smooth and they fill the entire flow field. Furthermore their ends almost meet, and material balances are satisfied. From this figure it appears that the best values for the boundary determining parameters are:

(1) XN4 = 0.5

(2) XNF = 0.9

(3) XN3 = 0.1

(4) FZO = 0

The above values are recommended values and they are relatively insensitive to impeller speed and diameter. The program is flexible

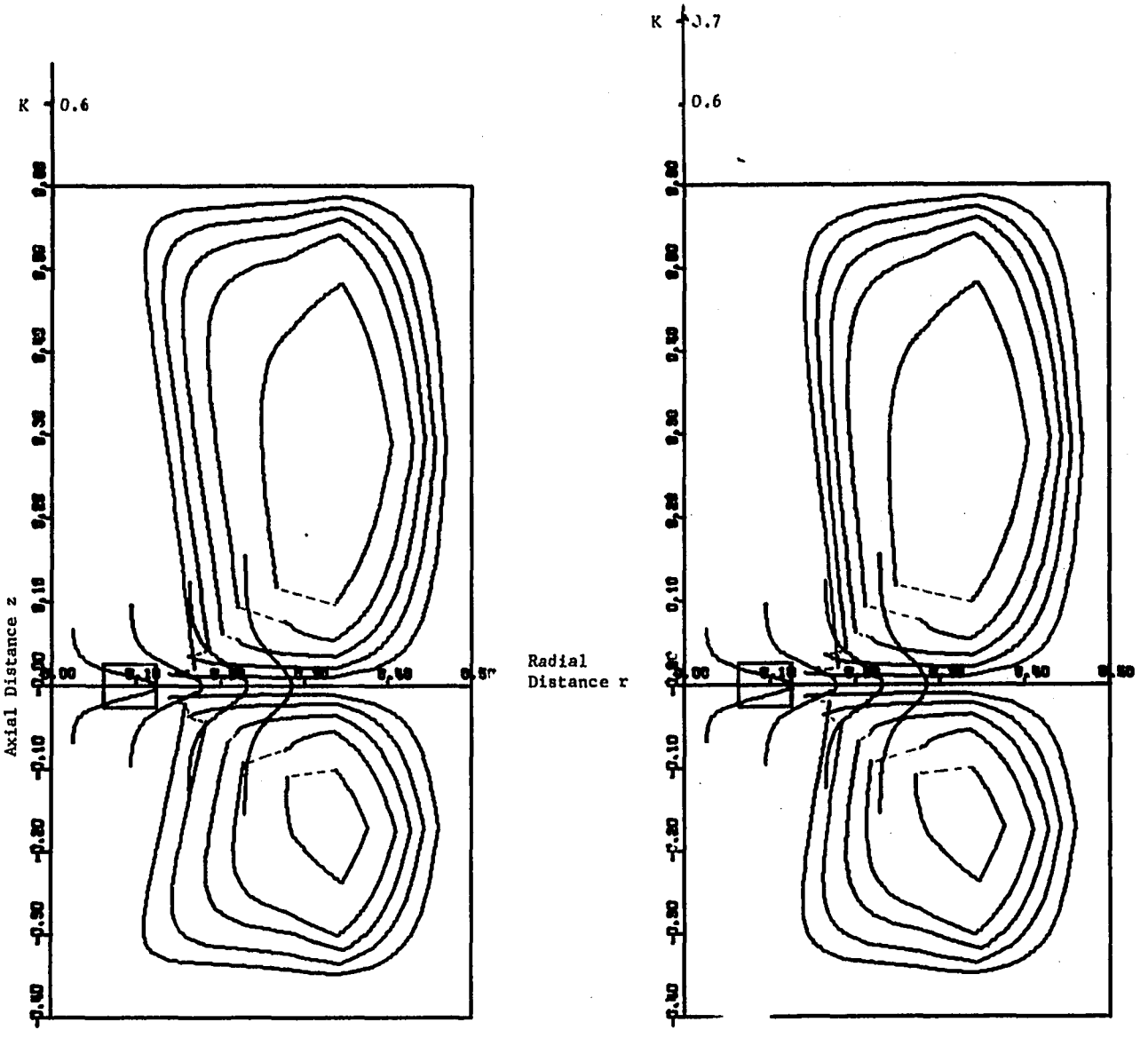

(a) FZO = 0.1

(b) FZO = 2.0

Scale: 1.0 = 1.0 ft.

Parameter Settings: XN2 = 0.9, XN3 = 0.2, XNF = 1.0, XN4 = 0.5

Figure II-11. Effect of Varying the Origin, K of the Circular Jet on the Theoretical Flow Patterns.

enough to take any desired value for the above boundary parameters. The tangential jet parameters are obtained from correlations given in Chapter IV. The flow pattern shown in Figure II-1 is for illustration purpose only and hence does not conform to the above recommended values, but is similar to that shown in Figure II-7 The reason for this is that in Figure II-1, Region IV is well defined and not truncated as in Figure II-9 (c).

4. Summary and Conclusions

In this chapter the theoretical basis for drawing flow patterns was developed in Section 1. In Section 2 the basis for the computer program that enables a Calcomp Plotter to draw the flow patterns was discussed. Several theoretical flow patterns were drawn in Section 3. The limits and capabilities of the mathematical model are thus shown. The boundaries of the various regions are shown to be flexible and suitable limits for these boundaries have been recommended.

The flow pattern as drawn by the program is not exactly similar to the one given by Nagata (19). First in Region V because of the circular jet model selected the streamlines are pulled towards the axis of the tank and are made somewhat square rather than rounded. This is clearly visible when Figures II-9 (c) and I-5 are compared. Second, the inner most streamlines suffer the maximum distortion, tending to have corners rather than being round and smooth. The reason for this can be seen if the profile of $\bar{v}_r$ in Region I is examined. These profiles have been scaled relative to the profile at the impeller periphery. The relative flattening of the profile with increasing r is thus visible. It will be recalled from Section

2.2 that Equation D-9, the potential flow model used in Regions II, III and IV is valid for uniform flow. If the tangential jet profile is examined in Figure II-7 through II-11, it is seen that at Region II although the jet has broadened, the uniform flow can be considered to hold approximately for three of the streamlines and is questionable for the rest of the streamlines. These inner streamlines are really a part of Region VI which has been modeled as a dead water region. This is not too severe a restriction since the velocities beyond the third streamline is less than half q_{max} evaluated at r_o. From the shape of the velocity profile, beyond this point the velocity falls rapidly to zero. This value of q_{max} in Figure II-7 (c) is approximately 135 ft/min. This means that velocities at the inner streamlines is at the most 60 ft/min which is relatively small, compared to the maximum velocity of 238.5 ft/min at the impeller periphery.

From the theoretical profiles it seems that Region VI occupies a considerable portion of the tank and the bulk flow is limited to the periphery of the tank. Examining Nagata's plot of representative streamlines for baffled tanks shown in Figure I-5 of Chapter I it is seen that the streamlines are close and crowned at the interface of Regions II and III, indicating that the bulk flow does occur at the periphery of the tank.

CHAPTER III

EXPERIMENTAL APPARATUS AND OPERATING PROCEDURE

In this chapter, the experimental apparatus used will be described. The procedures and steps involved in taking the data will be detailed. Some problems were encountered in operating the equipment. The method employed in solving these problems together with the limitations on the apparatus used will be discussed in the sections that follow.

3.1. Mixing Vessel

Two mixing vessels were used in this work. The first vessel used was a 12.5 in. i.d. by 18 in. pyrex glass vessel as shown in Figure III-1. The bottom of this vessel had a small crown. In order to have a truly flat bottom vessel a 1.0 in. thick plastic sheet was placed at a depth of 15.0 in. The tank was fitted with four baffles. The baffles were made of AISI 316 stainless steel flat, measuring 1.0 in. by 1/8 in. thick. These baffles are within the recommended baffle width range of 1/12 to 1/10 of the tank diameter, being closer to 1/12 of the tank diameter.

The tank was fitted at the top with a 1/2 in. thick steel cover. In order that the cover should not slide it was recessed into the tank by 1/4 in. The baffles were mounted by welding them to the tank cover at the top and fitting into slots in the plastic

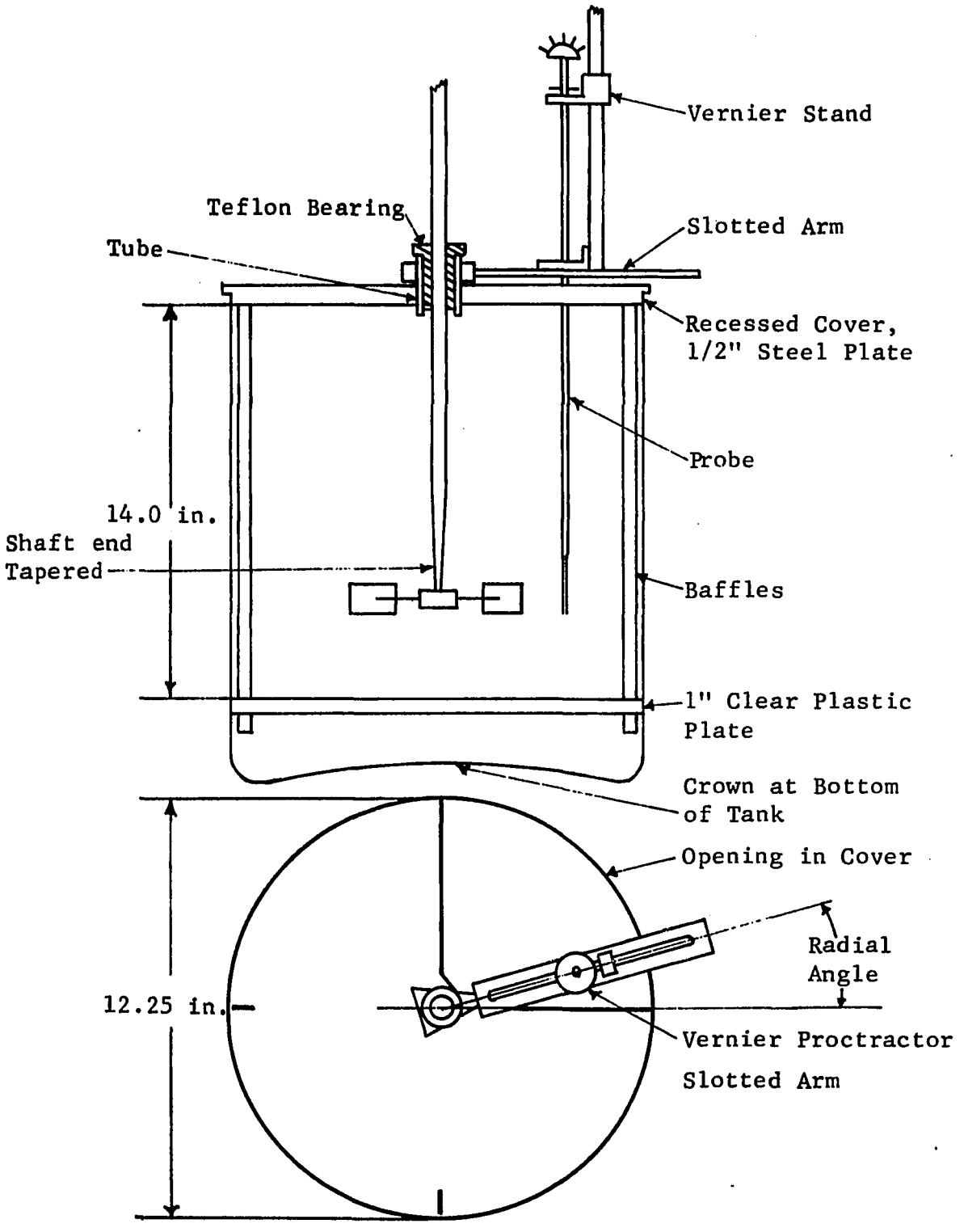

TOP VIEW

Figure III-1. Details of Stirred Tank and Probe Assembly.

sheet at the bottom. The tank cover had a 90° quadrant removed so as to have access to a region between two adjacent baffles. It was not necessary to have access to the rest of the tank since the flow is symmetrical in between adjacent baffles. The tank cover also had a cylinderical tube fitted exactly at the center to faciliate centering the impeller shaft by means of a simple teflon bearing. The tube also acts as a bearing for the probe assembly. The above details are shown in Figure III-1 which is not drawn to scale.

To measure velocity profiles in the region outside of the impeller, three holes were drilled in the sides of the tank wall as shown in Figure III-2. As this could not be done on the pyrex glass tank, a new tank was built out of plexiglass. A 11.5 in., inside diameter by 18.0 in. high, plexiglass pipe was used to make this tank. The diameter of the new tank was determined by the diameter of plexiglass pipe available which was closest to the diameter of the glass tank.

The velocity outside the impeller region reaches a maximum at approximately half the depth of the fluid above or below the impeller centerline. Since the impeller was centrally located the flow is symmetrical and the upper half of the tank was selected for measuring velocities outside the impeller region. Accordingly, three holes were drilled into the sides of the plexiglass tank at 8.0, 9.0 and 10.0 in. from the inner surface of the tank bottom. The 9.0 in. hole corresponds to the z-plane at which the velocities are a maximum. The other two holes are an inch apart above and below this hole to further explore the velocity field. A 5/8 in. diameter by 3.0 in. long nylon rod was glued to these holes. This

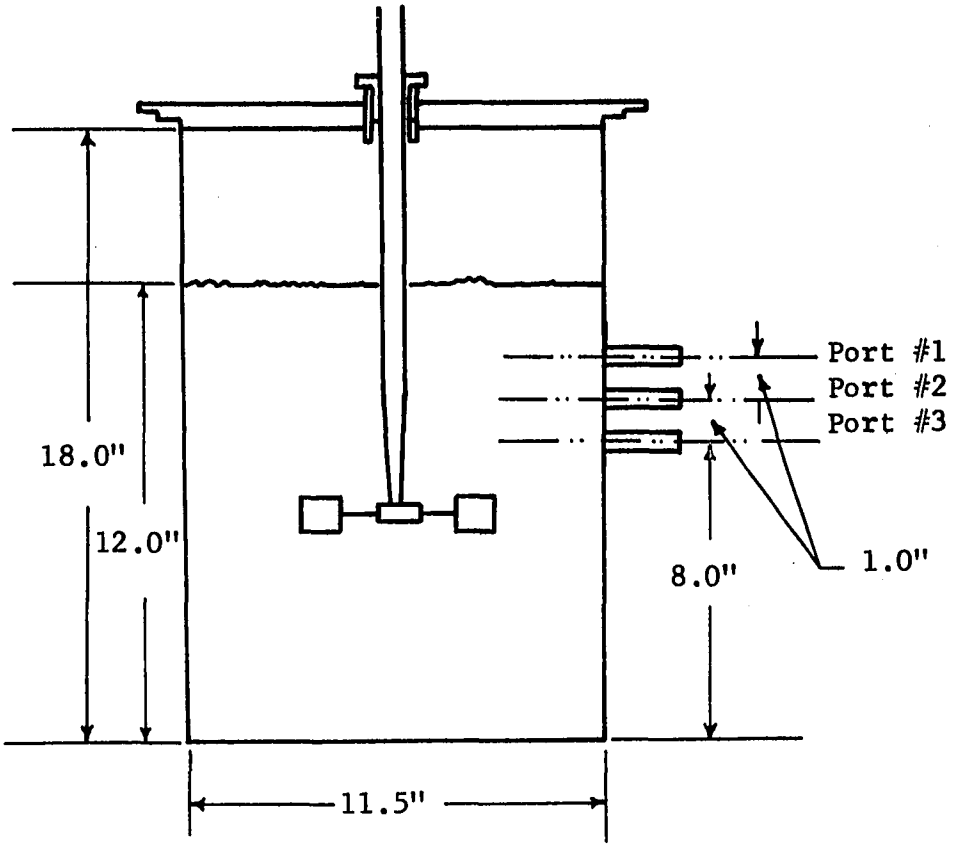

(a) Plexiglass Tank Showing Location of Horizontal Parts.

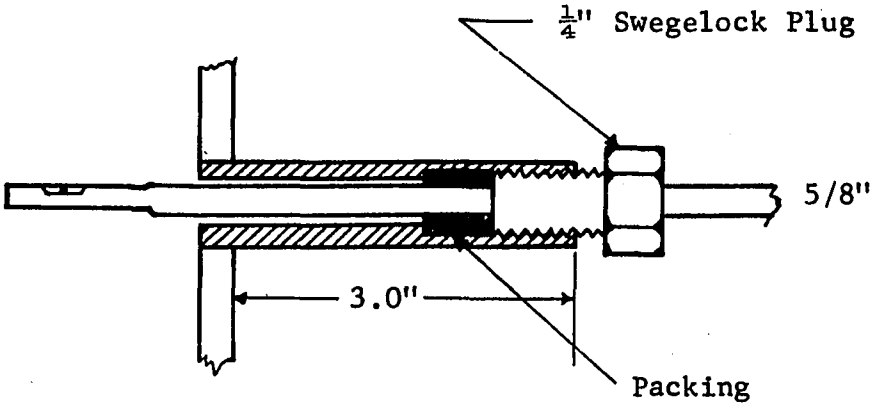

(b) Details of Port Assembly

Figure III-2. Plexiglass Tank.

rod was drilled and tapped such that it acted as a guide, support and sealing gland for the probe. The details of this assembly is also shown in Figure III-2. These holes are referred to as ports and are numbered 1, 2 and 3 as shown in Figure III-2.

The tank cover was machined down to 11.5 in. so that the rest of the tank assembly could be used with the plexiglass tank. The same baffles 1.0 in. wide as in the glass tank were used.

3.2. Impeller and Impeller Drive Assembly

A 3.0 in. Type A turbine made of AISI 316 stainless steel was used as the impeller. The blade dimensions are width, b, equal to 0.6 in., length of blade, l, equal to 0.75 in. and diameter of disk, d_1, equal to 2.0 in. The impeller shaft was made of 5/8 in. AISI 316 stainless steel. The impeller shaft was tapered from 5/8 in. to 1/2 in. for the last 6.0 in. of the shaft, and the bottom most 1/2 in. was turned to 5/16 in. so as to fit into the hub of the impeller where it was held fast by two screws.

The drive used was a Bench Scale Equipment Company (Dayton, Ohio) Model 4R Lab drive unit. It has continuously variable speed from 100 RPM to 1000 RPM. A higher speed range could be obtained by using a different chuck. The above range was adequate for this work. The entire drive was mounted on a 5 ft. vertical pipe which permitted raising and lowering the impeller. The drive mounting can be seen in Figure III-3 which is an overall photograph of the experimental apparatus. Figure III-4 is a close-up photograph of the glass tank and drive mechanism. In Figure III-5 is shown a close-up photograph of impeller and probe in the tank.

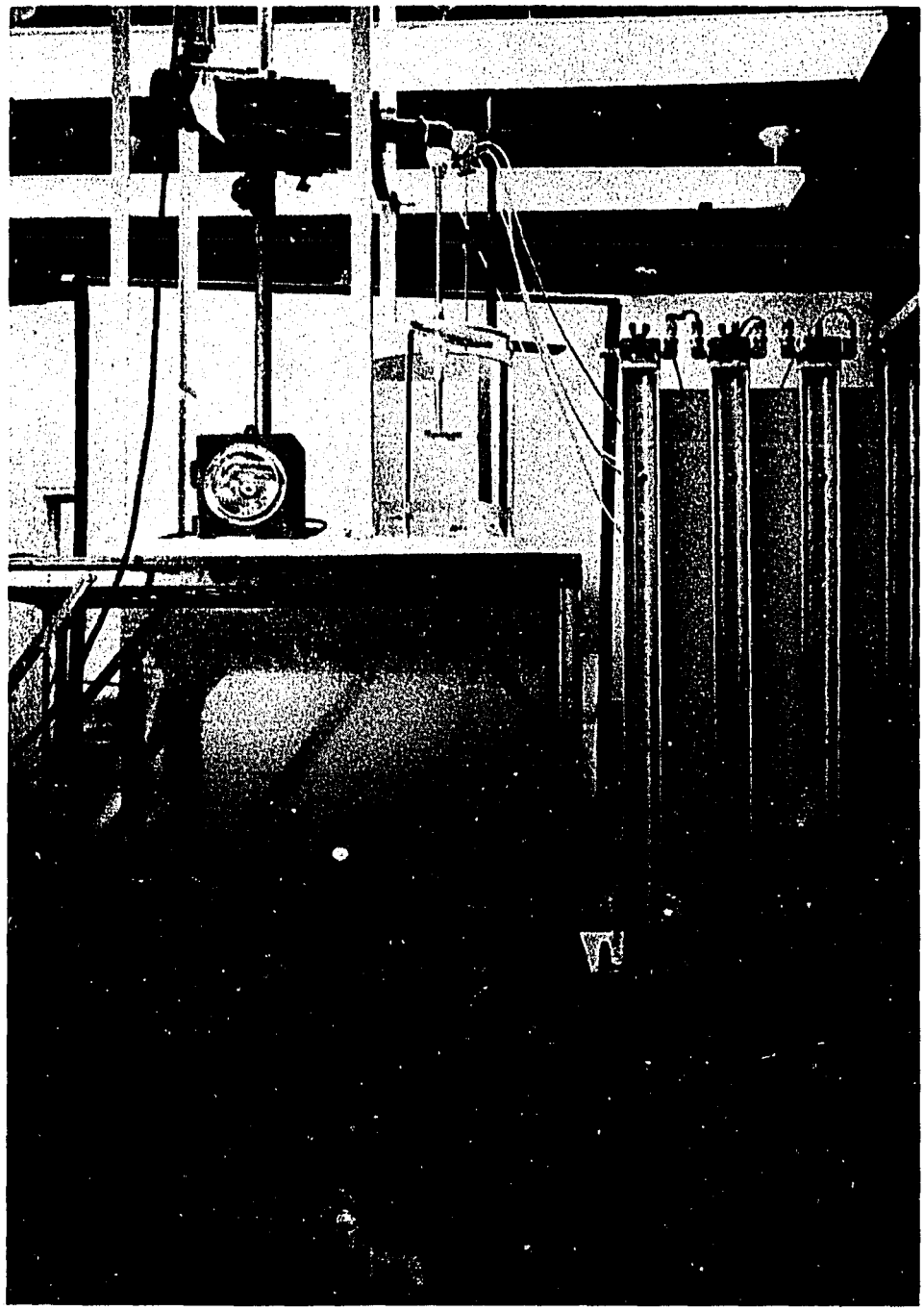

Figure III-3

Overall Views of the Experimental Apparatus

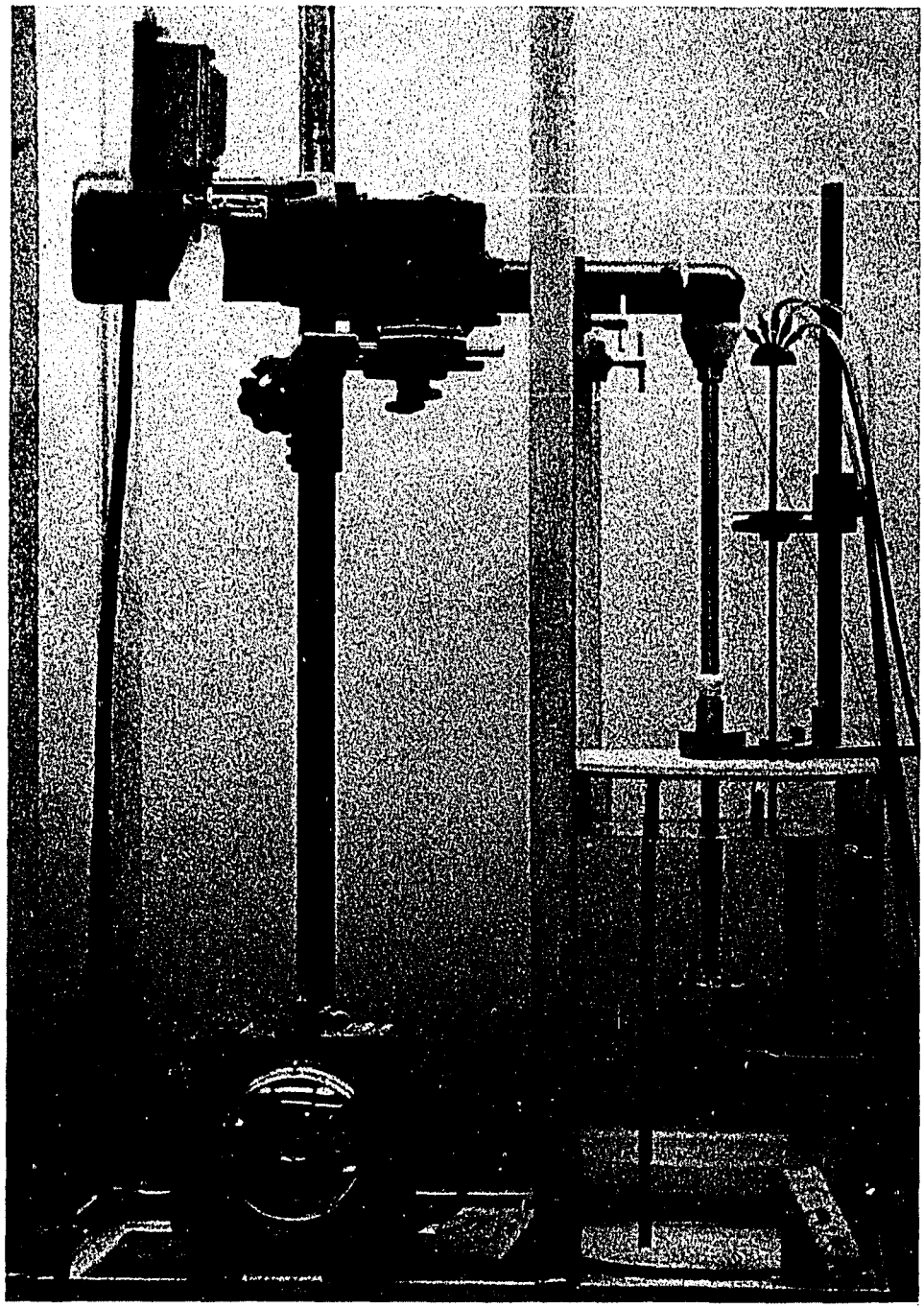

Figure III-4

Close-up View Showing Tank Drive,
Vernier Stand, Strobotac and Tank

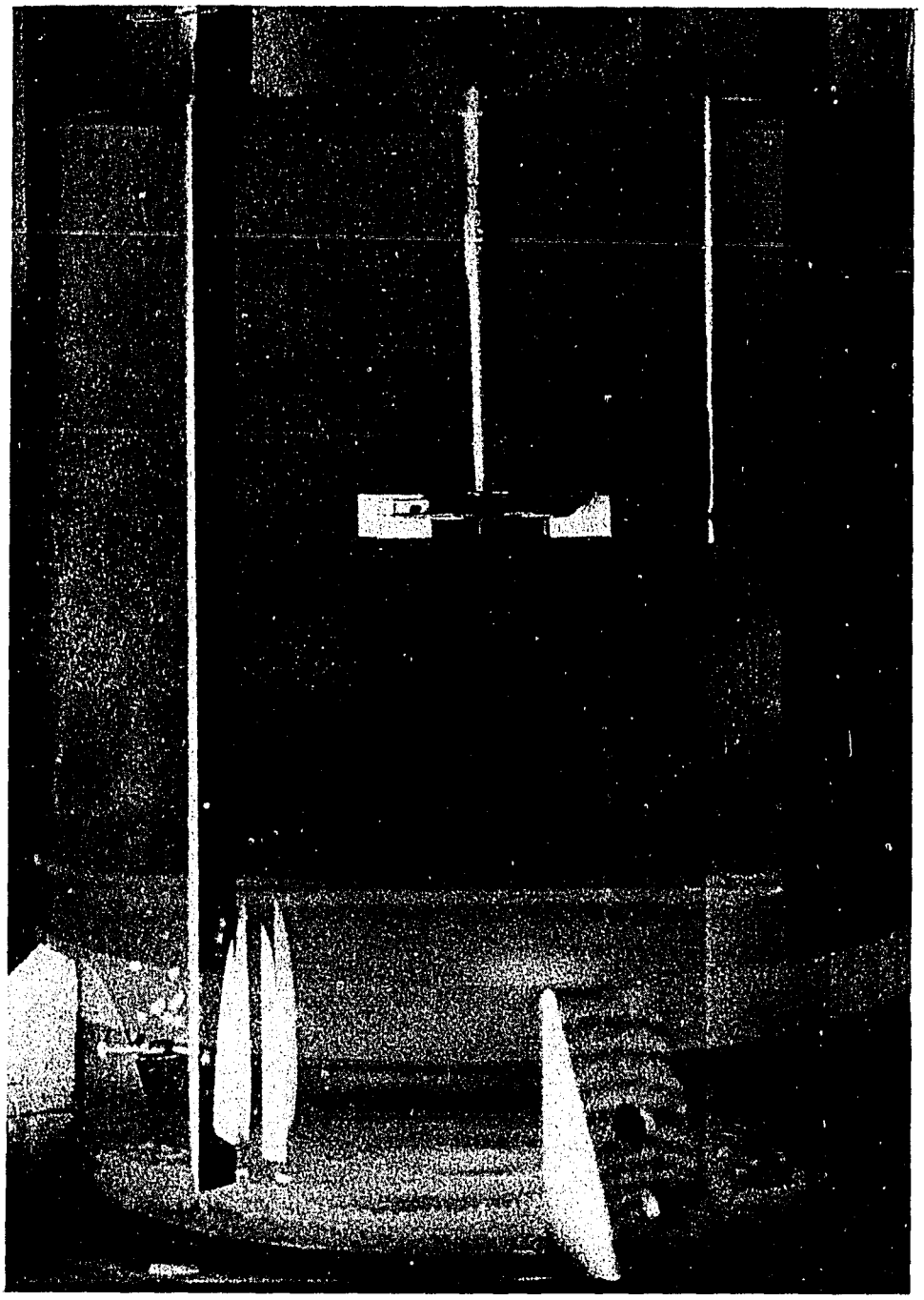

Figure III-5

Close-up Showing Impeller and Probe Tip

3.3. Velocity Measuring Probe and Probe Assembly

Velocities in the neighborhood of the impeller were measured with a three dimensional probe Model DA 187 made by United Sensor Corporation, Watertown, Massachusetts. The probe consists of a 3/16 in. tube ending in a 1/8 in. measuring tip. In the 1/8 in. diameter measuring section of the tube is a prism shaped section in which five pressure taps are located. The probe and the prism shaped section is shown in Figure III-6. Three of the pressure taps P_1, P_4, and P_5 are located in the same plane, but P_4 and P_5 are located in a slight overhang above and below P_1. The prism face on which P_1 is located is so fashioned that the tap P_1 does not move when the probe is rotated. Individual connections are made from each tap to five nipples located at the top of the probe. The nipples are labeled P_1, P_2, etc.

The pressure is measured by four manometers and the manometer connections are shown in Figure III-7. All connections are made through 1/4 in. polystyrene tubing with Swedgelock fittings. The manometers used are Merriam Instrument Company, Model 10AA25WM, 50 in. range manometers.

The probe mounting assembly consists of a slotted arm that rotates in a bearing about the tube mounted in the tank cover. On the slotted arm is mounted a vernier stand. The probe fits into a vernier protractor mounted on the stand. The entire assembly permits the following movements.

1. Rotating the slotted arm allows measurements in any desired radial plane.

2. The vernier stand slides in the slot of the slotted arm,

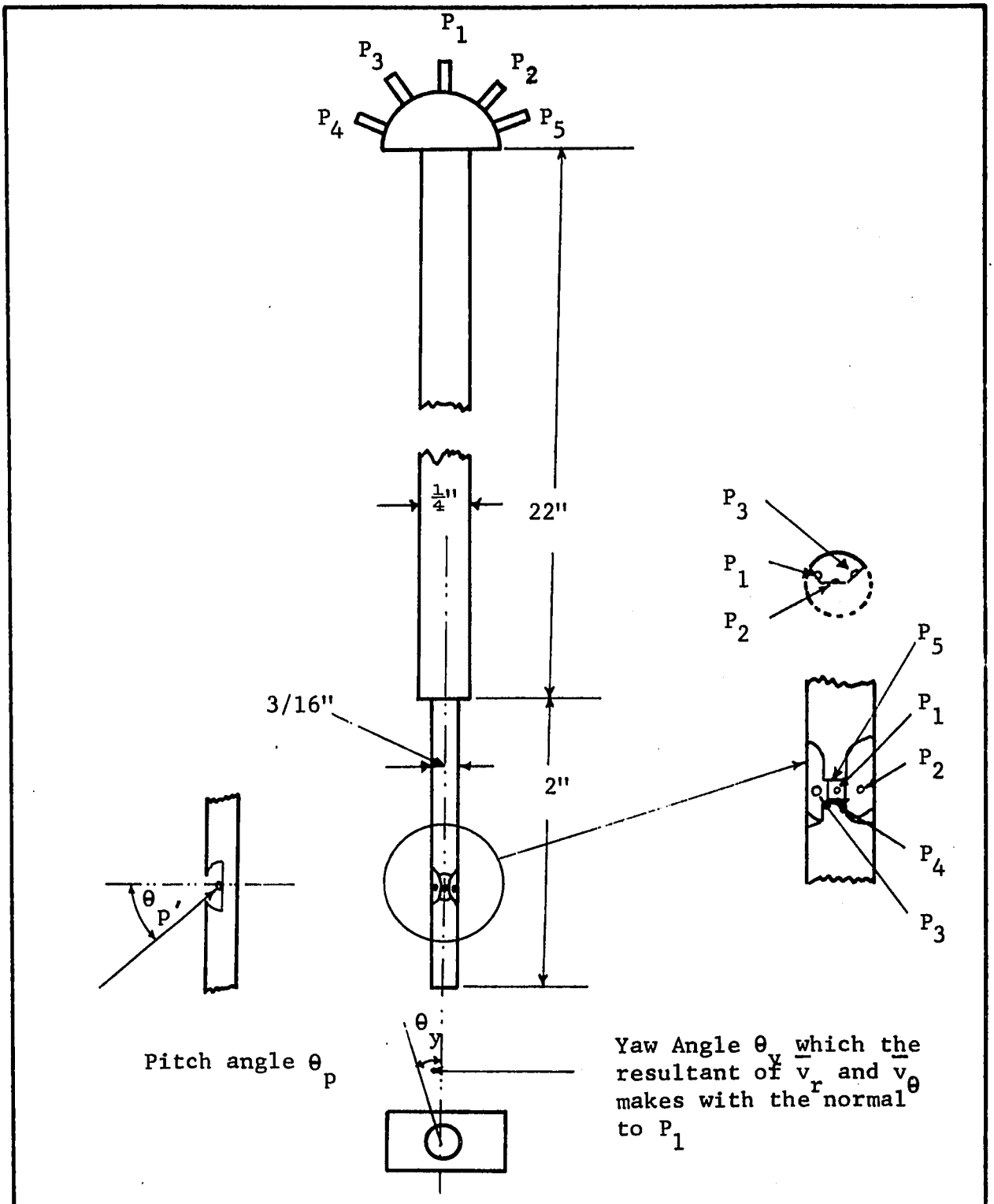

Figure III-6. Details of Three Dimensional Pitot Tube.

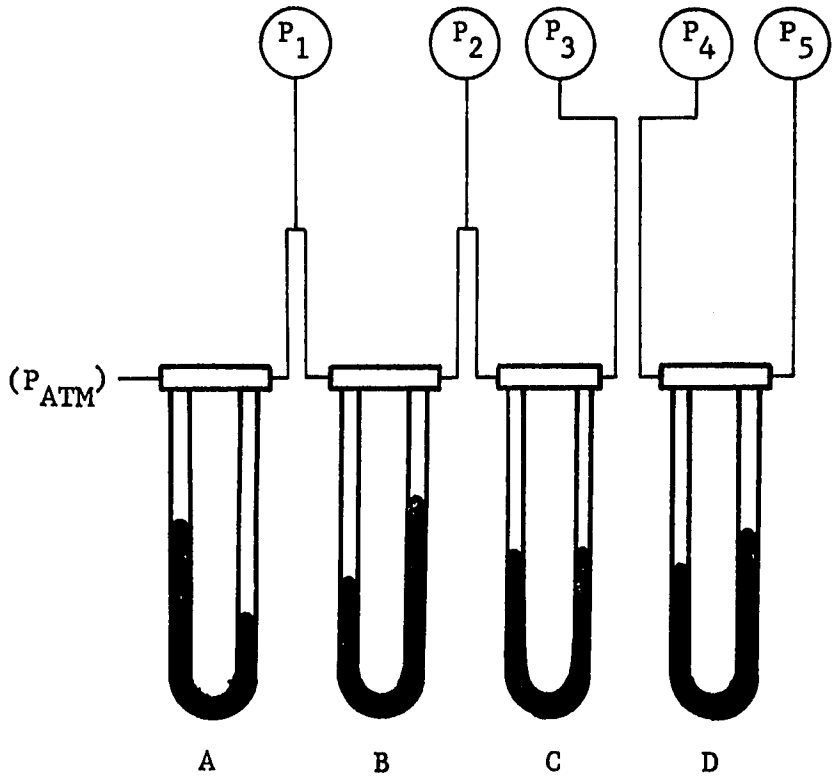

Figure III-7. Manometer Connections to Three-Dimensional Pitot Tubes.

thus allowing the probe to be placed at any desired radius in a given r-z plane.

3. The vernier stand permits locating the pressure tap P_1 at any desired level z from some reference level. This reference level is the impeller centerline where z is taken as zero. The vernier permits measurements to within 0.01 inch.

4. The vernier protractor is used to measure rotation of the probe and is accurate to 0.2 of a degree. This permits measurements of the yaw angle, θ_y, shown in Figure III-6. To obtain $\theta_y = 0$, the pressure tap P_1 is aligned with the center of the impeller by using the impeller blades as guides.

3.4. Measurement of Velocities

The probe is set for measurement by first fixing the slide arm in the desired radial plane. Two radial planes were selected for making measurements. These were 5.5° and 44.1°, the angles being measured relative to a baffle as shown in Figure III-1. The pressure tap P_1 is placed at the desired r,z coordinates by suitable movement of the stand and the probe (motions 2 and 3 of Section 3.3). The probe is now ready for making measurements.

In order to understand how the probe is used to measure the velocity, consider Figure III-6 in which the details of probe measuring section is shown. The pressure taps P_2 and P_3 are in the same plane as P_1 located on prism faces on either side of P_1. From the manometer connections shown in Figure III-7, it is seen that the taps P_2 and P_3 are connected to manometer C. If the probe is rotated such that manometer C is balanced, then the fluid velocity is affecting the pressure taps P_2 and P_3 equally and the normal to the

pressure tap P_1 is identical with the direction of the fluid velocity. Manometer B which is connected between P_1 and P_2 will thus act as a Pitot tube with P_2 and P_3 being the static tap and P_1, the dynamic tap, this differential pressure is measured by manometer B and referred to as P_1-P_2. In case of two dimensional flow field with probe vertical and $\bar{v}_z = 0$, P_1-P_2 measures the dynamic head due to the resultant velocity $\bar{q}$ (resultant of $\bar{v}_r$ and $\bar{v}_\theta$). In case of three dimensional flows the dynamic head does not give $\bar{q}$ since it is affected by $\bar{v}_z$. In this case the pressure tap P_3 and P_4 connected to manometer D will register a pressure drop, P_4-P_5. A manufacturers calibration chart relates the ratio $(P_4-P_5)/(P_1-P_2)$ with $\theta_p = \pm 40°$. Another calibration curve relates θ_p to the dimensionless pressure ration $(P_t-P_s)/(P_1-P_2)$. (P_t-P_s) is the true dynamic head due to the resultant velocity $\vec{V}$ whose components are $\bar{v}_r$, $\bar{v}_\theta$ and $\bar{v}_z$. From (P_t-P_s), $\vec{V}$ can be calculated. Knowing θ_y, θ_p and the geometry of the flow field the component velocities can be calculated. Since the flow field geometry varies, the details of each individual case is worked out, as needed in Chapter IV.

3.5. Manometers

From the manometer connections shown in Figure III-7 and the discussion in sections 3.3 and 3.4 the following conclusion can be drawn.

1. Manometer A is for measuring stagnation or total pressure at pressure tap P_1.

2. Manometer B measures the resultant of the component velocities $\bar{v}_r$ and $\bar{v}_\theta$ which is $\vec{q}$ for two dimensional flows in the r, θ plane. For three dimensional flows the manufacturers calibration

charts must be used.

3. Manometer C is used to locate the yaw angle θ_y, which is shown in Figure III-6. This is done by rotating the probe until manometer C is balanced. The protractor attached to the probe then gives the yaw angle θ_y. When manometer C is balanced manometer B measures $\vec{q}$ exactly in two dimensional flow fields and the yaw angle is used to determine $\overline{v}_r$ and $\overline{v}_\theta$.

4. Manometer D evaluates the pitch angle θ_p from the probe manufactures calibration curve, as explained in section 3.4.

The manometer fluid used is Merriam No. 3 of specific gravity 2.95 in manometer A. In Manometers B and C, Merriam No. D-7878 fluid was used having a specific gravity of 1.2. At first, in manometers B and C, α - chloronapthalene having a specific gravity of 1.2 was used. α-chloronapthalene is a colorless fluid, hence a dye, sudan brown of unknown origin, was used to colour it. Merriam Fluid No. D-7878 has a similar smell as α - chloronapthalene and appears identical. The additives in the Merriam fluid make it a better manometer fluid hence it was used in all but the first runs. In manometer D, the pressure drops were found to be very small hence a mixture of 90% α - chloronapthalene and 10% n-hexane was used, giving a resultant mixture of specific gravity 1.09 which was found to be satisfactory.

The densities of the manometer fluid was obtained by first filling a clean dry manometer with manometer fluid to the desired level. Water was then poured into one arm. The ratio of the column of manometer fluid that is balanced by the column of water then gives the manometer fluid density. The column of manometer fluid was

kept larger than 10 in. since at lower values the density obtained was not consistent. At least five readings were taken for each fluid. A t-test was used to obtain the 0.95 confidence limit on the average. The results are:

1. Density of fluid in manometer A = 2.93 $\pm$ 0.0014
2. Density of fluid in manometer B = 1.1957 $\pm$ 0.00000622
3. Density of fluid in manometer D = 1.0953 $\pm$ 0.00000588

Manometer C used the same fluid as manometer B. To interpret the manometer readings obtained by manometer D consider Figure III-8, in which is shown the pressure connections of pressure taps P_4 and P_5 of the probe connected to manometer D. Taking a force balance about plane A, the level of the manometer fluid in the right hand arm of manometer D, gives

$$\rho_m \Delta H_m + \rho_w h_a + P_4 = P_5 + \rho_w h_b + \rho_w \Delta H_w \qquad \text{III-1}$$

In equation III-1, ρ_m and ρ_w are the densities of the manometer fluid and water. ΔH_m, h_a, h_b are the heights above plane A as shown in Figure III-8. Rearranging III-1 to evaluate P_4-P_5 gives

$$P_4 - P_5 = \rho_w(h_a - h_b) - \Delta H_m(\rho_m - \rho_w) \qquad \text{III-2}$$

Equation III-2 gives the pressure drop $P_4 - P_5$ in terms of the manometer differential ΔH_m and the distance between the pressure taps in the probe $h_a - h_b$. ΔH_{21} is the manometer reading of manometer B, it is related to velocity by the Pitot tube equation (44), which is

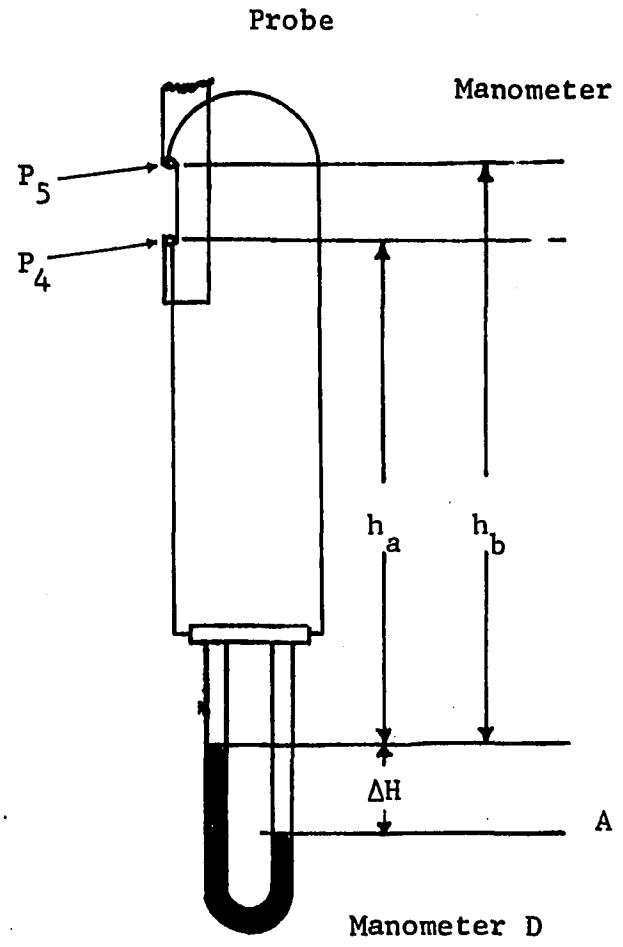

Figure III-8. Pressure Measurement of Pressure Taps P_4 and P_5 in High Shear Flows.

given by

$$\bar{q} = \left(2g\Delta H_{21}\left(\frac{\rho_m - \rho_w}{\rho_w}\right)\right)^{1/2} \qquad \text{III-3}$$

Equations III-2 and III-3 are used to calculate the pressure drops and velocity in Chapter IV.

3.6. Measurement of the Impeller Speed

The impeller speed was measured by a Strobotac made by a General Radio Company, Cambridge, Massachusetts. The instrument normally reads in the speed range of 600 to 14,500 RPM. This speed range is not in the range of speeds used in this work. However, as the impeller has six-fold symmetry the impeller could be stopped at six times its actual speed thus permitting use of this instrument. The strobotac was found very useful in checking speeds above 300 RPM, in which range of speeds the drive was observed to wander by $\pm$ 10 RPM. Hence, before recording a measurement the speed was checked and also at frequent intervals to insure that the RPM was maintained at the desired value.

3.7. Problems Encountered

In order to prevent air bubbles from being entrapped in manometer connections it was found necessary to raise the tank such that the level of fluid in the tank was above the top of the manometers. This can be seen in the photograph of the overall equipment shown in Figure III-2. It was also found convenient to install stop cocks on the manometer heads which helped in bleeding out entrapped air.

The manometers had to be cleaned frequently due to rust deposits from the cast iron manometer heads. This was prevented by coating the manometer heads with an epoxy paint. The tank cover was also painted with epoxy paint to prevent rusting and thus contaminating the distilled water in the tank.

The vessel was found to move with the torque generated by the impeller and to prevent this it had to be fixed firmly by four wooden blocks which are visible in Figure III-4. Since the tank was fixed the drive had to be made movable so as to vary the depth of the impeller in the tank. This was accomplished by mounting the drive on a pipe which was in turn mounted in an angle iron cage. Some residual vibration due to small misalignments in mounting the impeller shaft still remained. The vibrations when severe were observed to be transferred to the probe causing the measuring end of the probe to vibrate and hence move a considerable amount. Severe vibrations are thus undesirable and steps were taken to keep the vibrations a minimum.

3.8. Summary

In this chapter the experimental apparatus is described. Details of the three dimensional pitot tube probe used for measuring velocities in the tank were presented. Finally some observations on the problems involved in making the entire experimental set up work was also discussed.

CHAPTER IV

DISCUSSION AND ANALYSIS OF RESULTS

In Chapter II, the stirred tank was divided into several regions and a model was developed to describe the flow field in these regions. It will be recalled, that the computer solutions developed to draw the velocity profiles required several parameters to be specified. In this chapter the experimental data will be analysed to obtain these parameters. The mathematical models will also be examined to evaluate how good they predict the experimental data.

The experimental data is divided into two parts, that taken in the vicinity of the impeller and that in the rest of the tank. Following this, a detailed analysis of the experimental profiles will then be examined and a comparison made between this work and the results of investigators reviewed in Chapter I. The results of this comparison show that the tangential model gave a good prediction of the velocity profiles in the vicinity of the impeller.

The tangential jet model has four parameters, these are σ the jet width, A the volumetric flow parameter a, the radius of source; and z_o, the jet displacement. It will be shown that σ the jet width parameter is a constant, independent of tank diameter, impeller speed, the fluid used, and within limits the impeller location. The last observation is based on the fact that the jet width was found to be a constant resulting in a narrow stream of maximum width equal to 0.16T.

Within limits this width is constant independent of the height of the impeller above the tank bottom. The width of the jet was also found to be independent of impeller diameter for geometrically similar impellers.

The volumetric flow parameter A was found to be dependent on tank diameter; the best correlation for A was with $ND^3/((D/2)^2-a^2)^{\frac{1}{4}}$. The impeller discharge Q, was however found to be a function of ND^3 and independent of tank diameter or the fluid in the tank.

The radius of source, a, was found to be dependent on both tank diameter and impeller diameter. Finally the jet displacement showed no trend and its only purpose is to shift the theoretical profile so that a better fit is obtained. It does not affect the properties of the jet since the velocity profile which determine these properties is symmetrical, and the shape of the profile is not altered by varying z_o.

4.1. Velocity Profiles in the Region of the Impeller

The three dimensional pitot tube described in Chapter III was used to measure velocity profiles under different conditions to establish the validity of the tangential jet model. Velocity profile measurements were made with a 3.0 in diameter, type A impeller at two different impeller depths h, these are; (a) with impeller placed one impeller diameter off the bottom of the tank, which is the minimum recommended in the literature and (b) with the impeller centrally located. Two different radial planes were selected, one close to the baffle (5.5°) and the other in between baffles 44.1°.

These angular measurements are referred to as radial angles and are measured with respect to a baffle as shown in Figure III-1. Four different radial distances r were selected to evaluate the effect of this parameter on the jet profile.

Analysis of Velocity Profiles

A program FLOWANL was written to analyzed velocity profiles measured in the neighborhood of the impeller. Each velocity profile consists of a series of measurements of $\vec{q}$, the resultant of $\bar{v}_r$ and $\bar{v}_\theta$, as a function of z at constant r. These measurements are a result of making a vertical pass with the probe across the impeller stream. The number of data points in a profile depends on the thickness of the impeller stream. The closer the probe is to the impeller periphery the smaller the width of the stream resulting in a fewer number of data points since each data point is taken at a minimum spacing of 0.1 in. apart.

The analysis consists of evaluating the best values for the parameters in the tangential jet model so as to predict the experimentally determined velocity profiles. The correlation coefficient R is used to measure the goodness of fit and is defined by

$$R^2 = 1 - \frac{\Sigma(\vec{q}_{exp} - \vec{q}_{model})^2}{\Sigma(\vec{q}_{exp} - (\vec{q}_{exp})_{avg})^2} \qquad \text{(IV-1)}$$

In Equation IV-1, the numerator of the second term on the right is the sum of squares of deviation between the experimental velocity $\bar{q}_{exp}$

and the velocity predicted by the model $\bar{q}_{model}$. As this term is referred to frequently in the text it is called sum of squares SS and is identical to Equation C-2 of Appendix C. The denominator of the second term on the right of Equation IV-1 is the sum of squares of the deviation of $\bar{q}_{exp}$ from its average value $(\bar{q}_{exp})_{avg}$. For perfect agreement the deviation between the experimental value and the model given by SS will tend to zero and R will tend to one. In the case of a poor agreement or no agreement, the second term on the right of Equation IV-1 will tend to one, and R will thus tend to zero. In the present work, R values of 0.98 to 0.99 have been obtained indicating that the deviation of $\bar{q}_{exp}$ from the model is small and the prediction by the model is hence very good.

Of the four parameters σ, A, a and z_o that describe the tangential jet, three are obtained by a nonlinear least square fit. These are σ the jet width, A the volumetric flow and z_o the jet displacement. The fourth parameter, a, is obtained by a weighted average value of the yaw angle profile as explained in the next section.

The nonlinear least square fit uses Pattern Search to minimize the sum of squares SS resulting in a maximum value for R and thus the best possible fit of the data. Pattern Search is a procedure that perturbs the parameters a small amount, such that each small change in the parameters results in a reduction in the sum of square SS, eventually leading to maximum value of R. A theoretical discussion of Pattern Search and the subroutine PATERN that was written to

perform this search procedure is given in Appendix C. In future discussions a least square fit will refer to above procedure using Pattern Search.

In all, 39 velocity profiles were measured under varying conditions, summarized in Table IV-1. A detailed analysis of a velocity profile is given in Section 4.4. The analysis gives four pages of computer printout for each profile. This amount of information is needed to examine and evaluate a profile analysis in detail as done in Section 4.4. From this detail analysis seventeen items were considered as important factors that determine the character of the analysis. These are presented in tables and reported in Appendix A. In subsequent sections, pertinent information will be taken from Appendix G to support observations and conclusions that result from this velocity profile analysis.

Radius of Source Parameter a

It will be recalled from Chapter I That the velocity profile stream exhibited an angle profile (θ_y as a function of z), and this was first observed by Cooper (8). The tangential jet model on the other hand which is used in this work to predict the experimental data predicts a constant angle profile. This inconsistency was resolved by using an average angle for θ_y. Several averaging schemes were tried, the most successful was the weighted average θ_y, the weights being the velocity and is defined by,

$$\bar{\theta}_y = \frac{\Sigma \bar{q}_i (\theta_y)_i}{\Sigma \bar{q}_i} \qquad \text{(IV-2)}$$

TABLE IV-1

CONDITIONS UNDER WHICH VELOCITY PROFILES WERE MEASURED

Impeller Speed RPM	Tank Diameter T Inch	Height of Impeller Above Tank Bottom, h, in.	Radial Angle Degrees	Radial Distance r, in.	Table Number*
243	12.25	3.0	5.5	2.5	G-2
				3.0	and
				3.5	G-3
				4.0	
			44.1	2.5	
				3.0	
				3.5	
				4.0	
250		6.0	5.5	2.5	G-4
				3.0	and
			44.1	2.5	G-5
				3.0	
333.3		6.0	5.5	2.5	G-6
				3.0	and
			44.1	2.5	G-7
				3.0	
400		6.0	5.5	2.5	G-8
				3.0	and
			44.1	2.5	G-9
				3.0	
500		3.0	5.5	2.5	G-10
				3.0	and
			44.1	2.5	G-11
				3.0	
		6.0	5.5	2.5	
				3.0	
				3.5	
				4.0	
			44.1	2.5	
				3.0	
				3.5	
				4.0	
550		6.0	5.5	3.0	G-12
			44.1	3.0	G-13

TABLE IV-1 CONTINUED

Impeller Speed RPM	Tank Diameter T Inch	Height of Impeller Above Tank Bottom, h, in.	Radial Angle Degrees	Radial Distance r, in.	Table Number*
333.3	11.5	6.0	5.5	2.5	G-14
				3.0	and
			44.1	2.5	G-15
				3.0	

*Corresponds to table numbers in Appendix G where a summary of the detailed analysis at constant impeller speed is given.

The yaw angle θ_y determines the direction of the velocity vector $\vec{q}$ and is a function of r and the radius of source, a. This follows from Equation A-14 which gives θ_y as

$$\cos \theta_y = \left(\frac{r^2 - a^2}{r^2} \right)^{\frac{1}{2}} \qquad \text{(A-14)}$$

The value of, a, can now be determined from A-14 by using $(\bar{\theta}_y)$ for the yaw angle θ_y. In order to have some flexibility in selecting a, the radius of source, a velocity factor WT is defined as

$$WT = \frac{\bar{q}_i}{q_{max}} \qquad \text{(IV-3)}$$

In Equation IV-3 $\bar{q}_i$ is the velocity below which the angle profile is truncated in calculating the weighted average angle $\bar{\theta}_y$ from Equation IV-2. This is illustrated in Figure IV-1 (b) which is a rectangular plot of $\bar{q}$ versus θ_y for Run Number 29. It is seen that the angle profile is symmetrical above and below the impeller. $\bar{q}_i$ was calculated from Equation IV-3 as 66.2 ft/min for Run Number 29, with WT equal to 0.5 and q_{max} equal to 132.3 ft/min. A line is thus drawn through this point as shown in Figure IV-1 (b). In calculating $\bar{\theta}_y$ from Equation IV-2 only experimental points located above this line, indicated by the arrow, are used. Increasing WT raises the line reducing the number of points used for evaluating θ_y. The converse occurs when WT is lowered.

In Figure IV-1 (a) is shown a polar plot of $\bar{q}$ versus θ_y. The angle profile for the range of velocities measured lie in a narrow

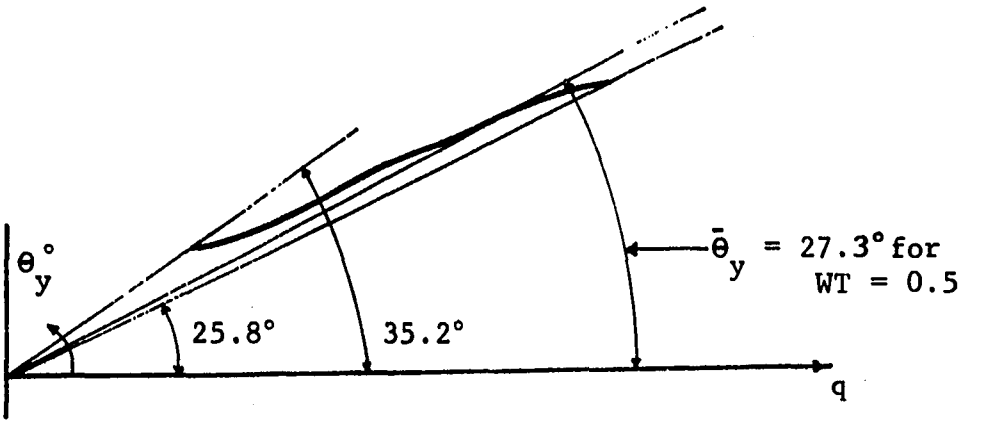

(a) Angle profile in Polar Coordinate

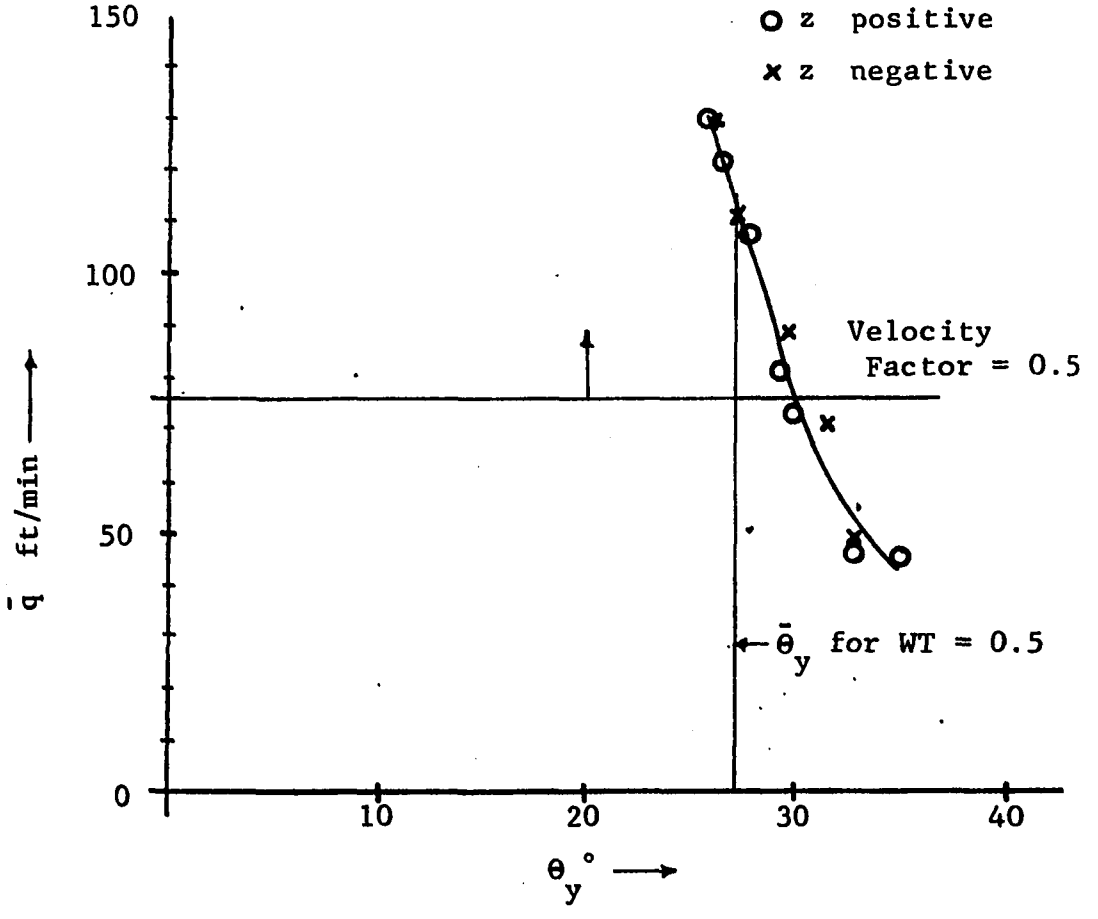

(b) Angle Profile in Rectangular Coordinates.

Figure IV-1: Angle Profile for Run Number 29, Illustrating the Definition of Velocity Factor

band of 10°, and is typical of the velocity profiles measured in this work. Also shown in the diagram is $\bar{\theta}_y$ the weighted average angle for WT equal to 0.5. $\bar{\theta}_y$ is seen to lie closer to θ_y corresponding to $\bar{q}_{max}$ and is a result of the weights being larger at the center, than at the ends of the velocity profile. $\bar{\theta}_y$ was found to increase with increasing .

Various values of the velocity factor were tried and WT equal to 0.5 was found to give the best prediction of the velocity profile in all cases. This is illustrated in Table IV-2 which shown four velocity profiles measured at constant impeller speed of 333.3 RPM and varying radial distance and radial angle. Three different velocity factors are selected and these are 0.6, 0.5 and 0.4.

Table IV-2 shows the effect of the velocity factor WT on the sum of square SS and the correlation coefficient R for both $\vec{q}$ and $\bar{v}_r$. Equations similar to C-2 and IV-1 can be written to define SS and R for $\bar{v}_r$. The velocity profile for $\bar{v}_r$ is obtained from Equation A-20 which is

$$\bar{v}_r = |\vec{q}| \cos \theta_y \qquad \text{(A-20)}$$

The need for examining SS and R for $\bar{v}_r$ in Table IV-2 is because $\bar{v}_r$ determines the pumping capacity and it is desirable that this quantity be also predicted as accurately as possible.

Examining Table IV-2 it is seen that the velocity factor WT has very little effect on SS for $\bar{q}$, for a given profile. For example, Profile Number 1 has a constant value of SS equal to 1167.41 for $\bar{q}$.

TABLE IV-2

EFFECT OF VELOCITY FACTOR ON LEAST SQUARE FIT OF A VELOCITY PROFILE FOR A 3.0 INCH DIAMETER IMPELLER AT 333.3 RPM IN A 12.25 INCH DIAMETER TANK

Profile Number	Radial Angle	Radial Distance r Inch	Sum of Squares SS		Correlation Coefficient R	
			$\vec{q}$	$\bar{v}_r$	$\vec{q}$	$\bar{v}_r$
(a) Velocity Factor = 0.6						
1	44.1	2.5	1167.41	1044.30	0.9782	0.9756
2	5.5	2.5	2155.45	1512.04	0.9669	0.9701
3	44.1	3.0	123.27	126.96	0.9935	0.9925
4	5.5	3.0	235.64	215.69	0.9919	0.9915
(b) Velocity factor = 0.5						
1	44.1	2.5	1167.41	1030.68	0.9782	0.9759
2	5.5	2.5	2155.45	1512.04	0.9669	0.9701
3	44.1	3.0	123.27	126.96	0.9935	0.9925
4	5.5	3.0	235.63	214.30	0.9919	0.9915
(c) Velocity factor = 0.4						
1	44.1	2.5	1167.41	1021.85	0.9782	0.9761
2	5.5	2.5	2155.45	1499.11	0.9669	0.9703
3	44.1	3.0	123.26	128.95	0.9935	0.9924
4	5.5	3.0	235.63	214.08	0.9919	0.9915

Small changes are seen in the sum of squares for $\bar{v}_r$. In general decreasing the velocity factor decreases the sum squares for $\bar{v}_r$ and increases the magnitude of the weighted average angle $\bar{\theta}_y$. In one profile (not shown in Table IV-2) $\bar{\theta}_y$ was increased to where it gave a value of a, the radius of source, just larger than the impeller radius. From Table IV-2 it is seen that the difference in sum squares for $\bar{v}_r$ between velocity factors of 0.5 and 0.4 are not very large. In some cases (for example Profile Number 3) the sum square is smaller with a velocity factor of 0.5. The trends noted above apply to all the profiles investigated, hence a velocity factor of 0.5 was chosen for all the profiles. The summary of results reported in Appendix G are based on this value of velocity factor.

In Table IV-2, the correlation coefficient reported for $\bar{v}_r$ of Profile Number 2 is slightly larger than that of $\vec{q}$. This is an exceptional case. In the majority of profiles it was found that the correlation coefficient was of the order of 0.98 to 0.99 for $\vec{q}$. The correlation coefficient for $\bar{v}_r$ was found to be slightly lower than that of $\vec{q}$ but very close as shown in Table IV-2.

Effect of Impeller Depth, Radial Angle, and Radial Distance on Tangential Jet Parameters

The tank geometry is an important consideration in the design of stirred tanks. With a veiw of finding the most important variables the impeller depth, radial angle and radial distance were varied at constant impeller speed. The impeller depth, h, is defined in this

work as the distanc h from the tank bottom to the impeller centerline. Two values of h were chosen; the impeller centrally located, h = 6.0 inches and the impeller at maximum depth of one impeller diameter off the tank bottom recommended in the literature, h = 3.0 inches.

Velocity profile measurements were made in two radial planes at radial angles of 5.5° and 44.5°. The angles are measured with respect to a baffle as shown in Figure III-1. These measurements were made to test the assumption of angular symmetry.

At fixed impeller depth and radial angle, velocity profile measurements were made at four different radial distance r from the impeller axis. The purpose of these measurements was to explore the radial distance to which the tangential jet model was valid.

In Table IV-3 are shown values of the tangential jet parameters σ, A and a for varying h, radial angle and radial distance r. Profiles 3, 4, 7 and 8 are measured at h = 6.0 in. The rest of the profiles are measured at h = 3.0 in. Table IV-3 is extracted from Table G-1; the radius of source, a is evaluated with a velocity factor of 0.5.

The volumetric parameter, A, and the radius of source parameter, a, show very little variation in Table IV-3 indicating that at constant RPM. These two parameters are not affected by varying h, r, or radial angle. This is more closely brought out when the average value variance and confidence limit of A for the twelve profiles is

TABLE IV-3

EFFECT OF IMPELLER DEPTH, RADIAL ANGLE, AND RADIAL DISTANCE ON TANGENTIAL JET PARAMETERS AT IMPELLER SPEED OF 500 RPM

Profile No.	h in.	Radial Angle Deg.	Radial Distance r, in.	σ	A	a
1	3.0	44.1	2.5	12.2	27.4	0.116
2		5.5		11.9	27.4	0.119
3	6.0	44.1		14.3	27.3	0.117
4		5.5		13.5	29.7	0.119
5	3.0	44.1	3.0	11.2	27.7	0.114
6		5.5		10.9	27.7	0.117
7	6.0	44.1		11.3	28.9	0.104
8		5.5		10.9	29.3	0.112
9	3.0	44.1	3.5	10.3	28.6	0.106
10		5.5		10.5	28.3	0.110
11		44.1	4.0	9.7	29.2	0.097
12		5.5		9.8	29.3	0.110

	Average	Variance	Confidence Limit
σ	11.4	1.98	$\pm$ 0.9
A	28.4	0.75	$\pm$ 0.6
a	0.112	0.00004	$\pm$ 0.004

examined at the bottom of Table IV-3. It is seen that both the variance and confidence limit are small indicating the low scatter or deviation of A about its mean value.

The variance S_x^2 reported at the bottom of Table IV-3 is defined by

$$S_x^2 = \frac{1}{N-1} \sum_{i=1}^{n} (x_i - \bar{x})^2 \qquad \text{(IV-4)}$$

where $\bar{x}$ is the average value of x. The confidence limit, DEVIATION, is calculated from the following equation:

$$\text{DEVIATION} = t_{0.95,N-1} S_{\bar{x}}^2 \qquad \text{(IV-5)}$$

where $t_{0.95,N-1}$ is obtained from a t-table at a 95% confidence level and N-1 degrees of freedom. $S_{\bar{x}}^2$ in IV-5 is the standard deviation on the mean and is given by

$$S_{\bar{x}}^2 = S_x^2/N \qquad \text{(IV-6)}$$

Table IV-3 also shows that, a, the radius of source is a constant equal to 0.112 ± 0.004 having a small value of variance and confidence limit.

The jet width σ in Table IV-3 has a high value for Profile Numbers 3 and 4 and a low value for Profile Numbers 11 and 12. The rest of the profiles are within the confidence limit of the average given as 11.4 ± 0.9 at the bottom of Table IV-3. It will be shown later that Profile Numbers 11 and 12 were taken at an r value close to r_o the limit of the tangential jet region. These two profiles

could hence be considered as not representative of the tangential jet region, and the low values of σ obtained could be the result of interference caused by the proximity of the stagnation flow region that follows the tangential jet. The high value of σ in Profile Number 3 and 4 could be due to the effect of h on the velocity profile. In general the velocity profiles gave a slightly higher value of σ for smaller values of r and this trend is clearly noticed in Table IV-3 . A case for σ being considered a constant is plausible although from Table IV-3 this conclusion is not as clear as in the case of A and a.

From the tangential jet model we have that the dimensionless velocity profile η is given by

$$\eta = \sigma \frac{z}{r} \qquad \text{(B-2)}$$

At constant r from B-2 it is seen that σ is scale factor on z, hence the name jet width parameter for σ. If σ is constant it follows that the width of the jet is a constant. If the width of the jet is constant then within limits it appears that it should not be affected by varying h.

To test this assumption the impeller speed was reduced by approximately half to 243 RPM and h was kept at its minimum value of one impeller diameter (3.0 in.). The resulting values of σ, A and a, are shown in Table IV-4. It is seen in Table IV-4 that A and a are constant given by 13.5 ± 0.2 and 0.114 ± 0.004 respectively. In Table IV-4, Profile Numbers 8 and 9 for r equal to 4 show a low

TABLE IV-4

EFFECT OF RADIAL DISTANCE ON TANGENTIAL JET PARAMETERS

FOR A 3.0 IN. IMPELLER AT 243 RPM AND IMPELLER DEPTH OF 3.0 IN.

Profile No.	Radial Angle Deg.	Radial Distance r in.	σ	A	a
1	44.1	2.5	11.5	13.5	0.114
2	44.1		11.6	13.3	0.116
3	5.5		11.1	13.4	0.112
4	44.1	3.0	10.8	13.0	0.115
5	5.5		10.5	13.4	0.120
6	44.1	3.5	10.4	13.4	0.107
7	5.5		10.3	13.5	0.116
8	44.1	4.0	8.7	14.0	0.103
9	5.5	4.0	9.7	13.9	0.115

	Average	Variance	Confidence Limit
σ	10.5	0.839	0.7
A	13.5	0.093	0.2
a	0.114	0.00003	0.004

for σ indicating that this point is close to the stagnation region. As in the case of Table IV-3 for small r, σ is found to be larger in magnitude. The average value of σ in Table IV-4 is seen to be within the confidence limit of σ reported in Table IV-3. It is thus concluded that an argument for σ being a constant exists. Since h has been varied in the profiles investigated in Tables IV-3 and IV-4 without significant effect on the jet parameters it was concluded that the impeller depth h had no effect and hence in subsequent runs the impeller was centerally located with h equal to 6.0 inches.

It is thus concluded that the tangential jet parameters are a function of impeller speed. In order to get a reasonable estimate of an average value, four profiles were taken at constant impeller speed. The four profiles were taken at two radial angles, 5.5° and 44.1° and two values of r, 2.5 in. and 3.0 in. Larger values of r were not selected since as noted above the value of σ was noticed to fall markedly being influenced by the flow in the next region. The summary of the analysis of these velocity profiles are given in Appendix G. Tables IV-5 to IV-7 give the average values of σ, A and a at varying impeller speeds and are obtained from Appendix G. Item 1-6 in these tables are taken in a 12.25 in. diameter tank, while Item 7 is taken in a 11.5 diameter tank.

Effect of Impeller Speed on Tangential Jet Parameter

The observations made and conclusions drawn for the tangential jet parameters obtained from profile measurements taken at constant

TABLE IV-5

AVERAGE VALUE OF JET WIDTH PARAMETER σ FOR

A 3.0 INCH DIAMETER IMPELLER

Item Number	Impeller Speed (RPM)	Average Value of σ	Variance	Confidence Limit	Number of Profiles
1	243	10.5	0.838	0.7	9
2	250	10.0	2.750	2.6	4
3	333.3	11.8	0.448	1.1	4
4	400	11.8	0.719	1.3	4
5	500	11.4	1.982	0.9	12
6	550.	11.6	0.064	2.3	2
7*	333.3	10.7	0.773	1.4	4

Tank diameter = 11.5 inches

TABLE IV-6

AVERAGE VALUE OF VOLUMETRIC FLOW PARAMETER

A, FOR A 3.0 IN. DIAMETER IMPELLER

Item No.	Impeller Speed RPM	Average Value of A	Variance	Confidence Limit	Number of Profiles
1	243	13.5	0.093	0.2	9
2	250	14.3	0.204	0.7	4
3	333.3	18.6	0.062	0.4	4
4	400	22.7	0.014	0.2	4
5	500	28.4	0.750	0.6	12
6	550	31.6	0.119	3.1	2
7*	333.3	17.9	0.170	0.6	4

*Tank Diameter = 11.5 in.

TABLE IV-7

AVERAGE VALUE OF RADIUS OF SOURCE a FOR A 3.0 INCH DIAMETER IMPELLER IN A 12.5 INCH DIAMETER TANK

Item Number	Impeller Speed	Average Value of a	Variance	Confidence Limit	Number of Profiles
1	243	0.114	0.000029	0.004	9
2	250	0.119	0.000024	0.008	4
3	333.3	0.115	0.000004	0.003	4
4	400	0.117	0.000012	0.005	4
5	500	0.112	0.000045	0.004	12
6	550	0.112	0.0000006	0.007	2
7*	333.3	0.122	0.000001	0.002	4

*Tank diameter = 11.5 inches

impeller speed of 500 and 243 RPM in the previous section are also valid at other impeller speeds. In Table IV-5 is shown the average values, variance and confidence for σ the jet width at different impeller speeds. The average value of σ is seen to fall in a narrow range indicating that σ is independent of impeller speed and tank diameter. The later observation is made from Item 7 of Table IV-5 which is taken in a different tank diameter. The constancy (low scatter) in the average value of σ is misleading since the confidence limit of these average values are rather large. The maximum confidence limit is 2.6 which is about 25% of the magnitude of σ. This means that assuming the model is correct the measurement made by the probe are not as accurate as desirable.

In Table IV-6 is shown the average value, variance and deviation for the volumetric flow parameter A, at varying impeller speed. Both variance and confidence limit are small indicating that the average value is a good estimate of this parameter. The only exception is Item 6 which will be discussed in the next section.

On examining Table IV-7 it is evident that the radius of source, a, is a constant independent of impeller speed but not of tank diameter. For the 12.25 in. diameter tank the average value is 0.115 ± 0.008. The confidence limit is taken as the largest deviation of Items 1 to 6 in Table IV-5. This is because the average value is based on components which are error bound themselves. A t-test taken on the average of the average values will reflect the variation between the averages, but will not account for the error in

in each component. In this case the t-test gave a confidence limit of 0.003 which is smaller than the confidence limits of individual averages reported in Table IV-7.

Effect of High Impeller Speed on Velocity Profiles Measurements

In Table IV-5, the rather large deviation for A shown in Item 6 is due partly because the sample size (number of profiles) is small and partly because the manometer B was observed to fluctuate erratically making it difficult to record the true pressure drop. The amplitude of the fluctuation ranged from 0.5 to as much as 2 cms, the larger value being observed for large ΔH_m. The period of the fluctuations was not fixed and varied in a random manner from 30 seconds to 2 minutes. Since the manometers have high inertia, such large fluctuations indicates that at this high impeller speed the intensity of turbulence is very high, and could be as much as 100%.

At this high speed with the impeller centrally located it was observed that considerable amount of air was entrained. The air remained in the system as large bubbles. The entrainment of air in the system was observed to begin at a little below 500 RPM. The air entrainment is due to the rotating vortex at the surface shown in Figure I-4 (c) and first observed by Nagata (19). It was noticed that the vortex is enhanced by high speed, small tank diameter, and large D/T ratio. However, if the liquid level is increased sufficiently it was observed that the vortex was reduced in strength and air entrainment eliminated. Lowering of the impeller (i.e., decreasing h) would also have the same effect. It is possible that the fluctuations of the manometer may be due to the excessive air entrainment.

The velocity profile data at this impeller speed reported in Appendix G is based on an average value of manometer differential ΔH_m. The average value of ΔH_m being eyed in since it fluctuated in an erratic manner as described above. In spite of these rough estimates of ΔH_m, the parameters are rather close for the two profiles measured as can be seen in Appendix G. This is reflected in a rather low value for the variance of the tangential jet parameters given in Tables IV-5 to IV-7 for Item 6. Two profiles were taken at this speed at two radial angles and r = 3.0. At r = 2.5 in (1.0 in. from impeller periphery), the probe was observed to vibrate excessively due to the large velocity and high intensity of turbulence at that point.

Effect of Tank Diameter

To measure velocity profiles in the rest of the tank, a tank was assembled from plexiglass having a diameter of 11.5 inches. A single impeller speed of 333.3 RPM was investigated to compare the effect of change in tank diameter. As in the other cases four profiles were measured. The results are in agreement with conclusions made earlier, namely that the tangential jet parameters are independent of radial angle and radial distance. The impeller depth was not varied. The results of this analysis is reported in Appendix G and the average value of the jet parameters are reported as Item 7 in Tables IV-5 to IV-7. From Table IV-5 it is seen that σ has the same order of magnitude and confidence limit as in the glass tank. This means that the width of the jet is approximately the

same and hence impeller depth should have no effect on the jet. In Table IV-6 comparing the average value of A at 333.3 RPM for the two tanks (Item Numbers 3 and 7), A is smaller in the smaller diameter tank. The difference in the two values is out of the range of their respective confidence limits and it is thus concluded that the diameter of the tank has an effect on the parameter A and hence the pumping capacity of the impeller. In Table IV-7 it is seen that while the average value of a is almost constant for the glass tank, its value for the plexiglass tank is much larger being very close to the impeller radius of 0.125 ft. It is thus concluded that the diameter of the tank has an effect on a, the radius of source.

Correlation of Tangential Jet Parameters

From Tables IV-5 to IV-7 and the discussion in the previous section the tangential jet parameters can be considered as independent of impeller depth, radial angle and radial distance (r should be less than 4.0 in.). These tables also indicate that the average values at constant impeller speed are good estimates of the parameters. They are a function of impeller speed, impeller diameter and tank diameter.

In Table IV-8, the average values of the parameter from Tables IV-5 to IV-7 are collected, and reported together with other information on the impeller stream. These are Q, the volumetric flow at the impeller periphery, calculated from Equation B-31 with r = D/2 and is given by,

$$Q = 4\pi A \left(\frac{D}{2\sigma}\right)^{\frac{1}{2}} \left((D/2)^2 - a^2\right)^{\frac{1}{2}} \qquad \text{(IV-7)}$$

TABLE IV-8

SUMMARY OF RESULTS OF TANGENTIAL JET PARAMETERS FOR A 3.0 INCH DIAMETER IMPELLER IN A 12.25 INCH DIAMETER TANK

Item Number	σ	A	a	Impeller Speed RPM	Q	Q/ND^3	$\bar{\theta}_y$	ND^3
1	10.5	13.5	0.114	243.0	4.18	1.10	65.8	3.80
2	10.1	14.3	0.119	250.0	3.92	1.00	72.2	3.91
3	11.8	18.6	0.115	333.3	5.28	1.01	67.3	5.21
4	11.8	22.7	0.117	400.0	6.18	0.988	69.3	6.25
5	11.4	28.4	0.112	500.0	8.87	1.14	63.3	7.81
6	11.6	31.6	0.112	550.0	9.81	1.41	63.1	8.59
7*	10.7	17.9	0.122	333.3	4.13	0.79	76.6	5.21

Correlating Equation	Correlation Coefficient R
$A = 3.47(ND^3)^{1.024}$	0.9996
$Q = 0.903(ND^3)^{1.09}$	0.9897
$A = 0.0004(N_{Re})^{1.024}$	0.9996
$Q = 0.0001(N_{Re})^{1.09}$	0.9897

	Average	Confidence Limit
σ	11.2	0.8
a	0.115	0.003
Q/ND^3	1.06	0.07

*Tank diameter 11.5 inches

Also given is the dimensionless pumping capacity $N_Q = Q/ND^3$, and the weighted average yaw angle, $\bar{\theta}_y$ at the impeller periphery. The angle $\bar{\theta}_y$ is calculated by inverting Equation A-14 with r = D/2 and is

$$\bar{\theta}_y = \cos^{-1}\left(\left[(D/2)^2 - r^2\right]^{\frac{1}{2}}/r\right) \qquad \text{(IV-8)}$$

In Figure IV-2 is shown a log-log plot of ND^3 versus σ; ND^3 versus A; and ND^3 versus Q. The best correlation for σ, the jet width parameter is a horizontal straight line drawn at the average value of 11.2 ± 2.6 for all seven points. This is shown in Figure IV-2. The deviation on σ is taken as the same as the largest deviation in Table IV-5 which is Item 2. It should be noted that tank diameter has no effect on σ as seen in Table IV-8.

Figure IV-2 shows that both A and Q correlate very well with ND^3 for the 12.25 in diameter tank. The correlation coefficient R for both these plots is 0.99. Item 7 of Table IV-8 has been plotted in Figure IV-2 as a cross. The deviation of this point from the regression line for A and σ is small showing that they correlate reasonably well. The point for Q shows a large deviation from the regression line indicating that the tank diameter has an effect on Q. The reason for this is that the radius of source parameter a is significantly different as can be seen in Table IV-8.

In Figure IV-2 it is seen that the slopes of A and Q are almost equal. This suggests that A is a scaled value of Q, hence the name volumetric flow parameter. In Table IV-8 is also given the regression

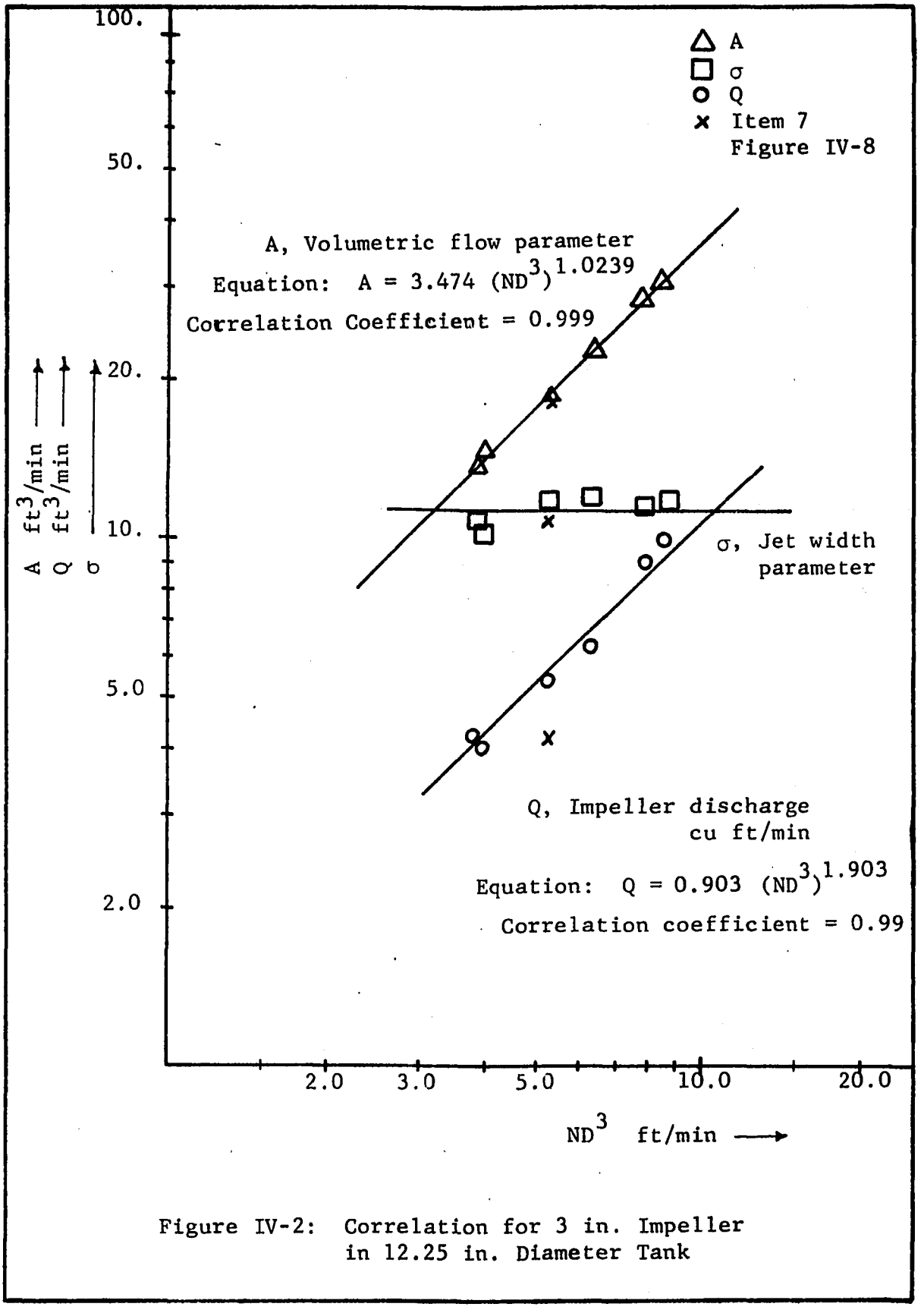

Figure IV-2: Correlation for 3 in. Impeller in 12.25 in. Diameter Tank

equations for the log-log plot. For convenience these are also reported in Figure IV-2. The equations reported in Table IV-8 are for the 12.25 in. diameter tank.

Log-log least square fits of A and Q versus N_{Re} the Reynolds number were also tried. The results for these equations are given in Table IV-8. Since $N_{Re} = ND^2\rho/\mu$ and, ρ and μ are constant for a given fluid, this in effect is a correlation with ND^2. Table IV-8 shows the correlation coefficient for N_{Re} or in effect ND^2, to be the same as for the correlation with ND^3.

In Table IV-8 it is seen that θ_y varies from 63.13° to 72.18° whereas the corresponding values of, a, vary only in the third significant place for the 12.25 in. diameter tank. This indicates the relative insensitivity of the tangential jet model to the angle profile and hence the good prediction of experimental velocity profiles by using a weighted average value of θ_y.

4.2. Effect of Constant Jet Width and Radius of Source on the Analysis

Since a reasonable estimate of σ, the jet width and, a, the radius of the tangential source were found to be overall average values, the entire analysis was repeated keeping σ and a constant at

$$\sigma = 11.2 \pm 2.6 \qquad \text{(IV-9)}$$

$$a = 0.115 \pm 0.008 \qquad \text{(IV-10)}$$

The results of this analysis is also given in Appendix G.

The result of fixing the parameters σ and a was to increase the sum of the squares SS by a small amount and thus decrease the

correlation coefficient R. A typical case is illustrated in Table IV-9 which shows a comparison of sum of squares SS and R the correlation coefficient for velocity profiles measured at a constant impeller speed of 243 RPM. The information is extracted from Tables G-2 and G-3 of Appendix G. The increase in SS in Table IV-9 is seen to result in a much larger change in R for $\bar{v}_r$ than for $\bar{q}$. This trend of small changes in R for $\bar{q}$ and slightly larger changes in R for $\bar{v}_r$ is seen in all the Tables of Appendix G. In those profiles where R has a relatively low value, the change in R will be proportionately larger. This is clearly seen in case of Profile Number 8 of Table IV-9 where R drops from 0.917 to 0.841.

In Table IV-10 the volumetric flow parameter A and z_o are presented to see the effect of keeping σ and a as constant. Both parameters A and z_o show very little variation as can be seen in Table IV-10. The fact that there is no variation in z_o is not significant, its only purpose is to shift the coordinates as pointed out at the beginning of this chapter. This trend is the case for all the profiles analyzed as can be verified in Appendix G. It is thus concluded that the parameters σ and a can be treated as constants independent of impeller speed, radial angle or impeller depth. In addition σ is independent of tank diameter.

The reason for the above behavior is a peculiarity of nonlinear least square fits. In general the larger the number of parameters the better the fit. However if one of these parameters is a constant the nonlinear least square fit will treat it as a variable

TABLE IV-9

EFFECT OF CONSTANT σ AND, a, ON THE SUM OF SQUARES SS, AND CORRELATION COEFFICIENT FOR $\bar{q}$ AND $\bar{v}_r$ AT IMPELLER SPEED OF 243 RPM

Profile Number	Radial Distance in.	Radial Angle	Sum of Square SS		Correlation Coefficient R	
			$\bar{q}$	$\bar{v}_r$	$\bar{q}$	$\bar{v}_r$
(a) σ and, a, constant						
1	2.5	44.1	201	319	0.988	0.979
2		44.1	77	279	0.996	0.982
3		5.5	23	212	0.999	0.988
4	3.0	44.1	52	36	0.995	0.996
5		5.5	114	59	0.989	0.994
6	3.5	44.1	51	49	0.990	0.989
7		5.5	85	55	0.986	0.990
8	4.0	44.1	635	537	0.841	0.862
9		5.5	110	78	0.960	0.971
(b) σ and, a, obtained by least square fit						
1	2.5	44.1	179	222	0.990	0.985
2		44.1	39	146	0.998	0.991
3		5.5	23	168	0.999	0.990
4	3.0	44.1	41	47	0.996	0.995
5		5.5	64	73	0.994	0.992
6	3.5	44.1	21	26	0.996	0.994
7		5.5	29	41	0.995	0.993
8	4.0	44.1	344	316	0.917	0.921
9		5.5	19	26	0.993	0.990

TABLE IV-10

EFFECT OF CONSTANT σ AND, a, ON THE VOLUMETRIC FLOW PARAMETER A AND JET DISPLACEMENT PARAMETER z_o AT IMPELLER SPEED OF 243 RPM

	σ and a Constant		σ and, a, obtained By Least Square Fit	
Profile Number	A ft^3/min	z_o,ft	A ft^3/min	z_o,ft
1	13.5	0.000457	13.5	0.00048
2	13.4	-0.000731	13.3	-0.00071
3	13.5	0.001305	13.4	0.00131
4	12.9	0.001954	13.0	0.00198
5	13.4	0.001570	13.4	0.00160
6	13.2	0.003100	13.4	0.00325
7	13.4	0.005407	13.5	0.00542
8	13.	0.006688	14.0	0.00621
9	13.6	0.005964	13.9	0.00612

to reduce the scatter in the data as measured by sum of squares SS about the regression line. It therefore becomes necessary to exercise proper judgement to get meaningful results from nonlinear least square fits.

The result of considering σ and a as constants has more revelance when the volumetric flow at the impeller periphery and at the point of measurement r is examined in Table IV-11. The volumetric flow at the impeller periphery (impeller discharge) exhibits some scatter when σ and a are free. For Profiles 8 and 9 where r is 4.0 in., the volumetric flow appears to be larger. This erratic behavior disappears when σ and a are taken as a constant. The volumetric flow at radial distance r is not affected appreciably up to r equal to 3.5 in. There is a significant difference in volumetric flow for r equal to 4.0. If Equation IV-7 is examined it is seen that keeping σ and a constant does not make the impeller discharge constant (at fixed impeller speed) unless A was a constant too.

In Table IV-12 is shown the average value of A, averaged over profiles obtained at a constant impeller speed. The number of profiles over which this average is taken is given in the last column. The variance and confidence limit in this table has small values. This indicates that A has a constant value at constant impeller speed, and this is the reason for constant Q values in Table IV-11 noted above. The large confidence limit in Item 6 is because of small sample size. The conditions under which the velocity profiles (Item 6) were obtained are questionable and were discussed in an

TABLE IV-11

EFFECT OF CONSTANT σ AND a ON VOLUMETRIC FLOW AT IMPELLER PERIPHERY AND AT RADIAL DISTANCE r FOR A CONSTANT IMPELLER SPEED OF 243 RPM

			σ and a Obtained by Least Sq. Fit		σ and a Constant	
Profile Number	Radial Distance r in.	Radial Angle	Flow at Impeller CFM	Flow at Radial Distance r, CFM	Flow at Impeller CFM	Flow at Radial Distance r, CFM
1	2.5	44.1	3.981	9.50	4.001	9.68
2		44.1	3.741	9.30	3.970	9.59
3		5.5	3.373	9.51	4.022	9.71
4	3.0	44.1	3.869	11.67	3.839	11.48
5		5.5	3.502	12.19	3.975	11.89
6	3.5	44.1	4.684	14.71	3.925	13.93
7		5.5	4.004	14.78	3.969	14.08
8	4.0	44.1	5.561	19.29	3.946	16.17
9		5.5	4.445	18.13	4.031	16.52

TABLE IV-12

EFFECT OF CONSTANT σ AND a ON THE AVERAGE

VALUES OF THE VOLUMETRIC FLOW PARAMETER A

Item No.	Impeller Speed RPM	Average Value of A	Variance	Confidence Limit	Number of Profiles
1	243	13.4	0.039	0.2	9
2	250	14.1	0,196	0.7	4
3	333.3	18.6	0.084	0.5	4
4	400	22.9	0.084	0.5	4
5	500	28.3	0.539	0.5	12
6	550	31.6	0,144	3.4	2
7*	333.3	17.8	0.236	0.8	4

* Tank diameter = 11.5 inches

earlier section. Comparing Tables IV-12 and IV-6 the value of A are not significantly different being within the estimates of their error bounds as reported by the deviation. Hence keeping σ and a constant has not materially affected the least square fit of the data.

Width of the Tangential Jet

An important conclusion that results from considering σ, the jet width parameter, constant can be obtained from considering Equation B-25 which is

$$\bar{v}_r = (\bar{v}_r)_{max} [\tanh^2 (\eta/2)] \qquad \text{(B-25)}$$

This equation can be rewritten as:

$$\frac{\bar{v}_r}{(\bar{v}_r)_{max}} = f(\eta) \qquad \text{(IV-11)}$$

where

$$\eta = \sigma \frac{r}{z} \qquad \text{(IV-12)}$$

Equation IV-11 is a restatement of the original assumption that the velocity profiles are similar. From IV-12 it is evident that since σ is independent of impeller speed, hence the width of the jet is also independent of impeller speed, and η is a function of r and z only. From IV-11 it then follows that $\bar{v}_r/(\bar{v}_r)_{max}$ is independent of the impeller speed and a function of r and z only. This result has been observed by Sachs (28) and Aiba (1) and Cutter (9), thus confirming the conclusion that σ is a constant.

In Chapter II, Section 2.2 it was shown that the maximum radial distance r_o, that the tangential jet model holds is given by Equation II-28,

$$r_o = \frac{T\sigma}{12 + 2\sigma} \qquad \text{(II-28)}$$

Substituting T = 12.25 in. and σ from IV-9, gives r_o = 4.2 in. In Table IV-3 profiles 11 and 12 are runs made at r equals 4 in., a radial distance close to r_o, where the tangential jet model breaks down. It is thus not surprising that the values of σ is much lower than the average value of σ. This effect was also noticed in Profiles 8 and 9 of Table IV-4. It is for this reason that in subsequent runs the maximum value of the radial distance r is limited to r equal to 3.0 in., well below r_o.

Jet Displacement Parameter

The parameter z_o is a measure of the displacement of the jet from the impeller centerline. It is obtained under all cases by a least square fit of the data and reported in the Tables of Appendix G under the column P(4). The value of z_o is extremely small ranging from 0.003 to 0.009 ft. and can be either positive or negative. In Table IV-10 where profiles 1 and 2 are replicate measurements made at exactly the same points, z_o has a positive value for Profile 1 and negative value for Profile 2. It is more often positive than negative and most cases shows about twice the displacement for profile measurements made near the baffle than in between baffles. The value of z_o is not affected appreciably by fixing σ and a at

their average values. This is because z_o can only cause a shift or displacement in the profile, it cannot alter the shape of the profile. Hence it does not affect the properties of jet which are determine by the shape of the velocity profile. The only anomalous result is in Profile 3 of Table G-11 (impeller speed 500 RPM) where z_o has an excessively high value of -0.94 in.. The correlation coefficient is rather low for this profile casting further doubts on this particular measurement.

4.3. Velocity Profile Measurements in the Rest of the Tank

Figure IV-3 shows a computer drawn solution, drawn by the program PLOTER described in Chapter II. This is a solution for a 3.0 in. diameter impeller, centrally located in a 11.5 in. diameter tank, depth of fluid is 12.0 in. and the impeller speed is 500 RPM. The values of the parameters needed for this solution are (a) the tangential jet parameters and (b) the geometric parameters that set the boundaries of the different flow regions into which the tank has been divided as explained in Chapter II. The tangential jet parameters have been evaluated in Section 4.2 and are; σ and a given by Equations IV-9 and IV-10 and the volumetric parameter A obtained from Figure IV-2. The geometric parameters are taken as that for Figure II-9 (c) with one exception. XN4 was set at 0.55 instead of 0.5, as this solution was considered the best representation of the flow field.

In Figure IV-3 it is seen that the streamlines in the region outside the impeller tend to stay close to the tank wall and the axis of the impeller. This is in agreement with Nagata's profile as can

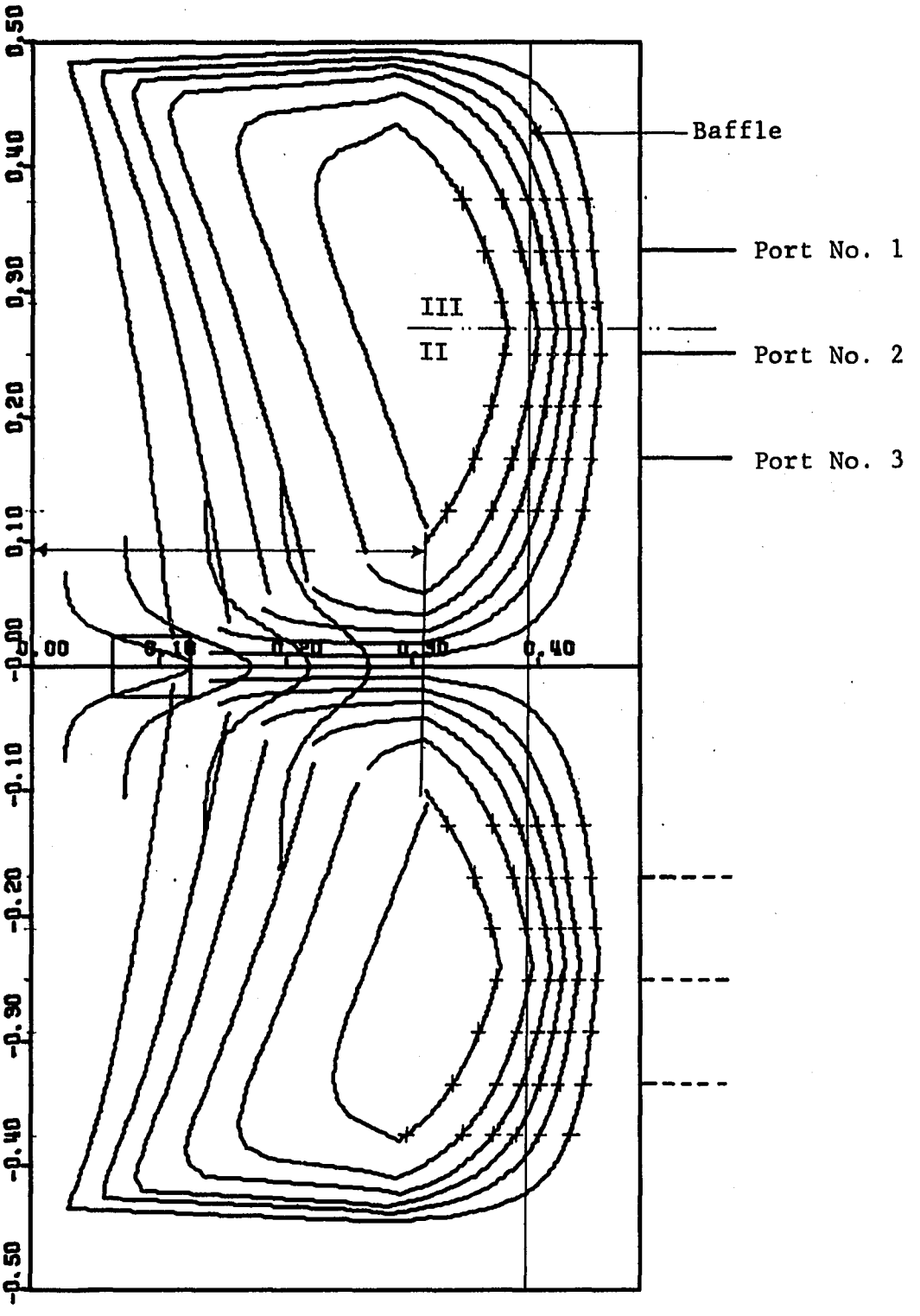

Figure IV-3:

Theoretical Streamlines for a 3.0 in. Impeller at 500 RPM Values of Parameters are = 11.192, A = 28.24, a = 0.1147, h = 6.0. Depth of Water 12.0 in. and Tank diameter = 11.5 in. Each Pair of Streamlines Enclose 5 ft^3/min of Water. This Theoretical Profile Illustrates a Boundary Layer at the Tank Bottom having a Width of 10% of the Fluid Depth.

be seen in Figure I-5. This is not exactly surprising since up to the radial distance r_o (the point where the tangential jet model ends) the flow in the rest of the tank is into the impeller and the jet. The peripherial region $T/2-r_o$ is thus left for the upward and downward flow out of the tangential jet. In our case, r_o was estimated to be 3.98 inches (see Section 4.2), hence the thickness of the upward and downward flow from the stagnation region is restricted to a narrow peripherial region of 1.9 inches. The flow as it leaves Region II tends to stay close to the wall as noticed by the crowding of the streamlines. The maximum crowding of the streamlines and thus the minimum width of the flow occurs roughly half way between the impeller center line and the liquid surface. The minimum width is of order of one baffle width thick, as seen in Figure IV-3 where the vertical line represents a 1 inch baffle. The theoretical solution shown in Figure IV-3 is for a 11.5 in diameter tank with impeller speed of 500 RPM. This represents the condition under which velocity profiles were measured outside the impeller region which will now be described. In order to get a quantative idea of the velocity profiles in the region outside of the impeller, three ports where drilled into a plexiglass tank 11.5 in. in diameter at 10, 8 and 9 inches from the bottome of the tank. These ports are numbered 1, 2, and 3 and their locations are marked on Figure IV-3. The three dimensional pitot tube was used to make a horizontal pass through these ports to measure velocity profiles. The flow is symmetrical and hence only one quadrant need be considered. Also

Port Number 2 is located where the velocities would be a maximum and hence the probe should give a maximum response. Ports 1 and 3 were placed 1.0 in. above and below Port 2 so as to further explore the velocity field.

Velocity Measurements in the Rest of the Tank

As noted in Chapter III, probe response is a function of flow geometry. In Figure IV-4 (a) is shown schematically the probe response close to the tank wall. θ_p is the pitch angle and θ_y is the yaw angle. The yaw angle θ_y is obtained by rotating the probe till the manometer C balances as explained in Chapter III. θ_y is taken as zero when the probe points vertically upwards. With this as a reference point, the component velocities can be calculated with their correct sign if in case (a) where the flow is upward

$$\theta_y = (\theta_y)_{exp} + 90° \qquad \text{(IV-13)}$$

and in case (b) where the flow is downward

$$\theta_y = 180 - (\theta_y)_{exp} \qquad \text{(IV-14)}$$

The above equations follow from the geometry of Figure IV-4 (a) and IV-4 (b).

The pitch angle θ_y is obtained from the manufactures calibration plot which is shown in Figure IV-5. Curve A is an empirical plot of $(P_4-P_5)/(P_1-P_2)$ versus θ_p; where (P_4-P_5) is the pressure drop recorded by manometer D and (P_1-P_2) is the pressure drop from manometer B. Curve B is an empirical plot of $(P_t-P_s)/(P_1-P_2)$ versus θ_p,

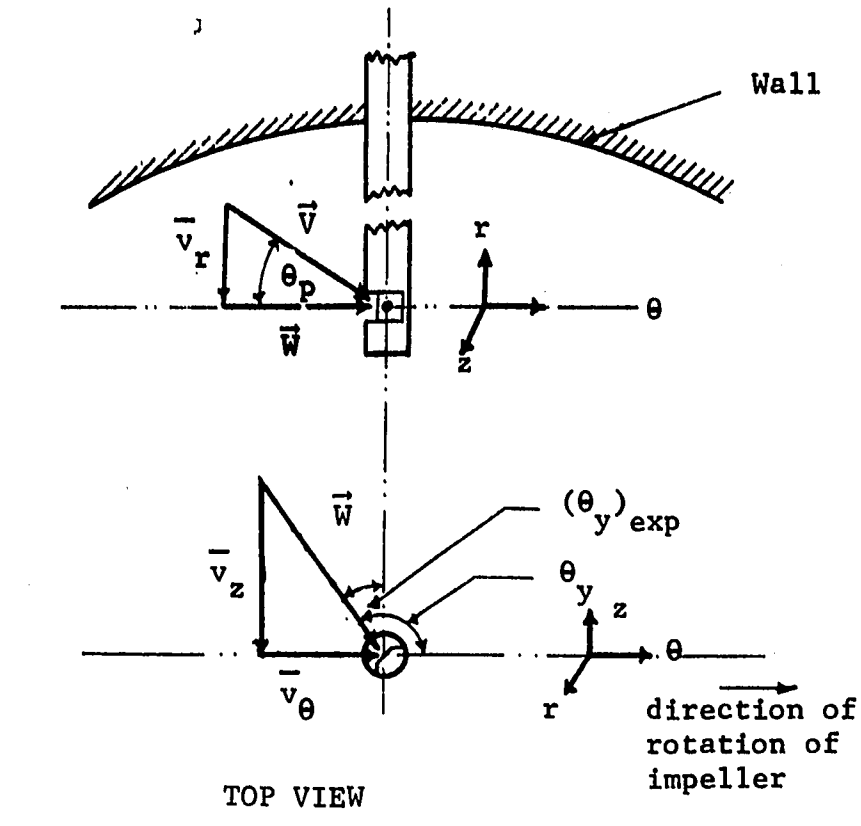

TOP VIEW

(a) Far from Tank Wall

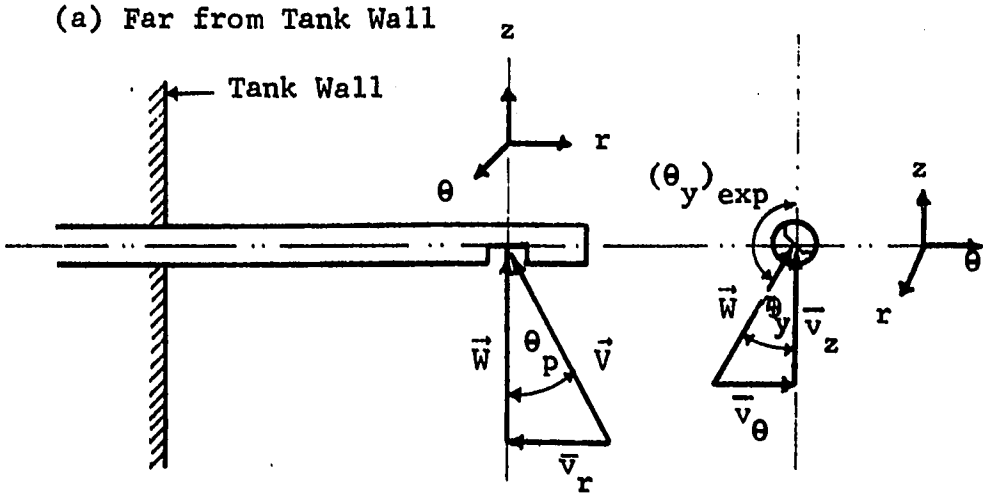

END VIEW

(b) Close to Tank Wall

Figure IV-4: Resolution of Velocity into its Components When the Three Dimensional Probe is in a Horizontal Position.

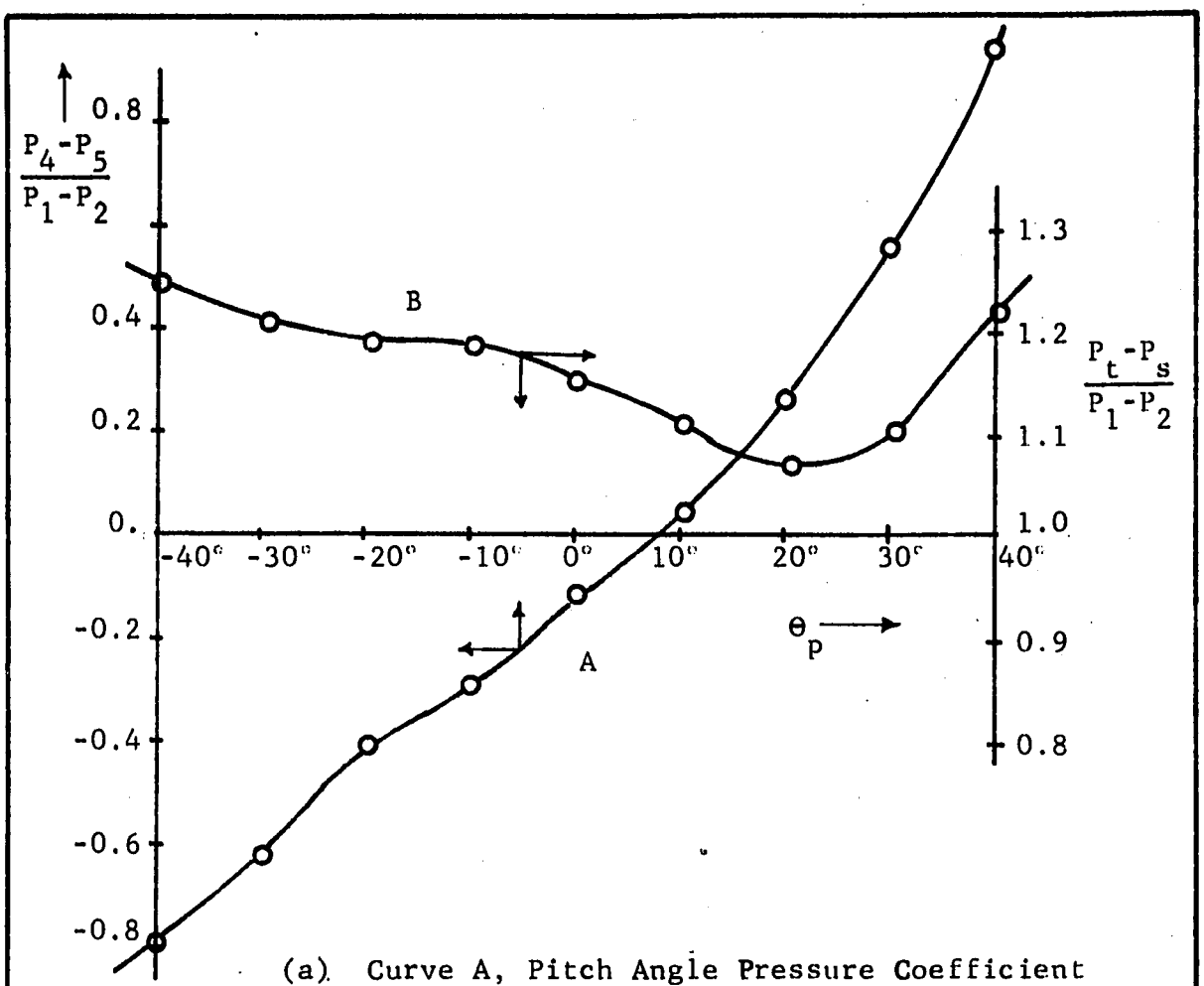

(a) Curve A, Pitch Angle Pressure Coefficient Versus Pitch Angle. Curve B, Velocity Pressure Coefficient Versus Pitch Angle.

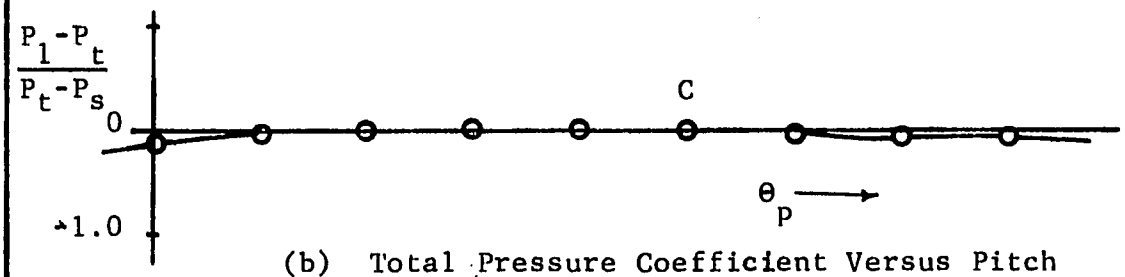

(b) Total Pressure Coefficient Versus Pitch Angle

Figure IV-5: Manufacturers Calibration Chart for Three-dimensional Pitot Tube (47)

where (P_t-P_s) is the true kinetic head and (P_1-P_2) is the actual kinetic head recorded by the instrument. Curve C indicates that the kinetic head (P_t-P_s) is the true kinetic head provided that $\theta_p \leq \pm 40°$.

A program called TANKANL was written that analyses the data obtained from the horizontal pitot tube runs. The program and the input data are given in Appendix F. The program uses Equations IV-13 and IV-14 to give correct value of θ_y. It next calculates (P_4-P_5), (P_1-P_2) and the ratio of $(P_4-P_5)/(P_1-P_2)$. Curve A is then interpolated by a three point Lagrange interpolation subprogram OMEGA to give θ_p. OMEGA is used again with θ_p as input to obtain $(P_t-P_s)/(P_1-P_2)$ from curve B. A logical trap omits calculations when the ratio $(P_4-P_5)/(P_1-P_2)$ is less than -0.8 or greater than 0.8 as these values are outside the range of the calibration chart. Let α be the values obtained from the calibration chart using curve B, then

$$\alpha = \frac{P_t-P_s}{P_1-P_2} \tag{IV-15}$$

The velocity $\vec{V}$ recorded by the three dimensional probe is then

$$\vec{V} = (2g\alpha(P_1-P_2))^{\frac{1}{2}} \tag{IV-16}$$

From Figure IV-3 and from geometry, the component velocities can be written as

$$\bar{v}_r = |\vec{V}| \sin \theta_p \tag{IV-17}$$

$$\bar{v}_z = |\vec{V}| \cos \theta_p \sin \theta_y \tag{IV-18}$$

$$\bar{v}_\theta = |\vec{V}| \cos \theta_p \cos \theta_y \qquad \text{(IV-19)}$$

where θ_y in IV-18 and IV-19 are given by Equations IV-3 or IV-14. The above equation gives the component velocities with their correct sign. $\bar{v}_\theta$ is considered positive in the direction of rotation of the impeller, and the positive values of $\bar{v}_z$ and $\bar{v}_r$ are shown in Figure IV-4.

Experimental Velocity Profiles

The results of the experimental velocity profiles are calculated by program TANKANL and are given in Appendix H. These velocity profiles are summarized here as plots of $\bar{v}_r$, $\bar{v}_\theta$ and $\bar{v}_z$ versus the distance from the tank wall, T-r, in Figures IV-6 to IV-8. The data points for these plots are taken from tables given in Appendix J. In Figure IV-6 is shown a plot of radial velocity $\bar{v}_r$ for Port Numbers 1, 2, and 3. The velocity profiles of Port Numbers 2 and 3 are approximately of the same magnitude, that of Port Number 2 being higher near the wall, while Port Number 3 is higher at the center of the tank. This behavior is reasonable since near the wall Port Number 3 is still in the stagnation region, while near the tank center, Port Number 3 is closer to the impeller and the fluid begins to turn and accelerate due to the impeller suction and entrainment in the jet. The profiles take a dip at 1.5 inches from the wall and this point corresponds to the stagnation region observed by Nagata. The $\bar{v}_r$ velocity profile for Port Number 1 shows peculiar behavior, showing a positive value between 0.5 and 1 inch. This behavior is possibly due to erratic probe response.

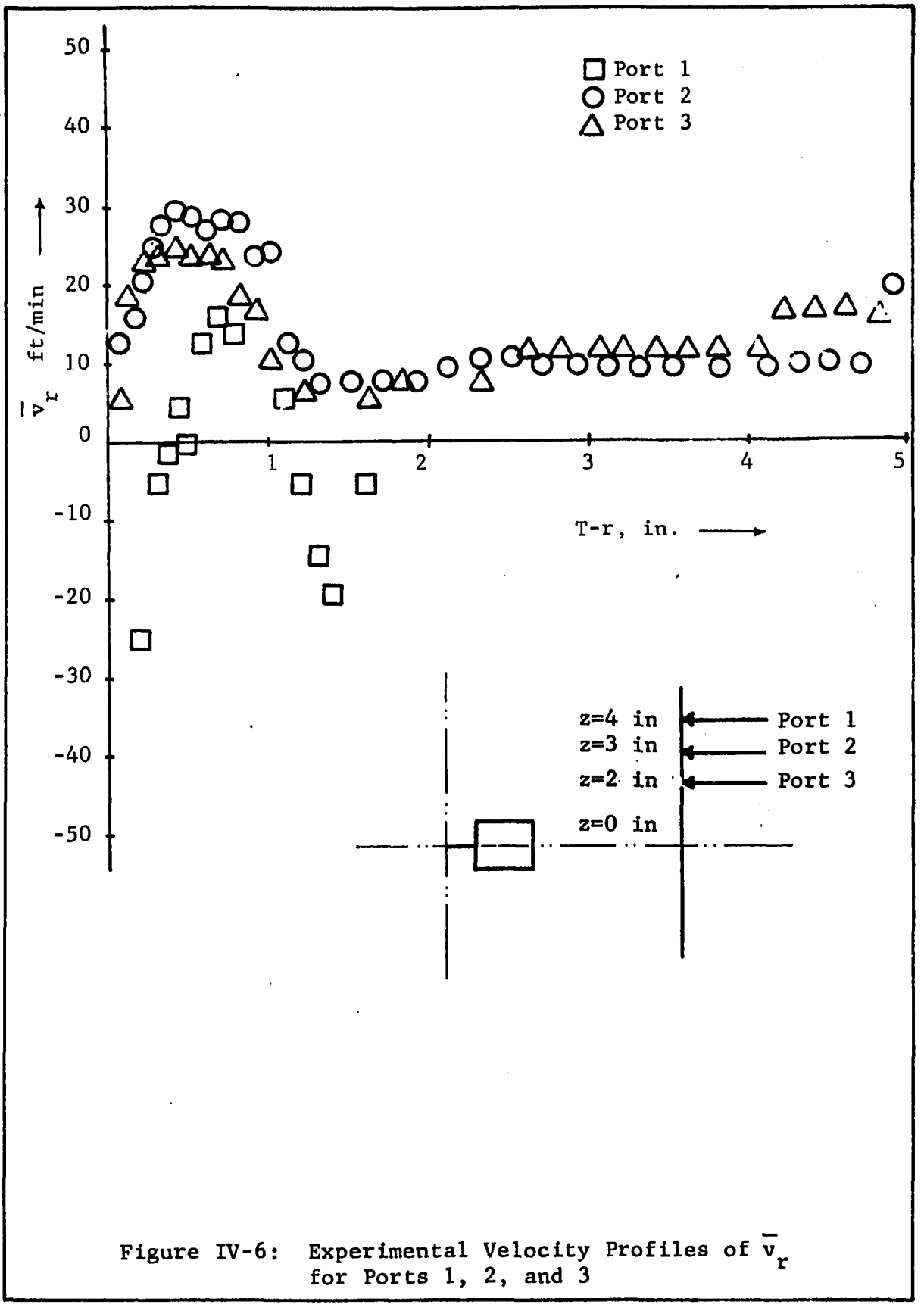

Figure IV-6: Experimental Velocity Profiles of $\bar{v}_r$ for Ports 1, 2, and 3

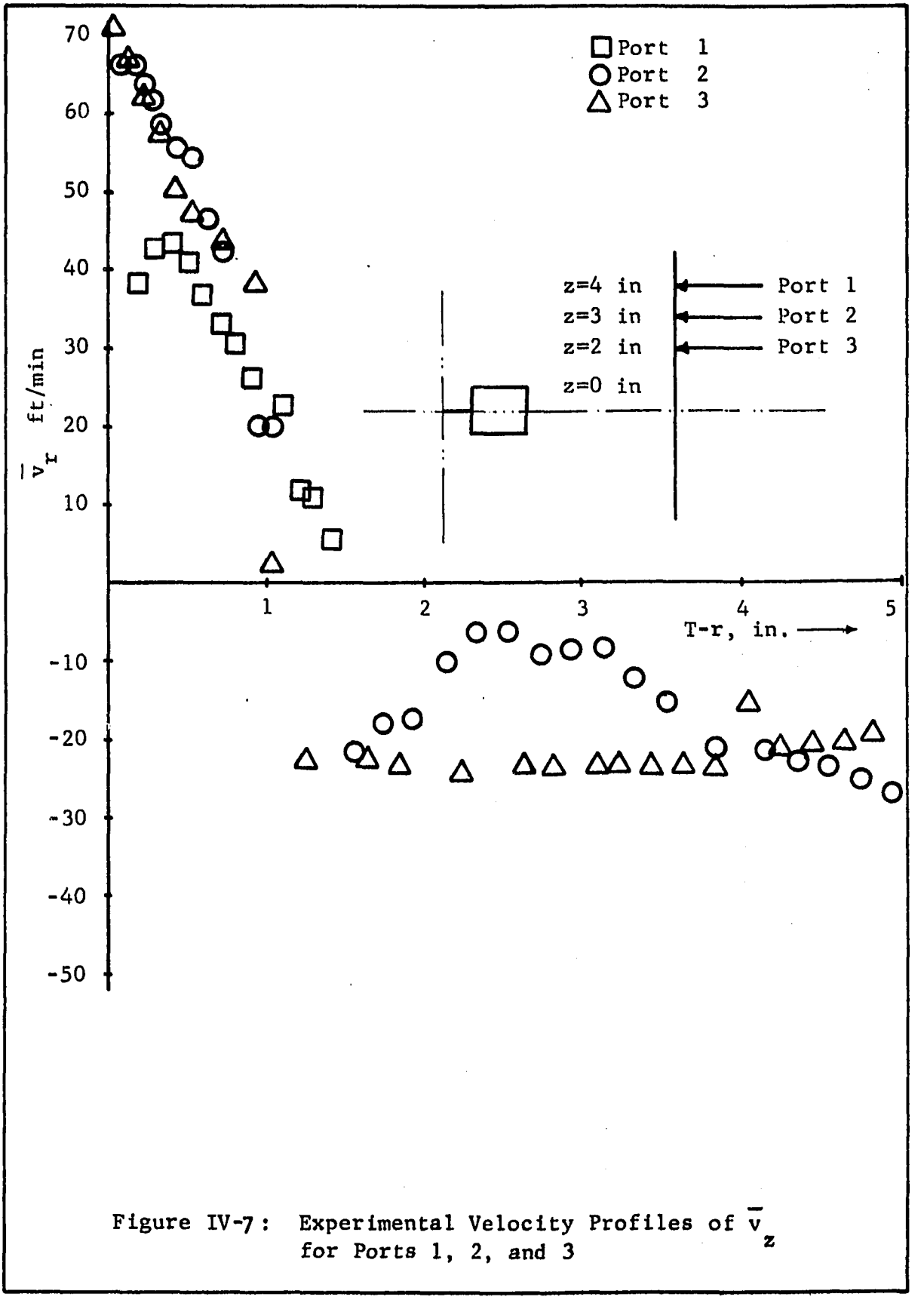

Figure IV-7: Experimental Velocity Profiles of $\bar{v}_z$ for Ports 1, 2, and 3

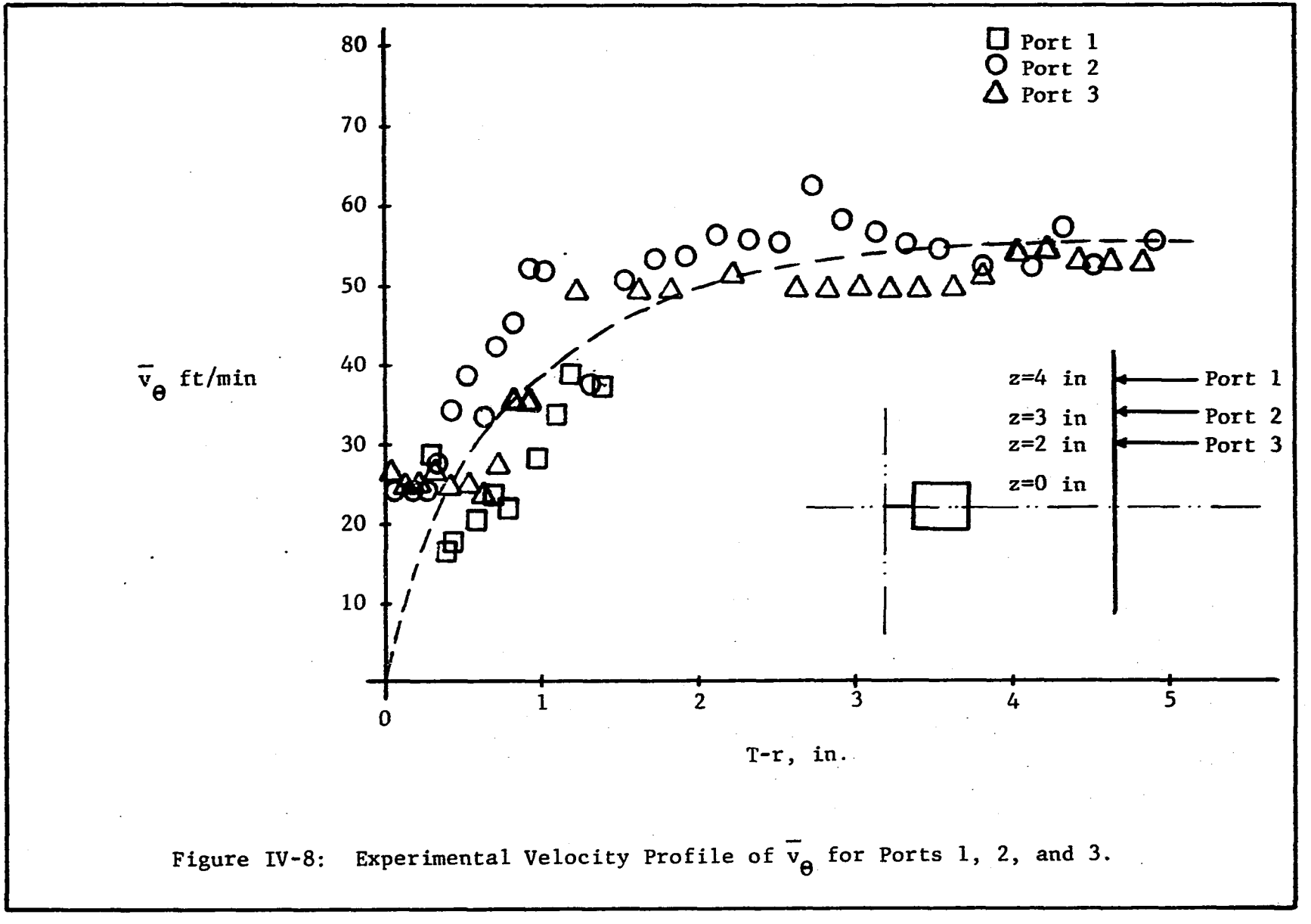

Figure IV-8: Experimental Velocity Profile of $\bar{v}_\theta$ for Ports 1, 2, and 3.

In Figure IV-7 is shown the vertical velocity profile $\bar{v}_z$. The velocity profile for Ports 2 and 3 are virtually indentically near the wall. For Port Number 1 (located 4.0 inches from impeller centerline), $\bar{v}_z$ is much smaller close to the wall and shows a manimum, at T-r of 0.4 inch. This indicates that at Port Number 1 the fluid is beginning to turn. Beyond T-r of 1.6 in. only one negative value at T-r equal to 1.6 could be analyzed. This is because the pitch angle θ_p was larger than 40°.

For T-r larger than 1.0 in., $\bar{v}_z$ for Port Numbers 2 and 3 deviate from one another. This is because Port Number 3 is closer to jet while Port Number 2 crosses the center of circulation. At the center of circulation the flow is largerly tangential, $\bar{v}_\theta$ being larger than $\bar{v}_r$ or $\bar{v}_z$. This can be seen in Figure IV-8 which shows $\bar{v}_\theta$ to have reached near its maximum value at T-r = 2.5 in. At this point $\bar{v}_z$ for Port Number 2 reaches its smallest value thus accounting for the stagnation point observed by Nagata in the r-z plane. From Figures IV-6 and IV-7 the stagnation point could be estimated at T-r of 1.5 to 2.0 inches. In our theoretical model, this point can be calculated from Equation II-28 and is found to have a value of 3.98 in., or T-r = 1.9 in. Considering the precision of the velocity measurements the calculated and experimental value of the circulation point are not significantly different. It will be recalled that Equation II-28 was obtained on the assumption that the tangential jet model breaks down at r_o, the r coordinate of the center of circulation. The above evidence supports this assumption.

In Figure IV-8 is shown the plot of $\bar{v}_\theta$ versus T-r. In this plot $\bar{v}_\theta$ decreases as it approaches the tank wall and reaches a maximum limiting value at 4.0 inches from the tank wall. $\bar{v}_\theta$ for all three ports have the same order of magnitude and a dotted line has been drawn through the data points as shown in Figure IV-8. This means that within the region covered by the three ports, $\bar{v}_\theta$ is independent of z and a function of r only. Figure IV-8 indicates that $\bar{v}_\theta$ is not small in the region outside the impeller. Comparing its magnitude with that of $\bar{v}_r$ in Figure IV-6 it is seen that $\bar{v}_\theta$ is larger than $\bar{v}_r$ except in a narrow region near the tank wall. In the case of $\bar{v}_z$, $\bar{v}_\theta$ is smaller than $\bar{v}_z$ near the tank wall and larger than $\bar{v}_z$ for from the tank wall. These observations indicate that $\bar{v}_\theta$ has an appreciable magnitude and thus cannot be neglected in comparison with $\bar{v}_r$ and $\bar{v}_z$. The flow field is thus three dimensional.

A clearer idea of the three dimensional structure of the flow field in the region outside the impeller is obtained on examining the values of $\vec{V}$ the resultant velocity in the tables given in Appendix H. It was found that for Port 1, $\vec{V}$ ranges from 56 ft/min near the wall steadily decreasing to 36 ft/min far from the wall. For Port Number 2 this range is 71 ft/min near the wall decreasing to 58 ft/min far from the wall. In the case of Port Number 3 $\vec{V}$ is 56 ft/min near the wall increasing to 74 ft/min far from the wall. The increase in velocity far from the wall for Port Number 3 reflects the acceleration of the fluid by impeller suction and jet entrainment.

It should be noted that probe readings very close to the tank wall are not reliable. This is because the probe interacts with the flow field tending to report higher values of velocity. The probe manufactureres recommends that readings be taken beyond 4 to 5 probe diameters for a 4.0 inch diameter duct. Since the tank is 11.5 in., in diameter this restriction could be relaxed somewhat, hence readings taken for T-r less than 0.5 inches are considered as biased.

Theoretical Velocity Profiles

For comparison, theoretical profiles at Port Numbers 1, 2, and 3 were also calculated and these are shown in Figures IV-9 and IV-10. No values for $\bar{v}_\theta$ exist as it was assumed to be zero in the theoretical model. Since the theoretical model as drawn by the program FOWANL and given in Figure IV-3 does not give the stream function explicitly it had to be calculated. For this purpose the program FLOWANL was made to punch out the value of ψ and the corresponding radial position r for seven different constant z values. These are shown by plus marks on the streamline in Figure IV-3. Since no additional effort is required to obtain the corresponding points in the bottom of the tank, these were also analyzed. These points are also marked in Figure IV-3. The answers will of course be different since the profile in bottom half of the tank was drawn with a boundary layer.

The program VELPRO was written to calculate $\bar{v}_r$ and $\bar{v}_z$ from the following definitions of ψ for stream surfaces

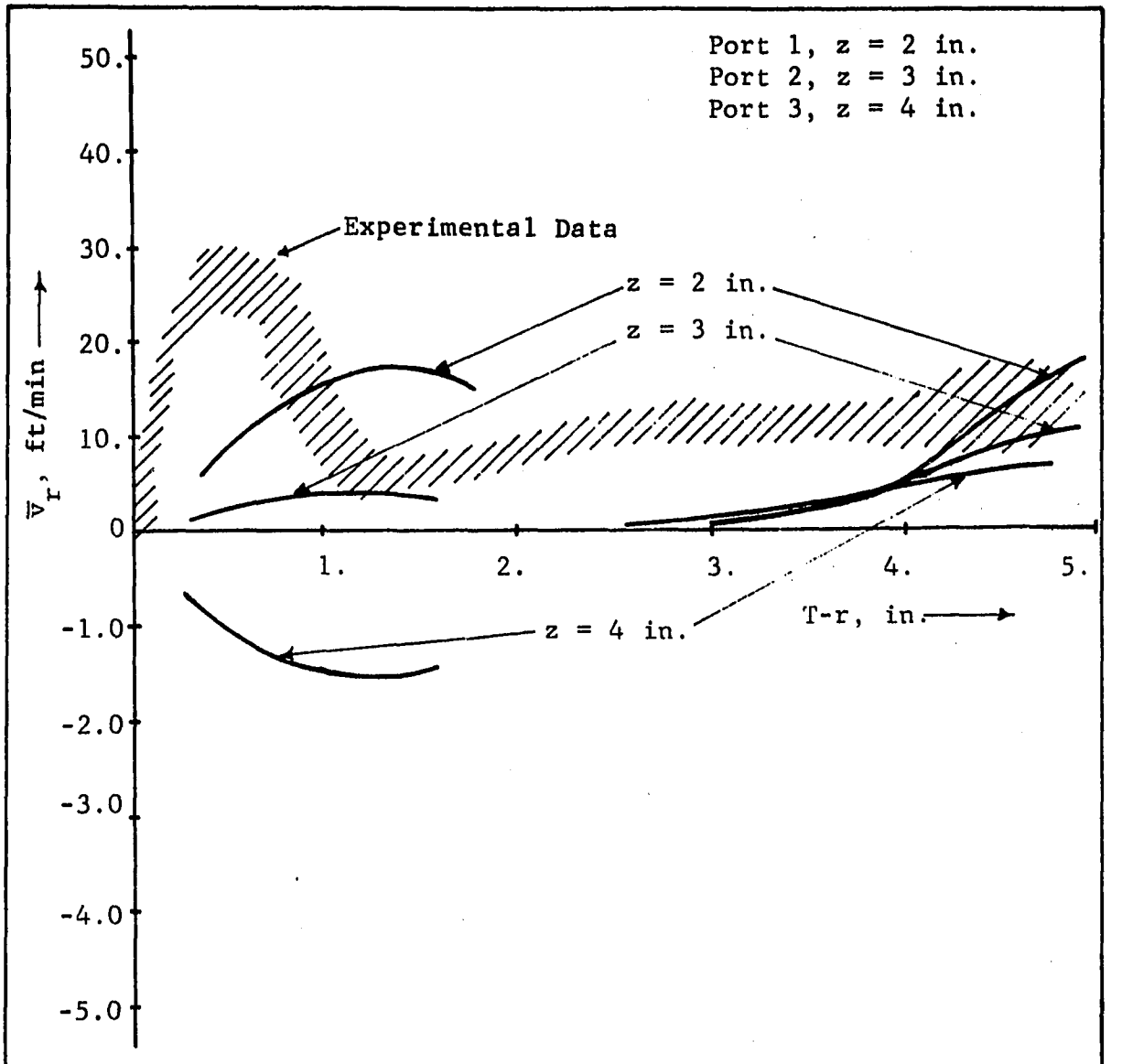

Figure IV-9: Comparison between Experimental and Theoretical Velocity Profiles for $\bar{v}_r$ for Ports 1, 2, and 3

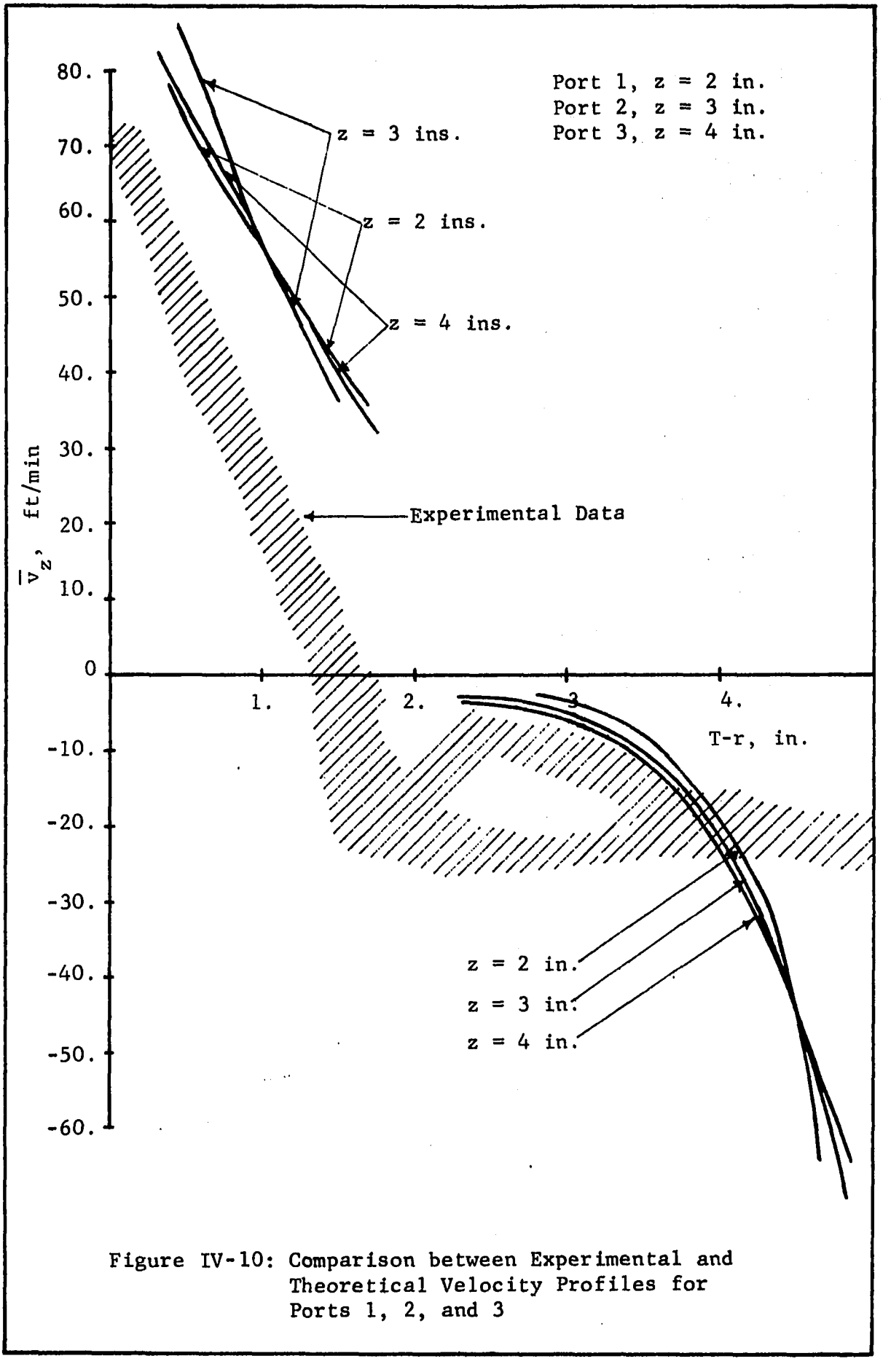

Figure IV-10: Comparison between Experimental and Theoretical Velocity Profiles for Ports 1, 2, and 3

$$\bar{v}_r = \frac{1}{2\pi r} \frac{\partial \psi}{\partial z} \qquad \text{(IV-20)}$$

$$\bar{v}_z = - \frac{1}{2\pi r} \frac{\partial \psi}{\partial r} \qquad \text{(IV-21)}$$

Program VELPRO and its input data is given in Appendix F. As a streamline in Figure IV-3 is given by r = f(z) at constant ψ, the derivatives of ψ in Equations IV-20 and IV-21 are obtained by a numerical method. This is done by fitting a third order polynomial through a row of points having a constant z value. Seven such rows are shown in Figure IV-2. The bottom most row is 1.0 in. from the impeller centerline (i.e., z = 1.0 inch). Each succeeding row is at a distance of 0.5 inch apart. Differentiating this polynomial gives $\frac{\partial \psi}{\partial r}$ and from Equation Iv-21, $\bar{v}_z$ is calculated.

To calculate $\bar{v}_r$, first we calculate ψ = f(r) at constant z by fitting a third order polynomial for each of the seven z-planes shown in Figure IV-3. Next, these seven polynomials are used to obtain seven values of ψ as a function of z at constant r. The constant value of r is determined by the coordinates of the point at which $\bar{v}_r$ is desired. A third order polynomial is then fitted through these seven points to obtain ψ = f(z) at constant r. $\frac{\partial \psi}{\partial z}$ can now be calculated and hence $\bar{v}_r$ from Equation IV-20. The goodness of fit for ψ = f(r) at constant z was greater than 0.99, while that for ψ = f(z) at constant r was greater than 0.98. Both these values indicate a good estimate of ψ. The final results

obtained by the program VELPRO is given in Table IV-13 for the upper quadrant while that for the lower quadrant is shown in Table IV-14. The crossover point in Figure IV-3 from Regions II to III was changed so that $\bar{v}_r$ shows a positive value rather than a negative value for Port Number 2. This is clearly seen in Figure IV-3, where Port Number 2 in the lower quadrant is located in Region III and hence $\bar{v}_r$ is negative as shown in Table IV-14 for z greater than 3.0 inches. The crossover point was changed in the upper quadrant by increasing XN4, one of the boundary parameters, from 0.5 to 0.55.

The probable range of the experimentally determined values of $\bar{v}_r$ and $\bar{v}_z$ are shown in Figure IV-9 and IV-10 as a crosshatch band. This permits comparison between experimental and theoretical velocity profiles. It is seen in Figure IV-9 that $\bar{v}_z$ theoretical for all three Ports are fairly close together having the same slope as the experimental values but are much larger in magnitude and thus appear to be displaced. The values of $\bar{v}_r$ are much lower and show little resemblance to the experimental profiles. This indicates that the analysis needs to include $\bar{v}_\theta$, which would lower the value of $\bar{v}_z$ and increase that of $\bar{v}_r$ for a constant value of $\vec{q}$.

Theoretical values of $\bar{v}_r$ and $\bar{v}_z$ in Region V were also obtained from the circular jet model used in this section of the tank. However it will be recalled from the analysis of Chapter II that the eddy viscosity ϵ_o was not needed for obtaining $\psi = f(r,z)$. This can be clearly seen when Equations II-38 and II-39 are examined. However

TABLE IV-13

THEORETICAL VELOCITY PROFILES CALCULATED BY PROGRAM VELPRO FOR REGIONS II AND III ABOVE THE IMPELLER

Velocity Profile at z = 2 in.

T-r(in.)	$\bar{v}_z$ (ft/min)	$\bar{v}_r$ (ft/min)	$\vec{V}$ (ft/min)
0.5	73.9	9.7	74.5
0.7	67.1	12.5	68.3
0.8	62.2	14.2	63.8
1.0	57.0	15.6	59.0
1.2	50.2	16.7	52.9
1.6	38.5	16.5	41.9

Velocity Profile at z = 3 in.

0.4	88.9	1.9	88.9
0.6	80.2	2.7	80.2
0.7	73.9	3.1	73.9
0.8	67.1	3.5	67.2
1.0	58.7	3.8	58.8
1.3	44.3	3.9	44.5

Velocity Profile at z = 4 in.

0.4	79.6	-8.7	80.0
0.6	72.1	-11.3	73.0
0.8	66.7	-12.8	68.0
0.9	61.2	-14.0	62.8
1.1	53.5	-15.0	55.5
1.5	40.4	-14.9	43.1

TABLE IV-14

THEORETICAL VELOCITY PROFILE CALCULATED BY PROGRAM VELPRO FOR REGIONS II AND III BELOW IMPELLER. SHOWS EFFECT OF CONSIDERING A BOUNDARY LAYER IN THE THEORETICAL MODEL.

T-r (in.)	$\bar{v}_z$ (ft/min)	$\bar{v}_r$ (ft/min)	$\vec{V}$ (ft/min)
	Velocity Profile at z = 2 in.		
0.5	74.3	8.3	74.7
0.7	67.2	10.3	68.0
0.8	62.2	11.7	63.3
1.0	56.8	12.9	58.3
1.2	50.2	14.0	52.1
1.6	39.1	14.4	41.7
	Velocity Profile At z = 3 in.		
0.5	76.2	-10.5	76.9
0.7	69.0	-10.8	69.8
0.8	63.9	-11.0	64.8
1.0	58.7	-11.3	59.8
1.2	51.4	-11.7	52.7
1.5	39.5	-11.8	41.2
	Velocity Profile At z = 4 in.		
0.7	59.1	-14.9	61.0
1.0	50.5	-29.2	58.3
1.2	45.5	-36.7	58.5
1.4	41.6	-42.2	59.3
1.7	38.4	-46.7	60.5
2.3	41.0	-47.7	62.9

in order to calculate $\bar{v}_r$ and $\bar{v}_z$, Equations II-14 and II-15 are used which are given below and require a value for ϵ_o.

$$\bar{v}_z = \frac{\epsilon_o}{z+z_o} \quad \frac{2\gamma^2}{(1+\frac{1}{4}\xi^2)^2} \tag{II-14}$$

$$\bar{v}_r = \frac{\epsilon_o}{z+z_o} \quad \gamma \frac{\xi - \frac{1}{4}\xi^2}{(1+\frac{1}{4}\xi^2)^2} \tag{II-15}$$

To evaluate ϵ_o, as a first approximation the momentum in the circular jet was equated to that of the tangential jet. This appears reasonable, since both these jets are connected in series and energy dissipation outside the impeller stream is small. The momentum in the tangential jet J_t is obtained from Equation A-32 which after simplication gives

$$J_t = \frac{4}{3} \pi \rho A^2 \tag{IV-22}$$

The momentum in the circular jet J_c is given by Equation II-18 and is

$$J_c = \frac{16}{3} \pi \rho r^2 \epsilon_o^2 \tag{II-18}$$

However to allow for some dissipation of the momentum in the tangential jet, a factor E_c was included where E_c is defined as

$$E_c = \frac{J_c}{J_t} \tag{IV-23}$$

It follows from the definition of E_c, that E_c is the fraction of the momentum transferred to the circular jet. Combining IV-22, II-18 and IV-23 gives

$$\epsilon_o = E_c \frac{A}{2\gamma} \qquad \text{(IV-26)}$$

The program FLOWANL was again used to evaluate $\bar{v}_z$ and $\bar{v}_r$ using Equations II-14, II-15, and IV-26. The result of these calculations are shown in Table IV-15 and are plotted on Figure IV-9 and IV-10 for comparison. The theoretical value of $\bar{v}_r$ are very small while those of $\bar{v}_z$ are grossly incorrect. $\bar{v}_z$ shows an extremely high value for T-r greater than 4.5 inches and being extremely low below 4.5 inches. Varying E_c the fraction of momentum transferred to the circular jet, does not alter the shape of the profile but merely scales the value of the velocities; large values of E_c gives large values of ϵ_o which in turn gives larger values of $\bar{v}_z$ and $\bar{v}_r$. The theoretical velocities shown in Figures IV-9 and IV-10 have been calculated with $E_c = 0.6$. Also shown in Table IV-15 is $\vec{V}$ the resultant velocity of $\bar{v}_r$ and $\bar{v}_\theta$, and is not constant but decreases as r increases.

The above analysis suggests that although the streamlines appear reasonable the velocity profiles obtained from them need not necessarily reflect a desired velocity profile. The flow in the region outside the impeller appears to have an approximately uniform resultant velocity which could be represented in potential flow. However this flow is a three dimensional flow field. Since in potential flow the Laplace equation holds, the superposition principle could be applied. Thus subtracting $\bar{v}_\theta$ from the total velocity

TABLE IV-15

THEORETICAL VELOCITY PROFILES IN REGION V
OBTAINED FROM THE CIRCULAR JET

T-r (in.)	$\bar{v}_z$ (ft/min)	$\bar{v}_r$ (ft/min)	$\vec{V}$ (ft/min)
	Velocity Profile at z = 2		
5.0	98.8	18.6	100.5
4.6	54.1	14.1	55.9
4.3	29.7	9.0	31.0
4.0	16.0	5.4	16.9
3.5	7.8	2.8	8.2
3.0	3.5	1.1	3.7
	Velocity Profile at z = 3 in.		
4.8	67.7	10.5	68.6
4.4	38.3	8.3	39.2
4.0	21.7	5.6	22.4
3.7	12.1	3.6	12.7
3.2	6.4	2.1	6.8
2.6	3.3	1.1	3.4
	Velocity Profile at z = 4 in.		
4.6	51.5	6.9	52.0
4.2	29.6	5.6	30.1
3.8	17.0	3.9	17.4
3.4	9.7	2.5	10.0
2.9	5.3	1.6	5.5
2.3	2.8	1.0	3.0

$\vec{V}$ would then result in two dimension flow field which could be modeled by the methods suggested in this section. In order to evaluates the results of this model a probe is needed that is not only sensitive to low velocity fields but also has directional properties such that the component velocities $\bar{v}_r$, $\bar{v}_\theta$ and $\bar{v}_z$ can be evaluated. A cross-wire, two channel, hotwire anemometer could be used for this purpose. Two different probes will be needed, one set of wires crossed in a horizontal plane to give $\bar{v}_r$ and $\bar{v}_\theta$ and another set crossed in a vertical plane to give $\bar{v}_r$ and $\bar{v}_z$.

4.4. Detailed Analyses of a Velocity Profile in the Neighborhood of the Impeller

In this section a velocity profile analysis will be presented in detail. The results of the analysis was performed by the program FLOWNAL. A description of the program, its FORTRAN source listing and a flow diagram is given in Appendix F. At the end of the program is given the raw data which is the input to the program.

A complete analysis of a single profile result in four pages of computer printout. To illustrate a typical printout, Run Number 29 was analyzed and the results are given in Tables H-1 to H-4 of Appendix H.

It will be recalled from Chapter II that the tangential jet model is a one dimensional flow in the direction of the velocity $\vec{q}$. This model was also found to give extremely small values of $\bar{v}_z$ of the order of 0.1 ft/min in a region of $\pm$ 0.5 inches about the impeller centerline. The flow in the region of the impeller

is thus essentially one dimensional in the direction of $\vec{q}$. However a velocity probe is needed to locate the direction of $\vec{q}$. The three dimensional pitot tube locates this direction from a yaw angle measurement θ_y. As $\bar{v}_z$ is very small, the pitch angle θ_p is essentially zero, and hence from a description of the probe in Chapter III the manometer D should show no response. However the manometer D was observed to give a measurable pressure drop indicating that the pitch angle θ_p was not zero. In Section 4.5 the reading from the manometer D will be analyzed and it will be shown the manometer D measures Δq^2 and not θ_p in this high shear flow field.

The flow in the impeller stream is thus two dimensional as far as the probe is concerned. The only measurable velocities are $\bar{v}_z$ and $\bar{v}_\theta$. Hence no additional information is obtained from measuring Δq^2 and a two dimensional probe can be used. This type of probe has been used by Cooper (8) for obtaining velocity profiles in the region of the impeller.

The program FLOWANL converts pressure drop readings of manometer B into velocities using Equation III-3. This procedure results in an experimental velocity profile of $\vec{q}_{exp}$ as a function of z. Table IV-16 shows the results of this calculation. In the first column is given values of z; in the next columns are given the corresponding value of $\vec{q}_{exp}$ and the yaw angle θ_y. It is noticed that θ_y is a function z and is plotted in Figure IV-1. This angle profile was first observed by Cooper (8).

A predicted value of $\bar{q}_{calc}$ is obtained from a least square fit of $\bar{q}_{exp}$ as a function of z by adjusting σ, a, and A as explained in

TABLE IV-16

TYPICAL RESULTS OF VELOCITY PROFILE ANALYSIS IN THE NEIGHBORHOOD OF THE IMPELLER FROM PROGRAM FLOWANL AND ILLUSTRATED FOR EXPERIMENTAL DATA FROM RUN NUMBER 29

z ft	$\bar{q}_{exp}$ ft/min	$\bar{\theta}_y$ Degrees	$\bar{q}_{calc}$ ft/min
0.058	44.8	35.2	36.9
0.050	45.6	32.8	50.2
0.042	62.8	30.0	66.5
0.033	80.9	29.4	85.0
0.025	108.4	28.0	103.9
0.017	122.0	26.6	120.1
0.008	130.2	26.4	130.2
0.000	130.5	25.8	131.8
-0.008	124.4	26.6	124.4
-0.017	111.8	27.4	109.9
-0.025	89.2	29.8	91.5
-0.033	72.2	31.6	72.6
-0.042	50.3	32.8	55.4
-0.050	48.8	32.8	41.0

Arithemetic average, $\bar{\theta}_y = 29.7°$

Weighted average, $\bar{\theta}_y = 27.8°$

Velocity factor, $WT = 0.5$

Correlation coefficient $R = 0.99$

Jet parameters

$\sigma = 11.28$
$A = 18.54\ ft^3/min$
$a = 0.116\ ft$
$z_o = 0.0027\ ft$

Half width of jet, $b_{\frac{1}{2}} = 1.6$ in

Section 4.1. $\bar{q}_{calc}$ is given by Equation II-10 and is reproduced here

$$\bar{q}_{calc} = \frac{A}{2}\left(\frac{\sigma}{r}\right)^{\frac{1}{2}} \frac{1}{(r^2-a^2)^{\frac{1}{4}}} \left[1-\tanh^2(\eta/2)\right] \qquad \text{(II-10)}$$

where η is given by

$$\eta = \sigma \frac{z-z_o}{r} \qquad \text{(II-21)}$$

As explained in Section 4.1, the parameters σ, A and z_o are obtained by a least square fit and a, the radius of source, is calculated from a weighted average angle and a velocity factor. The resulting parameters and other pertinent information obtained from Tables J-1 to J-4 are given in Table IV-16.

The theoretical velocity profile $\bar{q}_{calc}$ is also given in Table IV-16. In Figure IV-11 is shown a plot of $\bar{q}_{calc}$ versus z. Also shown on the plot is $\bar{q}_{exp}$. The correlation coefficient R is 0.99 and as can be seen in Figure IV-11 the agreement between experimental and theoretical values of q is excellant. Also shown on the plot is the jet displacement parameter z_o and the half width of the jet $b_{\frac{1}{2}}$. A quantity BHALF is also shown and should not be confused with $b_{\frac{1}{2}}$, the half width of the jet. BHALF is the z coordinate of $\frac{1}{2}\bar{q}_{max}$. It is noticed in Figure IV-11 that only two data points are measured for z greater than BHALF. This is because the probe has reached a velocity near 30 ft/min below which it will not respond. It is noticed that for z larger than BHALF the velocity profile falls off rapidly, the rate of fall is then gradual reaching 1% of $\bar{q}_{max}$ at z equal to $b_{\frac{1}{2}}$, the half width of the jet.

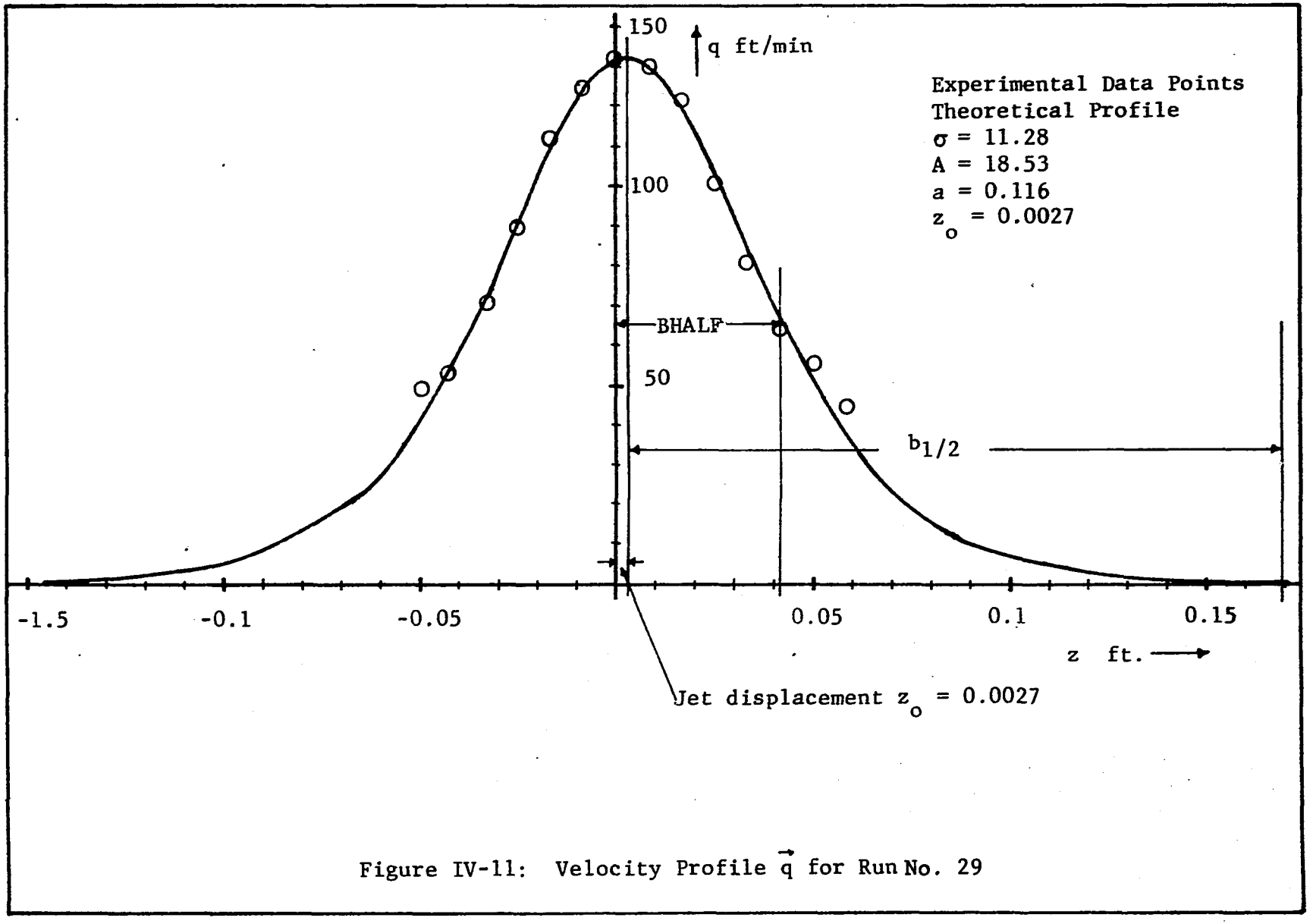

Figure IV-11: Velocity Profile $\vec{q}$ for Run No. 29

Radial Velocity Profile Analysis

The experimental value of the radial velocity is obtained from Equation A-20 which is

$$(\bar{v}_r)_{exp} = \bar{q}_{exp} \cos \theta_y \qquad \text{(A-20)}$$

Table IV-17 lists the value of $(\bar{v}_r)_{exp}$ for Run Number 29 calculated from A-20. The theoretical value of the radial velocity $(\bar{v}_r)_{calc}$ is obtained from Equation B-22,

$$(\bar{v}_r)_{calc} = \frac{A}{2}\left(\frac{\sigma}{r^3}\right)^{\frac{1}{2}} (r^2-a^2)[1-\tanh^2(\eta/2)] \qquad \text{(B-22)}$$

In Table IV-7, $(\bar{v}_r)_{calc}$ is obtained from B-22, using the values of σ, A, a and z_o from Table IV-16. A correlation coefficient R is also calculated from an equation similar to Equation IV-1 written for $\bar{v}_r$. The value of R is 0.99 indicating an excellant prediction of the data.

4.5. Interpretation of Manometer D

In Section 4.5, the experimental data obtained from the three dimensional pitot tube was analyzed on the basis that θ_p the pitch angle equals zero. In this section it will be shown that this is indeed the case and that the readings from manometer D must be interpreted as measuring Δq^2 because of the large velocity gradients in the impeller stream.

In Chapter III it was shown that the pressure difference between the pressure taps P_4 and P_5 is given by

$$P_4 - P_5 = \rho_w(h_a-h_b) - \Delta H_m(\rho_m-\rho_w) \qquad \text{(III-2)}$$

TABLE IV-17

TYPICAL RESULTS OF RADIAL VELOCITY PROFILE ANALYSIS ILLUSTRATED FOR EXPERIMENTAL DATA FROM RUN NUMBER 29.

z ft	$(v_r)_{exp}$ ft/min	$(v_r)_{calc}$ ft/min
0.058	36.6	32.7
0.050	38.4	44.4
0.042	54.4	58.9
0.033	70.5	75.3
0.025	95.7	92.0
0.017	109.2	106.4
0.008	116.7	115.4
0.000	117.5	116.8
-0.008	111.2	110.2
-0.017	99.3	97.3
-0.025	77.4	81.1
-0.033	61.5	64.4
-0.042	42.2	49.1
-0.050	41.0	36.4

Correlation coefficient R = 0.99

where $h_a - h_b$ is the linear distance between taps P_4 and P_5. This linear distance is small and hard to measure, however it is recognized that $\rho_w(h_a-h_b)$ is the static head recorded by the manometer under no flow conditions. This static head is called ΔH_s and was found equal to 1.0 in. of manometer fluid. In terms of the static head ΔH_s, h_a-h_b is given by

$$h_a - h_b = \Delta H_s(\rho_w-\rho_m)/\rho_w \qquad \text{(IV-25)}$$

Combining IV-25 and III-3 gives

$$P_4 - P_5 = (\Delta H_s - \Delta H_n)(\rho_m - \rho_w) \qquad \text{(IV-26)}$$

Hypothesize that the pressure drop $P_4 - P_5$ is the pressure differential due to the vertical component of velocity $\bar{v}_z$. Then as in Section 4.3, Figure IV-12 gives the geometry of the three dimensional flow field acting on the probe. The resultant velocity $\vec{V}$ approaches the probe at a pitch angle of θ_p and a yaw angle of θ_y. From the geometry of Figure IV-12 it follows that

$$\bar{v}_z = |\vec{V}| \sin \theta_p \qquad \text{(IV-27)(a)}$$

$$\bar{v}_r = |\vec{V}| \cos \theta_p \cos \theta_y \qquad \text{(IV-27)(b)}$$

$$\bar{v}_\theta = |\vec{V}| \cos \theta_p \sin \theta_y \qquad \text{(IV-27)(c)}$$

As in the case of Section 4.3, Equation IV-15 is used to calculate the pressure ratio α. Curves A and B of Figure IV-5 are then interpolated to evaluate the pitch angle θ_p and a corrected value of the pressure (ΔP_{12}) corrected. Equation IV-16 is then used to

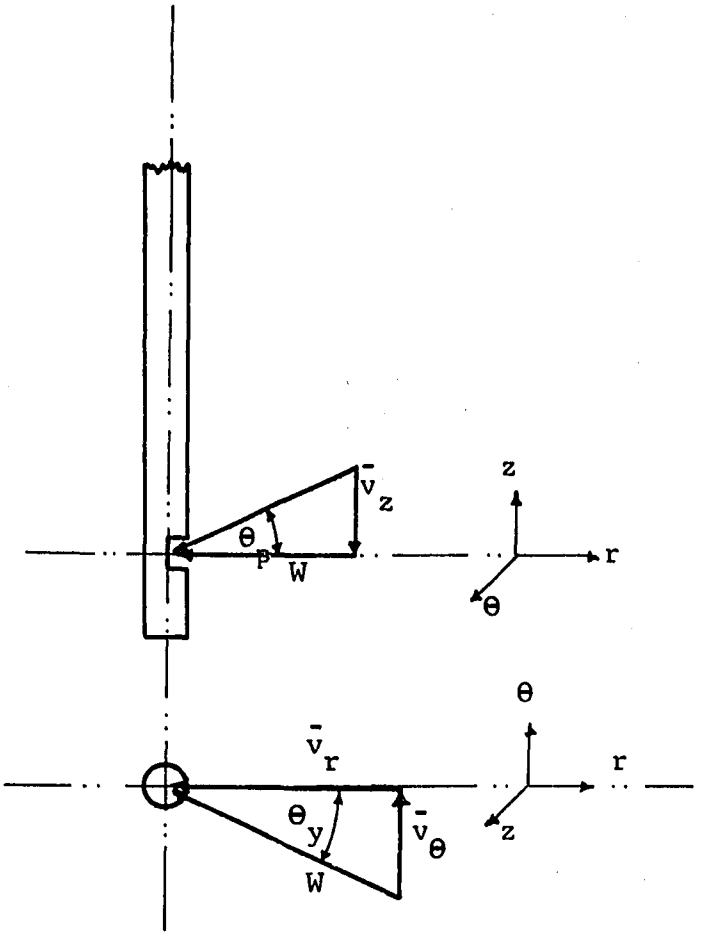

Figure IV-12: Resolution of Velocity $\vec{V}$ into its Components, when Probe is Placed in the Region of the Impeller

evaluate $\vec{V}$. The component velocities $\bar{v}_r$, $\bar{v}_\theta$ and $\bar{v}_z$ is then evaluated from Equations IV-27 to IV-29. These calculations are performed by the program YAWANL. The results of the calculations by YAWANL is given in Table IV-18 and is typical of the analysis obtained for a velocity profile measurement. Table IV-18 illustrates the results by analyzing the experimental data from Run Number 29.

Two things are evident in Table IV-18, (a) five of the points cannot be analyzed indicating that the pitch angle is larger than $\pm 40°$, (b) the valve of $\bar{v}_z$ is large and about the same magnitude as $\bar{v}_\theta$. Also $\bar{v}_z$ decreases as the magnitude of z increases. This behavior is inconsistent with the jet model which assumes $\bar{v}_z$ is small and that $\bar{v}_z$ increases with increasing magnitude of z. It is also physically impossible for the fluid in the impeller stream to have a pitch angle θ_p larger than 40°. The conclusion is that this hypothesis is not valid and some other phenomena is the cause of the pressure drop recorded by manometer D.

Since $P_4 - P_5$ is a kinetic head caused by the motion of the fluid, it was concluded that the pressure drop is due to the high velocity gradient present in the tangential jet. This is expected since the tangential jet is a high shear flow and the boundary layer assumptions hold.

Because of the velocity gradient, the velocities at the pressure taps P_4 and P_5 are different. Let these velocities be $\vec{q}_4$ and $\vec{q}_5$. If P_s is the stagnation pressure then from pitot tube theory (44) we can write the following relation

TABLE IV-18

RESULTS OF PROGRAM YAWANL WHICH TREATS THE IMPELLER REGION AS A THREE-DIMENSIONAL FLOW FIELD, AND ILLUSTRATED FOR EXPERIMENTAL DATA FROM RUN NUMBER 29

Item No.	z in.	ΔP_{12}*	ΔP_{45}*	(ΔP_{12})* Corrected
1	0.7	1.35	-0.8	1.6
2	0.6	1.40	-4.1	**
3	0.5	2.65	-7.6	**
4	0.4	4.40	-8.8	**
5	0.3	7.90	-9.8	9.5
6	0.2	10.00	-7.1	11.9
7	0.1	11.40	-1.1	12.9
8	-0.0	11.45	5.6	12.2
9	-0.1	10.40	10.0	11.3
10	-0.2	8.40	11.4	9.5
11	-0.3	5.35	10.8	**
12	-0.4	3.50	8.2	**
13	-0.5	1.70	4.7	**
14	-0.6	1.60	2.4	1.8

Item No.	z in.	$\bar{V}$ ft/min.	$\bar{v}_r$ ft/min.	$\bar{v}_z$ ft/min	$\bar{v}_\theta$ ft/min.	Pitch Angle θ_p°	Yaw Angle θ_y°
1	0.7	48.7	39.3	-7.9	27.7	-9.4	35.2
5	0.3	119.0	92.2	-57.1	49.0	-28.7	28.0
6	0.2	133.0	115.6	-31.1	57.9	-13.5	26.6
7	0.1	138.4	123.7	11.0	61.3	4.5	26.4
8	-0.0	135.0	114.9	44.2	55.5	19.1	25.8
9	-0.1	129.5	102.8	59.6	51.5	27.4	26.6
10	-0.2	118.8	88.1	65.3	45.7	33.4	27.4
14	-0.6	52.4	35.8	30.4	23.1	35.5	32.8

* Inches Manometer fluid
** Yaw Angle θ_p greater than 40°

$$\bar{q}_4^{-2} - \bar{q}_5^{-2} \doteq \frac{2g}{\rho_w}\left[(P_4-P_s) - P_5 - P_s\right] \qquad \text{(IV-28)(a)}$$

Since the pressure taps P_4 and P_5 are close together (about 0.1 in. apart) the stagnation pressure P_s is approximately constant. Lumping all the approximations in a coefficient of performance c_1 and noting that $q_4^2 - q_5^2$ is a change in $\bar{q}^{-2}$ in the z-direction we have

$$\Delta\bar{q}^{-2} = c_1 2g\,(P_4-P_5)/\rho w \qquad \text{(IV-28)(b)}$$

The coefficient of performance c_1 can be defined by

$$c_1 = \frac{\Delta q^2_{exp}}{\Delta q^2_{calc}} \qquad \text{(IV-29)(a)}$$

where Δq^2_{exp} is given by

$$\Delta\bar{q}^{-2}_{exp} = 2g(P_4-P_5)/\rho_w \qquad \text{(IV-29)(b)}$$

$\Delta\bar{q}^{-2}_{calc}$ is obtained by calculating $\bar{q}$ from Equation II-10 at a distance $\eta \pm \Delta\eta$ where $\Delta\eta$ is given by

$$\Delta\eta = \frac{h_a - h_b}{2r} \qquad \text{(IV-30)}$$

η is the value of the dimensionless velocity profile coordinate at the mid-point of the pressure taps P_4 and P_5. $\Delta\eta$ in Equation IV-30 then locates the pressure taps P_4 and P_5 relative to the dimensionless coordinate η. $\Delta\bar{q}^{-2}_{calc}$ can now be written as

$$\Delta\bar{q}^{-2}_{calc} = \bar{q}^{-2}_{max}\left[(1-\tanh^2(\eta+\Delta\eta)/2)^2 - (1-\tanh^2(\eta-\Delta\eta)/2\right] \qquad \text{(IV-31)}$$

From a plot of c_1 versus $1/\bar{q}^2_{exp}$ for a few points it appeared that a correlation exist. Hence a fourth order polynomial was fitted through the point c_1 versus $1/\bar{q}^2_{exp}$ using a Share Library program CURVEF. Next points which were located more than three times the standard error (which is an estimate of the standard deviation) were removed from the correlation. The remaining points gave an average value of 0.5216 and a variance of 0.0413 indicating that c_1 is a constant. The original data had 471 points the above procedure reduced the number of points to 440. Since such a large number of points were considered the variance will be considered as the best estimate of the standard deviation, hence with a 0.95 probability, and assuming a normal distribution the best estimate for c_1 is

$$c_1 = 0.52 \pm 0.02 \qquad \text{(IV-32)}$$

This value of c_1 was used in Equation IV-28 to obtain $\Delta\bar{q}^2$ which is shown in Table IV-19. The agreement between the experimental and theoretical values of $\Delta\bar{q}^2$ is fairly good with a deviation of ± 0.2 as seen in the last column which shows the difference between experimental and calculated values of $\Delta\bar{q}^2$. Both experimental and theoretical values show a maximum for $z = \pm 0.025$ ft, a strong evidence that the manometer D is recording $\Delta\bar{q}^2$. The value of $\bar{v}_z$ as obtained from the tangential jet model is also shown for comparison and are seen to be extremely small. The results of the above analysis which is shown in Table IV-19 is calculated by the subroutine YAW. This subroutine is part of program FLOWANL that analyses the experimental velocity profile data.

TABLE IV-19

RESULT OF ANALYSIS BY SUBROUTINE YAW THAT TREATS THE REGION OF THE IMPELLER AS A REGION OF HIGH SHEAR, FOR EXPERIMENTAL DATA OF RUN NUMBER 29

Item Number	z ft.	Δq^2 ft^2/min^2	Δq^2_{cal} ft^2/min^2	$(\bar{v}_z)_{calc}$ ft/min	$\Delta q^2 - \Delta q^2_{calc}$ ft^2/min^2
1	0.058	-0.23	-0.24	-0.24	-0.01
2	0.050	-0.57	-0.42	-0.15	0.15
3	0.042	-0.94	-0.66	-0.12	0.28
4	0.033	-1.07	-0.91	-0.08	0.16
5	0.025	-1.18	-1.05	-0.04	0.13
6	0.017	-0.89	-0.91	-0.02	-0.02
7	0.008	-0.26	-0.44	-0.00	-0.18
8	0.000	0.44	0.22	0.01	-0.22
9	-0.008	0.90	0.79	0.01	-0.11
10	-0.017	1.05	1.04	1.03	-0.02
11	-0.025	0.99	0.98	0.06	-0.01
12	-0.033	0.71	0.75	0.10	0.04
13	-0.042	0.25	0.50	0.14	0.15
14	-0.05	0.11	0.30	0.18	0.19

4.6. Accuracy of the Three-Dimensional Pitot Tube as a Measuring Device in Turbulent Flow Fields

On examining a recent dissertation by Rao (24), it was pointed out that the readings obrained by the three dimensional probe was in error. The error is due to distortion of the turbulence field; (a) by the probe (called nose effect) and (b) by suppression of the normal velocities in the neighborhood of the pitot tube surface (called surface effect). The distortion of the turbulence is also a function of the size of the eddies (defined by the macro-scale) and the radius of the Pitot tube. An analysis of these factors is given by Toomre (24), and a summary of the analysis is given by Rao. Rao checked the results of the pitot tube by a hot film anemometer.

The system in which Rao made his measurements consists of a 11 5/8 in. diameter pyrex glass cylinder. The bottom of the tank is a 10μ porous stainless steel plate that acts as a distributor for an upward flow of water at 6.625 liters per minute. The tank is baffled and the overflow water is collected by a weir, at the top of the tank. The reason for this upward draft of water is to sweep out the dye introduced into the tank for turbulence measurements. The impeller used is a Type B, 4.0 in. diameter turbine. At the bottom of the impeller is notched a 1.5 in. diameter recess, 0.4 cm thick, which serves to introduce the dye directly into the impeller at a rate of 1.753 liters per minute.

A three dimensional pitot tube similar to the one used in this work was used to measure velocity profiles in the neighborhood of

impeller. The impeller was run at a single speed of 300 RPM. The various pressure differentials from the five pressure taps were measured by a single differential pressure transducer, Model P7 (The Pace Engineering Company) using a system of three way stop cocks. The stop cocks permit connecting the transducer to any two pressure taps. An auxilliary manometer was used for calibration.

This three dimensional pitot tube was used to locate yaw angle θ_y and the pitch angle θ_p. the pitch angle was obtained from the manufacturers calibration chart of $(P_4-P_5)/(P_1-P_2)$ versus θ_y as explained in Section 4.3. The hot film probe was then introduced into the system at exactly the same point and directed along the yaw angle. A linearized signal E, in volts was obtained from the instrument and was a linearized form of King's law. As described in Chapter I, the hot film (or wire) is sensitive to the normal component of velocity. If $\vec{V}$ is the true velocity having a pitch angle θ_p then the anemometer will respond to the velocity normal to it namely $\bar{V} \cos \theta_p$ and from King's law we have

$$\bar{V} \cos \theta_p = A\bar{E} + B \qquad \text{(IV-33)}$$

$\bar{E}$ is the linearized average voltage from the anemometer, and A and B are calibration constants of the instrument. It can be shown that if if e' is the fluctuating voltage that, the intensity of turbulence v' is given by

$$v' \cos \theta_p = Ae' \qquad \text{(IV-34)}$$

$\bar{V}$ is thus obtained from IV-33. Knowing θ_p and θ_y, $\bar{v}_r$, $\bar{v}_\theta$ and $\bar{v}_z$ can be calculated from the geometry of the system. θ_p was evaluated by using the three dimensional pitot tube.

Using the above method, Rao obtained a value of $\bar{V}$ from IV-33 which is lower than $\bar{V}$ from the pitot tube by about 50%. $\bar{V}$ from the pitot tube was calculated from

$$\bar{V} = \sqrt{2g\Delta H_{12}} \qquad \text{(IV-35)}$$

where ΔH_{12} is the pressure drop across pressure taps P_1 and P_2. Apparently Rao uses the manufacturers calibration chart to calculate θ_p, however he did not use these charts to get a corrected ΔH_{12} as described in Section 4.3. Nor does he examine the flow geometry as was done in Figure IV-12.

On examining the velocity profile measured at four values of (2.5, 3.0, 3.5, and 4.0 inches) it was found that z_o the displacement of the jet ranged from 0.031 to 0.038 ft. above the impeller centerline. In our jet z_o is of the order of 0.003 and in only one case has an excessively large value of 0.079. The large value of z_o obtained by Rao is attributed to the upward flow of water and dye.

The quantity BHALF, the point at which the velocity equals half the maximum velocity was also calculated for these four profiles and was found to range from 0.038 to 0.11 feet. The value of BHALF is calculated relative to the maximum velocity where z is taken equal to zero. Our values for the tangential jet ranges

from 0.033 to 0.067. This indicates that the type B turbine exhibits a broader jet. The tangential jet model could thus still apply.

It was shown in Section 4.6 that for a tangential jet $\bar{v}_z$ is very small for z less than BHALF. Rao's profiles were measured a little beyond BHALF. Hence the pressure differential, P_4-P_5, is as was shown in the previous section due to $\Delta\bar{q}^2$; and the pitch angle which has been calculated is thus erroneous. Since cos θ_p is needed in Equation IV-33 as a correction factor, it is bound to give lower values of $\bar{V}$, for θ_p greater than zero. As the raw data is not given, it was not possible to check the above conclusions quantatively.

Rao used Toomre's analysis to estimate a correction factor for the pitot tube. The nose effect was assumed zero. Using a maximum possible value for the surface effect. Rao obtained a correction that was 10% lower than the experimental value. This calculation cannot be repeated for our work since it requires a knowledge of $\bar{v}'$, the intensity of turbulence.

It is possible that the surface effect could have an effect on the pitot tube reading and is perhaps a maximum of 10% as shown by Rao using Toomre's method (which is itself is an approximate method). We agree with Rao that it is necessary to know more quantatively the effect of turbulence on pitot tube measurements. In absence of any concrete evidence it was thought best to not include a correction

factor on the velocity profiles since it is small and may very well be within the precision of the subsequent analysis using the tangential jet model.

4.7. Comparison with Coopers (8) Data

From the review of Cooper's work in Chapter I, it will be recalled that Cooper used a similar measuring device as in this work and has measured velocity profiles only in the region of the impeller. Cooper however did not present his raw data, nor indicated by way of a sample calculation how the resulting velocity profiles $\vec{q}$, were obtained. Tables are presented of $\vec{q}$ in (in./sec.) for various cases together with the corresponding yaw angle θ_y. These tables have been conveniently punched on cards for making a nonlinear least square fit to the tangential jet model. The analysis was done by reading the data for a single table as a matrix and analyzing the several flow profiles in the table by the program COOPER. The program COOPER is very similar to FLOWANL, the difference is mainly in data processing. Since Cooper's data exists as a velocity profile, several profiles at constant impeller diameter are read in and stored. The program COOPER then analysed one profile at a time using the same subroutines as FLOWANL to obtain a least square fit of the data for the tangential jet model. The subroutines used are, PATERN, PROC, BOUNDS, and AVG. The program COOPER is given in Appendix F together with the input data.

To obtain the velocity profile data, Cooper used a two dimensional probe. This probe is similar to the probe used in this

TABLE IV-20: SUMMARY OF TANGENTIAL JET ANALYSIS FOR DATA OBTAINED WITH A DIRECTIONAL PITOT TUBE

Data Set Number	Item No.	σ	A ft^3/min	a ft.	Impeller Speed RPM	Q ft^3/min	Q/ND^3	$\bar{\theta}_y$ °	ND^3 ft^3/min
		T = 15.0 IN., D = 3.0 IN., FLUID USED IS WATER, COOPER (8)							
1	1	11.5	9.8	0.105	200.0	3.33	1.067	57.2	3.13
	2	11.8	14.1	0.105	300.0	4.74	1.012	57.0	4.69
	3	11.6	15.0	0.109	400.0	4.88	0.780	60.2	6.25
	4	14.4	19.2	0.101	500.0	6.11	0.782	53.9	7.81
	5	12.5	22.5	0.104	600.0	7.46	0.795	56.2	9.38
		T = 15.0 IN., D = 4.0 IN., FLUID USED IS WATER, COOPER (8)							
2	1	14.1	7.9	0.139	100.0	3.26	0.880	56.6	3.70
	2	12.1	11.9	0.142	150.0	5.20	0.935	58.5	5.56
	3	13.6	17.1	0.140	200.0	7.12	0.961	57.3	7.41
	4	11.3	20.6	0.145	250.0	8.98	0.969	60.7	9.26
	5	11.7	23.0	0.146	300.0	9.82	0.883	60.9	11.11
		T = 15.0 IN., D = 5.0 IN., FLUID USED IS WATER, COOPER (8)							
3	1	12.5	12.8	0.173	100.0	7.06	0.975	56.2	7.23
	2	12.7	20.1	0.171	150.0	11.13	1.025	55.4	10.85
	3	12.8	26.5	0.169	200.0	14.83	1.025	54.2	14.47
	4	12.6	34.0	0.170	250.0	19.04	1.053	54.7	18.08
	5	12.7	37.1	0.171	275.0	20.63	1.037	55.1	19.89
		T = 15.0 IN., D = 6.0 IN., FLUID USED IS WATER, COOPER (8)							
4	1	11.7	14.2	0.202	50.0	9.96	1.593	54.0	6.25
	2	11.8	19.5	0.203	100.0	13.67	1.093	54.3	12.50
	3	11.7	24.5	0.203	125.0	17.12	1.095	54.4	15.63
	4	12.6	29.4	0.204	150.0	19.86	1.059	54.6	18.75
	5	12.3	33.7	0.201	170.0	23.47	1.104	53.4	21.25
		T = 12.25 IN., D = 3.0 IN., FLUID USED IS WATER, THIS WORK							
5	1	10.5	13.5	0.114	243.0	4.18	1.101	65.8	3.80
	2	10.1	14.3	0.119	250.0	3.92	1.002	72.2	3.91
	3	11.8	18.6	0.115	333.3	5.28	1.014	67.3	5.29
	4	11.8	22.7	0.117	400.0	6.18	0.988	69.3	6.25
	5	11.4	28.4	0.112	500.0	8.87	1.135	63.3	7.81
	6	11.6	31.6	0.112	550.0	9.81	1.141	63.1	8.59
		T = 11.5 IN., D = 3.0 IN., FLUID USED IS WATER, THIS WORK							
6	1	10.7	17.9	0.122	333.3	4.13	0.793	76.6	5.21
		T = 15.0 IN., D = 4.0 IN., FLUID USED IS AIR , COOPER (8)							
7	1	13.7	13.3	0.143	200.0	5.40	0.729	58.9	7.41
	2	13.0	19.1	0.143	300.0	7.95	0.715	59.0	11.11
	3	14.3	26.4	0.143	366.0	10.49	0.774	58.8	13.56
	4	15.2	35.8	0.141	500.0	14.05	0.758	57.8	18.52
	5	14.6	43.9	0.141	600.0	17.51	0.788	57.9	22.22
		T = 15.0 IN., D = 5.0 IN., FLUID USED IS AIR , COOPER (8)							
8	1	12.9	20.5	0.169	200.0	11.43	0.790	54.1	14.47
	2	13.6	31.3	0.169	300.0	17.04	0.785	54.0	21.70
	3	14.1	43.8	0.169	400.0	23.36	0.807	54.0	28.94
	4	14.0	57.2	0.167	500.0	30.95	0.856	53.1	36.17
	5	14.0	67.6	0.169	600.0	36.29	0.836	54.0	43.40
		T = 15.0 IN., D = 6.0 IN., FLUID USED IS AIR , COOPER (8)							
9	1	11.9	18.1	0.202	100.0	12.68	1.014	53.7	12.50
	2	12.6	34.0	0.200	200.0	23.41	0.937	53.0	25.00
	3	12.9	46.6	0.200	300.0	31.64	0.844	53.0	37.50
	4	13.7	81.6	0.200	500.0	53.69	0.859	53.0	62.50
	5	13.6	95.3	0.200	600.0	63.09	0.841	53.0	75.00

work with the taps P_4 and P_5 removed. No serious loss of information results from using this probe as can be seen from our analysis of pitch angles in Section 4.5 and the discussion on velocity measurements in the impeller stream in Section 4.4. (The two dimensional probe is placed within a tenth of an inch off the impeller periphery, and hence the velocity profile measured can be considered as a good estimate of the velocity profile at the impeller periphery.)

As in the case of our data, a velocity factor was used to obtain, a, the radius of the tangential jet source. A velocity factor of 0.5 gave the best fit for the radial velocity profile. However the difference between the correlation coefficients of $\vec{q}$ and $\bar{v}_r$ is much larger for Cooper (8) than in ours. The correlation coefficient for $\vec{q}$ ranges from 0.97 to 0.99 while that of $\bar{v}_r$ range from 0.92 to 0.97. This indicates that the tangential jet model gives a good predication of the experimental data. As in our data, the velocity factor had very little effect on σ but caused small changes in A the volumetric factor and, a, the jet radius.

In Appendix G is given a detailed summary of the analysis of Cooper's data. Table IV-20 gives a summary of the results from Appendix G, and consists of nine sets of data, each set at a constant impeller diameter. Its purpose is to facilitate comparison of all Pitot tube measurements.

Examining these nine sets of data, some of the items are found to be approximately constant. These are σ, a, N_Q and $\bar{\theta}_y$. These quantities have been averaged and a 0.95 confidence limit using a t-test have also been calculated. The results are reported in

Table IV-21. The confidence limits are reported under the heading $\Delta\sigma$, Δa etc. The impeller diameter and tank diameter for which these average values correspond and the fluid used are also given in Table IV-21.

Jet Width σ

Various correlations were tried to relate the data presented in Table IV-20. In Figure IV-13 is shown a log-log plot of σ versus ND^3. The data correlates very well along a line drawn through the average value of σ, indicating that σ is a constant. Since the data consists of two fluids, air and water this means that turbulence and not viscosity is the significant variable in the impeller stream. The average value of σ for all the data in Table IV-20 is

$$\sigma = 12.621 \pm 0.066 \qquad \text{(IV-36)}$$

The confidence limit of 0.066 on σ might be misleading since the confidence limit on our data is rather large, equal to 2.66 (see Equation IV-9). It should be noted that Cooper reports only one profile for each condition investigated, hence it is not possible to estimate the confidence limit on the parameters obtained by the least square fit of a velocity profile from his data.

If the average value of σ at constant impeller diameter is examined in Table IV-21, these values are found to fall into three groups. Items 1 to 4 are Coopers data for water, Items 5 to 6 are, our data in water and Items 7 to 9 which are Coopers data in air. In each group the value of σ appears approximately constant. The

TABLE IV-21: AVERAGE VALUES OF JET WIDTH σ , RADIUS OF SOURCE a, DIMENSIONLESS PUMPING CAPACITY N_Q AND WEIGHTED AVERAGE YAW ANGLE $\bar{\theta}_y$ EXTRACTED FOR DATA SETS OF TABLE IV-20

Data Set Number	T in.	D in.	Fluid Used*	D/T	σ	$\Delta\sigma$	a ft.	Δa	N_Q ft^3/min	ΔN_Q	$\bar{\theta}_y$°	$\Delta\bar{\theta}_y$
1	15.00	3.00	W	0.20	12.4	1.5	0.105	0.003	0.887	0.174	56.9	2.8
2	15.00	4.00	W	0.27	12.6	1.5	0.143	0.004	0.926	0.052	58.8	2.4
3	15.00	5.00	W	0.33	12.7	0.1	0.171	0.002	1.023	0.036	55.0	0.9
4	15.00	6.00	W	0.40	12.0	0.5	0.203	0.002	1.189	0.281	54.1	0.6
5	12.25	3.00	W	0.24	11.2	0.8	0.115	0.003	1.064	0.074	66.8	3.7
6	11.50	3.00	W	0.26	10.7		0.122		0.793		76.6	
7	15.00	4.00	A	0.27	14.2	1.0	0.142	0.001	0.753	0.038	58.5	0.7
8	15.00	5.00	A	0.33	13.7	0.6	0.168	0.001	0.815	0.038	53.8	0.5
9	15.00	6.00	A	0.40	12.9	0.9	0.200	0.001	0.899	0.094	53.1	0.4

*W = water
A = air

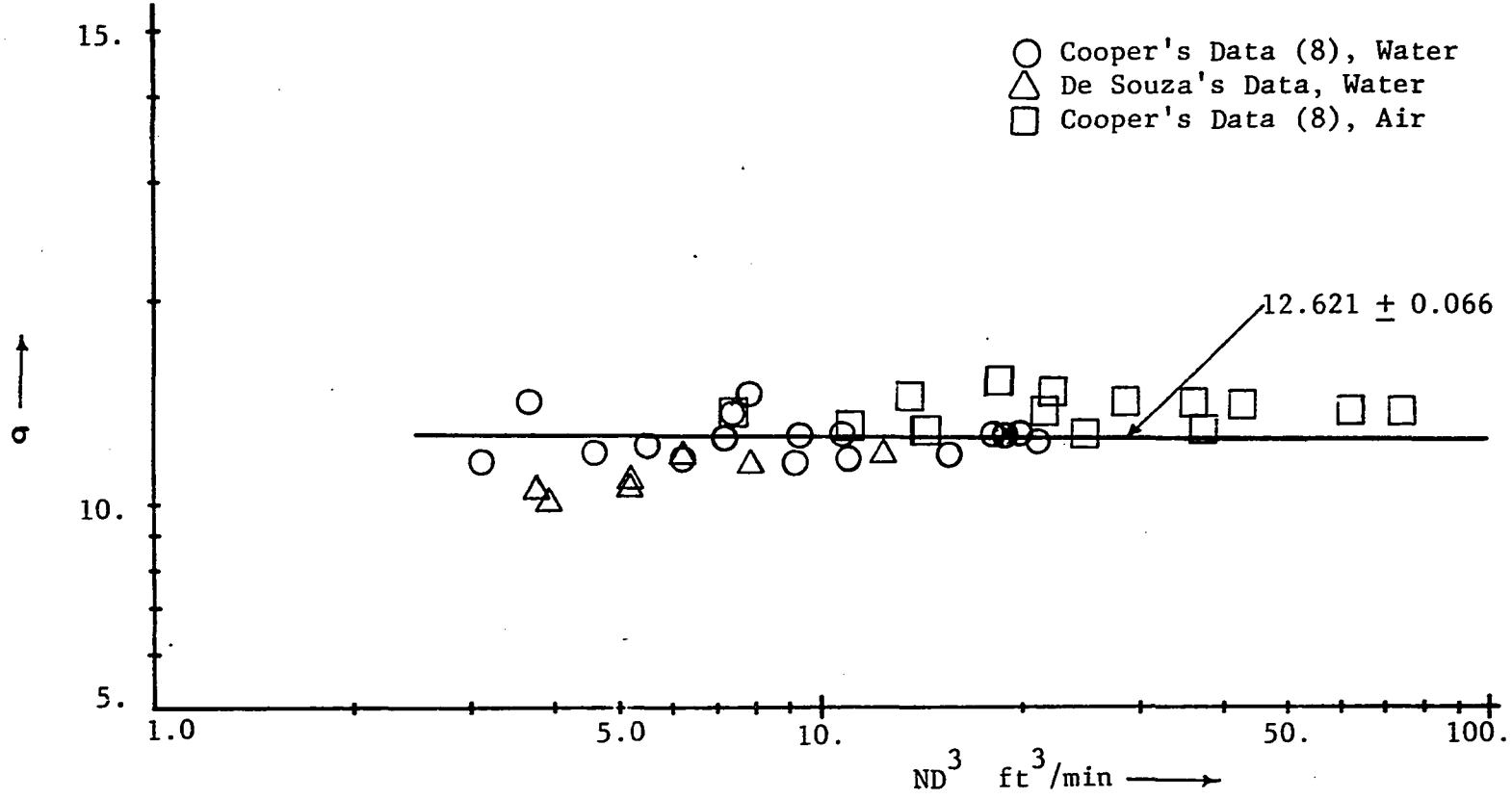

Figure IV-13: Correlation for jet width parameter σ

confidence limits for these nine items are also larger than that of the overall average given in Equation IV-36. These groupings are not visible when the individual data points are plotted in Figure IV-13. This suggests more exhaustive measurements are needed to conclude that σ is independent of tank diameter and fluid in the tank. The data presented here suggests that σ is a universal constant independent of tank geometry, impeller speed, and fluid used in the tank.

Radius of Source a

In Table IV-20 the radius of source, a, is reported for a number of profiles. It is observed that in each set of data at constant impeller diameter, a, is approximately constant. This is seen to be the case when the average value and confidence limit is examined in Table IV-21. The confidence limit is of the order of 0.003 indicating that, a, is constant to two significant figures.

From Table IV-20, a, is seen to be a function of both impeller diameter and tank diameter. In Figure IV-14 is shown a log-log plot of, a, versus D/T also shown is the regression line calculated by program GRAPH (for listing see Appendix F). The plot shows that, a, for both air and water are almost identical. However the points obtained by using a smaller tank does not correlate very well. The value predicted by the regression line for our data is found to be larger than D/2 the impeller radius. This violates the constraint on, a, which was discussed in Chapter II.

It thus appears that D/T is not a good criteria for correlating, a. As the flow occurs in the region between the periphery of the

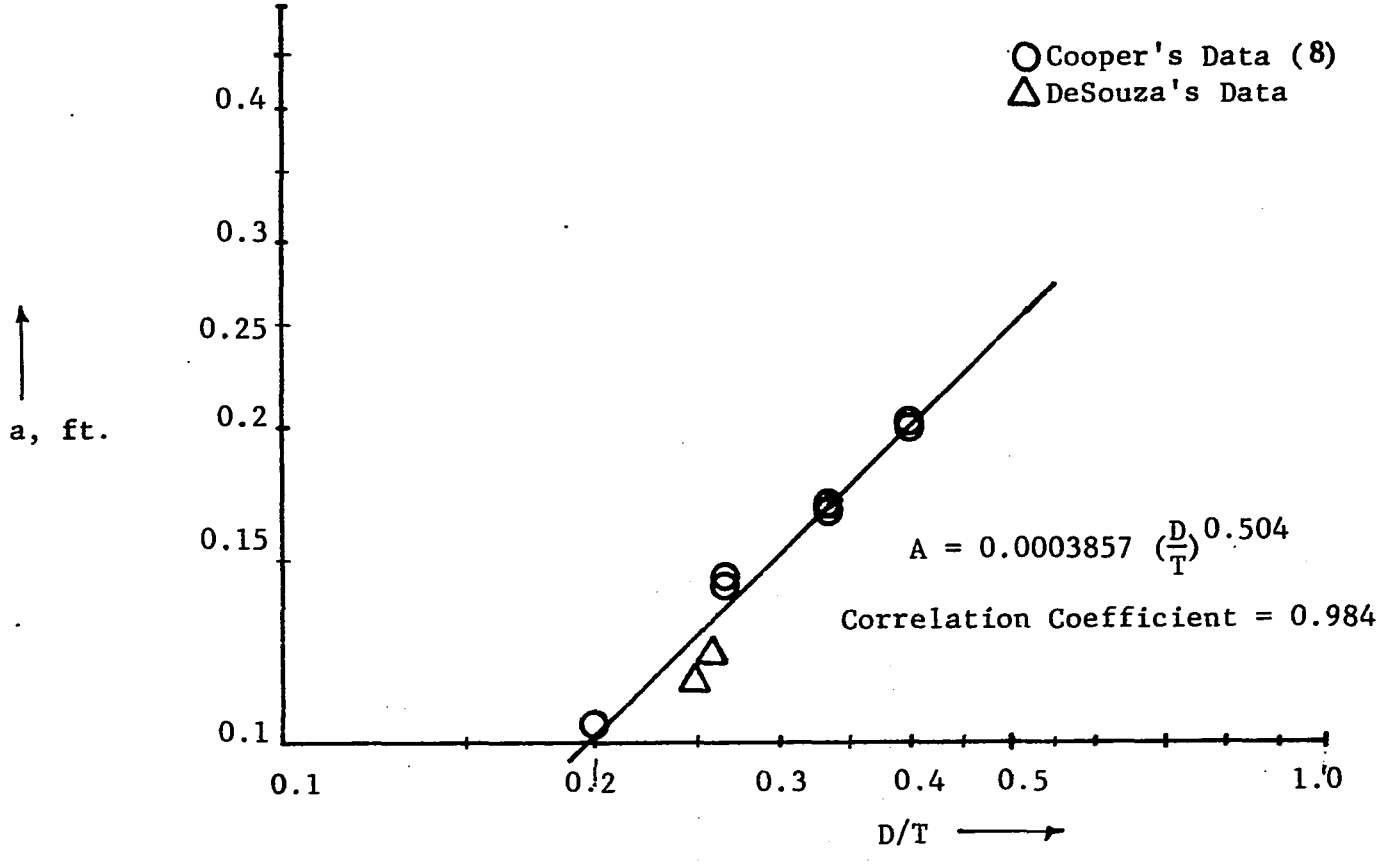

Figure IV-14: Correlation for Radius of Source a with D/T

impeller and the tank wall, changing the tank diameter would alter the length of this region which is measured by T-D. Accordingly Figure IV-15 shows a plot of a versus (D-T)/T. In this plot it is seen that the points at constant impeller diameter correlate better separately. The results are two separate correlations. One at constant impeller diameter of 3.0 inches given by

$$a = 0.06924 \left(\frac{T-D}{T}\right)^{-1.837} \qquad \text{(IV-37)}$$

and the second at constant tank diameter of 15.0 inches

$$a = 0.08354 \left(\frac{T-D}{T}\right)^{-1.7281} \qquad \text{(IV-38)}$$

This relationship can be seen more clearly in Table IV-22 where the value of, a, from Table IV-21 and the predicted value using one of the appropriate Equations IV-37 and IV-38 are also shown. The above two equations are thus useful for interpolating the value of a given in Table IV-20.

Equations IV-37 and IV-38 were used to calculate, a, for Nielson's data analyzed in Section 4.8. The tank diameter used by Nielson was 11.25 in. and is the smallest size tank investigated. It was found that both Equations IV-27 and IV-38 gave values of, a, larger than D/2, the impeller radius for all three impeller used by Nielson. The equations are thus not recommended for tank diameters smaller than 11.5 inches.

From the above discussion it will be necessary to investigate more fully the effect of tank diameter on the parameter, a. The data that is presently available is not sufficient to make a

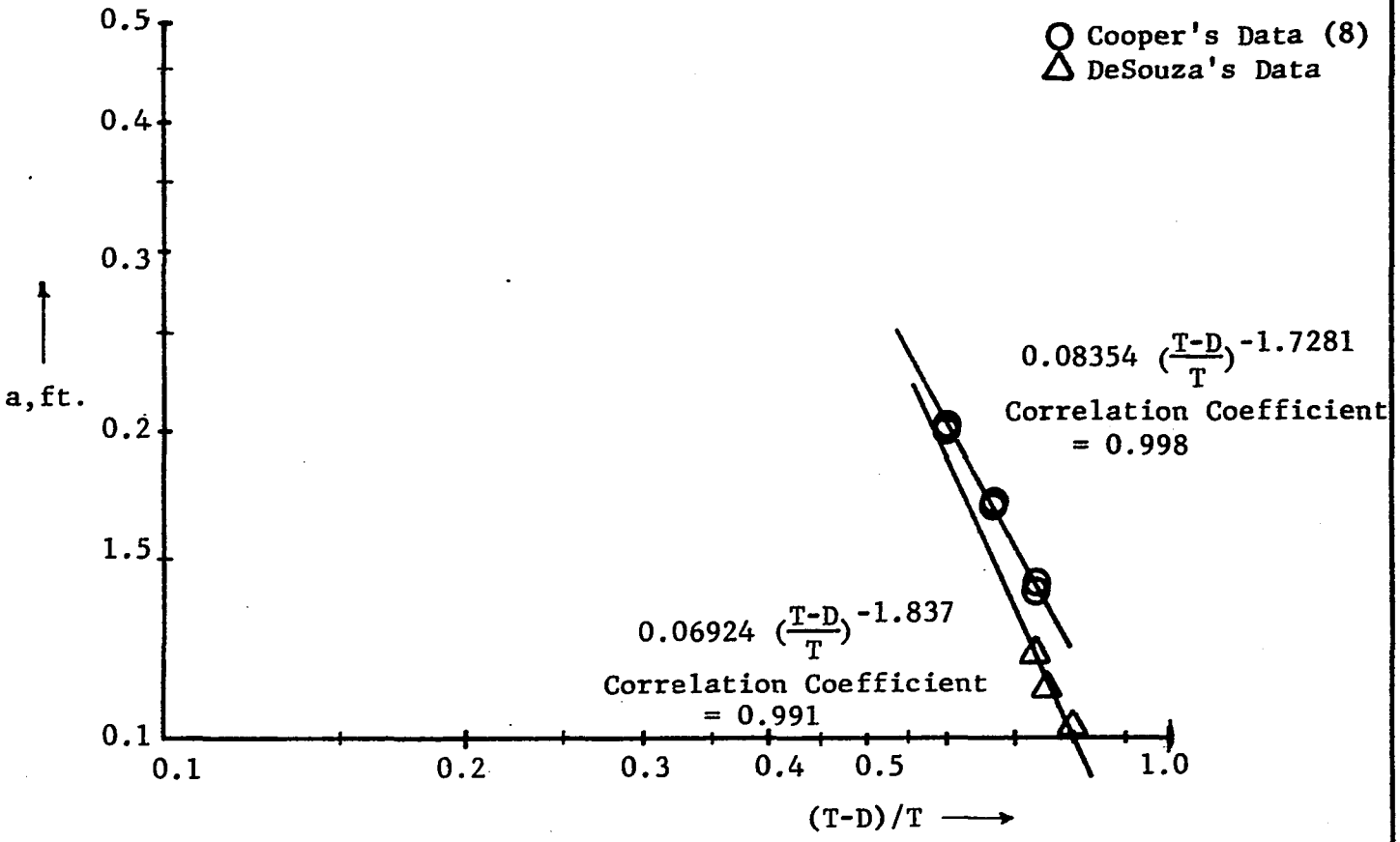

Figure IV-15: Correlation of Radius of Source a with (T-D)/T.

TABLE IV-22

PREDICTED AND EXPERIMENTALLY DETERMINED VALUES

OF a, THE RADIUS OF SOURCE

Item Number	D In.	T In.	(T-D)/T	a, ft. Obtained From Table IV-21	a, ft. Calculated From Equation IV-36	a, ft. Calculated From Equation IV-37
1	3.0	15.0	0.8	0.105	0.104	
2	4.0	15.0	0.73	0.143		0.143
3	5.0	15.0	0.67	0.171		0.168
4	6.0	15.0	0.6	0.203		0.202
5	3.0	12.25	0.76	0.115	0.116	
6	3.0	11.5	0.74	0.122	0.121	
7	4.0	15.0	0.73	0.142		0.143
8	5.0	15.0	0.67	0.168		0.168
9	6.0	15.0	0.6	0.200		0.202

conclusive statement for predicting the behavior of, a.

Dimensionless Pumping Capacity N_Q

The dimensionless pumping capacity $N_Q = Q/ND^3$ appears to be constant for a given impeller and tank diameter as seen in Table IV-21. The confidence limit of Data Sets 1 and 4 are large. Figure IV-16 shows a log-log plot of N_Q versus D/T. No apparent correlation exists. The line drawn through the points is an average value. The confidence limit for the average values is 0.01 which is much smaller than the confidence limits of the individual points given in Table IV-21. The best estimate of N_Q is thus an average value with the confidence limit of $\pm$ 0.28 corresponding to that of Data Set 4 of Table IV-21. Hence,

$$N_Q = 0.93 \pm 0.28 \qquad \text{(IV-39)}$$

This conclusion is in agreement with Equation I-34, Section 3.4 of Chapter I where it was shown that for geometrically similar impellers N_Q is a constant.

Pumping Capacity Q

It should be noted that there is a marked difference in the pumping capacity that was calculated by different investigators. (8,19) This is illustrated by consulting Figure IV-17 which shows the theoretical and experimental values of the radial velocity $\bar{v}_r$ for Run Number 29. This profile has been discussed in Section 4.4. The experimental values are from Table IV-17, and the theoretical line

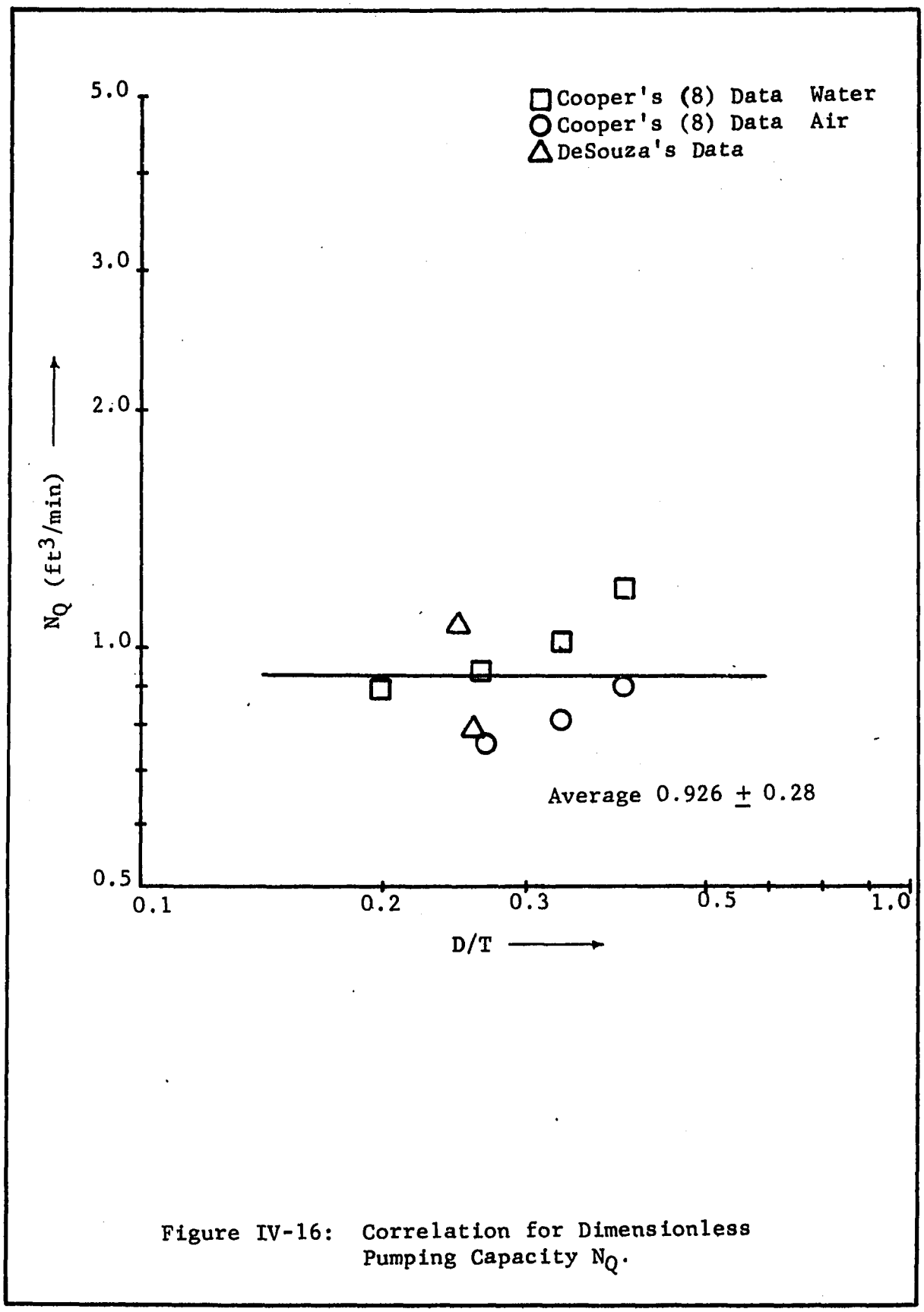

Figure IV-16: Correlation for Dimensionless Pumping Capacity N_Q.

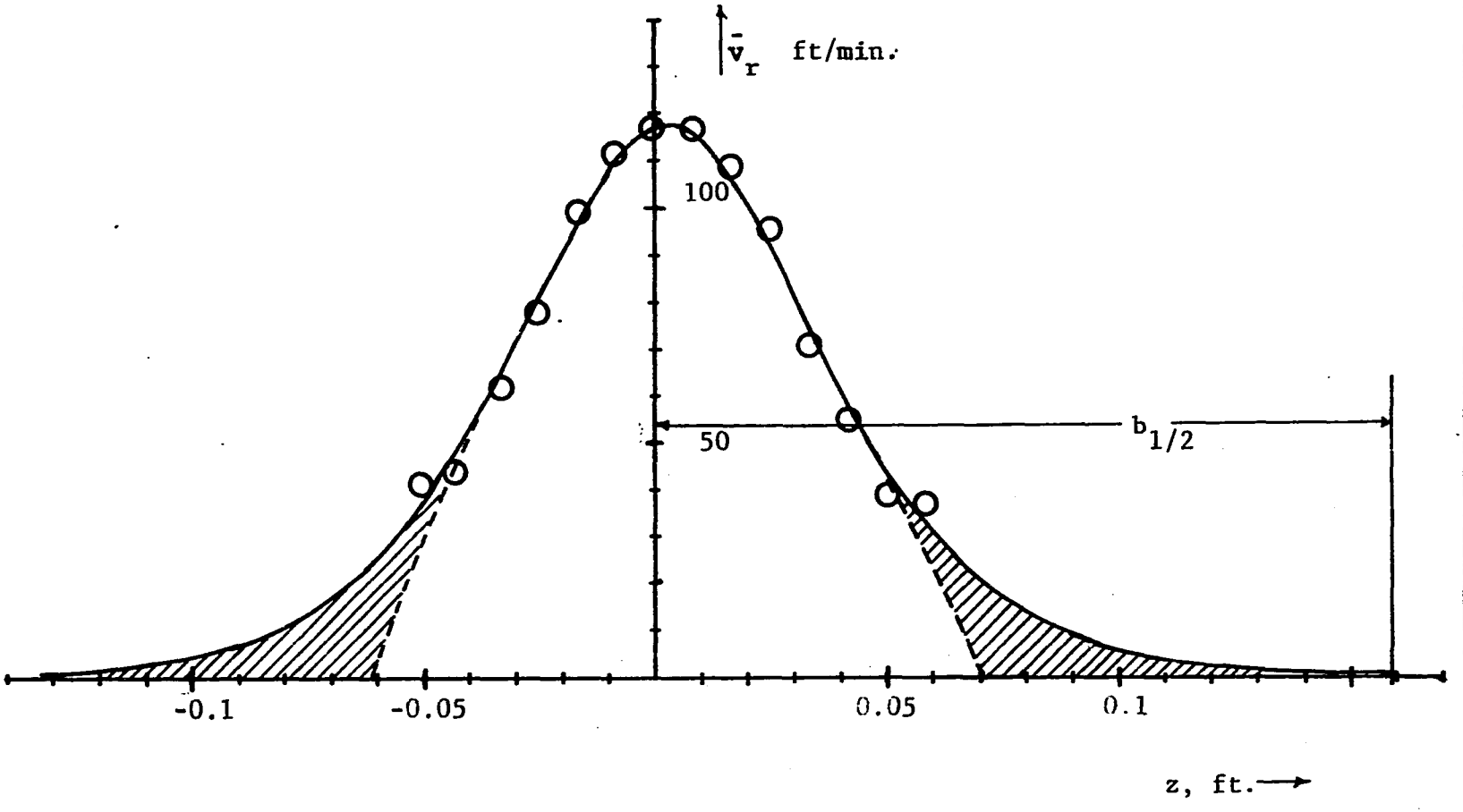

Figure IV-17. Velocity Profile $\bar{v}_r$ for Run Number 29.

line was drawn by using Equation B-22. The tangential jet parameters in Equation B-22 are taken from Table IV-17. Table IV-17 gives a correlation coefficient of 0.99 for $\bar{v}_r$ indicating that the fit is good and is verified by the plot in Figure IV-17. The fit, like that for $\vec{q}$ in Figure IV-11 deteriorates for low velocities.

Cooper in presenting his profiles extropolates the velocities to zero as shown by the dotted lines. As no sample calculations are given it is presumed that the crosshatched areas are omitted in calculating Q the impeller discharge. This is brought out by comparing our values for $\vec{q}$ with those reported by Cooper (8). In all cases our estimation of Q is larger than that of Cooper by 0.5 to as much as 5.0 ft^3/min. The discrepancy is large when $\bar{v}_r$ is large as in the case of the 6.0 inch impeller.

No investigators reviewed by us have measured velocity profiles very far beyond BHALF of Figure IV-11. This is also true of velocity profiles measured by the light streak method to be analyzed in the next section. The value of Q reported in Table IV-20 is calculated using Equation IV-7. This equation includes the crosshatched area of Figure IV-17. Although Equation IV-7 involves integrating $\bar{v}_r$ from $-\infty$ to $+\infty$, it is evident from Figure IV-17 that the contribution to Q beyond $b_{\frac{1}{2}}$ is negligible. $b_{\frac{1}{2}}$ in this case is 0.169 ft.

Figure IV-18 shows a plot of Q versus ND^3. The correlation coefficient for the plot is 0.99, indicating that the correlation is good as can be seen by the low scatter in Figure IV-18. The regression line from program GRAPH is

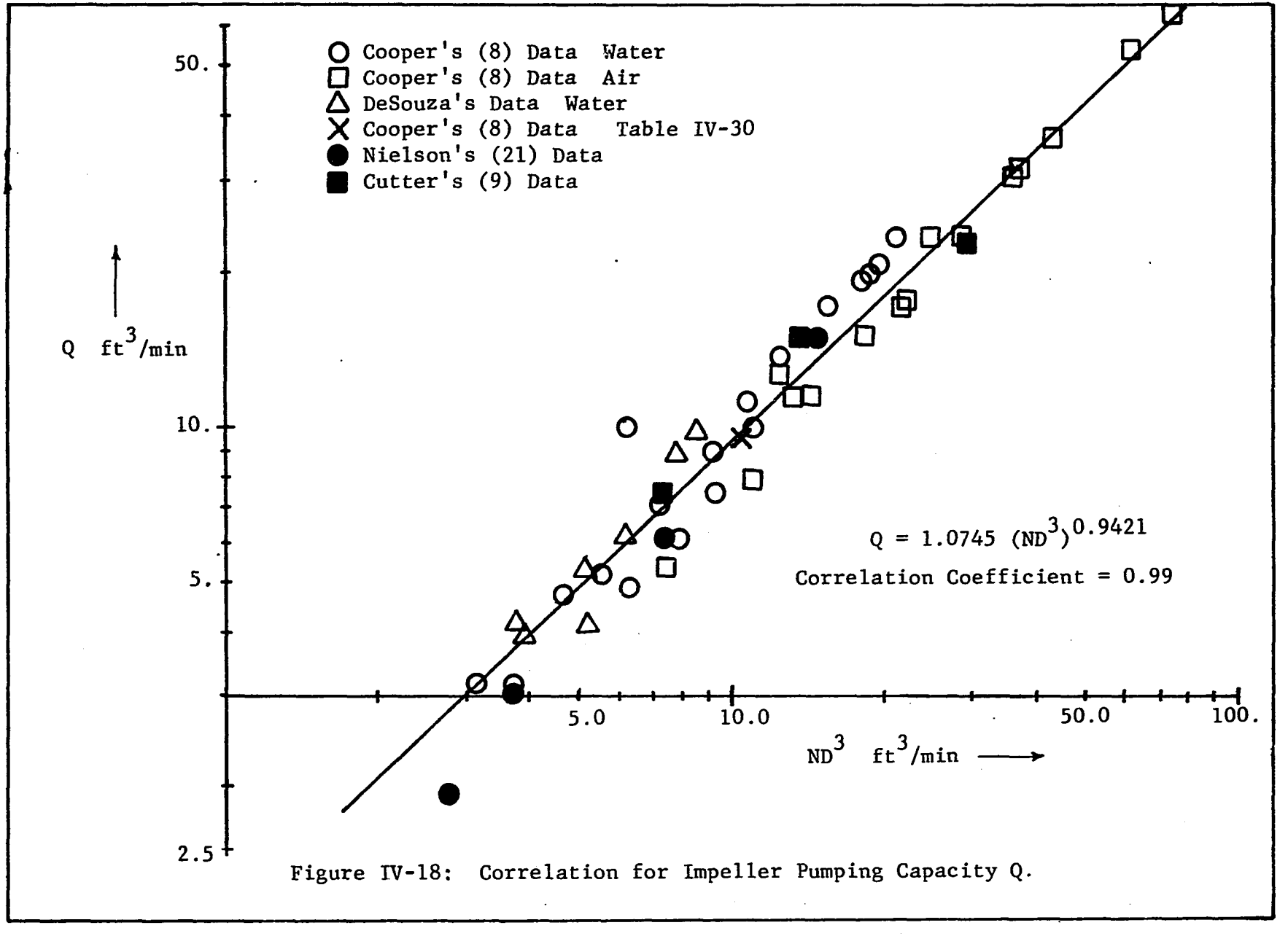

Figure IV-18: Correlation for Impeller Pumping Capacity Q.

$$Q = 1.075\ (ND^3)^{0.942} \qquad \text{(IV-40)}$$

Volumetric Flow Parameter A

The volumetric flow parameter reported in Table IV-20 for several profiles is plotted in Figure IV-19. This is a log-log plot of A versus ND^3. Also shown in the figure is the regression line whose correlation coefficient is 0.958. There is some scatter in the data which is the cause of a low correlation coefficient as compared to that for Q. Our data shown by triangles could be correlated by a separate line roughly parallel to Cooper's data. This shows that A is a function of tank diameter in addition to impeller diameter and impeller speed. We have noticed in Figure IV-2 that A is a scaled value of Q. Since Q correlates very well as shown in Figure IV-18, a logical choice for correlating A would be $ND^3/((D/2)^2-a^2)^{\frac{1}{4}}$. This follows from combining Equations IV-40 and IV-7. In Figure IV-20 is shown a log-log plot of a versus $ND^3/((D/2)^2-a^2)^{\frac{1}{4}}$. The value of, a, used in the above correlation is from Table IV-20. The regression line as calculated by program GRAPH is

$$A = 1.144\left(\frac{ND^3}{((D/2)^2-a^2)^{\frac{1}{4}}}\right)^{0.834} \qquad \text{(IV-41)}$$

The correlation is improved as measured by the correlation coefficient which has increased from 0.958 in Figure IV-19 to 0.986 in Figure IV-20.

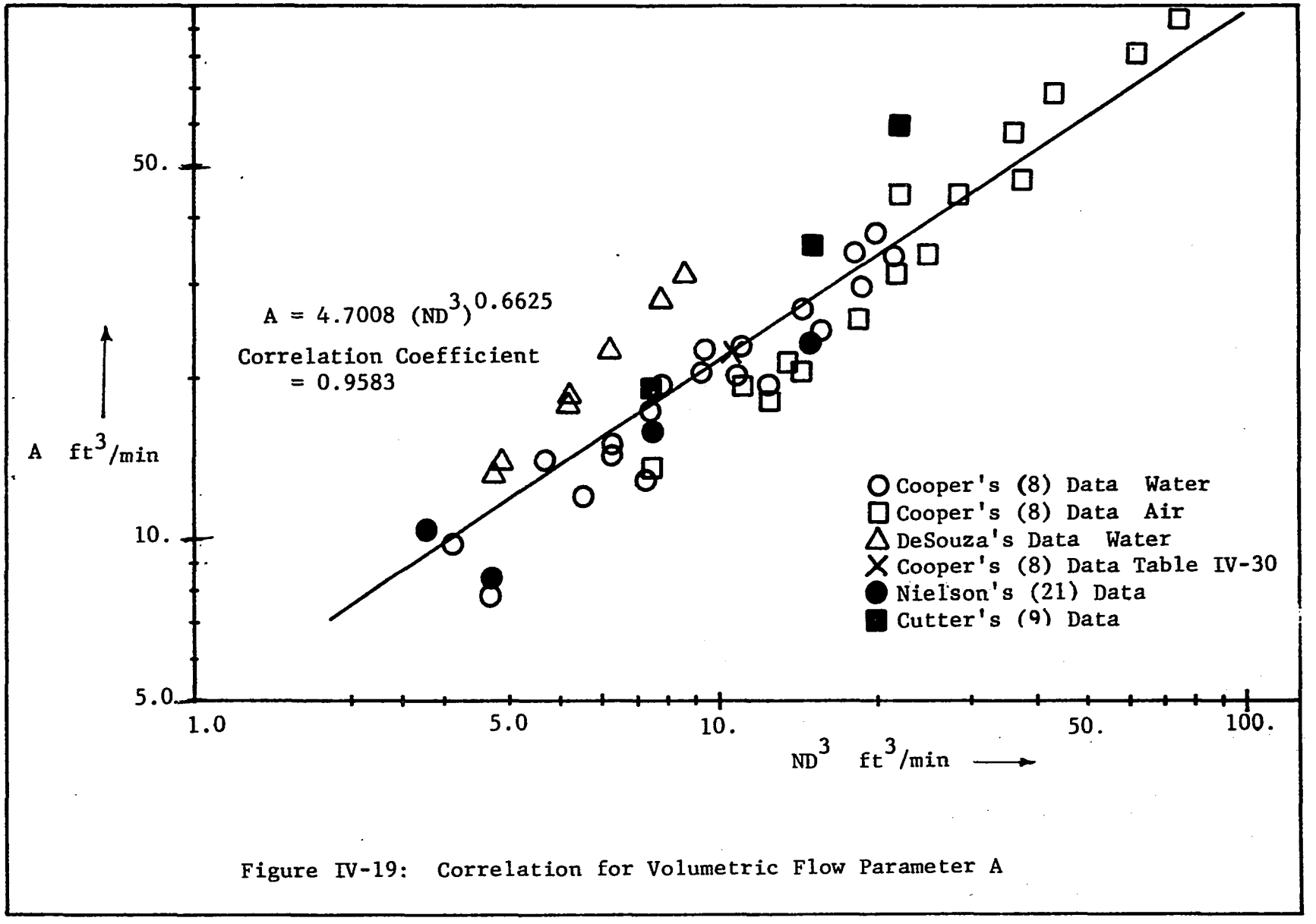

Figure IV-19: Correlation for Volumetric Flow Parameter A

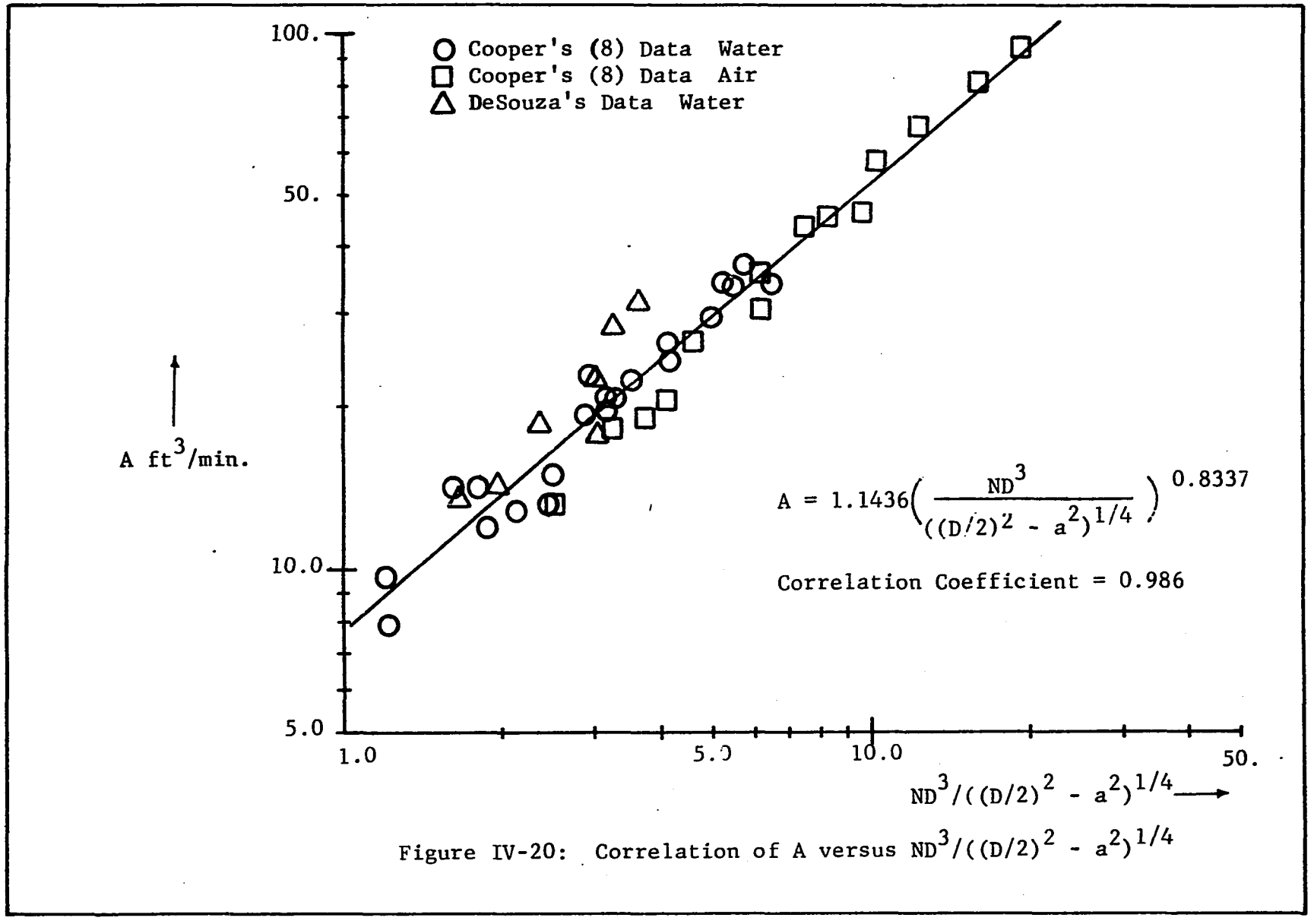

Figure IV-20: Correlation of A versus $ND^3/((D/2)^2 - a^2)^{1/4}$

Results of Correlating Tangential Jet Parameters

To test the usefulness of the correlations of the tangential jet parameters, these correlations were used to evaluate the impeller discharge Q given by Equation IV-7 and the eddy viscosity given by Equation B-15. A program RESULT was written for this purpose. For a listing of the program RESULT and the calculated output see Appendix F.

In Figure IV-21 is plotted Q_{calc} versus Q. Q_{calc} is obtained from Equation B-15 using Equation IV-36 for σ, one of the appropriate Equation IV-37 or IV-38 for, a, and Equation IV-41 for, A. The value of Q is calculated from the experimentally determined values of the jet parameters σ, A and a and given in Table IV-20. If Q_{calc} accurately predicts Q then the data should fall along a straight line inclined at 45° to the horizontal. It is seen that the data for air and water fall closely about this line with a low scatter. The prediction of Q by the correlated values of the tangential jet parameters is very good.

A similar calculation is performed for the eddy viscosity, ϵ, using Equation B-15. The predicted value ϵ_{calc} and experimentally determined value ϵ is given in Table IV-23. In Figure IV-22 is plotted ϵ_{calc} versus ϵ. It is seen that there is a relatively large scatter about the predicted line indicating that the prediction of the eddy viscosity is not as good as for the impeller dischange Q. The eddy viscosity is thus sensitive to small changes in the magnitude of the tangential jet parameters.

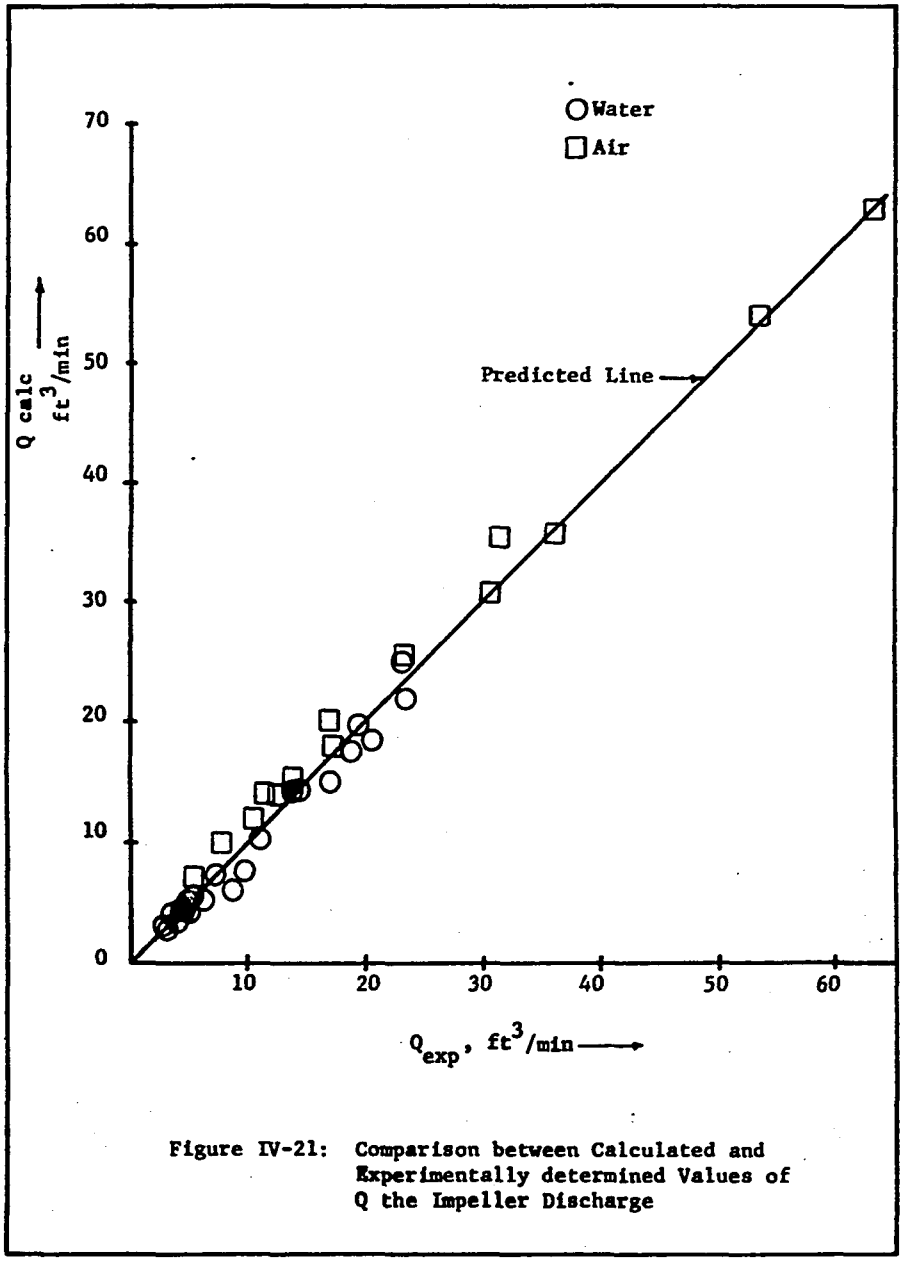

Figure IV-21: Comparison between Calculated and Experimentally determined Values of Q the Impeller Discharge

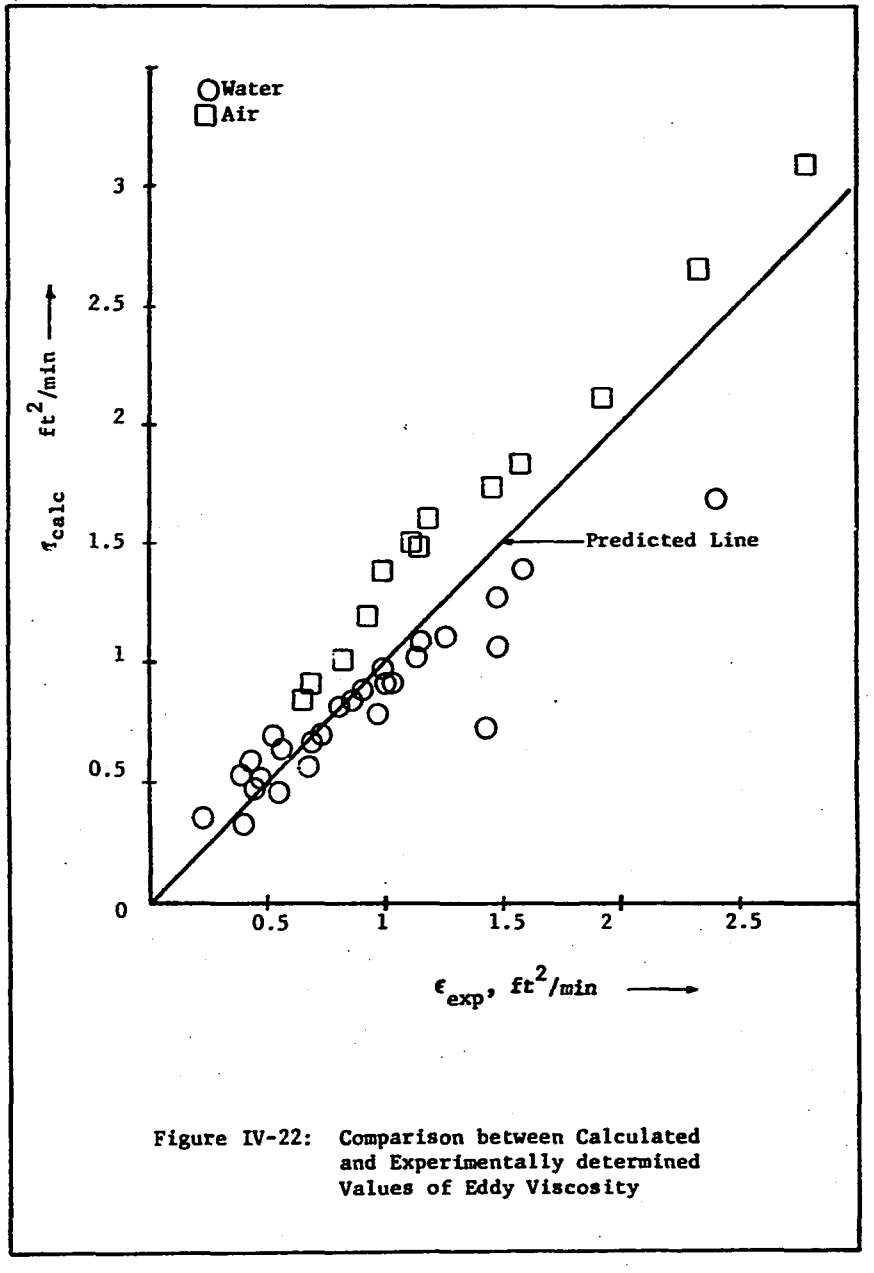

Figure IV-22: Comparison between Calculated and Experimentally determined Values of Eddy Viscosity

TABLE IV-23

EDDY VISCOSITY ϵ. CALCULATED FROM PREDICTED VALUES OF σ, A AND a

Item Number	T, inch	D, inch	Impeller Speed RPM	ϵ ft^2/min	ϵ_{calc} ft/min	Difference
1	15.00	3.00	200.0	0.407	0.321	0.086
2			300.0	0.557	0.450	0.107
3			400.0	0.676	0.572	0.105
4			500.0	0.523	0.688	-0.165
5			600.0	0.802	0.801	0.001
6			100.0	0.237	0.361	-0.124
7			150.0	0.478	0.506	-0.028
8			200.0	0.552	0.643	-0.092
9			250.0	0.979	0.775	0.204
10			300.0	1.048	0.902	0.146
11		5.00	100.0	0.455	0.474	-0.009
12			150.0	0.687	0.665	0.022
13			200.0	0.866	0.845	0.021
14			250.0	1.149	1.018	0.132
15			275.0	1.260	1.102	0.158
16		6.00	50.0	0.526	0.389	0.138
17			100.0	0.729	0.693	0.036
18			125.0	0.919	0.835	0.085
19			150.0	1.000	0.972	0.028
20			170.0	1.159	1.078	0.081
21	12.25	3.00	243.0	0.879	0.697	0.181
22			250.0	1.447	0.714	0.733
23			333.3	1.099	0.908	0.192
24			400.0	1.489	1.057	0.432
25			500.0	1.481	1.273	0.208
26			550.0	1.588	1.378	0.210
27*	11.50		333.3	2.412	1.677	0.735
28*	15.00	4.00	200.0	0.446	0.643	-0.197
29			300.0	0.693	0.902	-0.209
30			366.0	0.825	1.065	-0.240
31			500.0	0.999	1.381	-0.382
32			600.0	1.298	1.608	-0.310
33		5.00	200.0	0.660	0.845	-0.185
34			300.0	0.934	1.185	-0.251
35			400.0	1.228	1.506	-0.278
36			500.0	1.587	1.814	-0.227
37			600.0	1.929	2.112	-0.183

TABLE IV-23 CONTINUED

Item Number	T, inch	D, inch	Impeller Speed RPM	ϵ ft^2/min	ϵ_{calc} ft/min	Difference
38		6.00	100.0	0.653	0.693	-0.040
39			200.0	1.115	1.235	-0.120
40			300.0	1.468	1.732	-0.264
41			500.0	2.333	2.651	-0.318
42			600.0	2.780	3.086	-0.306

Examining the eddy viscosity in Table IV-23 it is seen that at constant impeller diameter it increases with impeller speed. At constant impeller diameter reducing the tank diameter results in an increase in eddy viscosity. This is clear on examining Items 2, 23 and 27 of Table IV-23. In Figure IV-22 it is seen that the predicted value of eddy viscosity is smaller for water and larger for air. On further examining of Table IV-23 it is observed that for a given impeller speed at constant tank diameter, increasing the diameter of the impeller increases the eddy viscosity. For example in Item 1 and 13 the RPM is 200 and the impeller diameters are 3.0 inches and 5.0 inches. The eddy viscosity is doubled when the diameter change form 3.0 inches to 5.0 inches. However, the pumping capacity was found to increase by 4.4 times. This means that the momentum transfer per unit volume is lower by a factor of two. Hence the well known fact that a large impeller at low speeds gives more circulation and less mixing, while a small impeller at high speeds gives a low circulation but intense mixing in the impeller stream. The eddy viscosity gives the rate ofmomentum transfer and its value can now be predicted and fixed at any desired level.

4.8. Analysis of Cooper's (8) Data at Varying Radial Distance and Varying Impeller Blade Width

Cooper has also reported velocity profiles for the 4.0 inch Type A impeller at 280 RPM and five different points along the radius. These are: 2.0, 2.5, 3,0, 4.5, and 5.0 inches. He has in addition reported velocity profiles at 100 RPM and 200 RPM for a 4.0 inch Type A impeller with five different blade widths b. The

dimension b is the length of the blade in the axial direction as shown in Figure I-2. These varying blade widths are 1.6, 1.4, 1.2, 1.0 and 0.6 inches. The normal value of b for a 4.0 inch impeller is 0.8 inch. This impeller has been used in the data reported in the previous section. Hence, six different blade widths at constant impeller diameter were investigated.

Analysis at Varying Radial Distance

In Table IV-24 (b) is shown the results of the analysis of Cooper's data for varying radial distance. In this Table σ, and A were obtained by a least square fit and the radius of source, a, from the weighted average angle $\bar{\theta}_y$. The velocity factor was 0.5. The fit on the data is excellent as noted by the high correlation coefficient of 0.99 for $\bar{q}$ and 0.96 to 0.98 for $\bar{v}_r$. The only exception is Profile Number 5 where r equals 5.0 inches. This profile does not correlate at all and was suspected to be located near r_o. This was indeed the case as r_o calculated from Equation II-28 with T equal to 15 inches and σ equal to 12.621, is found to be 5.08 inches.

Table IV-24 (b) shows a widely varying value for σ and the radius of source, a, increases with r. In Table IV-24 (a) are shown the analysis on the same data with σ kept constant at its universal value given in Equation IV-36, and, a, obtained from Equation IV-38. The correlation coefficient is smaller in Table IV-24 (a) than in IV-24 (b) for both $\bar{q}$ and $\bar{v}_r$. The lowering in the correlation coefficient is not large and the correlation is thus still very good.

TABLE IV-24

ANALYSIS OF COOPER'S DATA WITH VARYING RADIAL DISTANCE,

SHOWING EFFECT OF σ

(a) σ = 12.621, constant

Number	Radius	σ	A ft^3/min	a, ft.	Correlation Coefficient $\bar{q}$	Correlation Coefficient $\bar{v}_r$	Volumetric Flow Q_r, CFM
1	2.00	12.62	22.97	0.143	0.992	0.957	9.72
2	2.50		21.48	0.143	0.917	0.816	13.51
3	3.00		22.04	0.143	0.950	0.854	17.66
4	4.00		24.16	0.143	0.986	0.948	27.08
5	5.00		23.75	0.143	0.743	0.563	33.93

(b) σ obtained by least square fit

1	2.00	12.38	23.52	0.140	0.993	0.955	10.29
2	2.50	17.03	20.34	0.156	0.982	0.967	10.49
3	3.00	15.77	20.59	0.165	0.997	0.981	14.12
4	4.00	13.37	23.38	0.164	0.991	0.983	25.00
5	5.00	--	--	0.188	--	--	--

Profile Number 5 is also correlated indicating that a correct choice for σ and a was made.

The correlation coefficient on $\bar{v}_r$ is low, indicating that the profile is no longer in the tangential jet region as noted above. This shows that keeping σ constant is a valid argument and that Equation IV-38 predicts the correct value for a. The volumetric parameter A in Table IV-24 (a) is seen to be more nearly constant and independent of r, which is in agreement with the tangential jet model. The average value of A is 22.9 and is very close to the correlating line when plotted in Figure IV-19. The value of Q is also found to correlate well on Figure IV-18.

The complete results corresponding to Tables IV-24 (a) and IV-24 (b) are given in Appendix G, Tables G-30 and G-31.

Analysis at Varying Blade Widths

In Table IV-25 is shown the analysis for varying blade widths at 100 and 200 RPM. Profile Number 5 in this Table is for a normal 4.0 inch impeller and the results are reported from Table G-18. At 100 RPM the value of σ is seen to be fairly constant while at 200 RPM it is seen to increase with decreasing blade width. The value of A, the volumetric parameter decreases with decreasing blade width indicating that the impeller discharge is a function of the blade width. The radius of source parameter, a, shows a slight increase with decreasing blade width. Its value has the same order of magnitude at corresponding blade widths for the two impeller speeds.

TABLE IV-25

ANALYSIS OF COOPER'S DATA AT VARYING BLADE WIDTH AND RPM

(a) 100 RPM, 4.0 inch diameter impeller

Profile Number	Blade Width b	σ	ft^3/min A	a, ft	Correlation Coefficient $\overline{q}$	$\overline{v}_r$	Impeller Discharge Q, CFM
1	1.6	10.6	11.6	0.115	0.937	0.914	6.32
2	1.4	10.6	10.9	0.107	0.953	0.923	6.12
3	1.2	12.5	10.7	0.106	0.981	0.982	5.58
4	1.0	12.3	8.4	0.134	0.987	0.962	3.88
5	0.8	14.1	7.9	0.139	0.993	0.975	3.26
6	0.6	11.8	7.8	0.142	0.996	0.887	3.45

(b) 200 RPM, 4.0 inch diameter Impeller

1	1.6	8.5	22.7	0.112	0.938	0.902	13.98
2	1.4	11.0	22.3	0,105	0.938	0.929	12.43
3	1,2	11.8	21.7	0.107	0.963	0.964	11.58
4	1.0	12.4	17.8	0.132	0.993	0.982	8.27
5	0.8	13.6	17.1	0.140	0.994	0.963	7.12
6	0.6	13.0	14.3	0.141	0.996	0.922	6.11

Table IV-26 gives the results for keeping σ constant at its universal value of 12.621. In Table IV-26 (a), the radius of source, a, is predicted from IV-38. This value of a has a small effect on $\vec{q}$ as measured by the correlation coefficient being slightly smaller. Its effect on $\bar{v}_r$ is disasterous. Profile Number 1 of Table IV-25 shows no correlation for $\bar{v}_r$, while Profile Numbers 2 and 3 give an unacceptably low value for the correlation coefficient. Profile Numbers 4 and 6 are fairly good correlations. This means that the radius of source is sensitive to blade width and this factor should be included in the correlation for, a.

In Table IV-26 (b) the value of, a, is obtained from the weighted average angle $\bar{\theta}_y$. The correlation is excellant for Profile Numbers 4, 5, and 6, and deteriates for Profile Numbers 1 and 2. The indication is that σ is less sensitive for small variations in b. From Table IV-26 we conclude that the universal value of σ given by Equation IV-36 is valid for b ranging from 0.6 to 1.0 inch ($\pm$ 33% change). The value of, a, given by Equation IV-38 could be used for this range of b but is not as good for predicting the data as in the case of σ. For this reason the detail analysis in Appendix G, Tables G-32 and G-33 are reported for σ, A and z_o obtained by a least square fit and, a, from the weighted average angle $\bar{\theta}_y$.

Figure IV-23 shows a log-log plot of Q theimpeller discharge versus the blade width b. The value of Q is taken from Table IV-25 and is a good estimate of Q as measured by the large value of correlation coefficient on $\bar{v}_r$. In Figure IV-22, Q increases almost

TABLE IV-26

EFFECT OF CONSTANT σ EQUAL TO 12.621 ON VARYING BLADE WIDTH AT 100 RPM AND IMPELLER DIAMETER OF 4.0 INCH

(a) Radius of Source a, from Equation IV-38

Number	Blade Width	ft^3/min A	a,ft	Correlation Coefficient $\vec{q}$	Correlation Coefficient $\bar{v}_r$
1	1.6	9.8	0.143	0.8983	0.0000
2	1.4	8.8		0.9145	0.0996
3	1.2	8.7		0.9806	0.5093
4	1.0	7.9		0.9862	0.8887
5	0.8	7.6		0.9830	0.9414
6	0.6	7.7		0.9893	0.9144

(b) Radius of Source a, From Weighted Average Angle

1	1.6	11.4	0.115	0.8983	0.8462
2	1.4	10.7	0.107	0.9145	0.8900
3	1.2	10.7	0.106	0.9806	0.9813
4	1.0	8.4	0.134	0.9862	0.9687
5	0.8	7.9	0.139	0.9830	0.9459
6	0.6	7.8	0.142	0.9893	0.9169

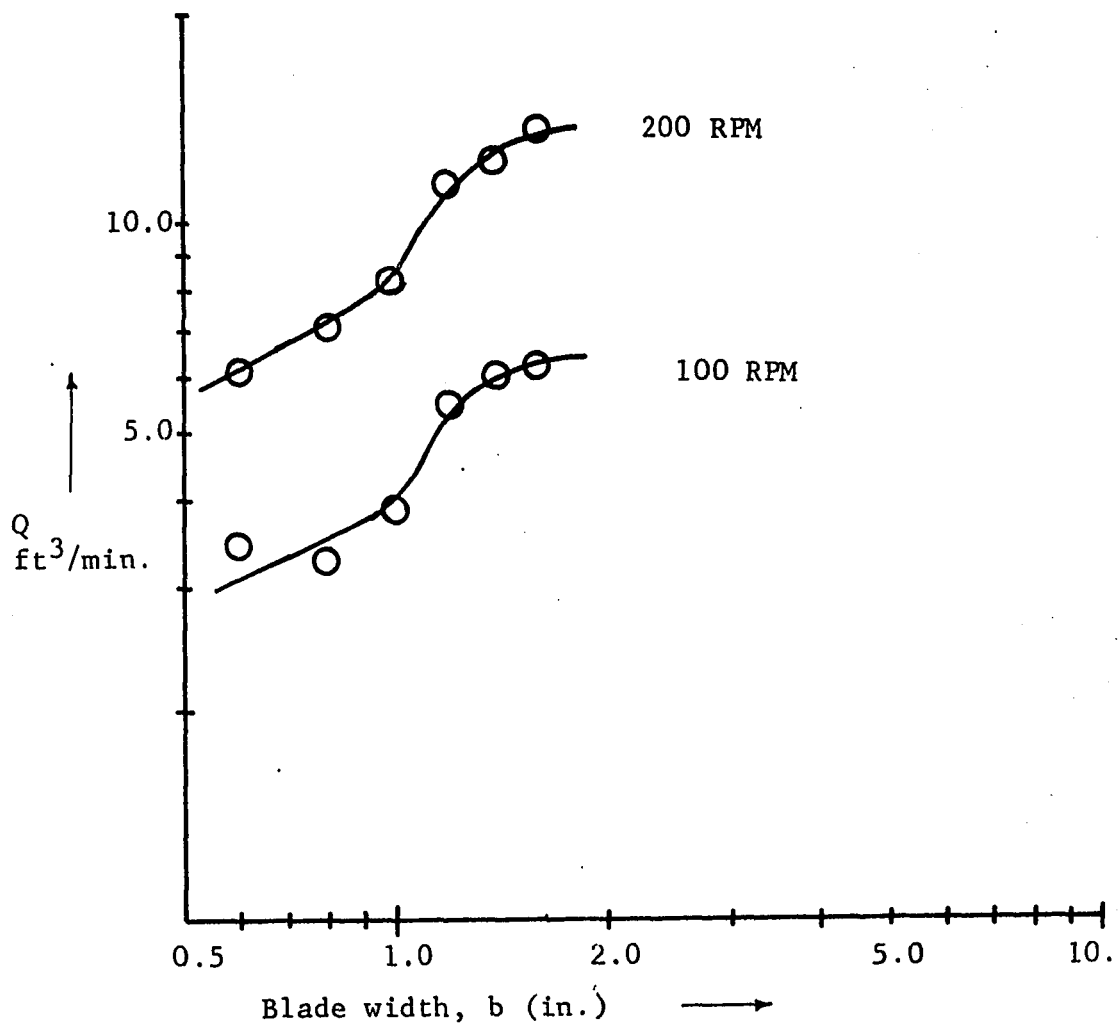

Figure IV-23: Effect of Blade Width on the Impeller Discharge Q for a 4.0 in. Impeller

linearly till b reaches 1.0 inch. After this point there is a sudden increase in b. This is the reason why σ the jet width and a are different from that obtained for the standard impeller with b equal 0.8 inches.

From the point of view of optimum value of Q, b equal to 1.0 in. appears a good choice. However other considerations such as power input which have not been determined, might be a significant factor in determining the optimum blade width. It is noticed that changing the impeller speed merely shifts the curve up indicating that Q is proportional to N, the impeller speed. The blade width is thus not an interacting factor with the impeller speed. It thus appears that Equation IV-40 could still be used to calculate Q for impellers have varying blade widths with a suitable scaling factor to account for b.

4.9. Analysis of Nielson's (21) and Cutter's (9) Data

Both Nielson and Cutter used the light streak method described in Chapter I to obtain velocity profiles in the neighborhood of the impeller. The experimentally determined velocity profiles were fitted to the tangential jet model. The results of this analysis is reported in this section.

The velocity profiles reported by Nielson and Cutter are for $\bar{v}_r$. From Chapter II, the equation for $\bar{v}_r$ is

$$\bar{v}_r = \frac{A}{2}\frac{\sigma^{\frac{1}{2}}}{r^3}(r^2-a^2)^{\frac{1}{4}}[1-\tanh^2(\eta/2)] \qquad \text{(II-9)}$$

In analyzing our data and that of Cooper, the value of, a, was fixed by a weighted average value of the angle profile. In the light streak method the angle profile was not detected nor is an average

angle given. Hence in analyzing Nielson's and Cutter's data an average angle $\bar{\theta}_y$ was estimated to evaluate a. It was noted earlier that Equations IV-37 and IV-38 could not be used to predict a, as they gave a value for, a, larger than D/2.

As a first trial $\bar{\theta}_y$ was selected using $\bar{\theta}_y$ given in Table IV-21 as a guide. It is noted in Table IV-21 that $\bar{\theta}_y$ for Cooper's data in a 12.0 inch diameter tank ranges from 53.0° to 59.0°. Our data in 12.25 inch and 11.5 inch diameter tanks gave $\bar{\theta}_y$ as 66.8° and 76.6°. From these observations a trend is noticed in which $\bar{\theta}_y$ increases as tank diameter decreases. As Nielson and Cutter used a 11.25 inch and 11.5 inch diameter tanks respectively, three values of $\bar{\theta}_y$ were tried. They are 60°, 65° and 70°.

The analysis of Nielson's and Cutter's data is done by the program NIELCUT. The listing of the program together with a listing of the raw data is given in Appendix F. The program NIELCUT is essentially the same as FLOWANL. The difference lies in processing the raw data, the way, a, the radius of source is calculated, and the regression is for $\bar{v}_r$ and not $\bar{q}$.

Analysis of Nielson's Data

Nielson measured seven velocity profiles. Profile Numbers 1, 2 and 3 are at three different radial distances r, for a 2.0 inch impeller in water at 600 RPM. Profile Numbers 4, 5, and 6 are with a 4.0 inch impeller. Profiles 4 and 6 are with water at 200 RPM, while Profile Number 5 is in corn syrup (viscosity 10 centipoise)

at 100 RPM. Finally Profile Number 7 is for a 7.0 inch diameter impeller at 75 RPM.

Table IV-27 shows the effect of varying $\bar{\theta}_y$ on Nielson's data. Comparing Tables IV-27 (a) and IV-27 (b) it is seen that changing $\bar{\theta}_y$, (from which a is calculated) results in a change in A the volumetric parameter only. No change is noticed in σ, the sum square SS and the correlation coefficient for the corresponding profiles in these tables.

Table IV-27 also gives a widely varying value for σ at constant impeller diameter. From the analysis presented in the previous section it was shown that σ is a universal constant. Hence in Table IV-28 is shown the result for Nielson's data with σ a constant given by Equation IV-36. The result of keeping σ a constant is to increase the sum of squares about the regression line and decrease the correlation coefficient. The decrease in correlation is not excessive and can be verified by comparing Tables IV-27 and IV-28. The value of A however is not affected. Here again it is seen that σ can be considered as a universal constant, without drastically affecting the fit.

Table IV-29 shows the final result of analyzing Nielson's data. In this table, the value of $\bar{\theta}_y$ was fixed at 70° for impeller diameter of 2.0 inches, since this gave a more nearly constant value of A = 10.67 for the Profile Numbers 1, 2, and 3 taken at different radial distances. Similarly for Profiles 4, 5, and 6 $\bar{\theta}_y$ was fixed at 60° as this gave a nearly constant value for A in Profile Numbers 4 and 6. These two profiles it will be recalled are for a 4.0 inch

TABLE IV-27

EFFECT OF $\bar{\theta}_y$ ON THE ANALYSIS OF NIELSON'S DATA

Profile Number	Impeller Speed RPM	Radial Distance	σ	A ft^3/min	a, ft	Sum Square SS	Correlation Coefficient R
(a) $\bar{\theta}_y$ = 60°							
1	600	1.0	22.4	8.6	0.072	3282	0.938
2		3.0	12.1	10.5	0.072	49	0.989
3		4.0	10.2	10.9	0.072	16	0.978
4	200	2.00	16.5	15.0	0.144	472	0.981
5	100	2.00	17.5	7.7	0.144	97	0.987
6	200	4.00	13.4	15.1	0.144	30	0.998
7	75	3.50	11.8	21.4	0.25	176	0.967
(b) $\bar{\theta}_y$ = 65°							
1	600	1.00	22.4	9.4	0.076	3282	0.938
2		3.00	12.2	10.6	0.076	49	0.989
3		4.00	10.1	10.9	0.076	16	0.978
4	200	2.00	16.5	16.4	0.151	472	0.981
5*	100	2.00	17.5	8.3	0.151	97.	0.987
6	200	4.00	13.4	15.23	0.151	30	0.998
7	75	3.50	11.8	23.22	0.264	176	0.967

*Profile measurements made in Corn Syrup, viscosity 10 centipoises.

TABLE IV-28

EFFECT OF KEEPING σ A CONSTANT VALUE OF 12.621

ON NIELSON'S DATA. $\overline{\theta}_y = 65°$

Number	Radial Distance Min.	σ	ft^3/min A	a,ft.	Sum Square SS	Correlation Coefficient R
1	1.00	12.621	9.9	0.076	9221	0.814
2	3.00		10.5	0.076	55	0.814
3	4.00		10.5	0.076	84	0.879
4	2.00		16.4	0.151	1586	0.934
5*	2.00		8.3	0.151	609	0.919
6	4.00		15.2	0.151	63	0.995
7	3.50		23.0	0.264	203	0.962

*For corn syrup

TABLE IV-29

ANALYSIS OF NIELSON'S DATA RESULTING FROM AN OPTIMUM SELECTION OF $\bar{\theta}_y$

Profile Number	Radial Distance r, in.	σ	ft^3/min A	a, ft.	$\bar{\theta}_y$	Correlation Coefficient R
1	1.00	12.621	11.0	0.078	70	0.814
2	3.00		10.6	0.078		0.987
3	4.00		10.5	0.078		0.879
4	2.00		15.1	0.144	60	0.934
5*	2.00		7.6	0.144		0.919
6	4.00		15.2	0.144		0.995
7	3.50		23.1	0.264	70	0.962

*For corn syrup

diameter impeller in water at 200 RPM. In case of Profile Number 7 the value of $\bar{\theta}_y$ was fixed at 70° since this gave a value of A that came very close to the regression line of Figure IV-18. The above observations can be checked by comparing Tables IV-28 and IV-29. In Table IV-28, $\bar{\theta}_y$ was selected equal to 65° so as to make this comparison possible and thus show the effect of a suitable choice in $\bar{\theta}_y$. The values of A reported in Table IV-34 are plotted in Figure IV-18. It is seen that the result for Profile Number 5 which is for corn syrup is not very much different, lending further support to the observation that the physical properties of the fluid is not an important variable in analyzing the flow in the stirred tank.

A summary of the detailed analysis from program NIELCUT for Table IV-29 is given in Appendix G. Tables for σ free and fixed by Equation IV-36 are included for comparison. The value of a, in these Tables are at the optimum values shown in Table IV-29.

Analysis of Cutters Data

Cutter reports average values of $\bar{v}_r$ for only positive values of z, or half a velocity profile. Velocity profiles are for a single 4.0 inch diameter impeller, and at several different radial distances. The data is obtained at three different impeller speeds. As for Nielson data a value of $\bar{\theta}_y$ had to be selected in order to calculate a, the radius of source.

In Table IV-30 is shown the analysis of Cutter's data at 200 RPM with two values of, a. The radius of source is calculated from $\bar{\theta}_y$ set at 65° and 70°. It is observed that changing, a, has a very

TABLE IV-30

ANALYSIS OF CUTTER'S DATA AT 200 RPM FOR A 4.0 INCH IMPELLER

SHOWING EFFECT OF VARYING $\bar{\theta}_y$

(a) $\bar{\theta}_y = 65°$

Number	Radial Distance r, in.	σ	A ft^3/min	a, ft	Sum Square SS	Correlation Coefficient R
1	2.00	9.7	33.7	0.151	112	0.995
2	2.75	18.1	12.0		315	0.976
3	3.38	13.7	18.5		196	0.985
4	4.13	6.5	24.0		166	0.896
5	4.38	23.6	15.3		114	0.877
6	5.13	7.8	24.8		177	0.647

(b) $\bar{\theta}_y = 70°$

1	2.00	9.5	40.1	0.157	112	0.995
2	2.75	18.4	12.0		314	0.976
3	3.38	14.0	18.2		195	0.985
4	4.13	6.9	22.0		168	0.894
5	4.38	23.6	15.3		114	0.877
6	5.13	6.8	28.7		172	0.661

small effect on σ, sum of squares about the correlation and the correlation coefficient. It has a proportionately larger effect on the volumetric parameter A. The parameter σ is seen to vary in an irregular manner. The tank diameter is 11.5 inches, taking σ at 12.621, r_o from II-28 is found to be 3.9 inches. Hence profiles 4, 5, and 5 are outside the tangential jet region as their values of r is larger than 3.9 inches. This is verified by the comparatively lower values of the correlation coefficient for these profiles. This trend is the profiles measured at 400 and 600 RPM and can be verified in Appendix G where a detail summary of the profiles are given.

In Table IV-31 is shown the velocity profiles measured at 200 RPM with σ constant and equal to 12.621. The results are presented for two values of, a, calculated from $\bar{\theta}_y$ set at 65° and 70°. Comparing this analysis with the previous analysis given in Table IV-30, it is seen that the sum of squares has increased and the correlation coefficient has been lowered a small amount. It is observed that the results with $\bar{\theta}_y$ equal to 65° gives a more nearly equal value for A in Profile Numbers 1, 2, and 3 than that obtained with $\bar{\theta}_y$ equal to 70°. Only Profile Numbers 1, 2 and 3 are considered since it has been noted above that these are the only profiles for which the tangential jet model is valid. The rest of the profiles are for r greater than 3.9 inches and are thus in the stagnation region, Region II. This observation is supported by the fact that Q decreases for r larger than 3.9 as seen in Tables IV-32 and IV-33.

TABLE IV-31

ANALYSIS OF CUTTER'S DATA AT 200 RPM FOR A 4.0 INCH IMPELLER, WITH σ CONSTANT AND VARYING $\bar{\theta}_y$

(a) $\bar{\theta}_y = 65°$

Profile Number	Radial Distance r	σ	ft^3/min A	a, ft.	Sum Square SS	Correlation Coefficient R
1	2.00	12.621	19.9	0.151	205	0.991
2	2.75		17.2		493	0.962
3	3.38		20.5		205	0.984
4	4.13		12.9		266	0.827
5	4.38		19.7		275	0.667
6	5.13		17.7		213	0.548

(b) $\bar{\theta}_y = 70°$

1	2.00	12.621	22.1	0.157	205	0.991
2	2.75		17.5		493	0.962
3	3.38		20.5		204	0.984
4	4.13		13.0		266	0.827
5	4.38		19.8		275	0.668
6	5.13		17.8		213	0.548

TABLE IV-32

RESULTS OF ANALYSIS OF CUTTER'S DATA AT 400 RPM, FOR A 4.0 INCH IMPELLER, σ CONSTANT AND $\bar{\theta}_y = 65°$

Number	Radial Distance r, in.	σ	ft^3/min A	a, ft.	Correlation Coefficient	Volumetric Flow at Corresponding r, cfm
1	2.00	12.621	42.9	0.151	0.963	16.4413
2	2.81		35.5		0.984	25.6676
3	2.86		39.7		0.985	29.4310
4	3.44		31.6		0.934	29.5016
5	3.56		29.5		0.982	28.7167
6	4.19		31.8		0.892	37.3338
7	4.75		21.8		0.885	29.3451
8	5.56		9.4		0.673	15.0565

TABLE IV-33

RESULTS OF ANALYSIS OF CUTTER'S DATA AT 600 RPM, FOR A 4.0 INCH IMPELLER, σ CONSTANT AND $\bar{\theta}_y = 65°$

Number	Radial Distance r, in.	σ	A	a	Correlation Coefficient	Volumetric Flow at Corresponding r, CFM
1	2.14	12.621	66.180	0.1511	0.989	30.4369
2	2.75		54.230		0.978	38.1213
3	3.38		59.044		0.951	54.0455
4	4.13		72.044		0.958	83.1381
5	4.38		62.255		0.889	76.6890
6	5.13		37.850		0.848	55.3585

The above observations were also noticed in the profiles measured at 400 and 600 RPM. The best estimate of, a, was obtained by setting $\bar{\theta}_y$ equal to 65°. Tables IV-32 and IV-33 show the results of profiles measured at 400 and 600 RPM with the parameter σ chosen at 12.621 and, a, calculated from $\bar{\theta}_y$ equal to 65°. These values of σ and a are the best estimates for these parameters.

From Tables IV-31 through IV-33, the average value of A for r less than 3.9 inches (value of r_o) was calculated and given in Table IV-36. In Appendix G is given the detailed summary for these profiles. The radius of source is obtained from $\bar{\theta}_y$ and the results for σ free and a constant are given for comparison.

4.10. Summary of Velocity Profiles Obtained by the Light Streak Method

In Table IV-34 is given the best estimates of the tangential jet parameters for Nielson's and Cutter's data. Item Numbers 1 to 4 were taken by Nielson and Profile Numbers 5 to 7 by Cutter. Item Numbers 2 and 5 are at the same impeller speed but different tank diameters. As in the case of our measurements the smaller tank gave lower values of A and Q. This is seen from our data in Table IV-20 Data Set 5, Item 3 and Data Set 6, Item 1. Data Set 6 is taken in the smaller diameter tank.

The value of Q, the impeller discharge reported in Table IV-34 is obtained from σ, A and a reported in the Table and using Equation IV-7. In Figure IV-18, Q has been plotted versus ND^3. Although there is some scatter in the data it is not excessive except at low

TABLE IV-34

SUMMARY OF RESULTS FOR THE TANGENTIAL JET BY THE LIGHT STREAK METHOD

No.	T in.	D in.	Impeller Speed (RPM)	σ	A ft^3/min	a ft	Q ft^3/min	ND^3 ft^3/min	Reference
1	11.25	2.0	600	12.621	10.3	0.0755	1.98	2.78	21
2		4.0	200		15.83	0.1511	6.06	7.41	21
3*		4.0	100		8.31	0.1511	3.18	3.7	21
4		7.0	75		23.084	0.2643	15.48	14.89	21
5	11.5	4.0	200		19.198	0.1511	7.35	7.41	9
6		4.0	400		35.82	0.1511	13.72	14.81	9
7		4.0	600		59.82	0.1511	22.91	22.22	9

* Taken in corn syrup.

values of ND^3. In Figure IV-19 is plotted the values of A versus ND^3. In this plot the scatter is larger than for Q. However it is within the scatter of the other points on the plot and thus would be acceptable for correlation. It should be noted that Profile Number 3 was measured by Nielson in corn syrup. This data point is also seen to correlate well confirming the observation made earlier that viscosity is not an important factor in the stirred tank. The correlation lines given in Figures IV-17 and IV-18 were calculated without using Nielson's and Cutter's data. This was because, the parameters σ and a were estimated and not obtained from the measured data.

The analysis presented in this section shows that the tangential jet model successfully predicts the data of Nielson and Cutter.

4.11. Extent of the Tangential Jet

Equation II-28 gives r_o the extent of the tangential jet as

$$r_o = \frac{\sigma T}{12 + 2\sigma} \qquad \text{(II-28)}$$

Substituting for σ equal to 12.621 from Equation IV-36 gives

$$r_o = 0.339\ T \qquad \text{(IV-41)}$$

In terms of radius of the tank this reduces to

$$r_o = 0.678\ (T/2) \qquad \text{(IV-42)}$$

Equation IV-42 gives the extent of the tangential jet as 67.8% of the tank radius. This leaves 32.2% of the tank radius for the return

flow at the perphery of the tank. Velocity profile measurements in Section 4.3 show this to be true as can be seen in the radial velocity profile for $\bar{v}_r$ given in Figure IV-6 and the axial velocity for $\bar{v}_z$ given in Figure IV-7. The maximum value of $\bar{v}_z$ and $\bar{v}_r$ occurs well beyond r_o in these figures. This indicates that the bulk of the flow at the periphery of the tank occurs in a region less than 32 % of the radius of the tank.

We can now determine the width of the baffle. The function of the baffle is to interfere with the flow and reduce the tangential component. Since the flow is restricted to the periphery of the tank its position should thus be at the tank periphery. Its width should be the thickness of the return flow which is estimated as maximum of 32 % of the tank radius. In the literature the recommended baffle width is 10 % of the tank diameter, i.e., 20% of the tank radius. As noted above the flow as it leaves the stagnation region, Region II, is reduced in width and is thus amply covered by a 10% baffle. This is the reason why at fully baffled conditions, increasing the baffle width or giving it a pitch has very little effect on the flow (36)

Jet Width

In Appendix B, the jet width was defined on the basis of the point where the velocity profile is less than 1% of $\bar{q}_{max}$, and given by

$$b_{\frac{1}{2}} = \frac{6r}{\sigma} \qquad \text{(B-34)}$$

The tangential jet model also defines a half width of the jet, and this value of $b_{\frac{1}{2}}$ is given by

$$b_{\frac{1}{2}} = \frac{2r^2-a^2}{(r^2-a^2)^{\frac{1}{2}}k'} \qquad \text{(II-12)}$$

Since, a, the radius of the jet source D/2, it is clear that for large r, II-12 reduces to

$$b_{\frac{1}{2}} = \frac{2r}{k'} \qquad \text{(IV-43)}$$

Comparing Equations IV-43 and B-34 it follows that

$$k' = \frac{3}{\sigma} \qquad \text{(IV-44)}$$

Hence II-12 becomes

$$b_{\frac{1}{2}} = \frac{3}{\sigma} \frac{(2r^2-a^2)}{(r^2-a^2)^{\frac{1}{2}}} \qquad \text{(IV-45)}$$

Equation IV-45 and B-34 are thus made identical for large r at the impeller periphery, it was found that Equation IV-45 with σ equal to 12.621 and, a, reported in Table IV-21 gave a slightly larger value of $b_{\frac{1}{2}}$ as compared to Equation B-34. As and example, for our data in a 12.25 diameter tank $b_{\frac{1}{2}}$ as calculated from Equation IV-45 is 0.077 feet as compared to 0.067 feet from Equation B-34.

4.12. Summary

In this chapter experimental evidence is presented and interpreted in terms of the mathematical model developed in Chapter II. Measurements were made with a three dimensional Pitot tube in the vicinity of the impeller and in the region outside the impeller. It was shown that the tangential jet model adequately describes the flow

in the region of the impeller. The angle profile is not predicted by the tangential jet model. The model however is relatively insensitive to the angle profile and a weighted average angle was found to give satisfactory results.

The significant velocity in the neighborhood of the impeller centerline was shown to be $\vec{q}$ the resultant of $\bar{v}_r$ and $\bar{v}_\theta$. It was also shown that the three dimensional pitot tube is not sensitive enough to make measurements beyond the point where $\vec{q} = \frac{1}{2}\bar{q}_{max}$. This was because for z larger than that corresponding to $\frac{1}{2}\bar{q}_{max}$ the velocity falls rapidly to less than 30 ft/min. This velocity is the lower limit of probe response. It was also found that the contribution to volumetric flow beyond this point is small. However for completeness it is desirable to obtain measurements in this region.

The readings from the three dimensional pitot tube was shown to be dependent on the flow geometry. It was pointed out by Rao (24) that the readings given by the pitot tube in a turbulent flow field are subject to error. However, these errors if any are small being of the order of less than 10% and could be neglected.

The tangential jet model was successfully fitted to the data taken by Cooper (8) and to a lesser extent by Nielson (21) and Cutter (9). In the latter case some of the parameters had to be estimated. The model has three parameters; these are: σ, the jet width parameter, A the volumetric flow parameter and, a, the radius

of source parameter. It was shown that the results for Cooper and our data for σ results in a constant value of σ. The data analyzed includes measurement made in air and water. The data also spans varying impeller diameter, tank diameter and impeller speeds. This means that for geometrically similar impellers σ, the jet width parameter is a universal constant. It follows that in such cases the width of the jet is also constant. The analysis of Cooper's data for a single impeller and varying blade widths showed that σ is dependent on the impeller blade width in the case of impellers that are not geometrically similar.

A correlation with $ND^3/((D/2)^2-a^2)^{\frac{1}{4}}$ was found satisfactory for A. In the case of the radius of source a, it was observed that the tank diameter had a significant effect. Two separate correlations are given for a, which are satisfactory for the purpose of interpolating the results analyzed in this work. The data is not enough to make a sweeping statement to cover all possible cases. The results of the correlation was shown to successfully predict the impeller discharge Q and to a lesser extent the eddy viscosity ϵ. The impeller discharge Q was found to correlate satisfactorily with ND^3.

It was also found that the dimensionless pumping capacity N_Q was a constant for geometrically similar impellers. The eddy viscosity as defined by Equaton B-15 was shown to increase with both impeller diameter and impeller speed. However as the impeller discharge Q, increased at a much faster rate with increasing speed

and impeller diameter, the net effect is a low momentum transfer per unit volume of fluid with a larger impeller at constant speed.

In the rest of the tank the model presented in Chapter II was shown to be inadequate. The model in Chapter II was based on a two dimensional potential flow. The measurements with the pitot tube was possible only at high impeller speed. The results of the analysis at three different horizontal planes showed that the flow was a three dimensional low velocity flow field. The stagnation zone shown by Nagata is not a true velocity flow field. The stagnation zone shown by Nagata is not a true stagnation zone, but appears to exist when the streamlines are plotted in the r-z plane.

It was also shown that the return flow of the impeller stream occupies a narrow region at the tank walls which ranges from 32.2% of the tank radius, at the impeller centerline and reduces to about 20% of the tank radius half way between the impeller centerline and the fluid surface. This was the reason for having a baffle width of 10% of the tank diameter.

CHAPTER V

CONCLUSIONS

In the preceding chapters the stirred tank with a Type A turbine impeller was investigated. The investigation reveals that the study of the stirred tank consists of two parts; first, selecting and evaluating a suitable probe to measure three dimensional velocity profiles and second to arrive at a suitable model to predict the measured flow field. Partial success has been achieved in both these areas.

5.1. Three-Dimensional Velocity Probe

A three-dimensional pitot tube probe has been used in this work and found to be a satisfactory device in the region of the impeller. The lower limit of probe response is 0.5 ft/sec and a maximum pitch angle θ_p of 40°. With this probe near the impeller centerline the predominant velocity was shown to be $\vec{q}$, the resultant of $\bar{v}_r$ and $\bar{v}_\theta$. The velocity profile $\vec{q}$ is a function of z and r and is symmetrical about a line parallel to the impeller centerline and displaced from it by approximately $\pm$ 0.036 in. An angle profile on $\vec{q}$ was measured and a typical profile is shown in Figure IV-1. The limits of measurement of the profile is a little beyond $\frac{1}{2}\bar{q}_{max}$, at which point the velocity profile decreases rapidly to less than 0.5 ft/sec.

The region of the impeller is a high velocity, high shear layer with the important velocities being $\bar{v}_r$ and $\bar{v}_\theta$. It should be noted that a single 3.0 inch diameter impeller was used in water. With this impeller the lowest impeller speed for which the probe gave an adequate response was 250 RPM. A lower limit of 200 RPM was reported by Cooper (8). At 200 RPM the Reynolds number is 21,600. The probe is thus suitable for measuring velocities only in fully turbulent flow.

In the region outside the impeller, measurements were made in three horizontal planes at 2.0, 3.0, and 4.0 inches above the impeller centerline, (the depth of fluid was 12.0 inches and the impeller was centerally located). The probe was found to respond for an impeller speed of 500 RPM (N_{Re} = 54,000). At higher impeller speeds excessive air entrainment occured which is not a normal operating condition. The flow was found to be three dimensional and fairly quiescent. The resultant velocity ranged between 30 to 70 ft/min. In the horizontal plane 4.0 inches above the impeller centerline, in some areas the probe could not be used as the pitch angle were larger than 40°. It is thus concluded that in the region outside the impeller, the three dimensional pitot tube probe is a poor measuring device. In this region a probe is required which is not only sensitive to low velocity fields but permits true three dimensional velocity profile measurements with large pitch angles. A quartz coated cross-wire hot wire anenrometer is recommended for this purpose. Two such probes will be needed. A probe

with wires crossed in a horizontal plane will permit measuring $\bar{v}_r$ and $\bar{v}_\theta$, and a second probe with wires crossed in a vertical plane to measure $\bar{v}_r$ and $\bar{v}_z$. The hot wire anemometer is not recommended for measuring velocities in the region of the impeller since the high shear layer will damage the wires. Other devices such as thermister beads are available for measuring low velocity fields; however these do not have directional properties and hence cannot be used to measure three-dimensional flow fields.

5.2. Flow Model for the Stirred Tank

In modeling the flow field generated by the stirred tank, it was convenient to devide the flow field into two regions. One region is the neighborhood of the impeller modeled by a tangential jet and the other is the rest of the tank modeled by potential flow.

Tangential Jet

In the region of the impeller the flow was represented by a tangential jet. It consists of a circular source of radius, a, smaller than the impeller diameter from which the fluid emerges at a tangent to the periphery of the source. The tangential jet model was first proposed by Nielson (21). The jet is a one dimensional flow in the direction of the tangent to circular source. An analytical solution giving the velocity $\vec{q}$ in explicit form was obtained from solving the equation of motion and using Prandtl's Second Hypothesis as a model for the turbulent shear stress. The resulting equations are

$$\bar{q} = \frac{A}{2}\left(\frac{\sigma}{r}\right)^{\frac{1}{2}} \frac{1}{(r^2-a^2)^{\frac{1}{4}}} \left[1 - \tanh^2(\eta/2)\right] \qquad \text{(II-10)}$$

where η is a dimensionless z coordinate and is given by

$$\eta = \sigma \frac{z-z_o}{r} \qquad \text{(II-21)}$$

Equation II-10 is a four parameter model, the parameters are σ the jet width, A the volumetric flow, a, the radius of source and z_o the jet displacement. The model does not predict the angle profile and a weighted average angle was found to be satisfactory to evaluate, a, the radius of source. The other three parameters were obtained by a nonlinear least square regression analysis, and the fit on the data was excellent. It should be noted that since velocity profiles are measured for a little beyond $\frac{1}{2}q_{max}$, the model could not be checked for accuracy at the tail ends of the profile.

Cooper (8) had measured velocity profile in water and air using essentially the same probe. His data was found to be compatible with the tangential jet model and the results were in agreement with the data taken by us. Cooper's and our data were thus combined together for the purpose of correlating the results. The combined data covers four geometrically similar type A turbines and three different tank diameters. Cooper's data is for air and water, thus the data includes two different fluids. The Reynolds number N_{Re} range is 19,000 to 358,000. The higher values for N_{Re} is for air.

The conclusions from data are:

1. The jet width is a constant, since σ was found to be a constant, independent of radial angle, radial distance and height of impeller off tank battom, h. The minimum value

of h recommended is twice the maximum jet width b_o and is given by Equation II-28 (since b_o is equal to r_o.)

2. A weighted average angle was found to give a value of a, the radius of source, which satisfactorily predicted the measured velocity profile.
3. The volumetric flow parameter, A, was found to be a scaled value of the impeller discharge Q.

The conclusions from the combined data of ours and that of Cooper's are:

1. The jet width σ was found to be a constant. Its value is 12.6 $\pm$ 1.5. It is thus also independent of tank diameter and the physical properties of the fluid. The independency with tank diameter is not conclusive; however, in the absence of adequate data this analysis indicates it to be approximately true.
2. The radius of source parameter, a, was found to be dependent on tank and impeller diameter. Two separate correlations were found that could satisfactorily interpolate the data, one at constant tank diameter and one at constant impeller diameter.
3. The impeller discharge, Q, was found to correlate well with ND^3, as the correlation coefficient was found to be 0.99. The equation for Q is

$$Q = 1.075(ND^3)^{0.942}$$

4. The volumetric flow parameter A was found to be dependent on the tank diameter it was found to correlate well with

$ND^3/((D/2)^2-a^2)^{\frac{1}{4}}$. The equation for A is

$$A = 1.144 \left(\frac{ND^3}{((D/2)^2-a^2)^{\frac{1}{4}}} \right)^{0.834}$$

and the correlation coefficient was found to be 0.986.

5. The extent of the tangential jet was successfully predicted as 34% of the tank diameter.

6. Cooper also measured velocity profiles for a 4.0 inch diameter impeller with varying blade widths, b. These impellers are not geometrically similar. The jet width σ is insensitive to small changes in b but in general is a function of b. The radius of source a is strongly dependent on b. Finally the impeller discharge Q was found to be proportional to a function of b. This means that the functional relationship with b does not interact with that of the impeller speed.

The tangential jet model was also tested on the velocity profile data of Nielson (21) and Cutter (9). This data was obtained by the light streak method and does not show an angle profile. Since geometrically similar impellers were used the results of the correlation were used to estimate σ. The correlation gave an erroneous value of a, the radius of source, indicating that a is strongly dependent on the tank diameter. The value of a was thus estimated. These estimates of a, gave a satisfactory fit of the velocity profile data, and the results of the analysis was in agreement with Cooper's and our data.

The tangential jet model gave a value for the eddy viscosity ϵ as

$$\epsilon = \frac{A}{2} \frac{1}{(\sigma^3 r)^{\frac{1}{3}}} \frac{2r^2-a^2}{(r^2-a^2)^{3/4}}$$

The correlations for σ, A and a was found to give a satisfactory prediction for the eddy viscosity and impeller discharge Q. The correlations for the tangential jet parameters are thus good estimates of these parameters.

The tangential jet model is a satisfactory model for predicting the flow in the region of the impeller. It does not predice the angle profile and is thus not a completely satisfactory model.

Potential Flow

Outside the impeller region two dimensional potential flow was used to model the flow field. The field was divided into five regions as shown in Figure II-1 and are:

1. Impeller stream impinging on tank wall, modeled by stagnation flow.
2. Upper and lower corners of the tank modeled by potential flow in a corner.
3. Flow at the top and bottom of the tank axis, also modeled by potential flow in a corner.
4. Flow at the center of the tank axis, modeled by a circular jet.
5. Two doughnut shaped regions on either side of the impeller stream modeled as dead water regions.

A Calcomp plotter was used to draw the flow patterns and is a useful method for obtaining flow patterns.

The agreement between the model and experimental data is poor because of the assumption of two dimensional flow. Velocity profile measurements indicate that a three dimensional flow field exists. Comparison of $\bar{v}_z$ between model and experimental data show a close resemblance in the shape but not in magnitude of the velocity profile in Regions II and III. There is no agreement between the model and experimental profiles for $\bar{v}_r$. It is thus concluded that potential flow is a valid flow model in this region. Since potential flow is a linear model, the inclusion of $\bar{v}_\theta$ in the model would scale the $\bar{v}_z$ profile correctly and bring an agreement of the profile for $\bar{v}_r$. No attempt was made to test this theory as adequate data could not be taken with the three dimensional probe.

In Region V the circular jet model was shown to be a poor representation of the velocity field. This model illustrates that the agreement in flow pattern by streamlines need not necessary give an agreement in velocity profiles as well.

The flow outside the impeller was shown to be a maximum at the walls of the tank. The width of this stream was shown to be the width of the 10% baffle used. This clearly shows that the width and location of the baffle was correctly determined for the purpose of modifying the flow.

Recommendation

The following are the recommendations based on the evaluation

and analysis of the experimental data presented in this dissertation, and the data available in the literature.

1. Hot wire anemometer is recommended to measure flow fields outside the impeller region.
2. Measurements of velocity profiles are needed near the boundary of the tangential jet region to test the validity of the model in this region. If the model is inadequate, it is not a serious error since this region can be modeled with Region VI, and the tangential jet could be used to model the present range of the velocity profile.
3. Velocity profile measurements are needed with varying tank diameters to adequately predict the radius of source a, and the effect if any on σ.
4. Exhaustive velocity profile measurements with at least one fluid other than air or water are needed to test conclusively the independence of the tangential jet parameters on the fluid used.
5. In the region outside the impeller a potential flow model is recommended. Since potential flow is a linear model it would be valid to subtract $\bar{v}_\theta$ from the resultant velocity $\vec{V}$ of the three dimensional flow field. $\bar{v}_\theta$ could be then modeled seperately as a vortex in combination with a solid rotating cylinder at the impeller axis. This model is suggested from the velocity profile for $\bar{v}_\theta$ given in Figure IV-9. The remaining two velocity components $\bar{v}_r$ and $\bar{v}_z$ could be handled as a two dimensional flow field as done in this work.

NOMENCLATURE

In the case of vectors and tensors, the symbols given in this nomenclature represents their magnitudes. Vectors and Tensors are distinguished in the text by overmarks and are given below under the heading overmarks.

Symbol	Description	Units
A	Volumetric flow parameter	ft^3/min
	Parameter in Equation I-10	
a	Radius of source of the tangential jet	ft.
	Constant Equation I-1	none
	Parameter Equation I-10	none
b	Width of impeller blade (Figure I-2)	in.
	Width of jet (Equation I-9)	ft.
$b_{\frac{1}{2}}$	Half width of the jet (Equation B-32)	ft.
C_1	Constant (Equation I-25)	none
c	Mixing length constant (Equation I-5)	none
	Constant (Equation B-3)	
D	Impeller diameter	ft.
d	Constant (Equation I-9)	none
d_1	Diameter of Type A impeller disc (Figure I-2)	in.
E	Voltage	volts

E_c	Fraction of momentum transferred, Equation IV-23	none
e'	Fluctuating component of E	volts
F	Function defined by Equation B-9	none
f	Function defined by Equation B-5	none
g_c	Standard acceleration of gravity (32.174 ft/sec^2)	ft/sec^2
H	Depth of fluid in tank	ft.
	Also used as length of column of manometer fluid in manometer calculations	ins.
h	Height of impeller of tank bottom	ins.
h_1	Height of blade above impeller plane (see Figure I-2)	ins.
J	Momentum	$(lb_m)(ft)/sec$
k	Constant	
k'	Constant defined by Equation IV-44	
	Constant, Equation I-33	
l	Length of impeller blade (Figure I-2)	in.
N	Impeller speed	RPM
N_P	Power number Pg_c/N^3D^5	none
N_Q	Dimensionless pumping capacity Q/ND^3	none
N_{Re}	Reynolds number for stirred tanks $\rho ND^2/\mu$	none
P	Power	$(lb_f)(ft)/sec$
	Pressure	lb_f/ft^2
P_t	Total Pressure	lb_f/ft^2
P_s	Stagnation pressure	lb_f/ft^2

Q	Volumetric flow	ft^3/min
Q_o	Volumetric flow increment on a streamline	ft^3/min
$\vec{q}$	Velocity, resultant of v_r, v_θ	ft/min
q	Relative slip in velocity between the fluid and impeller at impeller periphery, Equation I-27	none
r, θ, z	Lengths, in cylinderical coordinates	ft.
R	Impeller radius	ft.
	Correlation Coefficient defined by Equation IV-1	none
r_o	Extent of tangential jet model	ft.
r_c	Starting coordinate of a streamline in Region I. Also r coordinate of center of circulation (Figure I-3)	ft.
	Dimensionless coordinate for velocity profile defined by Equation I-6	none
S_x^2	Variance (see Equation IV-4)	none
s	Dimensionless z coordinate, (Equation I-6)	none
T	Tank diameter	ft.
t	Boundary layer thickness (Figure II-6)	ft.
$t_{0.95,(N-1)}$	t-test parameter 0.95 probability with (N01) degrees of freedom	none
V	Velocity	ft/min
v_r, v_θ, v_z	Velocity components, cylinderical coordinates	ft/min
v_x, v_y, v_z	Velocity components, cartesian coordinates	ft/min
W	Velocity, resultant of v_z and v_θ	ft/min
w	Angular velocity	radians/sec

x,y,z	Lengths, in cartesian coordinates	ft.
x_n,y_n	Local coordinates of boundary point between two regions, defined in Section 2.3	ft.
z_o	Displacement of tangential jet profile from impeller centerline	ft.
	z coordinate of center of circulation (Figure I-3)	
	Displacement of circular jet relative to tank bottom	

Greek

α	Angle	degrees
	Pressure ratio defined by Equation IV-15	none
γ	Circular jet width parameter, defined by Equation II-19	none
ΔH	Pressure drop in inches of manometer fluid	in.
ΔH_s	Static head	in.
ϵ	Eddy viscosity, tangential jet	ft^2/min
ϵ_o	Eddy viscosity, circular jet	ft^2/min
η	Dimensionless velocity profile coordinate for tangential jet defined by Equation II-13	none
θ	Angle	degrees
μ	Viscosity	$lb_m/(ft)(sec)$
ξ	Dimensionless velocity profile coordinate for circular jet defined by Equation II-19	none
ρ	Density	$lb_m/(ft)^3$
σ	Tangential jet width parameter defined by Equatio n II-13	none

$\overline{\overline{\tau}}$	Stress tensor	lb_f/ft^2
$\tau_{r,z}, \tau_{\theta,z}$ etc.	Components of stress tensor	lb_f/ft^2
τ	Resultant of $\tau_{r,z}$ and $\tau_{\theta,z}$	
ϕ	Potential function	lb_f/ft^2
ψ	Stream function	ft^3/min

Subscripts

AA	Boundary between Regions IV and V
BB	Boundary between Regions III and IV
CC	Boundary between Regions II and III
c	Circular jet
calc	Calculated from theoretical relationship
exp	Experimentally obtained value
m	Manometer
max	Maximum
min	Minimum
p	Pitch
s	Stagnation, Equation IV-15
	Static, Equation IV-25
t	Tangential jet
	Total
y	Yaw
1,2	On ΔH, refers to pressure drop across taps P_1 and P_2

Super Scripts

'	Derivative
°	Angular measurement or temperature in degrees

′	Fluctuating component

Overmarks

-	Time average quantity
→	Vector
=	Tensor

List of FØRTRAN Symbols Used in Text

A	A, volumetric flow parameter
AA	a, radius of source parameter
ANGLE	$\bar{\theta}_y$, weighted average angle
AVERAGE	Arithmetic average angle
AVG	Subroutine for calculating averages (List F-1)
AVG ANGLE	Arithmetic average of θ_y
BOUNDS	Subroutine required by PATERN (List F-1)
BCALC	z coordinate corresponding to $\frac{1}{2}q_{max}$ obtained by interpolating experimental data
BHALF	z coordinate corresponding to $\frac{1}{2}q_{max}$ from Equation H-1
CFM	Volumetric flow at r, calculated from Equation B-31 Impeller dischange calculated from Equation IV-1
COS(PHI)	COS $\bar{\theta}_y$
CORR COEF	Correlation coefficient defined by Equation IV-1
COOPER	Main program, to analysis Cooper's (8) data (List F-5)

CURVEF	Subroutine required by VELPRO (List F-2)
DEVIATION	95% confidence limit using t-test (Equation IV-5)
FK1=H/T	Scaled value of H, the depth of fluid in the tank
FK2=h/T	Scaled value of h, height of impeller off the tank bottom
FK3	Scale on $\bar{v}_r$ used for plotting velocity frofile in Region I
FLOWANL	Main program, analyses velocity profiles (List F-1)
GOLD	Subroutine for Golden section search (List E-1)
GRAPH	Main program to obtain linear regression coefficients (List F-7)
JGAMMA	Controls calculation of velocity profile in Regions II, III and V, needed for Figure IV-5 through IV-8
LIV	Controls shape of Regions IV, LIV = 0 gives Figure II-5, LIV = 1 gives Figures II-6 through II-9
LPRINT	Print control, LPRINT = 1 gives a detailed print out
NIELCUT	Main program, analyses Nielson's ( ) and Cutter's ( ) data (List F-6)
OMEGA	Subroutine, performs Lagrange interpolation (List F-1)
PATERN	Subroutine, performs Pattern Search (List F-1)
PLOTER	Main Program, plots theoretical velocity Profiles (List E-1)

PROC — Subroutine, minimization criteria function for PATERN (List F-1)

POLY — Subroutine, performs polynomial least square fit (List F-2)

PX,PY — Array, stores r and z coordinates of a complete streamline

P(4) — z_o, displacement parameter of tangential jet

RRX — Stores r coordinate of velocity profile analyses from theoretical streamlines of Regions II, III and V

SOLVE — Subroutine, needed by GRAPH (List F-6)

SPRINT — Subroutin, needed by PLOTER (List E-1)

SS — Sum of Squares about predicted line defined by Equation C-2

STREAM — Subroutine, calculates coordinates of a streamline (List E-1)

SY — Stores values of ψ in velocity profile analysis from theoretical streamlines of Regions II, III and V

T — Tank diameter, ft.

TANKANL — Main program, analyses three dimensional flow data from Pitot tube in the region outside the impeller (List F-3)

TB=FK2*T — Height of impeller of tank bottom

TF — Effect depth of fluid in potential flow region above or below impeller centerline (see Figure IV-6)

TL=(FK1-KF2)*T

Depth of fluid above impeller centerline

UHALF	$\frac{1}{2}q_{max}$
VARIANCE	Variance, S_x^2 (Equation IV-4)
VR,VZ	Stores $\bar{v}_r$ and $\bar{v}_z$ of velocity profile analysis from theoretical streamlines in Regions II, III and IV
WT	Velocity factor (Equation IV-3)
X,Y	Local frame of axis
XN	Extent of tangential jet solution r_o
XN2	Parameter, determined thickness of boundary layer given by XN2*TB
XN3	Parameter, determines boundary between Regions IV and V
XN4	Parameter, determines boundary between Regions II and III
XNF	Parameter, determines boundary between Regions III and IV
YAW	Subroutin, calculates results from manometer D (List F-1)
YAWANL	Main program, analyses three dimensional flow data from Pitot tube in the region of the impeller (List F-4)

BIBLIOGRAPHY

1. Aiba, S. "Flow Patterns of Liquids in Agitated Vessels", A.I.Ch.E. J., 4, 485 (1958).

2. Askew, Waren S., Beckman, Robert B., "Velocity Profiles and Transfer Operations at the Wall of an Agitated Vessel", I & EC Process Design and Development, 5 (3), 268 (1966).

3. Bates, Robert L., Fondy, Philip L., Corpstein, Robert R., "An Examination of Some Geometric Parameters of Impeller Power", Ind., Eng. Chem., Process Design and Development, 2, 310 (1963).

4. Bowers, R.H., "An Investigation of Flow Phenomena in Stirred Liquids", A.I.Ch.E. - I. Chem. E., Symposium Series 10, London (1965).

5. Bird, R. B., Stewart, W. E., Lightfoot, E. N., Transport Phenomena, John Wiley and Sons Inc., New York, p. 159 (1962).

6. Ibid, p. 83, 85.

7. Camps, Jorge A., Mixing Model and Measurements of Heptane-Sulfuric Acid Emulsions in a Continuous Flow Stirred Tank Reactor, M.S. Thesis, Louisiana State University (1968).

8. Cooper, R. G., Velocity Profiles and Pumping Capacities of Turbine Type Impellers, M. S. Thesis, McGill University (1966).

9. Cutter, L. A., Flow and Turbulence in a Stirred Tank, Ph.D. Thesis, Columbia University (1960).

10. Dell'osso, Luino Jr., Turbulence Measurement in Water in an Open Channel with the Hot-film Anemometer, Ph. D. Thesis, Rice University (1966).

11. Goldstein, R. J., Kreid, D. K., "Measurement of Laminar Flow Development in a Square Duct Using a Laser-Doppler Flowmeter", J. Applied Mech., Trans. of ASME, Paper No. 67, APM-37,(1967).

12. Holland, F. A., Chapman F. S., Liquid Mixing and Processing in Stirred Tanks, Reinhold Publishing Corporation, New York (1966).

13. Holmes, D. B., Voncken, R. M., Dekker, J. A., "Fluid Flow in Turbine-stirred, Baffled Tanks", Chem. Eng. Sc. 19, 201. (1964).

14. Larson, Paul Z., Flow Patterns and Velocity Profiles in an Agitated Vessel, Ph. D. Thesis, University of Delaware (1965).

15. Milne-Thompson, L.M., Theoretical Hydrodynamics, 5th Edition (1968), p. 351, Macmillian, New York.

16. Metzner, A. B., Taylor, J. S., "Flow Patterns in Agitated Vessels," A.I.Ch.E.J., 6 (1), 109 (1960).

17. Mujumdar, A.A. Huang, B., Wolf, D., Weber, M. E., Douglas, W. J. M., "Turbulence Parameters in a Stirred Tank", Preprint 25f, Chemical Engineering Conference, Triportite Meeting, Montreal Canada (Sept. 22-25, 1968).

18. Nagata, S., Yamamoto, K., Ujihara, M., "Flow Patterns of Liquids in a Cylinderical Mixing Vessel without Baffles", Mem. Fac. Eng., Kyoto University, 20, 336 (1958).

19. Nagata, S., Yamamoto, K., Hashimoto, K., Naruse, Y., "Flow Patterns of Liquids in a Cylinderical Mixing Vessel with Baffles", Mem. Fac. Eng., Kyoto University 21, 260 (1959).

20. Nagata, S., Yamamoto, K., Hashimoto, K., Naruse, Y., "Studies on the Flow Patterns of Liquids in a Cylinderical Mixing Vessel, Over a Wide Range of Reynolds Numbers", Mem. Fac. Eng., Kyoto University 22, 68 (1960).

21. Nielson, Hugo J., Flow and Turbulence form a Flat Blade Turbine Mixing Impeller, Ph. D. Thsis, Illinois Institute of Technology (1958).

22. Norwood, K. W., Metzner, A. W., "Flow Patterns and Mixing Rates In Agitated Vessels", A.I.Ch.E.J. 6, (3), 432 (1960).

23. Oldshue, J. Y., "Fermentation Mixing Scale-up Techniques", Biotechnology and Bioengineering, Vol. VIII, pp. 3-24, John Wiley and Sons, Inc., New York (1966).

24. Rao, A. M., Turbulence and Mixing in a Continuous Flow Stirred Tank, Ph. D. Thesis, The Ohio State University (1969).

25. Rolfe, E., Silk, J. K., Booth, S., Meister, K., Young, R. M., Laser Doppler Velocity Instrument, NASA CR-1199 (Dec. 1968).

26. Rushton, J. H., Costich, E. W., Everett, H.J., "Power Characteristics of Mixing Impellers", Chem. Eng. Prog. 46,(395) 467 (1950).

27. Rushton, J. H., Oldshue, J.Y., "Mixing of Liquids",Chem. Eng. Prog. 55 (25),181 (1959).

28. Sachs, J.P., Rushton, J.H., "Discharge Flow from Turbine-Type Mixing Impellers",Chem. Eng. Prog., 50, (12), 597 (1954).

29. Schlichtling, H., Boundary Layer Theory, 4th Edition, p. 482 McGrw-Hill Book Co, Inc., New York, (1960).

30. Ibid. p. 604-609.

31. Ibid. p. 182, 607.

32. Schumm, Jr., Brooke, A Mathematical Model for Wake-Type Fluid Flow from Turbine-Tube Impellers, Ph. D. Thesis, University of Rochester (1966).

33. Sterbacek, Z., Tausk, P., "Mixing in the Chemical Industry," Permagon Press Inc., New York (1965).

34. Uhl, V. W., Grey, J. B., Mixing, Theory and Practice, Vols. I and II, Academic Press, New York (1966).

35. Ibid., Vol I, p. 132.

36. Ibid., Vol I, p. 137, 157.

37. Ibid., Vol I, p. 181.

38. Ibid., Vol I, p. 187-200.

39. Ibid., Vol I, p. 207.

40. Ibid., Vol I, p. 209.

41. Van de Vusse, J. G., "Mixing by Agitation of Miscible Liquids", Chem. Eng. Sc. 4, 178, 209 (1955).

42. Wilde, D. J., Optimum Seeking Methods, Prentice-Hall, Inc., New Jersey (1964).

43. Yaun, S. W., Foundations of Fluid Mechanics, Prentice-Hall Inc. New Jersey, p. 74, (1967).

44. Ibid., p. 158.

45. Ibid., p. 200.

46. Ibid., p. 207, 208.

47. United Sensor and Control Corporation, 85 School Street, Water-Town, Massachusetts 02172. Calibration Data Sheet for USC-1086, probe type Da-187-24-F-22-CD, Serial No. A-402.

APPENDIX A

TANGENTIAL OR RING JET

Derivation of Differential Equation

This appendix will derive the equations that describe the motion of the tangential or ring jet. The approach used, is to simplify the time averaged continuity equation and equation of motion subject to geometric constraints and observations on the behavior of the flow. The time averaged equation of continuity and equation of motion are used to describe the energy dissapation due to turbulence.

The flow in the jet is similar to boundary layer flow in that both flows have high velocity gradients perpendicular to the direction of flow. The turbulence in the jet is free turbulence and will be modeled by using Prandtl's Second Hypothesis. The assumptions and constraints that apply to the tangential jet are:

1. Pressure gradients are negligible. The only pressure gradient that exists is in the z-direction due to gravity and does not influence the flow of the fluid.
2. Axial symmetry about z axis; hence $\bar{v}_r$, $\bar{v}_\theta$, $\bar{v}_z$ are independant of θ.
3. Steady State.
4. Incompressible isothermal flow, hence the density ρ is constant.
5. $\bar{v}_r$, $\bar{v}_\theta$ are of the same order of magnitude, $\bar{v}_z$ is of a lower

order. This will be recognized as the boundary layer approximation. Furthermore, the velocity gradient in the z direction is larger than in the r, and θ directions. This is because the flow is in the r, θ plane and in the r direction. The flow does not change rapidly with increasing r. However, the change in the velocity profile in the z direction is comparatively larger.

The time averaged equation of continuity in vector form (5) for an incompressible fluid and steady state conditions is

$$\vec{\nabla} \cdot \vec{V} = 0 \qquad \text{(A-1)}$$

The velocity $\vec{V}$ is the resultant of v_r, v_θ, and v_z. The arrow over V signified that it is a vector. The bar over $\bar{v}_r$ for example, indicates that it is a time averaged velocity. Writing A-1 in cylinderical coordinates,

$$\frac{1}{r}\frac{\partial}{\partial r}(r\,\bar{v}_r) + \frac{1}{r}\frac{\partial \bar{v}_\theta}{\partial \theta} + \frac{\partial \bar{v}_z}{\partial z} = 0 \qquad \text{(A-2)}$$

The second term in equation A-2 is zero from Assumption Two, rearranging A-2 gives

$$\frac{\partial}{\partial r}(r\bar{v}_r) + \frac{\partial}{\partial z}(r\bar{v}_z) = 0 \qquad \text{(A-3)}$$

Equation A-3 is the continuity equation for the tangential jet.

The time averaged equation of motion in vector form (5) for an incompressible fluid is

$$\rho \frac{D\vec{V}}{Dt} = -\vec{\nabla} \cdot \vec{p} \quad [\vec{\nabla} \cdot \overline{\overline{\tau}}^{(1)}] - [\vec{\nabla} \cdot \overline{\overline{\tau}}^{(t)}] + \rho\vec{g} \qquad \text{(A-4)}$$

where, $\overline{\overline{\tau}}^{(1)}$ and $\overline{\overline{\tau}}^{(t)}$ are the laminar and turbulent momentum fluxes. In fully turbulent flow $\overline{\overline{\tau}}^{(t)}$ is much larger than $\overline{\overline{\tau}}^{(1)}$, hence $\overline{\overline{\tau}}^{(1)}$ can be neglected in comparison. In future discussion the superscript on

$\bar{\bar{\tau}}$ will be dropped, since it is clear that $\bar{\bar{\tau}}$ refers to $\bar{\bar{\tau}}^{(t)}$. From Assumption one, the pressure $\bar{p}$ is constant hence A-4 reduces to

$$\rho \frac{D\vec{v}}{Dt} = - \vec{\nabla} \cdot \bar{\bar{\tau}} + \rho \vec{g} \tag{A-5}$$

Equation A-5 can be simplified further by writing it in cylinderical coordinates. The r-component is (6) given by,

$$\rho\left(\frac{\partial \bar{v}_r}{\partial t} + \bar{v}_r \frac{\partial \bar{v}_r}{\partial r} + \frac{\bar{v}_\theta}{r} \frac{\partial \bar{v}_r}{\partial \theta} - \frac{\bar{v}_\theta^2}{r} + v_z \frac{\partial \bar{v}_r}{\partial z} = \right.$$

$$\left. - \left(\frac{1}{r} \frac{\partial}{\partial r} (r\tau_{rr}) + \frac{1}{r} \frac{\partial \tau_{r\theta}}{\partial \theta} - \frac{\tau_{\theta\theta}}{\tau} + \frac{\partial \tau_{rz}}{\partial z}\right)\right) \tag{A-6}$$

In equation A-6 the first term on the left hand side is zero because of steady state and the third term is zero because of axial symmetry. From the boundary layer assumption, Assumption Five, it follows that τ_{rz} is much larger in comparison with τ_{rr} and $\tau_{r\theta}$, and hence the terms containing these quantities can be deleted from the equation. In the light of the above remarks A-6 reduces to

$$\bar{v}_r \frac{\partial \bar{v}_r}{\partial r} - \frac{\bar{v}_\theta^2}{r} + \bar{v}_z \frac{\partial \bar{v}_r}{\partial z} = - \frac{1}{\rho} \frac{\partial \tau_{rz}}{\partial z} \tag{A-7}$$

The θ-component of equation A-5 is

$$\rho\left(\frac{\partial \bar{v}_\theta}{\partial t} + \bar{v}_r \frac{\partial \bar{v}_\theta}{\partial r} + \frac{\bar{v}_\theta}{r} \frac{\partial \bar{v}_\theta}{\partial \theta} + \frac{\bar{v}_r \bar{v}_\theta}{r} + \bar{v}_z \frac{\partial \bar{v}_\theta}{\partial z}\right) =$$

$$- \frac{1}{\rho} \left(\frac{1}{r^2} \frac{\partial}{\partial r} (r^2 \tau_{r\theta}) + \frac{1}{r} \frac{\partial \tau_{\theta\theta}}{\partial \theta} + \frac{\partial \tau_{\theta z}}{\partial z}\right) \tag{A-8}$$

In equation A-9, the first term on the left hand side is zero because of steady state. Since $\bar{v}_\theta$ is not a function of θ the third term is zero. Examining the right had side of A-8 it is seen on using Assumption Five that $\tau_{\theta z}$ is much larger than $\tau_{\theta\theta}$ and $\tau_{\tau\theta}$ and terms containing them could thus be deleted. Equation A-8 thus simplifies to

$$\bar{v}_r \frac{\partial \bar{v}_\theta}{\partial \theta} + \frac{\bar{v}_r \bar{v}_\theta}{r} + \bar{v}_z \frac{\partial v_z}{\partial z} = - \frac{1}{\rho} \frac{\partial \tau_{\theta z}}{\partial z} \qquad \text{(A-9)}$$

The z-component of A-5 is given by

$$\rho \left(\frac{\partial \bar{v}_z}{\partial t} + \bar{v}_r \frac{\partial \bar{v}_z}{\partial r} + \frac{\bar{v}_\theta}{r} \frac{\partial \bar{v}_z}{\partial r} + \bar{v}_z \frac{\partial \bar{v}_z}{\partial z} \right) =$$

$$- \frac{1}{\rho} \left(\frac{1}{r} \frac{\partial}{\partial r} (r \tau_{rz}) + \frac{1}{r} \frac{\partial \tau_{\theta z}}{\partial \theta} + \frac{\partial \tau_{zz}}{\partial z} \right) + \rho g_z - \frac{\partial p}{\partial z} \qquad \text{(A-10)}$$

In equation A-10 all terms on the left hand side are small being functions of $\bar{v}_z$ and hence can be neglected from Assumption Five. The turbulent shear stresses are also functions of $\bar{v}_z$ and can be neglected. The two extra terms have been included in Equation A-10. These are the static pressure P and the acceleration due to gravity. These terms are a result of Assumption One. Equation A-10 thus simplifies to

$$- \frac{\partial p}{\partial z} + \rho g = 0 \qquad \text{(A-11)}$$

For convenience, the continuity equation and the equation of motion which have been simplified above are rewritten below.

$$\frac{\partial}{\partial r}(r\bar{v}_r) + \frac{\partial}{\partial z}(r\,\bar{v}_z) = 0 \qquad \text{(A-3)}$$

$$\bar{v}_r \frac{\partial \bar{v}_\theta}{\partial r} + \bar{v}_z \frac{\partial \bar{v}_r}{\partial_z} - \frac{\bar{v}_\theta^2}{r} = -\frac{1}{\rho}\frac{\partial \tau_{rz}}{\partial z} \qquad \text{(A-7)}$$

$$\bar{v}_r \frac{\partial \bar{v}_\theta}{\partial r} + \bar{v}_z \frac{\partial \bar{v}_\theta}{\partial z} + \frac{\bar{v}_r \bar{v}_\theta}{r} = -\frac{1}{\rho}\frac{\partial \tau_{\theta z}}{\partial z} \qquad \text{(A-9)}$$

$$-\frac{\partial P}{\partial z} + \rho g = 0 \qquad \text{(A-11)}$$

The above equations can also be used to describe axially-symmetric two dimensional boundary layer flows. These equations are partial differential equations and as such cannot be solved directly. Further simplification is possible when the tangential jet is examined. In Figure A-1 is shown the tangential jet. O is the center of the tangential source of radius a and height 2b. The fluid flows out of the source in a direction which is a tangent to the periphery of the source. When the fluid leaves the periphery such as from a point A in figure A-1 it has a magnitude, $\vec{q}$, and a fixed direction. Consider any arbitrary point B. The angle which the velocity of the fluid makes with the radius vector is θ_y. In chapter IV, this was referred to as a yaw angle. It is easily seen that $\theta_y = 90°$ at r = a and decreases as r increases. The radial and tangetial components are $\bar{v}_r$ and $\bar{v}_\theta$ and are shown in the figure. From the geometry of Figure A-1 it is clear that

$$\tan \theta_y = \frac{\bar{v}_\theta}{\bar{v}_r} \qquad \text{(A-12)}$$

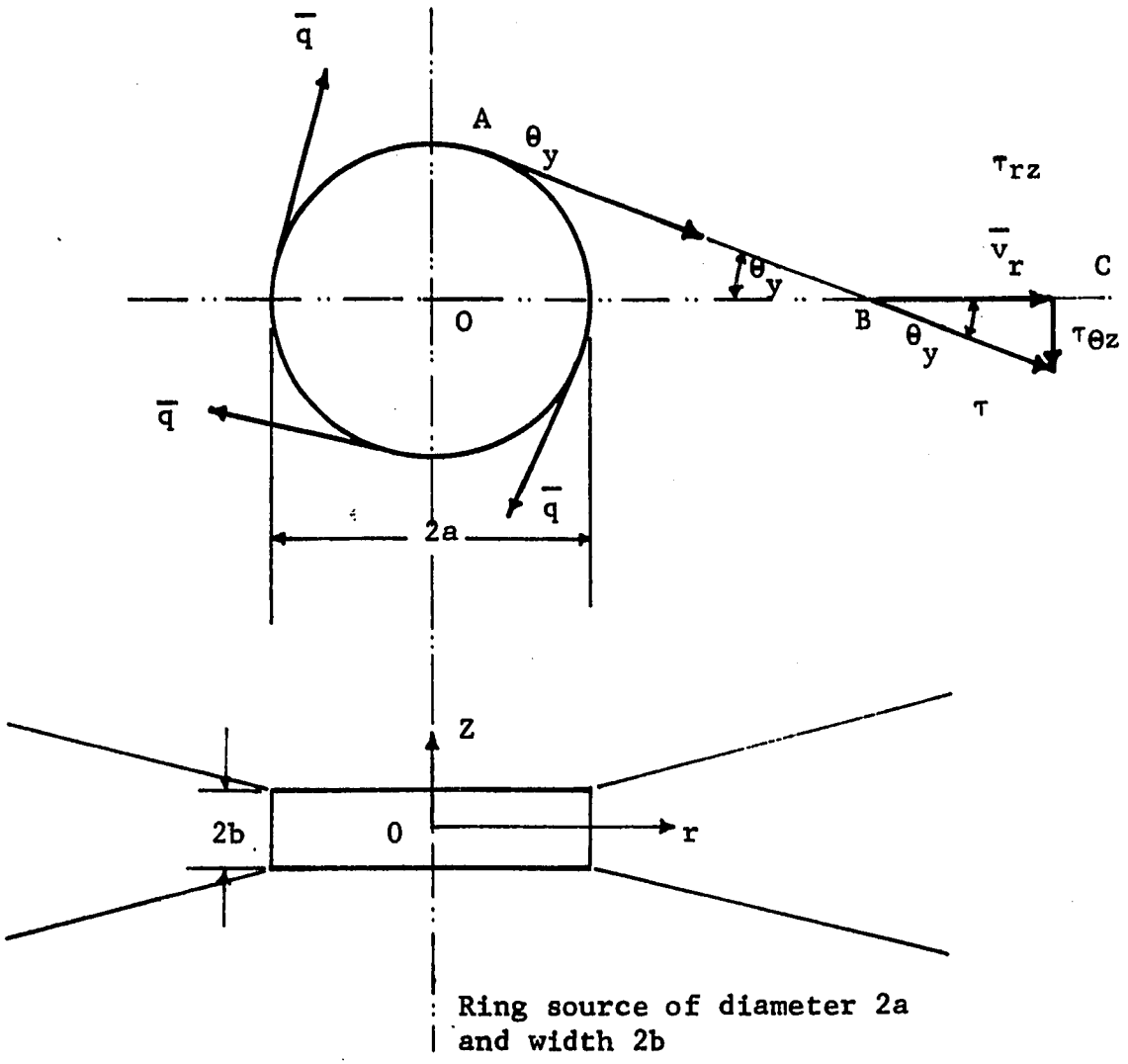

Ring source of diameter 2a and width 2b

Figure A-1. The Tangential Jet.

Since OB = r and OA = a, from the geometry of the figure it follows that

$$\tan \theta_y = \frac{a}{\sqrt{r^2 - a^2}} \tag{A-13}$$

$$\cos \theta_y = \frac{\sqrt{r^2 - a^2}}{r} \tag{A-14}$$

$$\sin \theta_y = \frac{a}{r} \tag{A-15}$$

In the equations of motion, A-7 and A-9, the process of simplification using Assumptions One to Five have reduced the stress tensor $\bar{\bar{\tau}}$ from nine components to two, τ_{rz} and $\tau_{\theta z}$. The stress tensor has thus been reduced to a vector $\vec{\tau}$. From Figure A-1 it is seen that the tangetial jet is clearly a one dimension flow in the direction of $\vec{q}$. The shear stress $\vec{\tau}$ is thus a result of the flow $\vec{q}$ and hence τ_{rz} and $\tau_{\theta z}$ are components of $\vec{\tau}$, as shown in Figure A-1.

$$\tau_{rz} = |\vec{\tau}| \text{ Cos } \theta_y \tag{A-16}$$

$$\tau_{\theta z} = |\vec{\tau}| \text{ Sin } \theta y \tag{A-17}$$

Substituting for Cos θ_y from A-14 and Sin θ_y from A-15 gives

$$\tau_{rz} = \frac{\sqrt{r^2 - a^2}}{r} \quad |\vec{\tau}| \tag{A-18}$$

and

$$\tau_{\theta z} = \frac{r}{a} \quad |\vec{\tau}| \tag{A-19}$$

From the geometry of Figure A-1 it follows that

$$\bar{v}_r = |\vec{q}| \quad \text{Cos } \theta_y \tag{A-20}$$

$$\bar{v}_\theta = |\vec{q}| \quad \text{Sin } \theta_y \tag{A-21}$$

We can now show that the two equations of motion, A-7 and A-9 are identical, reducing to a single equation. This is done as follows. Substituting for τ_{rz} from Equation A-18, $\bar{v}_\theta$ from A-21 into A-7 and simplifying gives

$$\bar{v}_r \frac{\partial \bar{v}_r}{\partial r} + \bar{v}_z \frac{\partial \bar{v}_r}{\partial z} - \frac{a^2}{r(r^2 - a^2)} \bar{v}_r^2 = -\frac{1}{\rho} \frac{\sqrt{r^2 - a^2}}{r} \frac{\partial |\vec{\tau}|}{\partial z} \qquad \text{(A-22)}$$

Similarly substituting $\tau_{\theta z}$ from A-19 and $\bar{v}_\theta$ from A-21 into A-9 and simplifying gives

$$\bar{v}_r \frac{\partial \bar{v}_r}{\partial r} + \bar{v}_r^2 \left[\frac{1}{r} - \frac{r}{r^2 - a^2} \right] + \bar{v}_z \frac{\partial \bar{v}_r}{\partial z} = \frac{1}{\rho} \frac{\sqrt{r^2 - a^2}}{r} \frac{\partial |\vec{\tau}|}{\partial z} \qquad \text{(A-23)}$$

On examining equations A-22 and A-23 we see they are identical. We thus have a single equation of motion, which is expected since the problem is a one dimensional flow field. The above analysis for a tangential jet was first obtained by Nielson (21).

Momentum of Tangential Jet.

Equation of motion A-22, the continuity equation A-3 and the boundary conditions are sufficient to obtain a solution for the tangential jet. An analytic solution will be obtained using the similarity principle. However in order to do this the momentum in the jet has to be evaluated. This is done by first considering the following identity from calculus.

$$\bar{v}_z \frac{\partial \bar{v}_r}{\partial z} = \frac{\partial (\bar{v}_r \bar{v}_z)}{\partial z} - \bar{v}_r \frac{\partial \bar{v}_z}{\partial z} \qquad \text{(A-24)}$$

Introducing the continuity equation A-3 into A-23,

$$\bar{v}_z \frac{\partial \bar{v}_r}{\partial z} = \frac{\partial (\bar{v}_r \bar{v}_z)}{\partial z} + \bar{v}_r \frac{\partial \bar{v}_r}{\partial r} + \frac{\bar{v}_r^2}{r} \qquad \text{(A-25)}$$

Combining A-22, the equation of motion, and A-25 and rearranging,

$$\frac{\partial \bar{v}_r^2}{\partial r} + \frac{\partial (\bar{v}_r \bar{v}_z)}{\partial z} + \frac{\bar{v}_r^2}{r} \left[1 - \frac{a^2}{r^2 - a^2} \right] = - \frac{1}{\rho} \frac{\sqrt{r^2 - a^2}}{r} \frac{\partial |\vec{\tau}|}{\partial z} \qquad \text{(A-26)}$$

Equation A-26 can be shown to reduce to

$$\frac{\partial \left(\frac{r^2 \bar{v}_r^2}{\sqrt{r^2 - a^2}} \right)}{\partial r} + \frac{r^2}{\sqrt{r^2 - a^2}} \frac{\partial (\bar{v}_r \bar{v}_z)}{\partial z} = - \frac{r}{\rho} \frac{\partial |\vec{\tau}|}{\partial z} \qquad \text{(A-27)}$$

The boundary conditions for the tangential jet are, at $z = \pm \infty$ the radial velocity is zero and so is the velocity gradient $\frac{\partial \bar{v}_r}{\partial z}$. At the centerline of the jet the radial velocity $\bar{v}_r$ is a maximum and $\bar{v}_z = 0$. These can be expressed mathematically as

$$z = \pm \infty \qquad \bar{v}_r = 0, \qquad \frac{\partial \bar{v}_r}{\partial z} = 0 \qquad \text{(A-28)}$$

$$z = 0 \qquad \frac{\partial \bar{v}_r}{\partial z} = 0, \quad \bar{v}_z = 0 \tag{A-29}$$

Integrating A-27 with respect to z from $-\infty$ to $+\infty$

$$\int_{-\infty}^{\infty} \frac{\dfrac{r^2 v_r^2}{\sqrt{r^2-a^2}}}{\partial r} dz + \frac{r^2}{\sqrt{r^2-a^2}} \bar{v}_r \bar{v}_z = -\frac{r}{\rho} |\vec{\tau}| \tag{A-30}$$

Applying the boundary conditions and noting that $|\vec{\tau}|$ is proportional to $\frac{\partial \bar{q}}{\partial z}$ which quantity is zero at $z = \pm \infty$, we have

$$\int_{\infty}^{\infty} \frac{\dfrac{r^2 \bar{v}_r^2}{\sqrt{r^2-a^2}}}{\partial r} dz = 0 \tag{A-31}$$

Integrating once again but with respect to r gives,

$$\frac{r^2}{\sqrt{r^2-a^2}} \int_{-\infty}^{\infty} \bar{v}_r^2 \, dz = c \tag{A-32}$$

Where c is a constant of integration.

The quantity under the integral sign is the momentum. Equation A-32 indicates that the total momentum in the jet is a constant. This should be so, since the only momentum received by the jet is that obtained from the impeller.

APPENDIX B

SIMILARITY SOLUTION FOR A TANGENTIAL JET

In Appendix A the equation of continuity and motion were developed that describe the flow in the tangential jet. In this appendix, these equations will be solved using the assumption of similarity of velocity profiles. Sachs (28), Aiba (1), and other workers have observed that the flow in a stirred tank can be described by a dimensionless velocity which is independent of impeller speed. This dimensionless velocity is the ratio of actual velocity to impeller tip speed. Cooper (8) plots $\bar{v}_r$, $\bar{v}_{r\ max}$ against z and finds that for a given turbine impeller this quantity is independent of impeller speed. If z is also normalized by dividing by the width of the jet then the flow profile data was found by Cooper to be independent of impeller size for geometrically similar impellers. These observations suggest that the flow profiles are similar and can be stated mathematically as

$$\frac{\bar{v}_r}{(\bar{v}_r)_{max}} = f(\eta) \qquad \text{(B-1)}$$

where η is given by

$$\eta = \sigma \frac{z}{r} \qquad \text{(B-2)}$$

The maximum velocity of jet $(\bar{v}_r)_{max}$ occurs at z equal to zero.

The jet spreading parameter is σ and, a large value of σ means a narrow jet. In Appendix A, the momentum of the tangential jet was evaluated as

$$\frac{r^2}{\sqrt{r^2 - a^2}} \int_{-\infty}^{\infty} \bar{v}_r^2 \, dz = c \qquad \text{(A-32)}$$

where c is a constant.

Substituting for $\bar{v}_r$ from B-1 and z from B-2 in A-32 results in

$$\frac{r^3 (\bar{v}_r)^2_{max}}{\sigma \sqrt{r^2 - a^2}} \int_{-\infty}^{\infty} f(\eta) \, d\eta = c \qquad \text{(B-3)}$$

Since $f(\eta)$ is a similar velocity profile independent of the coordinates of the system, the integral must be a constant. Defining A^2 as

$$A^2 = c / \int_{-\infty}^{\infty} f(\eta) \, d\eta,$$

and introducing A^2 into B-3 gives,

$$(\bar{v}_r)^2_{max} = \frac{A^2 \sigma (r^2 - a^2)^{\frac{1}{2}}}{r^3}$$

or

$$(v_r)_{max} = \frac{A\,\sigma^{\frac{1}{2}}\,(r^2 - a^2)^{\frac{1}{4}}}{r^{3/2}} \qquad \text{(B-4)}$$

Substituting for $(\bar{v}_r)_{max}$ in B-1,

$$\bar{v}_r = \frac{A\,\sigma^{\frac{1}{2}}\,(r^2 - a^2)^{\frac{1}{4}}}{r^{3/2}}\; f(\eta) \qquad \text{(B-5)}$$

The velocity $\bar{v}_r$ has thus been evaluated in terms of a dimensionless velicity profile $f(\eta)$.

As the tangential jet is a two-dimensional problem, the introduction of the stream function ψ into the equation of motion A-22 automatically insures that the continuity equation A-3 is satisfied. The appropriate form of ψ in cylinderical coordinates (46) is

$$\bar{v}_r = \frac{1}{r}\,\frac{\partial \psi}{\partial z} \qquad \text{(B-6)}$$

$$\bar{v}_z = -\frac{1}{r}\,\frac{\partial \psi}{\partial r} \qquad \text{(B-7)}$$

From B-6 it follows that

$$\psi = \int_0^z r\bar{v}_r\,dz \qquad \text{(B-8)}$$

Substituting for $\bar{v}_r$ and z from B-4 and B-2

$$\psi = A \left(\frac{r}{\sigma}\right)^{\frac{1}{2}} (r^2 - a^2)^{\frac{1}{4}} \int_0^{\eta} f(\eta)\, d\eta$$

if we let

$$F(\eta) = \int_0^{\eta} f(\eta)\, d\eta$$

then,

$$\psi = A \left(\frac{r}{\sigma}\right)^{\frac{1}{2}} \left(r^2 - a^2\right)^{\frac{1}{4}} F(\eta) \qquad \text{(B-9)}$$

From B-6, B-7, and B-9 the following quantities can be evaluated in terms of the function F and its derivatives

$$\bar{v}_r = \frac{A \sigma^{\frac{1}{2}}}{r^{3/2}} (r^2 - a^2)^{\frac{1}{4}} F' \qquad \text{(B-10)}$$

$$\bar{v}_z = - \frac{A (r^2 - a^2)^{\frac{1}{4}}}{2 \sigma^{\frac{1}{2}} r^{3/2}} \left(F + \frac{r^2}{r^2 - a^2} F - 2\eta F'\right) \qquad \text{(B-11)}$$

$$\frac{\partial \bar{v}_r}{\partial r} = \frac{A}{2} \frac{\sigma^{\frac{1}{2}}}{r^{5/2}} (r^2 - a^2)^{\frac{1}{4}} \left[-3F + \frac{r^2}{r^2 - a^2} F' - 2\eta F''\right] \qquad \text{(B-12)}$$

$$\frac{\partial \bar{v}_r}{\partial z} = A \frac{\sigma^{3/2}}{r^{5/2}} (r^2 - a^2)^{\frac{1}{4}} F'' \qquad \text{(B-13)}$$

$$\frac{\partial^2 \bar{v}_r}{\partial z} = A \frac{\sigma^{5/2}}{r^{7/2}} (r^2 - a^2)^{\frac{1}{4}} F''' \qquad \text{(B-14)}$$

In the above equations F is the same as F (η) and $F' = \frac{\partial F}{\partial \eta}$, $F'' = \frac{\partial^2 F}{\partial \eta^2}$ etc. All quantities of Equation II-9, the equation of motion, have been evaluated above in terms of the dimensionless quantity $F(\eta)$. Equation II-9 is reproduced here for convenience.

$$\bar{v}_r \frac{\partial \bar{v}_r}{\partial r} + \bar{v}_z \frac{\partial \bar{v}_r}{\partial z} - \frac{a^2}{r(r^2-a^2)} \bar{v}_r^2 = - \epsilon \frac{\partial^2 \bar{v}_r}{\partial z^2} \qquad \text{(II-9)}$$

Introducing equations B-10 to B-14 into II-9 and rearranging gives

$$\frac{A^2}{2} \frac{\sigma}{r^4} (r^2 - a^2)^{\frac{1}{2}} F' \left(-3F' + \frac{r}{r^2-a^2} F' - 2\eta F''\right)$$

$$- \frac{A^2\sigma}{r^4} (r^2-a^2)^{\frac{1}{2}} \frac{a^2}{r^2-a^2} (F')^2$$

$$- \frac{A^2\sigma}{2r^4} (r^2-a^2)^{\frac{1}{2}} F'' \left(F + \frac{r^2}{r^2-a^2} F - 2\eta F'\right)$$

$$= - A\epsilon (r^2-a^2)^{\frac{1}{4}} \frac{1}{r^{7/2}} \sigma^{5/2} F'''$$

Dividing through by $\frac{A^2\sigma}{2r^4}(r^2-a^2)^{\frac{1}{2}}$, and simplifying we get

$$(F')^2 + FF'' + \frac{2\epsilon}{A}\frac{(r^2-a^2)^{3/4}}{(2r^2-a^2)}(\sigma^3 r)^{\frac{1}{2}} F''' = 0$$

Since ϵ, A, a and σ are arbitrary constants to be set by boundary conditions, there is no loss in generality, if in the above third order differential equation we let

$$\epsilon = \frac{A}{2}\frac{1}{(\sigma^3 r)^{\frac{1}{2}}}\frac{2r^2-a^2}{(r^2-a^2)^{3/4}} \qquad \text{(B-15)}$$

We still have three independent constants A, σ and a which will be determined by three boundary conditions of the resulting third order differential equation.

$$F'^2 + FF'' + F''' = 0 \qquad \text{(B-16)}$$

The boundary conditions are given by Equation A-28 and A-29 of Appendix A and is reproduced here for convenience.

$$Z = \pm\infty \qquad \bar{v}_r = 0, \quad \frac{\partial \bar{v}_r}{\partial Z} = 0 \qquad \text{(A-28)}$$

$$Z = 0 \qquad \frac{\partial \bar{v}_r}{\partial Z} = 0, \quad \bar{v}_z = 0 \qquad \text{(A-29)}$$

From Equations B-2 and B-10 to B-14, it can be easily shown that the boundary conditions A-28 and A-29 transform to

$$F(0) = F''(0) = 0 \qquad \text{(B-17)}$$

$$F'(\infty) = 0 \qquad \text{(B-18)}$$

Equation B-16 can be rearranged to

$$\frac{d}{d\eta}(FF') + \frac{d}{d\eta}(F'') = 0$$

which on integrating and applying boundary condition B-17 reduces to

$$FF' + F'' = 0 \qquad \text{(B-19)}$$

Integrating once more results in

$$\tfrac{1}{2}F^2 + F' = C \qquad \text{(B-20)}$$

Since σ, A and a are independent constants to be determined from experimental data, the constant C in B-20 can be given any value without loss of generality. Let $C = \frac{1}{2}$, this is equivalent to saying $F(\infty) = 1$. Hence,

$$F' = \tfrac{1}{2}(1 - F^2)$$

The above equation integrates to yield

$$F = \tanh(\eta/2) \qquad \text{(B-21)}$$

The constant of integration is zero since $F(0) = 0$. We can now find $\bar{v}_r$ and $\bar{v}_z$ from B-10 and B-11 since the value of F is now known.

$$\bar{v}_r = \frac{A}{2}\left(\frac{\sigma}{3}\right)^{\frac{1}{2}}(r^2-a^2)^{\frac{1}{4}}\left[1-\tanh^2\left(\frac{\eta}{2}\right)\right] \qquad \text{(B-22)}$$

$$\bar{v}_z = -\frac{A(r^2-a^2)^{\frac{1}{4}}}{2\sigma^{\frac{1}{2}}r^{3/2}}\left[\frac{2r^2-a^2}{r^2-a^2}\tanh\left(\frac{\eta}{2}\right) - \eta\left(1-\tanh^2\left(\frac{\eta}{2}\right)\right)\right] \qquad \text{(B-23)}$$

Since at $\eta = 0$, $\tanh(\eta) = 0$, $\bar{v}_r$ has a maximum value at $\eta = 0$. B-22 can hence be written as

$$\bar{v}_r = (\bar{v}_r)_{max}\left[1-\tanh^2\left(\frac{\eta}{2}\right)\right] \qquad \text{(B-24)}$$

where

$$(\bar{v}_r)_{max} = \frac{A}{2}\left(\frac{\sigma}{r^3}\right)^{\frac{1}{2}} (r^2-a^2)^{\frac{1}{4}} \qquad \text{(B-25)}$$

Equation B-23 can also be written as

$$\bar{v}_z = - \frac{(\bar{v}_r)_{max}}{\sigma} \left(\frac{2r^2-a^2}{r^2-a^2} \tanh(\eta) - \eta \, (1-\tanh^2(\tfrac{\eta}{2})) \right) \qquad \text{(B-26)}$$

Properties of the Tangential Jet

In setting up a computer program to draw the streamlines in the stirred tank it is necessary to evaluate some of the properties of the tangential jet. These properties will be evaluated in this section.

(1) Pumping Capacity

The pumping capacity is the net flow of fluid out of the impeller. Consider a cylinderical surface of radius r (r larger than D/2) and of infinite length, surrounding the impeller. Then the net amount of fluid that flows out of this surface can be obtained by integrating the velocity normal to the surface. Hence Q the pumping capacity or the volume of fluid flowing out of the cylinderical surface of radius r is

$$Q = \int_{-\infty}^{\infty} 2\pi r \bar{v}_r dz \qquad \text{(B-27)}$$

Since $\bar{v}_r$ is an even function and a function of z only,

$$Q = 4\pi r \int_{o}^{\infty} \bar{v}_r dz \qquad \text{(B-28)}$$

Substituting for $\bar{v}_r$ from B-22 and z from B-2 gives,

$$Q = 4\pi A \left(\frac{r}{\sigma}\right)^{\frac{1}{2}} (r^2-a^2)^{\frac{1}{4}} \int_o^{\infty} (1-\tanh^2(\frac{\eta}{2}))d(\frac{\eta}{2}) \qquad \text{(B-29)}$$

which integrates to,

$$Q = 4\pi A(\frac{r}{\sigma})^{\frac{1}{2}}(r^2-a^2)^{\frac{1}{4}}\tanh\ (\frac{\eta}{2}) \qquad \text{(B-30)}$$

Equation B-30 gives the flow out of the tangential jet for a given value of r between the limits $\pm\ \eta$, since the lower limit of B-29 is zero. For $\eta = \infty$ we have the total pumping capacity of the jet which is

$$Q = 4\pi A(\frac{r}{\sigma})^{\frac{1}{2}}\ (r^2-a^2)^{\frac{1}{4}} \qquad \text{(B-31)}$$

From B-31 it is seen that for r, considered far from the source of the jet, Q is approximately proportional to r.

(2) Half Width of the Tangential Jet

The width of the jet is determined by the boundary of the jet. In order to determine the jet boundaries consider Equation B-24. From the properties of hyperbolic tangents it is seen from B-24 that $\bar{v}_r$ rapidly goes to zero for large η. It can be verified from a table of hyperbolic tangents that when $\eta = 6$, $\tanh^2(\eta/2) = 0.99102$ and hence from B-24, $\bar{v}_r/(\bar{v}_r)_{max}$ is equal to 0.00998. As in the case of boundary layers we can define the boundary of the jet as the point where $\bar{v}_r/(\bar{v}_r)_{max}$ is less than 0.01. From the above discussion this is obviously given by

$$\eta = \pm\ 6$$

Substituting for η from B-2 and rearranging

$$z = \frac{6r}{\sigma} \tag{B-33}$$

The above value of z is the half width of the jet and to avoid confusion is called $b_{\frac{1}{2}}$, hence

$$b_{\frac{1}{2}} = \frac{6r}{\sigma} \tag{B-34}$$

From the above discussion it follows that the boundary of the jet is given by

$$z = b_{\frac{1}{2}}$$

It should be noted that $b_{\frac{1}{2}}$ as defined by Equation B-34 is not the same as that defined by II-12. In Section 4.11 it is shown that by defining k′ by Equation IV-44, Equation II-12 and B-34 are identical for values of r of the order of r_o or larger.

APPENDIX C

NON-LINEAR LEAST SQUARE FIT OF EXPERIMENTAL VELOCITY PROFILE

In this appendix the procedure that will be used to obtain the best values of the parameters of Equation II-13 from experimental data will be developed. The best fit of experimental velocity profile data will be considered one in which the least square criteria is satisfied. If q_i is the experimentally determined velocities and $\hat{q}_i$ is the corresponding velocity obtained from Equation II-10, the sam of squares, SS of the deviation between q_i and q_i is given by

$$SS = \sum_{i=1}^{N} (\hat{q}_i - q_i)^2 \qquad \text{(C-1)}$$

Substituting for $\hat{q}_i$ from Equation II-10:

$$SS = \Sigma \left[\frac{A}{2} \left(\frac{\sigma}{r}\right)^{\frac{1}{2}} \frac{1}{(r^2-a^2)^{\frac{1}{4}}} \left(1 - \tanh^2 \left(\frac{\sigma(z_i-z_o)}{r}\right)\right) - q_i \right] \qquad \text{(C-2)}$$

In equation C-2 it is understood that the summation of i is from 1 to n, where n is the number of experimental observations or data points. The least square criteria requires that the parameters σ, A, a and z_o be chosen such that SS has a minimum value. Equation C-2 is non-linear with four parameters, one of which has a constraint.

The constraint is

$$- D/2 < a < D/2 \qquad \text{(C-3)}$$

An optimization technique know as Pattern Search was used to obtain the parameters of Equation C-2 subject to constraint C-3. The constraint feature of Pattern Search was not needed since the parameter a was evaluated from the weighted average angle $\bar{\theta}_y$ as described in Chapter IV, Section 4.1. Wilde has given an excellent account of how pattern search works. His comment that D. Himmelblau, of the University of Texas, found Pattern Search as an excellent least-square minimization technique is confirmed from the innumerable runs that were made using this method.

The least square criteria equation C-2 raises the power of the parameters to at the most two. This is equivalent to generating a surface in multidimension coordinates. Pattern Search treats the parameters of the model as an n-dimensional vector $\vec{P}$ that moves from point to point on this least square surface by perturbing $\vec{P}$ till a minimum is reached. Since in multidimension surfaces several local minimas may exist, the minimum value obtained by this method (or by any optimization method) will depend on the initial value of $\vec{P}$ selected.

Briefly, Pattern Search starts with an arbitrary point P_{1j}. The first subscript refers to the point under consideration, the second subscrip to the dimension of the vector $\vec{P}$. Let Δp_i be the amount by which each vector component of $\vec{P}$ (orparameter) will be perturbed. Consider perturbing P_{11} by Δp_i. The sum of the square SS (also known as the criteria function) is calculated. If SS decreases then this new value of $P_{11} = P_{11} + \Delta p_i$ is accepted. If SS does not

decrease, P_{11} is perturbed in the negative direction or $P_{11} = P_{11} - \Delta p_i$. If perturbing P_{11} does not give a decrease in SS, P_{11} is left unchanged and the next parameter is perturbed. When all parameters are perturbed point P_{2i} is reached. The above logic is easily generalized and the algorithim for the i-th parameter is

$$P_{2i} = \begin{cases} P_{1i} + \Delta p_1 \\ P_{1i} - \Delta pi \\ P_{1i} \end{cases} \quad \text{if} \quad \begin{pmatrix} SS(P_{1i} + \Delta p_i) < SS\ (P_{1i}) \\ SS(P_{1i} - \Delta p_i) < SS(P_{1i}) \\ SS(P_{1i}) < \text{Min}\left[SS(P_{1i} + \Delta p_i), SS(P_{1i} - \Delta p_i)\right] \end{pmatrix} \qquad \text{(C-4)}$$

At Point P_{2i} the algorithim C-4 is not repeated but an acceleration step is taken. This is based on the reasoning that the point P_{2i} is in the direction of a trend or pattern. The point P_{3i} is obtained by moving a linear distance equal to $P_{1i}\ P_{2i}$ in the direction P_{1i} to P_{2i}. Vectorially this is given as

$$P_{3i} = P_{2i} + F\ (P_{2i} - P_{1i}) \qquad \text{(C-5)}$$

The factor F as indicated above is unity. However if a constraint on $\vec{P}$ is violated, then F is reduced by a suitable amount. In our program this amount is in steps of 0.1. The minimum value of F is of course zero (i.e. acceleration step is omitted).

In Figure C-1, the above reasoning is illustrated for the two dimensional or two parameter case. P_{11} is perturbed by $-\Delta p_1$ to give a decrease in the criteria function SS. A further decrease in

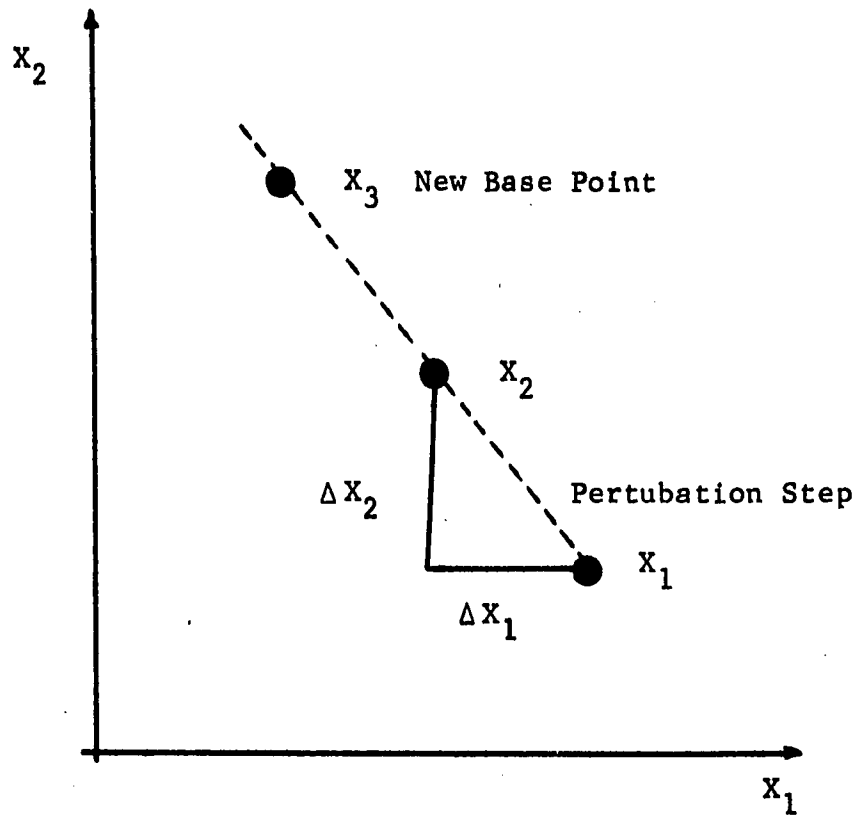

Figure C-1. Pattern Search in Two Dimension.

SS is obtained by perturbing P_{12} by Δp_2. We thus arrive at P_2. The acceleration step is then taken to arrive at P_3. The procedure is then repeated until no futher decrease in SS is observed.

If the initial step size Δp_i are large, the above prodedure will quickly bring the search in the region of the minimum. However for a more precise evaluation of the minimum, the pattern search prodedure is repeated with a smaller step size. In the program used by us, the initial step size is decreased by a factor of 10, four times. The number of times is purely arbitrary. In spite of this excessive reduction, the running time for fitting a single velocity profile in no case exceeded 30.0 seconds on the IBM 7040 Computer. This figure does not include the compiling time. The time is also dependant on the initial value selected. After some experience it is not too difficult to select an initial value close to the desired optimum.

In Figure C-2 is presented a flow diagram of the Pattern Search subroutine. The flow diagram outlines a general flow of information. In the program itself several other steps are included so as to make the program work under all possible conditions. The Pattern Search subroutine was written as a general optimization program and to do this it requires two other subroutines that depend on the problem being solved. These sub-programs are PROC in which the criteria function, C-2, is specified and BOUNDS in which the constraints, if any are specified. To illustrate the general nature of the program, it could have been used to evaluate the four parameters using some other criteria. For example to minimize the absolute value of the deviation $(\hat{q}_i - q_i)$. The details of the actual program used for evaluating the

parameters and other pertinent information from experimental data is treated in Chapter IV.

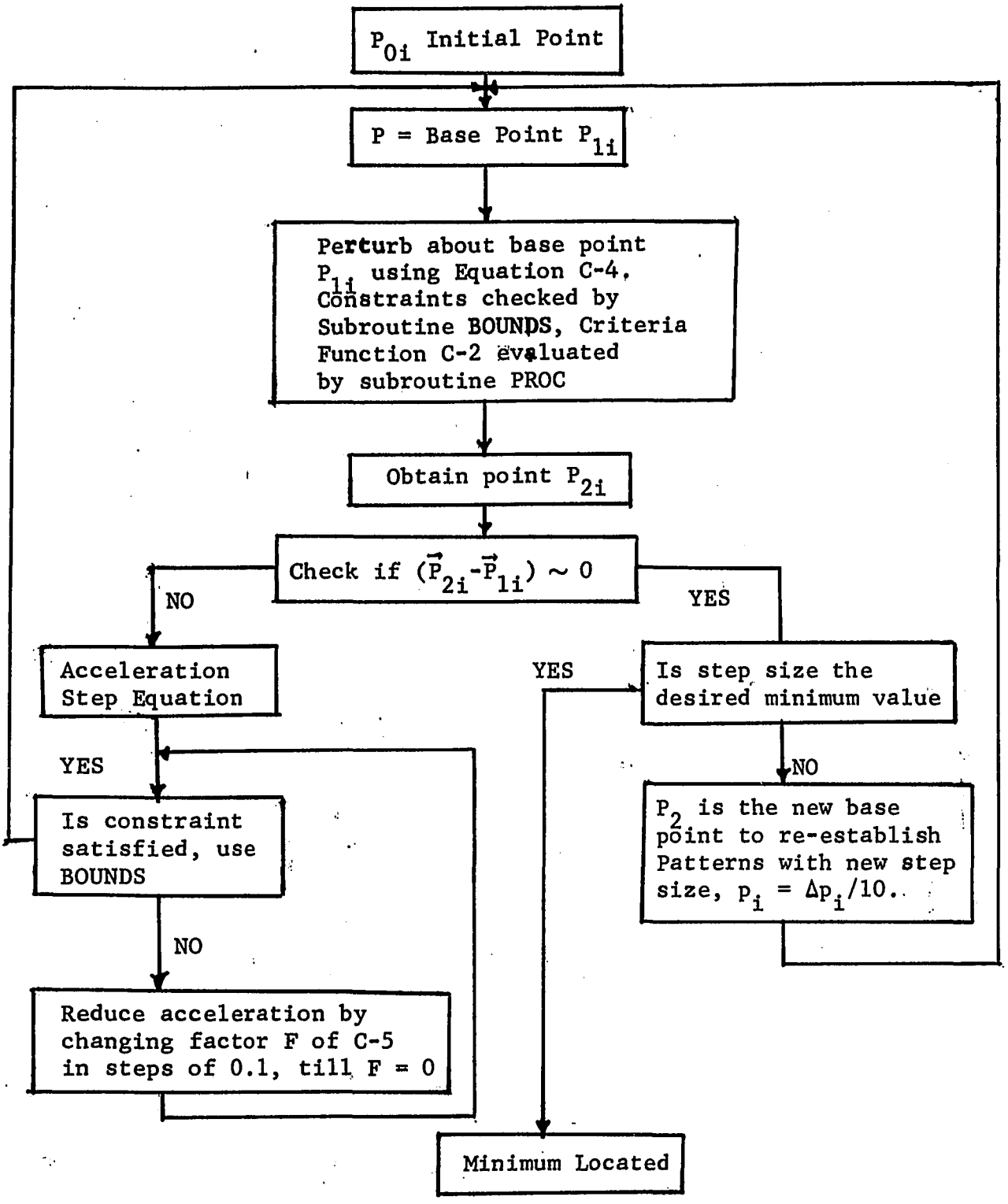

Figure C-2. Flow Diagram for Pattern Search Subroutine.

APPENDIX D

TWO DIMENSIONAL POTENTIAL FLOW IN r-z PLANE

In this appendix the stream function for two dimensional potential flow in cylinderical coordinates for the r-z plane will be derived. In potential flow the following assumptions hold which are: viscous forces are not important, and the flow is irrotational. In the stirred tank the above conditions are approximately true, except in the region of the impeller and at the walls of the tank. In addition the flow in the stirred tank is in steady state.

The continuity equation thus reduces to,

$$\vec{\nabla} \cdot \vec{V} = 0 \qquad \text{(D-1)}$$

Neglecting the viscous forces in Equation A-4, the equation of motion reduces to

$$(\vec{V} \cdot \vec{\nabla})\ \vec{V} = -\frac{1}{\rho}\vec{\nabla} P + \frac{1}{\rho}\vec{g} \qquad \text{(D-2)}$$

In potential flow a potential function $\emptyset$ is defined as,

$$\vec{V} = \vec{\nabla}\emptyset \qquad \text{(D-3)}$$

The existence of $\emptyset$ stems from the condition of irrotationality Combining D-1 and D-3 results in the Laplace equation

$$\nabla^2\emptyset = 0 \qquad \text{(D-4)}$$

The problem reduces to finding a suitable function $\emptyset$ which satisfies Equation D-4 and the boundary conditions. The velocity field can

then be evaluated from D-3, and pressure field from D-2.

In the present case it is more convenient to use the stream function ψ than the potential function ϕ. These are related by the following equations (46) in cylindrical coordinates.

$$\frac{\partial \phi}{\partial Z} = \frac{1}{r} \frac{\partial \psi}{\partial r} \qquad \text{(D-5)}$$

$$\frac{\partial \phi}{\partial r} = - \frac{1}{r} \frac{\partial \psi}{\partial Z} \qquad \text{(D-6)}$$

The stream function is a more useful quantity since it can be used to obtain the streamlines directly. The relationship between velocity and streamlines in the r-z plane is

$$\bar{v}_z = \frac{1}{r} \frac{\partial \psi}{\partial r} \qquad \text{(D-7)}$$

$$\bar{v}_r = - \frac{1}{r} \frac{\partial \psi}{\partial Z} \qquad \text{(D-8)}$$

In the literature several solutions to the potential function are available. One such solution in terms of the stream function ψ is (45)

$$\psi = r^2 Z \qquad \text{(D-9)}$$

Equation D-9 was chosen because it represents stagnation flow in cylinderical coordinates. This is evident when the streamlines are drawn for Equation D-9 as in Figure II-3(a) that Equation D-9 satisfies the boundary conditions in Region II of Figure II-1.

Since a streamline is a line across which no flow takes place, it can thus be replaced by a solid boundary. In Figure II-3(b) is shown the streamlines for Equation D-9 with OR now a solid boundary.

The flow is now seen to take place in a corner and could thus represent the flow in Regions III and IV of Figure II-1.

APPENDIX E

DESCRIPTION OF PROGRAM PLOTER USED FOR PLOTTING STREAMLINES

This appendix presents the flow diagram for the computer program PLOTTER. The program is written in FORTRAN IV compatible with the IBM Systems/360. Originally the program was written for the IBM 7040 computer and was converted to the IBM Systems/360 with minor additions. The additions are print statements which are not compatible with the IBM 7040 machine.

Figure E-1 shows a flow diagram for the main program PLOTER, Figure E-2 is the flow diagram for the subroutine STREAM and Figure E-3 is the flow diagram for the subroutine GOLD. In List E-1 is a printout of the entire program with a sample output. The program contains a print control variable LPRINT. A value of LPRINT = 1 gives detailed printout. In the program given in List E-1, LPRINT = 0 which gives a minimum printout. The symbols used in the program are explained in comment cards at the beginning of the main program and each subprogram.

Golden Section Search. Golden section is a one dimensional search procedure and is used to locate r_c the start of the streamline in Region I. For a detailed analysis of the theory the reader is referred to Wilde (42). The method is well suited for locating single roots of an equation in a known interval. It can also be used

for locating maxima and minima of functions that have a unique optimia in a given interval. The subroutine GOLD has been written to locate roots in a given interval.

To obtain an idea of how the method works, consider Figure E-4 (a). In the Figure X1 and X2 are the boundaries of the given interval. The points DG1 and DG2 are located by the following equations:

$$DG1 = X1 + (X2-X1)/1.618032 \qquad (E-1)$$

$$DG2 = X1 + (DG/-X1)/1.618034 \qquad (E-2)$$

In Equation E-1 and E-2, the constant 1.618034 is the Golden section ratio.

The value of the function of DG1 and DG2 are f(DG1) and f(DG2). These values are compared with kQ_o the desired root. Since both these values are larger than kQ_o it is obvious that the root does not lie in the interval between X2 and DG1. This interval is then eliminated by shifting X2 to DG1 as shown in Figure E-4 (b). The crossed out section indicates intervals eliminated.

New values of DG1 and DG2 are calculated using Equations E-1 and E-2. These points are shown in Figure E-4 (b). The quantities of f(DG1) and f(DG2) are then computed. These values are compared with kQ_o and found to be on either side of it. It follows then that the root lies within the interval DG1 and DG2. In two iterations the original interval X1, X2, of Figure E-4 (a) have been reduced to DG1, DG2 of Figure E-4 (b). By repeating the above procedure the final interval can be made as small as desired. In our program the final interval is reduced to 0.001 of (X2-X1) the original interval

in seven iterations. The subroutine GOLD is written in a general manner to cover all possible cases including if the function Q = f(r) is decreasing in the interval X1 to X2 rather than increasing as shown in Figure E-1. With slight modifications it could be used to locate an extremum for a unimodal function.

Evaluation of Velocity Profiles. In Chapter IV velocity profiles from the theoretical solution were needed for the purpose of comparison with the experimentally determined profile. These are also obtained from the program PLOTER. Small modifications were made in the subroutine STREAM to permit calculating and storing the values of $\bar{v}_r$ and at constant z. These values are stored in the arrays VR, SY, VZ, RRX, RVZ. The subroutine SPRINT permits printing the results in a suitable tabular form. This could not be done at the moment of calculation since subrouitne STREAM evaluates one streamline at a time. The fixed point variable JGAMMA controls operation or deletion of velocity profile calculations. To delete this option JGAMMA is set equal to zero as shown in sample list in Table E-1.

Sample Printout from PLOTER. At the end of the program is given the input data necessary for plotting Figure II-7 (a). It should be noted that the parameter LIV controls truncation of Region IV. This is because two different calculation procedures are needed to obtain Figure II-7 and Figures II-8 through II-11. To obtain Figure II-7 put LIV equal to zero, otherwise equal to one. Also given in the listing is the sample printout. This printout is the minimum desirable information. If LPRINT, print control parameter is put equal to 1 a detailed printout of practically every step in

the program will be given. This was found useful in debugging. It should be noted that Figure E-3 showing the flow diagram of subroutine STREAM does not include the details of branching to obtain Figure II-7 as opposed to Figures II-8 through II-11. It also does not include the details of the output to program SPRINT for velocity profile data from the streamlines. Both these changes are minor and can be better seen in the program listing itself where it is clearly pointed out by comment statements.

The printout gives first the print control, a value of less than 5 means program should be recalled for another plot. Next, the input parameters and data are printed. This is followed by a list of important variables that give information about the flow such as Reynolds number RE, eddy viscosity EDVIS etc. Next is given TF, TB etc. defined in Figure II-6 which are overall scaled dimensions of the quadrant being plotted. This is followed by the iteration sequence that determines γ, and discussed in Section 2.4. A starting value of γ equal to 1.87 is selected. With this value of γ, the γ for each streamline is then calculated and listed. The numbers below γ are the number of points evaluated for each streamline required for plotting. The average value of γ for all the streamlines is then taken and called new value of γ which is 1.048. This value is used as a new starting value to calculate another average value of γ. In two iteration the average value of γ has converged to 1.01 (within 1% of the previous value) and is used for plotting the streamlines in Region V.

The next series of print statements is for plotting in the quadrant above the impeller centerline. The iteration sequence for γ is given and it should be noted that since the quadrant dimension are different , (see Figure II-7 (a)), the final value of γ is also different.

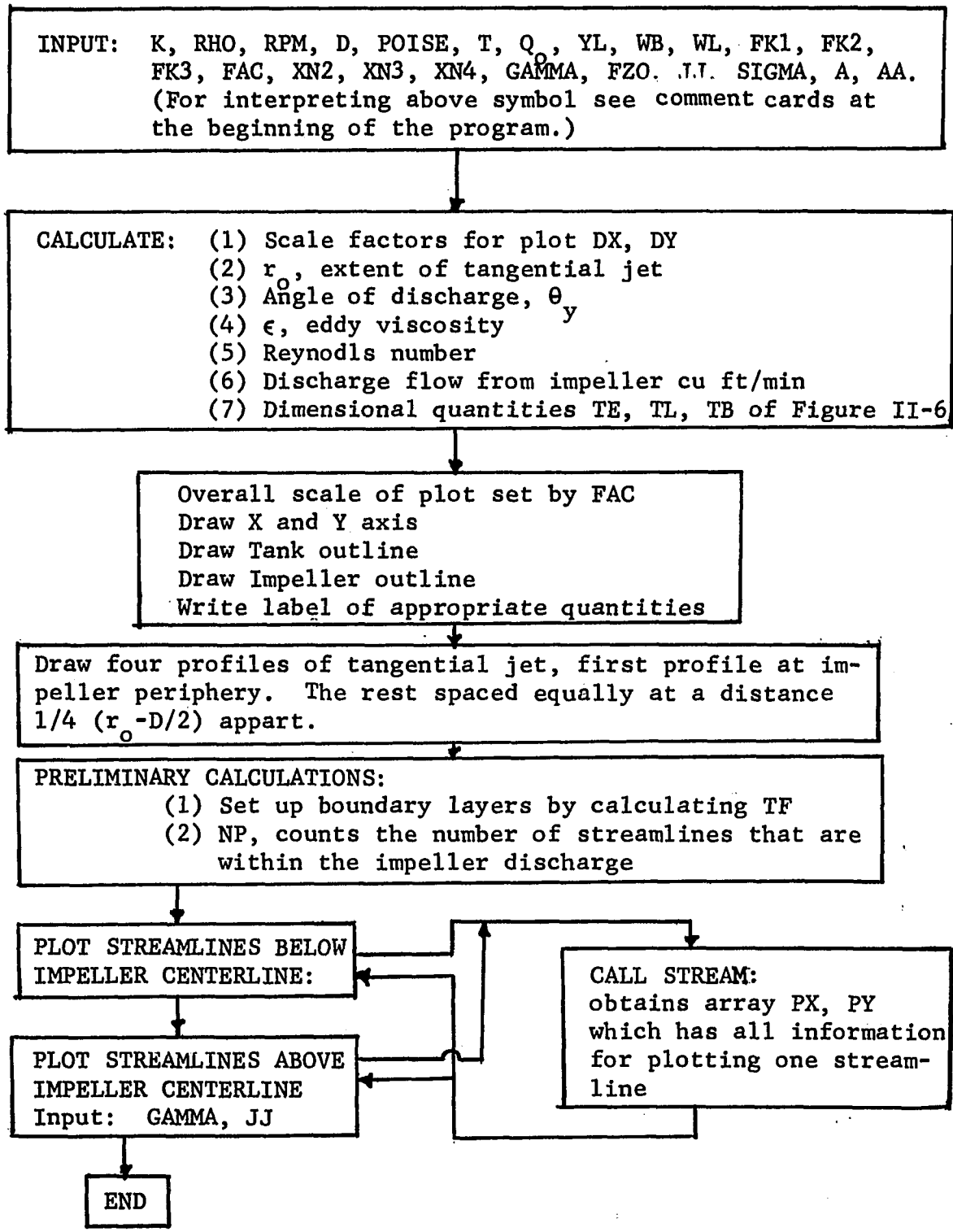

Figure E-1. Flow Diagram for Main Program PLOTER.

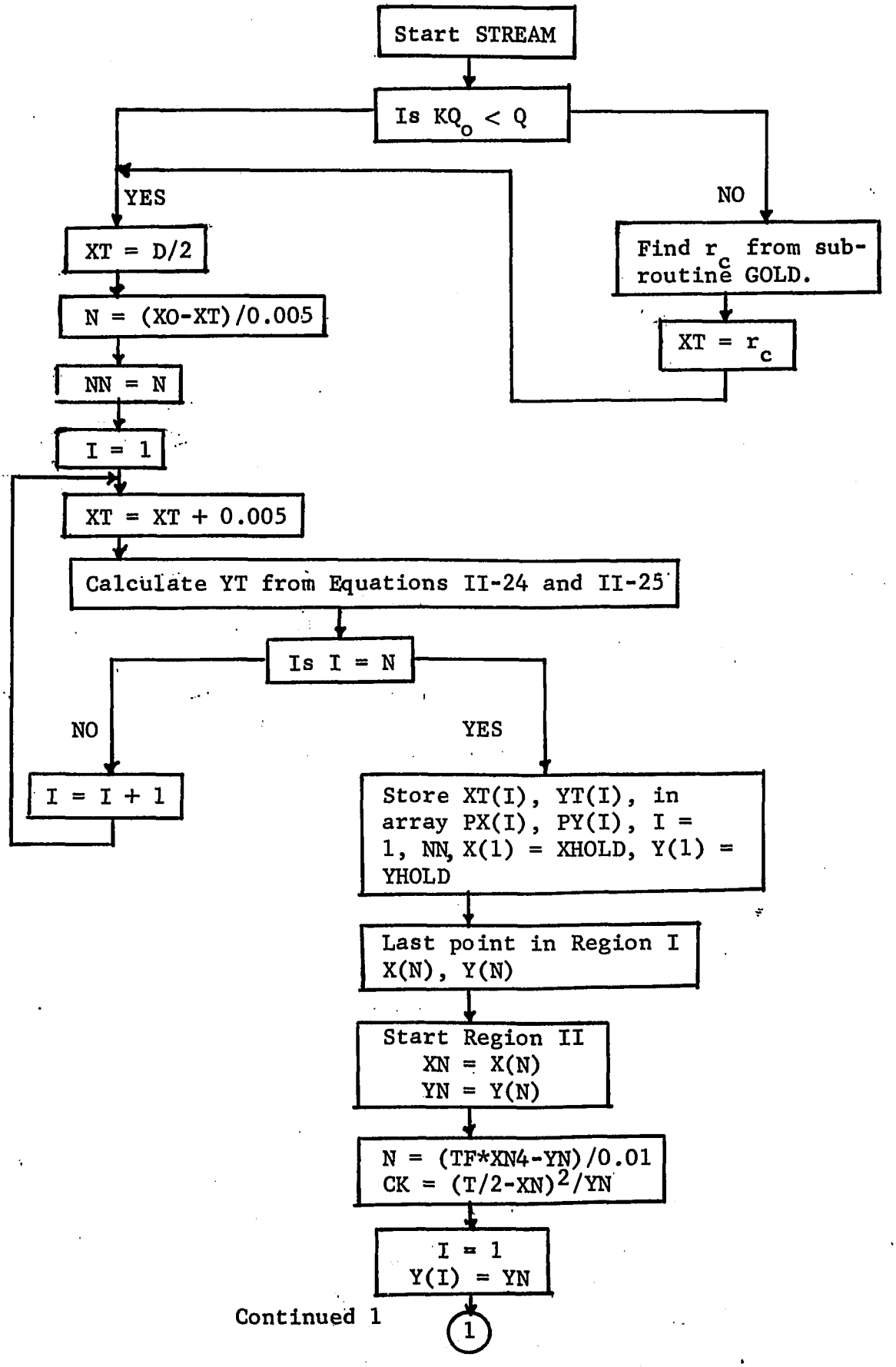
Start STREAM
Is $KQ_o < Q$
YES
NO
XT = D/2
N = (XO-XT)/0.005
NN = N
I = 1
XT = XT + 0.005
Calculate YT from Equations II-24 and II-25
Is I = N
NO
YES
I = I + 1
Store XT(I), YT(I), in array PX(I), PY(I), I = 1, NN, X(1) = XHOLD, Y(1) = YHOLD
Last point in Region I X(N), Y(N)
Start Region II
XN = X(N)
YN = Y(N)
N = (TF*XN4-YN)/0.01
CK = $(T/2-XN)^2/YN$
I = 1
Y(I) = YN
Continued 1
1
Find r_c from subroutine GOLD.
XT = r_c

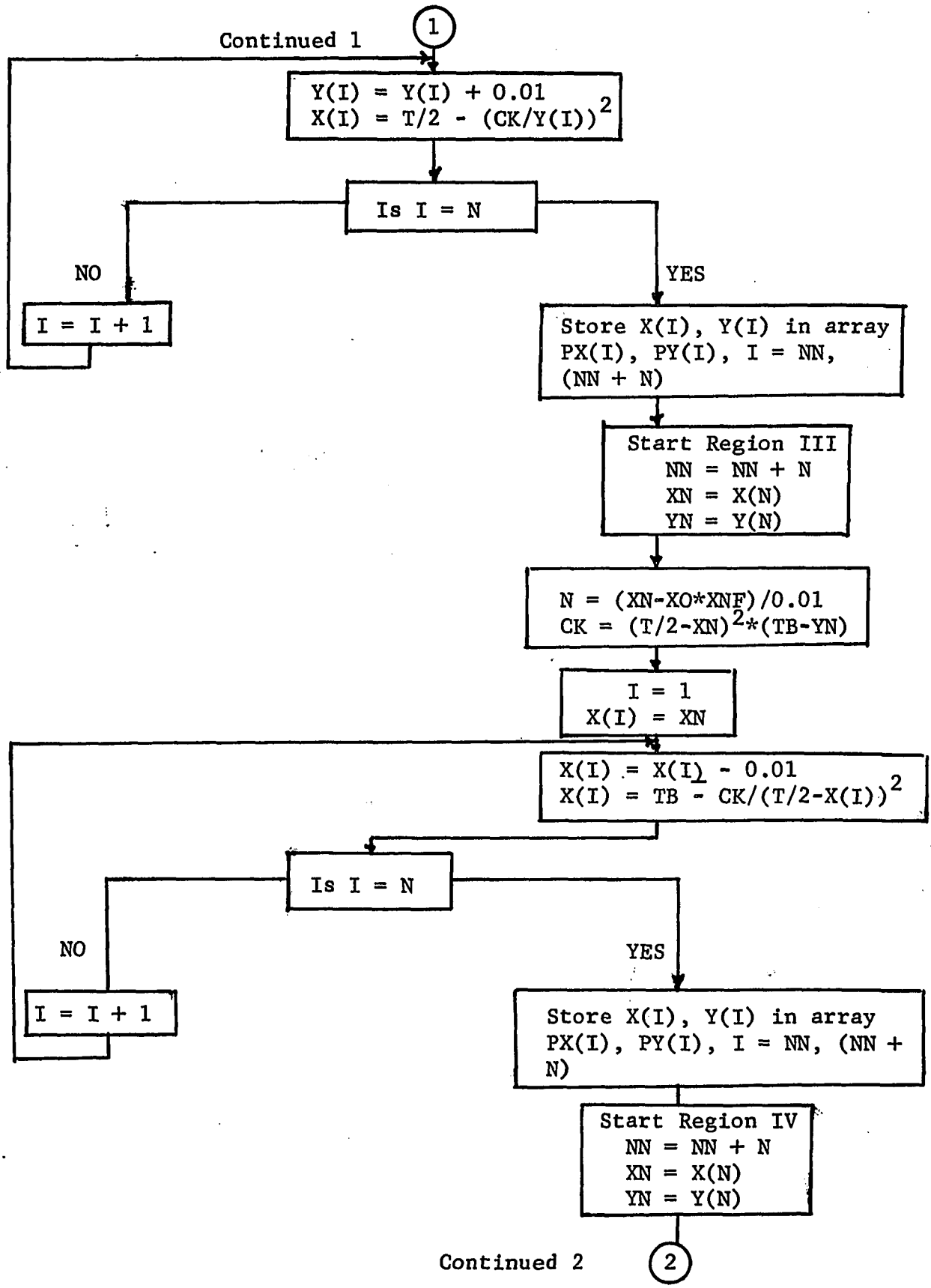
Continued 1
1
Y(I) = Y(I) + 0.01
X(I) = T/2 - (CK/Y(I))^2
Is I = N
NO
YES
I = I + 1
Store X(I), Y(I) in array PX(I), PY(I), I = NN, (NN + N)
Start Region III
NN = NN + N
XN = X(N)
YN = Y(N)
N = (XN-XO*XNF)/0.01
CK = (T/2-XN)^2*(TB-YN)
I = 1
X(I) = XN
X(I) = X(I) - 0.01
X(I) = TB - CK/(T/2-X(I))^2
Is I = N
NO
YES
I = I + 1
Store X(I), Y(I) in array PX(I), PY(I), I = NN, (NN + N)
Start Region IV
NN = NN + N
XN = X(N)
YN = Y(N)
Continued 2
2

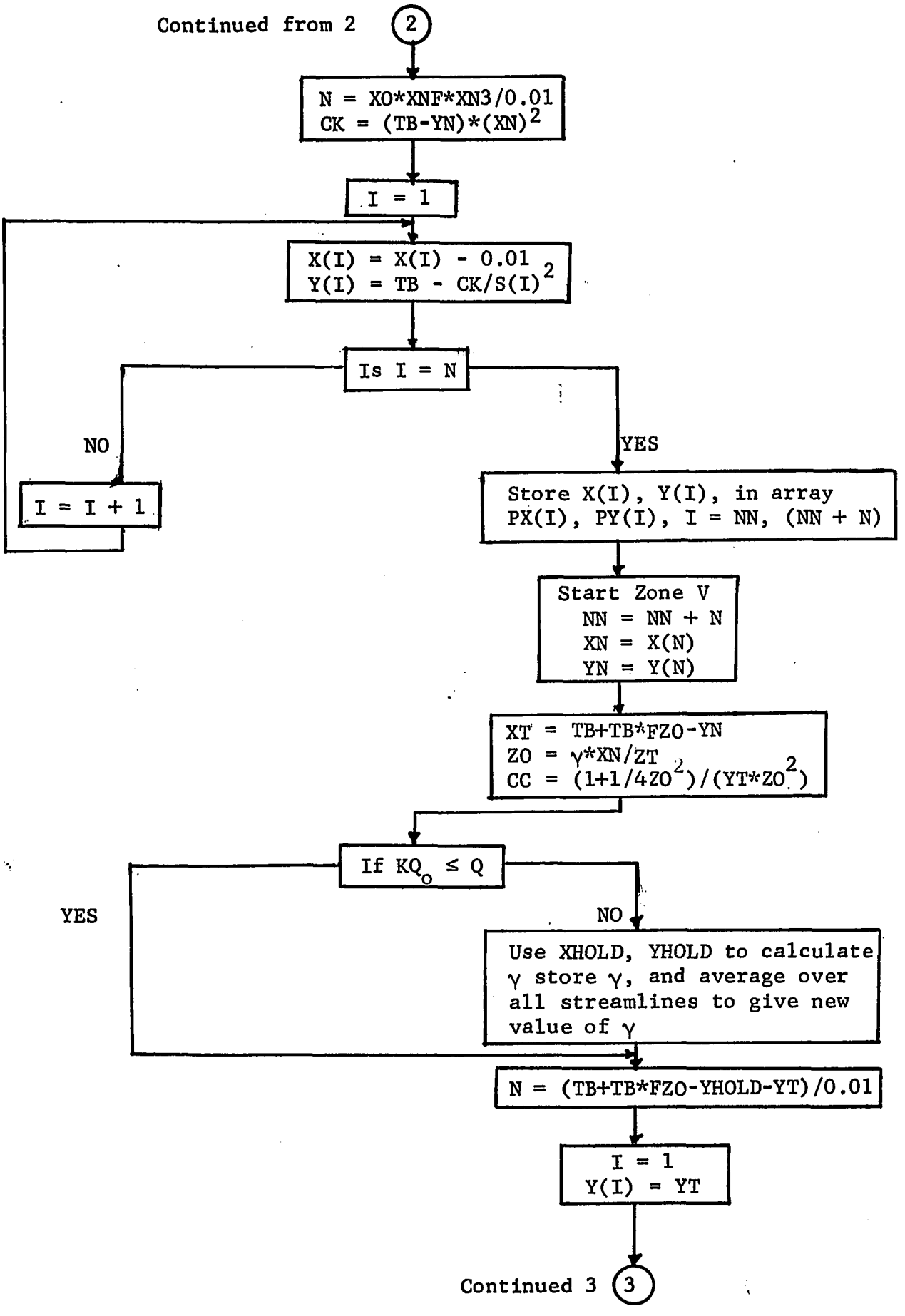
Continued from 2
2
N = XO*XNF*XN3/0.01
CK = (TB-YN)*(XN)^2
I = 1
X(I) = X(I) - 0.01
Y(I) = TB - CK/S(I)^2
Is I = N
NO
YES
I = I + 1
Store X(I), Y(I), in array
PX(I), PY(I), I = NN, (NN + N)
Start Zone V
NN = NN + N
XN = X(N)
YN = Y(N)
XT = TB+TB*FZO-YN
ZO = γ*XN/ZT
CC = (1+1/4ZO^2)/(YT*ZO^2)
If KQo ≤ Q
YES
NO
Use XHOLD, YHOLD to calculate
γ store γ, and average over
all streamlines to give new
value of γ
N = (TB+TB*FZO-YHOLD-YT)/0.01
I = 1
Y(I) = YT
Continued 3
3

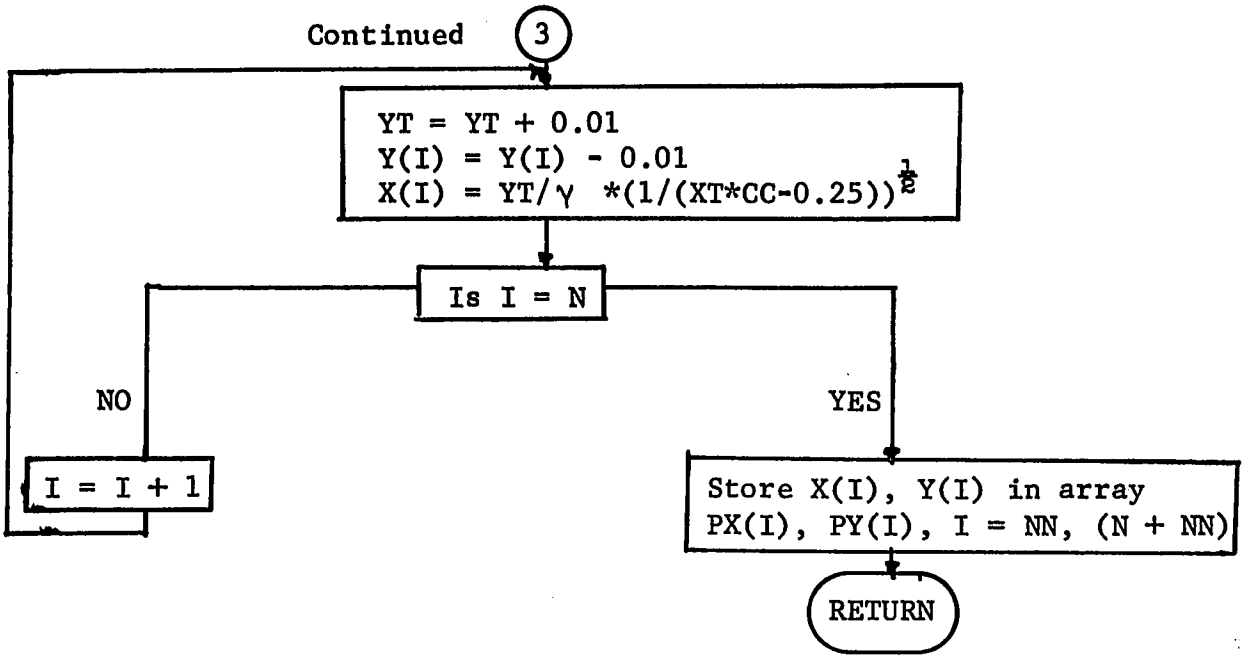

Figure E-2. Flow Diagram for Subroutine STREAM.

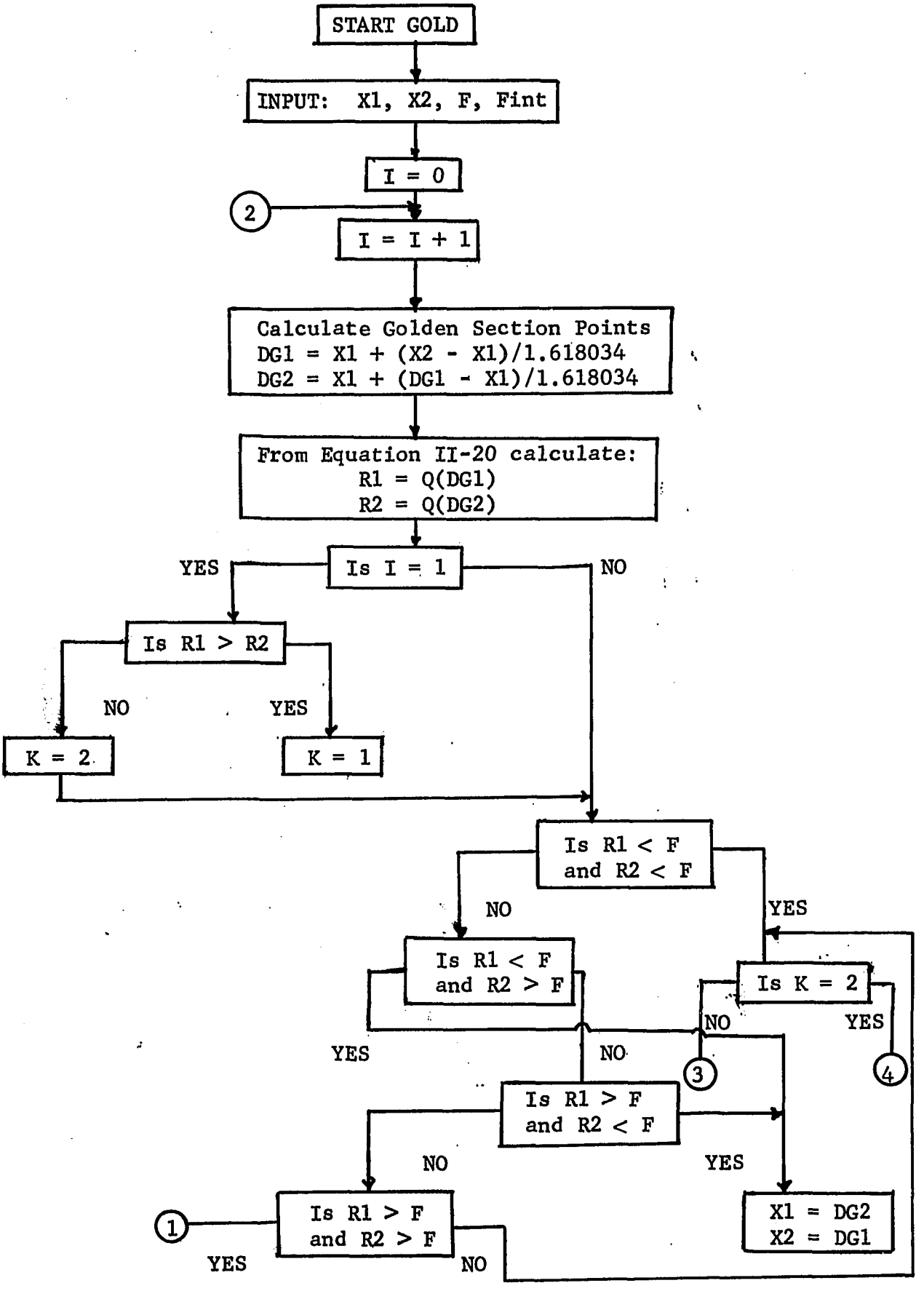
START GOLD
INPUT: X1, X2, F, Fint
I = 0
2
I = I + 1
Calculate Golden Section Points
DG1 = X1 + (X2 - X1)/1.618034
DG2 = X1 + (DG1 - X1)/1.618034
From Equation II-20 calculate:
R1 = Q(DG1)
R2 = Q(DG2)
Is I = 1
YES
NO
Is R1 > R2
NO
YES
K = 2
K = 1
Is R1 < F
and R2 < F
NO
YES
Is R1 < F
and R2 > F
Is K = 2
NO
YES
YES
NO
3
4
Is R1 > F
and R2 < F
NO
YES
1
Is R1 > F
and R2 > F
X1 = DG2
X2 = DG1
YES
NO

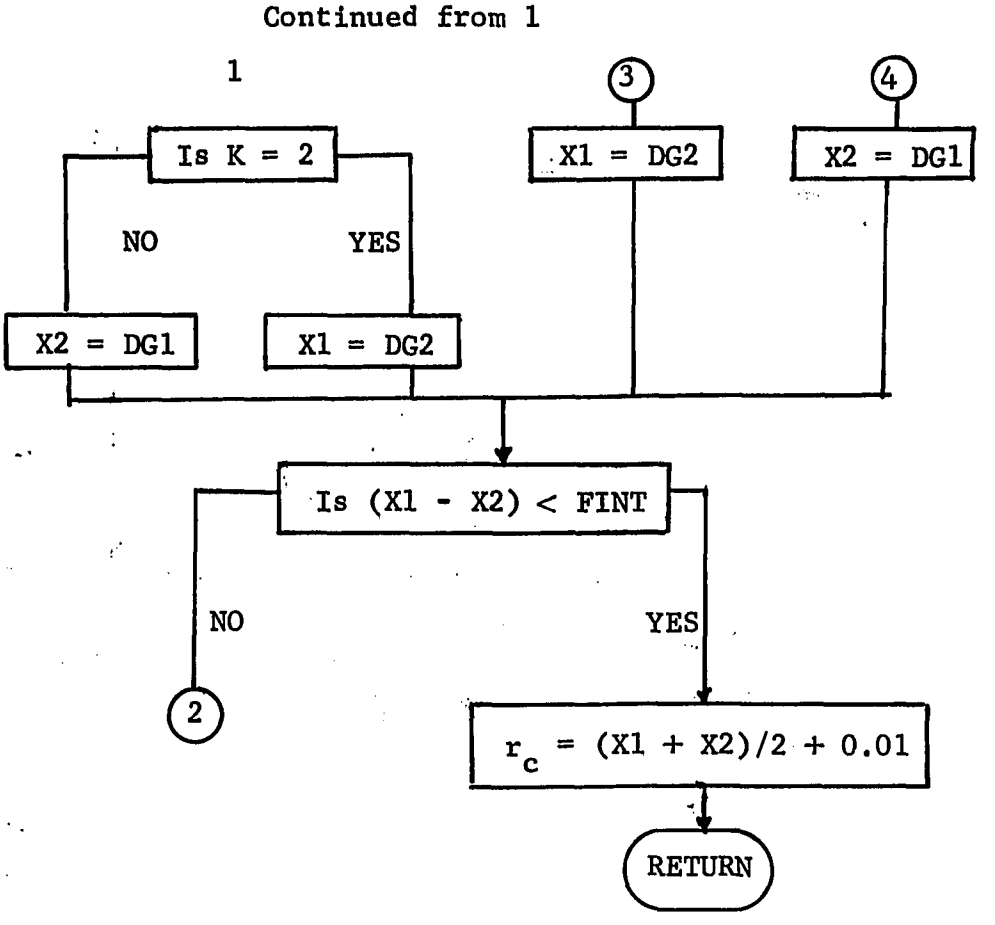

Figure E-3. Flow Diagram for Subroutine GOLD.

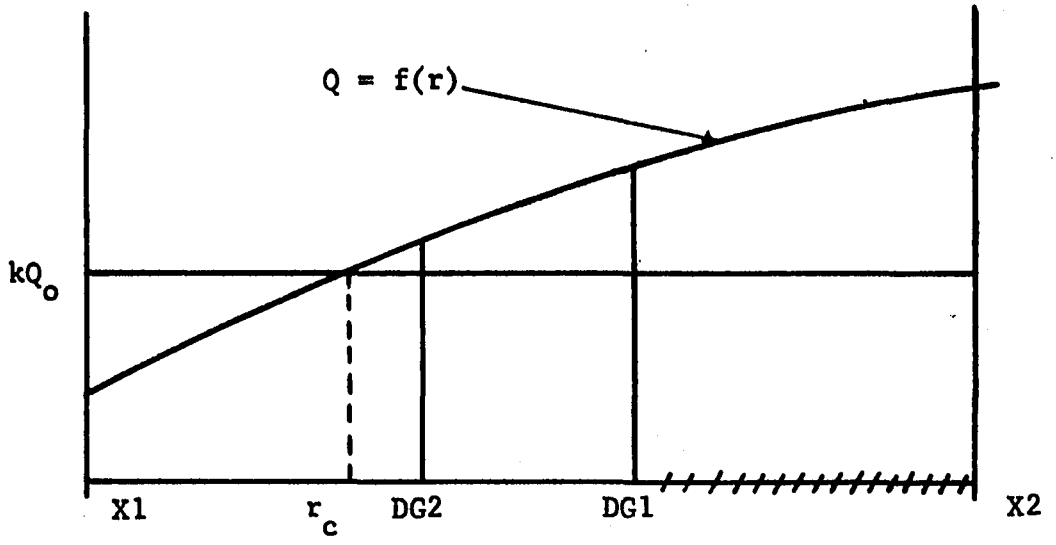

(a) First Iteration for Golden Section Search

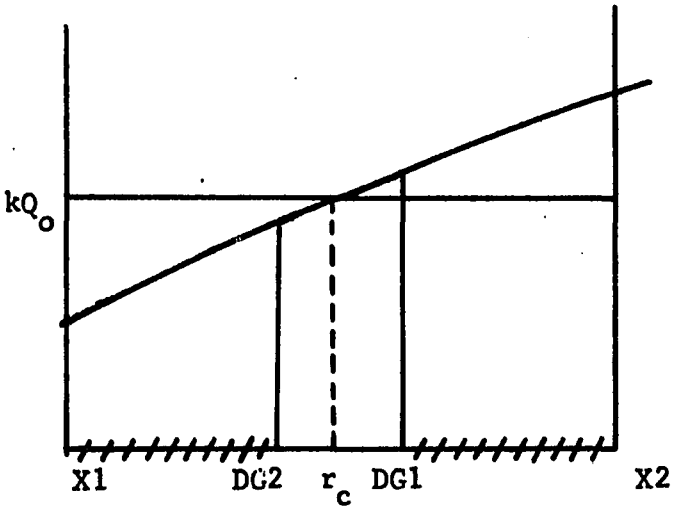

(b) Second Iteration for Golden Section Search

Figure E-4. Illustration of Golden Section Search Procedure

LIST E-1

FORTRAN LIST OF PROGRAM PLOTER, WITH SUPPORTING SUBROUTINES STREAM, GOLD AND SPRINT, AND SAMPLE OUTPUT

```
**********************************************************************************

                              MAIN PROGRAM PLOTTER

**********************************************************************************

C                                                                          PLOT    1
C--------ALL PROPERTIES MEASURED AT 25 DEG. C                             PLOT    2
C                                                                          PLOT    3
C                                                                          PLOT    4
C       K - JOB CONTROL, .LT. 5 FOR MULTIPLE JOBS                          PLOT    5
C       RHO - SPECIFIC GRAVITY                                             PLOT    6
C       RPM - REVOLUTIONS PER MINUTE                                       PLOT    7
C       D - IMPELLER DIAMETER, IN.                                         PLOT    8
C       POISE - VISCOSITY, CENTIPOISES                                     PLOT    9
C       T - TANK DIAMETER, TAKEN AS 1. FT.                                 PLOT   10
C       QO - VALUE OF STREAMLINE, FT**3/MIN.                               PLOT   11
C                                                                          PLOT   12
C                                                                          PLOT   13
C       YL - LENGTH OF Y-AXIS                                              PLOT   14
C       WB, WL - WIDTH AND LENGTH OF IMPELLER BLADE, RATIO OF D            PLOT   15
C       FK2 - HEIGHT OF IMPELLER FROM TANK BOTTOM, RATIO OF T              PLOT   16
C       FK3 - SCALE FACTOR OF JET PROFILE                                  PLOT   17
C       FAC - SCALE FACTOR OVERALL PLOT                                    PLOT   18
C                                                                          PLOT   19
C                                                                          PLOT   20
C       XN2 - BOUNDARY LAYER THICKNESS, RATIO OF T8                        PLOT   21
C       XN3 - EXTENT OF ZONE IV, RATIO OF XO                               PLOT   22
C       XNF - EXTENT OF ZONE III RATIO OF RATIO OF XO                      PLOT   23
C       XN4 - EXTENT OF ZONE II, RATIO OF XO                               PLOT   24
C       GAMMA - JET EXPANSION FACTOR OF CIRCULAR JET, ZONE V               PLOT   25
C       FZO - DISPLACEMENT OF ORIGIN OF CIRCULAR JET, RATIO OF T8          PLOT   26
C       JJ, LPRINT - CONTROLS PRINTOUT                                     PLOT   27
C                                                                          PLOT   28
C                                                                          PLOT   29
C       SIGMA, A, AA - TANGENTIAL JET PARAMETERS                           PLOT   30
C                                                                          PLOT   31
C                                                                          PLOT   32
C       DX - SCALE FACTOR FOR X-AXIS                                       PLOT   33
C       DY - SCALE FACTOR FOR Y-AXIS                                       PLOT   34
```

```
C       TB, TL - HEIGHT OF LIQUID BELOW AND ABOVE IMPELLER                PLOT  35
C              CENTERLINE, RATIO OF T                                     PLOT  36
C       TF - HEIGHT ABOVE OR BELOW IMPELLER CENTERLINE EXCLUDING          PLOT  37
C            BOUNDARY LAYER                                               PLOT  38
C       EDVIS - KINEMATIC EDDY VISCOSITY, FT**2/MIN.                      PLOT  39
C       Q - TOTAL FLOW AT IMPELLER PERIPHERY, FT**3/MIN.                  PLOT  40
C       TF = T/2. - XD                                                    PLOT  41
C       XA, YA - ARRAYS THAT STORES COORDINATES OF JET VELOCITY PROFILE   PLOT  42
C       X3 - CONTROLS PRINTOUT OF MULTIPLE PLOTS                          PLOT  43
C                                                                         PLOT  44
C                                                                         PLOT  45
      DIMENSIONBUF(5000),XA(100),YA(100),TT(5),ETA(40),JRATIO(40)         PLOT  46
      DIMENSIONSA(4),SB(4),SC(4),SD(4),SE(4),SF(4),SG(4),SH(4)            PLOT  47
      DIMENSIONSI(4),SJ(4),PX(300),PY(300)                                PLOT  48
      DIMENSION  SY(20,7),RRX(20,7),VZ(20,3),VR(20,3),RVZ(20,3)           PLOT  49
      COMMON PX,PY,XN,QQ,Q,D,T,TF,XN2,XNF,TB,SIGMA,GAMMA,XN3,REC,XHOLD    PLOT  50
      COMMON TGAM,XN4,A,AA,F70                                            PLOT  51
      COMMON SY,RRX,VZ,VR,RVZ                                             PLOT  52
      COMMON CONST,NPP,NP,NN,LPRINT,JGAMMA                                PLOT  53
      DATASA,SB,SC,SD,SE,SF,SG,SH,SI,SJ/'IMPE','LLER',' DIA','  =','RE',PLOT  54
     1' ',' ','  =','RPM',' ',' ',' ','  =','EDDY',' VIS','COSI','TY=',  PLOT  55
     2'Q, F','LOW ','AT I','MP=','STRE','AMLI','NE',' ','  =','SIGM','A',PLOT  56
     3' ',' ','  =','A',' ',' ',' ','  =','AA',' ',' ',' ','  =','DISC','HARG',PLOT  57
     4'E AN','GLE'/                                                       PLOT  58
      X3=0.                                                               PLOT  59
      Y3=0.                                                               PLOT  60
9     READ(5,100)K,RHO,RPM,D,POISE,T,QQ                                   PLOT  61
100   FORMAT(I2,6F10.2)                                                   PLOT  62
      READ(5,100)NOPLOT,PRTPLT                                            PLOT  63
      WRITE(6,114)K                                                       PLOT  64
114   FORMAT(1H1,'PRINT CONTROL=',T20,I2)                                 PLOT  65
      READ(5,109)YL,WB,WL,FK1,FK2,FK3,FAC                                 PLOT  66
109   FORMAT(7F10.2)                                                      PLOT  67
      READ(5,204)XN2,XN3,XNF,XN4,GAMMA,F70,JJ                             PLOT  68
204   FORMAT(6F10.2,I2)                                                   PLOT  69
      WRITE(6,400) RHO,RPM,D,POISE,T,QQ                                   PLOT  70
400   FORMAT(20X,'INPUT PARAMETERS'//20X,'FLUID AND TANK CONSTANTS'/      PLOT  71
     120X,'RHO   =',F5.4,10X,'RPM   =',F6.2,9X,'D     =',F5.2/            PLOT  72
     220X,'POISE =',F5.4,10X,'TANK DIA =',F5.2,6X,'STREAM LINE INC =',   PLOT  73
     3F5.2//)                                                             PLOT  74
      WRITE(6,401)YL,WB,WL,FK1,FK2,FK3,FAC,XN2                            PLOT  75
401   FORMAT(20X,'IMPELLER AND BOUNDARY PARAMETERS'//                     PLOT  76
     120X,'LENGTH OF X AXIS=',F5.2,T50,'WIDTH OF IMPELLER BLADE =',F5.2/PLOT  77
     220X,'LENGTH OF IMP BLADE =',F5.2,T50,'FLUID DEPTH RATIO ='        PLOT  78
     3,F5.2/20X,'IMPELLER DEPTH =',F5.2,T50,'SCALE FACTOR JET PROFILE ='PLOT  79
     4,F5.2/20X,'SCALE FACTOR OF PLOT =',F5.2,T50,'BOUNDARY LAYER THICKNPLOT  80
     5ESS RATIO =',F5.2)                                                  PLOT  81
      WRITE(6,402)XN3,XNF,XN4                                             PLOT  82
402   FORMAT(20X,'EXTENT OF ZONE IV =',F5.2,T50,'EXTENT OF ZONE III = ',  PLOT  83
     1F5.2/20X,'EXTENT OF ZONE II =',F5.2)                                PLOT  84
      READ(5,110)SIGMA,A,AA                                               PLOT  85
110   FORMAT(3F10.2)                                                      PLOT  86
      DBYT=D/12.                                                          PLOT  87
```

```
      D=DBYT                                                            PLOT  89
      XO=T*SIGMA/(12.+2.*SIGMA)                                         PLOT  89
      XN=XO                                                             PLOT  90
      X=DBYT/2.                                                         PLOT  91
      TEMP=X**2-AA**2                                                   PLOT  92
      COSPHI=SQRT(TEMP)/X                                               PLOT  93
      PI=ARCOS(COSPHI)*180./3.1416                                      PLOT  94
      EDVIS=A*(TEMP+X**2)/(SQRT(SIGMA**3*X)*TEMP**0.75*2)               PLOT  95
      TE=T/2.-XO                                                        PLOT  96
      TL=(EK1-EK2)*T                                                    PLOT  97
      TR=EK2*T                                                          PLOT  98
      DY=EK1*T/YL                                                       PLOT  99
      XL=T/(2.*DY)                                                      PLOT 100
      DX=DY                                                             PLOT 101
      RHO=RHO*62.43                                                     PLOT 102
      V=POISE*6.72*0.006/RHO                                            PLOT 103
      RE=RPM*D**2/V                                                     PLOT 104
      Q=12.5663706*A*SQRT(D/(2.*SIGMA))*((D/2.)**2-AA**2)**0.25         PLOT 105
903   WRITE(6,3)D,PI,AA,SIGMA,A,RPM,EDVIS,RE,Q                         PLOT 106
3     FORMAT(1H0,6HD     =,F10.5,/1H0,6HANGLE=,F10.5,/1H0,6HAA    =,    PLOT 107
     1F10.5,/1H0,6HSIGMA=, F10.5,/1H0,6HA     =,F10.5,/1H0,6HRPM   =,F10.5PLOT 108
     2,/1H0,6HEDVIS=,F10.5,/1H0,6HRE    =,F20.8,/1H0,6HQ     =,F20.8///)  PLOT 109
      IF(QQ.GT.0.1)GOTO44                                               PLOT 110
      IF(Q.LT.1.  )GOTO40                                               PLOT 111
      IF(Q.LT.5.  )GOTO41                                               PLOT 112
      IF(Q.LT.10. )GOTO42                                               PLOT 113
      QQ=10.                                                            PLOT 114
      GOTO44                                                            PLOT 115
40    QQ=1.                                                             PLOT 116
      GOTO44                                                            PLOT 117
41    QQ=2.                                                             PLOT 118
      GOTO44                                                            PLOT 119
42    QQ=5.                                                             PLOT 120
44    CONTINUE                                                          PLOT 121
C                                                                       PLOT 122
C--------START OF CALCULATION FOR ZONE II                               PLOT 123
C          XO= X COORDINATE OF FLOW CIRCULATION POINT                   PLOT 124
C         YO= Y COORDINATE OF FLOW CIRCULATION POINT                    PLOT 125
C                                                                       PLOT 126
C                                                                       PLOT 127
C--------PLOTTING OF FLOW PROFILE AT SELECTED POINTS IN ZONE I          PLOT 128
C                                                                       PLOT 129
      IF(NOPLOT.EQ.1)GOTO405                                            PLOT 130
      CALL FACTOR(FAC)                                                  PLOT 131
907   CALL PLOTS(BUF, 5000)                                             PLOT 132
908   CALL PLOT(X3,Y3,-3)                                               PLOT 133
      X3=0.                                                             PLOT 134
      Y3=0.                                                             PLOT 135
C                                                                       PLOT 136
C--------DRAW IMPELLER OUTLINE, AND X,Y AXIS                            PLOT 137
C         NOTE,  LENGTH/WIDTH/IMPELLER DIA = WL/WB/D = 4/5/20           PLOT 138
C                                                                       PLOT 139
909   CALL AXIS(0.,0.,1H ,1,XL ,0.,0.,DX)                               PLOT 140
```

```
      CALL AXIS(0.,-FK2*T/DY,1H ,1,YL,90.,-FK2*T,DY)                    PLOT 141
910   CALL PLOT(0.,-TB/DY,3)                                            PLOT 142
      CALL PLOT(XL,-TB/DY,2)                                            PLOT 143
911   CALL PLOT(XL, TL/DY,2)                                            PLOT 144
      CALL PLOT(0., TL/DY,2)                                            PLOT 145
C                                                                       PLOT 146
C---------PRTPLT CONTROLS PRINTOUT ON PLOT                              PLOT 147
C                                                                       PLOT 148
      IF(PRTPLT.LT.1)GOTO920                                            PLOT 149
912   AX=XL+2.5                                                         PLOT 150
      BY=-TB/2.                                                         PLOT 151
913   CALL SYMBOL(AX,BY ,0.2,SA,0.,15)                                  PLOT 152
      BY=BY-0.3                                                         PLOT 153
      CALL SYMBOL(AX,BY ,0.2,SB,0.,15)                                  PLOT 154
914   BY=BY-0.3                                                         PLOT 155
      CALL SYMBOL(AX,BY ,0.2,SC,0.,15)                                  PLOT 156
      BY=BY-0.3                                                         PLOT 157
      CALL SYMBOL(AX,BY ,0.2,SD,0.,15)                                  PLOT 158
      BY=BY-0.3                                                         PLOT 159
915   CALL SYMBOL(AX,BY ,0.2,SE,0.,15)                                  PLOT 160
      BY=BY-0.3                                                         PLOT 161
      CALL SYMBOL(AX,BY ,0.2,SF,0.,15)                                  PLOT 162
      BY=BY-0.3                                                         PLOT 163
916   CALL SYMBOL(AX,BY ,0.2,SG,0.,15)                                  PLOT 164
      BY=BY-0.3                                                         PLOT 165
      CALL SYMBOL(AX,BY ,0.2,SH,0.,15)                                  PLOT 166
      BY=BY-0.3                                                         PLOT 167
      CALL SYMBOL(AX,BY ,0.2,SI,0.,15)                                  PLOT 168
      BY=BY-0.3                                                         PLOT 169
      CALL SYMBOL(AX,BY ,0.2,SJ,0.,15)                                  PLOT 170
      AX=AX+3.5                                                         PLOT 171
917   BY=-TB/2.                                                         PLOT 172
      CALL NUMBER(AX,BY  ,0.2,D,0.,4)                                   PLOT 173
      BY=BY-0.3                                                         PLOT 174
      CALL NUMBER(AX,BY  ,0.2,RE,0.,4)                                  PLOT 175
      BY=BY-0.3                                                         PLOT 176
      CALL NUMBER(AX,BY  ,0.2,RPM,0.,4)                                 PLOT 177
      BY=BY-0.3                                                         PLOT 178
      CALL NUMBER(AX,BY  ,0.2,EDVIS,0.,4)                               PLOT 179
918   BY=BY-0.3                                                         PLOT 180
      CALL NUMBER(AX,BY  ,0.2,Q    ,0.,4)                               PLOT 181
      BY=BY-0.3                                                         PLOT 182
      CALL NUMBER(AX,BY  ,0.2,OO   ,0.,4)                               PLOT 183
      BY=BY-0.3                                                         PLOT 184
      CALL NUMBER(AX,BY  ,0.2,SIGMA,0.,4)                               PLOT 185
      BY=BY-0.3                                                         PLOT 186
919   CALL NUMBER(AX,BY  ,0.2,A    ,0.,4)                               PLOT 187
      BY=BY-0.3                                                         PLOT 188
      CALL NUMBER(AX,BY  ,0.2,AA   ,0.,4)                               PLOT 189
      BY=BY-0.3                                                         PLOT 190
      CALL NUMBER(AX,BY  ,0.2,PI   ,0.,4)                               PLOT 191
920   CALL PLOT( D/(2.*DX),D/(WB*DY*2.),3)                              PLOT 192
      CALL PLOT((D/2.-D/WL)/DX,D/(WB*DY*2.),2)                          PLOT 193
```

```
      CALL PLOT((D/2.-D/WL)/DX,-D/(WB*DY*2.),2)                          PLOT 194
921   CALL PLOT( D/(2.*DX),-D/(WB*DY*2.),2)                              PLOT 195
      CALL PLOT( D/(2.*DX), D/(WB*DY*2.),2)                              PLOT 196
C                                                                        PLOT 197
C--------DRAW SELECTED PROFILES ON X-AXIS                               PLOT 198
C         SCALE FOR PROFILE,FK3 = U(MAX), AT IMPELLER TIP, INCHES        PLOT 199
C                                                                        PLOT 200
900   R=D/2.                                                             PLOT 201
      VRMAX=A/2.*SQRT(SIGMA/R**3)*(R**2-AA**2)**0.25                     PLOT 202
      TEMP=(XO-R)/4.                                                     PLOT 203
      TT(1)=D/2.-TEMP                                                    PLOT 204
      DO14J=1,4                                                          PLOT 205
      TT(J+1)=TT(J)+TEMP                                                 PLOT 206
      XA(35)=TT(J+1)/DX                                                  PLOT 207
      YA(35)=0.                                                          PLOT 208
      ETA(1)=0.                                                          PLOT 209
      DO15I=2,35                                                         PLOT 210
      VRR=A/2.*SQRT(SIGMA/TT(J+1)**3)*(TT(J+1)**2-AA**2)**0.25           PLOT 211
      KU=34+I                                                            PLOT 212
      KB=36-I                                                            PLOT 213
      ETA(I)=ETA(I-1)+0.2                                                PLOT 214
      URATIO(I)=1.-(TANH(ETA(I)/2.))**2                                  PLOT 215
      XA( KU )=(TT(J+1)-VRR/VRMAX*FK3*(1.-URATIO(I)))/DX                 PLOT 216
      XA( KB )=XA( KU )                                                  PLOT 217
      YA( KU )=ETA(I)*TT(J+1)/(SIGMA*DY)                                 PLOT 218
15    YA( KB )=-YA( KU )                                                 PLOT 219
      XA(70)=0.0                                                         PLOT 220
      YA(70)=0.0                                                         PLOT 221
      XA(71)=1.                                                          PLOT 222
      YA(71)=1.                                                          PLOT 223
      CALL LINE(XA,YA,69,1,0,0)                                          PLOT 224
14    CONTINUE                                                           PLOT 225
C                                                                        PLOT 226
C--------PRELIMINARY  CALCULATIONS                                       PLOT 227
C                                                                        PLOT 228
405   TF=TB                                                              PLOT 229
      TB=TF*XN2                                                          PLOT 230
      WRITE(6,115)TF,TB,TL,XO                                            PLOT 231
115   FORMAT(1X,'STREAMLINE PARAMETERS'//1X,'TF = 'F15.8,5X,'TB = 'F15.8PLOT 232
     1,5X,'TL = 'F15.8,5X,'XO =',F15.8///)                               PLOT 233
      IF(Q.LT.00)GOTO27                                                  PLOT 234
      PN=Q/QO                                                            PLOT 235
      NP=PN                                                              PLOT 236
      WRITE(6,113)NP                                                     PLOT 237
113   FORMAT(1X,I5)                                                      PLOT 238
      GOTO26                                                             PLOT 239
27    NP=0                                                               PLOT 240
26    PEC=0.                                                             PLOT 241
      WRITE(6,1)GAMMA                                                    PLOT 242
1     FORMAT(1H0,5X,7HGAMMA =,F20.8)                                     PLOT 243
C                                                                        PLOT 244
C--------PLOT STREAMLINES BELOW IMPELLER CENTER-LINE                     PLOT 245
C                                                                        PLOT 246
```

```
      J=0                                                               PLOT 247
      IF(JJ.EQ.1)J=1                                                    PLOT 248
      JGAMMA=J                                                          PLOT 249
31    TGAM=0.                                                           PLOT 250
      LPRINT=J                                                          PLOT 251
      PEC=0.                                                            PLOT 252
      NPP=0                                                             PLOT 253
      DO16I=1,20                                                        PLOT 254
      CALL STREAM                                                       PLOT 255
      IF(XHOLD.GE.XN)GOTO28                                             PLOT 256
      IF(J.EQ.0)GOTO16                                                  PLOT 257
      IF(NN.GT.300)GOTO21                                               PLOT 258
      PX(NN+1)=0.                                                       PLOT 259
      PY(NN+1)=0.                                                       PLOT 260
      PX(NN+2)=DX                                                       PLOT 261
      PY(NN+2)=DY                                                       PLOT 262
      DO13L=1,NN                                                        PLOT 263
13    PY(L)=-PY(L)                                                      PLOT 264
      IF(NOPLOT.EQ.1)GOTO16                                             PLOT 265
      CALL LINE(PX,PY,NN,1,0,0)                                         PLOT 266
16    CONTINUE                                                          PLOT 267
28    IF(J.EQ.1)GOTO29                                                  PLOT 268
      IF(ABS(TGAM-GAMMA).LE.(0.01*GAMMA))GOTO30                         PLOT 269
      GAMMA=TGAM                                                        PLOT 270
      GOTO31                                                            PLOT 271
30    J=1                                                               PLOT 272
      JGAMMA=J                                                          PLOT 273
      GAMMA=TGAM                                                        PLOT 274
      GOTO31                                                            PLOT 275
C                                                                       PLOT 276
C---------STREAMLINES ABOVE IMPELLER CENTERLINE                         PLOT 277
C                                                                       PLOT 278
29    READ(5,37)GAMMA,XN2,JJ                                            PLOT 279
      IF(JGAMMA.EQ.1)CALLSPRINT                                         PLOT 280
37    FORMAT(2F10.2,I2)                                                 PLOT 281
      WRITE(6,36)                                                       PLOT 282
36    FORMAT(1X,///1X,T15,'STREAMLINES ABOVE CENTER-LINE',///)          PLOT 283
      TB=TL*XN2                                                         PLOT 284
      WRITE(6,115)TF,TB,TL,XO                                           PLOT 285
      WRITE(6,1)GAMMA                                                   PLOT 286
      J=0                                                               PLOT 287
      IF(JJ.EQ.1)J=1                                                    PLOT 288
      JGAMMA=J                                                          PLOT 289
34    TGAM=0.                                                           PLOT 290
      LPRINT=J                                                          PLOT 291
      PEC=0.                                                            PLOT 292
      NPP=0                                                             PLOT 293
      DO17I=1,20                                                        PLOT 294
      CALL STREAM                                                       PLOT 295
      IF(XHOLD.GE.XN)GOTO32                                             PLOT 296
      IF(J.EQ.0)GOTO17                                                  PLOT 297
      IF(NN.GT.300)GOTO21                                               PLOT 298
      PX(NN+1)=0.                                                       PLOT 299
```

```
      PY(NN+1)=0.                                                        PLOT 300
      PX(NN+2)=DX                                                        PLOT 301
      PY(NN+2)=DY                                                        PLOT 302
      IF(NOPLOT.EQ.1)GOTO17                                              PLOT 303
      CALL LINE(PX,PY,NN,1,0,0)                                          PLOT 304
17    CONTINUE                                                           PLOT 305
32    IF(J.EQ.1)GOTO10                                                   PLOT 306
      IF(ABS(TGAM-GAMMA).LE.(0.01*GAMMA))GOTO33                          PLOT 307
      GAMMA=TGAM                                                         PLOT 308
      GOTO34                                                             PLOT 309
33    J=1                                                                PLOT 310
      JGAMMA=J                                                           PLOT 311
      GAMMA=TGAM                                                         PLOT 312
      GOTO34                                                             PLOT 313
21    WRITE(6,12)NN                                                      PLOT 314
12    FORMAT(1H0,5X,29HNN IS GREATER THAN 300, AND =,I4)                 PLOT 315
10    IF(JGAMMA.EQ.1)CALLSPRINT                                          PLOT 316
      IF(NOPLOT.EQ.0)CALL PLOT(0.,0.,-3)                                 PLOT 317
      X3=X3+XL+2.5                                                       PLOT 318
18    IF(K.LT.5)GOTO9                                                    PLOT 319
22    IF(NOPLOT.EQ.0)CALL PLOT(0.,0.,999)                                PLOT 320
      WRITE(6,114)K                                                      PLOT 321
      STOP                                                               PLOT 322
      END                                                                PLOT 323
```

****

SUBROUTINE STREAM

****

```
      SUBROUTINE STREAM                                                  STRE   1
C                                                                        STRE   2
C                                                                        STRE   3
C        XO = XN - EXTENT OF TANGENTIAL JET, EQUATION II-29              STRE   4
C        PEC - FRACTION OF FLUID FLOWING IN TANGENTIAL JET, RATIO OF Q   STRE   5
C        XHOLD, YHOLD - COORDINATES OF START OF STREAM LINE              STRE   6
C        TGAM - TEMPORARY STORAGE FOR EVALUATING GAMMA                   STRE   7
C        PX, PY - ARRAYS THAT HOLD COORDINATES OF ONE ENTIRE STREAMLINE  STRE   8
C        CK - VALUE OF PSI IN EQUATION II-30                             STRE   9
C        ZO - SEE EQUATION II-38                                         STRE  10
C        JGAMMA CONTROLS VELOCITY PROFILE ANALYSIS IN SELECTED Z PLANES  STRE  12
C        JGAMMA= 0, DELETE ANALYSIS                                      STRE  13
C                                                                        STRE  14
C                                                                        STRE  15
      DIMENSION PX(300),PY(300)                                          STRE  16
      DIMENSION  SY(20,7),RRX(20,7),VZ(20,3),VR(20,3),RVZ(20,3)          STRE  17
      COMMON PX,PY,XN,QO,Q,D,T,TF,XN2,XNF,TB,SIGMA,GAMMA,XN3,PEC,XHOLD   STRE  18
      COMMON TGAM,XN4,A,AA,FZO                                           STRE  19
      COMMON SY,RRX,VZ,VR,RVZ                                            STRE  20
      COMMON CONST,NPP,NP,NN,LPRINT,JGAMMA                               STRE  21
      F(R)=Q*SQRT(SIGMA*R)/(12.5663706*A*(R**2-AA**2)**0.25)             STRE  22
      JGAMMA=0                                                           STRE  23
```

```
      LIV=1                                                              STRE  24
      LPRINT=0                                                           STRE  25
      IF(NPP.EQ.0)77=2.                                                  STRE  26
      DD=D/2.                                                            STRE  27
      JC=0                                                               STRE  28
      QQ=QQ                                                              STRE  29
      XO=XN                                                              STRE  30
      IF(NPP.GE.NP)GOTO28                                                STRE  31
      NPP=NPP+1                                                          STRE  32
      PEC=PEC+QQ/Q                                                       STRE  33
      QX=PEC                                                             STRE  34
      XT=D/2.+0.01                                                       STRE  35
      DK=QX*F(XT)                                                        STRE  36
      GOTO19                                                             STRE  37
28    NPP=NPP+1                                                          STRE  38
      PN=NPP                                                             STRE  39
      QX=QQ*PN                                                           STRE  40
      CALL GOLD(DD,XO,QX,.001,RR)                                        STRE  41
      XT=RR                                                              STRE  42
      QX=QX/Q                                                            STRE  43
      DK=QX*F(XT)                                                        STRE  44
19    TOP=XT+DK                                                          STRE  45
      BOT=XT-DK                                                          STRE  46
      XHOLD=XT                                                           STRE  47
      IF(XHOLD.GE.XN)GOTO16                                              STRE  48
      YT=XT/SIGMA*ALOG(TOP/BOT)                                          STRE  49
      YHOLD=YT                                                           STRE  50
      IF(LPRINT.EQ.1)WRITE(6,100)XHOLD,YHOLD,DK                          STRE  51
100   FORMAT(1X,7HXHOLD =,F20.8,10X,7HYHOLD =,F20.8,/                    STRE  52
     11X,7HDK     =,F20.8)                                              STRE  53
      TEMP=(XN-XT)/.005                                                  STRE  54
      N=TEMP                                                             STRE  55
      NN=N                                                               STRE  56
      DO17J=1,N                                                          STRE  57
      XT=XT+.005                                                         STRE  58
      DK=QX*F(XT)                                                        STRE  59
      TOP=XT+DK                                                          STRE  60
      BOT=XT-DK                                                          STRE  61
      YT=XT/SIGMA*ALOG(TOP/BOT)                                          STRE  62
      PX(J)=XT                                                           STRE  63
      PY(J)=YT                                                           STRE  64
17    CONTINUE                                                           STRE  65
C                                                                        STRE  66
C---------PLOT STREAM LINES OF ZONE II                                   STRE  67
C                                                                        STRE  68
      X=XT                                                               STRE  69
      Y=YT                                                               STRE  70
      TF=T/2.-XN                                                         STRE  71
      CK=(T/2.-X)**2*Y                                                   STRE  72
C                                                                        STRE  73
C---------CALCULATE, R AND STREAM FUNCTION IN SELECTED 7 PLANES          STRE  74
C         TO EVALUATE VELOCITY PROFILES                                  STRE  75
C                                                                        STRE  76
```

```
      IF(JGAMMA.EQ.0)GOTO31                                              STRE  77
      SCALER=11.5/T                                                      STRE  78
      TINC=TB/(12.*XN2)                                                  STRE  79
      TRR=0.5*TB/XN2-4.*TINC                                             STRE  80
      TQQ=QQ/2.*NPP                                                      STRE  81
      DO30JK=1,7                                                         STRE  82
      TRR=TRR+TINC                                                       STRE  83
      TEMP=TRR*XN2*6./TB                                                 STRE  84
      IF(LPRINT.EQ.1)WRITE(406)TEMP                                      STRE  85
406   FORMAT(20X,'TRR='F15.2)                                            STRE  86
      IF(TRR.GT.(TB*XN4))GOTO31                                          STRE  87
      RRX(NPP,JK)=SQRT(CK/TRR)*SCALER                                    STRE  88
30    SY(NPP,JK)=TQQ                                                     STRE  89
31    IF(LPRINT.EQ.1)WRITE(6,106)CK                                      STRE  90
106   FORMAT(1X,4HCK =,F20.8,//)                                         STRE  91
      TEMP=(TB*XN4-Y)/0.01                                               STRE  92
      N=TEMP                                                             STRE  93
      DO11J=1,N                                                          STRE  94
      Y=Y+0.01                                                           STRE  95
      X=T/2.-(CK/Y)**0.5                                                 STRE  96
      JN=J+NN                                                            STRE  97
      PX(JN)=X                                                           STRE  98
      PY(JN)=Y                                                           STRE  99
11    CONTINUE                                                           STRE 100
C                                                                        STRE 101
C--------PLOT STREAM LINES OF ZONE III, TAKEN AS MIRROR IMAGE OF         STRE 102
C         ZONE II                                                        STRE 103
C                                                                        STRE 104
      NN=NN+N                                                            STRE 105
      XQ=XN*XNF                                                          STRE 106
      XR=T/2.-X                                                          STRE 107
      CK=XR**2*(TB-Y)                                                    STRE 108
C                                                                        STRE 109
C--------CONTINUE R AND STREAM FUNCTION CALCULATIONS IN SELECTED 7 PLANESTRE 110
C                                                                        STRE 111
      IF(JGAMMA.EQ.0)GOTO35                                              STRE 112
      JL=JK                                                              STRE 113
      TRR=TRR-TINC                                                       STRE 114
      DO32JK=JL,7                                                        STRE 115
      TRR=TRR+TINC                                                       STRE 116
      TEMP=TRR*XN2*6./TB                                                 STRE 117
      TEP=TB*XN2-TRR                                                     STRE 118
      IF(LPRINT.EQ.1)WRITE(406)TEMP                                      STRE 119
      RRX(NPP,JK)=SQRT(CK/TEP)*SCALER                                    STRE 120
32    SY(NPP,JK)=TQQ                                                     STRE 121
      IF(LPRINT.EQ.0)GOTO35                                              STRE 122
      IPR=7                                                              STRE 123
      WRITE(6,403)NPP                                                    STRE 124
403   FORMAT(1X/19X,I3/)                                                 STRE 125
      WRITE(IPR,400)(SY(NPP,JK),JK=1,7)                                  STRE 126
400   FORMAT(1X,7F10.2)                                                  STRE 127
      WRITE(IPR,401)(RRX(NPP,JK),JK=1,7)                                 STRE 128
401   FORMAT(1X,7F10.5)                                                  STRE 129
```

```
35    IF(LPRINT.EQ.1)WRITE(6,106)CK                                          STRE 130
      TEMP=(X-X0)/0.01                                                       STRE 131
      N=TEMP                                                                 STRE 132
      DO12J=1,N                                                              STRE 133
      XR=XR+0.01                                                             STRE 134
      X=X-0.01                                                               STRE 135
      Y=TB-CK/(XR**2)                                                        STRE 136
      JN=J+NN                                                                STRE 137
      PX(JN)=X                                                               STRE 138
      PY(JN)=Y                                                               STRE 139
12    CONTINUE                                                               STRE 140
C                                                                            STRE 141
C--------PLOT STREAM LINES OF ZONE IV                                        STRE 142
C         TO DRAW ZONE IV AS IN FIGURE II-5, PUT LIV=1, OTHERWISE LIV=0      STRE 143
C                                                                            STRE 144
      NN=NN+N                                                                STRE 145
      X0=XN*XNF                                                              STRE 146
      YR=TB-Y                                                                STRE 147
      CK=YR*X**2                                                             STRE 148
      IF(LPRINT.EQ.1)WRITE(6,106)CK                                          STRE 149
      TEMP=X0*XN3/0.01                                                       STRE 150
      IF(LIV.EQ.0)GOTO60                                                     STRE 151
      IF(YR.GT.(XN3*TB))GOTO120                                              STRE 152
      TEMP=(XN3*TB-YR)/0.01                                                  STRE 153
60    N=TEMP                                                                 STRE 154
      DO21J=1,N                                                              STRE 155
      IF(LIV.EQ.0)GOTO61                                                     STRE 156
      YR=YR+0.01                                                             STRE 157
      Y=Y-0.01                                                               STRE 158
      X=SQRT(CK/YR)                                                          STRE 159
      GOTO62                                                                 STRE 160
61    X=X-0.01                                                               STRE 161
      Y=TB-CK/(X**2)                                                         STRE 162
62    JN=J+NN                                                                STRE 163
      PX(JN)=X                                                               STRE 164
      PY(JN)=Y                                                               STRE 165
21    CONTINUE                                                               STRE 166
C                                                                            STRE 167
C--------CONTINUATION OF ZONE IV, TREATED AS CIRCULAR JET                   STRE 168
C                                                                            STRE 169
      IF(LPRINT.EQ.1)WRITE(6,109)(PX(K),PY(K),K=1,JN)                        STRE 170
109   FORMAT(1X//1H0,T5,'X(I)',T20,'Y(I)'/1X,(2F15.8))                       STRE 171
      NN=NN+N                                                                STRE 172
120   ZF=TB*FZ0                                                              STRE 173
      XT=TB-Y+ZF                                                             STRE 174
      Z0=GAMMA*X/XT                                                          STRE 175
      IF(ZZ.GT.Z0)ZZ=Z0                                                      STRE 176
      CC=(1.+0.25*Z0**2)/(XT*Z0**2)                                          STRE 177
      TC=TB-YHOLD+ZF                                                         STRE 178
      IF(LPRINT.EQ.1)WRITE(6,105)Z0,TC,CC                                    STRE 179
105   FORMAT(1X,4HZ0 =,F20.8,10X,4HTC =,F20.8,10X,4HCC =,F20.8)              STRE 180
      IF(NPP.LT.NP)GOTO29                                                    STRE 181
      IF(JGAMMA.EQ.1)GOTO33                                                  STRE 182
```

```
      IF((TC*CC).LE.0.25)GOTO49                                          STRE 183
42    TEMP=TC/XHOLD*SQRT(1./(TC*CC-0.25))                                STRE 184
      TGAM=TGAM+TEMP                                                     STRE 185
      WRITE(6,205)TEMP                                                   STRE 186
205   FORMAT(1X,7HGAMMA =,F20.8)                                         STRE 187
      GOTO29                                                             STRE 188
C                                                                        STRE 189
C---------CALCULATE VELOCITY PROFILES IN REGION V IN SELECTED 7 PLANES   STRE 190
C         (1.-ECONST) DETERMINES FRACTION OF MOMENTUM IN TANGENTIAL      STRE 191
C                     JET THAT HAS BEEN DISSIPATED                       STRE 192
C                                                                        STRE 193
33    IF(NPP.EQ.1)EZO=A /(2.*GAMMA)                                      STRE 194
      ECONST=.4                                                          STRE 195
      EZO=EZO*ECONST                                                     STRE 196
      TINC=2.*TINC                                                       STRE 197
      ZX=0.5*TB/XN2+ZF-2*TINC                                            STRE 198
      TEMP=ZX                                                            STRE 199
      DO34JK=1,3                                                         STRE 200
      TEMP=TEMP+TINC                                                     STRE 201
      ZX=TEMP                                                            STRE 202
      RVZ(NPP,JK)=ZX/GAMMA*SQRT(1./(ZX*CC-0.25))                         STRE 203
      CSY=GAMMA*RVZ(NPP,JK)/ZX                                           STRE 204
      RVZ(NPP,JK)=11.50/2.-RVZ(NPP,JK)*SCALER                            STRE 205
      CTEMP=EZO/(1.+0.25*CSY**2)**2                                      STRE 206
      ZX=ZX*6./TB*XN2                                                    STRE 207
      ZX=ZX/12.                                                          STRE 208
      VZ(NPP,JK)=2.*GAMMA**2*CTEMP/ZX                                   STRE 209
34    VR(NPP,JK)=CTEMP/ZX*(CSY-0.25*CSY**3)*GAMMA                        STRE 210
      IF(LPRINT.EQ.0)GOTO29                                              STRE 211
      WRITE(6,411)EZO                                                    STRE 212
411   FORMAT(20X,'EZO =',F15.8)                                          STRE 213
      IPR=6                                                              STRE 214
      WRITE(IPR,501)   (RVZ(NPP,JK),VZ(NPP,JK),VR(NPP,JK),JK=1,3)       STRE 215
501   FORMAT(1X,3F12.5)                                                  STRE 216
29    TEMP=(TC-XT)/0.01                                                  STRE 217
      N=TEMP                                                             STRE 218
      DO25J=1,N                                                          STRE 219
      Y=Y-0.01                                                           STRE 220
      XT=XT+0.01                                                         STRE 221
      YT=XT/GAMMA*SQRT(1./(XT*CC-0.25))                                  STRE 222
      X=YT                                                               STRE 223
      JN=J+NN                                                            STRE 224
      PX(JN)=X                                                           STRE 225
      PY(JN)=Y                                                           STRE 226
25    CONTINUE                                                           STRE 227
      NN=NN+N                                                            STRE 228
      WRITE(6,113)NN                                                     STRE 229
113   FORMAT(1X,I5)                                                      STRE 230
      IF(LPRINT.EQ.1)WRITE(6,104)(PX(J),PY(J),J=1,NN)                    STRE 231
104   FORMAT(1X,//// (1X,6F15.4))                                        STRE 232
      GOTO27                                                             STRE 233
16    N=NPP-NP                                                           STRE 234
      IF(NP.EQ.0)N=N-1                                                   STRE 235
```

```
      TGAM=TGAM/FLOAT(N)                                                STRE 236
      IF(7Z.LT.1.)GAMMA=TGAM                                            STRE 237
      WRITE(6,26)TGAM                                                   STRE 238
26    FORMAT(1H0,20HNEW VALUE OF GAMMA =,F20.8)                         STRE 239
      GOTO27                                                            STRE 240
49    TEMP=TC*CC                                                        STRE 241
      WRITE(6,108)TEMP                                                  STRE 242
108   FORMAT(1H0,'TC*CC =',T15,F15.8)                                   STRE 243
      CALL PLOT(0.,0.,999)                                              STRE 244
      STOP                                                              STRE 245
27    RETURN                                                            STRE 246
      END                                                               STRE 247
```

```
*************************************************************************************
                                SUBROUTINE GOLD
*************************************************************************************

      SUBROUTINE GOLD(X1,X2,F,FINT,XT)                                  GOLD   1
C                                                                       GOLD   2
C        THIS SUBROUTINE EVALUATES A ROOT OF  AN EQUATION USING         GOLD   3
C        GOLDEN SECTION                                                 GOLD   4
C        S = EQUATION WHOSE ROOT IS DESIRED                             GOLD   5
C        X1 = INITIAL VALUE OF INTERVAL                                 GOLD   6
C        X2 = FINAL VALUE OF INTERVAL                                   GOLD   7
C        F = VALUE OF S AT DESIRED ROOT                                 GOLD   8
C        FINT = INTERVAL OF UNCERTAINITY                                GOLD   9
C                                                                       GOLD  10
      DIMENSION PX(300),PY(300)                                         GOLD  11
      DIMENSION  SY(20,7),RRX(20,7),VZ(20,3),VR(20,3),RVZ(20,3)         GOLD  12
      COMMON PX,PY,XN,QD,Q,D,T,TF,XN2,XNF,TB,SIGMA,GAMMA,XN3,PEC,XHOLD  GOLD  13
      COMMON TGAM,XN4,A,AA,FZO                                          GOLD  14
      COMMON SY,RRX,VZ,VR,RVZ                                           GOLD  15
      COMMON CONST,NPP,NP,NN,LPRINT,JGAMMA                              GOLD  16
      S(R)=12.5663706*A*SQRT(R/SIGMA)*(R**2-AA**2)**0.25                GOLD  17
      I=0                                                               GOLD  18
8     I=I+1                                                             GOLD  19
      DG1=X1+(X2-X1)/1.618034                                           GOLD  20
      DG2=X1+(DG1-X1)/1.618034                                          GOLD  21
      R1=S(DG1)                                                         GOLD  22
      R2=S(DG2)                                                         GOLD  23
      IF(I.NE.1)GOTO1                                                   GOLD  24
      K=2                                                               GOLD  25
      IF(R1.GT.R2)K=1                                                   GOLD  26
1     IF(R1.LE.F.AND.R2.LE.F)GOTO2                                      GOLD  27
      IF(R1.LE.F.AND.R2.GT.F)GOTO3                                      GOLD  28
      IF(R1.GT.F.AND.R2.LE.F)GOTO3                                      GOLD  29
      IF(R1.GT.F.AND.R2.GT.F)GOTO4                                      GOLD  30
2     IF(K.EQ.2)GOTO5                                                   GOLD  31
6     X1=DG2                                                            GOLD  32
      GOTO7                                                             GOLD  33
3     X1=DG2                                                            GOLD  34
      X2=DG1                                                            GOLD  35
```

```
      GOTO7                                                              GOLD   36
4     IF(K.EQ.2)GOTO6                                                    GOLD   37
5     X2=DGI                                                             GOLD   38
      GOTO7                                                              GOLD   39
7     TEST=X2-X1                                                         GOLD   40
      IF(LPRINT.EQ.1)WRITE(6,9)X1,X2,TEST                                GOLD   41
9     FORMAT(1X,3E15.8)                                                  GOLD   42
      IF(TEST.GE.FINT)GOTO8                                              GOLD   43
      XT=(X2+X1)/2.+0.01                                                 GOLD   44
      RETURN                                                             GOLD   45
      END                                                                GOLD   46
```

****

SUBROUTINE SPRINT

****

```
      SUBROUTINE SPRINT                                                  SPRI    1
      DIMENSION PX(300),PY(300)                                          SPRI    2
      DIMENSION  SY(20,7),RRX(20,7),VZ(20,3),VR(20,3),RVZ(20,3),VT(20,3)SPRI    3
      COMMON PX,PY,XN,QD,Q,D,T,TF,XN2,XNF,TB,SIGMA,GAMMA,XN3,PEC,XHOLD   SPRI    4
      COMMON TGAM,XN4,A,AA,FZO                                           SPRI    5
      COMMON SY,RRX,VZ,VR,RVZ                                            SPRI    6
      COMMON CONST,NPP,NP,NN,LPRINT,JGAMMA                               SPRI    7
C                                                                        SPRI    8
C---------SUMMARY OF PROFILE ANALYSIS IN REGION V                        SPRI    9
C                                                                        SPRI   10
407   LTEMP=NPP-1                                                        SPRI   11
      DO406LQ=1,3                                                        SPRI   12
      DO406LP=1,LTEMP                                                    SPRI   13
406   VT(LP,LQ)=SQRT(VZ(LP,LQ)**2+VR(LP,LQ)**2)                          SPRI   14
      WRITE(6,403)(RVZ(I,1),VZ(I,1),VR(I,1),VT(I,1),I=1,LTEMP)          SPRI   15
      WRITE(6,404)(RVZ(I,2),VZ(I,2),VR(I,2),VT(I,2),I=1,LTEMP)          SPRI   16
      WRITE(6,405)(RVZ(I,3),VZ(I,3),VR(I,3),VT(I,3),I=1,LTEMP)          SPRI   17
403   FORMAT(1H1//30X,'VELOCITY PROFILE IN REGION V AT Z= 2 IN.'/        SPRI   18
     1/35X,'R',8X,'VZ',8X,'VR',8X,'V'/(28X,4F10.3))                     SPRI   19
404   FORMAT(1X //30X,'VELOCITY PROFILE IN REGION V AT Z= 3 IN.'//       SPRI   20
     1(28X,4F10.3))                                                     SPRI   21
405   FORMAT(1X //30X,'VELOCITY PROFILE IN REGION V AT Z= 4 IN.'//       SPRI   22
     1(28X,4F10.3))                                                     SPRI   23
      WRITE(6,401)(( SY(I,J),J=1,7),I=1,LTEMP)                           SPRI   24
      WRITE(6,402)((RRX(I,J),J=1,7),I=1,LTEMP)                           SPRI   25
401   FORMAT(1H1,30X,'STREAM FUNCTION MATRIX'//(20X,7F10.3))             SPRI   26
402   FORMAT(1X///30X,'CORESPONDING RADIAL MATRIX',//(20X,7F10.3))       SPRI   27
      WRITE(6,400)                                                       SPRI   28
400   FORMAT(1H1)                                                        SPRI   29
      RETURN                                                             SPRI   30
      END                                                                SPRI   31
```

****

INPUT DATA FOR FIGURE II-5(A)

```
*************************************************************************************

 10.99708    500.       3.          0.8937     1.          5.

10.          5.0        4.0         1.          0.4        1.0         0.5
0.9          0.3        1.          0.5         1.87       0.0          0
12.621       19.273     0.1009
2.5          1.          0

*************************************************************************************
```

INPUT DATA FOR FIGURE II-5(B)

```
*************************************************************************************

 90.99708    500.       3.          0.8937     1.          3.
   2.
10.          5.0        4.0         1.          0.4        1.0         0.5
0.9          0.5        1.          0.5         1.87       0.0          0
12.621       19.273     0.1009
2.5          1.          0
```

SAMPLE OUTPUT

```
PRINT CONTROL=      9
                    INPUT PARAMETERS

                    FLUID AND TANK CONSTANTS
                    RHO   =.0971          RPM   =500.00          D     = 3.00
                    POISE =.8937          TANK DIA = 0.96        STREAM LINE INC = 5.00


                    IMPELLER AND BOUNDARY PARAMETERS

                    LENGTH OF X AXIS=10.00        WIDTH OF IMPELLER BLADE = 5.00
                    LENGTH OF IMP BLADE = 4.00    FLUID DEPTH RATIO = 1.04
                    IMPELLER DEPTH = 0.52         SCALE FACTOR JET PROFILE = 0.10
                    SCALE FACTOR OF PLOT = 0.70   BOUNDARY LAYER THICKNESS RATIO = 0.90
                    EXTENT OF ZONE IV = 0.10      EXTENT OF ZONE III =  0.90
                    EXTENT OF ZONE II = 0.55

D     =   0.25000

ANGLE=  66.57747

AA    =   0.11470

SIGMA=  11.19200

A     =  28.23859

RPM   = 500.00000

EQVIS=   1.74240

RE    =      53983.52343750

Q     =          8.35951233
```

(a) Streamlines Above Impeller Centerline

```
STREAMLINE PARAMETERS

TF =      0.50083190     TR =      0.45074868     TL =      0.49948782     XO =      0.31248027


    1

     GAMMA =          1.86999989
GAMMA =          0.82881755
  119
GAMMA =          1.09923363
  112
GAMMA =          1.07112598
  101
GAMMA =          1.06623840
   87
GAMMA =          1.04436398
```

```
   72
GAMMA =          1.17652225
   51

NEW VALUE OF GAMMA =          1.04771614
GAMMA =          0.82809001
  119
GAMMA =          1.09507275
  112
GAMMA =          1.06200027
  101
GAMMA =          1.04611969
   87
GAMMA =          1.00335789
   72
GAMMA =          1.04719353
   51

NEW VALUE OF GAMMA =          1.01363850
GAMMA =          0.82801771
  119
GAMMA =          1.09466076
  112
GAMMA =          1.06110382
  101
GAMMA =          1.04417706
   87
GAMMA =          0.99953204
   72
GAMMA =          1.03651905
   51

NEW VALUE OF GAMMA =          1.01066780

                    1

  119

                    2

  112

                    3

  101

                    4

   87

                    5

   72

                    6
```

51

NEW VALUE OF GAMMA = 0.0

VELOCITY PROFILE IN REGION V AT Z= 2 IN.

R	VZ	VR	V
4.921	94.289	18.683	96.122
4.548	51.676	14.095	53.563
4.261	28.379	9.071	29.794
3.868	14.762	5.375	15.710
3.481	7.543	2.873	8.072
2.783	3.275	1.064	3.443

VELOCITY PROFILE IN REGION V AT Z= 3 IN.

4.742	64.711	10.557	65.567
4.300	36.601	8.317	37.534
3.968	20.748	5.609	21.493
3.527	11.381	3.625	11.944
3.112	6.191	2.184	6.565
2.415	3.078	1.171	3.293

VELOCITY PROFILE IN REGION V AT Z= 4 IN.

4.590	49.235	6.984	49.728
4.088	28.275	5.615	28.828
3.715	16.271	3.866	16.724
3.227	9.144	2.591	9.504
2.777	5.113	1.632	5.367
2.043	2.687	0.972	2.857

STREAM FUNCTION MATRIX

2.500	2.500	2.500	2.500	2.500	2.500	2.500
5.000	5.000	5.000	5.000	5.000	5.000	5.000
7.500	7.500	7.500	7.500	7.500	7.500	7.500
10.000	10.000	10.000	10.000	10.000	10.000	10.000
12.500	12.500	12.500	12.500	12.500	12.500	12.500
15.000	15.000	15.000	15.000	15.000	15.000	15.000

CORESPONDING RADIAL MATRIX

0.540	0.468	0.418	0.457	0.535	0.672	1.039
0.785	0.680	0.608	0.666	0.779	0.980	1.515
0.963	0.834	0.746	0.816	0.955	1.200	1.855
1.155	1.000	0.895	0.968	1.132	1.423	2.199
1.399	1.212	1.084	1.182	1.382	1.738	2.686
1.821	1.577	1.410	1.533	1.793	2.255	3.485

(b) STREAMLINES ABOVE CENTER-LINE

STREAMLINE PARAMETERS

TF = 0.50083190 TB = 0.49948782 TL = 0.49948782 XO = 0.31248027

```
     GAMMA =          2.50000000
GAMMA =          0.86653042
  126
GAMMA =          1.15571308
  120
GAMMA =          1.13208771
  109
GAMMA =          1.07725239
   97
GAMMA =          1.12177372
   80
GAMMA =          1.22035503
   60

NEW VALUE OF GAMMA =          1.09561825
GAMMA =          0.86574781
  126
GAMMA =          1.15118217
  120
GAMMA =          1.12202644
  109
GAMMA =          1.05829620
   97
GAMMA =          1.07476425
   80
GAMMA =          1.08933163
   60

NEW VALUE OF GAMMA =          1.06022453
GAMMA =          0.86568201
  126
GAMMA =          1.15080357
  120
GAMMA =          1.12119293
  109
GAMMA =          1.05674839
   97
GAMMA =          1.07107830
   80
GAMMA =          1.08015060
```

```
 60
NEW VALUF OF GAMMA =          1.05760860
                    1
126
                    2
120
                    3
109
                    4
 97
                    5
 80
                    6
 60
NEW VALUE OF GAMMA =          0.0
```

VELOCITY PROFILE IN REGION V AT Z= 2 IN.

R	VZ	VR	V
4.965	98.772	18.597	100.507
4.607	54.112	14.082	55.915
4.327	29.664	9.074	31.021
4.039	15.973	5.441	16.875
3.548	7.751	2.820	8.248
2.961	3.495	1.107	3.666

VELOCITY PROFILE IN REGION V AT Z= 3 IN.

4.795	67.763	10.503	68.573
4.371	38.318	8.306	39.208
4.048	21.697	5.614	22.411
3.723	12.160	3.591	12.679
3.195	6.408	2.178	6.768
2.609	3.256	1.182	3.464

VELOCITY PROFILE IN REGION V AT Z= 4 IN.

4.652	51.549	6.947	52.015
4.169	29.598	5.607	30.125
3.806	17.017	3.871	17.452
3.446	9.715	2.544	10.042
2.872	5.309	1.636	5.555
2.255	2.833	0.975	2.996

STREAM FUNCTION MATRIX

2.500	2.500	2.500	2.500	2.500	2.500	2.500
5.000	5.000	5.000	5.000	5.000	5.000	5.000
7.500	7.500	7.500	7.500	7.500	7.500	7.500
10.000	10.000	10.000	10.000	10.000	10.000	10.000
12.500	12.500	12.500	12.500	12.500	12.500	12.500
15.000	15.000	15.000	15.000	15.000	15.000	15.000

CORESPONDING RADIAL MATRIX

0.541	0.469	0.419	0.383	0.388	0.434	0.501
0.786	0.681	0.609	0.556	0.566	0.633	0.730
0.965	0.835	0.747	0.682	0.693	0.775	0.895
1.157	1.002	0.896	0.818	0.823	0.920	1.062
1.401	1.213	1.085	0.991	1.004	1.122	1.296
1.823	1.579	1.412	1.289	1.303	1.456	1.682

APPENDIX F

LISTING AND DESCRIPTION OF COMPUTER PROGRAMS

This Appendix contains a listing of all the programs used in Chapter IV. The listing consists of the FORTRAN IV source list compatible with a IBM 360/65 computer. At the end of the source list is given sets of imput data read into the program and a sample output. Each set of data is for one pass through the program and is in the order called for by the source list. For example in list F-1 is presented the program FLOWANL. Two types of initial input data is shown for two modes of operation. Next is given data sets at constant impeller speed. Each data set contains a number of velocity profiles all taken at the same impeller speed.

In presenting the source list, subroutines are sometimes used in more than one program. In such cases, the listing of the subroutines is given only in the first program that it appears. The subroutine CURVEF performs a polynomial fit and is obtained from the LSU Computer Center Share Library. A similar program is assumed readily available (see for example IBM Scientific Subroutine Package) and is hence not listed.

A flow diagram of the flow of information in the computer is also provided were it is considered necessary. In other programs the comment cards in the listing are descriptive of the calculations performed, hence flow diagrams were not needed. The flow diagrams are closely associated with the comment cards that are liberally

distributed throughout the program. In the listing, only those statements with the first four letters of the program name followed by a serial number are a part of the program. Other statements are there to help make the listing more readable.

Program FLOWANL: This program is given in List F-1 and the flow diagram in Figure F-1. The program output is in two modes (a) To obtain a detail printout of complete profile analysis, and to print out a summary of the important pieces of information of all profiles run at constant impeller speed (b) To printout only the summary of the profile analysis at constant impeller speed.

FLOWANL reads in the raw data, converts this data into $\bar{q}$ versus z, (where z = 0 is the impeller centerline), performs a nonlinear least square fit on $\bar{q}$ using the Tangential jet model and prints the result in desired format. The nonlinear fit is done by pattern search program subroutine PATTERN, with its supporting subroutines PROC and BOUNDS. The flow diagram and theoretical treatment of subroutine PATTERN is given in Appendix C. The flow diagram for FLOWANL is given in Figure F-1.

In Figure F-2 is given the flow diagram for subroutine YAW, which analyses the information from manometer D. The flow diagram is a direct application of Equations IV-31, IV-32 and IV-28(b). Subroutine BOUNDS is self explanatory. Subroutine PROC is again straight forward although it might appear complex. It calculates a criteria for minimization which is Equation C-2. It has two additional features (1) Allows keeping σ and a constant though the variable P1 whose value is controlled by FLOWANL (2) Gives a printout if desired of every 30th evaluation of the criteria function. The

second feature permits following the search procedure as it proceeds to locate the minimum of the sum of squares.

Subroutine OMEGA is a Lagrange interpolation Program. It was obtained from the Share Library; a listing is given since one was available. A flow diagram will not be given as this is a library program and not written by the author. The program is designed to handle unequal step size and the number of points desired for interpolation is specified by NPTS. In the present case NPTS = 3, resulting in the three closest points being used for interpolation. It was found that use of this program is equivalent to drawing a smooth curve through the data and interpolating with the help of this curve.

The flow diagram for subroutine AVG is given in Table F-3. The subroutine is designed to take a one dimensional array and calculate an average value and variance. From the variance it calculates a 0.96 confidence limit for the average using a t-test.

Program VELPRO. This program calculates velocity profiles from the theoretical model in Regions II and III as explained in Section 4. Figure F-4 gives the flow diagram for VELPRO. Supportin subroutines are POLY and CURVEF. Subroutine POLY is a service program that was written to throw out points whose diviation from the regression line is larger than three times the standard error. This has no effect on the imput data to VELPRO, since the data correlates very well. It calls LSU Share Library program CURVEF that performs the polynomial fit and prints out detail results useful in debugging.

Program TANLANL and YAWANL. Programs TANKANL and YAWANL calculate the component velocities $\bar{v}_r$, $\bar{v}_\theta$, and $\bar{v}_z$ from the manometer readings recorded by the three dimensional pitot tube. The resulting analysis of the data it is recalled, is dependent on the flow geometry. The flow diagram is identical for both programs. The difference lies in the final equations used to calculate $\bar{v}_r$, $\bar{v}_z$, and $\bar{v}_\theta$. TANKANL computes component velocities from data obtained from Ports 1, 2, 3. YAWANL analyses data obtained in the neighborhood of the impeller.

Program COOPER and NIELCUT. Program COOPER analyses Cooper's (8) data, while Program NIELCUT analyses Nielson's (21) and Cutter's (9) data. The flow diagram is identical to FLOWANL hence no flow diagram is given. The difference lies in reading th input data and initial calculation of $\bar{q} = f(z)$. In the case of NIELCUT the least square anlysis is performed on $\bar{v}_r = f(z)$. This causes a change in the criteria function hence subroutine PROC is different and was rewritten. The comment statements in the program closely follows the flow diagram of Figure F-1 and notes the differences as they occur.

Program GRAPH. This program correlates the parameters of the tangential jet model. The main program is mainly data processing. Provision exists for getting correlations at constant impeller diameter or lumping all the data together. The regression is done by subroutine SOLVE. Subroutine SOLVE is designed to obtain three types of plots.

(1) Log-log

(2) Semilog

(3) Rectangular

No flow diagram is given for GRAPH or SOLVE since the program

is not complicated and is mainly used for processing the data. The reason for including a listing is to serve as a sample calculation so that the results quoted could be checked if desired.

The following log-log correlations are obtained from GRAPH, and quoted in Chapter IV

(1) ND^3 versus A

(2) $ND^3 / ((D/2)^2 - a^2)^{\frac{1}{4}}$ versus A

(3) N_{Re} versus A

(4) ND^3 versus Q

(5) N_{Re} versus Q

Program RESULT: Like Program GRAPH, RESULT processes data. It calculates experimental and calculated values of impeller discharge Q and eddy viscosity ϵ. Again a listing is given to serve as sample calculations.

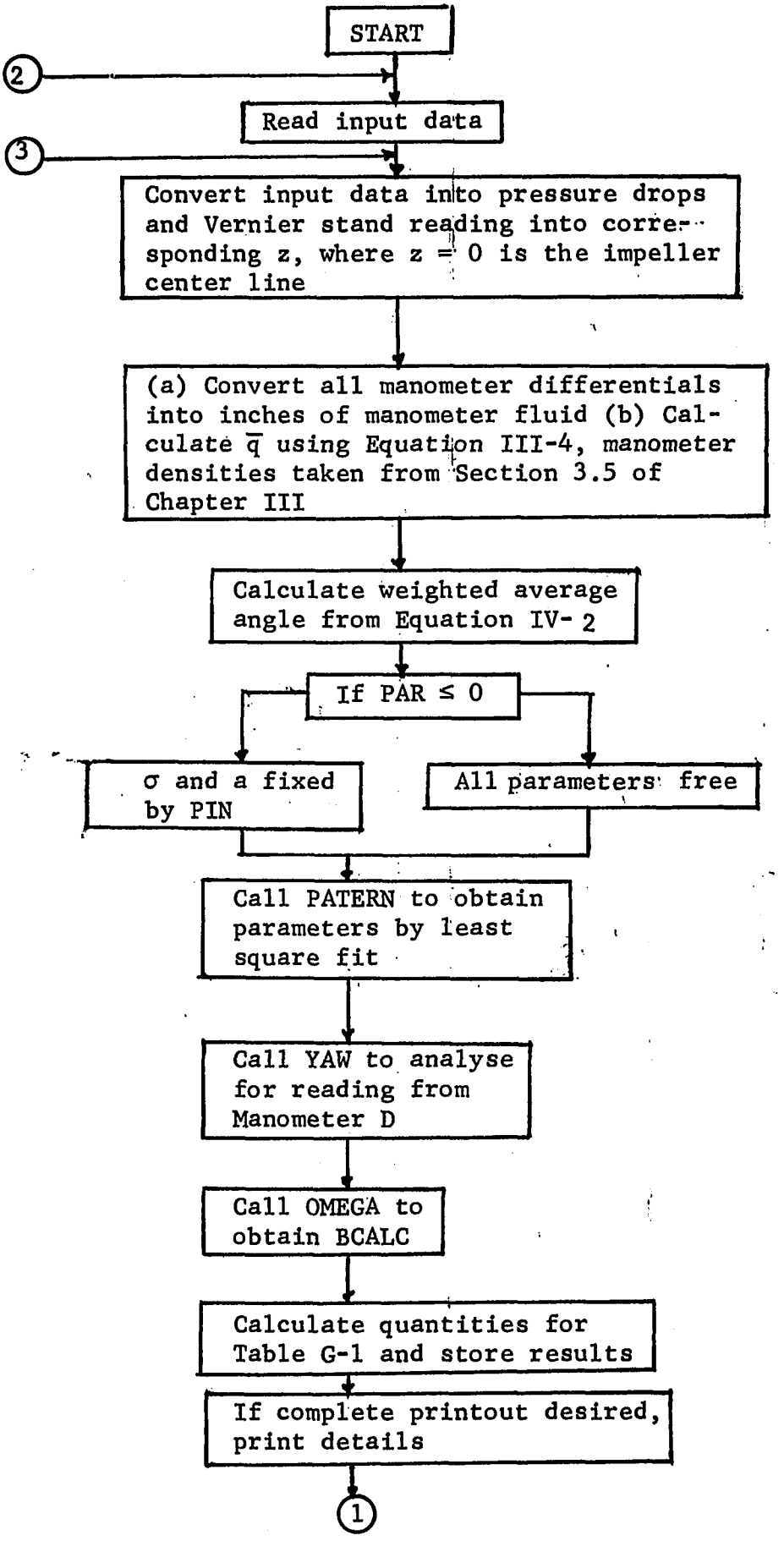
START
2
Read input data
3
Convert input data into pressure drops and Vernier stand reading into corresponding z, where z = 0 is the impeller center line
(a) Convert all manometer differentials into inches of manometer fluid (b) Calculate $\overline{q}$ using Equation III-4, manometer densities taken from Section 3.5 of Chapter III
Calculate weighted average angle from Equation IV-2
If PAR ≤ 0
σ and a fixed by PIN
All parameters free
Call PATERN to obtain parameters by least square fit
Call YAW to analyse for reading from Manometer D
Call OMEGA to obtain BCALC
Calculate quantities for Table G-1 and store results
If complete printout desired, print details
1

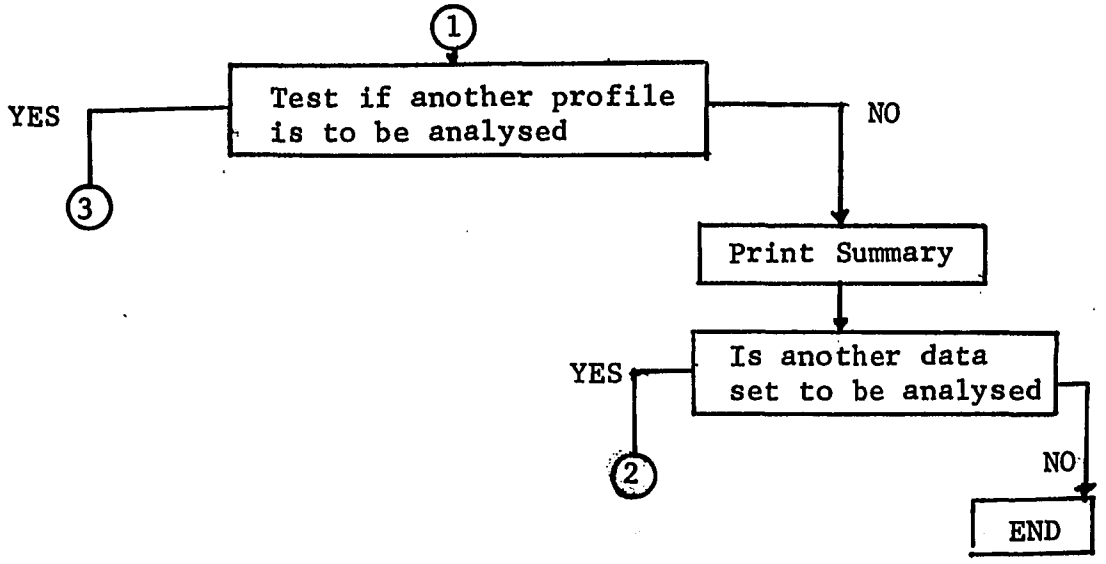

Figure F-1. Flow Diagram For Program FLOWANL.

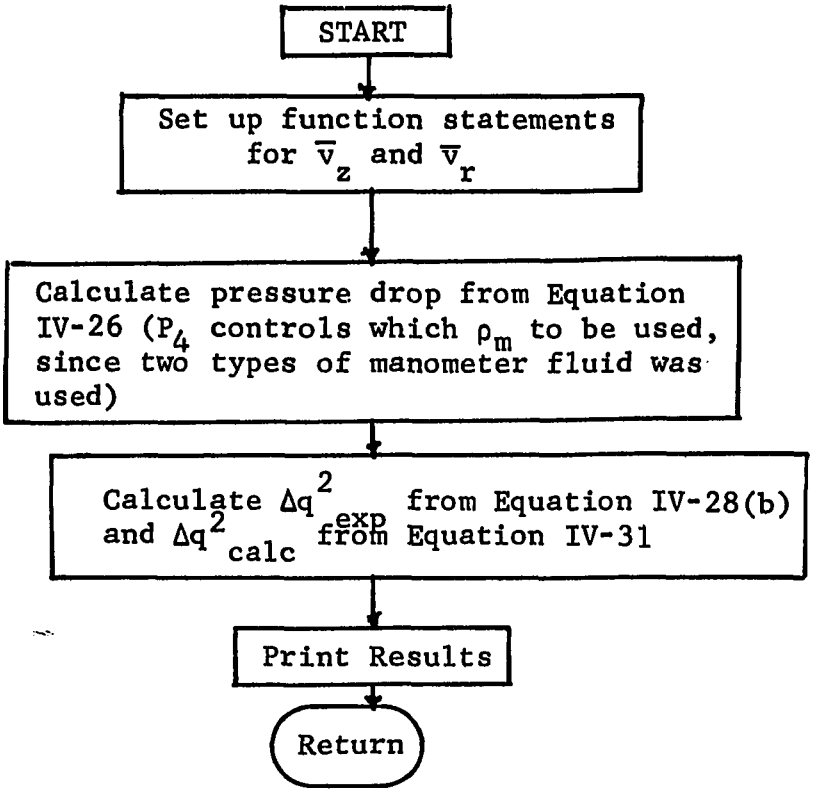

Figure F-2. Flow Diagram For Program YAW.

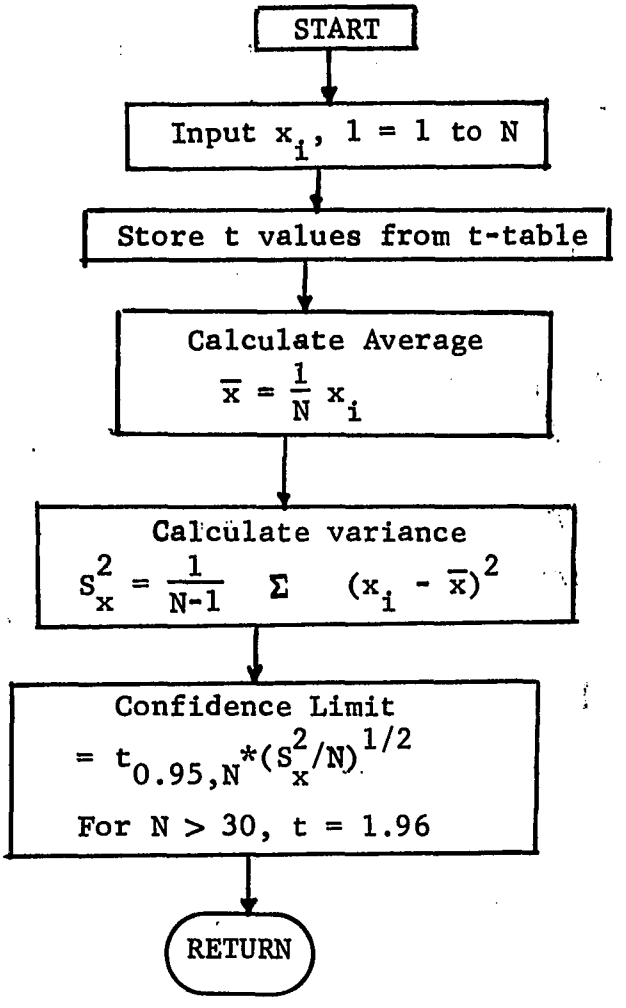

Figure F-3. Flow Diagram for Subroutine AVG.

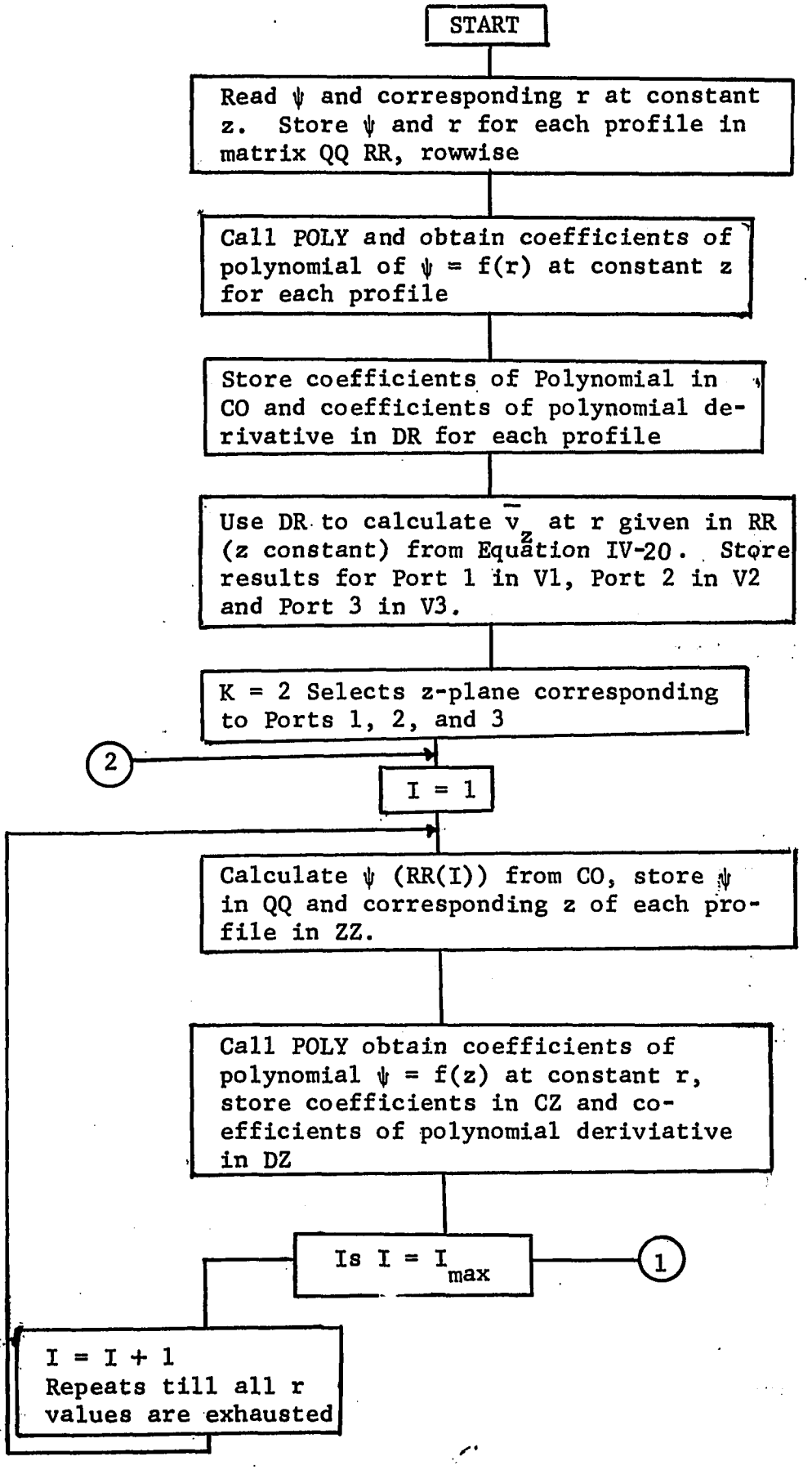
START
Read ψ and corresponding r at constant z. Store ψ and r for each profile in matrix QQ RR, rowwise
Call POLY and obtain coefficients of polynomial of ψ = f(r) at constant z for each profile
Store coefficients of Polynomial in CO and coefficients of polynomial derivative in DR for each profile
Use DR to calculate $\bar{v}_z$ at r given in RR (z constant) from Equation IV-20. Store results for Port 1 in V1, Port 2 in V2 and Port 3 in V3.
K = 2 Selects z-plane corresponding to Ports 1, 2, and 3
2
I = 1
Calculate ψ (RR(I)) from CO, store ψ in QQ and corresponding z of each profile in ZZ.
Call POLY obtain coefficients of polynomial ψ = f(z) at constant r, store coefficients in CZ and coefficients of polynomial deriviative in DZ
Is I = I_{max}
1
I = I + 1
Repeats till all r values are exhausted

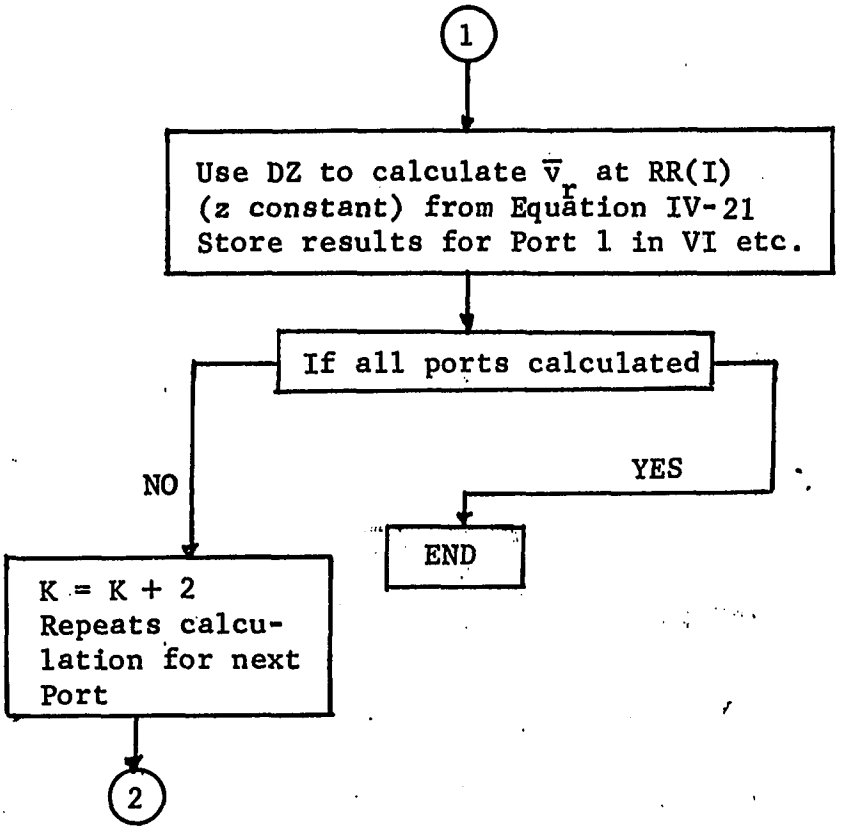

Figure F-4. Flow Diagram For Program VELPRO.

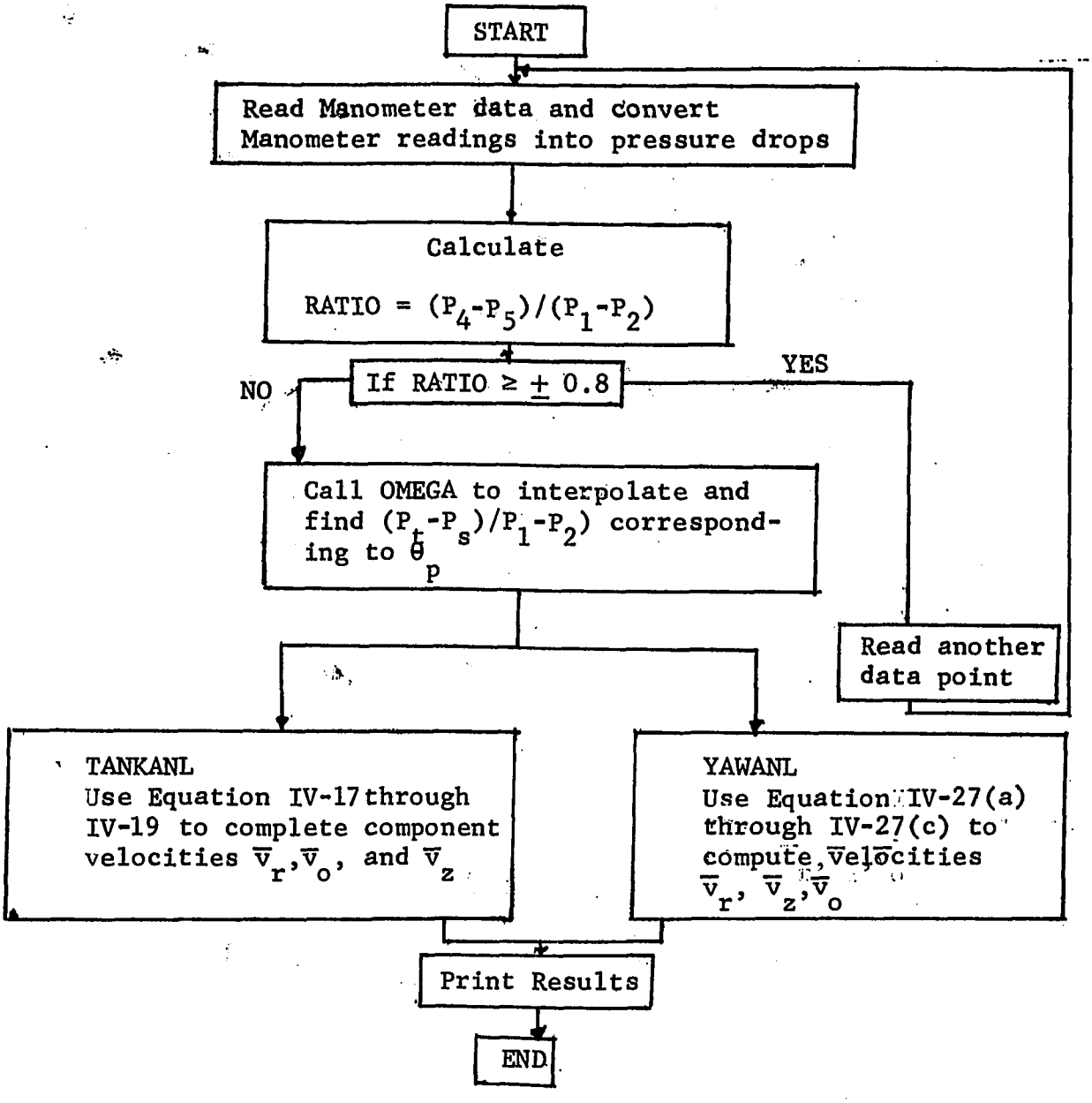

Figure F-5: Flow Diagram for Program TANKANL and YAWANL

LIST F-1

FORTRAN LISTING PROGRAM FLOWANL WITH SUPPORTING SUBROUTINES YAW, AVG, PROC, BOUNDS, OMEGA AND PATERN. THIS LISTING ALSO GIVES RAW DATA WHICH IS THE INPUT TO THE PROGRAM AND A DETAILED SAMPLE OUTPUT FOR RUN NUMBER 29.

MAIN PROGRAM FLOWANL

```
**************************************************************************************

$$$$$$$$$$$$$$$$$$$$$$$$$$$$$$$$$$$$$$$$$$$$$$$$$$$$$$$$$$$$$$$$$$$$$$$$$$$$$$$$$$$
C                                                                                FLOW    1
C--------KK = 0, GIVES PRINT AT EVERY 30TH POINT FROM SUBROUTINE PROC              FLOW    2
C        KK .GT. 30, NO PRINT FROM SUBROUTINE PROC                               FLOW    3
C        LPRINT= 1, SKIPS PRINT FOR INDIVIDUAL PROFILES                          FLOW    4
C        ANY OTHER VALUE GIVES COMPLETE PRINT                                    FLOW    5
C        KVR= 0, PRINTS RADIAL VELOCITY PROFILE ANALYSIS                         FLOW    6
C        PAR .GT. 0, SIGMA AND AA FIXED BY PIN(I)                                FLOW    7
C        PAR .LE. 0 ALL PARAMETERS FREE                                          FLOW    8
C        DX - THE DISTANCE BETWEEN MANOMETER HOLES P4 AND P5                     FLOW    9
C        RHOM= DENSITY CORRECTION FACTOR FOR OBTAINING VELOCITY FROM             FLOW   10
C              MANOMETER READING                                                 FLOW   11
C                                                                                FLOW   12
      DIMENSIONX(20),Y(20),YC(20),P(6),STEP(6),PIN(6),YR(20),PH(50)              FLOW   13
      DIMENSIONXR(20),SIGMA(20),A(20),AA(20),SQ(20),GF(20),Q(20)                 FLOW   14
      DIMENSIONT(15,15),ANG(20),PA(50),PB(50),PC(50),PD(50),PE(50)               FLOW   15
      DIMENSION RPM(50),DA(3),D(50,50),PF(50),QI(20),XNG(20),PG(50)              FLOW   16
      COMMONDIA,X,Y,YC,XX,N,KK,P1,P2,P3,P4                                       FLOW   17
      READ(5,42)LPRINT,KK,KVR,DX,PAR,WT,RHOM                                     FLOW   18
42    FORMAT(3I2,5F10.2)                                                         FLOW   19
      DX=DX/12.                                                                  FLOW   20
C                                                                                FLOW   21
C--------READ INITIAL VALUES OF PARAMETER AND STEP SIZE                          FLOW   22
C        PIN STORES INITIAL VALUES OF PARAMETER FOR ANALYSIS OF MULTIPLE         FLOW   23
C        FLOW PROFILES                                                           FLOW   24
C        KGROUP  .LT. 5 REPEATS THE PROGRAM FOR A NOTHER DATA SET                FLOW   25
C        K .LT. 5 REPEATS PROGRAM FOR ANOTHER PROFILE WHICH IS A                 FLOW   26
C                 PART OF A DATA SET                                             FLOW   27
C        NP= NO OF FREE PARAMETERS                                               FLOW   28
C        N= NO OF DATA POINTS IN A FLOW PROFILE                                  FLOW   29
C        DA= DATE ON WHICH FLOW PROFILE DATA WAS TAKEN                           FLOW   30
C        FAC= 1, MANOMETER B AND READINGS ARE IN INCHES                          FLOW   31
C        FAC= 2.54, MANOMETER B AND D READINGS ARE IN CMS                        FLOW   32
C                                                                                FLOW   33
      READ(5,16)(PIN(I),STEP(I),I=1,4)                                           FLOW   34
16    FORMAT(2F10.2)                                                             FLOW   35
```

```
70    READ(5,15)KGROUP                                                    FLOW  36
      M=0                                                                 FLOW  37
7     READ(5,15)K,NP                                                      FLOW  38
15    FORMAT(2I2)                                                         FLOW  39
      DO47I=1,NP                                                          FLOW  40
47    P(I)=PIN(I)                                                         FLOW  41
      READ(5,100)N,DA,FAC                                                 FLOW  42
100   FORMAT(I2,3A4,F10.2)                                                FLOW  43
      READ(5,102)L,(D(1,J),J=1,10)                                        FLOW  44
102   FORMAT(I7,10F7.2)                                                   FLOW  45
C                                                                         FLOW  46
C--------PRINT RAW DATA FOR A PROFILE                                     FLOW  47
C                                                                         FLOW  48
      IF(LPRINT.EQ.1)GOTO48                                               FLOW  49
      WRITE(6,101)DA                                                      FLOW  50
101   FORMAT(1H1,30X,8HRAW DATA,   10X,3A4,///)                           FLOW  51
      WRITE(6,103) L,(D(1,J),J=1,10)                                      FLOW  52
103   FORMAT(21X,10HRUN NUMBER,29X,1H=,I2/1HO,20X,8HIMPELLER,             FLOW  53
     19H DIAMETER,22X,1H=,F5.2/1HO,20X,30HIMPELLER HT OF TANK BOTTOM      FLOW  54
     2,9X,1H=,F5.2/1HO,20X,22HLEVEL OF WATER IN TANK,17X,1H=,F5.2/1HO,    FLOW  55
     320X,36HHEIGHT OF PITOT TUBE OFF TANK BOTTOM,3X,1H=,F5.2/1HO,20X,    FLOW  56
     4'VERNIER STAND READING',19X,'=',F5.2/1HO,20X,'ZERO ERROR FOR ',     FLOW  57
     5'ANGLE'19X,'=',F5.2/1HO,20X,'DIST PROBE TO AXIS',T61,'=',F5.2/      FLOW  58
     61HO,20X,'RPM SETTING',T61,'=',F6.2/1HO,20X,'FLUID TEMP',T61,'=',    FLOW  59
     7F5.2,'  DEG F'/1HO,20X,'ANGULAR POSITION FROM BAFFLE',T61,'=',      FLOW  60
     8F5.2,'  DEG'///)                                                    FLOW  61
48    XD=D(1,7)                                                           FLOW  62
      DD=D(1,1)                                                           FLOW  63
      DIA=DD/12.                                                          FLOW  64
      XX=XD/12.                                                           FLOW  65
      ANGPO=D(1,10)                                                       FLOW  66
C                                                                         FLOW  67
C--------CANGLE= CORRECTION FACTOR FOR OBTAINING TRUE ANGLE              FLOW  68
C        REFL= CORRECTION FACTOR FOR OBTAINING Z COORDINATE               FLOW  69
C        ANGPO= RADIAL ANGLE WITH RESPECT TO BAFFLE AT WHICH PROFILE      FLOW  70
C               WAS MEASURED                                              FLOW  71
C                                                                         FLOW  72
      CANGLE=D(1,6)                                                       FLOW  73
      REFL=D(1,5)+D(1,4)-D(1,2)                                           FLOW  74
      REV=D(1,8)                                                          FLOW  75
      READ(5,104)((D(I,J),J=1,10),I=1,N)                                  FLOW  76
104   FORMAT(10F7.2)                                                      FLOW  77
      IF(LPRINT.EQ.1)GOTO49                                               FLOW  78
      WRITE(6,105)((D(I,J),J=1,10),I=1,N)                                 FLOW  79
105   FORMAT(24X,11HP(1)-P(ATM),5X,9HP(1)-P(2),4X,9HP(2)-P(3),3X,         FLOW  80
     19HP(4)-P(5),5X,1HH,4X,5HANGLE,/ 24X,11HLEFT  RIGHT,4X,              FLOW  81
     211HLEFT  RIGHT ,2X,10HLEFT RIGHT,3X,10HLEFT RIGHT,///              FLOW  82
     3(20X,2F7.2,F8.2,F7.2,1X,2F5.2,4F7.2))                              FLOW  83
C                                                                         FLOW  84
C--------CALCULATE Y(I) IN FT/MIN FORM EQUATION III-3                    FLOW  85
C        CALCULATE X(I),FT                                                FLOW  86
C        NOTE, X,Y ARE DUMMY NAMES FOR Z AND Q                            FLOW  87
C        CONVERT ALL MANOMETER READINGS TO INCHES OF MANOMETER FLUID      FLOW  88
```

```
C                                                                       FLOW  89
49    DO106I=1,N                                                        FLOW  90
      X(I)=(REFL-D(I,9))/12.                                            FLOW  91
      D(I,10)=D(I,10)-CANGLE                                            FLOW  92
      DELZ=D(I,4)-D(I,3)                                                FLOW  93
      IF(FAC.EQ.1.)GOTO106                                              FLOW  94
      DELZ=DELZ/FAC                                                     FLOW  95
      D(I,3)=D(I,3)/FAC                                                 FLOW  96
      D(I,4)=D(I,4)/FAC                                                 FLOW  97
      D(I,7)=D(I,7)/FAC                                                 FLOW  98
      D(I,8)=D(I,8)/FAC                                                 FLOW  99
106   Y(I)=SQRT(2.*32.174*DELZ* RHOM /12.)*60.                          FLOW 100
C                                                                       FLOW 101
C--------CALCULATE WEIGHTED AVERAGE ANGLE AND AVERAGE ANGLE            FLOW 102
C         WT= RATIO OF VELOCITIES FOR WHICH WEIGHT IS ZERO,             FLOW 103
C             CHOSEN AS 0.7                                             FLOW 104
C         YM= AVERAGE VALUE OF Y                                        FLOW 105
C                                                                       FLOW 106
      YM=0.                                                             FLOW 107
      ANGLE=0.                                                          FLOW 108
      NK=N/2                                                            FLOW 109
      ANGL=0.                                                           FLOW 110
      YMM=0.                                                            FLOW 111
      M=M+1                                                             FLOW 112
      DO22I=1,N                                                         FLOW 113
      IF((Y(I)/Y(NK)).LT.WT )GOTO34                                     FLOW 114
      ANGL=ANGL+D(I,10)*Y(I)                                            FLOW 115
      YMM=YMM+Y(I)                                                      FLOW 116
34    ANGLE=ANGLE+D(I,10)                                               FLOW 117
22    YM=YM+Y(I)                                                        FLOW 118
      ANGLE=ANGLE/FLOAT(N)                                              FLOW 119
      YM=YM/FLOAT(N)                                                    FLOW 120
      ANGL=ANGL/YMM                                                     FLOW 121
C                                                                       FLOW 122
C--------LOGIC BRANCH FOR ONE DIMENSIONAL SEARCH ON PARAMETER P(2)      FLOW 123
C         OTHER PARAMETERS FIXED THROUGH PIN                            FLOW 124
C                                                                       FLOW 125
      IF(PAR)51,51,52                                                   FLOW 126
52    P1=PIN(1)                                                         FLOW 127
      P2=PIN(2)                                                         FLOW 128
      P3=PIN(3)                                                         FLOW 129
      P4=PIN(4)                                                         FLOW 130
      GOTO53                                                            FLOW 131
51    P1=0.                                                             FLOW 132
      P3=    XX*SIN(ANGL *3.1416/180.)                                  FLOW 133
      IF(P3.GT.(DIA/2.))GOTO60                                          FLOW 134
C                                                                       FLOW 135
C--------CALCULATE SUM OF SQUARES ABOUT MEAN                           FLOW 136
C                                                                       FLOW 137
53    SSM=0.                                                            FLOW 138
      DO12I=1,N                                                         FLOW 139
12    SSM=SSM+(Y(I)-YM)**2                                              FLOW 140
      B=0.                                                              FLOW 141
```

```
29    IF(KK.GT.30)GOTO46                                                FLOW 142
      KK=0                                                              FLOW 143
      WRITE(6,19)                                                       FLOW 144
19    FORMAT(1H1,6X,4HP(1), 9X,4HP(2), 9X,4HP(3), 8X,4HP(4),            FLOW 145
     18X,10HSUM SQ REG,//)                                              FLOW 146
C                                                                       FLOW 147
C---------CALL PATTERN SEARCH SUBROUTINE                                FLOW 148
C                                                                       FLOW 149
46    CALL PATERN(NP,P,STEP,4,0,COST)                                   FLOW 150
      IF(PAR)58,58,59                                                   FLOW 151
59    P(1)=P1                                                           FLOW 152
58    P(3)=P3                                                           FLOW 153
C                                                                       FLOW 154
C---------CALCULATE CORRELATION COEFFICIENT R                           FLOW 155
C         CALCULATE HALF WIDTH OF JET BHALF                             FLOW 156
C         CALCULATE VELOCITY AT BHALF, UHALF                            FLOW 157
C         CALL OMEGA TO FIND HALF WIDTH CORRESPONDING TO UHALF BY THREE FLOW 158
C         POINT LAGRANGE INTERPOLATION                                  FLOW 159
C         CORRECT FOR DISPLACEMENT OF ORIGIN BY SUBRACTING P(4)         FLOW 160
C                                                                       FLOW 161
      R=SQRT(1.-COST/SSM)                                               FLOW 162
      BHALF=1.762747*XX/P(1)                                            FLOW 163
      IF(B.EQ.0.)B=BHALF                                                FLOW 164
      UHALF=P(2)*SQRT(P(1)/XX)/((XX**2-P(3)**2)**0.25*4.)               FLOW 165
      CALL OMEGA(UHALF,Y,X,N,25,BCALC)                                  FLOW 166
      BCALC=BCALC-P(4)                                                  FLOW 167
      BXX=6.*XX/P(1)*12.                                                FLOW 168
      IF(LPRINT.EQ.1)GOTO30                                             FLOW 169
C                                                                       FLOW 170
C---------PRINT COMPLETE ANALYSIS OF A PROFILE                          FLOW 171
C                                                                       FLOW 172
      WRITE(6,18)DD,XD                                                  FLOW 173
18    FORMAT(1H1,20X,4HD  =,F10.5,/1H0,20X,4HR  =,F10.5,/)              FLOW 174
      WRITE(6,2)(X(I),Y(I),D(I,10),I=1,N)                               FLOW 175
2     FORMAT(1H0,27X,1HZ,8X,1HQ,6X,5HANGLE/(20X,3F10.5))                FLOW 176
      WRITE(6,17)(I,P(I),I=1,NP)                                        FLOW 177
17    FORMAT(1H0,30X10HPARAMETERS,/(    20X,I2,F20.8))                  FLOW 178
      WRITE(6,25)ANGLE,ANGL,WT                                          FLOW 179
25    FORMAT(1X,//20X,'AVG ANGLE   =',F15.8/20X,'WT AVG ANGLE=',F15.8,  FLOW 180
     15X,'VELOCITY FACTOR=',F5.2)                                       FLOW 181
      WRITE(6,13)(Y(I),YC(I),I=1,N)                                     FLOW 182
13    FORMAT(1H0,32X,1HQ,19X,2HQC/(20X,2F20.8))                         FLOW 183
      WRITE(6,14)COST,R                                                 FLOW 184
14    FORMAT(1H0,20X,27HSUM OF SQUARES OF (Q-QCALC),F20.8,/1H0,20X,     FLOW 185
     127HGOODNESS OF FIT              ,F20.8)                           FLOW 186
      WRITE(6,31)BHALF,BCALC,UHALF                                      FLOW 187
31    FORMAT(1H0,20X,7HBHALF =,F20.8,10X,7HBCALC =,F20.8,/1H0,30X,      FLOW 188
     17HUHALF =,F20.8)                                                  FLOW 189
      WRITE(6,41)XD,BXX                                                 FLOW 190
41    FORMAT(1H0,20X,25HHALF WIDTH OF JET AT XD =,F4.2,1H,,4X,F10.2,     FLOW 191
     12X,6HINCHES,//)                                                  FLOW 192
C                                                                       FLOW 193
C---------STORE IMPORTANT RESULTS OF A PROFILE ANALYSIS FOR SUMMARY     FLOW 194
```

```
C                                                                       FLOW 195
30      ANG(M)=SQRT(XX**2-P(3)**2)/XX                                   FLOW 196
        PA(M)=ARCOS(ANG(M))*180./3.1416                                 FLOW 197
33      Q(M)=4.*3.1416*P(2)*(XX**2-P(3)**2)**0.25*SQRT(XX/P(1))         FLOW 198
        XR(M)=XD                                                        FLOW 199
        SIGMA(M)=P(1)                                                   FLOW 200
        A(M)=P(2)                                                       FLOW 201
        AA(M)=P(3)                                                      FLOW 202
        SQ(M)=COST                                                      FLOW 203
        GE(M)=R                                                         FLOW 204
        PB(M)=P(4)                                                      FLOW 205
        PC(M)=BHALF                                                     FLOW 206
        RPM(M)=REV*DIA**3                                               FLOW 207
        PD(M)=BCALC                                                     FLOW 208
        PE(M)=ANGLE                                                     FLOW 209
        PF(M)=UHALF                                                     FLOW 210
        XNG(M)=ANGPO                                                    FLOW 211
        XT=DIA/2.                                                       FLOW 212
        TEMP=4.*3.1416*P(2)*(XT**2-P(3)**2)**0.25*SQRT(XT/P(1))         FLOW 213
        QI(M)=TEMP                                                      FLOW 214
        P4=K                                                            FLOW 215
C                                                                       FLOW 216
C--------CALL YAW TO ANALYSE FOR DATA FROM MANOMETER D                  FLOW 217
C                                                                       FLOW 218
        IF(LPRINT.EQ.1)GOTO62                                           FLOW 219
        CALL YAW(D,P,DX)                                                FLOW 220
C                                                                       FLOW 221
C--------ANALYSE DIFFERENCE IN CALCULATED AND TRUE RADIAL VELOCITY       FLOW 222
C                                                                       FLOW 223
62      VRMAX=P(2)/2.*SQRT(P(1)/XX**3)*(XX**2-P(3)**2)**0.25            FLOW 224
        TEMP=P(1)/(2.*XX)                                               FLOW 225
        DO63I=1,N                                                       FLOW 226
        ALP=D(I,10)*3.1416/180.                                         FLOW 227
        Y(I)=Y(I)*COS(ALP)                                              FLOW 228
63      YR(I)=VRMAX*(1.-(TANH(TEMP*(X(I)-P(4))))**2)                    FLOW 229
        CALL AVG(Y ,N,YM ,BR,BB)                                        FLOW 230
        SSM=0.                                                          FLOW 231
        SSR=0.                                                          FLOW 232
        DO64I=1,N                                                       FLOW 233
        SSR=SSR+(YR(I)-Y(I))**2                                         FLOW 234
64      SSM=SSM+(Y(I)-YM)**2                                            FLOW 235
        COST=SSR                                                        FLOW 236
        IF(SSR.GT.SSM)GOTO68                                            FLOW 237
        R=SQRT(1.-SSR/SSM)                                              FLOW 238
        GOTO69                                                          FLOW 239
68      R=0.                                                            FLOW 240
        WRITE(6,67)SSR,SSM                                              FLOW 241
67      FORMAT(1HO,20X,'SSR =',F15.8/20X,'SSM =',F15.8/)                FLOW 242
69      PG(M)=R                                                         FLOW 243
        PH(M)=SSR                                                       FLOW 244
        IF(KVR.EQ.1)GOTO44                                              FLOW 245
        WRITE(6,65)                                                     FLOW 246
65      FORMAT(1H1,/////,30X,'RADIAL VELOCITY ANALYSIS'//)              FLOW 247
```

```
      WRITE(6,13)(Y(I),YR(I),I=1,N)                                          FLOW 248
      WRITE(6,14)COST,R                                                      FLOW 249
      GOTO44                                                                 FLOW 250
C                                                                            FLOW 251
C--------PRINTOUT, WHEN P(3) DID NOT SATISFY CONSTRAINTS                     FLOW 252
C                                                                            FLOW 253
60    WRITE(6,18)DD,XD                                                       FLOW 254
      WRITE(6,2)(X(I),Y(I),D(I,10),I=1,N)                                    FLOW 255
      WRITE(6,61)P3                                                          FLOW 256
61    FORMAT(1HO,'AA IS GT D/2, AA =',F15.8)                                 FLOW 257
44    IF(K.LT.5)GOTO7                                                        FLOW 258
C                                                                            FLOW 259
C--------PRINT SUMMARY OF A SET OF PROFILES                                  FLOW 260
C                                                                            FLOW 261
23    WRITE(6,20)(N,XNG(N),XR(N),SIGMA(N),A(N),AA(N),SQ(N),PH(N),GF(N),      FLOW 262
     1PG(N),N=1,M)                                                           FLOW 263
20    FORMAT(1H1,25X,'RADIAL ', 6HRADIUS,2X,5HSIGMA,6X,1HA, 7X,2HAA,11X,FLOW 264
     1'SUM SQ', 8X,'CORR COEF',/22X,'NO  ANGLE',40X,'Q',8X,'VR',7X,'O',     FLOW 265
     25X,'VR',//(22X,I2,1X,2F6.2,2F9.3,F9.4,2F10.2,1X,2F7.4))               FLOW 266
      WRITE(6,21)(N,QI(N),Q(N),ANG(N),PA(N),PB(N),N=1,M)                     FLOW 267
21    FORMAT(1X,// 20X,'  NO'  ,4X,7HCFM IMP, 4X,3HCFM, 5X8HCOS(PHI),3X,FLOW 268
     15HANGLE,10X,4HP(4),// (22X,I2,4F10.4,F15.8))                          FLOW 269
      WRITE(6,40)(I,PE(I),PC(I),PD(I),PF(I),RPM(I),I=1,M)                    FLOW 270
40    FORMAT(1X,// 20X,'  NO'  ,4X,5HUHALF, 6X,5HBHALF, 6X,5HBCALC,         FLOW 271
     1 2X,9HAVG ANGLE,3X,5HND**3,// (22X,I2,F9.2,2F11.4,F9.2,F10.3))        FLOW 272
C                                                                            FLOW 273
C--------CALL AVG, TO OBTAIN AVERAGE, VARIANCE AND DEVIATION               FLOW 274
C        DEVIATION CALCULATED USING 'T-TEST', WITH 0.95 PROBABILITY         FLOW 275
C                                                                            FLOW 276
      CALL AVG(A,M,AAVG,SQD,VARAA)                                           FLOW 277
      WRITE(6,50)AAVG,SQD,VARAA                                              FLOW 278
      IF(PAR.GT.0.)GOTO80                                                    FLOW 279
50    FORMAT(1X//1HO,37X,'AVERAGE',8X,'VARIANCE',6X,'DEVIATION',/            FLOW 280
     1/25X,'A',4X,2F15.4,F13.3)                                              FLOW 281
      CALL AVG(SIGMA,M,SIGM,SQSGM,VARSGM)                                    FLOW 282
      CALL AVG(AA,M,ALVG,SQAA,VARAA)                                         FLOW 283
      WRITE(6,45)SIGM,SQSGM,VARSGM,ALVG,SQAA,VARAA                           FLOW 284
45    FORMAT(25X,'SIGMA',2F15.4,F13.3/25X,'AA',3X,F15.4,F15.8,F15.5)         FLOW 285
      WRITE(6,76)WT                                                          FLOW 286
76    FORMAT(1X//,30X,'VELOCITY FACTOR=',F5.2)                               FLOW 287
C                                                                            FLOW 288
C--------CHECK IF ANOTHER DATA SET IS TO BE ANALYSED                         FLOW 289
C                                                                            FLOW 290
80    IF(KGROUP.LT.5)GOTO70                                                  FLOW 291
8     STOP                                                                   FLOW 292
      END                                                                    FLOW 293
```

****

SUBROUTINE YAW

****

```
      SUBROUTINE YAW(D,P,DX)                                                YAW    1
C                                                                           YAW    2
C--------WS AND YCAL ARE FUNCTION STATEMENTS THAT CALCULATES THE            YAW    3
C         VELOCITY COMPONENTS V(Z) AND V(R)                                 YAW    4
C         DUSQE DELTA V(R)**2 EXPERIMENTAL                                  YAW    5
C         DUSQC DELTA V(R)**2 CALCULATED, OBTAINED BY CALCULATING           YAW    6
C         TWO VALUES OF V(R) SEPARATED A DISTANCE DX APART                  YAW    7
C         DP45= CORRECTION FACTOR FOR MANOMETER D                           YAW    8
C                                                                           YAW    9
      DIMENSIONX(20),Y(20),YC(20),P(6),D(50,50),WCALC(20)                   YAW   10
      DIMENSION XDU(20),YCF(20)                                             YAW   11
      COMMONDIA,X,Y,YC,XX,N,KK,P1,P2,P3,P4                                  YAW   12
      EE(A)=P1/XX*(A-CC)                                                    YAW   13
      WS(A,B)=-P2*TT**.25/(2.*SQRT(P1/XX**3))* ((TT+XX**2)*A/TT-            YAW   14
     1B*(1.-A**2))                                                          YAW   15
      YCAL(A)=P2*SQRT(P1/XX)*(1.-A**2)/(TT**.25*2.)                         YAW   16
      P1=P(1)                                                               YAW   17
      P2=P(2)                                                               YAW   18
      CC=P(4)                                                               YAW   19
      TT=XX**2-P(3)**2                                                      YAW   20
      DP45=1./2.54                                                          YAW   21
      LPRINT=1                                                              YAW   22
      WRITE(6,5)                                                            YAW   23
5     FORMAT(1H1,////////26X,9HP(1)-P(2),3X,9HP(4)-P(5),3X,8HDEL U**2,      YAW   24
     14X,8HDEL U**2,8X,2HVZ,/52X,3HEXP, 9X,4HCALC, 8X,4HCALC,               YAW   25
     24X,'DIFF OF U**2',//)                                                 YAW   26
      IF(P4.GE.2..AND.P4.LE.9.)GOTO9                                        YAW   27
      RHOM=0.19579                                                          YAW   28
      GOTO8                                                                 YAW   29
9     RHOM=0.0953                                                           YAW   30
8     DO1I=1,N                                                              YAW   31
      DELP=D(I,4)-D(I,3)                                                    YAW   32
      DEL=D(I,7)-D(I,8)-DP45                                                YAW   33
6     TEMP=X(I)                                                             YAW   34
      ETA=EE(TEMP)                                                          YAW   35
      T=TANH(ETA/2.)                                                        YAW   36
      WCALC(I)=WS(T,ETA)                                                    YAW   37
      TEMP=X(I)-DX/2.                                                       YAW   38
      E1=EE(TEMP)                                                           YAW   39
      TA=TANH(E1/2.)                                                        YAW   40
      YCA=YCAL(TA)                                                          YAW   41
      TEMP=X(I)+DX/2.                                                       YAW   42
      E2=EE(TEMP)                                                           YAW   43
      TB=TANH(E2/2.)                                                        YAW   44
      YCB=YCAL(TB)                                                          YAW   45
      DUSQE=2.*32.174*DEL*RHOM/12.                                          YAW   46
      DUSQC=(YCB**2-YCA**2)/3600.                                           YAW   47
      CFDD=DUSQC/DUSQE                                                      YAW   48
      DUSQE=DUSQE*0.5217                                                    YAW   49
      CFD=DUSQC-DUSQE                                                       YAW   50
      IF(LPRINT.EQ.1)GOTO13                                                 YAW   51
      XDU(I)=DUSQE                                                          YAW   52
      YCF(I)=CFDD                                                           YAW   53
```

```
      CFD=CFDD                                                          YAW    54
13    WRITE(6,3)DELP,DEL,DUSOF,DUSOC,WCALC(I),CFD                       YAW    55
3     FORMAT(21X,6F12.4)                                                YAW    56
1     CONTINUE                                                          YAW    57
      IF(LPRINT.EQ.1)GOTO12                                             YAW    58
      WRITE(7,11)N                                                      YAW    59
11    FORMAT(I2)                                                        YAW    60
      WRITE(7,10)( XDU(I),YCF(I),I=1,N)                                 YAW    61
10    FORMAT(8F10.6)                                                    YAW    62
12    RETURN                                                            YAW    63
      END                                                               YAW    64
```

****

SUBROUTINE AVG

****

```
      SUBROUTINE AVG(X,N,XM,SSM,VAR,DEV)                                AVG     1
C                                                                       AVG     2
C--------T= VALUE OF TWO TAILED 'T' TEST WITH 0.95 PROBABILITY         AVG     3
C                                                                       AVG     4
      DIMENSIONX(50),T(30)                                              AVG     5
      DATA T/12.706,4.303,3.182,2.776,2.571,2.447,2.365,2.306,2.262,    AVG     6
     12.228,2.201,2.179,2.160,2.145,2.131,2.12,2.11,2.101,2.093,        AVG     7
     22.086,2.08,2.074,2.069,2.064,2.06,2.056,2.052,2.048,2.045,2.042/  AVG     8
      LPRINT=1                                                          AVG     9
      XM=0.                                                             AVG    10
      DO1I=1,N                                                          AVG    11
1     XM=XM+X(I)                                                        AVG    12
      XM=XM/FLOAT(N)                                                    AVG    13
      SSM=0.                                                            AVG    14
      IF(N.LE.1)GOTO3                                                   AVG    15
      DO2I=1,N                                                          AVG    16
2     SSM=SSM+(X(I)-XM)**2                                              AVG    17
      VAR=SSM/(FLOAT(N)-1.)                                             AVG    18
      IF(N-30)6,6,7                                                     AVG    19
6     DEV=SQRT(VAR/N)*T(N-1)                                            AVG    20
      GOTO4                                                             AVG    21
7     DEV=VAR*1.96/N                                                    AVG    22
      GOTO4                                                             AVG    23
3     VAR=0.                                                            AVG    24
      DEV=0.                                                            AVG    25
4     IF(LPRINT.EQ.1)GOTO55                                             AVG    26
      WRITE(6,5)XM,VAR,DEV                                              AVG    27
5     FORMAT(28X,3F15.8)                                                AVG    28
55    RETURN                                                            AVG    29
      END                                                               AVG    30
```

****

SUBROUTINE PROC

```
*******************************************************************************

      SUBROUTINE PROC(P,COST)                                          PROC   1
      DIMENSIONX(20),Y(20),YC(20),P(6)                                 PROC   2
      COMMONDIA,X,Y,YC,XX,N,KK,P1,P2,P3,P4                             PROC   3
      IF(P1)7,7,8                                                      PROC   4
8     P(1)=P1
7     P(3)=P3                                                          PROC   6
      COST=0.                                                          PROC   7
      DOII=1,N                                                         PROC   8
      ETA=P(1)*(X(I)-P(4))/XX                                          PROC   9
      T=1.-(TANH(ETA/2.))**2                                           PROC  10
      YC(I)=P(2)*SQRT(P(1)/XX)*T/(XX**2-P(3)**2)**0.25/2.              PROC  11
      COST=COST+(YC(I)-Y(I))**2                                        PROC  12
1     CONTINUE                                                         PROC  13
      IF(KK.GT.30)GOTO5                                                PROC  14
      IF(KK.NE.0)GOTO4                                                 PROC  15
      WRITE(6,2)P(1),P(2),P(3),P(4),COST                               PROC  16
2     FORMAT(1X,5(1PE15.7))                                            PROC  17
4     KK=KK+1                                                          PROC  18
      IF(KK.LE.30)GOTO5                                                PROC  19
      KK=0                                                             PROC  20
5     RETURN                                                           PROC  21
      END                                                              PROC  22

*******************************************************************************

                              SUBROUTINE BOUNDS

*******************************************************************************

      SUBROUTINE BOUNDS(P,I)                                           BOUN   1
      DIMENSION P(6),X(20),Y(20),YC(20)                                BOUN   2
      COMMONDIA,X,Y,YC,XX,N,KK,P1,P2,P3,P4                             BOUN   3
      D=DIA                                                            BOUN   4
      IF(P(1).LT.0.)GOTO2                                              BOUN   5
      IF(P(3).LT.(-D/2.).OR.P(3).GT.D/2.)GOTO2                         BOUN   6
      I=0                                                              BOUN   7
      GOTO3                                                            BOUN   8
2     I=1                                                              BOUN   9
3     RETURN                                                           BOUN  10
      END                                                              BOUN  11

*******************************************************************************

                              SUBROUTINE OMEGA

*******************************************************************************

      SUBROUTINE OMEGA (VAR,X,F,IMAX,NAME,SOM)                         OMEG   1
C                                                                      OMEG   2
C---------THIS PROGROM PERFORMS LAGRANGE INTERPOLATION WITH NON-EQUAL   OMEG   3
C         STEP SIZE BETWEEN POINTS                                     OMEG   4
```

```
C         F - DEPENDANT VARIABLE                                                OMEG   5
C         X - INDEPENDANT VARIABLE                                              OMEG   6
C         VAR - VALUE OF X FOR WHICH CORRESPONDING VALUE OF F IS DESIRED        OMEG   7
C         INTERPOLATION                                                         OMEG   8
C         IMAX - NUMBER OF POINTS IN ARRAY X OR F                               OMEG   9
C         NAME - DIMENSION  OF ARRAY X OR F                                     OMEG  10
C         SOM - VALUE OF INTERPOLATED DEPENDANT VARIABLE                        OMEG  11
C         NPTS - NUMBER OF POINTS USED FOR INTERPOLATION                        OMEG  12
C                                                                               OMEG  13
      DIMENSION X(NAME),F(NAME),XN(300),FN(300)                                 OMEG  14
      NPTS=3                                                                    OMEG  15
  607 XUP=1.E30                                                                 OMEG  16
      DO611 I=1,IMAX                                                            OMEG  17
      T=VAR-X(I)                                                                OMEG  18
      IF(T)608,609,609                                                          OMEG  19
  608 T=-T                                                                      OMEG  20
  609 IF(T-XUP)610,611,611                                                      OMEG  21
  610 IP=I                                                                      OMEG  22
      XUP=T                                                                     OMEG  23
  611 CONTINUE                                                                  OMEG  24
      IN=1                                                                      OMEG  25
      NPP=NPTS+1                                                                OMEG  26
      DO618I=1,NPP                                                              OMEG  27
      FN(I)=F(IP)                                                               OMEG  28
      XN(I)=X(IP)                                                               OMEG  29
      IF(IN)612,612,613                                                         OMEG  30
  612 IQ=IP-I                                                                   OMEG  31
      GO TO 615                                                                 OMEG  32
  613 IQ=IP+I                                                                   OMEG  33
      IF(IMAX-IQ)614,615,615                                                    OMEG  34
  614 IP=IP-1                                                                   OMEG  35
      GO TO 618                                                                 OMEG  36
  615 IF(IQ)616,616,617                                                         OMEG  37
  616 IP=IP+1                                                                   OMEG  38
      GO TO 618                                                                 OMEG  39
  617 IP=IQ                                                                     OMEG  40
      IN=-IN                                                                    OMEG  41
  618 CONTINUE                                                                  OMEG  42
      SOM=0.0                                                                   OMEG  43
      FACT=1.0                                                                  OMEG  44
      DO620 J=1,NPTS                                                            OMEG  45
      SOM=SOM+FACT*FN(I)                                                        OMEG  46
      DO619 I=J,NPTS                                                            OMEG  47
      IQ=I-J+1                                                                  OMEG  48
  619 FN(IQ)=(FN(IQ+1)-FN(IQ))/(XN(I+1)-XN(IQ))                                 OMEG  49
  620 FACT=FACT*(VAR-XN(J))                                                     OMEG  50
      RETURN                                                                    OMEG  51
      END                                                                       OMEG  52
```

****

SUBROUTINE PATERN

```
*************************************************************************************

      SUBROUTINE PATERN(NP,P,STEP,NRD,IO,COST)                                PATE   1
C--------PATTERN SEARCH PROGRAMMED BY C. F. MOORE, LSU                        PATE   2
C        NP= NUMBER OF PARAMETERS                                             PATE   3
C        P= INITIAL VA                                                        PATE   4
C        P= INITIAL VECTOR OF PARAMETERS, MUST BE WITHIN STABLE REGION        PATE   5
C        STEP= INITIAL STEP SIZE                                              PATE   6
C        NRD= NUMBER OF TIMES H                                               PATE   7
C        NRD= NUMBER OF TIMES THE STEP SIZE IS REDUCED BY A FACTOR            PATE   8
C             OF TEN                                                          PATE   9
C        IO= PRINT CONTROL                                                    PATE  10
C        IO= 0    NO PRINT OUTPUT                                             PATE  11
C        IO= 1    ONLY THE ANSWER IS PRINTED                                  PATE  12
C        IO= 2    PRINT OUTPUT FOR EACH ITERATION                             PATE  13
C        IO= 3    PRINT OUTPUT FOR EACH TRIAL STEP                            PATE  14
C        COST= VALUE OF CRITERION FUNCTION                                    PATE  15
      DIMENSION P(NP),STEP(NP),B1(1000),B2(1000),T(1000),S(1000)              PATE  16
C-----STARTING POINT                                                          PATE  17
      L=1                                                                     PATE  18
      ICK=2                                                                   PATE  19
      ITTER=0                                                                 PATE  20
      DO5 I=1,NP                                                              PATE  21
      B1(I)=P(I)                                                              PATE  22
      B2(I)=P(I)                                                              PATE  23
      T(I)=P(I)                                                               PATE  24
  5   S(I)=STEP(I)*10.                                                        PATE  25
C-----INITIAL BOUNDARY CHECK AND COST EVALUATION                              PATE  26
      CALL BOUNDS(P,IOUT)                                                     PATE  27
      IF(IOUT.LE.0)GOTO10                                                     PATE  28
                   IF(IO.LE.0)GOTO6                                           PATE  29
                   WRITE(6,1005)                                              PATE  30
                   WRITE(6,1000)(J,P(J),J=1,NP)                               PATE  31
  6   RETURN                                                                  PATE  32
 10   CALL PROC(P,C1)                                                         PATE  33
                   IF(IO.LE.0)GOTO11                                          PATE  34
                   WRITE(6,1001)ITTER,C1                                      PATE  35
                   WRITE(6,1000)(J,P(J),J=1,NP)                               PATE  36
C-------BEGINNING OF PATTERN SEARCH STRATEGY                                  PATE  37
 11   DO99 INRD=1,NRD                                                         PATE  38
      DO12 I=1,NP                                                             PATE  39
 12   S(I)=S(I)/10.                                                           PATE  40
                   IF(IO.LE.0)GOTO20                                          PATE  41
                   WRITE(6,1003)                                              PATE  42
                   WRITE(6,1000)(J,S(J),J=1,NP)                               PATE  43
 20   IFAIL=0.0                                                               PATE  44
C-----PRETURBATION ABOUT T                                                    PATE  45
      DO30 I=1,NP                                                             PATE  46
      IC=0                                                                    PATE  47
 21   P(I)=T(I)+S(I)                                                          PATE  48
      IC=IC+1                                                                 PATE  49
      CALL BOUNDS(P,IOUT)                                                     PATE  50
      IF(IOUT.GT.0)GOTO23                                                     PATE  51
```

```
      CALL PROC(P,C2)                                                    PATE  52
                    L=L+1                                                PATE  53
                    IF(IO.LT.3)GOTO22                                    PATE  54
                    WRITE(6,1002)L,C2                                    PATE  55
                    WRITE(6,1000)(J,P(J),J=1,NP)                         PATE  56
   22   IF(C1-C2)23,23,25                                                PATE  57
   23   IF(IC.GE.2)GOTO24                                                PATE  58
        S(I)=-S(I)                                                       PATE  59
        GOTO21                                                           PATE  60
   24   IFAIL=IFAIL+1                                                    PATE  61
        P(I)=T(I)                                                        PATE  62
        GOTO30                                                           PATE  63
   25   T(I)=P(I)                                                        PATE  64
        C1=C2                                                            PATE  65
   30   CONTINUE                                                         PATE  66
        IF(IFAIL.LT.NP)GOTO35                                            PATE  67
        IF(ICK.EQ.2)GOTO90                                               PATE  68
        IF(ICK.EQ.1)GOTO35                                               PATE  69
        CALL PROC(T,C2)                                                  PATE  70
                    L=L+1                                                PATE  71
                    IF(IO.LT.2)GOTO31                                    PATE  72
                    WRITE(6,1002)L,C2                                    PATE  73
                    WRITE(6,1000)(J,T(J),J=1,NP)                         PATE  74
   31   IF(C1-C2)32,34,34                                                PATE  75
   32   ICK=1                                                            PATE  76
        DO33 I=1,NP                                                      PATE  77
        B1(I)=B2(I)                                                      PATE  78
        P(I)=B2(I)                                                       PATE  79
   33   T(I)=B2(I)                                                       PATE  80
        GOTO20                                                           PATE  81
   34   C1=C2                                                            PATE  82
   35   IB1=0                                                            PATE  83
        DO39 I=1,NP                                                      PATE  84
        B2(I)=T(I)                                                       PATE  85
        IF(ABS(B1(I)-B2(I)).LT..01*ABS(S(I))) IB1=IB1+1                  PATE  86
   39   CONTINUE                                                         PATE  87
        IF(IB1.EQ.NP)GOTO90                                              PATE  88
        ICK=0                                                            PATE  89
                    ITTER=ITTER+1                                        PATE  90
                    IF(IO.LT.2)GOTO40                                    PATE  91
                    WRITE(6,1001)ITTER,C1                                PATE  92
                    WRITE(6,1000)(J,T(J),J=1,NP)                         PATE  93
C-----ACCELERATION STEP                                                  PATE  94
   40   SJ=1.0                                                           PATE  95
        DO45 II=1,11                                                     PATE  96
        DO42 I=1,NP                                                      PATE  97
        T(I)=B2(I)+SJ*(B2(I)-B1(I))                                      PATE  98
   42   P(I)=T(I)                                                        PATE  99
        SJ=SJ-.1                                                         PATE 100
        CALL BOUNDS(T,IOUT)                                              PATE 101
        IF(IOUT.LT.1)GOTO46                                              PATE 102
        IF(II.EQ.11)ICK=1                                                PATE 103
   45   CONTINUE                                                         PATE 104
```

```
 46    DO47 I=1,NP                                                    PATE 105
 47    B1(I)=B2(I)                                                    PATE 106
       GOTO20                                                         PATE 107
 90    DO91 I=1,NP                                                    PATE 108
 91    T(I)=B2(I)                                                     PATE 109
 99    CONTINUE                                                       PATE 110
       DO100 I=1,NP                                                   PATE 111
100    P(I)=T(I)                                                      PATE 112
       COST=C1                                                        PATE 113
                    IF(IO.LE.0)RETURN                                 PATE 114
                    WRITE(6,1004)L,C1                                 PATE 115
                    WRITE(6,1000)(J,P(J),J=1,NP)                      PATE 116
       RETURN                                                         PATE 117
1000   FORMAT(10X,5(I7,E13.6)/)                                       PATE 118
1001   FORMAT(//1X14HITTERATION NO.  ,I5/5X,5HCOST= ,E15.6,20X,       PATE 119
      1   10HPARAMETERS)                                             PATE 120
1002   FORMAT(10X3HNO.,I4, 8X5HCOST=,E15.6)                           PATE 121
1003   FORMAT(/1X28HSTEP SIZE FOR EACH PARAMETER   )                  PATE 122
1004   FORMAT(1H113HANSWERS AFTER ,I3,2X,23HFUNCTIONAL EVALUATIONS   //  PATE 123
      1   5X5HCOST=,E15.6,20X,18HOPTIMAL PARAMETERS  )                PATE 124
1005   FORMAT(1H135HINITIAL PARAMETERS OUT OF BOUNDS        )         PATE 125
       END                                                            PATE 126
```

****

INPUT DATA

****

****

CONTROL PARAMETERS TO OBTAIN CONDENSED TABLES OF
APPENDIX G

****

```
 140 1  0.1015  1.        0.5       0.19579
11.121    0.5
18.       0.5
0.1147    0.01
0.001     0.0001
```

****

CONTROL PARAMETERS TO OBTAIN DETAIL PRINTOUT OF
SECTION 4.4

****

```
 240 2  0.1015  0.        0.5       0.19579
```

```
11.121      0.5
18.         0.5
0.1147      0.01
0.001       0.0001

*****************************************************************************

                VELOCITY PROFILES MEASURED AT 243 RPM
                    TANK DIAMETER= 12.25 IN.

*****************************************************************************

 1
 1 4
11NOV 22, 1968 1.
      1  3.000  3.000 12.000  3.250 13.950 16.8002.5    243.    75.6    44.1
5.75    -8.95   .2      .8      0.      0.      .3      -.1     14.68   58.6
5.8     -8.95   0.      .9      0.      0.      .4      -.2     14.6    56.6
5.8     -9.     -.04    1.25    0.      0.      .65     -.55    14.49   54.
5.95    -8.9    -.95    1.7     0.      0.      .65     -.6     14.38   51.
6.      -8.9    -1.35   2.1     0.      0.      .5      -.4     14.3    49.2
6.      -8.9    -1.45   2.3     0.      0.      .05     .1      14.2    47.
6.      -8.9    -1.4    2.25    0.      0.      -.35    .55     14.1    47.
5.95    -8.85   -.95    1.8     0.      0.      -.65    .9      14.     49.
5.9     -8.85   -.3     1.15    0.      0.      -.6     .8      13.9    52.
5.85    -8.85   .05     .8      0.      0.      -.45    .7      13.8    54.8
5.75    -8.9    .03     .55     0.      0.      -.15    .32     13.7    62.4
 1 4
11DEC  9, 1968 1.
      9  3.000  3.000 12.000  3.250 13.950 16.8002.5    243.    74.5    44.1
5.5     -9.3    .2      .65     0.      0.      1.4     -.2     14.7    60.6
5.5     -9.3    0.      .85     0.      0.      1.7     -.5     14.6    58.
5.5     -9.35   -.4     1.2     0.      0.      1.8     -.65    14.5    56.
5.6     -9.4    -.9     1.7     0.      0.      1.75    -.6     14.4    52.8
5.6     -9.45   -1.35   2.1     0.      0.      1.1     .1      14.3    49.6
5.65    -9.45   -1.4    2.2     0.      0.      .4      .9      14.2    48.
5.6     -9.4    -1.3    2.1     0.      0.      -.3     1.65    14.1    47.8
5.6     -9.4    -.8     1.6     0.      0.      -.6     1.95    14.     49.8
5.5     -9.3    -.35    1.25    0.      0.      -.4     1.8     13.9    53.
5.5     -9.3    .05     .8      0.      0.      .0      1.3     13.8    56.
5.5     -9.3    .3      .6      0.      0.      .45     .85     13.7    62.2
 1 4
12NOV 26, 1968 1.
      2  3.000  3.000 12.000  3.250 13.950 16.8002.5    243.    76.4    5.5
5.8     -8.95   .2      .7      0.      0.      .25     -.1     14.68   60.8
5.8     -8.96   .05     .85     0.      0.      .4      -.25    14.6    59.2
5.8     -9.     -.3     1.2     0.      0.      .65     -.05    14.5    59.8
5.85    -9.     -.8     1.65    0.      0.      .8      -.75    14.4    54.4
5.85    -9.1    -1.2    2.      0.      0.      .5      -.4     14.3    51.
5.9     -9.     -1.4    2.2     0.      0.      .15     0.      14.2    48.8
5.9     -9.     -1.35   2.2     0.      0.      -.25    .4      14.1    48.6
5.85    -9.     -.95    1.8     0.      0.      -.55    .75     14.     49.6
5.8     -9.     -.4     1.35    0.      0.      -.6     .8      13.9    51.8
```

```
5.8     -9.     -.1     .95     0.      0.      -.5     .7      13.8    55.8
5.75    -8.95   .2      .7      0.      0.      -.25    .45     13.7    60.
5.7     -8.95   .35     .55     0.      0.      -.05    .25     13.6    63.2
 1 4
13DEC  3, 1968 1.
       8  3.000  3.000 12.000  3.250 13.950 16.8003.      243.    74.5    44.1
5.5     -9.25   .3      .55     0.      0.      1.25    -.1     14.8    46.6
5.5     -9.25   .2      .65     0.      0.      1.3     -.1     14.7    46.2
5.5     -9.3    .05     .75     0.      0.      1.4     -.2     14.6    45.8
5.5     -9.25   -.2     1.      0.      0.      1.5     -.3     14.5    45.2
5.55    -9.3    -.45    1.25    0.      0.      1.55    -.35    14.4    44.
5.55    -9.3    -.55    1.35    0.      0.      1.45    -.25    14.3    43.
5.6     -9.35   -.65    1.4     0.      0.      1.2     0.      14.2    43.
5.5     -9.35   -.6     1.4     0.      0.      .8      .5      14.1    42.4
5.5     -9.35   -.525   1.3     0.      0.      .35     1.      14.     43.
5.55    -9.35   -.3     1.1     0.      0.      .25     1.1     13.9    44.4
5.5     -9.3    -.1     .9      0.      0.      .25     1.1     13.8    46.
5.5     -9.3    0.15    .7      0.      0.      .3      1.      13.7    48.8
5.5     -9.3    .3      .6      0.      0.      .45     .9      13.6    50.8
 1 4
13NOV  27, 1968 1.
       3  3.000  3.000 12.000  3.250 13.950 16.8003.      243.    78.     5.5
5.7     -9.     .3      .6      0.      0.      .1      .05     14.8    52.
5.7     -9.     .2      .8      0.      0.      .15     0.      14.7    50.4
5.75    -9.     .05     .85     0.      0.      .25     -.1     14.6    48.4
5.8     -9.     -.2     1.1     0.      0.      .3      -.15    14.5    46.8
5.8     -9.     -.4     1.3     0.      0.      .3      -.1     14.4    45.8
5.8     -9.05   -.6     1.45    0.      0.      .2      -.05    14.3    44.
5.81    -9.01   -.6     1.5     0.      0.      .05     .15     14.2    43.4
5.8     -9.     -.65    1.5     0.      0.      -.1     .3      14.1    42.6
5.8     -9.     -.55    1.4     0.      0.      -.3     .5      14.     43.8
5.75    -9.     -.3     1.2     0.      0.      -.35    .55     13.9    44.6
5.75    -9.     -.1     1.      0.      0.      -.3     .5      13.8    46.6
5.75    -9.     .15     .75     0.      0.      -.25    .4      13.7    48.2
5.75    -8.95   .3      .6      0.      0.      -.1     .3      13.6    50.4
 1 4
13DEC  3, 1968 1.
       7  3.000  3.000 12.000  3.250 13.950 16.8003.5     243.    75.5    44.1
5.6     -9.1    .25     .6      0.      0.      .15     -.05    14.8    37.4
5.55    -9.2    .175    .7      0.      0.      .15     -.05    14.7    37.6
5.55    -9.2    .1      .75     0.      0.      .175    -.1     14.6    37.6
5.6     -9.2    -.05    .9      0.      0.      .2      -.1     14.5    38.4
5.6     -9.24   -.15    1.05    0.      0.      .2      -.1     14.4    38.4
5.6     -9.2    -.3     1.15    0.      0.      .15     -.05    14.3    37.8
5.6     -9.2    -.35    1.2     0.      0.      .15     -.05    14.2    37.4
5.6     -9.2    -.35    1.2     0.      0.      .05     .05     14.1    37.4
5.6     -9.25   -.3     1.125   0.      0.      -.05    .15     14.     37.6
5.6     -9.25   -.15    1.      0.      0.      -.1     .2      13.9    38.8
5.6     -9.25   -.075   .9      0.      0.      -.15    .25     13.8    38.8
5.55    -9.25   .1      .75     0.      0.      -.15    .25     13.7    40.4
5.55    -9.25   .25     .65     0.      0.      -.1     .25     13.6    42.6
 1 4
14NOV  28, 1968 1.
```

```
      4  3.000  3.000 12.000  3.250 13.950 16.8003.5      243.    75.6    5.5
5.65   -9.     .275    .6      0.      0.      .05     .05     14.8    41.4
5.65   -9.     .2      .7      0.      0.      .1      .05     14.7    41.
5.7    -9.     .1      .75     0.      0.      .1      0.      14.6    40.6
5.7    -9.     0.      .9      0.      0.      .15     0.      14.5    40.2
5.7    -9.     -.15    1.      0.      0.      .15     0.      14.4    39.8
5.7    -9.05   -.25    1.1     0.      0.      .1      .05     14.3    39.4
5.7    -9.05   -.35    1.2     0.      0.      .1      .075    14.2    39.
5.7    -9.05   -.35    1.2     0.      0.      0.      .15     14.1    38.6
5.7    -9.05   -.3     1.2     0.      0.      -.05    .3      14.     39.4
5.7    -9.05   -.2     1.1     0.      0.      -.15    .3      13.9    39.8
5.7    -9.07   -.1     1.      0.      0.      -.15    .4      13.8    41.
5.7    -9.04   .1      .8      0.      0.      -.15    .35     13.7    43.4
5.7    -9.04   .2      .7      0.      0.      -.1     .3      13.6    44.6
5.7    -9.02   .3      .6      0.      0.      -.05    .25     13.5    47.
 1 4
16NOV 30, 1968 1.
      6  3.000  3.000 12.000  3.250 13.950 16.8004.      243.    76.     44.1
5.65   -9.05   .25     .65     0.      0.      .05     .05     14.8    35.
5.65   -9.05   .2      .7      0.      0.      .075    .05     14.7    34.6
5.65   -9.05   .15     .7      0.      0.      .05     .05     14.6    34.
5.65   -9.05   .05     .8      0.      0.      .05     .05     14.5    33.2
5.65   -9.1    0.      .9      0.      0.      .05     .075    14.4    33.8
5.65   -9.1    -.01    .95     0.      0.      .05     .05     14.3    33.8
5.65   -9.1    -.15    1.      0.      0.      .05     .1      14.2    33.8
5.65   -9.1    -.15    1.      0.      0.      0.      .15     14.1    33.8
5.65   -9.1    -.125   .975    0.      0.      -.05    .2      14.     33.8
5.65   -9.1    -.1     .9      0.      0.      -.075   .2      13.9    34.6
5.65   -9.1    0.      .85     0.      0.      -.1     .25     13.8    36.2
5.65   -9.1    .1      .75     0.      0.      -.1     .25     13.7    35.6
5.65   -9.1    .2      .7      0.      0.      -.1     .25     13.6    36.8
5.65   -9.1    .275    .6      0.      0.      -.05    .2      13.5    39.4
5.65   -9.1    .3      .55     0.      0.      -.025   .175    13.4    39.4
5.65   -9.1    .3      .6      0.      0.      -.05    .1      13.     39.
11 4
14NOV 28, 1968 1.
      5  3.000  3.000 12.000  3.250 13.950 16.8004.      243.    76.8    5.5
5.75   -9.05   .25     .65     0.      0.      .1      .1      14.8    36.8
5.75   -9.05   .2      .7      0.      0.      .1      .1      14.7    36.8
5.7    -9.05   .15     .75     0.      0.      .1      .05     14.6    36.8
5.7    -9.05   .05     .85     0.      0.      .1      .05     14.5    36.
5.7    -9.05   0.      .9      0.      0.      .1      .075    14.4    36.
5.7    -9.05   -.1     1.      0.      0.      .1      .1      14.3    35.4
5.7    -9.05   -.15    1.      0.      0.      .05     .1      14.2    35.4
5.7    -9.05   -.15    1.05    0.      0.      0.      .15     14.1    36.4
5.7    -9.05   -.15    1.      0.      0.      0.      .2      14.     35.6
5.7    -9.05   -.1     1.      0.      0.      -.05    .25     13.9    36.2
5.7    -9.05   0.      .9      0.      0.      -.1     .275    13.8    37.2
5.7    -9.05   .1      .8      0.      0.      -.1     .3      13.7    38.
5.7    -9.05   .175    .7      0.      0.      -.1     .3      13.6    40.4
5.7    -9.     .25     .65     0.      0.      -.05    .25     13.5    43.
```

****

VELOCITY PROFILES MEASURED AT 250 RPM
TANK DIAMETER= 12.25 IN.

****

```
 1
 2 4
11JAN 24, 1969 2.54
     25  3.000  6.000 12.000  3.250 13.950 27.2002.5     250.    76.     44.1
4.2     -11.2  -.05    1.1     0.      0.      -.5     1.15    10.7    71.4
4.22    -11.27 -.6     1.2     0.      0.      -1.9    3.25    10.8    68.
4.3     -11.31 -1.4    2.      0.      0.      -4.     5.5     10.9    66.
4.31    -11.4  -3.1    3.4     0.      0.      -4.5    6.05    11.     62.8
4.35    -11.46 -4.4    4.9     0.      0.      -2.9    4.1     11.1    59.9
4.4     -11.5  -5.     5.45    0.      0.      1.      .2      11.2    58.4
4.4     -11.48 -4.8    5.2     0.      0.      4.12    -3.2    11.3    59.2
4.3     -11.4  -3.6    4.1     0.      0.      5.8     -5.1    11.4    62.
3.75    -12.1  -1.3    2.      0.      0.      4.8     -4.2    11.5    67.6
3.72    -12.08 -.6     1.2     0.      0.      3.3     -2.4    11.6    70.4
3.7     -12.03 -.5     1.1     0.      0.      2.      -1.     11.7    73.2
 2 4
14JAN 17, 1969 2.54
     22  3.000  6.000 12.000  3.250 13.950 27.2002.5     250.    75.6    5.5
4.2     -11.2  -.35    .9      0.      0.      -.1     1.2     10.5    95.4
4.25    -11.17 -.2     0.8     0.      0.      -.2     1.5     10.6    72.2
4.3     -11.8  -.2     .95     0.      0.      -1.1    2.4     10.7    72.
4.3     -11.2  -.6     1.25    0.      0.      -2.9    4.3     10.8    70.8
4.4     -11.23 -2.1    2.8     0.      0.      -4.95   6.5     10.9    66.4
4.45    -11.3  -3.9    4.5     0.      0.      -4.45   6.1     11.     63.
4.45    -11.48 -5.2    5.7     0.      0.      -1.8    3.2     11.1    59.8
4.5     -11.4  -5.55   6.05    0.      0.      2.2     -1.1    11.2    59.2
4.45    -11.35 -5.05   5.55    0.      0.      5.4     -4.6    11.3    61.8
4.35    -11.3  -2.95   3.45    0.      0.      6.3     -5.8    11.4    64.6
4.3     -11.25 -1.6    2.1     0.      0.      5.1     -4.3    11.5    68.8
4.25    -11.2  -.85    1.4     0.      0.      3.5     -2.55   11.6    71.
4.25    -11.2  -.6     1.15    0.      0.      2.      -1.1    11.7    72.
4.25    -11.2  -.5     1.1     0.      0.      1.25    -.3     11.9    72.
 2 4
12MAR 24, 1969 2.54
     24  3.000  6.000 12.000  3.250 13.950 27.2003.0     250.    77.5    44.1
2.95    -13.17 -.8     1.25    0.      0.      -1.2    2.35    10.7    58.4
3.01    -13.1  -.9     1.45    0.      0.      -2.05   3.3     10.8    55.
3.09    -13.14 -1.4    1.9     0.      0.      -2.3    3.6     10.9    54.2
3.1     -13.16 -1.9    2.5     0.      0.      -1.9    3.15    11.     53.4
3.12    -13.18 -2.2    2.65    0.      0.      -1.     2.2     11.1    52.2
3.15    -13.18 -2.55   3.1     0.      0.      1.3     -.4     11.2    52.2
3.1     -13.15 -2.45   3.      0.      0.      2.6     -1.8    11.3    52.8
3.1     -13.15 -2.15   2.7     0.      0.      3.35    -2.6    11.4    53.6
3.05    -13.1  -1.7    2.2     0.      0.      3.35    -2.6    11.5    54.6
3.05    -13.1  -1.25   1.8     0.      0.      2.85    -2.1    11.6    55.
3.05    -13.05 -.9     1.5     0.      0.      2.1     -1.3    11.7    55.
3.02    -13.05 -.75    1.4     0.      0.      1.3     -.4     11.8    55.
```

```
 9 4
13JAN 22, 1969 2.54
      23  3.000  6.000 12.000  3.250 13.950 27.2003.0      250.    76.     5.5
4.27    -11.2  -.45    1.05    0.      0.      -.1     1.4     10.6    63.9
4.28    -11.2  -.45    1.2     0.      0.      -1.     2.45    10.7    60.
4.29    -11.23 -.6     1.4     0.      0.      -1.5    2.7     10.8    58.4
4.31    -11.28 -1.4    2.1     0.      0.      -1.75   3.1     10.9    58.
4.37    -11.3  -2.1    2.7     0.      0.      -1.2    2.58    11.     54.8
4.39    -11.3  -2.58   3.3     0.      0.      -.15    1.45    11.1    53.8
4.39    -11.3  -2.6    3.28    0.      0.      1.45    -.3     11.2    53.8
4.35    -11.3  -2.6    3.2     0.      0.      3.      -1.9    11.3    54.
4.35    -11.3  -2.3    2.85    0.      0.      3.1     -2.7    11.4    55.4
4.32    -11.25 -1.6    2.3     0.      0.      3.1     -2.7    11.5    56.6
4.25    -11.2  -1.     1.7     0.      0.      3.2     -2.8    11.6    59.
4.25    -11.2  -.7     1.9     0.      0.      2.4     -1.3    11.7    60.6
4.2     -11.2  -.5     1.05    0.      0.      1.3     -.3     11.8    62.4

*******************************************************************************

                VELOCITY PROFILES MEASURED AT 333.3 PPM
                        TANK DIAMETER= 12.25 IN.

*******************************************************************************

 1
 2 4
13MAR  6, 1969 2.54
      27  3.000  6.000 12.000  3.250 13.950 27.2002.5      333.33 75.     44.1
3.2     -12.8  -.4     1.      0.      0.      2.7     -1.9    11.7    72.4
3.25    -12.8  -.6     1.3     0.      0.      5.3     -4.65   11.6    69.4
3.3     -12.9  -2.7    3.1     0.      0.      8.1     -7.7    11.5    65.8
3.35    -12.95 -5.3    5.7     0.      0.      10.3    -10.    11.4    62.2
3.55    -13.1  -8.3    8.6     0.      0.      8.4     -8.     11.3    60.
3.6     -13.2  -9.4    9.75    0.      0.      3.5     -2.7    11.2    58.6
3.5     -13.1  -9.1    9.4     0.      0.      -4.1    5.5     11.1    60.
3.45    -13.05 -6.8    7.25    0.      0.      -8.15   9.8     11.     62.4
3.35    -12.95 -3.7    4.1     0.      0.      -8.7    10.2    10.9    65.
3.25    -12.9  -1.8    2.3     0.      0.      -5.7    7.3     10.8    68.
3.2     -12.85 -1.     1.5     0.      0.      -2.8    4.1     10.7    68.8
3.2     -12.8  -.7     1.25    0.      0.      -.7     1.9     10.6    70.4
3.2     -12.8  -.6     1.15    0.      0.      .3      .8      10.5    70.4
 2 4
13MAR  8, 1969 2.54
      28  3.000  6.000 12.000  3.250 13.950 27.2002.5      333.33 76.     5.5
3.1     -12.85 -.3     .8      0.      0.      -.8     1.7     10.6    68.2
3.12    -12.85 -.4     .9      0.      0.      -3.     4.15    10.7    68.2
3.2     -12.9  -2.     2.6     0.      0.      -6.55   8.1     10.8    67.
3.45    -13.   -4.75   5.2     0.      0.      -9.8    11.6    10.9    64.8
3.5     -13.15 -8.     8.4     0.      0.      -7.5    9.3     11.     61.6
3.55    -13.2  -9.8    10.2    0.      0.      -1.9    3.5     11.1    59.2
3.55    -13.25 -9.9    10.4    0.      0.      5.3     -4.5    11.2    58.
3.45    -13.15 -8.1    8.6     0.      0.      10.5    -10.    11.3    60.4
3.3     -13.05 -5.2    5.6     0.      0.      10.4    -10.2   11.4    62.8
```

```
3.15    -12.95 -1.95  2.4     0.      0.      7.1     -6.7    11.5    67.6
3.1     -12.9  -.6    1.1     0.      0.      3.7     -3.     11.6    68.4
3.1     -12.9  -.7    1.15    0.      0.      1.9     -1.     11.7    68.6
3.1     -12.9  -.5    1.1     0.      0.      0.6     .45     12.     68.6
 2 4
12MAR 15,1969  2.54
      26  3.000  6.000 12.000  3.250 13.950 27.2    3.0     333.33 77.     44.1
2.95    -13.1  -.6    1.1     0.      0.      -1.2    2.4     10.6    60.2
3.0     -13.15 -.7    1.25    0.      0.      -2.35   3.65    10.7    59.
3.0     -13.15 -1.7   2.2     0.      0.      -4.     5.45    10.8    55.4
3.1     -13.2  -3.1   3.6     0.      0.      -4.9    6.3     10.9    55.
3.15    -13.26 -4.2   4.6     0.      0.      -4.     5.4     11.     54.
3.2     -13.3  -5.1   5.5     0.      0.      -1.5    2.7     11.1    52.6
3.15    -13.3  -5.25  5.6     0.      0.      1.25    -.4     11.2    52.2
3.15    -13.3  -5.1   5.45    0.      0.      4.0     -3.3    11.3    53.
3.1     -13.25 -4.2   4.6     0.      0.      5.6     -5.05   11.4    53.4
3.05    -13.2  -2.9   3.35    0.      0.      5.7    -5.25    11.5    55.
3.05    -13.15 -1.85  2.4     0.      0.      4.95    -4.35   11.6    57.4
2.95    -13.15 -.8    1.2     0.      0.      2.9     -2.45   11.7    59.8
 9 4
14MAR 10, 1969 2.54
      29  3.000  6.000 12.000  3.250 13.950 27.2003.     333.33 75.     5.5
3.1     -12.9  -.4    .95     0.      0.      .4      1.6     10.5    62.4
3.1     -12.9  -.4    1.      0.      0.      -1.6    2.85    10.6    60.
3.15    -12.95 -1.05  1.6     0.      0.      -3.3    4.7     10.7    57.2
3.2     -13.   -1.7   2.7     0.      0.      -3.9    5.3     10.8    56.6
3.25    -13.05 -3.7   4.2     0.      0.      -4.4    5.8     10.9    55.2
3.3     -13.1  -4.8   5.2     0.      0.      -3.1    4.4     11.     53.8
3.3     -13.15 -5.5   5.9     0.      0.      -.15    1.3     11.1    53.6
3.3     -13.1  -5.55  5.9     0.      0.      3.      -2.2    11.2    53.
3.25    -13.05 -5.    5.4     0.      0.      5.1     -4.5    11.3    53.8
3.25    -13.05 -4.    4.4     0.      0.      5.8     -5.25   11.4    54.6
3.2     -13.   -2.45  2.9     0.      0.      5.5     -4.9    11.5    57.
3.12    -12.94 -1.5   2.      0.      0.      4.2     -3.6    11.6    58.8
3.1     -12.96 -0.65  1.05    0.      0.      2.5     -1.85   11.7    60.
3.05    -12.95 -.6    1.      0.      0.      1.45    -.6     11.8    60.
```

****

VELOCITY PROFILES MEASURED AT 400 RPM
TANK DIAMETER= 12.25 IN.

****

```
 1
 2 4
12MAR 12, 1969 2.54
      32  3.000  6.000 12.000  3.250 13.950 27.2002.5    400.    78.     44.1
3.05    -13.   -.6    1.2     0.      0.      4.      -3.2    11.7    68.4
3.1     -13.03 -1.4   2.      0.      0.      7.      -6.4    11.6    67.4
3.18    -13.1  -4.5   5.      0.      0.      12.7    -12.55  11.5    66.
3.4     -13.4  -9.1   9.65    0.      0.      16.85   -17.    11.4    62.6
3.55    -13.45 -12.8  13.25   0.      0.      13.1    -13.    11.3    60.
```

```
3.55   -13.5  -14.5  14.8   0.     0.     5.     -4.2   11.2   58.6
3.5    -13.5  -13.5  13.7   0.     0.     -5.3   6.75   11.1   60.6
3.45   -13.41 -10.4  10.6   0.     0.     -13.   14.7   11.    63.6
3.3    -13.26 -6.    6.3    0.     0.     -13.3  15.    10.9   66.6
3.15   -13.1  -2.5   3.     0.     0.     -8.    9.6    10.8   68.8
3.05   -13.06 -1.1   1.55   0.     0.     -3.5   4.85   10.7   69.
3.02   -13.   -.8    1.3    0.     0.     -1.3   2.6    10.6   69.8
 2 4
12MAR 11, 1969 2.54
     31  3.000  6.000 12.000  3.250 13.950 27.2002.5     400.   78.    5.5
3.05   -12.9  -.55   1.1    0.     0.     .1     1.     10.5   67.8
3.05   -12.95 -.6    1.15   0.     0.     -1.3   2.5    10.6   67.6
3.1    -13.   -.8    1.35   0.     0.     -4.    5.4    10.7   68.2
3.15   -13.05 -2.75  3.8    0.     0.     -9.5   11.2   10.8   68.6
3.35   -13.25 -7.7   8.1    0.     0.     -14.2  15.9   10.9   66.
3.5    -13.4  -12.05 12.2   0.     0.     -12.   13.6   11.    62.4
3.6    -13.5  -14.7  15.    0.     0.     -3.3   4.75   11.1   59.4
3.6    -13.52 -14.9  15.15  0.     0.     7.4    -7.    11.2   58.8
3.45   -13.35 -12.   12.35  0.     0.     14.7   -14.6  11.3   60.
3.32   -13.25 -7.6   7.95   0.     0.     16.2   -16.3  11.4   63.6
3.15   -13.05 -3.7   4.1    0.     0.     11.8   -11.5  11.5   67.6
3.1    -13.   -1.55  2.2    0.     0.     6.6    -6.    11.6   68.4
 2 4
15MAR 13, 1969 2.54
     33  3.000  6.000 12.000  3.250 13.950 27.2003.0     400.   78.    44.1
3.05   -13.   -.5    1.1    0.     0.     -.9    2.2    10.5   62.
3.1    -13.05 -.6    1.2    0.     0.     -1.9   3.3    10.6   59.6
3.1    -13.05 -1.2   1.8    0.     0.     -4.    5.5    10.7   58.2
3.15   -13.1  -2.5   3.05   0.     0.     -5.7   7.3    10.8   55.6
3.25   -13.2  -4.8   5.3    0.     0.     -6.7   8.3    10.9   54.6
3.32   -13.3  -6.7   7.2    0.     0.     -5.6   7.3    11.    54.2
3.35   -13.3  -8.1   8.5    0.     0.     -2.5   4.1    11.1   53.4
3.4    -13.3  -8.2   8.75   0.     0.     2.35   -1.3   11.2   52.4
3.35   -13.3  -7.7   8.25   0.     0.     5.5    -4.75  11.3   52.4
3.3    -13.25 -6.6   7.1    0.     0.     7.25   -6.7   11.4   54.
3.1    -13.2  -4.2   4.7    0.     0.     7.7    -7.2   11.5   55.2
3.1    -13.1  -2.6   3.1    0.     0.     6.6    -6.3   11.6   56.4
3.1    -13.1  -1.5   2.     0.     0.     4.5    -3.8   11.7   58.4
3.02   -13.05 -.9    1.5    0.     0.     2.7    -1.85  11.8   60.6
3.0    -13.05 -.8    1.3    0.     0.     1.4    -.5    11.9   65.8
 9 4
15MAR 10, 1969 2.54
     30  3.000  6.000 12.000  3.250 13.950 27.2003.     400.   78.    5.5
3.05   -12.95 -.6    1.     0.     0.     1.9    -1.2   11.8   61.
3.06   -12.96 -.7    1.05   0.     0.     3.1    -2.6   11.7   60.
3.12   -13.   -1.5   1.9    0.     0.     5.45   -5.1   11.6   58.
3.15   -13.05 -3.2   3.65   0.     0.     7.     -6.7   11.5   55.6
3.25   -13.1  -4.7   4.95   0.     0.     7.6    -7.4   11.4   53.8
3.3    -13.2  -7.3   7.5    0.     0.     6.9    -6.65  11.3   53.8
3.4    -13.25 -8.3   8.5    0.     0.     4.7    -4.3   11.2   53.2
3.3    -13.25 -8.65  8.9    0.     0.     -.4    1.5    11.1   53.
3.4    -13.21 -8.    8.3    0.     0.     -4.4   5.9    11.    53.6
3.3    -13.15 -6.1   6.5    0.     0.     -6.4   8.     10.9   56.
```

```
3.2     -13.05 -4.25  4.7     0.      0.      -6.5    8.15    10.8    57.
3.15    -13.    -2.5  3.05    0.      0.      -5.1    6.7     10.7    59.8
3.1     -12.95 -1.2   1.8     0.      0.      -2.7    4.2     10.6    62.
3.1     -12.95 -.85   1.5     0.      0.      -1.     2.3     10.5    64.2
3.05    -12.95 -.7    1.4     0.      0.      0.      1.3     10.4    71.
```

****

VELOCITY PROFILES MEASURED AT 500 RPM
TANK DIAMETER= 12.25 IN.

****

```
 1
 2 4
15DEC  5, 1968 1.
     10  3.000  3.000 12.000  3.250 13.950 16.800  2.500500.000 76.500 44.1
  5.500 -9.300  0.200  0.650  0.000  0.000  1.150  0.200 14.900 58.800
  5.500 -9.300  0.100  0.800  0.000  0.000  1.250 -0.050 14.800 57.600
  5.500 -9.300 -0.250  1.150  0.000  0.000  2.250 -1.000 14.700 57.600
  5.600 -9.400 -1.050  1.900  0.000  0.000  4.200 -3.200 14.600 57.200
  5.700 -9.550 -2.550  3.350  0.000  0.000  6.450 -5.600 14.500 56.400
  5.950 -9.750 -4.750  5.400  0.000  0.000  7.450 -6.600 14.400 53.600
  6.150 -9.950 -6.850  7.500  0.000  0.000  6.300 -5.500 14.300 50.000
  6.250-10.050 -7.950  8.600  0.000  0.000  1.850 -0.700 14.200 48.000
6.25   -10.05  -7.800  8.500  0.000  0.000 -0.400  1.800 14.150 47.800
  6.200-10.000 -7.250  7.900  0.000  0.000 -3.200  4.750 14.100 47.800
  6.000 -9.800 -5.450  6.100  0.000  0.000 -6.800  8.500 14.000 49.400
  5.800 -9.600 -3.250  4.000  0.000  0.000 -7.100  8.750 13.900 52.200
  5.650 -9.450 -1.500  2.250  0.000  0.000 -5.150  6.800 13.800 56.000
  5.500 -9.350 -0.150  1.050  0.000  0.000  1.500  2.050 13.700 61.000
  5.500 -9.300  0.300  0.600  0.000  0.000  0.450  1.900 13.600 69.200
 2 4
14DEC 18, 1968 1.
     17  3.000  3.000 12.000  3.250 13.950 16.800  2.500500.000 76.750  5.500
  5.150 -9.800 -0.050  0.500  0.000  0.000  0.800  0.500 14.900 73.400
  5.200 -9.900 -0.200  0.650  0.000  0.000  1.600 -0.400 14.800 65.000
  5.200 -9.900 -0.500  0.900  0.000  0.000  2.300 -1.200 14.700 62.000
  5.250 -9.950 -1.100  1.500  0.000  0.000  3.950 -3.000 14.600 61.400
  5.450-10.000 -2.600  2.950  0.000  0.000  6.700 -5.850 14.500 58.600
  5.600-10.200 -4.500  4.800  0.000  0.000  8.100 -7.300 14.400 55.200
  5.850-10.400 -6.750  7.000  0.000  0.000  6.950 -6.150 14.300 51.600
  5.900-10.600 -7.900  8.150  0.000  0.000  3.100 -2.050 14.200 48.600
  5.900-10.600 -7.750  8.000  0.000  0.000 -2.200  3.700 14.100 45.600
  5.700-10.400 -5.950  6.200  0.000  0.000 -6.650  8.350 14.000 49.600
  5.550-10.200 -3.950  4.250  0.000  0.000 -7.200  8.900 13.900 52.400
  5.300 -9.950 -1.850  2.200  0.000  0.000 -5.000  6.650 13.800 56.600
  5.200 -9.850 -0.500  1.000  0.000  0.000 -2.150  3.700 13.700 61.600
  5.100 -9.800  0.000  0.400  0.000  0.000 -0.050  1.200 13.600 65.800
 2 4
12DEC 22, 1968 2.54
     18  3.000  6.000 12.000  3.250 13. 50 16.8002.5    500.   76.6   44.1
  5.050 -9.900  0.254  1.143  0.000  0.000  4.445 -1.397 11.800 60.000
```

```
  5.100 -9.950 -0.635  1.778  0.000  0.000  6.731 -3.937 11.700 58.800
  5.250-10.050 -4.445  5.461  0.000  0.000 15.494-13.091 11.600 58.800
  5.500-10.300-10.160 10.922  0.000  0.000 24.892-23.114 11.500 56.600
  5.700-10.600-17.018 17.780  0.000  0.000 27.559-26.162 11.400 53.400
  5.900-10.900-22.733 23.495  0.000  0.000 16.764-14.986 11.300 48.400
  5.950-10.900-23.622 24.384  0.000  0.000  0.889  2.796 11.200 47.600
  5.700-10.650-17.145 17.780  0.000  0.000-16.002 19.939 11.100 49.600
  5.400-10.400 -9.144  9.906  0.000  0.000-18.796 22.987 11.000 52.400
  5.150-10.200 -5.207  6.096  0.000  0.000-14.605 18.542 10.900 54.200
  5.000-10.000 -0.635  1.651  0.000  0.000 -5.588  9.017 10.800 56.600
  4.950-10.050 -0.127  1.143  0.000  0.000 -1.778  4.953 10.700 56.600
 2 4
13JAN 12, 1969 2.54
     21  3.000  6.000 12.000  3.250 13.950 16.8002.5     500.    75.6    5.5
4.46   -10.83 -.4    1.25   0.      0.      1.9     .15    11.8    57.4
4.45   -10.85 -.8    1.6    0.      0.      4.      -2.9   11.7    57.4
4.55   -10.9  -1.8   2.5    0.      0.      10.5    -9.4   11.6    57.4
4.65   -11.05 -6.15  6.75   0.      0.      20.5    -19.5  11.5    56.6
4.9    -11.3  -13.3  13.7   0.      0.      27.4    -26.9  11.4    52.4
5.15   -11.5  -20.6  21.05  0.      0.      26.15   -25.6  11.3    49.4
5.5    -11.85 -26.75 27.35  0.      0.      11.2    -10.15 11.2    48.
5.5    -11.8  -25.3  25.9   0.      0.      -7.5    9.95   11.1    48.4
5.3    -11.7  -19.8  20.25  0.      0.      -22.1   25.3   11.     51.2
4.95   -11.3  -11.8  12.4   0.      0.      -24.2   27.2   10.9    55.4
4.65   -11.05 -5.15  5.65   0.      0.      -15.4   18.15  10.8    57.8
4.5    -10.9  -1.05  1.8    0.      0.      -6.1    8.6    10.7    58.2
4.45   -10.85 -.6    1.35   0.      0.      -1.85   3.9    10.6    58.2
 2 4
14DEC  6, 1968 1.
     11  3.000  3.000 12.000  3.250 13.950 16.800  3.000500.000 78.000 44.1
  5.500 -9.350 -0.200  1.100  0.000  0.000  1.400 -0.100 14.800 43.200
  5.550 -9.400 -0.425  1.400  0.000  0.000  2.200 -0.900 14.700 44.200
  5.600 -9.450-1.325 2.15     0.000  0.000  3.100 -2.000 14.600 44.600
  5.700 -9.500-2.175 3.       0.000  0.000  3.700 -2.600 14.500 44.600
  5.800 -9.600 -3.200  3.900  0.000  0.000  3.800 -2.700 14.400 44.000
  5.850 -9.700 -4.050  4.800  0.000  0.000  3.050 -1.900 14.300 43.800
  5.900 -9.750 -4.600  5.300  0.000  0.000  1.300  0.000 14.200 42.400
  5.900 -9.750 -4.450  5.200  0.000  0.000 -0.800  2.350 14.100 42.400
  5.850 -9.700 -3.900  4.650  0.000  0.000 -2.700  4.300 14.000 42.800
  5.650 -9.700 -2.950  3.600  0.000  0.000 -3.550  5.100 13.900 44.000
  5.500 -9.600 -1.900  2.650  0.000  0.000 -3.500  5.050 13.800 45.800
  5.450 -9.500 -0.900  1.650  0.000  0.000 -2.500  4.000 13.700 48.000
  5.400 -9.450 -0.200  1.100  0.000  0.000 -1.200  2.600 13.600 51.600
  5.350 -9.400  0.175  0.650  0.000  0.000 -0.300  1.650 13.500 55.800
 2 4
16DEC 16, 1968 1.
     16  3.000  3.000 12.000  3.250 13.950 16.800  3.000500.000 74.200  5.500
  5.150 -9.800  0.000  0.350  0.000  0.000  0.600  0.600 15.100 65.800
  5.150 -9.800 -0.150  0.600  0.000  0.000  0.800  0.350 14.900 54.600
  5.150 -9.800 -0.350  0.700  0.000  0.000  1.200 -0.150 14.800 51.400
  5.200 -9.900 -0.650  0.950  0.000  0.000  1.900 -0.850 14.700 49.400
  5.200 -9.950 -1.250  1.550  0.000  0.000  2.700 -1.750 14.600 47.600
  5.300-10.000 -2.200  2.450  0.000  0.000  3.700 -2.800 14.500 46.600
```

```
5.4     -10.05  -3.100  3.350  0.000  0.000  3.900 -3.000 14.400 45.400
  5.500-10.200 -4.150  4.300  0.000  0.000  3.400 -2.600 14.300 45.200
  5.600-10.200 -4.800  5.000  0.000  0.000  1.900 -0.800 14.200 43.200
  5.600-10.200 -4.900  5.100  0.000  0.000 -0.150  1.400 14.100 42.600
  5.500-10.200 -4.300  4.500  0.000  0.000 -2.450  3.900 14.000 43.000
5.45    -10.15  -3.550  3.700  0.000  0.000 -3.450  5.050 13.900 44.000
  5.350-10.000 -2.350  2.650  0.000  0.000 -3.550  5.000 13.800 45.600
  5.250 -9.900 -1.350  1.700  0.000  0.000 -2.700  4.100 13.700 48.400
  5.150 -9.800 -0.600  0.950  0.000  0.000 -1.600  3.000 13.600 51.000
  5.150 -9.800 -0.200  0.550  0.000  0.000 -0.450  1.700 13.500 57.000
 2 4
17DEC 30, 1968 2.54
     19  3.000  6.000 12.000  3.250 13.950 16.8003.      500.    76.     44.1
4.85    -10.3  .15    1.8     0.      0.      .45     1.6     12.1    55.
4.85    -10.3  .1     1.9     0.      0.      1.3     .7      11.9    50.8
4.85    -10.3  -.15   2.15    0.      0.      4.      -2.3    11.8    46.8
4.85    -10.35 -1.4   3.2     0.      0.      6.6     -5.25   11.7    46.2
5.      -10.4  -3.6   5.4     0.      0.      9.8     -8.2    11.6    43.2
5.1     -10.6  -8.1   9.9     0.      0.      13.     -11.1   11.5    43.6
5.2     -10.7  -9.4   11.2    0.      0.      11.5    -10.4   11.4    40.6
5.25    -10.75 -11.2  12.95   0.      0.      8.1     -6.85   11.3    39.
5.3     -10.85 -12.75 14.5    0.      0.      3.3     -1.6    11.2    39.4
5.25    -10.75 -12.3  14.05   0.      0.      -3.5    5.8     11.1    40.2
5.1     -10.6  -10.   11.8    0.      0.      -7.75   10.4    11.     41.
5.1     -10.6  -7.6   9.45    0.      0.      -9.8    12.6    10.9    42.6
4.9     -10.45 -4.3   6.15    0.      0.      -9.1    11.7    10.8    42.2
4.9     -10.4  -2.1   4.1     0.      0.      -6.8    9.9     10.7    45.2
4.8     -10.4  -.45   1.85    0.      0.      -3.1    5.3     10.6    47.4
4.75    -10.35 0.05   1.4     0.      0.      -1.15   3.25    10.5    51.
4.75    -10.35 .2     1.3     0.      0.      .45     1.6     10.3    59.6
 2 4
16JAN  7, 1969 2.54
     20  3.000  6.000 12.000  3.250 13.950 16.8003.      500.    77.5    5.5
4.55    -10.65 -.4    1.8     0.      0.      1.3     .7      11.9    49.
4.54    -10.7  -.65   2.      0.      0.      3.9     -2.3    11.8    49.
4.6     -10.75 -1.6   2.85    0.      0.      6.75    -5.25   11.7    48.4
4.65    -10.75 -3.3   4.55    0.      0.      10.3    -9.     11.6    46.
4.75    -10.85 -6.05  7.2     0.      0.      13.2    -12.05  11.5    44.
4.9     -10.9  -8.15  10.     0.      0.      13.5    -12.25  11.4    42.4
5.05    -11.1  -12.   13.     0.      0.      11.5    -10.3   11.3    41.4
5.1     -11.1  -13.1  14.25   0.      0.      5.45    -3.8    11.2    41.
5.1     -11.15 -13.35 14.3    0.      0.      -2.     4.2     11.1    41.4
5.0     -11.1  -11.9  12.95   0.      0.      -7.     9.6     11.0    42.
4.95    -11.05 -9.65  10.75   0.      0.      -11.1   13.9    10.9    44.6
4.8     -10.9  -6.3   7.35    0.      0.      -10.75  13.55   10.8    46.4
4.7     -10.8  -3.3   4.5     0.      0.      -7.7    10.15   10.7    48.2
4.65    -10.7  -1.35  2.5     0.      0.      -4.3    6.6     10.6    52.2
4.6     -10.65 -.6    1.9     0.      0.      -2.3    4.6     10.5    56.8
4.55    -10.6  -.2    1.5     0.      0.      .7      1.3     10.3    68.
 2 4
17DEC  9, 1968 1.
     12  3.000  3.000 12.000  3.250 13.950 16.800  3.500500.000 77.000 44.1
  5.200 -9.600 -0.300  0.550  0.000  0.000  0.750  0.300 15.000 36.400
```

```
  5.200 -9.600 -0.400  0.650  0.000  0.000  0.800  0.250 14.900 36.400
  5.350 -9.550 -0.550  0.950  0.000  0.000  1.400 -0.200 14.800 34.600
  5.400 -9.550 -0.950  1.400  0.000  0.000  1.900 -0.750 14.700 36.400
  5.400 -9.600 -1.300  1.800  0.000  0.000  2.200 -1.050 14.600 37.000
  5.5   -9.600 -1.800  2.200  0.000  0.000  2.400 -1.250 14.500 37.400
  5.400 -9.800 -2.400  2.600  0.000  0.000  2.000 -1.100 14.400 37.400
  5.600 -9.700 -2.950  3.300  0.000  0.000  1.700 -0.600 14.300 37.600
  5.600 -9.750 -3.350  3.650  0.000  0.000  0.800  0.400 14.200 37.600
  5.600 -9.750 -3.300  3.600  0.000  0.000 -0.300  1.650 14.100 37.600
  5.600 -9.750 -3.200  3.500  0.000  0.000 -1.250  2.700 14.000 38.000
  5.550 -9.700 -2.700  3.000  0.000  0.000 -1.700  3.100 13.900 39.400
  5.450 -9.700 -2.100  2.350  0.000  0.000 -2.150  3.500 13.800 39.400
  5.400 -9.650 -1.400  1.700  0.000  0.000 -1.950  3.250 13.700 40.600
  5.350 -9.550 -0.800  1.150  0.000  0.000 -1.500  2.800 13.600 42.400
  5.350 -9.550 -0.450  0.800  0.000  0.000 -1.000  2.300 13.500 44.600
  5.300 -9.500 -0.100  0.500  0.000  0.000 -0.200  0.500 13.400 47.000
 2 4
17DEC 13, 1968 1.
     15  3.000  3.000 12.000  3.250 13.950 16.800  3.500500.000 75.000  5.500
  5.150 -9.850 -0.150  0.500  0.000  0.000  0.800  0.400 15.000 44.800
  5.200 -9.900 -0.500  0.850  0.000  0.000  1.450 -0.300 14.800 40.800
  5.200 -9.850 -0.750  1.100  0.000  0.000  1.850 -0.700 14.700 40.200
  5.250 -9.900 -1.100  1.500  0.000  0.000  2.000 -1.050 14.600 39.400
  5.350 -9.800 -1.800  2.150  0.000  0.000  2.350 -1.250 14.500 39.000
  5.400 -9.900 -2.400  2.700  0.000  0.000  2.350 -1.300 14.400 38.600
  5.450 -9.900 -2.850  3.200  0.000  0.000  2.050 -0.950 14.300 38.200
  5.500 -9.950 -3.200  3.500  0.000  0.000  1.050  0.100 14.200 38.000
  5.500 -9.950 -3.300  3.600  0.000  0.000  0.300  0.900 14.100 38.000
  5.500 -9.900 -3.200  3.500  0.000  0.000 -0.900  2.300 14.000 38.000
  5.500 -9.900 -2.750  3.100  0.000  0.000 -1.700  3.150 13.900 38.400
  5.400 -9.800 -2.200  2.550  0.000  0.000 -2.000  3.450 13.800 39.400
  5.350 -9.800 -1.550  1.900  0.000  0.000 -1.800  3.200 13.700 40.800
  5.300 -9.700 -0.850  1.250  0.000  0.000 -1.200  2.650 13.600 43.000
  5.300 -9.650 -0.500  0.950  0.000  0.000 -0.700  2.100 13.500 45.600
  5.250 -9.650 -0.150  0.600  0.000  0.000 -0.050  1.300 13.400 49.400
  5.250 -9.600  0.100  0.400  0.000  0.000  0.650  0.750 13.200 59.600
 2 4
19DEC 10, 1968 1.
     13  3.000  3.000 12.000  3.250 13.950 16.800  4.000500.000 76.000 44.1
  5.300 -9.550 -0.150  0.550  0.000  0.000  0.700  0.600 15.200 40.200
  5.300 -9.550 -0.350  0.750  0.000  0.000  0.700  0.550 15.000 34.600
  5.250 -9.600 -0.700  0.900  0.000  0.000  1.200 -0.200 14.800 32.600
  5.300 -9.600 -0.850  1.150  0.000  0.000  1.350 -0.350 14.700 32.800
  5.350 -9.600 -1.200  1.500  0.000  0.000  1.600 -0.500 14.600 32.000
  5.400 -9.650 -1.500  1.850  0.000  0.000  1.600 -0.550 14.500 32.400
  5.400 -9.650 -1.800  2.150  0.000  0.000  1.650 -0.550 14.400 32.400
  5.450 -9.700 -2.150  2.500  0.000  0.000  1.200 -0.100 14.300 33.000
  5.500 -9.700 -2.350  2.700  0.000  0.000  1.050  0.150 14.200 33.400
  5.500 -9.750 -2.400  2.750  0.000  0.000  0.650  0.700 14.100 33.400
  5.500 -9.750 -2.350  2.700  0.000  0.000  0.000  1.300 14.000 33.800
  5.500 -9.700 -2.100  2.450  0.000  0.000 -0.600  2.000 13.900 34.000
  5.450 -9.700 -1.800  2.200  0.000  0.000 -0.950  2.350 13.800 34.400
  5.400 -9.650 -1.450  1.850  0.000  0.000 -1.050  2.450 13.700 35.000
```

```
  5.400 -9.600 -1.000  1.400  0.000  0.000 -0.950  2.400 13.600 35.800
  5.300 -9.600 -0.550  0.950  0.000  0.000 -0.600  1.900 13.500 37.400
  5.300 -9.600 -0.350  0.750  0.000  0.000 -0.400  1.750 13.400 38.000
  5.300 -9.550 -0.100  0.550  0.000  0.000 -0.050  1.300 13.300 39.800
  5.300 -9.550  0.000  0.450  0.000  0.000  0.300  1.000 13.200 41.400
11 4
18DEC 12  1968 1.
     14  3.000  3.000 12.000  3.250 13.950 16.800  4.000500.000 78.200  5.500
  5.250 -9.550  0.050  0.400  0.000  0.000  0.750  0.550 15.200 50.400
  5.250 -9.550 -0.150  0.600  0.000  0.000  0.800  0.450 15.000 39.400
  5.300 -9.600 -0.500  0.950  0.000  0.000  1.200  0.000 14.800 36.000
  5.300 -9.600-0.65  1.1       0.000  0.000  1.350 -0.200 14.700 35.000
  5.350 -9.600 -1.000  1.400  0.000  0.000  1.700 -0.500 14.600 34.600
  5.350 -9.750 -1.350  1.800  0.000  0.000  1.800 -0.600 14.500 34.200
  5.400 -9.700 -1.700  2.100  0.000  0.000  1.850 -0.700 14.400 34.600
  5.450 -9.750 -2.100  2.500  0.000  0.000  1.700 -0.500 14.300 34.600
  5.450 -9.750 -2.350  2.750  0.000  0.000  1.250 -0.050 14.200 34.600
  5.450 -9.750 -2.500  2.850  0.000  0.000  0.750  0.650 14.100 35.000
  5.450 -9.750 -2.350  2.700  0.000  0.000  0.200  1.100 14.000 35.200
  5.450 -9.750 -2.300  2.700  0.000  0.000 -0.300  1.700 13.900 35.800
  5.450 -9.750 -2.000  2.400  0.000  0.000 -0.850  2.300 13.800 36.400
  5.400 -9.700 -1.650  2.050  0.000  0.000 -1.050  2.500 13.700 37.400
  5.350 -9.650 -1.200  1.600  0.000  0.000 -1.050  2.500 13.600 38.800
  5.300 -9.650 -0.800  1.200  0.000  0.000 -0.800  2.200 13.500 40.800
  5.300 -9.600 -0.500  0.900  0.000  0.000 -0.500  1.900 13.400 42.600
  5.250 -9.600 -0.050  0.500  0.000  0.000  0.400  0.850 13.200 52.000
```

****

VELOCITY PROFILES MEASURED AT 550 RPM
TANK DIAMETER= 12.25 IN.

****

```
 9
 2 4
15MAR 16, 1969 2.54
     35  3.000  6.000 12.000  3.250 13.950 27.2  3.     550.   78.    44.1
2.95   -13.15 -1.    1.5    0.     0.     -2.6   3.85   10.5   67.6
3.     -13.15 -1.6   2.1    0.     0.     -4.9   6.35   10.6   61.2          3
3.1    -13.25 -3.8   4.25   0.     0.     -9.7   11.15  10.7   58.4
3.1    -13.3  -6.9   7.2    0.     0.     -13.   14.7   10.8   56.2
3.3    -13.52 -10.15 10.4   0.     0.     -13.5  15.2   10.9   55.2
3.4    -13.6  -13.1  13.35  0.     0.     -10.9  12.6   11.    52.2
3.55   -13.7  -16.1  16.35  0.     0.     -3.7   5.     11.1   52.2
3.55   -13.75 -17.1  17.3   0.     0.     3.6    -3.05  11.2   53.2
3.45   -13.66 -14.4  14.6   0.     0.     10.3   -10.1  11.3   53.2
3.35   -13.52 -12.2  12.4   0.     0.     13.9   -13.9  11.4   53.2
3.25   -13.45 -7.9   8.15   0.     0.     14.1   -14.1  11.5   55.2
3.05   -13.25 -4.8   5.25   0.     0.     11.    -10.8  11.6   56.
3.     -13.2  -2.5   2.95   0.     0.     7.6    -7.3   11.7   59.2
2.95   -13.15 -1.3   1.8    0.     0.     4.1    -3.5   11.8   62.6
2.95   -13.15 -.95   1.45   0.     0.     1.1    -.7    11.9   65.4
```

```
 9 4
14MAR 17, 1969 2.54
     36  3.000  6.000 12.000   3.250 13.950 27.2   3.      550.    78.     5.5
2.95    -13.15 -.9    1.45    0.      0.     2.1    -1.4    11.9    62.8
3.0     -13.2  -2.    2.6     0.      0.     6.9    -6.5    11.7    58.2
3.1     -13.3  -4.    4.5     0.      0.     9.     -9.2    11.6    55.8
3.2     -13.45 -7.3   7.7     0.      0.     14.    -14.    11.5    54.
3.3     -13.5  -11.4  11.7    0.      0.     14.8   -14.8   11.4    53.2
3.45    -13.65 -14.5  14.7    0.      0.     11.    -10.8   11.3    52.6
3.55    -13.8  -17.6  18.     0.      0.     3.8    -3.1    11.2    53.
3.5     -13.8  -17.9  18.     0.      0.     -3.6   5.      11.1    52.4
3.4     -13.7  -15.35 15.7    0.      0.     -11.5  13.3    11.     53.2
3.4     -13.6  -11.4  11.6    0.      0.     -14.5  16.4    10.9    54.2
3.2     -13.4  -6.6   7.      0.      0.     -13.3  15.1    10.8    57.4
3.0     -13.25 -4.1   4.6     0.      0.     -10.2  11.9    10.7    60.
2.95    -13.25 -1.6   2.1     0.      0.     -4.6   5.9     10.6    60.6
2.9     -13.2  -.8    1.35    0.      0.     -.8    2.      10.4    64.

*******************************************************************************

                VELOCITY PROFILES MEASURED AT 333.3 RPM
                      TANK DIAMETER= 11.5 IN.

*******************************************************************************

 9
 2 4
11MAR 20, 1969 2.54
     37  3.000  6.000 12.000   6.0   14.75  26.8   2.5     333.33 78.6    44.1
2.12    -12.55 -1.05  .7      0.      0.     -2.3   3.1     14.3    76.8
2.2     -12.65 -1.9   1.5     0.      0.     -5.6   6.5     14.4    70.
2.3     -12.7  -4.3   3.8     0.      0.     -7.8   8.9     14.5    64.
2.4     -12.8  -7.3   6.7     0.      0.     -6.7   7.8     14.6    60.6
2.5     -12.75 -9.1   8.5     0.      0.     -2.4   3.2     14.7    59.
2.5     -12.9  -9.1   8.6     0.      0.     3.4    -3.15   14.8    58.8
2.4     -12.85 -8.4   7.8     0.      0.     8.1    -8.2    14.9    61.2
2.25    -12.7  -5.6   5.      0.      0.     9.6    -9.8    15.     65.2
2.2     -12.7  -3.6   3.2     0.      0.     8.1    -8.2    15.1    69.2
2.15    -12.6  -2.1   1.7     0.      0.     5.6    -5.5    15.2    73.2
2.1     -12.6  -1.    1.15    0.      0.     3.3    -3.0    15.3    81.4
 2 4
13MAR 23, 1969 2.54
     40  3.000  6.000 12.000   6.0   14.75  26.8   2.5     333.33 75.75   5.5
2.02    -12.7  -1.1   .6      0.      0.     1.3    -1.     15.4    79.2
2.02    -12.7  -1.15  .65     0.      0.     2.6    -2.3    15.3    77.4
2.08    -12.75 -1.7   1.15    0.      0.     5.3    -5.3    15.2    70.6
2.15    -12.8  -3.2   2.6     0.      0.     7.6    -7.8    15.1    67.4
2.2     -12.9  -5.5   4.9     0.      0.     9.15   -9.45   15.     64.
2.35    -13.   -7.7   7.05    0.      0.     7.75   -7.9    14.9    60.8
2.35    -13.   -8.75  8.1     0.      0.     3.6    -3.4    14.8    59.
2.35    -13.   -8.65  8.      0.      0.     -1.05  2.15    14.7    59.8
2.3     -12.9  -6.9   6.3     0.      0.     -6.5   7.4     14.6    61.4
2.2     -12.85 -4.65  4.1     0.      0.     -7.25  8.25    14.5    65.2
```

```
2.1     -12.75 -2.65  2.25    0.      0.      -5.25  6.1     14.4    68.2
2.05    -12.7  -1.6   1.15    0.      0.      -2.45  3.2     14.3    72.4
2.03    -12.65 -1.1   .75     0.      0.      -.7    1.3     14.2    75.4
 2 4
12MAR 21, 1969 2.54
     38  3.000  6.000 12.000  6.0    14.75  26.8   3.      333.33  78.     44.1
2.15    -12.6  -1.1   .9      0.      0.      3.4    -3.     15.3    60.4
2.15    -12.6  -1.5   1.2     0.      0.      4.4    -4.     15.2    59.6
2.2     -12.65 -2.7   2.235   0.      0.      5.3    -5.1    15.1    56.6
2.25    -12.75 -3.7   3.25    0.      0.      4.9    -4.75   15.     55.4
2.27    -12.75 -4.6   4.05    0.      0.      3.95   -3.6    14.9    54.4
2.3     -12.75 -4.95  4.45    0.      0.      1.8    -1.35   14.8    54.4
2.25    -12.77 -4.85  4.4     0.      0.      -1.15  1.9     14.7    53.6
2.25    -12.75 -4.45  3.95    0.      0.      -3.15  3.95    14.6    55.4
2.2     -12.7  -3.55  3.1     0.      0.      -3.95  4.85    14.5    56.4
2.15    -12.65 -2.4   2.      0.      0.      -3.7   4.55    14.4    58.
2.1     -12.6  -1.75  1.4     0.      0.      -2.4   3.15    14.3    61.
2.1     -12.6  -1.3   .9      0.      0.      -1.25  1.9     14.2    62.8
 9 4
13MAR 22, 1969 2.54
     39  3.000  6.000 12.000  6.0    14.75  26.8   3.      333.33  77.     5.5
2.05    -12.6  -1.    .7      0.      0.      -.9    1.6     14.2    62.6
2.1     -12.6  -1.1   .8      0.      0.      -2.    2.8     14.3    58.6
2.1     -12.65 -1.6   1.2     0.      0.      3.1    -3.95   14.4    56.6
2.15    -12.7  -2.9   2.5     0.      0.      -3.8   4.7     14.5    55.6
2.2     -12.7  -4.    3.55    0.      0.      -3.5   4.3     14.6    53.8
2.2     -12.75 -4.7   4.25    0.      0.      -1.6   2.3     14.7    53.4
2.25    -12.8  -4.9   4.5     0.      0.      .9     -.4     14.8    53.4
2.25    -12.8  -4.9   4.45    0.      0.      3.     -2.7    14.9    53.8
2.2     -12.75 -4.8   4.3     0.      0.      4.8    -4.5    15.     55.2
2.16    -12.72 -3.1   2.65    0.      0.      4.8    -4.6    15.1    56.4
22.1    -12.66 -2.6   2.2     0.      0.      4.4    -4.2    15.2    58.6
2.1     -12.65 -2.2   1.75    0.      0.      3.5    -3.3    15.3    62.
2.05    -12.65 -1.65  1.3     0.      0.      2.4    -2.1    15.4    64.6
```

SAMPLE OUTPUT FOR RUN NUMBER 29

RAW DATA MAR 10, 1969

RUN NUMBER	=29	
IMPELLER DIAMETER	= 3.00	
IMPELLER HT OF TANK BOTTOM	= 6.00	
LEVEL OF WATER IN TANK	=12.00	
HEIGHT OF PITOT TUBE OFF TANK BOTTOM	= 3.25	
VERNIER STAND READING	=13.95	
ZERO ERROR FOR ANGLE	=27.20	
DIST PROBE TO AXIS	= 3.00	
RPM SETTING	=333.33	
FLUID TEMP	=75.00	DEG F
ANGULAR POSITION FROM BAFFLE	= 5.50	DEG

P(1)-P(ATM) LEFT	P(1)-P(ATM) RIGHT	P(1)-P(2) LEFT	P(1)-P(2) RIGHT	P(2)-P(3) LEFT	P(2)-P(3) RIGHT	P(4)-P(5) LEFT	P(4)-P(5) RIGHT	H	ANGLE
3.10	-12.90	-0.40	0.95	0.0	0.0	0.40	1.60	10.50	62.40
3.10	-12.90	-0.40	1.00	0.0	0.0	-1.60	2.85	10.60	60.00
3.15	-12.95	-1.05	1.60	0.0	0.0	-3.30	4.70	10.70	57.20
3.20	-13.00	-1.70	2.70	0.0	0.0	-3.90	5.30	10.80	56.60
3.25	-13.05	-3.70	4.20	0.0	0.0	-4.40	5.80	10.90	55.20
3.30	-13.10	-4.80	5.20	0.0	0.0	-3.10	4.40	11.00	53.80
3.30	-13.15	-5.50	5.90	0.0	0.0	-0.15	1.30	11.10	53.60
3.30	-13.10	-5.55	5.90	0.0	0.0	3.00	-2.20	11.20	53.00
3.25	-13.05	-5.00	5.40	0.0	0.0	5.10	-4.50	11.30	53.80
3.25	-13.05	-4.00	4.40	0.0	0.0	5.80	-5.25	11.40	54.60
3.20	-13.00	-2.45	2.90	0.0	0.0	5.50	-4.90	11.50	57.00
3.12	-12.94	-1.50	2.00	0.0	0.0	4.20	-3.60	11.60	58.80
3.10	-12.96	-0.65	1.05	0.0	0.0	2.50	-1.85	11.70	60.00
3.05	-12.95	-0.60	1.00	0.0	0.0	1.45	-0.60	11.80	60.00

P(1)	P(2)	P(3)	P(4)	SUM SQ REG
1.1191999E 01	1.8000000E 01	1.1587989E-01	9.9999993E-04	4.7790601E 02
1.0791992E 01	1.8500000E 01	1.1587989E-01	2.9999965E-03	2.9860718E 02
1.1591991E 01	1.8500000E 01	1.1587989E-01	2.7999969E-03	2.5867212E 02
1.1261989E 01	1.8499954E 01	1.1587989E-01	2.7499963E-03	2.3648961E 02
1.1281989E 01	1.8549973E 01	1.1587989E-01	2.7499963E-03	2.3564842E 02
1.1275987E 01	1.8544972E 01	1.1587989E-01	2.7429950E-03	2.3563470E 02

The above is the value of the parameters σ, A, a, and z_o at every 30th evaluation of SS as defined by Equation C-2.

D = 3.00000

R = 3.00000

Y	Q	ANGLE
0.05833	44.82013	35.20000
0.05000	45.64259	32.80000
0.04167	62.79556	30.00000
0.03333	80.91562	29.39999
0.02500	108.42258	28.00000
0.01667	121.98497	26.59999
0.00833	130.24434	26.39999
-0.00000	130.52959	25.80000
-0.00833	124.40071	26.59999
-0.01667	111.80104	27.39999
-0.02500	89.22432	29.80000
-0.03333	72.16724	31.59999
-0.04167	50.29568	32.80000
-0.05000	48.79399	32.80000

	PARAMETERS
1	11.27798748
2	18.54493713
3	0.11587989
4	0.00274200

AVG ANGLE = 29.65705872
WT AVG ANGLE= 27.61441040 VELOCITY FACTOR= 0.50

Q	QC
44.82012939	36.85945129
45.64259338	50.17221069
62.79556274	66.47894287
80.91561890	85.00456238
108.42257690	103.86741638
121.98497009	120.08189392
130.24433899	130.23974609
130.52958679	131.81726074
124.40071106	124.39604187
111.80104065	109.88250732
89.22431946	91.54614258
72.16723633	72.63247681
50.29568481	55.42958069
48.79399109	41.06221008

SUM OF SQUARES OF (Q-QCALC) 235.63095093

GOODNESS OF FIT 0.99190027

BHALF = 0.03907494 BCALC = 0.03734012

UHALF = 66.16113281

HALF WIDTH OF JET AT XD =3.00, 1.60 INCHES

P(1)-P(2)	P(4)-P(5)	DEL U**2 EXP	DEL U**2 CALC	VZ CALC	DIFF OF J**2
0.5315	-0.8661	-0.2309	-0.2475	-0.2002	-0.0165
0.5512	-2.1457	-0.5720	-0.4234	-0.1597	0.1487
1.0433	-3.5433	-0.9447	-0.6617	-0.1172	0.2829
1.7323	-4.0157	-1.0706	-0.9114	-0.0768	0.1592
3.1102	-4.4094	-1.1756	-1.0484	-0.0432	0.1271
3.9370	-3.3465	-0.8922	-0.9140	-0.0197	-0.0218
4.4882	-0.9646	-0.2572	-0.4419	-0.0060	-0.1848
4.5079	1.6535	0.4408	0.2228	0.0028	-0.2180
4.0945	3.3858	0.9027	0.7881	0.0141	-0.1145
3.3071	3.9567	1.0549	1.0399	0.0340	-0.0150
2.1063	3.7008	0.9866	0.9791	0.0644	-0.0076
1.3780	2.6772	0.7137	0.7505	0.1029	0.0368
0.6693	1.3189	0.3516	0.4990	0.1452	0.1474
0.6299	0.4134	0.1102	0.2998	0.1868	0.1896

RADIAL VELOCITY ANALYSIS

Q	QC
36.62449646	32.66082764
38.36560059	44.45713806
54.38250732	59.90635681
70.49476624	75.32167053
95.73139954	92.03572083
109.07333374	106.40310669
116.66134644	115.40379333
117.51817322	116.80154419
111.23338318	110.22555542
99.25863647	97.36524963
77.42572021	81.11764526
61.46673584	64.35850525
42.27684021	49.11526489
41.01455688	36.38455200

SUM OF SQUARES OF (Q-QCALC) 214.25904846

GOODNESS OF FIT 0.99151355

LIST F-2

FORTRAN LISTING FOR PROGRAM VELPRO, SUPPORTING SUBSTANCES ARE POLY AND CURVEF.

ALSO GIVEN ARE THE NECESSARY INPUT DATA AND SAMPLE OUTPUT.

```
C*******************************************************************************
C                          MAIN PROGRAM VELPRO
C*******************************************************************************

      DIMENSION R(10),Q(10),RR(10,7),QQ(10,7),COEFS(10),CO(10,6)          VELP   1
      DIMENSION DR(10,6),ZZ(10,7),VR(10),Z(10),CZ(10,6),DZ(10,6)          VELP   2
      DIMENSION V1(10,4),V2(10,4),V3(10,4)                                VELP   3
      COMMON COEFS,LPRINT                                                 VELP   4
C                                                                         VELP   5
C--------L= ORDER OF POLYNOMIAL FIT                                       VELP   6
C         N= NUMBER OF PROFILES EXAMINED                                  VELP   7
C         M= NUMBER OF Z PLANES IN WHICH PROFILES ARE EXAMINED            VELP   8
C         Q= ARRAY HOLDS STREAM FUNCTION AT CONSTANT R OR Z               VELP   9
C         R= ARRAY HOLDS R OR Z                                           VELP  10
C                                                                         VELP  11
      LPRINT=0                                                            VELP  12
      LPRINT=1                                                            VELP  13
12    READ(5,11)KGROUP                                                    VELP  14
11    FORMAT(I2,F10.2)                                                    VELP  15
      SCALER=1./12.*SQRT(2.*3.1416)                                       VELP  16
      IF(LPRINT.EQ.1)WRITE(6,100)SCALER                                   VELP  17
100   FORMAT(1X ,10X,'SCALER =',F10.4)                                    VELP  18
101   FORMAT(1H1,15(/))                                                   VELP  19
      WRITE(6,101)                                                        VELP  20
      M=7                                                                 VELP  21
      N=6                                                                 VELP  22
      L=3                                                                 VELP  23
      LL=L+1                                                              VELP  24
C                                                                         VELP  25
C--------START CALCULATION OF STREAM FUNCTION AT CONSTANT Z               VELP  26
C                                                                         VELP  27
      DO6I=1,N                                                            VELP  28
      READ(5,1)(Q(K),K=1,M)                                               VELP  29
      READ(5,1)(R(K),K=1,M)                                               VELP  30
1     FORMAT(1X,7F10.2)                                                   VELP  31
C                                                                         VELP  32
C--------STORE STREAM FUNCTION IN QQ AND RADIUS IN RR                     VELP  33
C                                                                         VELP  34
```

```
      T=11.5/2.                                                          VELP  35
      DO6J=1,M                                                           VELP  36
      RR(J,I)=T-R(J)                                                     VELP  37
6     QQ(J,I)=Q(J)                                                       VELP  38
      IF(LPRINT.EQ.1)GOTO30                                              VELP  39
      WRITE(6,20)((QQ(I,J),J=1,N),I=1,M)                                 VELP  40
20    FORMAT(1X/30X,'PSI MATRIX AT CONSTANT Z'//(10X,6E10.4))            VELP  41
      WRITE(6,21)((RR(I,J),J=1,N),I=1,M)                                 VELP  42
21    FORMAT(1X/30X,'CORESPONDING R MATRIX   '//(10X,6E10.4))            VELP  43
30    DO2I=1,M                                                           VELP  44
      DO29K=1,N                                                          VELP  45
      R(K)=RR(I,K)                                                       VELP  46
29    Q(K)=QQ(I,K)                                                       VELP  47
      CALL POLY(R,Q,L,N,0.5)                                             VELP  48
C                                                                        VELP  49
C--------STORE POLYNOMIAL COEFFICIENTS IN CO                            VELP  50
C         STORE DERIVATIVES OF POLYNOMIAL IN DR                          VELP  51
C                                                                        VELP  52
      DO2J=1,LL                                                          VELP  53
      LF=J-1                                                             VELP  54
      CO(I,J)=COEFS(J)                                                   VELP  55
      IF(J.GE.2)DR(I,LF)=COEFS(J)*LF                                     VELP  56
2     CONTINUE                                                           VELP  57
      IF(LPRINT.EQ.1)GOTO31                                              VELP  58
      WRITE(6,3)((CO(I,J),J=1,LL),I=1,M)                                 VELP  59
3     FORMAT(1X//20X,'PSI COEFFICIENT MATRIX'//(10X,4E15.6))             VELP  60
      WRITE(6,4)((DR(I,J),J=1,L),I=1,M)                                  VELP  61
4     FORMAT(1X//20X,'VEL COEFFICIENT MATRIX'//(10X,3E15.6))             VELP  62
C                                                                        VELP  63
C--------CALCULATE VZ FUNCTION OF R AT CONSTANT Z                       VELP  64
C                                                                        VELP  65
31    DO13K=2,M,2                                                        VELP  66
      DO8I=1,N                                                           VELP  67
      R(I)=  RR(K,I)                                                     VELP  68
      TEMP=DR(K,1)                                                       VELP  69
      DO10J=2,L                                                          VELP  70
10    TEMP=TEMP+DR(K,J)*R(I)**(J-1)                                      VELP  71
      VR(I)=TEMP*(-1./(R(I)*SCALER**2))                                  VELP  72
      IF(K-4)33,34,35                                                    VELP  73
33    V1(I,1)=T-R(I)                                                     VELP  74
      V1(I,2)=VR(I)                                                      VELP  75
      GOTO8                                                              VELP  76
34    V2(I,1)=T-R(I)                                                     VELP  77
      V2(I,2)=VR(I)                                                      VELP  78
      GOTO8                                                              VELP  79
35    V3(I,1)=T-R(I)                                                     VELP  80
      V3(I,2)=VR(I)                                                      VELP  81
8     CONTINUE                                                           VELP  82
      IF(LPRINT.EQ.1)GOTO13                                              VELP  83
      WRITE(6,14)(R(J),VR(J),J=1,N)                                      VELP  84
14    FORMAT(20X,'VELOCITY PROFILE, VZ VERSUS R'/30X,'R',10X,'VR'//      VELP  85
     1(20X,2F15.4))                                                      VELP  86
13    CONTINUE                                                           VELP  87
```

```
C                                                                       VELP  98
C--------START CALCULATION OF STREAM FUNCTION AT CONSTANT R            VELP  99
C         K, SELECTS ALTERNATE ROW                                      VELP  90
C         J, COUNTS COLUMNS IN SELECTED ROW                             VELP  91
C         I, EVALUATES NEW ELEMENTS OF Z AND STREAM FUNCTION PSI        VELP  92
C         STORE POLYNOMIAL COEFFICIENTS AT CONSTANT Z IN CZ             VELP  93
C         STORE DERIVATIVES OF POLYNOMIAL AT CONSTANT Z IN DZ           VELP  94
C                                                                       VELP  95
      DO15K=2,M,2                                                       VELP  96
      DO9J=1,N                                                          VELP  97
      RTEM=RR(K,J)                                                      VELP  98
      ZZ(M+1,J)=RTEM                                                    VELP  99
      TEMP=1.                                                           VELP 100
      DO5I=1,M                                                          VELP 101
      QTEM=CO(I,1)                                                      VELP 102
      DO7KK=1,L                                                         VELP 103
7     QTEM=QTEM+CO(I,KK+1)*RTEM**KK                                     VELP 104
      Q(I)=QTEM                                                         VELP 105
      TEMP=TEMP+0.5                                                     VELP 106
      R(I)=TEMP                                                         VELP 107
      QQ(I,J)=Q(I)                                                      VELP 108
5     ZZ(I,J)=R(I)                                                      VELP 109
      CALL POLY(R,Q,L,M,0.5)                                            VELP 110
      DO8KK=1,LL                                                        VELP 111
      LF=KK-1                                                           VELP 112
      CZ(J,KK)=COEFS(KK)                                                VELP 113
      IF(KK.GE.2)DZ(J,LF)=COEFS(KK)*LF                                  VELP 114
9     CONTINUE                                                          VELP 115
      IF(LPRINT.EQ.1)GOTO32                                             VELP 116
      WRITE(6,22)((QQ(I,J),J=1,N),I=1,M)                                VELP 117
22    FORMAT(1X/30X,'PSI MATRIX AT CONSTANT R'/(10X,6F10.4))            VELP 118
      WRITE(6,23)((ZZ(I,J),J=1,N),I=1,M)                                VELP 119
23    FORMAT(1X/30X,'CORESPONDING Z MATRIX   '/(10X,6F10.2))            VELP 120
      WRITE(6,24)(ZZ(M+1,J),J=1,N)                                      VELP 121
24    FORMAT(1X/30X,'CORESPONDING VALUES OF R, WHEN CONSTANT'/          VELP 122
     1(10X,7F10.4))                                                     VELP 123
      WRITE(6,3)((CZ(I,J),J=1,(L),I=1,N)                                VELP 124
      WRITE(6,4)((DZ(I,J),J=1,L),I=1,N)                                 VELP 125
C                                                                       VELP 126
C--------CALCULATE VR FUNCTION OF Z AT CONSTANT R                       VELP 127
C         KL SELECTS POINTS IN DESIRED ROW                              VELP 128
C         I EVALUATES STREAM FUNCTION, FUNCTION OF Z AT DESIRED POINT   VELP 129
C                                                                       VELP 130
32    ZTEM=ZZ(K,1)                                                      VELP 131
      DO16KL=1,N                                                        VELP 132
      R(KL)=ZZ(M+1,KL)                                                  VELP 133
      TEMP=DZ(KL,1)                                                     VELP 134
      DO18J=2,L                                                         VELP 135
18    TEMP=TEMP+DZ(KL,J)*ZTEM**(J-1)                                    VELP 136
      VR(KL)=TEMP/(R(KL)*SCALER**2)                                     VELP 137
      IF(K-4)37,38,39                                                   VELP 138
37    V1(KL,3)=VR(KL)                                                   VELP 139
      GOTO16                                                            VELP 140
```

```
38    V2(KL,3)=VR(KL)                                                    VELP 141
      GOTO16                                                             VELP 142
39    V3(KL,3)=VR(KL)                                                    VELP 143
16    CONTINUE                                                           VELP 144
      IF(LPRINT.EQ.1)GOTO15                                              VELP 145
      WRITE(6,19)(R(J),VR(J),J=1,N)                                      VELP 146
19    FORMAT(20X,'VELOCITY PROFILE, VZ VERSUS R'/30X,'R',10X,'VR'//      VELP 147
     1(20X,2F15.4))                                                      VELP 148
15    CONTINUE                                                           VELP 149
      DO40I=1,N                                                          VELP 150
      V1(I,4)=SQRT(V1(I,2)**2+V1(I,3)**2)                                VELP 151
      V2(I,4)=SQRT(V2(I,2)**2+V2(I,3)**2)                                VELP 152
40    V3(I,4)=SQRT(V3(I,2)**2+V3(I,3)**2)                                VELP 153
      WRITE(6,41)((V1(I,J),J=1,4),I=1,N)                                 VELP 154
      WRITE(6,42)((V2(I,J),J=1,4),I=1,N)                                 VELP 155
      WRITE(6,43)((V3(I,J),J=1,4),I=1,N)                                 VELP 156
41    FORMAT(1X/20X,'VELOCITY PROFILE AT Z=2 INS.'/                      VELP 157
     1/18X,'R',8X,'VZ',8X,'VR',8X,'V'/(10X,4F10.3))                      VELP 158
42    FORMAT(1X/20X,'VELOCITY PROFILE AT Z=3 INS.'//(10X,4F10.3))        VELP 159
43    FORMAT(1X/20X,'VELOCITY PROFILE AT Z=4 INS.'//(10X,4F10.3))        VELP 160
      IF(KGROUP.LT.5)GOTO12                                              VELP 161
      STOP                                                               VELP 162
      END                                                                VELP 163
```

****

SUBROUTINE POLY

```
**********                                                                POLY   1
      SUBROUTINE POLY(X,Y,L,N,TOL)                                       POLY   2
C                                                                        POLY   3
C--------L=DEGREE OF POLYNOMIAL                                          POLY   4
C         N= NUMBER OF DATA POINTS                                       POLY   5
C         TOL= MAXIMUM DESIRED STANDARD ERROR                            POLY   6
C         SE= STANDARD ERROR, SQRT(SSR/DEG. FREEDOM)                     POLY   7
C         INDIK= 1, IF SE, FOR A POLYNOMIAL OF LOWER DEGREE IS LESS      POLY   8
C                THAN TOL                                                POLY   9
C                                                                        POLY  10
      DIMENSION X(500),Y(500),YC(500),COEFS(10)                          POLY  11
      COMMON COEFS,LPRINT                                                POLY  12
16    CALL CURVEF(N,TOL,L,X,Y,SE,YC,COEFS,INDIK)                         POLY  13
      JJ=0                                                               POLY  14
      ERROR=3.*SE                                                        POLY  15
      YM=0                                                               POLY  16
      IF(LPRINT.EQ.1)GOTO64                                              POLY  17
      WRITE(6,7)                                                         POLY  18
7     FORMAT(1H1,     'BEGIN POLYNOMIAL FIT'//)                          POLY  19
      WRITE(6,4)SE,INDIK                                                 POLY  20
4     FORMAT(1HO,7HSE     =,F20.8,//1X,7HINDIK =,I10,////,               POLY  21
     13X,1HI,10X,4HX(I),16X,5HY-OBS,17X,6HY-CALC)                        POLY  22
      WRITE(6,61)                                                        POLY  23
61    FORMAT(1X///)                                                      POLY  24
```

```
64      DO10I=1,N                                                       POLY  24
        JJ=JJ+1                                                         POLY  25
        Y(JJ)=Y(I)                                                      POLY  26
        DIFF=ABS(Y(I)-YC(I))                                            POLY  27
        IF(DIFF.LT.ERROR)GOTO10                                         POLY  28
        JJ=JJ-1                                                         POLY  29
        WRITE(6,5)I,X(I),Y(I),YC(I)                                     POLY  30
10      YM=YM+Y(I)                                                      POLY  31
        IF((JJ+1).GE.N)GOTO15                                           POLY  32
        IF(INDIK.EQ.1)L=3                                               POLY  33
        N=JJ                                                            POLY  34
        GOTO16                                                          POLY  35
15      IF(LPRINT.EQ.1)GOTO14                                           POLY  36
        WRITE(6,62)N,JJ                                                 POLY  37
62      FORMAT(1HO,10X,'NO OF DATA POINTS =',I3,10X,I2//)               POLY  38
        WRITE(6,5)(I,X(I),Y(I),YC(I),I=1,N)                             POLY  39
5       FORMAT(1X,I3,3F20.8)                                            POLY  40
14      YM=YM/FLOAT(N)                                                  POLY  41
        SSR=0.                                                          POLY  42
        SSM=0.                                                          POLY  43
        DO11I=1,N                                                       POLY  44
        SSR=SSR+(Y(I)-YC(I))**2                                         POLY  45
11      SSM=SSM+(Y(I)-YM)**2                                            POLY  46
        COST=0.                                                         POLY  47
        IF(SSR.GT.SSM)GOTO12                                            POLY  48
        COST=SQRT(1.-SSR/SSM)                                           POLY  49
12      IF(LPRINT.EQ.1)GOTO63                                           POLY  50
        WRITE(6,13)YM,SSR,SSM,COST                                      POLY  51
13      FORMAT(1HO,1X,5H YM =,F20.8,/2X,5HSSR =,F20.8,/2X               POLY  52
       1,5HSSM =,F20.8,/1X,'CORR COEF =',F14.8/)                        POLY  53
        LL=L+1                                                          POLY  54
        WRITE(6,6)(I,COEFS(I),I=1,LL)                                   POLY  55
6       FORMAT(1HO,10X ,6HCOEFS(,I2,3H) =,F20.8)                        POLY  56
63      RETURN                                                          POLY  57
        END                                                             POLY  58
```

****

SUBROUTINE CURVFF
THIS SUBROUTINE IS A PART OF LSU SHARE LIBRARY

****

****

INPUT DATA
PUNCHED OUTPUT FROM SUBROUTINE SPRINT OF PROGRAM FLOWANL
FOR LISTING SEE LIST F-1

****

****

STREAMFUNCTION PSI VERSUS R FOR MATRIX OF POINTS (FIGURE IV-2)
BELOW IMPELLER CENTERLINE

****

2.50	2.50	2.50	2.50	2.50	2.50	2.50
0.54028	0.46790	0.41850	0.45707	0.53453	0.67219	1.03933
5.00	5.00	5.00	5.00	5.00	5.00	5.00
0.78518	0.67999	0.60820	0.66631	0.77923	0.97990	1.51454
7.50	7.50	7.50	7.50	7.50	7.50	7.50
0.96330	0.83424	0.74617	0.81623	0.95455	1.20038	1.85531
10.00	10.00	10.00	10.00	10.00	10.00	10.00
1.15527	1.00049	0.89487	0.96761	1.13159	1.42301	2.19940
12.50	12.50	12.50	12.50	12.50	12.50	12.50
1.39912	1.21167	1.08375	1.19181	1.38209	1.73802	2.68629
15.00	15.00	15.00	15.00	15.00	15.00	15.00
1.82058	1.57667	1.41021	1.53309	1.79289	2.25462	3.48474

****

STREAMFUNCTION PSI VERSUS R FOR MATRIX OF POINTS (FIGURE IV-2)
ABOVE IMPELLER CENTERLINE

****

2.50	2.50	2.50	2.50	2.50	2.50	2.50
0.54101	0.46853	0.41906	0.38255	0.38820	0.43402	0.50116
5.00	5.00	5.00	5.00	5.00	5.00	5.00
0.78624	0.68090	0.60902	0.55595	0.56574	0.63252	0.73037
7.50	7.50	7.50	7.50	7.50	7.50	7.50
0.96459	0.83536	0.74717	0.68207	0.69314	0.77495	0.89483
10.00	10.00	10.00	10.00	10.00	10.00	10.00
1.15683	1.00184	0.89607	0.81800	0.82260	0.91969	1.06197
12.50	12.50	12.50	12.50	12.50	12.50	12.50
1.40100	1.21330	1.08521	0.99066	1.00389	1.12238	1.29601
15.00	15.00	15.00	15.00	15.00	15.00	15.00
1.82302	1.57879	1.41211	1.28907	1.30266	1.45642	1.68172

SAMPLE OUTPUT FOR PROGRAM VELPRO

VELOCITY PROFILE AT Z=2 INS.

R	VZ	VR	V
0.5	74.3	8.3	74.7
0.7	67.2	10.3	68.0
0.8	62.2	11.7	63.3
1.0	56.8	12.9	58.3
1.2	50.2	14.0	52.1
1.6	39.1	14.4	41.7

VELOCITY PROFILE AT Z=3 INS.

0.5	76.2	-10.5	76.9
0.7	69.0	-10.8	69.8
0.8	63.9	-11.0	64.8
1.0	58.7	-11.3	59.8
1.2	51.4	-11.7	52.7
1.5	39.5	-11.8	41.2

VELOCITY PROFILE AT Z=4 INS.

0.7	59.1	-14.9	61.0
1.0	50.5	-29.2	58.3
1.2	45.5	-36.7	58.5
1.4	41.6	-42.2	59.3
1.7	38.4	-46.7	60.5
2.3	41.0	-47.7	62.9

VELOCITY PROFILE AT Z=2 INS.

R	VZ	VR	V
0.5	73.9	9.7	74.5
0.7	67.1	12.5	68.3
0.8	62.2	14.2	63.8
1.0	57.0	15.6	59.0
1.2	50.2	16.7	52.9
1.6	38.5	16.5	41.9

VELOCITY PROFILE AT Z=3 INS.

0.4	88.9	1.9	88.9
0.6	80.2	2.7	80.2
0.7	73.9	3.1	73.9
0.8	67.1	3.5	67.2
1.0	58.7	3.8	58.8
1.3	44.3	3.9	44.5

VELOCITY PROFILE AT Z=4 INS.

0.4	79.6	-8.7	80.0
0.6	72.1	-11.3	73.0
0.8	66.7	-12.8	68.0
0.9	61.2	-14.0	62.8
1.1	53.5	-15.0	55.5
1.5	40.4	-14.9	43.1

LIST F-3

FORTRAN LISTING FOR PROGRAM TANKANL WITH SUPPORTING SUBROUTINES OMEGA. ALSO GIVEN ARE THE RAW DATA AND A SAMPLE OUTPUT FOR PORT 1.

```
**********************************************************************************

                              MAIN PROGRAM TANKANL

**********************************************************************************

C                                                                          TANK   1
C--------THIS PROGRAM ANALYSES VELOCITY PROFILE DATA OBTAINED WITH          TANK   2
C         A HORIZONTAL PASS OF THE PROBE. FOR RUN NO. 45, PROBE WAS        TANK   3
C         REMOUNTED AND A NEW MANOMETER WAS USED FOR MANOMETER D.          TANK   4
C         MANOMETER A READINGS WERE DELETED AS THEY SERVED NO USEFUL       TANK   5
C         PURPOSE                                                          TANK   6
C                                                                          TANK   7
      DIMENSION DELP4(9),DELPT(9),THETA(9),D(50,10),DA(4),P12(50)          TANK   8
      DIMENSION P45(50)                                                    TANK   9
C                                                                          TANK  10
C--------DATA STATEMENT CONTAINS EXPERIMENTAL POINTS FROM FIGURE IV-4      TANK  11
C         THETA, EXPERIMENTAL POINTS FROM CURVE C                          TANK  12
C         DELPT, EXPERIMENTAL POINTS FROM CURVE B                          TANK  13
C         DELP4, EXPERIMENTAL POINTS FROM CURVE A                          TANK  14
C                                                                          TANK  15
      DATA THETA/-40.,-30.,-20.,-10.,0.,10.,20.,30.,40./,                  TANK  16
     1DELPT/1.25,1.21,1.185,1.185,1.15,1.1,1.07,1.1,1.215/,                TANK  17
     2DELP4/-.8,-.63,-.42,-.3,-.12,.04,.26,.55,.93/                        TANK  18
      TEMP=2.*32.17*0.19579/(12.*2.54)                                     TANK  19
      TE=3.1416/180.                                                       TANK  20
10    READ(5,1)KK                                                          TANK  21
      READ(5,1)N,DA,NR,NP                                                  TANK  22
      REFH=11.47                                                           TANK  23
      IF(NR.GE.45)REFH=12.1                                                TANK  24
1     FORMAT(I2,4A4,2I2)                                                   TANK  25
      WRITE(6,20)                                                          TANK  26
20    FORMAT(1H1)                                                          TANK  27
      WRITE(6,8)DA,NR,NP                                                   TANK  28
8     FORMAT(20X,'RAW DATA',10X,4A4//20X,'RUN NUMBER=',I3,5X,'PORT',       TANK  29
     1' NUMBER=',I2//)                                                     TANK  30
      READ(5,2)((D(I,J),J=1,10),I=1,N)                                     TANK  31
2     FORMAT(10F7.2)                                                       TANK  32
      WRITE(6,9)(I,(D(I,J),J=1,10),I=1,N)                                  TANK  33
9     FORMAT(20X,I2,3X,10F10.2)                                            TANK  34
```

```
C                                                                       TANK  35
C---------TRANSFORM RAW DATA INTO PRESSURE DROPS VERSUS DISTANCE FROM     TANK  36
C          TANK WALL                                                    TANK  37
       DO3I=1,N                                                         TANK  38
       P12(I)=D(I,4)-D(I,3)                                             TANK  39
       P45(I)=D(I,7)-D(I,8)                                             TANK  40
       IF(NR.GE.45)P45(I)=P45(I)*2.54                                   TANK  41
       IF(D(I,10).GT.90.)GOTO11                                         TANK  42
       D(I,10)= D(I,10)+90.                                             TANK  43
       GOTO3                                                            TANK  44
11     D(I,10)=180.-D(I,10)                                             TANK  45
3      D(I,9)=D(I,9)-REF1                                               TANK  46
       WRITE(6,4)(I,D(I,9),P12(I),P45(I),I=1,N)                         TANK  47
4      FORMAT(1H1///33X,'T-R', 7X,'DEL P12', 5X,'DEL P45'//(20X12,3X,   TANK  48
      13F12.4))                                                         TANK  49
       WRITE(6,20)                                                      TANK  50
       WRITE(6,6)                                                       TANK  51
6      FORMAT(1X//,26X,'T-R',5X,'V', 7X,'VR', 6X,'VZ', 4X,'VTHETA',3X,  TANK  52
      1  'PITCH',3X,'YAW',3X,'CORRECTED'/65X,'ANGLE',2X,'ANGLE',3X,      TANK  53
      2'DEL P12'//)                                                     TANK  54
C                                                                       TANK  55
C---------CALCULATE VELOCITY PROFILE USING EQUATIONS IV-15 TO IV-19      TANK  56
C                                                                       TANK  57
       DO5I=1,N                                                         TANK  58
       RATIO=P45(I)*0.09537/(P12(I)*0.19579)                            TANK  59
C                                                                       TANK  60
C---------CHECK IF PRESSURE RATIOS ARE OUT OF RANGE OF FIGURE IV-5      TANK  61
C                                                                       TANK  62
       IF(RATIO.LT.(-.8).OR.RATIO.GT..8)GOTO5                           TANK  63
C                                                                       TANK  64
C---------INTERPOLATE TO OBTAIN TRUE KINETIC HEAD, P(T)-P(S).           TANK  65
C          EQUIVALENT TO LOOKING UP FIGURE IV-4                         TANK  66
C                                                                       TANK  67
       CALL OMEGA(RATIO,DELP4,THETA,9,9,ANGLE)                          TANK  68
       TP=ANGLE*TE                                                      TANK  69
       TY=D(I,10)*TE                                                    TANK  70
       CALL OMEGA(ANGLE,THETA,DELPT,9,9,DELTA)                          TANK  71
       DELTA=DELTA*P12(I)                                               TANK  72
       V=SQRT(TEMP*DELTA)*60.                                           TANK  73
       VR=V*SIN(TP)                                                     TANK  74
       VTE=V*COS(TP)                                                    TANK  75
       VZ=VTE*COS(TY)                                                   TANK  76
       VTHETA=VTE*SIN(TY)                                               TANK  77
       WRITE(6,7)I,D(I,9),V,VR,VZ,VTHETA,ANGLE,D(I,10),DELTA            TANK  78
7      FORMAT(20X,I2,8F8.3)                                             TANK  79
5      CONTINUE                                                         TANK  80
       IF(KK.LT.5)GOTO10                                                TANK  81
99     STOP                                                             TANK  82
       END                                                              TANK  83
```

****

SUBROUTINE OMEGA

FOR LISTING SEE LIST F-1

****

****

INPUT DATA

****

****

PORT NO. 1

****

1
34MAY 14, 1969 45 1

-.9	.6	-7.08	-5.87	12.2	146.
-.9	.65	-6.85	-6.1	12.3	146.
-.9	.65	-6.61	-6.31	12.4	146.
-.8	.45	-6.56	-6.4	12.5	158.8
-.75	.5	-6.5	-6.46	12.55	157.6
-.75	.4	-6.6	-6.48	12.6	157.6
-.7	.5	-6.39	-6.56	12.7	151.2
-.7	.5	-6.32	-6.6	12.8	144.2
-0.6	.4	-6.35	-6.55	12.9	144.8
-.6	-.4	-6.35	-6.55	13.	138.2
-.6	.4	-6.4	-6.5	13.1	132.8
-.6	.4	-6.45	-6.45	13.2	124.
-.55	.4	-6.56	-6.35	13.3	106.
-.65	.35	-6.65	-6.3	13.4	105.4
-.7	.3	-6.71	-6.24	13.5	99.
-.55	.25	-6.8	-6.15	13.6	94.
-.55	.2	-6.28	-6.11	13.7	89.4
-.2	0.	-6.75	-6.15	13.9	2.
-.2	0.	-6.78	-6.15	14.1	2.
-.4	.1	-6.8	-6.12	14.3	23.
-.5	.1	-6.82	-6.11	14.5	7.2
-.5	.1	-6.85	-6.1	14.7	12.8
-.45	.1	-6.85	-6.1	14.9	17.4
-.45	.1	-6.85	-6.1	15.1	17.4
-.45	.1	-6.82	-6.1	15.3	26.2
-.45	.05	-6.85	-6.1	15.5	21.6
-.55	.15	-6.9	-6.05	15.7	31.8
-.55	.2	-6.9	-6.05	15.9	31.8
-.6	.35	-7.6	-5.3	16.1	31.4
-.55	.3	-7.5	-5.4	16.3	33.8
-.55	-.3	-7.4	-5.5	16.5	39.
-.6	.3	-7.39	-5.51	16.7	39.

		-0.55	0.3	-7.4	-5.5	16.9	43.2
		-0.55	0.3	-7.4	-5.5	17.1	43.2

****

PORT NO. 2

****

1
32APRIL 14, 1969 42 2

6.1	-6.45	-1.75	1.4	-18.	-18.3	11.55	160.
6.1	-6.45	-1.8	1.4	-17.9	-18.5	11.65	160.
6.1	-6.45	-1.75	1.4	-17.65	-18.8	11.7	160.
6.1	-6.45	-1.75	1.35	-17.5	-19.15	11.75	158.6
6.1	-6.45	-1.75	1.35	-17.4	-19.5	11.8	155.
6.08	-6.45	-1.8	1.4	-17.4	-19.8	11.9	148.4
6.05	-6.42	-1.9	1.4	-17.4	-19.7	12.	144.6
6.05	-6.42	-1.45	1.05	-18.95	-21.	12.1	144.6
6.05	-6.4	-1.55	1.15	-18.95	-21.2	12.2	135.
6.05	-6.4	-1.5	1.15	-19.	-21.15	12.3	130.
6.04	-6.4	-1.3	1.	-19.6	-21.2	12.4	111.
6.05	-6.4	-1.3	1.	-19.6	-21.25	12.5	111.
5.95	-6.5	-1.1	.8	-24.9	-25.3	12.6	82.
5.95	-6.5	-1.1	.8	-25.	-25.2	12.7	89.2
5.95	-6.5	-1.1	.8	-25.1	-25.1	12.8	48.
5.95	-6.5	-1.1	.75	-25.	-25.	13.	23.4
5.95	-6.55	-1.15	.8	-25.	-25.	13.2	18.8
5.95	-6.53	-1.15	.8	-24.9	-24.9	13.4	17.8
5.95	-6.55	-1.2	.85	-24.9	-25.	13.6	10.6
5.95	-6.55	-1.2	.8	-24.8	-25.	13.8	6.6
5.95	-6.55	-1.2	.8	-24.8	-25.	14.	6.6
6.0	-6.52	-1.4	1.1	-24.3	-24.4	14.2	8.6
6.	-6.5	-1.2	.95	-24.3	-24.4	14.4	8.6
6.	-6.51	-1.15	.9	-24.25	-24.35	14.6	8.6
6.	-6.52	-1.15	.85	-24.25	-24.35	14.8	12.8
6.	-6.55	-1.15	.85	-24.25	-24.35	15.	15.6
6.	-6.55	-1.15	.85	-24.25	-24.35	15.3	22.2
6.	-6.55	-1.15	0.85	-24.25	-24.35	15.6	22.2
6.	-6.55	-1.55	.85	-24.25	-24.35	15.8	21.6
6.	-6.55	-1.2	.9	-24.2	-24.35	16.	24.2
6.	-6.55	-1.2	.9	-24.2	-24.3	16.2	26.
6.09	-6.4	-1.45	1.2	-20.	-21.1	16.4	26.

****

PORT NO. 3

****

9
28APRIL 14, 1969 43 3

5.95	-6.8	-1.85	1.6	-27.6	-27.2	11.5	159.8

5.95	-6.78	-1.85	1.55			-27.	-27.9	11.6	159.8
5.9	-6.75	-1.75	1.4			-26.7	-28.2	11.7	158.
5.9	-6.75	-1.6	1.3			-26.6	-28.2	11.8	155.4
5.9	-6.7	-1.35	1.			-26.	-27.75	11.9	154.2
5.9	-6.7	-1.25	0.9			-26.05	-27.65	12.	152.4
5.9	-6.7	-1.2	0.8			-26.05	-27.65	12.1	152.4
5.9	-6.68	-1.2	0.8			-26.1	-27.6	12.2	148.2
5.9	-6.65	-1.1	0.8	0.	0.	-26.3	-27.3	12.3	137.
5.85	-6.65	-1.15	0.75	0.	0.	-26.4	-27.2	12.4	137.
5.95	-6.65	-1.05	0.7	0.	0.	-26.6	-26.85	12.5	92.9
5.95	-6.65	-1.1	0.7			-26.75	-26.7	12.7	25.
5.95	-6.65	-1.1	0.7			-26.7	-26.6	13.1	25.
5.85	-6.65	-1.15	0.7	0.	0.	-26.3	-26.3	13.3	25.
5.92	-6.6	-1.15	0.85	0.	0.	-26.1	-26.1	13.7	25.
5.95	-6.6	-1.15	.85			-26.	-21.1	13.9	25.
5.91	-6.62	-1.15	0.8	0.	0.	-25.8	-26.1	14.1	25.
5.91	-6.62	-1.15	0.8	0.	0.	-25.8	-26.1	14.3	25.
5.91	-6.62	-1.15	0.8	0.	0.	-25.8	-26.1	14.5	25.
5.91	-6.62	-1.15	0.8	0.	0.	-25.8	-26.1	14.7	25.
5.91	-6.62	-1.15	0.8	0.	0.	-25.8	-26.1	14.9	25.
5.91	-6.62	-1.15	0.8	0.	0.	-25.8	-26.1	15.1	25.
5.95	-6.6	-1.2	0.85	0.	0.	-25.8	-26.1	15.3	25.
5.95	6.6	-1.2	0.85	0.	0.	-25.8	-26.1	15.5	17.
5.95	6.63	-1.4	0.9	0.	0.	-25.15	-25.9	15.7	21.2
5.95	6.64	-1.4	0.8	0.	0.	-25.1	-25.9	15.9	21.2
5.95	6.63	-1.4	0.8	0.	0.	-25.1	-25.9	16.1	21.2
5.95	6.64	-1.35	0.8	0.	0.	-25.0	-25.7	16.3	20.2

SAMPLE OUTPUT OF PROGRAM TANKANL FOR PORT 1

RAW DATA MAY 14, 1969

RUN NUMBER= 45 PORT NUMBER= 1

1	0.0	0.0	-0.90	0.60	0.0	0.0	-7.08	-5.87	12.20	146.00
2	0.0	0.0	-0.90	0.65	0.0	0.0	-6.85	-6.10	12.30	146.00
3	0.0	0.0	-0.90	0.65	0.0	0.0	-6.61	-6.31	12.40	146.00
4	0.0	0.0	-0.80	0.45	0.0	0.0	-6.56	-6.40	12.50	158.80
5	0.0	0.0	-0.75	0.50	0.0	0.0	-6.50	-6.46	12.55	157.60
6	0.0	0.0	-0.75	0.40	0.0	0.0	-6.60	-6.48	12.60	157.60
7	0.0	0.0	-0.70	0.50	0.0	0.0	-6.39	-6.56	12.70	151.20
8	0.0	0.0	-0.70	0.50	0.0	0.0	-6.32	-6.60	12.80	144.20
9	0.0	0.0	-0.60	0.40	0.0	0.0	-6.35	-6.55	12.90	144.80
10	0.0	0.0	-0.60	-0.40	0.0	0.0	-6.35	-6.55	13.00	138.20
11	0.0	0.0	-0.60	0.40	0.0	0.0	-6.40	-6.50	13.10	132.80
12	0.0	0.0	-0.60	0.40	0.0	0.0	-6.45	-6.45	13.20	124.00
13	0.0	0.0	-0.55	0.40	0.0	0.0	-6.56	-6.35	13.30	106.00
14	0.0	0.0	-0.65	0.35	0.0	0.0	-6.65	-6.30	13.40	105.40
15	0.0	0.0	-0.70	0.30	0.0	0.0	-6.71	-6.24	13.50	99.00
16	0.0	0.0	-0.55	0.25	0.0	0.0	-6.80	-6.15	13.60	94.00
17	0.0	0.0	-0.55	0.20	0.0	0.0	-6.28	-6.11	13.70	89.40
18	0.0	0.0	-0.20	0.0	0.0	0.0	-6.75	-6.15	13.90	2.00
19	0.0	0.0	-0.20	0.0	0.0	0.0	-6.78	-6.15	14.10	2.00
20	0.0	0.0	-0.40	0.10	0.0	0.0	-6.80	-6.12	14.30	23.00
21	0.0	0.0	-0.50	0.10	0.0	0.0	-6.82	-6.11	14.50	7.20
22	0.0	0.0	-0.50	0.10	0.0	0.0	-6.85	-6.10	14.70	12.80
23	0.0	0.0	-0.45	0.10	0.0	0.0	-6.85	-6.10	14.90	17.40
24	0.0	0.0	-0.45	0.10	0.0	0.0	-6.85	-6.10	15.10	17.40
25	0.0	0.0	-0.45	0.10	0.0	0.0	-6.82	-6.10	15.30	26.20
26	0.0	0.0	-0.45	0.05	0.0	0.0	-6.85	-6.10	15.50	21.60
27	0.0	0.0	-0.55	0.15	0.0	0.0	-6.90	-6.05	15.70	31.80
28	0.0	0.0	-0.55	0.20	0.0	0.0	-6.90	-6.05	15.90	31.80
29	0.0	0.0	-0.60	0.35	0.0	0.0	-7.60	-5.30	16.10	31.40
30	0.0	0.0	-0.55	0.30	0.0	0.0	-7.50	-5.40	16.30	33.80
31	0.0	0.0	-0.55	-0.30	0.0	0.0	-7.40	-5.50	16.50	39.00
32	0.0	0.0	-0.60	0.30	0.0	0.0	-7.39	-5.51	16.70	39.00
33	0.0	0.0	-0.55	0.30	0.0	0.0	-7.40	-5.50	16.90	43.20
34	0.0	0.0	-0.55	0.30	0.0	0.0	-7.40	-5.50	17.10	43.20

	T-P	DEL P12	DEL P45
1	0.1000	1.5000	-3.0734
2	0.2000	1.5500	-1.9050
3	0.3000	1.5500	-0.7620
4	0.4000	1.2500	-0.4064
5	0.4500	1.2500	-0.1016
6	0.5000	1.1500	-0.3048
7	0.6000	1.2000	0.4318
8	0.7000	1.2000	0.7112
9	0.8000	1.0000	0.5080
10	0.9000	0.2000	0.5080
11	1.0000	1.0000	0.2540
12	1.1000	1.0000	0.0
13	1.2000	0.9500	-0.5334
14	1.3000	1.0000	-0.8890
15	1.4000	1.0000	-1.1938
16	1.5000	0.8000	-1.6510
17	1.6000	0.7500	-0.4318
18	1.8000	0.2000	-1.5240
19	2.0000	0.2000	-1.6002
20	2.2000	0.5000	-1.7272
21	2.4000	0.6000	-1.8034
22	2.6000	0.6000	-1.9050
23	2.8000	0.5500	-1.9050
24	3.0000	0.5500	-1.9050
25	3.2000	0.5500	-1.8288
26	3.4000	0.5000	-1.9050
27	3.6000	0.7000	-2.1590
28	3.8000	0.7500	-2.1590
29	4.0000	0.9500	-5.8420
30	4.2000	0.8500	-5.3340
31	4.4000	0.2500	-4.8260
32	4.6000	0.9000	-4.7752
33	4.8000	0.8500	-4.8260
34	5.0000	0.8500	-4.8260

	T-R	V	VR	VZ	VTHETA	PITCH ANGLE	YAW ANGLE	CORRECTED DEL PI?
2	0.200	52.712	-25.025	38.461	25.942	-28.343	34.000	1.867
3	0.300	52.057	-5.412	42.924	28.952	-5.967	34.000	1.821
4	0.400	46.431	-1.817	43.255	16.778	-2.242	21.200	1.449
5	0.450	45.659	4.228	42.033	17.325	5.313	22.400	1.401
6	0.500	44.402	-0.417	41.050	16.920	-0.538	22.400	1.325
7	0.600	43.788	12.360	36.811	20.237	16.395	28.800	1.289
8	0.700	43.716	15.774	33.068	23.849	21.151	35.800	1.284
9	0.800	39.901	13.310	30.738	21.683	19.485	35.200	1.070
11	1.000	40.171	9.934	26.446	28.559	14.317	47.200	1.085
12	1.100	40.633	5.455	22.516	33.381	7.715	56.000	1.110
13	1.200	40.860	-5.793	11.149	38.880	-8.151	74.000	1.122
14	1.300	42.011	-14.986	10.422	37.838	-20.899	74.600	1.186
15	1.400	42.293	-19.503	5.871	37.066	-27.460	81.000	1.202
17	1.600	36.322	-5.446	-35.909	0.376	-8.623	179.400	0.887

LIST F-4

FORTRAN LISTING FOR PROGRAM YAWANL WITH SUPPORTING SUBROUTINE OMEGA AND ILLUSTRATED WITH SAMPLE OUTPUT FOR EXPERIMENTAL DATA FROM RUN NUMBER 29.

```
**********************************************************************************

                              MAIN PROGRAM YAWANL

**********************************************************************************

C                                                                          YAWA   1
C--------THIS PROGRAM ANALYSES VELOCITY PROFILE DATA OBTAINED WITH         YAWA   2
C         A VERTICAL PASS OF THE PROBE IN THE REGION OF THE IMPELLER.      YAWA   3
C         INPUT DATA IS IDENTICAL IN FORMAT TO PROGRAM FLOWANL             YAWA   4
C                                                                          YAWA   5
      DIMENSION DELP4(9),DELPT(9),THETA(9),D(50,10),DA(3),P12(50)          YAWA   6
      DIMENSION P45(50)                                                    YAWA   7
C                                                                          YAWA   8
C--------DATA STATEMENT CONTAINS EXPERIMENTAL POINTS FROM FIGURE IV-5      YAWA   9
C         THETA, EXPERIMENTAL POINTS FROM CURVE C                          YAWA  10
C         DELPT, EXPERIMENTAL POINTS FROM CURVE B                          YAWA  11
C         DELP4, EXPERIMENTAL POINTS FROM CURVE A                          YAWA  12
C                                                                          YAWA  13
      DATA THETA/-40.,-30.,-20.,-10.,0.,10.,20.,30.,40./,                  YAWA  14
     1DELPT/1.25,1.21,1.185,1.185,1.15,1.1,1.07,1.1,1.215/,                YAWA  15
     2DELP4/-.8,-.63,-.42,-.3,-.12,.04,.26,.55,.93/                        YAWA  16
      DP45=-1./2.54                                                        YAWA  17
      TEMP=2.*32.17*0.19579/(12.*2.54)                                     YAWA  18
      TE=3.1416/180.                                                       YAWA  19
10    READ(5,15)KK,LPRINT                                                  YAWA  20
15    FORMAT(2I2)                                                          YAWA  21
      READ(5,100)N,DA(1),DA(2),DA(3),FAC                                   YAWA  22
100   FORMAT(I2,3A4,F10.2)                                                 YAWA  23
      READ(5,102)L,(D(1,J),J=1,10)                                         YAWA  24
102   FORMAT(I7,10F7.2)                                                    YAWA  25
      WRITE(6,401)L,DA                                                     YAWA  26
401   FORMAT('1',10(/),20X,'RUN NO=',I3,' TAKEN ON, ',3A4)                 YAWA  27
      ANGPO=D(1,10)                                                        YAWA  28
      CANGLE=D(1,6)                                                        YAWA  29
      REFL=D(1,5)+D(1,4)-D(1,2)                                            YAWA  30
      REV=D(1,8)                                                           YAWA  31
      WRITE(6,402)D(1,1),D(1,7),REV                                        YAWA  32
402   FORMAT(1X//20X,'IMPELLER DIAMETER =',F5.2/20X,'RADIAL DISTANCE',     YAWA  33
     1'   =',F5.2/20X,'RPM',T39,1H=,F7.2//)                                YAWA  34
```

```
      READ(5,104)((D(I,J),J=1,10),I=1,N)                                YAWA  35
104   FORMAT(10F7.2)                                                    YAWA  36
      IF(LPRINT.EQ.4)GOTO16                                             YAWA  37
      WRITE(6,105)((D(I,J),J=1,10),I=1,N)                               YAWA  38
105   FORMAT(24X,11HP(1)-P(ATM),5X,9HP(1)-P(2),4X,9HP(2)-P(3),3X,       YAWA  39
     19HP(4)-P(5),5X,1HH,4X,5HANGLE,/ 24X,11HLEFT  RIGHT,4X,            YAWA  40
     211HLEFT  RIGHT ,2X,10HLEFT RIGHT,3X,10HLEFT RIGHT,///             YAWA  41
     3(20X,2F7.2,F8.2,F7.2,1X,2F5.2,4F7.2))                             YAWA  42
C                                                                       YAWA  43
C--------TRANSFORM RAW DATA INTO PRESSURE DROPS VERSUS DISTANCE FROM    YAWA  44
C         TANK WALL                                                     YAWA  45
C                                                                       YAWA  46
16    DO106I=1,N                                                        YAWA  47
      D(I,9)=(REFL-D(I,9))                                              YAWA  48
      D(I,10)=D(I,10)-CANGLE                                            YAWA  49
      IF(FAC.NE.1.)GOTO107                                              YAWA  50
      D(I,3)=D(I,3)*2.54                                                YAWA  51
      D(I,4)=D(I,4)*2.54                                                YAWA  52
      D(I,7)=D(I,7)*2.54                                                YAWA  53
      D(I,8)=D(I,8)*2.54                                                YAWA  54
107   P12(I)=D(I,4)-D(I,3)                                              YAWA  55
      P45(I)=D(I,7)-D(I,8)-DP45                                         YAWA  56
106   CONTINUE                                                          YAWA  57
      WRITE(6,4)(I,D(I,9),P12(I),P45(I),I=1,N)                          YAWA  58
4     FORMAT(1X///33X,' Z ', 7X,'DEL P12', 5X,'DEL P45'//(20XI2,3X,     YAWA  59
     13F12.4))                                                          YAWA  60
      WRITE(6,6)                                                        YAWA  61
6     FORMAT(1X//,26X,' Z ',5X,'V', 7X,'VR', 6X,'VZ', 4X,'VTHETA',3X,   YAWA  62
     1  'PITCH',3X,'YAW',3X,'CORRECTED'/65X,'ANGLE',2X,'ANGLE',3X,       YAWA  63
     2'DEL P12'//)                                                      YAWA  64
C                                                                       YAWA  65
C--------CALCULATE VELOCITY PROFILE USING EQUATIONS IV-27(a) TO IV-27(c) YAWA  66
C                                                                       YAWA  67
      DO5I=1,N                                                          YAWA  68
      RATIO=P45(I)*0.09537/(P12(I)*0.19579)                             YAWA  69
C                                                                       YAWA  70
C--------CHECK IF PRESSURE RATIOS ARE OUT OF RANGE OF FIGURE IV-5       YAWA  71
C                                                                       YAWA  72
      IF(RATIO.LT.(-.8).OR.RATIO.GT.1.)GOTO5                            YAWA  73
C                                                                       YAWA  74
C--------INTERPOLATE TO OBTAIN TRUE KINETIC HEAD, P(T)-P(S).           YAWA  75
C         EQUIVALENT TO LOOKING UP FIGURE IV-4                          YAWA  76
C                                                                       YAWA  77
      CALL OMEGA(RATIO,DELP4,THETA,9,9,ANGLE)                           YAWA  78
      TP=ANGLE*TE                                                       YAWA  79
      TY=D(I,10)*TE                                                     YAWA  80
      CALL OMEGA(ANGLE,THETA,DELPT,9,9,DELTA)                           YAWA  81
      DELTA=DELTA*P12(I)                                                YAWA  82
      V=SQRT(TEMP*DELTA)*60.                                            YAWA  83
      VZ=V*SIN(TP)                                                      YAWA  84
      VTE=V*COS(TP)                                                     YAWA  85
      VR=VTE*COS(TY)                                                    YAWA  86
      VTHETA=VTE*SIN(TY)                                                YAWA  87
      WRITE(6,7)I,D(I,9),V,VR,VZ,VTHETA,ANGLE,D(I,10),DELTA             YAWA  88
```

```
7       FORMAT(20X,I2,8F8.3)                                    YAWA  89
5       CONTINUE                                                YAWA  90
        IF(KK.LT.5)GOTO10                                       YAWA  91
99      STOP                                                    YAWA  92
        END                                                     YAWA  93
```

****

SUBROUTINE OMEGA
FOR LISTING SEE LIST F-1

****

****

INPUT DATA
SAME AS FOR PROGRAM FLOWANL, SEE LIST F-1

****

SAMPLE OUTPUT

RUN NO= 29 TAKEN ON, MAR 10, 1969

IMPELLER DIAMETER = 3.00
RADIAL DISTANCE = 3.00
RPM = 333.33

	Z	DEL P12	DEL P45
1	0.7000	1.3500	-0.8063
2	0.6000	1.4000	-4.0563
3	0.5000	2.6500	-7.6063
4	0.4000	4.4000	-8.8063
5	0.3000	7.9000	-9.8063
6	0.2000	10.0000	-7.1063
7	0.1000	11.4000	-1.0563
8	-0.0000	11.4500	5.5937
9	-0.1000	10.4000	9.9937
10	-0.2000	8.4000	11.4437
11	-0.3000	5.3500	10.7937
12	-0.4000	3.5000	8.1937
13	-0.5000	1.7000	4.7437
14	-0.6000	1.6000	2.4437

	Z	V	VR	VZ	VTHETA	PITCH ANGLE	YAW ANGLE	CORRECTED DEL P12
1	0.700	48.762	39.316	-7.924	27.735	-9.352	35.200	1.598
5	0.300	119.048	92.240	-57.087	49.045	-28.654	28.000	9.526
6	0.200	133.006	115.627	-31.118	57.902	-13.530	26.600	11.890
7	0.100	138.389	123.566	10.976	61.339	4.549	26.400	12.872
8	-0.000	135.028	114.881	44.166	55.536	19.092	25.800	12.254
9	-0.100	129.508	102.825	59.565	51.491	27.383	26.600	11.273
10	-0.200	118.794	88.091	65.322	45.662	33.358	27.400	9.485
11	-0.300	99.069	64.773	65.138	37.096	41.110	29.800	6.597
14	-0.600	52.396	35.836	30.460	23.095	35.544	32.800	1.845

LIST F-5

FORTRAN LISTING FOR PROGRAM COOPER WITH SUPPORTING SUBROUTINES PATERN, PROC, BOUNDS, AVG AND OMEGA. ALSO GIVEN IS COOPER'S (8) VELOCITY PROFILE DATA.

```
**********************************************************************************

                              MAIN PROGRAM COOPER

**********************************************************************************

C                                                                          COOP   1
C--------THIS PROGRAM ANALYSES COOPERS DATA                               COOP   2
C         K=1, PROCESSES COOPERS REGULAR DATA                              COOP   3
C         K GT 5 NO RERUNS                                                 COOP   4
C         K=2, PROCESSES CUTTERS DATA FOR VARYING BLADE WIDTH              COOP   5
C         LPRINT = 1, SKIPS PRINT IN MAIN PROGROM,                         COOP   6
C         ANY OTHER VALUE GIVES COMPLETE PRINT                             COOP   7
C         KK = 0, GIVES PRINT AT EVERY 30TH POINT FROM SUBROUTINE PROC     COOP   8
C         KK .GT. 30, NO PRINT FROM SUBROUTINE PROC                        COOP   9
C         KVR= 0, PRINTS RADIAL VELOCITY PROFILE ANALYSIS                  COOP  10
C         PAR .GT. 0, SIGMA AND AA FIXED BY PIN(I)                         COOP  11
C         PAR .LE. 0 ALL PARAMETERS FREE                                   COOP  12
C                                                                          COOP  13
C                                                                          COOP  14
      DIMENSIONX(20),Y(20),YC(20),P(6),STEP(6),YR(20)                      COOP  15
      DIMENSIONXR(20),SIGMA(20),A(20),AA(20),SQ(20),GF(20),Q(20)           COOP  16
      DIMENSIONT(15,15),ANG(20),PA(50),PB(50),PC(50),PD(50),PE(50)         COOP  17
      DIMENSION RPM(10),PF(50),PIN(6),RR(10),PG(50),PH(50)                 COOP  18
      COMMONDIA,X,Y,YC,XX,N,KK,P1,P2,P3,P4                                 COOP  19
      READ(5,55)LPRINT,LPUNCH,KK, KVR,WT,PAR                               COOP  20
55    FORMAT(4I2,2F10.2)                                                   COOP  21
      M=0                                                                  COOP  22
C                                                                          COOP  23
C--------READ INITIAL VALUES OF PARAMETERS AND STEP SIZE                   COOP  24
C         PIN STORES INITIAL VALUES OF PARAMETER FOR ANALYSIS OF MULTIPLE  COOP  25
C         FLOW PROFILES                                                    COOP  26
C                                                                          COOP  27
      READ(5,16)(PIN(I),STEP(I),I=1,4)                                    COOP  28
16    FORMAT(2F10.2)                                                       COOP  29
7     READ(5,15)K,NP,KB                                                    COOP  30
15    FORMAT(3I2)                                                          COOP  31
      IF(KB.EQ.1)READ(5,32)(RR(I),I=1,5)                                   COOP  32
      READ(5,60)(PIN(I),I=1,3)                                             COOP  33
60    FORMAT(3F15.8)                                                       COOP  34
```

```
      READ(5,32)(RPM(I),I=1,5)                                          COMP  35
32    FORMAT(5F10.2)                                                    COMP  36
      READ(5,11)N,NN,D,XD                                               COMP  37
11    FORMAT(2I2,2F10.2)                                                COMP  38
      DIA=D/12.                                                         COMP  39
      L=2                                                               COMP  40
C                                                                       COMP  41
C--------READ VELOCITY PROFILE MATRIX                                   COMP  42
C                                                                       COMP  43
      READ(5,6)((T(I,J),J=1,NN),I=1,N)                                  COMP  44
6     FORMAT(11F5.2)                                                    COMP  45
      IF(LPRINT.EQ.1)GOTO54                                             COMP  46
      WRITE(6,3)((T(I,J),J=1,NN),I=1,N)                                 COMP  47
3     FORMAT(1H1,10X,4HDATA,///(1X,11F6.1))                             COMP  48
54    ANGLE=0.                                                          COMP  49
      YM=0.                                                             COMP  50
      ANGL=0.                                                           COMP  51
      YMM=0.                                                            COMP  52
      M=M+1                                                             COMP  53
      IF(KB.EQ.1)XD=PR(L/2)                                             COMP  54
      XX=XD/12.                                                         COMP  55
C                                                                       COMP  56
C--------LOGIC BRANCH TO READ A VELOCITY PROFILE FROM VELOCITY          COMP  57
C         PROFILE MATRIX, DELETES ZERO VALUES WHEN SUCH VALUES OCCUR    COMP  58
C                                                                       COMP  59
      IF(K.EQ.2.AND.M.GT.3)GOTO42                                       COMP  60
      IF(K.EQ.3)GOTO44                                                  COMP  61
45    NI=0                                                              COMP  62
      NII=N                                                             COMP  63
      NT=0.                                                             COMP  64
      GOTO43                                                            COMP  65
42    NI=1                                                              COMP  66
      NII=N-1                                                           COMP  67
      N=N-2                                                             COMP  68
      NT=2.                                                             COMP  69
      GOTO43                                                            COMP  70
44    IF(M-4)42,45,46                                                   COMP  71
46    NI=2                                                              COMP  72
      NII=N-2                                                           COMP  73
      N=N-4                                                             COMP  74
      NT=4.                                                             COMP  75
43    NK=NII/2+1                                                        COMP  76
C                                                                       COMP  77
C--------Z COORDINATE= X(I), FT                                        COMP  78
C         RESULTANT VELOCITY Q= Y(I), FT/MIN                            COMP  79
C                                                                       COMP  80
      DO22I=1,NII                                                       COMP  81
      KI=I+NI                                                           COMP  82
      X(I)=T(KI,1)/12.                                                  COMP  83
      Y(I)=T(KI,L)*5.                                                   COMP  84
      ANGLE=ANGLE+T(KI,L+1)                                             COMP  85
22    YM=YM+Y(I)                                                        COMP  86
      YM=YM/FLOAT(N)                                                    COMP  87
```

```
      ANGLE=ANGLE/FLOAT(N)                                              COOP  88
C                                                                       COOP  89
C---------CALCULATE WEIGHTED AVERAGE ANGLE AND AVERAGE ANGLE           COOP  90
C         WT= RATIO OF VELOCITIES FOR WHICH WEIGHT IS ZERO              COOP  91
C             CHOSEN AS 0.7                                             COOP  92
C         YM= AVERAGE VALUE OF Y                                        COOP  93
      DO34I=1,NII                                                       COOP  94
      KI=I+NI                                                           COOP  95
      IF((Y(I)/Y(NK)).LT.WT)GOTO34                                      COOP  96
      ANGL=ANGL+T(KI,L+1)*Y(I)                                          COOP  97
      YMM=YMM+Y(I)                                                      COOP  98
34    CONTINUE                                                          COOP  99
      ANGL=ANGL/YMM                                                     COOP 100
      RPM(M)=RPM(M)*DIA**3                                              COOP 101
C                                                                       COOP 102
C                                                                       COOP 103
C---------LOGIC BRANCH FOR ONE DIMENSIONAL SEARCH ON PARAMETER P(2)     COOP 104
C         OTHER PARAMETERS FIXED THROUGH PIN                            COOP 105
C                                                                       COOP 106
      DO47I=1,NP                                                        COOP 107
47    P(I)=PIN(I)                                                       COOP 108
      IF(PAR)51,51,52                                                   COOP 109
52    P1=PIN(1)                                                         COOP 110
      P2=PIN(2)                                                         COOP 111
      P3=PIN(3)                                                         COOP 112
      P3=    XX*SIN(ANGL *3.1416/180.)                                  COOP 113
      P4=PIN(4)                                                         COOP 114
      GOTO53                                                            COOP 115
51    P1=0.                                                             COOP 116
      P3=    XX*SIN(ANGL *3.1416/180.)                                  COOP 117
C                                                                       COOP 118
C---------CALCULATE SUM OF SQUARES ABOUT MEAN                          COOP 119
C                                                                       COOP 120
53    SSM=0.                                                            COOP 121
      DO12I=1,N                                                         COOP 122
12    SSM=SSM+(Y(I)-YM)**2                                              COOP 123
      R=0.                                                              COOP 124
C                                                                       COOP 125
C---------CALL PATTERN SEARCH SUBROUTINE                               COOP 126
C                                                                       COOP 127
29    IF(KK.GT.30)GOTO57                                                COOP 128
      KK=0                                                              COOP 129
      WRITE(6,19)                                                       COOP 130
19    FORMAT(1H1,6X,4HP(1), 9X,4HP(2), 9X,4HP(3), 8X,4HP(4),            COOP 131
     18X,10HSUM SQ REG,//)                                              COOP 132
57    CALL PATERN(NP,P,STEP,4,0,COST)                                   COOP 133
      IF(PAR)58,58,59                                                   COOP 134
59    P(1)=P1                                                           COOP 135
58    P(3)=P3                                                           COOP 136
      IF(COST.GT.SSM)GOTO75                                             COOP 137
      R=SQRT(1.-COST/SSM)                                               COOP 138
      GOTO74                                                            COOP 139
75    R=0.                                                              COOP 140
```

```
74    BHALF=1.762747*XX/P(1)                                          COOP 141
      IF(B.EQ.0.)B=BHALF                                              COOP 142
      UHALF=P(2)*SQRT(P(1)/XX)/((XX**2-P(3)**2)**0.25*4.)             COOP 143
      IF(UHALF.LT.Y(1).OR.UHALF.LT.Y(N))GOTO71                        COOP 144
      CALL OMEGA(UHALF,Y,X,NII,25,BCALC)                              COOP 145
      BCALC=BCALC-P(4)                                                COOP 146
      GOTO72                                                          COOP 147
71    BCALC=0.                                                        COOP 148
72    BXX=6.*XX/P(1)*12.                                              COOP 149
      IF(LPRINT.EQ.1)GOTO30                                           COOP 150
C                                                                     COOP 151
C--------PRINT COMPLETE ANALYSIS OF A PROFILE                         COOP 152
C                                                                     COOP 153
      IF(K.EQ.1)GOTO56                                                COOP 154
      NTE=NT+N                                                        COOP 155
      WRITE(6,2)(T(I,L),T(I,L+1),I=1,NTE)                             COOP 156
56    WRITE(6,18)D,XD                                                 COOP 157
18    FORMAT(1H1,4HD  =,F10.5,/1H0,4HR  =,F10.5,///)                  COOP 158
      WRITE(6,2)(X(I),Y(I),I=1,N)                                     COOP 159
2     FORMAT(1H0,7X,1HZ,9X,1HQ/(1X,2F10.5))                           COOP 160
      WRITE(6,17)(I,P(I),I=1,NP)                                      COOP 161
17    FORMAT(1H0,10X10HPARAMETERS,/(1H0,I2,F20.8))                    COOP 162
      WRITE(6,25)ANGLE,ANGL,WT                                        COOP 163
25    FORMAT(1X,//20X,'AVG ANGLE    =',F15.8/20X,'WT AVG ANGLE=',F15.8, COOP 164
     15X,'VELOCITY FACTOR=',F5.2)                                     COOP 165
      WRITE(6,13)(Y(I),YC(I),I=1,N)                                   COOP 166
13    FORMAT(1H0,9X,1HQ,19X,2HQC/(1X,2F20.8))                         COOP 167
      WRITE(6,14)COST,R                                               COOP 168
14    FORMAT(1H0,27HSUM OF SQUARES OF (Y-YCALC),F20.8,/1H0,           COOP 169
     127HGOODNESS OF FIT              ,F20.8)                         COOP 170
      WRITE(6,31)BHALF,BCALC,UHALF                                    COOP 171
31    FORMAT(1H0,7HBHALF =,F20.8,10X,7HBCALC =,F20.8,/1H0,10X,        COOP 172
     17HUHALF =,F20.8)                                                COOP 173
      WRITE(6,41)XD,BXX                                               COOP 174
41    FORMAT(1H0,25HHALF WIDTH OF JET AT XD =,F4.2,1H,,4X,F10.2,       COOP 175
     12X,6HINCHES,//)                                                 COOP 176
C                                                                     COOP 177
C--------STORE IMPORTANT RESULTS OF A PROFILE ANALYSIS FOR SUMMARY    COOP 178
C                                                                     COOP 179
30    Q(M)=4.*3.1416*P(2)*(XX**2-P(3)**2)**0.25*SQRT(XX/P(1))         COOP 180
      XR(M)=XD                                                        COOP 181
      SIGMA(M)=P(1)                                                   COOP 182
      A(M)=P(2)                                                       COOP 183
      AA(M)=P(3)                                                      COOP 184
      ANG(M)=SQRT(XX**2-P(3)**2)/XX                                   COOP 185
      PA(M)=ARCOS(ANG(M))*180./3.1416                                 COOP 186
      SQ(M)=COST                                                      COOP 187
      GF(M)=R                                                         COOP 188
      PB(M)=P(4)                                                      COOP 189
      PC(M)=BHALF                                                     COOP 190
      PD(M)=BCALC                                                     COOP 191
      PE(M)=UHALF                                                     COOP 192
      PF(M)=ANGLE                                                     COOP 193
```

```
C                                                                       COOP 194
C---------ANALYSE DIFFERENCE IN CALCULATED AND TRUE RADIAL VELOCITY      COOP 195
C                                                                       COOP 196
      VRMAX=P(2)/2.*SQRT(P(1)/XX**3)*(XX**2-P(3)**2)**0.25              COOP 197
      TEMP=P(1)/(2.*XX)                                                 COOP 198
      DO63I=1,N                                                         COOP 199
      Y(I)=Y(I)*COS(T(I+NT,L+1)*3.1416/180.)                            COOP 200
63    YR(I)=VRMAX*(1.-(TANH(TEMP*(X(I)-P(4))))**2)                      COOP 201
      CALL AVG(Y ,N,YM ,BB,BB)                                          COOP 202
      SSM=0.                                                            COOP 203
      SSR=0.                                                            COOP 204
      DO64I=1,N                                                         COOP 205
      SSR=SSR+(YR(I)-Y(I))**2                                           COOP 206
64    SSM=SSM+(Y(I)-YM)**2                                              COOP 207
      IF(SSR.GT.SSM)GOTO68                                              COOP 208
      R=SQRT(1.-SSR/SSM)                                                COOP 209
      GOTO69                                                            COOP 210
68    R=0.                                                              COOP 211
      WRITE(6,67)SSR,SSM                                                COOP 212
67    FORMAT(1H0,20X,'SSR =',F15.8/20X,'SSM =',F15.8/)                  COOP 213
69    PG(M)=R                                                           COOP 214
      PH(M)=SSR                                                         COOP 215
      IF(KVR.EQ.1)GOTO66                                                COOP 216
      WRITE(6,65)                                                       COOP 217
65    FORMAT(1H1,/////,30X,'RADIAL VELOCITY ANALYSIS'//)                COOP 218
      WRITE(6,13)(Y(I),YR(I),I=1,N)                                     COOP 219
      WRITE(6,14)COST,R                                                 COOP 220
C                                                                       COOP 221
C---------CHECK IF ANOTHER PROFILE IS TO BE ANALYSED FROM VELOCITY      COOP 222
C         PROFILE MATRIX                                                COOP 223
C                                                                       COOP 224
66    IF(L.GE.(NN-1))GOTO23                                             COOP 225
      L=L+2                                                             COOP 226
      N=N+NT                                                            COOP 227
      GOTO54                                                            COOP 228
C                                                                       COOP 229
C---------PRINT SUMMARY OF A SET OF PROFILES                            COOP 230
C                                                                       COOP 231
23    WRITE(6,20)(N,XR(N),SIGMA(N),A(N),AA(N),SQ(N),PH(N),GF(N),PG(N),  COOP 232
     1N=1,M)                                                            COOP 233
20    FORMAT(1H1,20X,' NO '6HRADIUS,2X,5HSIGMA,5X,1HA, 7X,2HAA, 9X,     COOP 234
     1'SUM SQ',10X,9HCORR COEF,/61X,'Q',8X,'VR',6X,'Q',6X,'VR'//        COOP 235
     2(22X,I2,F6.2,2F8.3,F9.4,2F10.2,1X,2F7.4))                         COOP 236
      WRITE(6,21)(N,XR(N),Q(N),ANG(N),PA(N),PB(N),N=1,M)                COOP 237
21    FORMAT(1X,///21X,' NO ',2X,6HRADIUS,2X,'IMP CFM',3X,'COS(PHI)',   COOP 238
     13X,5HANGLE, 7X,4HP(4),// (22X,I2,2X,F6.2,F9.2,F11.4,F9.2,F15.8))  COOP 239
      IF(LPUNCH.EQ.1)GOTO70                                             COOP 240
      PUNCH 26,(SIGMA(N),A(N),AA(N),PB(N),Q(N),ANG(N),N=1,M)            COOP 241
26    FORMAT(6F13.8)                                                    COOP 242
70    WRITE(6,40)(I,PE(I),PC(I),PD(I),PF(I),RPM(I),I=1,M)               COOP 243
40    FORMAT(1X,///21X,' NO ',5X,5HUHALF, 6X,5HBHALF, 6X,5HBCALC,       COOP 244
     1 2X,9HAVG ANGLE,3X,5HN0**3,///(22X,I2,2X,F9.2,2F11.4,F9.2,F10.3)) COOP 245
      M=0                                                               COOP 246
```

```
C                                                                       COMP 247
C--------CHECK IF ANOTHER VELOCITY PROFILE MATRIX IS TO BE ANALYSED      COMP 248
C                                                                       COMP 249
      WRITE(6,76)WT                                                     COMP 250
76    FORMAT(1X//,30X,'VELOCITY FACTOR=',F5.2)                          COMP 251
      IF(K.LT.5)GOTO7                                                   COMP 252
      WRITE(6,80)                                                       COMP 253
80    FORMAT(1H1)                                                       COMP 254
8     STOP                                                              COMP 255
      END                                                               COMP 256
```

****

THE FOLLOWING SUPPORTING SUBROUTINE ARE USED
IN COMMON WITH FLOWANL, FOR LISTING SEE LIST F-1

SUBROUTINE PATERN
SUBROUTINE PROC
SUBROUTINE BOUNDS
SUBROUTINE AVG
SUBROUTINE OMEGA

****

INPUT DATA

****

PRELIMINARY DATA, CONTROLS MODE OF OPERATION
FOR INSTRUCTIONS SEE COMMENT CARDS AT THE BEGINING
OF THE PROGRAM

****

```
 1 140 10.5         0.
15.26      .01
6.5        .1
0.125      0.001
.05        .001
```

****

VELOCITY PROFILE DATA, 4 INCH TURBINE AT 280 RPM AND
VARYING RADIAL DISTANCE R

****

```
 1 4 1
2.0        2.5         3.0         4.0         5.0
12.36537         15.               0.1024979
280.       280.        280.        280.        280.
 9114.0         280.
```

```
0.4   14.4 64.   5.5  71.   14.4 54.   16.4 34.   15.4 30.
 0.3  33.2 65.   19.7 62.   21.8 46.   21.8 30.   19.7 26.
0.2   49.1 62.   35.  54.   28.4 44.   23.8 30.   19.7 26.
0.1   61.5 54.   43.3 48.   34.1 40.   26.2 29.   19.7 26.
0.    65.8 50.   46.7 44.   38.2 38.   27.3 28.   19.7 26.
-0.1  60.6 56.   44.7 47.   35.8 38.   26.8 28.   19.7 26.
-0.2  49.4 63.   36.2 52.   29.9 42.   25.6 28.   19.7 26.
-0.3  32.8 68.   21.8 60.   20.4 46.   22.5 28.   19.7 26.
-0.4  18.1 68.   9.5  71.   15.4 50.   18.9 32.   17.3 30.
```

****

VELOCITY PROFILE DATA, 4 INCH TURBINE AT 100 RPM, VARYING BLADE WIDTHS

****

```
 2 4
12.36537        15.             0.1024979
100.        100.        100.        100.        100.
 9114.0         2.
0.4   6.7  40.   7.7  50.   5.5  38.   0.   0.   0.   0.
0.3   16.4 40.   16.4 36.   12.2 38.   9.5  62.   10.9 72.
0.2   22.5 44.   19.7 42.   18.9 39.   16.4 56.   16.4 62.
0.1   23.8 45.   22.5 41.   23.2 40.   21.2 52.   20.4 54.
0.    24.4 45.   23.2 40.   23.8 39.   21.8 49.   21.8 50.
-0.1  24.4 45.   21.8 42.   23.8 40.   21.8 52.   21.1 53.
-0.2  22.5 44.   19.7 42.   20.4 40.   17.3 56.   16.4 62.
-0.3  18.1 40.   15.4 36.   12.2 38.   10.9 62.   10.9 72.
-0.4  6.7  40.   5.5  50.   5.5  38.   0.   0.   0.   0.
```

****

VELOCITY PROFILE DATA, 4 INCH TURBINE AT 200 RPM, VARYING BLADE WIDTHS

****

```
 3 4
12.36537        15.             0.1024979
200.        200.        200.        200.        200.
11114.0         2.
0.5   0.   0.   0.   0.   0.   0.   5.5  72.   0.   0.
0.4   23.8 34.   12.2 32.   10.9 45.   12.2 64.   0.   0.
0.3   33.2 40.   30.9 36.   27.3 40.   23.2 56.   18.1 70.
0.2   40.9 44.   42.3 39.   41.2 40.   35.8 56.   27.8 64.
0.1   42.7 44.   45.4 40.   46.  41.   43.  51.   38.6 56.
0.    44.4 44.   45.4 40.   46.7 38.   45.7 46.   40.9 51.
-0.1  43.  44.   45.4 40.   46.3 40.   44.4 51.   39.4 56.
-0.2  40.9 44.   43.  39.   41.2 41.   36.6 56.   29.4 64.
-0.3  36.2 40.   30.9 36.   27.8 40.   23.2 56.   18.1 70.
-0.4  17.3 34.   10.9 30.   10.9 44.   13.4 63.   0.   0.
-0.5  0.   0.   0.   0.   0.   0.   5.5  72.   0.   0.
```

****

VELOCITY PROFILE DATA 3 INCH TURBINE IN WATER

****

```
 1 4
12.36537        15.             0.1024979
200.        300.        400.        500.        600.
13113.          1.5
.3    7.7   61.   14.4  67.   9.5   65.   5.5   60.   18.1  66.
.25   15.4  66.   22.5  68.   25.6  72.   21.2  58.   34.5  71.
.2    20.4  64.   27.3  66.   35.4  70.   37.4  62.   46.7  69.
.15   25.   62.   38.6  63.   44.4  66.   52.1  58.   62.3  67.
.1    31.8  56.   46.   58.   50.6  60.   63.9  54.   74.   56.
.05   34.5  52.   50.   52.   54.6  54.   70.1  50.   80.8  50.
0.0   34.4  51.   50.9  50.   55.2  51.   71.4  49.   82.1  48.
-.05  34.5  51.   50.3  52.   54.1  55.   69.3  51.   80.3  50.
-.1   31.8  57.   46.   56.   50.6  60.   62.3  52.   73.3  55.
-.15  28.9  60.   38.6  61.   45.7  65.   51.8  57.   60.6  61.
-.2   23.2  64.   29.9  64.   36.2  69.   38.6  60.   47.   67.
-.25  18.1  66.   24.4  68.   26.2  72.   22.5  58.   34.1  69.
-.3   12.2  66.   16.4  68.   18.9  66.   5.5   60.   20.4  72.
```

****

VELOCITY PROFILE DATA 4 INCH TURBINE IN WATER

****

```
 1 4
12.56403        15.             0.140107
100.        150.        200.        250.        300.
 9114.          2.
.4    3.9   67.   9.5   62.   9.5   62.   18.9  66.   21.2  62.
0.3   10.2  61.   16.4  67.   20.8  66.   32.3  67.   33.7  66.
.2    14.4  61.   23.8  65.   33.2  65.   46.7  63.   49.1  65.
.1    21.2  58.   31.4  58.   45.7  56.   56.   56.   61.1  58.
0.    23.2  51.   34.1  52.   48.8  51.   57.5  52.   66.2  53.
-.1   21.5  55.   31.4  54.   47.   55.   53.5  60.   63.2  58.
-.2   16.4  61.   25.6  62.   37.4  63.   45.4  66.   50.9  66.
-.3   9.5   64.   18.1  66.   20.4  68.   28.9  69.   34.5  68.
-.4   3.9   68.   9.5   64.   10.9  68.   19.7  69.   20.4  68.
```

****

VELOCITY PROFILE DATA 5 INCH TURBINE IN WATER

****

```
 1 4
12.66316        25.             0.1669657
```

```
100.        150.        200.        250.        275.
11115.          2.5
.5    7.7  62.   12.2 62.   15.4 58.   21.8 57.   22.5 59.
.4   10.9  69.   17.3 63.   22.5 60.   31.4 60.   34.5 60.
.3   17.3  63.   27.3 63.   37.8 61.   47.  61.   50.9 61.
.2   22.5  59.   35.8 59.   47.  58.   62.  57.   66.7 59.
.1   26.8  53.   41.9 52.   55.4 51.   70.6 52.   77.4 52.
0.0  28.9  49.   44.4 48.   58.1 47.   74.1 48.   81.2 48.
-.1  27.3  53.   42.7 51.   55.4 50.   71.  52.   78.8 52.
-.2  23.8  60.   37.  58.   47.9 58.   62.  57.   67.8 57.
-.3  18.1  62.   28.4 63.   35.8 60.   47.3 61.   50.6 62.
-.4  13.4  68.   18.9 63.   23.2 64.   28.9 65.   32.8 63.
-.5   7.7  62.   10.9 62.   13.4 58.   16.4 55.   19.7 59.
```

****

VELOCITY PROFILE DATA 6 INCH TURBINE IN WATER

****

```
 1 4
12.01391        24.             0.1998177
50.         100.        125.        150.        175.
13116.          3.
.6    7.7  62.   10.9 62.   13.4 55.   14.4 64.   17.3 62.
.5   10.9  60.   14.4 60.   18.1 59.   19.7 59.   23.8 58.
.4   14.4  58.   19.7 59.   24.4 60.   27.8 61.   33.2 60.
.3   18.9  58.   25.  59.   31.4 59.   39.  61.   44.4 58.
.2   21.8  56.   29.9 55.   38.2 56.   45.7 55.   53.2 54.
.1   23.8  50.   33.2 50.   41.6 50.   51.2 51.   58.1 49.
0.   25.6  48.   34.5 48.   43.  48.   53.8 48.   59.8 47.
-.1  24.4  50.   34.1 50.   41.9 50.   52.7 50.   58.6 49.
-.2  21.8  56.   31.4 55.   39.4 54.   47.6 54.   52.9 54.
-.3  18.1  58.   25.6 59.   32.8 59.   40.5 58.   44.7 57.
-.4  15.4  58.   21.2 61.   26.2 61.   29.9 62.   34.5 60.
-.5  10.9  58.   15.4 62.   18.9 61.   21.1 63.   23.8 60.
-.6   7.7  58.   10.9 63.   14.4 57.   15.4 56.   17.3 56.
```

****

VELOCITY PROFILE DATA 4 INCH TURBINE IN AIR

****

```
 1 4
14.17233        20.             0.1383935
200.        300.        366.        500.        600.
 9114.0          2.
0.4   13.1 68.   21.3 68.   22.8 68.   28.4 68.   35.  68.
0.3   15.6 66.   22.8 66.   30.9 66.   37.9 66.   46.  66.
0.2   22.3 65.   35.  65.   43.4 65.   56.3 65.   70.7 65.
0.1   35.  58.   51.4 58.   73.1 58.   91.9 58.   109.158.
0.    43.4 53.   60.5 53.   86.2 53.   121.253.   144.253.
```

```
-0.1 37.9 58.  53.3 58.  75.6 58.  104.258.  130.458.
-0.2 24.9 66.  35.  66.  48.6 66.  64.9 66.  86.2 66.
-0.3 16.4 68.  22.8 68.  30.9 68.  40.2 68.  53.3 68.
-0.4 12.4 68.  19.  68.  22.8 68.  29.6 68.  35.7 68.
```

****

VELOCITY PROFILE DATA 5 INCH TURBINE IN AIR

****

```
 1 4
13.73586        40.             0.1650288
200.        300.        400.        500.        600.
11115.          2.5
0.5  14.8 59.  21.6 59.  27.8 59.  35.3 59.  43.3 59.
0.4  18.6 60.  26.  60.  35.3 60.  46.  60.  54.7 60.
0.3  23.7 61.  35.3 61.  46.  61.  61.2 61.  73.2 61.
0.2  33.8 59.  50.7 59.  71.9 59.  92.9 59.  112.859.
0.1  43.3 52.  68.2 52.  94.5 52.  123.952.  148.452.
0.   47.8 48.  73.2 48.  105.948.  133.748.  159.648.
-0.1 44.2 52.  68.2 52.  97.6 52.  125.852.  150.652.
-0.2 35.3 57.  56.8 57.  75.8 57.  100.957.  118.257.
-0.3 25.4 62.  37.6 62.  53.7 62.  65.8 62.  79.9 62.
-0.4 18.6 63.  26.6 63.  36.  63.  47.8 63.  56.8 63.
-0.5 14.4 59.  20.1 59.  27.2 59.  35.3 59.  42.5 59.
```

****

VELOCITY PROFILE DATA 6 INCH TURBINE IN AIR

****

```
 9 4
12.93968        40.             0.1951546
100.        200.        300.        500.        600.
13116.          3.
0.6  11.8 62.  21.5 62.  28.9 62.  45.9 62.  53.5 62.
0.5  14.5 60.  25.6 60.  33.  60.  53.5 60.  63.1 60.
0.4  16.  59.  30.  59.  39.8 59.  64.1 59.  77.4 59.
0.3  21.3 59.  38.4 59.  54.4 59.  90.  59.  108.559.
0.2  25.5 55.  50.  55.  71.6 55.  123. 55.  140.755.
0.1  30.9 50.  61.1 50.  83.5 50.  148.250.  172.850.
0.   34.3 48.  65.2 48.  90.  48.  160.248.  186.248.
-0.1 32.9 50.  61.1 50.  83.5 50.  152.150.  177.250.
-0.2 27.8 55.  51.7 55.  71.6 55.  129.855.  150.355.
-0.3 23.9 59.  41.2 59.  56.3 59.  101.159.  116.459.
-0.4 18.1 61.  31.2 61.  41.2 61.  68.3 61.  83.5 61.
-0.5 14.1 62.  25.6 62.  33.  62.  56.3 62.  66.2 62.
-0.6 11.8 63.  21.3 63.  28.9 63.  46.7 63.  53.5 63.
```

LIST F-6

FORTRAN LISTING FOR PROGRAM NIELCUT WITH SUPPORTING SUBROUTINES, PATERN, BOUNDS AND OMEGA.

ALSO GIVEN ARE VELOCITY PROFILE DATA OF NIELSON (21) AND CUTTER (9).

```
**********************************************************************************

                                MAIN PROGRAM NIELCUT

**********************************************************************************
C                                                                          NIEL   1
C                                                                          NIEL   2
C--------THIS PROGRAM ANALYSES NIELSON'S AND CUTTER'S DATA                 NIEL   3
C        LPRINT = 1, SKIPS PRINT IN MAIN PROGROM,                          NIEL   4
C        KK .GT. 30, NO PRINT FROM SUBROUTINE PROC                         NIEL   5
C        K .GT. 5, LAST PROFILE IN A DATA SET                              NIEL   6
C        KK .GT. 5 LAST SET OF VELOCITY PROFILES                           NIEL   7
C                                                                          NIEL   8
C                                                                          NIEL   9
      DIMENSIONX(20),Y(20),YC(20),P(6),STEP(6)                             NIEL  10
      DIMENSIONXR(50),SIGMA(50),A(50),AA(50),SQ(50),GF(50),Q(50)           NIEL  11
      DIMENSION ANG(50),PA(50),PB(50),PC(50),PD(50),PE(50)                 NIEL  12
      DIMENSION PIN(6)                                                     NIEL  13
      COMMONDIA,X,Y,YC,XX,N,KK,P1,P2,P3,P4                                 NIEL  14
      ARCOS(C)=ATAN(SQRT(1.-C**2)/C)                                       NIEL  15
      READ(5,15)LPRINT,KK                                                  NIEL  16
      LPUNCH=1                                                             NIEL  17
      READ(5,16)(PIN(I),STEP(I),I=1,4)                                     NIEL  18
16    FORMAT(2F10.2)                                                       NIEL  19
70    READ(5,22)KGROUP,T                                                   NIEL  20
22    FORMAT(I2,F10.2)                                                     NIEL  21
      M=0                                                                  NIEL  22
7     READ(5,15)K,NP,RPM                                                   NIEL  23
15    FORMAT(2I2,F10.2)                                                    NIEL  24
      DO47I=1,NP                                                           NIEL  25
47    P(I)=PIN(I)                                                          NIEL  26
      P1=P(1)                                                              NIEL  27
      P2=P(2)                                                              NIEL  28
      P3=P(3)                                                              NIEL  29
      P4=P(4)                                                              NIEL  30
      READ(5,28)P3                                                         NIEL  31
28    FORMAT(F10.2)                                                        NIEL  32
      READ(5,11)N,D,XD                                                     NIEL  33
11    FORMAT(I2,2F10.2)                                                    NIEL  34
      M=M+1                                                                NIEL  35
```

```
      DIA=D/12.                                                          NIEL  36
      XX=DIA/2.                                                          NIEL  37
C                                                                        NIEL  38
C--------CALCULATE AA FROM A GIVEN VALUE OF ANGLE                       NIEL  39
C                                                                        NIEL  40
      ANGLE=65.                                                          NIEL  41
      P3=XX*SIN(ANGLE*3.1416/180.)                                       NIEL  42
42    P(3)=P3                                                            NIEL  43
      XX=XD/12.                                                          NIEL  44
      ENQ=RPM*DIA**3                                                     NIEL  45
C                                                                        NIEL  46
C--------READ IN VELOCITY PROFILE                                       NIEL  47
C         NOTE FOR CUTTER'S DATA Z IS READ FIRST, THEN VR                NIEL  48
C         SWITCH IN READ IS DONE BY KGROUP= 2                            NIEL  49
C                                                                        NIEL  50
      IF(KGROUP.GT.1)GOTO43                                              NIEL  51
      READ(5,6)(Y(I),X(I),I=1,N)                                         NIEL  52
      GOTO44                                                             NIEL  53
43    READ(5,6)(X(I),Y(I),I=1,N)                                         NIEL  54
6     FORMAT(2F10.2)                                                     NIEL  55
44    IF(LPRINT.NE.1)WRITE(6,3)(X(I),Y(I),I=1,N)                         NIEL  56
3     FORMAT(1H1,7X,1HX,9X,1HY/(1X,2F10.5))                              NIEL  57
      YM=0.                                                              NIEL  58
C                                                                        NIEL  59
C--------CALCULATE VR IN FT/MIN AND CORRESPONDING VALUE OF Z IN FT       NIEL  60
C                                                                        NIEL  61
      DO10I=1,N                                                          NIEL  62
      X(I)=X(I)/12.                                                      NIEL  63
      Y(I)=Y(I)*60.                                                      NIEL  64
10    YM=YM+Y(I)                                                         NIEL  65
      YM=YM/FLOAT(N)                                                     NIEL  66
C                                                                        NIEL  67
C--------CALCULATE SUM OF SQUARES ABOUT MEAN                            NIEL  68
C                                                                        NIEL  69
      SSM=0.                                                             NIEL  70
      DO12I=1,N                                                          NIEL  71
12    SSM=SSM+(Y(I)-YM)**2                                               NIEL  72
      B=0.                                                               NIEL  73
C                                                                        NIEL  74
C--------CALL PATTERN SEARCH SUBROUTINE                                 NIEL  75
C                                                                        NIEL  76
      IF(KK.GT.30)GOTO29                                                 NIEL  77
      KK=0                                                               NIEL  78
      WRITE(6,19)                                                        NIEL  79
19    FORMAT(1HO,8X,4HP(1),11X,4HP(2),11X,4HP(3), 8X,10HSUM SQ REG,//)   NIEL  80
29    CALL PATERN(NP,P,STEP,4,0,COST)                                    NIEL  81
      P(3)=P3                                                            NIEL  82
      R=SQRT(1.-COST/SSM)                                                NIEL  83
      BHALF=1.762747*XX/P(1)                                             NIEL  84
      UHALF=P(2)*SQRT(P(1)/XX**3)*(XX**2-P(3)**2)**0.25/4.               NIEL  85
      CALL OMEGA(UHALF,Y,X,N,25,BCALC)                                   NIEL  86
      BCALC=BCALC-P(4)                                                   NIEL  87
      BXX=6.*XX/P(1)*12.                                                 NIEL  88
```

```
C                                                                       NIEL  89
C---------PRINT COMPLETE ANALYSIS OF A PROFILE                          NIEL  90
C                                                                       NIEL  91
      IF(LPRINT.EQ.1)GOTO30                                             NIEL  92
      WRITE(6,18)D,XD                                                   NIEL  93
18    FORMAT(1H1,4HD  =,F10.5,/1H0,4HXD =,F10.5,///)                    NIEL  94
      WRITE(6,2)(X(I),Y(I),I=1,N)                                       NIEL  95
2     FORMAT(1H0,7X,1HX,9X,1HY/(1X,2F10.5))                             NIEL  96
      WRITE(6,17)(I,P(I),I=1,NP)                                        NIEL  97
17    FORMAT(1H0,10X10HPARAMETERS,/(1H0,I2,F20.8))                      NIEL  98
      WRITE(6,13)(Y(I),YC(I),I=1,N)                                     NIEL  99
13    FORMAT(1H0,9X,1HY,19X,2HYC/(1X,2F20.8))                           NIEL 100
      WRITE(6,14)COST,R                                                 NIEL 101
14    FORMAT(1H0,27HSUM OF SQUARES OF (Y-YCALC),F20.8,/1H0,             NIEL 102
     127HGOODNESS OF FIT              ,F20.8)                          NIEL 103
      WRITE(6,31)BHALF,BCALC,UHALF                                      NIEL 104
31    FORMAT(1H0,7HBHALF =,F20.8,10X,7HBCALC =,F20.8,/1H0,10X,          NIEL 105
     17HUHALF =,F20.8)                                                  NIEL 106
      WRITE(6,41)XD,BXX                                                 NIEL 107
41    FORMAT(1H0,20X,25HHALF WIDTH OF JET AT XD =,F4.2,1H,,4X,F10.2,    NIEL 108
     12X,6HINCHES,//)                                                   NIEL 109
30    Q(M)=4.*3.1416*P(2)*(XX**2-P(3)**2)**0.25*SQRT(XX/P(1))           NIEL 110
      XR(M)=XD                                                          NIEL 111
      SIGMA(M)=P(1)                                                     NIEL 112
      A(M)=P(2)                                                         NIEL 113
      AA(M)=P(3)                                                        NIEL 114
      ANG(M)=SQRT(XX**2-P(3)**2)/XX                                     NIEL 115
      PA(M)=ARCOS(ANG(M))*180./3.1416                                   NIEL 116
      SQ(M)=COST                                                        NIEL 117
      GF(M)=R                                                           NIEL 118
      PB(M)=P(4)                                                        NIEL 119
      PC(M)=BHALF                                                       NIEL 120
      PD(M)=BCALC                                                       NIEL 121
      PE(M)=UHALF                                                       NIEL 122
C                                                                       NIEL 123
C---------CHECK IF ANOTHER PROFILE IS TO BE ANALYSED                    NIEL 124
C                                                                       NIEL 125
      IF(K.LT.5)GOTO7                                                   NIEL 126
C                                                                       NIEL 127
C---------PRINT SUMMARY OF A SET OF PROFILES                            NIEL 128
C                                                                       NIEL 129
23    WRITE(6,20)(N,XR(N),SIGMA(N),A(N),AA(N),SQ(N),GF(N),N=1,M)        NIEL 130
20    FORMAT(1H1,22X,'NO',1X,6HRADIUS,2X,5HSIGMA,6X,1HA,7X,'AA',5X,     NIEL 131
     1'SUM SQ',4X,'CORR COFF'//(22X,I2,F6.2,2F9.3,F9.4,2F10.3))         NIEL 132
      WRITE(6,21)(N,XR(N),Q(N),ANG(N),PA(N),PB(N),N=1,M)                NIEL 133
21    FORMAT(1X,//20X,'  NO',2X,'RADIUS'  ,4X,'CFM',5X,'COS(PHI)',3X    NIEL 134
     1'ANGLE',10X,'P(4)',//(22X,I2,F6.2,3F10.4,F15.8))                  NIEL 135
      IF(LPUNCH.EQ.1)GOTO71                                             NIEL 136
      PUNCH 26,(SIGMA(N),A(N),AA(N),PB(N),Q(N),ANG(N),N=1,M)            NIEL 137
26    FORMAT(6F12.4)                                                    NIEL 138
71    WRITE(6,40)(I,PE(I),PC(I),PD(I),I=1,M)                            NIEL 139
40    FORMAT(1X,//20X,'  NO',4X,5HUHALF, 6X,5HBHALF, 6X,5HBCALC,///     NIEL 140
     1(22X,I2,F9.2,2F11.4))                                             NIEL 141
```

```
C                                                                       NIEL 142
C--------CHECK IF ANOTHER VELOCITY PROFILE DATA SET IS TO BE ANALYSED    NIEL 143
C                                                                       NIEL 144
      IF(KGROUP.LT.5)GOTO70                                             NIEL 145
8     STOP                                                              NIEL 146
      END                                                               NIEL 147
```

****

SUBROUTINE PROC

****

```
      SUBROUTINE PROC(P,COST)                                           PROC   1
      DIMENSIONX(20),Y(20),YC(20),P(6)                                  PROC   2
      COMMONDIA,X,Y,YC,XX,N,KK,P1,P2,P3,P4                              PROC   3
      P(3)=P3                                                           PROC   4
      P(1)=P1                                                           PROC   5
      COST=0.                                                           PROC   6
      DO1I=1,N                                                          PROC   7
      ETA=P(1)*(X(I)-P(4))/XX                                           PROC   8
      T=1.-(TANH(ETA/2.))**2                                            PROC   9
      YC(I)=P(2)*SQRT(P(1))*(XX**2-P(3)**2)**0.25*T/(XX**1.5*2.)        PROC  10
      COST=COST+(YC(I)-Y(I))**2                                         PROC  11
1     CONTINUE                                                          PROC  12
      IF(KK.GT.30)GOTO5                                                 PROC  13
      IF(KK.NE.0)GOTO4                                                  PROC  14
      WRITE(6,2)P(1),P(2),P(3),P(4),COST                                PROC  15
2     FORMAT(1X,5(1PE13.4))                                             PROC  16
4     KK=KK+1                                                           PROC  17
      IF(KK.LE.30)GOTO5                                                 PROC  18
      KK=0                                                              PROC  19
5     RETURN                                                            PROC  20
      END                                                               PROC  21
```

****

THE FOLLOWING SUPPORTING SUBROUTINE ARE USED
IN COMMON WITH FLOWANL, FOR LISTING SEE LIST F-1

SUBROUTINE PATERN
SUBROUTINE BOUNDS
SUBROUTINE OMEGA

****

****

INPUT DATA

****

```
**************************************************************************

                    PRELIMINARY DATA, CONTROLS MODE OF OPERATION
                    FOR INSTRUCTIONS SEE COMMENT CARDS AT THE BEGINING
                    OF THE PROGRAM

**************************************************************************

 140
12.621      .01
18.         0.5
0.1165      0.0001
0.001       0.0001

**************************************************************************

                                NIELSON'S DATA

**************************************************************************

 1 11.25

**************************************************************************

          VELOCITY PROFILE DATA, 2 INCH TURBINE AT 600 RPM AND
          VARYING RADIAL DISTANCE R

**************************************************************************

 1 4600.

 72.0          1.0
0.38        0.166667
1.32        0.1
2.41        0.03333333
3.47        0.0
1.67        -0.033333
1.01        -0.1
0.34        -0.166667
 1 4600.

 72.0          3.0
0.54        .5571429
0.89        .3714286
1.15        .1857143
1.21        0.0
0.81        -.1857143
0.54        -.3714286
0.37        -.5571429
 1 4600.
```

```
 72.0        4.0
0.55        .5541426
0.71        .3694284
0.81        .1847142
0.9         .0
0.78        -.1847142
0.65        -.3694284
0.56        -.5541426

*************************************************************************************

         VELOCITY PROFILE DATA, 4 INCH TURBINE AT 200 RPM IN WATER
         RADIAL DISTANCE R= 2 INCH

*************************************************************************************

 1 4200.

 94.0        2.0
0.54        .355555556
1.01        .266666667
1.53        .177777778
2.07        .088888889
2.22        .0
1.60        -.08888889
0.83        -.17777778
0.81        -.2666667
0.42        -.35555556

*************************************************************************************

         VELOCITY PROFILE DATA, 4 INCH TURBINE AT 100 RPM IN CORN
         SYRUP. RADIAL DISTANCE R= 2 INCH

*************************************************************************************

 1 4100.

 94.0        2.0
0.22        .355555556
0.33        .266666667
0.74        .177777778
0.88        .088888889
1.14        .0
1.02        -.08888889
0.68        -.17777778
0.34        -.2666667
0.12        -.35555556

*************************************************************************************

         VELOCITY PROFILE DATA, 4 INCH TURBINE AT 200 RPM IN WATER
         RADIAL DISTANCE R= 4
```

```
**********************************************************************************

 1 4200.

114.0         4.0
0.31        .9409090909
0.45        .7527272727
0.75        .5645454545
1.14        .3763636364
1.27        .1881818191
1.26        .0
1.06        -.188181818
0.7         -.376363636
0.47        -.564545454
0.28        -.752727273
0.13        -.940909091

**********************************************************************************

          VELOCITY PROFILE DATA, 7 INCH TURBINE IN WATER,
          RADIAL DISTANCE R= 3.5 INCH

**********************************************************************************

 9 475.

 77.0         3.5
0.61        .6
0.74        .4
1.37        .2
1.5         .0
1.33        -.2
1.          -.4
0.75        -.6

**********************************************************************************

                                    CUTTER'S DATA

**********************************************************************************


**********************************************************************************

          VELOCITY PROFILE DATA, 4 INCH TURBINE AT 200 RPM IN WATER
          AT VARYING RADIAL DISTANCE

**********************************************************************************

 2 11.5
 1 4200.
0.13101295
```

```
 94.          2.
.483          .34
.414          .4
.345          .65
.276          .65
.207          1.11
.138          1.32
.069          1.77
0.0           2.16
 1 4200.
0.13101295
 94.          2.75
.438          .37
.414          .46
.345          .56
.276          .73
.207          1.08
.138          1.22
.069          1.77
0.0           1.51
 1 4200.
0.13101295
 94.          3.38
.552          .51
.483          .57
.414          .69
.345          .84
.276          1.04
.207          1.13
.138          1.53
.069          1.76
0.0           1.67
 1 4200.
0.13101295
 94.          4.13
.552          .72
.483          .78
.414          .59
.345          .79
.276          .88
.207          .87
.138          1.03
.069          1.08
0.0           1.09
 1 4200.
0.13101295
 64.          4.38
.345          1.25
.276          1.34
.207          1.71
.138          1.57
.069          1.51
0.            1.41
```

```
 9 4200.
0.13101295
 64.          5.13
.345         .98
.276         1.09
.207         .99
.138         1.03
.069         1.04
0.0          1.33
```

****

VELOCITY PROFILE DATA, 4 INCH TURBINE AT 400 RPM IN WATER
AT VARYING RADIAL DISTANCE

****

```
 2 11.5
 1 4400.
0.12355394
 74.          2.
.414         .62
.345         1.26
.276         2.70
.207         3.65
.138         4.68
.069         4.47
0.0          4.84
 1 4400.
0.12355394
 64.          2.81
.345         1.87
.276         2.50
.207         2.70
.138         3.04
.069         3.54
0.0          3.94
 1 4400.
0.12355394
 64.          2.86
.345         2.14
.276         2.21
.207         2.81
.138         3.32
.069         3.97
0.0          4.11
 1 4400.
0.12355394
 74.          3.44
.414         1.86
.345         2.13
.276         1.98
.207         2.56
```

```
.138        2.64
.069        2.87
0.0         3.14
 1 4400.
0.12355394
 84.          3.56
.483        1.29
.414        1.30
.345        1.71
.276        1.74
.207        2.26
.138        2.46
.069        2.62
0.0         2.62
 1 4400.
0.12355394
 84.          4.19
.483        1.85
.414        2.3
.345        2.36
.276        2.36
.207        2.39
.138        2.53
.069        2.53
0.0         2.58
 1 4400.
0.12355394
 74.          4.75
.414        1.07
.345        1.08
.276        1.42
.207        1.45
.138        1.40
.069        1.41
0.0         1.63
 9 4400.
0.12355394
 64.          5.56
.345        .33
.276        .44
.207        .55
.138        .42
.069        .45
0.0         .58
```

****

VELOCITY PROFILE DATA, 4 INCH TURBINE AT 600 RPM IN WATER
AT VARYING RADIAL DISTANCE

****

```
 9 11.5
```

```
 1 4600.
0.12180995
 94.          2.14
.552          .07
.483          .87
.414          1.85
.345          2.06
.276          3.
.207          4.91
.138          6.11
.069          7.02
0.0           7.46
 1 4600.
0.12180995
 84.          2.75
.483          1.70
.414          1.72
.345          2.98
.276          3.95
.207          4.33
.138          5.61
.069          5.82
0.0           5.66
 1 4600.
0.12180995
 74.          3.38
.414          2.6
.345          2.66
.276          2.78
.207          3.28
.138          3.84
.069          5.05
.0            5.14
 1 4600.
0.12180995
 84.          4.13
.483          2.19
.414          1.99
.345          2.42
.276          2.62
.207          3.08
.138          4.38
.069          4.21
.0            4.71
 1 4600.
0.12180995
 64.          4.38
.345          2.9
.276          3.02
.207          3.93
.138          4.21
.069          3.76
.0            4.74
```

```
 0 4600.
0.12180995
 64.          5.13
.345          1.97
.276          2.04
.207          2.13
.138          2.48
.069          2.65
.0            2.34
```

LIST F-7

FORTRAN LISTING FOR GRAPH WITH SUPPORTING SUBROUTINE SOLVE AND SAMPLE INPUT. TYPICAL OUTPUT FROM PROGRAM IS ALSO GIVEN

```
**********************************************************************************

                              MAIN PROGRAM GRAPH

**********************************************************************************

C                                                                          GRAP   1
C--------THIS PROGRAM CORRELATES THE PARAMETERS OF THE TANGENTIAL JET      GRAP   2
C         LPRINT= 1, COMPLETE PRINTOUT                                     GRAP   3
C                                                                          GRAP   4
      DIMENSIONX(50),A(50),AA(50),Q(50),SLOPE(50),C(50),RE(50)             GRAP   5
      DIMENSION SIGMA(50),ANG(50),DIA(50),CORR(50),DDA(7)                  GRAP   6
      DIMENSION QND3(50),QAVG(10),DBT(10),ASIG(20),AQND(20),AAA(20)        GRAP   7
      DIMENSION DSIG(10),DQND(10),DAA(10),QTN(50),AANG(20),ADEV(20)        GRAP   8
      DIMENSION DIM(20),TT(20)                                             GRAP   9
      COMMON IS,LPRINT                                                     GRAP  10
      LPRINT=0                                                             GRAP  11
      IS=1                                                                 GRAP  12
      KL=0                                                                 GRAP  13
      KG=0                                                                 GRAP  14
C                                                                          GRAP  15
C--------READ TANK PARAMETERS FOR A SET OF PROFILES                        GRAP  16
C                                                                          GRAP  17
33    I=0                                                                  GRAP  18
17    READ(5,5)KGROUP,T,POISE,RHO                                          GRAP  19
      V=POISE*6.72*0.006/(RHO*62.43)                                       GRAP  20
      IF(I.EQ.0)WRITE(6,15)                                                GRAP  21
C                                                                          GRAP  22
C--------SET UP COUNTER FOR STORING AVERAGE OF SEVERAL PROFILES AT          GRAP  23
C         CONSTANT IMPELLER DIAMETER                                       GRAP  24
C                                                                          GRAP  25
      IF(KGROUP.EQ.2)GOTO1                                                 GRAP  26
      KL=KL+1                                                              GRAP  27
      KG=KG+5                                                              GRAP  28
      IF(KG.EQ.5)KG=1                                                      GRAP  29
15    FORMAT(1H1//     ,20X,'NO',3X,'SIGMA',6X,'A',9X,'AA',6X,'RPM',4X,    GRAP  30
     23X,'Q',4X,'Q/ND**3',2X,'ANGLE',3X,'ND**3'/)                          GRAP  31
C                                                                          GRAP  32
C--------READ PROFILE PARAMETERS                                           GRAP  33
C         IF KGROUP = 2 DELETE AVERAGE                                     GRAP  34
```

```
C                                                                       GRAP  35
1     READ(5,2)A1,A2,A3                                                 GRAP  36
2     FORMAT(3F13.8)                                                    GRAP  37
      READ(5,5)K,RPM,D                                                  GRAP  38
5     FORMAT(I2,3F10.2)                                                 GRAP  39
      IF(KGROUP.EQ.2)GOTO32                                             GRAP  40
      DO24J=1,5                                                         GRAP  41
      JJ=KG-1+J                                                         GRAP  42
24    DIA(JJ)=D                                                         GRAP  43
32    DIM(KL)=D                                                         GRAP  44
      TT(KL)=T                                                          GRAP  45
      DBT(KL)=D/T                                                       GRAP  46
      R=D/24.                                                           GRAP  47
C                                                                       GRAP  48
C--------I, COUNTS NUMBER PROFILES EXAMINED                            GRAP  49
C         START, CALCULATIONS OF ITEMS DESIRED                          GRAP  50
C                                                                       GRAP  51
      I=I+1                                                             GRAP  52
      X(I)=RPM*(D/12.)**3                                               GRAP  53
      RE(I)=RPM*(D/12.)**2/V                                            GRAP  54
      SIGMA(I)=A1                                                       GRAP  55
      A(I)=A2                                                           GRAP  56
      AA(I)=A3                                                          GRAP  57
      ANG(I)=ARCOS (SQRT(R**2-A3**2)/R)*180./3.1416                     GRAP  58
      Q(I)=4.*3.1416*A2*(R**2-A3**2)**0.25*SQRT(R/A1)                   GRAP  59
      QND3(I)=Q(I)/X(I)                                                 GRAP  60
      TEMP=A3                                                           GRAP  61
      QTN(I)=X(I)/(R**2-TEMP**2)**0.25                                  GRAP  62
      WRITE(6,16)I,A1,A2,A3,RPM,Q(I),QND3(I),ANG(I),X(I)                GRAP  63
16    FORMAT(20X,I2,2F9.3,F10.4,F9.2,2F8.3,F8.2,F8.3)                   GRAP  64
      IF(K.LT.5)GOTO1                                                   GRAP  65
      IF(LPRINT.EQ.1)WRITE(6,25)                                        GRAP  66
      IF(KGROUP.EQ.2)GOTO17                                             GRAP  67
C                                                                       GRAP  68
C--------CALCULATE AVERAGE VALUE OF SIGMA AA, AND ND**3                 GRAP  69
C                                                                       GRAP  70
      IF(LPRINT.EQ.1)WRITE(6,30)                                        GRAP  71
30    FORMAT(1H1,8X,'AVERAGE',8X,'VARIANCE',6X,'DEVIATION',/)           GRAP  72
      CALL AVG(SIGMA,I,XM,SSM,VAR,DEV)                                  GRAP  73
      ASIG(KL)=XM                                                       GRAP  74
      DSIG(KL)=DEV                                                      GRAP  75
      CALL AVG(AA  ,I,XM,SSM,VAR,DEV)                                   GRAP  76
      AAA (KL)=XM                                                       GRAP  77
      DAA (KL)=DEV                                                      GRAP  78
      CALL AVG(QND3,I,XM,SSM,VAR,DEV)                                   GRAP  79
      DQND(KL)=DEV                                                      GRAP  80
      QAVG(KL)=XM                                                       GRAP  81
      CALL AVG(ANG ,I,XM,SSM,VAR,DEV)                                   GRAP  82
      AANG(KL)=XM                                                       GRAP  83
      ADEV(KL)=DEV                                                      GRAP  84
      IF(LPRINT.EQ.1)WRITE(6,18)                                        GRAP  85
18    FORMAT(1X//)                                                      GRAP  86
      IF(I.LE.2)GOTO28                                                  GRAP  87
```

```
C                                                                       GRAP  88
C--------FIND EQUATION FOR ND**3 VERSUS A                               GRAP  89
C                                                                       GRAP  90
      IF(LPRINT.EQ.1)WRITE(6,7)                                         GRAP  91
7     FORMAT(1H1,5HND**3,10X,5HSIGMA,9X,10HSIGMA CALC,10X,4HDIFF,/)     GRAP  92
      CALL SOLVE(X  ,A    ,I,C1,C2,COST)                                GRAP  93
      SLOPE(KG  )=C1                                                    GRAP  94
      C(KG  )=C2                                                        GRAP  95
      CORR(KG  )=COST                                                   GRAP  96
      IF(LPRINT.EQ.1)WRITE(6,8)                                         GRAP  97
8     FORMAT(1H1,5HND**3,10X,5H  A  ,9X,10H    A CALC ,10X,4HDIFF,/)    GRAP  98
C                                                                       GRAP  99
C--------FIND EQUATION FOR ND**3/(R**2-AA**2)  VERSUS A                 GRAP 100
C                                                                       GRAP 101
      CALL SOLVE(QTN,A    ,I,C1,C2,COST)                                GRAP 102
      SLOPE(KG+1)=C1                                                    GRAP 103
      C(KG+1)=C2                                                        GRAP 104
      CORR(KG+1)=COST                                                   GRAP 105
C                                                                       GRAP 106
C--------FIND EQUATION FOR RE VERSUS A                                  GRAP 107
C                                                                       GRAP 108
      IF(LPRINT.EQ.1)WRITE(6,12)                                        GRAP 109
12    FORMAT(1H1,5HRE NO,10X,5H  A  ,9X,10H    A CALC ,10X,4HDIFF,/)    GRAP 110
      CALL SOLVE(RE,A     ,I,C1,C2,COST)                                GRAP 111
      SLOPE(KG+2)=C1                                                    GRAP 112
      C(KG+2)=C2                                                        GRAP 113
      CORR(KG+2)=COST                                                   GRAP 114
C                                                                       GRAP 115
C--------FIND EQUATION FOR ND**3 VERSUS Q                               GRAP 116
C                                                                       GRAP 117
      IF(LPRINT.EQ.1)WRITE(6,10)                                        GRAP 118
10    FORMAT(1H1,5HND**3,10X,5H  Q  ,9X,10H    Q CALC ,10X,4HDIFF,/)    GRAP 119
      CALL SOLVE(X,Q      ,I,C1,C2,COST)                                GRAP 120
      SLOPE(KG+3)=C1                                                    GRAP 121
      C(KG+3)=C2                                                        GRAP 122
      CORR(KG+3)=COST                                                   GRAP 123
C                                                                       GRAP 124
C--------FIND EQUATION FOR RE VERSUS Q                                  GRAP 125
C                                                                       GRAP 126
      IF(LPRINT.EQ.1)WRITE(6,13)                                        GRAP 127
13    FORMAT(1H1,5HRE NO,10X,5H  Q  ,9X,10H    Q CALC ,10X,4HDIFF,/)    GRAP 128
      CALL SOLVE(RE,Q     ,I,C1,C2,COST)                                GRAP 129
      SLOPE(KG+4)=C1                                                    GRAP 130
      C(KG+4)=C2                                                        GRAP 131
      CORR(KG+4)=COST                                                   GRAP 132
      GOTO29                                                            GRAP 133
28    KG=KG-5                                                           GRAP 134
29    IF(KGROUP.LT.5)GOTO33                                             GRAP 135
      IF(KL.LT.3)GOTO26                                                 GRAP 136
      IF(LPRINT.EQ.1)WRITE(6,25)                                        GRAP 137
C                                                                       GRAP 138
C--------FIND EQUATION FOR D/T  VERSUS  Q/ND**3                         GRAP 139
C                                                                       GRAP 140
```

```
      CALL SOLVE(DRT,QAVG,KL,C1,C2,COST)                                GRAP 141
      IF(LPRINT.EQ.1)WRITE(6,27)C1,C2,COST                              GRAP 142
27    FORMAT(1X ,'SLOPE =',5X,F15.8/1X,'INTERCEPT =',1X,F15.8,/         GRAP 143
     11X,'CORR COEF =',1X,F15.8/)                                       GRAP 144
      IS=0                                                              GRAP 145
C                                                                       GRAP 146
C--------FIND EQUATION FOR D/T  VERSUS  AVG AA                          GRAP 147
C                                                                       GRAP 148
      CALL SOLVE(DRT,AAA ,KL,C1,C2,COST)                                GRAP 149
      IF(LPRINT.EQ.1)WRITE(6,27)C1,C2,COST                              GRAP 150
C                                                                       GRAP 151
C--------WRITE SUMMARY OF RESULTS                                       GRAP 152
C                                                                       GRAP 153
26    WRITE(6,25)                                                       GRAP 154
25    FORMAT(1H1)                                                       GRAP 155
      DO20J=1,5                                                         GRAP 156
      READ(5,23)DDA                                                     GRAP 157
23    FORMAT(7A4)                                                       GRAP 158
      WRITE(6,21)DDA                                                    GRAP 159
21    FORMAT(1HO,41X,7A4/1HO,29X,'DIA',8X,'SLOPE',10X,'INTERCEPT',6X,   GRAP 160
     1'CORR COEF')                                                      GRAP 161
      IG=KG+J-1                                                         GRAP 162
      DO20I=J,IG,4                                                      GRAP 163
      WRITE(6,22)DIA(I),SLOPE(I),C(I),CORR(I)                           GRAP 164
22    FORMAT(25X,F9.2,F13.4,1X,F15.4,F15.4)                             GRAP 165
20    CONTINUE                                                          GRAP 166
      WRITE(6,31)                                                       GRAP 167
31    FORMAT(1H1,10(/),25X,'NO',3X,'T',6X,'D',6X,'D/T',4X,'SIGMA',4X,   GRAP 168
     1'DEV',5X,'A', 7X,'DEV',6X,'N(Q)',5X,'DEV',5X,'ANGLE',2X,'DEV'/)   GRAP 169
      DO36I=1,KL                                                        GRAP 170
36    WRITE(6,37)I,TT(I),DIM(I),DRT(I),ASIG(I),DSIG(I),AAA(I),DAA(I),   GRAP 171
     1QAVG(I),DQND(I),AANG(I),ADEV(I)                                   GRAP 172
37    FORMAT(25X,I2,2F6.2,F8.4,F9.3,F7.3,F9.4,F9.5,2F9.4,F8.2,F6.2)     GRAP 173
      STOP                                                              GRAP 174
      END                                                               GRAP 175
```

****

SUBROUTINE SOLVE

****

```
      SUBROUTINE SOLVE(X,Y,N,CS,CI,COST)                                SOLV   1
C                                                                       SOLV   2
C        SUBROUTINE SOLVE COMPUTES PARAMETERS FOR A LOG-LOG             SOLV   3
C        LEAST SQUARE FIT                                               SOLV   4
C        MODEL Y=M*X+C                                                  SOLV   5
C                                                                       SOLV   6
C        CS = SLOPE OF LOG-LOG PLOT                                     SOLV   7
C        CI = INTERCEPT OF LOG-LOG PLOT                                 SOLV   8
C        IS, CONTROLS TYPE OF PLOT                                      SOLV   9
C        IS=1 LOG -LOG PLOT                                             SOLV  10
C        IS=-1 SEMILOG                                                  SOLV  11
```

```
C         IS=0 RECTANGULAR PLOT                                          SOLV  12
C                                                                        SOLV  13
      DIMENSION X(50),Y(50),YC(50),DIFF(50)                              SOLV  14
      COMMON IS,LPRINT                                                   SOLV  15
      A1=0.                                                              SOLV  16
      A3=0.                                                              SOLV  17
      B1=0.                                                              SOLV  18
      B2=0.                                                              SOLV  19
      DO30I=1,N                                                          SOLV  20
      TEMP1=X(I)                                                         SOLV  21
      TEMP2=Y(I)                                                         SOLV  22
      IF(IS)11,10,12                                                     SOLV  23
12    TEMP1=ALOG(X(I))                                                   SOLV  24
11    TEMP2=ALOG(Y(I))                                                   SOLV  25
 10   A1=A1+TEMP1                                                        SOLV  26
      A3=A3+TEMP1**2                                                     SOLV  27
      B1=B1+TEMP2                                                        SOLV  28
30    B2=B2+TEMP1*TEMP2                                                  SOLV  29
      A2=N                                                               SOLV  30
      A4=A1                                                              SOLV  31
      DET=A1*A4-A3*A2                                                    SOLV  32
      C1=(B1*A4-B2*A2)/DET                                               SOLV  33
      C2=(A1*B2-A3*B1)/DET                                               SOLV  34
      CS=C1                                                              SOLV  35
      CI=C2                                                              SOLV  36
      IF(IS.NE.0)CI=EXP(C2)                                              SOLV  37
      YM=0.                                                              SOLV  38
      DO4I=1,N                                                           SOLV  39
4     YM=YM+Y(I)                                                         SOLV  40
      YM=YM/FLOAT(N)                                                     SOLV  41
      SSR=0.                                                             SOLV  42
      SSM=0.                                                             SOLV  43
      DO1I=1,N                                                           SOLV  44
      IF(IS)13,14,15                                                     SOLV  45
13    YC(I)=CI*2.71828**(CS*X(I))                                        SOLV  46
      GOTO17                                                             SOLV  47
14    YC(I)=CS*X(I)+CI                                                   SOLV  48
      GOTO17                                                             SOLV  49
15    YC(I)=CI*X(I)**CS                                                  SOLV  50
17    DIFF(I)=Y(I)-YC(I)                                                 SOLV  51
      SSM=SSM+(Y(I)-YM)**2                                               SOLV  52
1     SSR=DIFF(I)**2+SSR                                                 SOLV  53
      IF(LPRINT.NE.1)GOTO7                                               SOLV  54
      WRITE(6,2)(X(I),Y(I),YC(I),DIFF(I),I=1,N)                          SOLV  55
2     FORMAT(1X,4F15.4)                                                  SOLV  56
7     IF(SSR.GT.SSM)GOTO5                                                SOLV  57
      COST=SQRT(1.-SSR/SSM)                                              SOLV  58
5     IF(LPRINT.NE.1)GOTO8                                               SOLV  59
      WRITE(6,6)YM,SSR,SSM,COST                                          SOLV  60
6     FORMAT(1HO,1X,5H YM =,F20.8,/2X,5HSSR =,F20.8,/2X                  SOLV  61
     1,5HSSM =,F20.8,/1X,'CORR COEF =',F14.8/)                           SOLV  62
8     RETURN                                                             SOLV  63
      END                                                                SOLV  64
```

****

SUBROUTINE AVG
FOR LISTING SEE LIST F-1

****

****

INPUT DATA

****

****

TANGENTIAL JET PARAMETERS OBTAINED IN A 12.25 INCH
DIAMETER TANK

****

```
 112.25      0.8937     0.99708
10.5175       13.4772      0.114
 1243.       3.
10.0544       14.285        0.119
 1250.       3.
11.7746       18.557        0.1153
 1333.33     3.
11.8492       22.7386       0.1169
 1400.       3.
11.3673       28.412        0.1117
 1500.       3.
11.5885       31.6168       0.1115
 9550.       3.
```

(a) Results of Analysis for Data Sets Given in Table IV-20.

N*D**3 VERSUS A

DIA	SLOPE	INTERCEPT	CORR COEF
3.00	0.7252	4.3155	0.9851
3.00	0.6786	0.0038	0.9728
4.00	1.0313	0.8706	0.9901
5.00	1.0516	0.0003	0.9996
6.00	0.6966	1.9184	0.9717
3.00	1.0239	3.4737	0.9996
3.00	1.0931	0.0001	0.9897
4.00	1.0731	0.6218	0.9987
5.00	1.1035	0.0000	0.9992

ND**3/(R**2-AA**2) VERSUS A

DIA	SLOPE	INTERCEPT	CORR COEF
3.00	0.7308	1.6014	0.9728
4.00	1.0040	2.1553	0.9913
4.00	1.0306	0.0001	0.9902
5.00	1.0638	0.8673	0.9995
6.00	0.6967	0.0128	0.9742
3.00	1.1558	0.4820	0.9878
4.00	1.1085	1.4082	0.9978
4.00	1.0724	0.0000	0.9986
5.00	1.0708	0.6449	0.9986

RE VERSUS A

DIA	SLOPE	INTERCEPT	CORR COEF
3.00	0.7248	0.0071	0.9851
4.00	0.9488	0.7498	0.9881
5.00	1.0523	1.6058	0.9996
5.00	1.0630	0.0001	0.9995
6.00	0.6768	2.7376	0.9731
3.00	1.0238	0.0004	0.9996
4.00	1.1254	0.3414	0.9978
5.00	1.1042	1.0644	0.9992
5.00	1.0702	0.0000	0.9986

N*D**3 VERSUS Q

DIA	SLOPE	INTERCEPT	CORR COEF
3.00	0.6790	1.5467	0.9728
4.00	1.0034	0.0004	0.9914
5.00	1.0705	0.4907	0.9994
6.00	0.6968	3.7437	0.9742
6.00	0.6766	0.0111	0.9731
3.00	1.0934	0.9031	0.9897
4.00	1.1079	0.0000	0.9977
5.00	1.1094	0.3271	0.9985
6.00	0.9301	1.6988	0.9984

RE VERSUS Q

DIA	SLOPE	INTERCEPT	CORR COEF
3.00	0.6786	0.0038	0.9728
4.00	1.0313	0.8706	0.9901
5.00	1.0516	0.0003	0.9996
6.00	0.6966	1.9184	0.9717
3.00	1.0239	3.4737	0.9996
3.00	1.0931	0.0001	0.9897
4.00	1.0731	0.6218	0.9987
5.00	1.1035	0.0000	0.9992
6.00	0.9345	0.6892	0.9985

NO	T	D	D/T	SIGMA	DEV	A	DEV	N(Q)	DEV	ANGLE	DEV
1	15.00	3.00	0.2000	12.366	1.501	0.1046	0.00335	0.8872	0.1742	56.88	2.83
2	15.00	4.00	0.2667	12.564	1.528	0.1425	0.00362	0.9257	0.0524	58.79	2.41
3	15.00	5.00	0.3333	12.661	0.142	0.1708	0.00191	1.0232	0.0361	55.09	0.92
4	15.00	6.00	0.4000	12.013	0.483	0.2026	0.00155	1.1891	0.2814	54.15	0.60
5	12.25	3.00	0.2449	11.192	0.772	0.1147	0.00309	1.0636	0.0736	66.83	3.69
6	11.50	3.00	0.2609	10.696	0.0	0.1216	0.0	0.7926	0.0	76.61	0.0
7	15.00	4.00	0.2667	14.170	1.037	0.1420	0.00106	0.7529	0.0377	58.46	0.69
8	15.00	5.00	0.3333	13.736	0.624	0.1682	0.00114	0.8148	0.0377	53.84	0.53
9	15.00	6.00	0.4000	12.939	0.927	0.2000	0.00113	0.8990	0.0936	53.12	0.43

(b) Results of Analysis of (1) Tangential Jet Parameters from Table IV-20 and (2) Tangential Jet Parameters Obtained by Keeping σ Constant.

NO	SIGMA	A	AA	RPM	Q	Q/ND**3	ANGLE	ND**3
1	11.502	9.784	0.1051	200.00	3.334	1.067	57.22	3.125
2	11.832	14.062	0.1048	300.00	4.742	1.012	56.96	4.688
3	11.580	14.977	0.1085	400.00	4.875	0.780	60.19	6.250
4	14.410	19.226	0.1009	500.00	6.110	0.782	53.85	7.813
5	12.506	22.496	0.1038	600.00	7.456	0.795	56.17	9.375
6	14.110	7.876	0.1392	100.00	3.259	0.880	56.61	3.704
7	12.097	11.939	0.1421	150.00	5.196	0.935	59.51	5.556
8	13.617	17.050	0.1402	200.00	7.115	0.961	57.27	7.407
9	11.315	20.599	0.1453	250.00	8.977	0.969	60.67	9.259
10	11.682	22.966	0.1456	300.00	9.817	0.883	60.88	11.111
11	12.513	12.776	0.1731	100.00	7.055	0.975	56.17	7.234
12	12.661	20.059	0.1714	150.00	11.127	1.025	55.36	10.851
13	12.833	26.537	0.1690	200.00	14.834	1.025	54.19	14.468
14	12.638	34.011	0.1700	250.00	19.039	1.053	54.70	18.084
15	12.661	37.051	0.1708	275.00	20.632	1.037	55.05	19.893
16	11.744	14.176	0.2024	50.00	9.958	1.593	54.04	6.250
17	11.762	19.539	0.2031	100.00	13.667	1.093	54.33	12.500
18	11.717	24.450	0.2033	125.00	17.116	1.095	54.42	15.625
19	12.577	29.446	0.2037	150.00	19.857	1.059	54.59	18.750
20	12.267	33.860	0.2006	170.00	23.455	1.104	53.35	21.250
21	10.517	13.477	0.1140	243.00	4.181	1.101	65.78	3.797
22	10.054	14.285	0.1190	250.00	3.915	1.002	72.18	3.906
23	11.775	18.557	0.1153	333.33	5.279	1.014	67.28	5.208
24	11.849	22.739	0.1169	400.00	6.175	0.988	69.26	6.250
25	11.367	28.412	0.1117	500.00	8.869	1.135	63.33	7.813
26	11.588	31.617	0.1115	550.00	9.809	1.141	63.13	8.594
27	10.696	17.858	0.1216	333.33	4.128	0.793	76.61	5.208
28	13.678	13.256	0.1426	200.00	5.400	0.729	58.85	7.407
29	13.024	19.066	0.1428	300.00	7.947	0.715	58.95	11.111
30	14.340	26.351	0.1426	366.00	10.490	0.774	58.80	13.556
31	15.158	35.755	0.1410	500.00	14.046	0.758	57.77	18.518
32	14.649	43.917	0.1412	600.00	17.511	0.788	57.93	22.222
33	12.920	20.485	0.1687	200.00	11.429	0.790	54.07	14.468
34	13.587	31.302	0.1686	300.00	17.038	0.785	54.04	21.701
35	14.139	43.751	0.1685	400.00	23.355	0.807	53.99	28.935
36	14.043	57.158	0.1665	500.00	30.951	0.856	53.07	36.169
37	13.991	67.628	0.1686	600.00	36.289	0.836	54.00	43.403
38	11.922	18.123	0.2016	100.00	12.681	1.014	53.74	12.500
39	12.554	34.027	0.1996	200.00	23.413	0.937	52.97	25.000
40	12.904	46.640	0.1997	300.00	31.644	0.844	53.00	37.500
41	13.749	81.635	0.1995	500.00	53.691	0.859	52.94	62.500
42	13.564	95.794	0.1995	600.00	63.094	0.841	52.95	75.000

NO	SIGMA	A	AA	RPM	Q	Q/ND**3	ANGLE	ND**3
1	12.621	10.117	0.1012	200.00	3.428	1.097	54.04	3.125
2	12.621	14.527	0.1012	300.00	4.922	1.050	54.04	4.688
3	12.621	16.171	0.1012	400.00	5.479	0.877	54.04	6.250
4	12.621	19.230	0.1012	500.00	6.515	0.834	54.04	7.813
5	12.621	23.090	0.1012	600.00	7.823	0.834	54.04	9.375
6	12.621	8.159	0.1348	100.00	3.689	0.996	53.97	3.704
7	12.621	12.640	0.1348	150.00	5.715	1.029	53.97	5.556
8	12.621	17.824	0.1348	200.00	8.059	1.088	53.97	7.407
9	12.621	22.396	0.1348	250.00	10.127	1.094	53.97	9.259
10	12.621	25.125	0.1348	300.00	11.361	1.022	53.97	11.111
11	12.621	13.134	0.1684	100.00	7.427	1.027	53.92	7.234
12	12.621	20.421	0.1684	150.00	11.548	1.064	53.92	10.851
13	12.621	26.645	0.1684	200.00	15.068	1.042	53.92	14.468
14	12.621	34.340	0.1684	250.00	19.420	1.074	53.92	18.084
15	12.621	37.575	0.1684	275.00	21.249	1.068	53.92	19.893
16	12.621	14.129	0.2020	50.00	9.592	1.535	53.89	6.250
17	12.621	19.546	0.2020	100.00	13.269	1.062	53.89	12.500
18	12.621	24.476	0.2020	125.00	16.616	1.063	53.89	15.625
19	12.621	29.688	0.2020	150.00	20.154	1.075	53.89	18.750
20	12.621	33.585	0.2020	170.00	22.800	1.073	53.89	21.250
21	12.621	14.166	0.1348	200.00	6.405	0.865	53.97	7.407
22	12.621	20.383	0.1348	300.00	9.216	0.829	53.97	11.111
23	12.621	28.140	0.1348	366.00	12.724	0.939	53.97	13.556
24	12.621	37.600	0.1348	500.00	17.001	0.918	53.97	18.518
25	12.621	46.330	0.1348	600.00	20.949	0.943	53.97	22.222
26	12.621	20.540	0.1684	200.00	11.616	0.803	53.92	14.468
27	12.621	31.429	0.1684	300.00	17.774	0.819	53.92	21.701
28	12.621	43.910	0.1684	400.00	24.832	0.858	53.92	28.935
29	12.621	56.740	0.1684	500.00	32.087	0.887	53.92	36.169
30	12.621	67.882	0.1684	600.00	38.388	0.884	53.92	43.403
31	12.621	19.022	0.2020	100.00	12.234	0.979	53.89	12.500
32	12.621	33.643	0.2020	200.00	22.839	0.914	53.89	25.000
33	12.621	46.200	0.2020	300.00	31.363	0.836	53.89	37.500
34	12.621	80.971	0.2020	500.00	54.968	0.879	53.89	62.500
35	12.621	94.510	0.2020	600.00	64.159	0.855	53.89	75.000

N*D**3 VERSUS A

DIA	SLOPE	INTERCEPT	CORR COFF
6.00	0.6625	4.7008	0.9583
6.00	0.7316	3.7712	0.9771

RE VERSUS A

DIA	SLOPE	INTERCEPT	CORR COEF
6.00	0.2397	1.2031	0.7098
6.00	0.2424	1.3471	0.7564

N*D**3 VERSUS Q

DIA	SLOPE	INTERCEPT	CORR COEF

6.00	0.9421	1.0745	0.9904
6.00	0.9293	1.1665	0.9941

RE VERSUS Q

DIA	SLOPE	INTERCEPT	CORR COEF
6.00	0.3822	0.0921	0.7926
6.00	0.2861	0.4114	0.7108

	AVG	DEVIATION
SIGMA	12.621	0.066
A	0.1539	0.00006
QND**3	0.944	0.0012

	AVG	DEVIATION
SIGMA	12.621	0.000
A	0.1588	0.00007
QND**3	0.977	0.0011

LIST F-8

FORTRAN LISTING FOR MAIN PROGRAM RESULT WITH SUPPORTING SUBROUTINE VARI AND SAMPLE OUTPUT.

```
**********************************************************************************

                              MAIN PROGRAM RESULT

**********************************************************************************

C                                                                          RESU   1
C--------THIS PROGRAM EVALUATES THE PREDICTION OF IMPELLER DISCHARGE       RESU   2
C         Q, AND EDDY VISCOSITY EDVIS                                      RESU   3
C                                                                          RESU   4
      DIMENSION X(50),SIGMA(50),A(50),AA(50),Q(50)                         RESU   5
      DIMENSION E(50),EC(50),QC(50),AC(50),AAC(50)                         RESU   6
      COMMON TDIA(50),DIA(50),FN(50)                                       RESU   7
      I=0                                                                  RESU   8
C                                                                          RESU   9
C--------READ EXPERIMENTALLY OBTAINED VALUES OF TANGENTIAL JET             RESU  10
C         PARAMETERS                                                       RESU  11
C                                                                          RESU  12
17    READ(5,5)KGROUP,T                                                    RESU  13
1     READ(5,2)A1,A2,A3                                                    RESU  14
2     FORMAT(3F13.8)                                                       RESU  15
      READ(5,5)K,RPM,D                                                     RESU  16
5     FORMAT(I2,3F10.2)                                                    RESU  17
      R=D/24.                                                              RESU  18
      I=I+1                                                                RESU  19
      TDIA(I)=T                                                            RESU  20
      DIA(I)=D                                                             RESU  21
      FN(I)=RPM                                                            RESU  22
      X(I)=RPM*(D/12.)**3                                                  RESU  23
      SIGMA(I)=A1                                                          RESU  24
      A(I)=A2                                                              RESU  25
      AA(I)=A3                                                             RESU  26
      TEMP=SQRT(R**2-A3**2)/R                                              RESU  27
C                                                                          RESU  28
C--------CALCULATE EXPERIMENTAL VALUES OF EDVIS AND Q                      RESU  29
C                                                                          RESU  30
      Q(I)=4.*3.1416*A2*(R**2-A3**2)**0.25*SQRT(R/A1)                      RESU  31
      E(I)=A2/(2.*SQRT(A1**3*R))*(2.*R**2-A3**2)/(R**2-A3**2)**0.75        RESU  32
C                                                                          RESU  33
C--------CALCULATE PREDICTED VALUES OF TANGENTIAL JET PARAMETERS FROM      RESU  34
C         CORRELATING EQUATIONS                                            RESU  35
```

```
C                                                                       RESU  36
      A1=12.621                                                         RESU  37
      DBT=(T-D)/T                                                       RESU  38
      TA=DBT                                                            RESU  39
      IF(DBT-0.735)6,6,7                                                RESU  40
7     A3=     0.06924*TA**(-1.837)                                      RESU  41
      GOTO8                                                             RESU  42
6     A3=     0.08354*TA**(-1.7281)                                     RESU  43
8     TEMP=X(I)/(R**2-A3**2)**0.25                                      RESU  44
      A2=1.1436*TEMP**0.8337                                            RESU  45
      TEMP=SQRT(R**2-A3**2)/R                                           RESU  46
C                                                                       RESU  47
C--------CALCULATE PREDICTED VALUES OF Q AND EDVIS                      RESU  48
C                                                                       RESU  49
      QC(I)=4.*3.1416*A2*(R**2-A3**2)**0.25*SQRT(R/A1)                  RESU  50
      EC(I)=A2/(2.*SQRT(A1**3*R))*(2.*R**2-A3**2)/(R**2-A3**2)**0.75    RESU  51
      AC(I)=A2                                                          RESU  52
      AAC(I)=A3                                                         RESU  53
      IF(K.LT.5)GOTO1                                                   RESU  54
      IF(KGROUP.EQ.1)GOTO17                                             RESU  55
C                                                                       RESU  56
C--------CALCULATE DIFFERENCE BETWEEN CALCULATED AND PREDICTED          RESU  57
C         VALUE AND PRINT RESULTS                                       RESU  58
C                                                                       RESU  59
      WRITE(6,20)                                                       RESU  60
20    FORMAT(1H1,28X,'ANALYSIS FOR IMPELLER DISCHARGE Q'//              RESU  61
     120X,'NO',4X,'T',6X,'D',6X,'RPM',8X,'Q',8X,'QC',5X,'DIFF'//)       RESU  62
      CALL VARI(Q,QC,I)                                                 RESU  63
      WRITE(6,21)                                                       RESU  64
21    FORMAT(1H1,20X,'ANALYSIS FOR VOLUMETRIC FLOW, A',//)              RESU  65
      CALL VARI(A,AC,I)                                                 RESU  66
      WRITE(6,22)                                                       RESU  67
22    FORMAT(1H1,20X,'ANALYSIS FOR RADIUS OF SOURCE AA',//)             RESU  68
      CALL VARI(AA,AAC,I)                                               RESU  69
      WRITE(6,23)                                                       RESU  70
23    FORMAT(1H1,28X,'ANALYSIS FOR EDDY VISCOSITY',//                   RESU  71
     120X,'NO',4X,'T',6X,'D',6X,'RPM',8X,'E',8X,'EC',5X,'DIFF'//)       RESU  72
      CALL VARI(E,EC,I)                                                 RESU  73
      STOP                                                              RESU  74
      END                                                               RESU  75
```

****

SUBROUTINE VARI

****

```
      SUBROUTINE VARI(X,Y,N)                                            VARI   1
C                                                                       VARI   2
C--------THIS SUBROUTINE CALCULATES DIFFERENCE BETWEEN CALCULATED       VARI   3
C         AND PREDICTED VALUES OF A VARIABLE AND PRINTS RESULTS         VARI   4
C                                                                       VARI   5
      DIMENSION X(50),Y(50),DIFF(50)                                    VARI   6
      COMMON TDIA(50),DIA(50),FN(50)                                    VARI   7
```

```
      VAR=0.                                                              VARI    8
      DO1I=1,N                                                            VARI    9
      DIFF(I)=X(I)-Y(I)                                                   VARI   10
      WRITE(6,2)I,TDIA(I),DIA(I),FN(I),X(I),Y(I),DIFF(I)                  VARI   11
1     VAR=VAR+DIFF(I)**2                                                  VARI   12
2     FORMAT(20X,I2,2F7.2,F9.2,3F9.3)                                     VARI   13
      WRITE(6,3)VAR                                                       VARI   14
3     FORMAT(1X//,20X,'SUM SQ DIFF =',F15.8)                              VARI   15
      RETURN                                                              VARI   16
      END                                                                 VARI   17
```

****

INPUT DATA
SAME AS IN PROGRAM GRAPH

****

RESULTS OF ANALYSIS BY PROGRAM RESULT

ANALYSIS FOR EDDY VISCOSITY

NO	T	D	RPM	F	FC	DIFF
1	15.00	3.00	200.00	0.407	0.321	0.086
2	15.00	3.00	300.00	0.557	0.450	0.107
3	15.00	3.00	400.00	0.676	0.572	0.105
4	15.00	3.00	500.00	0.523	0.688	-0.165
5	15.00	3.00	600.00	0.802	0.801	0.001
6	15.00	4.00	100.00	0.237	0.361	-0.124
7	15.00	4.00	150.00	0.478	0.506	-0.028
8	15.00	4.00	200.00	0.552	0.643	-0.092
9	15.00	4.00	250.00	0.979	0.775	0.204
10	15.00	4.00	300.00	1.048	0.902	0.146
11	15.00	5.00	100.00	0.455	0.474	-0.019
12	15.00	5.00	150.00	0.687	0.665	0.022
13	15.00	5.00	200.00	0.866	0.845	0.021
14	15.00	5.00	250.00	1.149	1.018	0.132
15	15.00	5.00	275.00	1.260	1.102	0.158
16	15.00	6.00	50.00	0.526	0.389	0.138
17	15.00	6.00	100.00	0.729	0.693	0.036
18	15.00	6.00	125.00	0.919	0.835	0.085
19	15.00	6.00	150.00	1.000	0.972	0.028
20	15.00	6.00	170.00	1.159	1.078	0.081
21	12.25	3.00	243.00	0.879	0.697	0.181
22	12.25	3.00	250.00	1.447	0.714	0.733
23	12.25	3.00	333.33	1.099	0.908	0.192
24	12.25	3.00	400.00	1.489	1.057	0.432
25	12.25	3.00	500.00	1.481	1.273	0.208
26	12.25	3.00	550.00	1.588	1.378	0.210
27	11.50	3.00	333.33	2.412	1.677	0.735
28	15.00	4.00	200.00	0.446	0.643	-0.197
29	15.00	4.00	300.00	0.693	0.902	-0.209
30	15.00	4.00	366.00	0.825	1.065	-0.240
31	15.00	4.00	500.00	0.999	1.381	-0.382
32	15.00	4.00	600.00	1.298	1.608	-0.310
33	15.00	5.00	200.00	0.660	0.845	-0.185
34	15.00	5.00	300.00	0.934	1.185	-0.251
35	15.00	5.00	400.00	1.228	1.506	-0.278
36	15.00	5.00	500.00	1.587	1.814	-0.227
37	15.00	5.00	600.00	1.929	2.112	-0.183
38	15.00	6.00	100.00	0.653	0.693	-0.040
39	15.00	6.00	200.00	1.115	1.235	-0.120
40	15.00	6.00	300.00	1.468	1.732	-0.264
41	15.00	6.00	500.00	2.333	2.651	-0.318
42	15.00	6.00	600.00	2.780	3.086	-0.306

SUM SQ DIFF = 2.56500435

ANALYSIS FOR IMPELLER DISCHARGE Q

NO	T	D	RPM	Q	QC	DIFF
1	15.00	3.00	200.00	3.334	2.960	0.374
2	15.00	3.00	300.00	4.742	4.151	0.591
3	15.00	3.00	400.00	4.875	5.276	-0.401
4	15.00	3.00	500.00	6.110	6.355	-0.245
5	15.00	3.00	600.00	7.456	7.398	0.058
6	15.00	4.00	100.00	3.258	4.012	-0.754
7	15.00	4.00	150.00	5.196	5.625	-0.429
8	15.00	4.00	200.00	7.115	7.150	-0.034
9	15.00	4.00	250.00	8.977	8.612	0.365
10	15.00	4.00	300.00	9.817	10.025	-0.209
11	15.00	5.00	100.00	7.055	8.073	-1.017
12	15.00	5.00	150.00	11.127	11.319	-0.193
13	15.00	5.00	200.00	14.834	14.388	0.447
14	15.00	5.00	250.00	19.039	17.329	1.710
15	15.00	5.00	275.00	20.632	18.762	1.870
16	15.00	6.00	50.00	9.958	7.948	2.010
17	15.00	6.00	100.00	13.667	14.166	-0.499
18	15.00	6.00	125.00	17.116	17.062	0.053
19	15.00	6.00	150.00	19.857	19.863	-0.007
20	15.00	6.00	170.00	23.465	22.048	1.416
21	12.25	3.00	243.00	4.181	3.371	0.810
22	12.25	3.00	250.00	3.915	3.451	0.464
23	12.25	3.00	333.33	5.279	4.387	0.893
24	12.25	3.00	400.00	6.175	5.107	1.068
25	12.25	3.00	500.00	8.869	6.151	2.717
26	12.25	3.00	550.00	9.809	6.660	3.149
27	11.50	3.00	333.33	4.128	4.260	-0.132
28	15.00	4.00	200.00	5.400	7.150	-1.750
29	15.00	4.00	300.00	7.947	10.025	-2.078
30	15.00	4.00	366.00	10.490	11.833	-1.344
31	15.00	4.00	500.00	14.046	15.348	-1.302
32	15.00	4.00	600.00	17.511	17.868	-0.357
33	15.00	5.00	200.00	11.429	14.388	-2.958
34	15.00	5.00	300.00	17.038	20.174	-3.136
35	15.00	5.00	400.00	23.355	25.642	-2.287
36	15.00	5.00	500.00	30.951	30.885	0.066
37	15.00	5.00	600.00	36.288	35.955	0.333
38	15.00	6.00	100.00	12.681	14.166	-1.485
39	15.00	6.00	200.00	23.413	25.247	-1.834
40	15.00	6.00	300.00	31.644	35.402	-3.758
41	15.00	6.00	500.00	53.691	54.198	-0.506
42	15.00	6.00	600.00	63.094	63.095	-0.001

SUM SQ DIFF = 90.65058899

ANALYSIS FOR RADIUS OF SOURCE AA

1	15.00	3.00	200.00	0.105	0.104	0.001
2	15.00	3.00	300.00	0.105	0.104	0.000
3	15.00	3.00	400.00	0.108	0.104	0.004
4	15.00	3.00	500.00	0.101	0.104	-0.003
5	15.00	3.00	600.00	0.104	0.104	-0.000
6	15.00	4.00	100.00	0.139	0.143	-0.004
7	15.00	4.00	150.00	0.142	0.143	-0.001
8	15.00	4.00	200.00	0.140	0.143	-0.003
9	15.00	4.00	250.00	0.145	0.143	0.003
10	15.00	4.00	300.00	0.146	0.143	0.003
11	15.00	5.00	100.00	0.173	0.168	0.005
12	15.00	5.00	150.00	0.171	0.168	0.003
13	15.00	5.00	200.00	0.169	0.168	0.001
14	15.00	5.00	250.00	0.170	0.168	0.002
15	15.00	5.00	275.00	0.171	0.168	0.002
16	15.00	6.00	50.00	0.202	0.202	0.000
17	15.00	6.00	100.00	0.203	0.202	0.001
18	15.00	6.00	125.00	0.203	0.202	0.001
19	15.00	6.00	150.00	0.204	0.202	0.002
20	15.00	6.00	170.00	0.201	0.202	-0.001
21	12.25	3.00	243.00	0.114	0.116	-0.002
22	12.25	3.00	250.00	0.119	0.116	0.003
23	12.25	3.00	333.33	0.115	0.116	-0.001
24	12.25	3.00	400.00	0.117	0.116	0.001
25	12.25	3.00	500.00	0.112	0.116	-0.004
26	12.25	3.00	550.00	0.111	0.116	-0.005
27	11.50	3.00	333.33	0.122	0.121	0.001
28	15.00	4.00	200.00	0.143	0.143	-0.000
29	15.00	4.00	300.00	0.143	0.143	0.000
30	15.00	4.00	366.00	0.143	0.143	-0.000
31	15.00	4.00	500.00	0.141	0.143	-0.002
32	15.00	4.00	600.00	0.141	0.143	-0.002
33	15.00	5.00	200.00	0.169	0.168	0.000
34	15.00	5.00	300.00	0.169	0.168	0.000
35	15.00	5.00	400.00	0.169	0.168	0.000
36	15.00	5.00	500.00	0.167	0.168	-0.002
37	15.00	5.00	600.00	0.169	0.168	0.000
38	15.00	6.00	100.00	0.202	0.202	-0.000
39	15.00	6.00	200.00	0.200	0.202	-0.002
40	15.00	6.00	300.00	0.200	0.202	-0.002
41	15.00	6.00	500.00	0.200	0.202	-0.002
42	15.00	6.00	600.00	0.200	0.202	-0.002

SUM SQ DIFF = 0.00019938

ANALYSIS FOR VOLUMETRIC FLOW, A

1	15.00	3.00	200.00	9.784	9.020	0.764
2	15.00	3.00	300.00	14.062	12.648	1.413
3	15.00	3.00	400.00	14.977	16.077	-1.100
4	15.00	3.00	500.00	19.226	19.364	-0.137
5	15.00	3.00	600.00	22.496	22.542	-0.046
6	15.00	4.00	100.00	7.876	9.474	-1.599
7	15.00	4.00	150.00	11.939	13.285	-1.346
8	15.00	4.00	200.00	17.050	16.886	0.164
9	15.00	4.00	250.00	20.599	20.338	0.261
10	15.00	4.00	300.00	22.966	23.677	-0.711
11	15.00	5.00	100.00	12.776	14.272	-1.496
12	15.00	5.00	150.00	20.059	20.013	0.046
13	15.00	5.00	200.00	26.537	25.437	1.100
14	15.00	5.00	250.00	34.011	30.638	3.373
15	15.00	5.00	275.00	37.051	33.172	3.880
16	15.00	6.00	50.00	14.176	11.708	2.468
17	15.00	6.00	100.00	19.539	20.866	-1.328
18	15.00	6.00	125.00	24.450	25.133	-0.683
19	15.00	6.00	150.00	29.446	29.258	0.187
20	15.00	6.00	170.00	33.860	32.477	1.383
21	12.25	3.00	243.00	13.477	12.489	0.988
22	12.25	3.00	250.00	14.285	12.789	1.496
23	12.25	3.00	333.33	18.557	16.255	2.302
24	12.25	3.00	400.00	22.739	18.923	3.815
25	12.25	3.00	500.00	28.412	22.792	5.620
26	12.25	3.00	550.00	31.617	24.677	6.939
27	11.50	3.00	333.33	17.858	18.836	-0.978
28	15.00	4.00	200.00	13.256	16.886	-3.629
29	15.00	4.00	300.00	19.066	23.677	-4.611
30	15.00	4.00	366.00	26.351	27.946	-1.595
31	15.00	4.00	500.00	35.755	36.248	-0.493
32	15.00	4.00	600.00	43.917	42.198	1.719
33	15.00	5.00	200.00	20.485	25.437	-4.952
34	15.00	5.00	300.00	31.302	35.667	-4.365
35	15.00	5.00	400.00	43.751	45.335	-1.584
36	15.00	5.00	500.00	57.158	54.604	2.554
37	15.00	5.00	600.00	67.628	63.568	4.060
38	15.00	6.00	100.00	18.123	20.866	-2.743
39	15.00	6.00	200.00	34.027	37.189	-3.162
40	15.00	6.00	300.00	46.640	52.146	-5.506
41	15.00	6.00	500.00	81.635	79.832	1.803
42	15.00	6.00	600.00	95.294	92.937	2.357

SUM SQ DIFF = 318.60253906

ANALYSIS FOR IMPELLER DISCHARGE Q

NO	T	D	RPM	Q	QC	DIFF
1	15.00	3.00	200.00	3.334	2.960	0.374
2	15.00	3.00	300.00	4.742	4.151	0.591
3	15.00	3.00	400.00	4.875	5.276	-0.401
4	15.00	3.00	500.00	6.110	6.355	-0.245
5	15.00	3.00	600.00	7.456	7.398	0.058
6	15.00	4.00	100.00	3.258	4.012	-0.754
7	15.00	4.00	150.00	5.196	5.625	-0.429
8	15.00	4.00	200.00	7.115	7.150	-0.034
9	15.00	4.00	250.00	8.977	8.612	0.365
10	15.00	4.00	300.00	9.817	10.025	-0.209
11	15.00	5.00	100.00	7.055	8.073	-1.017
12	15.00	5.00	150.00	11.127	11.319	-0.193
13	15.00	5.00	200.00	14.834	14.388	0.447
14	15.00	5.00	250.00	19.039	17.329	1.710
15	15.00	5.00	275.00	20.632	18.762	1.870
16	15.00	6.00	50.00	9.958	7.948	2.010
17	15.00	6.00	100.00	13.667	14.166	-0.499
18	15.00	6.00	125.00	17.116	17.062	0.053
19	15.00	6.00	150.00	19.857	19.863	-0.007
20	15.00	6.00	170.00	23.465	22.048	1.416
21	12.25	3.00	243.00	4.181	3.371	0.810
22	12.25	3.00	250.00	3.915	3.451	0.464
23	12.25	3.00	333.33	5.279	4.387	0.893
24	12.25	3.00	400.00	6.175	5.107	1.068
25	12.25	3.00	500.00	8.869	6.151	2.717
26	12.25	3.00	550.00	9.809	6.660	3.149
27	11.50	3.00	333.33	4.128	4.260	-0.132
28	15.00	4.00	200.00	5.400	7.150	-1.750
29	15.00	4.00	300.00	7.947	10.025	-2.078
30	15.00	4.00	366.00	10.490	11.833	-1.344
31	15.00	4.00	500.00	14.046	15.348	-1.302
32	15.00	4.00	600.00	17.511	17.868	-0.357
33	15.00	5.00	200.00	11.429	14.388	-2.958
34	15.00	5.00	300.00	17.038	20.174	-3.136
35	15.00	5.00	400.00	23.355	25.642	-2.287
36	15.00	5.00	500.00	30.951	30.885	0.066
37	15.00	5.00	600.00	36.288	35.955	0.333
38	15.00	6.00	100.00	12.681	14.166	-1.485
39	15.00	6.00	200.00	23.413	25.247	-1.834
40	15.00	6.00	300.00	31.644	35.402	-3.758
41	15.00	6.00	500.00	53.691	54.198	-0.506
42	15.00	6.00	600.00	63.094	63.095	-0.001

SUM SQ DIFF = 90.65058899

APPENDIX G

SUMMARY OF TANGENTIAL JET ANALYSIS

This appendix gives the summary of results obtained from velocity profile data analyzed by the program FLOWANL. The listing of the program and the input data were given in Appendix F. The velocity profile summary is presented in Tables which are used in Chapter IV.

Section 4.1 of Chapter IV draws important conclusions and comments on the material given in the tables of this section. Section 4.4, 4.5 and Appendix H form the basis of the tables in this section. Appendix H presents the analysis of a single velocity profile in four tables. A typical set of tables for a velocity profile are Tables H-1, H-2, H-3, and H-4. Seventeen items from these tables are considered to be of interest and form a single line of a table in this appendix.

In Section 4.2 it was shown that the average values of σ the jet width parameter and a the radius of source parameter are reasonable estimates of these parameters, independent of impeller speed. The profile analysis was thus repeated with σ and a as constants, their values being given by Equations IV-9, and IV-10. The results of their analysis are presented back to back with corresponding tables where these parameters were originally free. This point will be made clear when the tables are presented.

In Table G-1 is given a list of abbreviations that form the column headings of the tables presented in this section. These abbreviations were needed because of use of upper case letters by the computer and the need to keep these headings as brief as possible. The abbreviations are in most cases the variables names used in the program FLOWANL. Each pair of tables that follow are for a constant impeller speed. The first table in the pair is with σ, and a (AA) obtained by a least square fit. The second table of the pair is with σ and a (AA) fixed by Equations IV-9 and IV-10 as noted above. Thus for example, Table G-2 and G-3 is for impeller speed at 243 RPM, and h = 3.0 inches, G-4 and G-5 at 250 RPM and h = 6.0 inches, etc. Tables G-2 to G-13 are for velocity profiles taken in 12.25 inch diameter tank while Tables G-14 and G-15, the data was taken in 11.5 inch diameter tank.

Summary of Cooper's Data

In Tables G-16 to G-33 are summarized the result of velocity profile analysis obtained from the program COOPER. The program and input data are given in Appendix F. Tables G-16 to G-23 are for velocity profiles obtained in water, Tables G-23 to G-29 are for profiles obtained in air, and Tables G-30 to G-33 are for varying radial distance and impeller blade width. Profile measurements in air are made with a hot wire anemometer.

In Section 4.7 of Chapter IV, Figure IV-13 suggests that σ is a constant independent of impeller diameter, impeller speed, tank diameter and fluid in the tank. The constant value of σ was estimated as

12.621 ± 0.066. Hence the analysis was repeated with σ kept constant at this value for Cooper's data. The result of this analysis is presented back to back with the case for σ obtained by a least square fit. This facilitates comparison between the two different cases. Thus for example, pairs of Tables G-16 and G-17, G-18 and G-19, etc. are results of analysis of the same data. The first table in the pair G-16 is for σ free while the second table is with σ constant.

In some of these tables a zero value is recorded for BALC and for the correlation coefficient. This occurs for example in Table G-30, Profile Number 5. This means that both these quantities coule not be calculated and were set equal to zero.

Summary of Nielson's and Cutter's Data

The summary of Nielson's data is given in Tables G-34 and G-35, while that of Cutter's data is given in Tables G-36 through G-41. In the analysis of the data the radius of source a, was selected by choosing a value for $\bar{\theta}_y$. The value of $\bar{\theta}_y$ is given under the heading ANGLE and is calculated from A-14. It is a function of r and it will be noticed that it decreases with increasing r. The value of $\bar{\theta}_y$ selected for evaluating a can be found in these tables by looking up $\bar{\theta}_y$ corresponding to r equal to D/2.

TABLE G-1

LIST OF ABBREVIATIONS USED FOR COLUMN HEADINGS

IN TABLES OF APPENDIX G

NO	=	Profile Number
RADIAL ANGLE	=	Angular position of radial plane in which velocity profile measurements are made. The angle is measured with respect to a baffle as shown in Figure III-1. (degrees)
SIGMA	=	σ
A	=	A, (ft^3/min)
AA	=	a, (ft.)
SUM SQ	=	Sum of Squares defined by Equation IV-1
Q	=	$\vec{q}$
VR	=	$\bar{v}_r$
CORR COEF	=	Correlation Coefficient R, defined by Equation IV-
CFM IMP	=	Volumetric flow at impeller periphery from Equation IV-7 (ft^3/min)
CFM	=	Volumetric flow at radial distance r from Equatio nB-31 (ft^3/min)
COS(PH1)	=	Cos θ_y

TABLE G-1 CONTINUED

ANGLE	=	$\bar{\theta}_y$ obtained from Equation A-14, (degrees)
P(4)	=	z_o, (ft)
UHALD	=	$\frac{1}{2}\bar{q}_{max}$, (ft^3/min)
BHALF	=	z, corresponding to $\bar{q} = \frac{1}{2}\bar{q}_{max}$ from Equation H-1, (ft)
BCALC	=	BHALF obtained by direct interpolation of the data (ft)
AVG ANGLE	=	Arithmetic average angle of angle profile θ_y (degrees)
NAD**3	=	ND^3 (ft^3/min)

At the bottom of the tables the following headings are used:

AVERAGE	=	Arithmetic Average
VARIANCE	=	Variance S_x^2, defined by Equation IV-
DEVIATION	=	0.95 confidence limit from t-test from Equation IV-5

TABLE G-2

SUMMARY OF VELOCITY PROFILE ANALYSIS AT 243 RPM, IN

A 12.25 INCH DIAMETER TANK

NO	RADIAL ANGLE	RADIUS	SIGMA	A	AA	SUM SQ Q	SUM SQ VR	CORR COEF Q	CORR COEF VR
1	44.10	2.50	11.520	13.466	0.1141	179.21	222.93	0.9895	0.9851
2	44.10	2.50	11.635	13.293	0.1160	39.10	145.90	0.9979	0.9905
3	5.50	2.50	11.151	13.406	0.1198	22.73	168.13	0.9989	0.9903
4	44.10	3.00	10.798	12.956	0.1151	40.87	46.75	0.9961	0.9949
5	5.50	3.00	10.453	13.390	0.1196	63.73	73.11	0.9938	0.9920
6	44.10	3.50	10.411	13.424	0.1073	20.71	25.82	0.9958	0.9942
7	5.50	3.50	10.267	13.485	0.1163	29.34	40.82	0.9952	0.9928
8	44.10	4.00	8.720	13.951	0.1034	343.97	316.05	0.9171	0.9214
9	5.50	4.00	9.709	13.920	0.1145	19.22	26.36	0.9932	0.9903

NO	CFM IMP	CFM	COS(PHI)	ANGLE	P(4)
1	3.9816	9.5009	0.8366	33.2126	0.00047730
2	3.7412	9.2995	0.8308	33.8195	-0.00070210
3	3.3729	9.5069	0.8182	35.0942	0.00131070
4	3.8702	11.6712	0.8878	27.4070	0.00198500
5	3.5019	12.1920	0.8781	28.5906	0.00159400
6	4.6838	14.7053	0.9299	21.5750	0.00324489
7	4.0014	14.7720	0.9170	23.5017	0.00541996
8	5.5616	19.2957	0.9506	18.0759	0.00621194
9	4.4450	18.1347	0.9392	20.0897	0.00612583

TABLE G-2 CONTINUED

NO	UHALF	BHALF	RCALC	AVG ANGLE	ND**3
1	59.96	0.0319	-0.0326	36.07	3.797
2	59.69	0.0316	-0.0312	37.18	3.797
3	59.39	0.0329	0.0336	38.45	3.797
4	45.19	0.0408	0.0399	28.52	3.797
5	46.20	0.0422	-0.0446	29.89	3.797
6	38.50	0.0494	0.0471	21.68	3.797
7	38.68	0.0501	-0.0523	24.29	3.797
8	31.69	0.0674	0.0895	18.63	3.797
9	33.57	0.0605	-0.0646	20.34	3.797

	AVERAGE	VARIANCE	DEVIATION
A	13.4770	0.0927	0.234
SIGMA	10.5182	0.8370	0.703
AA	0.1140	0.00002914	0.00415

VELOCITY FACTOR= 0.50

TABLE G-3

SUMMARY OF VELOCITY PROFILE ANALYSIS AT 243 RPM σ AND A CONSTANT,

IN A 12.25 INCH DIAMETER TANK

NO	RADIAL ANGLE	RADIUS	SIGMA	A	AA	SUM SQ O	SUM SQ VR	CORR COEF O	CORR COEF VR
1	44.10	2.50	11.192	13.483	0.1147	194.14	299.07	0.9896	0.9839
2	44.10	2.50	11.192	13.361	0.1147	67.56	259.28	0.9963	0.9931
3	5.50	2.50	11.192	13.539	0.1147	23.03	194.93	0.9989	0.9887
4	44.10	3.00	11.192	12.919	0.1147	57.12	35.93	0.9946	0.9961
5	5.50	3.00	11.192	13.377	0.1147	124.94	61.86	0.9879	0.9932
6	44.10	3.50	11.192	13.204	0.1147	57.65	53.55	0.9883	0.9879
7	5.50	3.50	11.192	13.355	0.1147	94.10	50.31	0.9846	0.9893
8	44.10	4.00	11.192	13.275	0.1147	652.03	551.76	0.8359	0.8581
9	5.50	4.00	11.192	13.560	0.1147	119.72	85.44	0.9569	0.9683

NO	CFM IMP	CFM	COS(PHI)	ANGLE	P(4)
1	3.9915	9.6407	0.8348	33.4053	0.00046300
2	3.9554	9.5535	0.8348	33.4053	-0.00073120
3	4.0080	9.6804	0.8348	33.4053	0.00131400
4	3.8244	11.4357	0.8885	27.3096	0.00195000
5	3.9600	11.8411	0.8885	27.3096	0.00157000
6	3.9088	13.8710	0.9194	23.1573	0.00309000
7	3.9535	14.0296	0.9194	23.1573	0.00540906
8	3.9298	16.1060	0.9389	20.1269	0.00669693
9	4.0143	16.4524	0.9389	20.1269	0.00596895

TABLE G-3 CONTINUED

NO	UHALF	BHALF	RCALC	AVG ANGLE	ND**3
1	59.24	0.0328	-0.0331	36.07	3.797
2	58.71	0.0328	-0.0316	37.18	3.797
3	59.49	0.0328	0.0336	38.45	3.797
4	45.85	0.0394	0.0396	28.52	3.797
5	47.48	0.0394	-0.0434	29.89	3.797
6	39.49	0.0459	0.0464	21.68	3.797
7	39.94	0.0459	-0.0510	24.29	3.797
8	34.37	0.0525	0.0528	18.63	3.797
9	35.11	0.0525	-0.0621	20.34	3.797

	AVERAGE	VARIANCE	DEVIATION
A	13.3416	0.0389	0.152

TABLE G-4

SUMMARY OF VELOCITY PROFILE ANALYSIS AT 250 RPM IN A 12.25 INCH DIAMETER TANK

NO	RADIAL ANGLE	RADIUS	SIGMA	A	AA	SUM SQ O	SUM SQ VR	CORR COEF O	CORR COEF VR
1	44.10	2.50	12.133	13.639	0.1177	283.65	347.16	0.9863	0.9804
2	5.50	2.50	10.525	14.600	0.1212	1684.47	1304.71	0.9455	0.9524
3	44.10	3.00	8.312	14.590	0.1129	72.46	71.78	0.9814	0.9799
4	5.50	3.00	9.251	14.310	0.1242	172.84	167.02	0.9778	0.9772

NO	CFM IMP	CFM	COS(PHI)	ANGLE	P(4)
1	3.5677	9.3114	0.8251	34.4034	-0.00076299
2	3.5063	10.6265	0.8135	35.5601	0.00059800
3	5.2095	15.0174	0.8923	26.8422	-0.00362798
4	2.4513	13.7689	0.8678	29.7993	-0.00243599

NO	UHALF	RHALF	RCALC	AVG ANGLE	ND**3
1	62.76	0.0303	-0.0272	38.15	3.906
2	63.02	0.0349	-0.0295	42.01	3.906
3	44.53	0.0530	0.0826	27.08	3.906
4	46.72	0.0476	0.0547	30.55	3.906

	AVERAGE	VARIANCE	DEVIATION
A	14.2847	0.2034	0.718
SIGMA	10.0553	2.7412	2.634
AA	0.1190	0.00002373	0.00775

VELOCITY FACTOR= 0.50

TABLE G-5

SUMMARY OF VELOCITY PROFILE ANALYSIS AT 250 RPM σ AND A CONSTANT

NO	RADIAL ANGLE	RADIUS	SIGMA	A	AA	SUM SQ Q	SUM SQ VR	CORR COEF Q	CORR COEF VR
1	44.10	2.50	11.192	13.785	0.1147	410.55	684.31	0.9801	0.9611
2	5.50	2.50	11.192	14.744	0.1147	1772.89	1147.34	0.9426	0.9583
3	44.10	3.00	11.192	13.819	0.1147	823.19	545.45	0.7661	0.8354
4	5.50	3.00	11.192	14.126	0.1147	611.03	272.48	0.9191	0.9625

NO	CFM IMP	CFM	COS(PHI)	ANGLE	P(4)
1	4.0808	9.8563	0.8348	33.4053	-0.00078600
2	4.3648	10.5423	0.8348	33.4053	0.00075880
3	4.0909	12.2324	0.8885	27.3096	-0.00364210
4	4.1817	12.5042	0.8885	27.3096	-0.00210720

NO	UHALF	BHALF	BCALC	AVG ANGLE	NO**3
1	60.57	0.0328	0.0292	38.15	3.906
2	64.79	0.0328	-0.0286	42.01	3.906
3	49.04	0.0394	0.0643	27.08	3.906
4	50.13	0.0394	0.0421	30.55	3.906

	AVERAGE	VARIANCE	DEVIATION
A	14.1186	0.1976	0.707

TABLE G-6

SUMMARY OF VELOCITY PROFILE ANALYSIS AT 333.3 RPM IN A 12.25 INCH DIAMETER TANK

NO	RADIAL ANGLE	RADIUS	SIGMA	A	AA	SUM SQ Q	SUM SQ VP	CORR COEF Q	CORR COEF VP
1	44.10	2.50	11.777	18.540	0.1175	1167.41	1030.48	0.9782	0.9759
2	5.50	2.50	12.716	18.872	0.1154	2155.44	1513.15	0.9669	0.9700
3	44.10	3.00	11.323	18.267	0.1126	123.26	127.14	0.9935	0.9925
4	5.50	3.00	11.278	18.545	0.1159	235.63	214.26	0.9919	0.9915

NO	CFM IMP	CFM	COS(PHI)	ANGLE	P(4)
1	4.9626	12.8536	0.8259	34.3206	0.00319199
2	5.1509	12.6419	0.8325	33.6435	0.00345199
3	5.6174	16.1148	0.8928	26.7737	0.00022360
4	5.3116	16.3304	0.8861	27.6144	0.00274200

NO	UHALF	BHALF	BCALC	AVG ANGLE	ND**3
1	84.01	0.0312	0.0279	38.45	5.208
2	88.51	0.0289	0.0286	37.68	5.208
3	65.05	0.0389	-0.0390	28.38	5.208
4	66.16	0.0391	0.0373	29.66	5.208

	AVERAGE	VARIANCE	DEVIATION
A	18.5561	0.0613	0.394
SIGMA	11.7734	0.4457	1.062
AA	0.1153	0.00000407	0.00321

VELOCITY FACTOR= 0.50

TABLE G-7

SUMMARY OF VELOCITY PROFILE ANALYSIS AT 333.3 RPM σ AND A CONSTANT

NO	RADIAL ANGLE	RADIUS	SIGMA	A	AA	SUM SQ Q	SUM SQ VP	CORR COEF Q	CORR COEF VR
1	44.10	2.50	11.192	18.671	0.1147	1278.12	1401.56	0.9761	0.9671
2	5.50	2.50	11.192	18.960	0.1147	2853.65	2578.72	0.9559	0.9484
3	44.10	3.00	11.192	18.247	0.1147	125.96	146.10	0.9934	0.9914
4	5.50	3.00	11.192	18.580	0.1147	237.39	232.98	0.9918	0.9908

NO	CFM IMP	CFM	COS(PHI)	ANGLE	P(4)
1	5.5273	13.3500	0.8348	33.4053	0.00321520
2	5.6128	13.5564	0.8348	33.4053	0.00329900
3	5.4017	16.1519	0.8885	27.3096	0.00019010
4	5.5004	16.4471	0.8885	27.3096	0.00273499

NO	UHALF	BHALF	BCALC	AVG ANGLE	ND**3
1	82.04	0.0328	0.0286	38.45	5.208
2	83.31	0.0328	0.0299	37.68	5.208
3	64.76	0.0394	-0.0390	28.38	5.209
4	65.94	0.0394	0.0374	29.66	5.208

	AVERAGE	VARIANCE	DEVIATION
A	18.6146	0.0863	0.467

TABLE G-8

SUMMARY OF VELOCITY PROFILE ANALYSIS AT 400 RPM IN A 12.25 INCH DIAMETER TANK

NO	RADIAL ANGLE	RADIUS	SIGMA	A	AA	SUM SQ Q	SUM SQ VR	CORR COEF Q	CORR COEF VR
1	44.10	2.50	12.563	22.645	0.1191	456.91	544.34	0.9944	0.9912
2	5.50	2.50	12.603	22.909	0.1202	777.34	777.94	0.9911	0.9884
3	44.10	3.00	11.095	22.671	0.1128	479.71	356.76	0.9902	0.9918
4	5.50	3.00	11.137	22.730	0.1157	501.97	421.70	0.9900	0.9906

NO	CFM IMP	CFM	COS(PHI)	ANGLE	P(4)
1	5.5214	15.1493	0.8204	34.8793	0.00174900
2	5.3045	15.2675	0.8167	35.2442	0.00378898
3	7.0236	20.2004	0.8925	26.8101	-0.00025910
4	6.5864	20.1470	0.8865	27.5616	0.00759289

NO	UHALF	BHALF	BCALC	AVG ANGLE	ND**3
1	106.34	0.0292	-0.0289	37.92	6.250
2	107.99	0.0291	-0.0287	37.67	6.250
3	79.93	0.0397	-0.0374	29.65	6.250
4	80.56	0.0396	-0.0378	30.93	6.250

	AVERAGE	VARIANCE	DEVIATION
A	22.7387	0.0142	0.189
SIGMA	11.8495	0.7180	1.348
AA	0.1169	0.00001156	0.00541

VELOCITY FACTOR= 0.50

TABLE G-9

SUMMARY OF VELOCITY PROFILE ANALYSIS AT 400 RPM σ AND A CONSTANT

NO	RADIAL ANGLE	RADIUS	SIGMA	A	AA	SUM SQ O	SUM SQ VP	CORR COEF O	CORR COEF VP
1	44.10	2.50	11.192	22.924	0.1147	1347.72	1944.56	0.9833	0.9684
2	5.50	2.50	11.192	23.285	0.1147	1664.98	2177.71	0.9809	0.9671
3	44.10	3.00	11.192	22.610	0.1147	483.41	324.84	0.9901	0.9925
4	5.50	3.00	11.192	22.750	0.1147	503.12	405.33	0.9900	0.9910

NO	CFM IMP	CFM	COS(PHI)	ANGLE	P(4)
1	6.7864	16.3909	0.8348	33.4053	0.00173600
2	6.8931	16.6487	0.8348	33.4053	0.00342999
3	6.6933	20.0140	0.8885	27.3096	-0.00025000
4	6.7347	20.1380	0.8885	27.3096	0.00758693

NO	UHALF	BHALF	BCALC	AVG ANGLE	NO**3
1	100.73	0.0328	0.0291	37.92	6.250
2	102.31	0.0328	0.0293	37.67	6.250
3	80.24	0.0394	-0.0373	29.65	6.250
4	80.74	0.0394	-0.0377	30.93	6.250

	AVERAGE	VARIANCE	DEVIATION
A	22.8923	0.0851	0.464

TABLE G-10

SUMMARY OF VELOCITY PROFILE ANALYSIS AT 500 RPM IN A 12.25 INCH DIAMETER TANK

NO	RADIAL ANGLE	RADIUS	SIGMA	A	AA	SUM SQ Q	SUM SQ VR	CORR COEF Q	CORR COEF VR
1	44.10	2.50	12.187	27.425	0.1158	654.33	1111.17	0.9964	0.9922
2	5.50	2.50	11.939	27.380	0.1185	912.57	1540.54	0.9940	0.9875
3	44.10	2.50	14.318	27.339	0.1168	730.47	747.26	0.9955	0.9939
4	5.50	2.50	13.460	29.654	0.1186	759.04	856.23	0.9961	0.9941
5	44.10	3.00	11.165	27.726	0.1141	311.34	422.72	0.9953	0.9926
6	5.50	3.00	10.886	27.729	0.1173	441.62	483.93	0.9951	0.9939
7	44.10	3.00	11.265	28.910	0.1039	1527.45	1071.78	0.9869	0.9899
8	5.50	3.00	10.940	29.331	0.1115	603.73	633.12	0.9938	0.9929
9	44.10	3.50	10.270	28.608	0.1064	377.70	448.53	0.9924	0.9900
10	5.50	3.50	10.486	28.325	0.1102	200.12	314.76	0.9965	0.9942
11	44.10	4.00	9.646	29.215	0.0967	555.15	498.50	0.9859	0.9868
12	5.50	4.00	9.844	29.304	0.1102	150.41	232.44	0.9962	0.9940

NO	CFM IMP	CFM	COS(PHI)	ANGLE	P(4)
1	7.5681	18.7510	0.8312	33.7755	0.00070500
2	7.0092	18.8120	0.8223	34.6829	0.00188900
3	6.7753	17.2132	0.8281	34.0977	-0.07912266
4	7.1447	19.1879	0.8223	34.6889	0.00321010
5	8.3371	24.5910	0.8899	27.1446	0.00203899
6	7.7484	24.8097	0.8830	27.9948	0.00432395
7	10.0924	25.8084	0.9096	24.5481	0.00055100
8	9.3682	26.3574	0.8951	26.4831	0.00434996
9	10.1638	31.5723	0.9311	21.3866	0.00351099
10	9.4345	30.8479	0.9258	22.2064	0.00593193
11	11.7609	38.5453	0.9570	16.8662	0.00459896
12	10.0857	38.0085	0.9438	19.2982	0.00967098

TABLE G-10 CONTINUED

NO	UHALF	BHALF	BCALC	AVG ANGLE	ND**3
1	126.01	0.0301	0.0314	38.04	7.813
2	125.19	0.0308	0.0312	40.87	7.813
3	136.42	0.0256	0.0279	37.62	7.813
4	143.97	0.0273	-0.0275	37.65	7.813
5	98.21	0.0395	0.0396	28.71	7.813
6	97.36	0.0405	-0.0394	32.00	7.813
7	101.74	0.0391	0.0396	28.72	7.813
8	102.54	0.0403	0.0386	30.75	7.813
9	81.44	0.0501	0.0485	21.95	7.813
10	81.71	0.0490	-0.0488	25.04	7.813
11	69.56	0.0609	-0.0648	18.27	7.813
12	70.98	0.0597	0.0580	21.39	7.813

	AVERAGE	VARIANCE	DEVIATION
A	28.4122	0.7499	0.550
SIGMA	11.3672	1.9830	0.895
AA	0.1117	0.00004487	0.00426

VELOCITY FACTOR= 0.50

TABLE G-11

SUMMARY OF VELOCITY PROFILE ANALYSIS AT 500 RPM, σ AND A CONSTANT

NO	RADIAL ANGLE	RADIUS	SIGMA	A	AA	SUM SQ Q	SUM SQ VP	CORR COEF Q	CORR COEF VP
1	44.10	2.50	11.192	27.669	0.1147	1569.98	2794.25	0.9913	0.9802
2	5.50	2.50	11.192	27.620	0.1147	1378.70	2994.58	0.9908	0.9756
3	44.10	2.50	11.192	27.428	0.1147	7341.79	7417.90	0.9539	0.9373
4	5.50	2.50	11.192	29.875	0.1147	5203.06	6055.44	0.9727	0.9578
5	44.10	3.00	11.192	27.700	0.1147	311.73	416.15	0.9953	0.9927
6	5.50	3.00	11.192	27.775	0.1147	499.49	369.38	0.9945	0.9954
7	44.10	3.00	11.192	28.580	0.1147	1531.09	1206.83	0.9869	0.9886
8	5.50	3.00	11.192	29.194	0.1147	647.88	466.86	0.9933	0.9948
9	44.10	3.50	11.192	28.240	0.1147	801.58	757.67	0.9839	0.9839
10	5.50	3.50	11.192	28.074	0.1147	443.68	309.28	0.9923	0.9943
11	44.10	4.00	11.192	28.470	0.1147	1518.92	1277.50	0.9611	0.9659
12	5.50	4.00	11.192	28.779	0.1147	937.39	539.58	0.9788	0.9861

NO	CFM IMP	CFM	COS(PHI)	ANGLE	P(4)
1	8.1909	19.7832	0.8348	33.4053	0.00075100
2	8.1764	19.7482	0.8348	33.4053	0.00188100
3	8.1195	19.6109	0.8348	33.4053	-0.07906894
4	8.8441	21.3609	0.8348	33.4053	0.00326399
5	8.2001	24.5196	0.8885	27.3096	0.00205010
6	8.2223	24.5860	0.8885	27.3096	0.00430297
7	8.4606	25.2985	0.8885	27.3096	0.00054000
8	8.6425	25.8425	0.8885	27.3096	0.00434007
9	8.3599	29.6664	0.9194	23.1573	0.00354009
10	8.3108	29.4921	0.9194	23.1573	0.00607395
11	8.4280	34.5413	0.9389	20.1269	0.00545494
12	8.5195	34.9162	0.9389	20.1269	0.00956588

TABLE G-11 CONTINUED

NO	UHALF	BHALF	BCALC	AVG ANGLE	ND**3
1	121.57	0.0328	0.0322	38.04	7.813
2	121.36	0.0328	0.0319	40.87	7.813
3	120.51	0.0328	-0.0294	37.62	7.813
4	131.27	0.0328	0.0295	37.65	7.813
5	98.31	0.0394	0.0396	28.71	7.813
6	98.58	0.0394	-0.0390	32.00	7.813
7	101.43	0.0394	0.0397	28.72	7.813
8	103.61	0.0394	0.0384	30.75	7.813
9	84.45	0.0459	0.0471	21.95	7.813
10	83.96	0.0459	-0.0475	25.04	7.813
11	73.72	0.0525	0.0539	18.27	7.813
12	74.52	0.0525	-0.0590	21.39	7.813

	AVERAGE	VARIANCE	DEVIATION
A	28.2836	0.5398	0.466

TABLE G-12

SUMMARY OF THE VELOCITY PROFILE ANALYSIS AT 550 RPM IN A 12.25 INCH DIAMETER TANK

NO	RADIAL ANGLE	RADIUS	SIGMA	A	AA	SUM SQ O	SUM SQ VR	CORR COEF O	CORR COEF VR
1	44.10	3.00	11.408	31.373	0.1120	244.46	371.16	0.9976	0.9960
2	5.50	3.00	11.765	31.860	0.1110	614.37	572.06	0.9942	0.9938

NO	CFM IMP	CFM	COS(PHI)	ANGLE	P(4)
1	9.7193	27.5912	0.8940	26.6205	0.00218699
2	9.8984	27.6235	0.8961	26.3530	0.00389098

NO	UHALF	BHALF	BCALC	AVG ANGLE	ND**3
1	112.07	0.0386	0.0389	30.20	8.594
2	115.44	0.0375	0.0373	29.33	8.594

	AVERAGE	VARIANCE	DEVIATION
A	31.6166	0.1189	3.098
SIGMA	11.5864	0.0638	2.269
AA	0.1115	0.00000055	0.00664

VELOCITY FACTOR= 0.50

TABLE G-13

SUMMARY OF VELOCITY PROFILE ANALYSIS AT 550 RPM, σ AND A CONSTANT

NO	RADIAL ANGLE	RADIUS	SIGMA	A	AA	SUM SQ Q	SUM SQ VP	CORR COEF Q	CORR COEF VP
1	44.10	3.00	11.192	31.303	0.1147	279.86	534.23	0.9973	0.9942
2	5.50	3.00	11.192	31.834	0.1147	824.55	1023.84	0.9922	0.9889

NO	CFM IMP	CFM	COS(PHI)	ANGLE	P(4)
1	9.2668	27.7094	0.8885	27.3096	0.00220019
2	9.4239	28.1790	0.8885	27.3096	0.00397009

NO	UHALF	BHALF	BCALC	AVG ANGLE	ND**3
1	111.10	0.0394	0.0391	30.20	8.594
2	112.98	0.0394	-0.0371	29.33	8.594

	AVERAGE	VARIANCE	DEVIATION
A	31.5687	0.1407	3.371

TABLE G-14

SUMMARY OF VELOCITY PROFILE ANALYSIS AT 333.3 RPM IN A 11.5 INCH DIAMETER TANK

NO	RADIAL ANGLE	RADIUS	SIGMA	A	AA	SUM SQ O	SUM SQ VR	CORR COEF O	CORR COEF VR
1	44.10	2.50	11.823	18.210	0.1201	225.89	673.10	0.9937	0.9794
2	5.50	2.50	10.810	18.080	0.1217	360.08	596.46	0.9915	0.9837
3	44.10	3.00	10.426	17.278	0.1221	61.63	90.46	0.9952	0.9921
4	5.50	3.00	9.712	17.866	0.1223	328.04	289.59	0.9779	0.9787

NO	CFM IMP	CFM	COS(PHI)	ANGLE	P(4)
1	4.3724	12.5321	0.8170	35.2152	-0.00323699
2	4.1207	12.9693	0.8116	35.7503	-0.00131700
3	3.8776	15.7025	0.8725	29.2449	-0.00004790
4	4.0891	16.8199	0.8721	29.2917	-0.00863706

NO	UHALF	BHALF	BCALC	AVG ANGLE	ND**3
1	83.13	0.0311	-0.0313	40.42	5.208
2	79.18	0.0340	0.0327	40.95	5.208
3	59.73	0.0423	0.0440	30.53	5.208
4	59.62	0.0454	0.0411	30.48	5.208

	AVERAGE	VARIANCE	DEVIATION
A	17.8584	0.1699	0.656
SIGMA	10.6927	0.7750	1.401
AA	0.1216	0.00000098	0.00158

VELOCITY FACTOR= 0.50

TABLE G-15

SUMMARY OF VELOCITY PROFILE ANALYSIS AT 333.3 RPM, σ AND A CONSTANT IN A 11.5 INCH DIAMETER TANK

NO	RADIAL ANGLE	RADIUS	SIGMA	A	AA	SUM SQ Q	SUM SQ VR	CORR COEF Q	CORR COEF VR
1	44.10	2.50	11.192	18.220	0.1216	334.24	1090.77	0.9907	0.9663
2	5.50	2.50	11.192	18.053	0.1216	409.49	387.88	0.9903	0.9895
3	44.10	3.00	11.192	17.137	0.1216	150.27	51.68	0.9882	0.9955
4	5.50	3.00	11.192	17.576	0.1216	731.47	301.44	0.9500	0.9778

NO	CFM IMP	CFM	COS(PHI)	ANGLE	P(4)
1	4.1174	12.8480	0.8120	35.7097	-0.00326300
2	4.0798	12.7306	0.8120	35.7097	-0.00133920
3	3.8728	15.0429	0.8737	29.1042	-0.00007560
4	3.9720	15.4283	0.8737	29.1042	-0.00813694

NO	UHALF	BHALF	BCALC	AVG ANGLE	ND**3
1	81.17	0.0328	-0.0320	40.42	5.208
2	80.43	0.0328	0.0323	40.95	5.208
3	61.34	0.0394	-0.0391	30.53	5.208
4	62.91	0.0394	0.0383	30.48	5.208

	AVERAGE	VARIANCE	DEVIATION
A	17.7468	0.2394	0.778

TABLE G-16

ANALYSIS OF COOPER'S DATA IN WATER FOR A 3.0 INCH DIAMETER IMPELLER

NO	RADIUS	SIGMA	A	AA	SUM SQ Q	SUM SQ VR	CORR COEF Q	CORR COEF VR
1	1.50	11.502	9.785	0.1051	534.07	1218.80	0.9893	0.9516
2	1.50	11.833	14.062	0.1048	402.25	3256.81	0.9962	0.9434
3	1.50	11.575	14.978	0.1085	2991.78	4682.07	0.9777	0.9262
4	1.50	14.408	19.225	0.1009	7993.67	2895.59	0.9767	0.9806
5	1.50	12.509	22.497	0.1038	2038.88	11763.60	0.9936	0.9373

NO	RADIUS	IMP CFM	COS(PHI)	ANGLE	P(4)
1	1.50	3.33	0.5414	57.22	-0.00116810
2	1.50	4.74	0.5453	56.96	-0.00036510
3	1.50	4.88	0.4972	60.19	-0.00053811
4	1.50	6.11	0.5898	53.85	0.00001489
5	1.50	7.45	0.5567	56.17	0.00004690

NO	UHALF	BHALF	BCALC	AVG ANGLE	ND**3
1	90.20	0.0192	-0.0197	59.69	3.125
2	131.01	0.0186	0.0179	61.00	4.688
3	144.54	0.0190	-0.0190	63.46	6.250
4	190.04	0.0153	-0.0169	56.08	7.813
5	213.28	0.0176	0.0179	61.23	9.375

VELOCITY FACTOR= 0.50

TABLE G-17

ANALYSIS OF COOPER'S DATA FOR A 3.0 INCH DIAMETER IMPELLER IN WATER, σ CONSTANT

NO	RADIUS	SIGMA	A	AA	SUM SQ Q	SUM SQ VR	CORR COEF Q	CORR COEF VR
1	1.50	12.621	9.714	0.1051	1030.51	590.29	0.9792	0.9768
2	1.50	12.621	13.999	0.1048	892.26	2081.05	0.9915	0.9642
3	1.50	12.621	14.881	0.1085	4123.14	2833.70	0.9692	0.9560
4	1.50	12.621	19.272	0.1009	12686.66	7579.75	0.9628	0.9484
5	1.50	12.621	22.485	0.1038	2065.06	11188.33	0.9935	0.9405

NO	RADIUS	IMP CFM	COS(PHI)	ANGLE	P(4)
1	1.50	3.16	0.5414	57.22	-0.00109310
2	1.50	4.57	0.5453	56.96	-0.00034411
3	1.50	4.64	0.4972	60.19	-0.00047911
4	1.50	6.54	0.5898	53.85	-0.00000211
5	1.50	7.42	0.5567	56.17	0.00004690

NO	UHALF	BHALF	BCALC	AVG ANGLE	ND**3
1	93.80	0.0175	-0.0192	59.69	3.125
2	134.70	0.0175	0.0173	61.00	4.688
3	149.95	0.0175	-0.0186	63.46	6.250
4	178.29	0.0175	0.0171	56.08	7.813
5	214.12	0.0175	0.0179	61.23	9.375

VELOCITY FACTOR= 0.50

TABLE G-18

ANALYSIS OF COOPER'S DATA IN WATER FOR A 4.0 INCH DIAMETER IMPELLER

NO	RADIUS	SIGMA	A	AA	SUM SQ Q	SUM SQ VR	CORR COEF Q	CORR COEF VR
1	2.00	14.106	7.876	0.1392	153.27	212.73	0.9930	0.9757
2	2.00	12.095	11.940	0.1421	90.20	705.60	0.9974	0.9538
3	2.00	13.611	17.052	0.1402	621.11	1507.36	0.9935	0.9631
4	2.00	11.317	20.599	0.1453	514.96	2643.61	0.9944	0.9374
5	2.00	11.680	22.967	0.1456	209.50	2869.09	0.9983	0.9443

NO	RADIUS	IMP CFM	COS(PHI)	ANGLE	P(4)
1	2.00	3.26	0.5503	56.61	-0.00044112
2	2.00	5.20	0.5224	58.51	-0.00064011
3	2.00	7.12	0.5407	57.27	-0.00070011
4	2.00	8.98	0.4898	60.67	0.00063988
5	2.00	9.82	0.4866	60.88	-0.00033811

NO	UHALF	BHALF	BCALC	AVG ANGLE	ND**3
1	59.81	0.0208	0.0222	60.67	3.704
2	86.18	0.0243	0.0247	61.11	5.556
3	128.34	0.0216	0.0223	61.56	7.407
4	148.52	0.0260	-0.0250	63.11	9.259
5	168.78	0.0252	0.0253	62.67	11.111

VELOCITY FACTOR= 0.50

TABLE G-19

ANALYSIS OF COOPER'S DATA FOR A 4.0 INCH DIAMETER IMPELLER IN WATER, σ CONSTANT

NO	RADIUS	SIGMA	A	AA	SUM SQ Q	SUM SQ VR	CORR COEF Q	CORR COEF VR
1	2.00	12.621	7.891	0.1392	368.35	466.56	0.9830	0.9459
2	2.00	12.621	11.911	0.1421	156.09	528.57	0.9955	0.9656
3	2.00	12.621	17.086	0.1402	1087.90	2446.82	0.9886	0.9393
4	2.00	12.621	20.439	0.1453	1820.71	1333.69	0.9802	0.9689
5	2.00	12.621	22.850	0.1456	1042.06	1811.36	0.9916	0.9652

NO	RADIUS	IMP CFM	COS(PHI)	ANGLE	P(4)
1	2.00	3.45	0.5503	56.61	-0.00042112
2	2.00	5.08	0.5224	58.51	-0.00063011
3	2.00	7.41	0.5407	57.27	-0.00069511
4	2.00	8.43	0.4898	60.67	0.00063888
5	2.00	9.40	0.4866	60.88	-0.00035011

NO	UHALF	BHALF	BCALC	AVG ANGLE	ND**3
1	56.68	0.0233	0.0234	60.67	3.704
2	87.82	0.0233	-0.0249	61.11	5.556
3	123.83	0.0233	0.0229	61.56	7.407
4	155.62	0.0233	0.0251	63.11	9.259
5	174.56	0.0233	-0.0244	62.67	11.111

VELOCITY FACTOR= 0.50

TABLE G-20

ANALYSIS OF COOPER'S DATA IN WATER FOR A 5.0 INCH DIAMETER IMPELLER

NO	RADIUS	SIGMA	A	AA	SUM SQ Q	SUM SQ VR	CORR COEF Q	CORR COEF VR
1	2.50	12.507	12.777	0.1731	62.31	731.97	0.9980	0.9924
2	2.50	12.660	20.058	0.1714	237.91	1447.64	0.9969	0.9826
3	2.50	12.833	26.538	0.1690	633.01	2042.89	0.9954	0.9699
4	2.50	12.639	34.010	0.1700	1253.35	2705.31	0.9943	0.9735
5	2.50	12.658	37.050	0.1708	783.04	3605.89	0.9970	0.9707

NO	RADIUS	IMP CFM	COS(PHI)	ANGLE	P(4)
1	2.50	7.06	0.5567	56.17	-0.00099511
2	2.50	11.13	0.5684	55.36	-0.00046711
3	2.50	14.83	0.5851	54.19	0.00019889
4	2.50	19.04	0.5778	54.70	0.00040989
5	2.50	20.63	0.5728	55.05	0.00011789

NO	UHALF	BHALF	BCALC	AVG ANGLE	ND**3
1	72.67	0.0294	-0.0304	60.00	7.234
2	113.59	0.0290	-0.0293	58.55	10.851
3	149.15	0.0286	-0.0292	56.82	14.468
4	190.87	0.0291	0.0285	56.82	18.084
5	209.00	0.0290	0.0291	57.45	19.893

VELOCITY FACTOR= 0.50

TABLE G-21

ANALYSIS OF COOPER'S DATA FOR A 5.0 INCH DIAMETER IMPELLER IN WATER, σ CONSTANT

NO	RADIUS	SIGMA	A	AA	SUM SQ D	SUM SQ VR	CORR COEF D	CORR COEF VR
1	2.50	12.621	12.770	0.1731	64.55	690.13	0.9979	0.9552
2	2.50	12.621	20.063	0.1714	238.71	1481.36	0.9969	0.9617
3	2.50	12.621	26.560	0.1690	669.70	2335.19	0.9951	0.9654
4	2.50	12.621	34.013	0.1700	1253.74	2739.71	0.9943	0.9732
5	2.50	12.621	37.060	0.1709	785.63	3694.81	0.9970	0.9700

NO	RADIUS	IMP CFM	COS(PHI)	ANGLE	P(4)
1	2.50	7.02	0.5567	56.17	-0.00099311
2	2.50	11.15	0.5684	55.36	-0.00046711
3	2.50	14.97	0.5851	54.19	0.00018989
4	2.50	19.05	0.5778	54.70	0.00041488
5	2.50	20.67	0.5728	55.05	0.00011989

NO	UHALF	BHALF	BCALC	AVG ANGLE	ND**3
1	72.96	0.0291	-0.0304	60.00	7.234
2	113.44	0.0291	-0.0293	58.55	10.851
3	148.03	0.0291	-0.0293	56.82	14.468
4	190.75	0.0291	0.0285	56.82	18.084
5	208.75	0.0291	0.0291	57.45	19.893

VELOCITY FACTOR= 0.50

TABLE G-22

ANALYSIS OF COOPER'S DATA IN WATER FOR A 6.0 INCH DIAMETER IMPELLER

NO	RADIUS	SIGMA	A	AA	SUM SQ Q	SUM SQ VR	CORR COEF Q	CORR COEF VR
1	3.00	11.740	14.177	0.2024	48.23	362.20	0.9980	0.9698
2	3.00	11.769	19.538	0.2031	53.13	870.38	0.9988	0.9647
3	3.00	11.721	24.449	0.2033	114.33	1153.47	0.9984	0.9675
4	3.00	12.581	29.445	0.2037	301.83	1950.14	0.9976	0.9696
5	3.00	12.264	33.861	0.2006	353.79	2098.11	0.9978	0.9738

NO	RADIUS	IMP CFM	COS(PHI)	ANGLE	P(4)
1	3.00	9.96	0.5872	54.04	-0.00013011
2	3.00	13.66	0.5831	54.33	-0.00089711
3	3.00	17.11	0.5818	54.42	-0.00088097
4	3.00	19.85	0.5795	54.59	-0.00092111
5	3.00	23.47	0.5969	53.35	-0.00016911

NO	UHALF	BHALF	BCALC	AVG ANGLE	ND**3
1	63.39	0.0375	0.0374	56.15	6.250
2	87.78	0.0374	0.0376	57.15	12.500
3	109.74	0.0376	0.0374	56.08	15.625
4	137.20	0.0350	0.0346	57.08	18.750
5	153.49	0.0359	0.0356	55.69	21.875

VELOCITY FACTOR= 0.50

TABLE G-23

ANALYSIS OF COOPER'S DATA FOR A 6.0 DIAMETER IMPELLER IN WATER, σ CONSTANT

NO	RADIUS	SIGMA	A	AA	SUM SQ Q	SUM SQ VR	CORR COEF Q	CORR COEF VR
1	3.00	12.621	14.103	0.2024	190.55	191.97	0.9921	0.9841
2	3.00	12.621	19.441	0.2031	312.66	451.68	0.9932	0.9818
3	3.00	12.621	24.319	0.2033	568.33	604.85	0.9921	0.9831
4	3.00	12.621	29.439	0.2037	303.47	1898.18	0.9976	0.9705
5	3.00	12.621	33.801	0.2006	465.94	1563.86	0.9970	0.9805

NO	RADIUS	IMP CFM	COS(PHI)	ANGLE	P(4)
1	3.00	9.56	0.5872	54.04	-0.00012211
2	3.00	13.13	0.5831	54.33	-0.00088011
3	3.00	16.40	0.5818	54.42	-0.00086111
4	3.00	19.82	0.5795	54.59	-0.00091911
5	3.00	23.09	0.5969	53.35	-0.00017011

NO	UHALF	BHALF	BCALC	AVG ANGLE	ND**3
1	65.38	0.0349	0.0364	56.15	6.250
2	90.45	0.0349	0.0367	57.15	12.500
3	113.27	0.0349	0.0364	56.08	15.625
4	137.39	0.0349	0.0345	57.08	18.750
5	155.43	0.0349	0.0353	55.69	21.875

VELOCITY FACTOR= 0.50

TABLE G-24

ANALYSIS OF COOPER'S DATA IN AIR FOR A 4.0 DIAMETER IMPELLER

NO	RADIUS	SIGMA	A	AA	SUM SQ		CORR COEF	
					O	VR	O	VR
1	2.00	13.679	13.255	0.1426	1232.42	1692.41	0.9768	0.9281
2	2.00	13.024	19.066	0.1428	2726.08	3492.60	0.9722	0.9219
3	2.00	14.345	26.350	0.1426	3796.08	5903.01	0.9838	0.9410
4	2.00	15.165	35.760	0.1410	8293.19	11505.16	0.9822	0.9413
5	2.00	14.649	43.920	0.1412	8318.10	15939.76	0.9876	0.9428

NO	RADIUS	IMP CFM	COS(PHI)	ANGLE	P(4)
1	2.00	5.40	0.5173	58.85	-0.00077011
2	2.00	7.95	0.5158	58.95	-0.00001011
3	2.00	10.49	0.5180	58.80	-0.00053011
4	2.00	14.04	0.5333	57.77	-0.00109011
5	2.00	17.51	0.5309	57.93	-0.00169011

NO	UHALF	BHALF	BCALC	AVG ANGLE	ND**3
1	102.24	0.0215	0.0195	63.33	7.407
2	143.70	0.0226	0.0077	63.33	11.111
3	207.99	0.0205	0.0182	63.33	13.556
4	286.04	0.0194	0.0174	63.33	18.518
5	346.05	0.0201	0.0188	63.33	22.222

VELOCITY FACTOR= 0.50

TABLE G-25

ANALYSIS OF COOPER'S DATA FOR A 4.0 INCH DIAMETER IMPELLER IN AIR, σ CONSTANT

NO	RADIUS	SIGMA	A	AA	SUM SQ Q	SUM SQ VR	CORR COEF Q	CORR COEF VR
1	2.00	12.621	13.284	0.1426	1505.28	2287.29	0.9715	0.9914
2	2.00	12.621	19.090	0.1428	2810.84	3936.13	0.9714	0.9915
3	2.00	12.621	26.410	0.1426	6614.67	9901.80	0.9716	0.9988
4	2.00	12.621	35.800	0.1410	18718.75	22887.32	0.9595	0.9794
5	2.00	12.621	44.000	0.1412	18910.02	29030.61	0.9715	0.9931

NO	RADIUS	IMP RPM	COS(PHI)	ANGLE	P(4)
1	2.00	5.63	0.5173	58.85	-0.00076411
2	2.00	8.08	0.5158	59.05	0.00000089
3	2.00	11.21	0.5180	58.80	-0.00052011
4	2.00	15.41	0.5333	57.77	-0.00108011
5	2.00	19.90	0.5309	57.93	-0.00169011

NO	UHALF	BHALF	BCALC	AVG ANGLE	NO**3
1	98.42	0.0233	0.0204	63.33	7.407
2	141.64	0.0233	0.0081	63.33	11.111
3	195.54	0.0233	0.0197	63.33	13.556
4	261.24	0.0233	0.0193	63.33	18.519
5	321.80	0.0233	0.0203	63.33	22.222

VELOCITY FACTOR= 0.50

TABLE G-26

ANALYSIS OF COOPER'S DATA IN AIR FOR A 5.0 INCH DIAMETER IMPELLER

NO	RADIUS	SIGMA	A	AA	SUM SQ Q	SUM SQ VR	CORR COEF Q	CORR COEF VR
1	2.50	12.920	20.484	0.1687	733.93	2095.38	0.9903	0.9454
2	2.50	13.588	31.306	0.1686	1740.72	4475.00	0.9914	0.9547
3	2.50	14.137	43.750	0.1685	3329.38	8864.42	0.9922	0.9575
4	2.50	14.039	57.150	0.1665	5130.23	14640.25	0.9928	0.9573
5	2.50	13.994	67.621	0.1686	7367.27	20039.58	0.9927	0.9589

NO	RADIUS	IMP CFM	COS(PHI)	ANGLE	P(4)
1	2.50	11.43	0.5868	54.07	-0.00047211
2	2.50	17.04	0.5873	54.04	-0.00068008
3	2.50	23.36	0.5879	53.99	-0.00081011
4	2.50	30.95	0.6008	53.07	-0.00070011
5	2.50	36.28	0.5877	54.00	-0.00056011

NO	UHALF	BHALF	BCALC	AVG ANGLE	ND**3
1	115.34	0.0284	0.0264	57.45	14.468
2	190.71	0.0270	0.0250	57.45	21.701
3	257.45	0.0260	-0.0251	57.45	28.935
4	331.51	0.0262	-0.0241	57.45	36.169
5	395.95	0.0262	-0.0247	57.45	43.403

VELOCITY FACTOR= 0.50

TABLE G-27

ANALYSIS OF COOPER'S DATA FOR A 5.0 DIAMETER IMPELLER IN AIR, - CONSTANT

NO	RADIUS	SIGMA	A	AA	SUM SQ		CORR COEF	
					Q	VR	Q	VR
1	2.50	12.621	20.505	0.1697	771.97	2333.74	0.9899	0.9390
2	2.50	12.621	31.380	0.1686	2670.15	6453.91	0.9847	0.9340
3	2.50	12.621	43.879	0.1695	7697.40	15425.88	0.9823	0.9249
4	2.50	12.621	57.313	0.1665	11592.66	24894.07	0.9836	0.9263
5	2.50	12.621	67.810	0.1686	15975.32	33912.89	0.9843	0.9294

NO	RADIUS	IMP CFM	COS(PHI)	ANGLE	P(4)
1	2.50	11.57	0.5868	54.07	-0.00047311
2	2.50	17.72	0.5873	54.04	-0.00066911
3	2.50	24.79	0.5879	53.99	-0.00091611
4	2.50	32.74	0.6008	53.07	-0.00069811
5	2.50	38.31	0.5877	54.00	-0.00057011

NO	UHALF	RHALF	RCALC	AVG ANGLE	NO**3
1	114.12	0.0291	0.0267	57.45	14.468
2	174.57	0.0291	0.0260	57.45	21.701
3	243.97	0.0291	0.0241	57.45	28.935
4	315.23	0.0291	0.0249	57.45	36.169
5	377.07	0.0291	0.0248	57.45	43.403

VELOCITY FACTOR= 0.50

TABLE G-28

ANALYSIS OF COOPER'S DATA IN AIR FOR A 6.0 INCH DIAMETER IMPELLER

NO	RADIUS	SIGMA	A	AA	SUM SQ Q	SUM SQ VR	COPR COEF Q	COPR COEF VR
1	3.00	11.926	18.124	0.2016	537.92	1257.60	0.9860	0.9424
2	3.00	12.559	34.020	0.1996	2268.21	4646.09	0.9850	0.9449
3	3.00	12.905	46.640	0.1997	3719.09	7792.27	0.9878	0.9531
4	3.00	13.747	81.630	0.1995	12066.85	22783.27	0.9890	0.9603
5	3.00	13.563	95.297	0.1995	12704.00	30668.21	0.9912	0.9598

NO	RADIUS	IMP CFM	COS(PHI)	ANGLE	P(4)
1	3.00	12.68	0.5914	53.74	-0.00149011
2	3.00	23.40	0.6023	52.97	-0.00055310
3	3.00	31.64	0.6018	53.00	-0.00024010
4	3.00	53.69	0.6026	52.94	-0.00104009
5	3.00	63.10	0.6025	52.95	-0.00094009

NO	UHALF	BHALF	BCALC	AVG ANGLE	ND**3
1	81.39	0.0370	0.0336	57.15	12.500
2	155.36	0.0351	-0.0329	57.15	25.000
3	215.98	0.0341	-0.0315	57.15	37.500
4	389.89	0.0321	-0.0276	57.15	62.500
5	452.16	0.0325	-0.0298	57.15	75.000

VELOCITY FACTOR= 0.50

TABLE G-29

ANALYSIS OF COOPER'S DATA FOR A 6.0 INCH DIAMETER IMPELLER IN AIR, σ CONSTANT

NO	RADIUS	SIGMA	A	AA	SUM SQ Q	SUM SQ VR	CORR COEF Q	CORR COEF VR
1	3.00	12.621	18.055	0.2016	670.57	934.39	0.9826	0.9576
2	3.00	12.621	34.010	0.1996	2271.84	4532.17	0.9850	0.9462
3	3.00	12.621	46.692	0.1997	3858.02	8820.49	0.9874	0.9467
4	3.00	12.621	81.872	0.1995	18747.68	36633.19	0.9828	0.9353
5	3.00	12.621	95.550	0.1995	19132.46	46129.21	0.9868	0.9390

NO	RADIUS	IMP CFM	COS(PHI)	ANGLE	P(4)
1	3.00	12.28	0.5914	53.74	-0.00148911
2	3.00	23.34	0.6023	52.97	-0.00056011
3	3.00	32.03	0.6018	53.00	-0.00024010
4	3.00	56.20	0.6026	52.94	-0.00105311
5	3.00	65.58	0.6025	52.95	-0.00094510

NO	UHALF	BHALF	BCALC	AVG ANGLE	ND**3
1	83.41	0.0349	0.0319	57.15	12.500
2	155.69	0.0349	-0.0329	57.15	25.000
3	213.82	0.0349	-0.0318	57.15	37.500
4	374.69	0.0349	-0.0289	57.15	62.500
5	437.33	0.0349	-0.0309	57.15	75.000

VELOCITY FACTOR= 0.50

TABLE G-30

ANALYSIS OF COOPER'S DATA FOR A 4.0 INCH IMPELLER AT 280 RPM AND VARYING RADIAL DISTANCE

NO	RADIUS	SIGMA	A	AA	SUM SQ Q	SUM SQ VR	CORR COEF Q	CORR COEF VR
1	2.00	12.376	23.520	0.1403	1069.62	3035.51	0.9926	0.9553
2	2.50	17.031	20.341	0.1563	1702.71	1882.94	0.9821	0.9669
3	3.00	15.769	20.591	0.1651	104.89	479.83	0.9966	0.9807
4	4.00	13.372	23.383	0.1636	51.44	86.58	0.9908	0.9831
5	5.00	19.953	15.000	0.1876	7274.54	5724.68	0.0	0.0

NO	RADIUS	IMP CFM	COS(PHI)	ANGLE	P(4)
1	2.00	10.29	0.5400	57.32	-0.00016011
2	2.50	10.49	0.6613	48.60	-0.00078911
3	3.00	14.12	0.7509	41.34	-0.00036711
4	4.00	25.00	0.8713	29.39	-0.00213909
5	5.00	16.61	0.8928	26.77	-0.00070621

NO	UHALF	RHALF	RCALC	AVG ANGLE	ND**3
1	168.90	0.0237	0.0249	61.11	10.370
2	123.87	0.0216	-0.0224	56.56	10.370
3	94.36	0.0279	-0.0269	44.22	10.370
4	68.70	0.0439	0.0	29.67	10.370
5	42.55	0.0368	0.0	26.89	10.370

VELOCITY FACTOR= 0.50

TABLE G-31

ANALYSIS OF COOPER'S DATA FOR A 4.0 INCH IMPELLER AT 280 RPM AND VARYING DISTANCE,

σ CONSTANT AND a EVALUATED FROM EQUATION IV-38

NO	RADIUS	SIGMA	A	AA	SUM SQ Q	SUM SQ VR	CORR COEF Q	CORR COEF VR
1	2.00	12.621	22.961	0.1428	1124.54	2902.53	0.9922	0.9573
2	2.50	12.621	21.478	0.1428	7685.15	9657.66	0.9166	0.9160
3	3.00	12.621	22.040	0.1428	1521.29	3383.90	0.9501	0.8545
4	4.00	12.621	24.163	0.1428	78.72	263.09	0.9858	0.9477
5	5.00	12.621	23.753	0.1428	215.76	356.83	0.7429	0.5637

NO	RADIUS	IMP CFM	COS(PHI)	ANGLE	P(4)
1	2.00	9.72	0.5156	58.96	-0.00015211
2	2.50	13.51	0.7281	43.27	-0.00100911
3	3.00	17.66	0.8208	34.83	-0.00039011
4	4.00	27.08	0.9036	25.37	-0.00230110
5	5.00	33.93	0.9394	20.04	-0.00190110

NO	UHALF	BHALF	BCALC	AVG ANGLE	NO**3
1	170.39	0.0233	0.0247	61.11	10.370
2	107.30	0.0291	-0.0242	56.56	10.370
3	86.42	0.0349	-0.0295	44.22	10.370
4	67.73	0.0466	0.0	29.67	10.370
5	52.24	0.0582	0.0	26.89	10.370

VELOCITY FACTOR= 0.50

TABLE G-32

ANALYSIS OF COOPER'S DATA FOR A 4.0 INCH IMPELLER AT 100 RPM WITH VARYING BLADE WIDTHS

NO	RADIUS	SIGMA	A	AA	SUM SQ Q	SUM SQ VR	CORR COEF Q	CORR COEF VR
1	2.00	10.622	11.560	0.1149	1268.99	797.51	0.9365	0.9144
2	2.00	10.630	10.887	0.1074	755.03	770.84	0.9528	0.9230
3	2.00	12.473	10.690	0.1056	429.39	237.30	0.9807	0.9817
4	2.00	12.318	8.440	0.1342	101.92	178.62	0.9870	0.9616
5	2.00	11.764	7.838	0.1423	22.75	605.85	0.9964	0.9873

NO	RADIUS	IMP CFM	COS(PHI)	ANGLE	P(4)
1	2.00	6.32	0.7245	43.57	-0.00055011
2	2.00	6.12	0.7646	40.13	0.00092289
3	2.00	5.58	0.7736	39.32	-0.00049011
4	2.00	3.88	0.5930	53.63	-0.00086111
5	2.00	3.45	0.5205	58.64	-0.00017309

NO	UHALF	BHALF	BCALC	AVG ANGLE	NO**3
1	66.39	0.0277	0.0289	42.56	3.704
2	60.89	0.0276	-0.0303	42.11	3.704
3	64.39	0.0236	0.0246	38.89	3.704
4	57.70	0.0238	-0.0234	55.57	3.704
5	55.90	0.0250	0.0249	60.71	3.704

VELOCITY FACTOR= 0.50

TABLE G-33

ANALYSIS OF COOPER'S DATA FOR A 4.0 INCH IMPELLER AT 200 RPM WITH VARYING BLADE WIDTHS

NO	RADIUS	SIGMA	A	AA	SUM SQ Q	SUM SQ VR	CORR COEF Q	CORR COEF VR
1	2.00	8.539	22.680	0.1122	2139.78	1303.72	0.9386	0.9022
2	2.00	10.961	22.270	0.1045	4743.79	2924.26	0.9375	0.9287
3	2.00	11.751	21.660	0.1071	3086.62	1869.22	0.9631	0.9636
4	2.00	12.427	17.829	0.1321	898.80	1035.75	0.9926	0.9923
5	2.00	13.032	14.346	0.1405	107.40	1379.01	0.9962	0.9236

NO	RADIUS	IMP CFM	COS(PHI)	ANGLE	P(4)
1	2.00	13.98	0.7395	42.31	0.00054988
2	2.00	12.43	0.7790	38.83	0.00003789
3	2.00	11.58	0.7663	39.98	-0.00009011
4	2.00	9.27	0.6094	52.45	-0.00033011
5	2.00	6.11	0.5382	57.44	-0.00038311

NO	UHALF	BHALF	BCALC	AVG ANGLE	ND**3
1	115.60	0.0344	0.0	40.89	7.407
2	125.30	0.0268	0.0283	36.89	7.407
3	127.23	0.0250	0.0261	41.00	7.407
4	120.76	0.0236	0.0247	58.45	7.407
5	105.89	0.0225	0.0227	61.57	7.407

VELOCITY FACTOR= 0.50

TABLE G-34

ANALYSIS OF NIELSON'S DATA AT VARYING IMPELLER DIAMETER, IMPELLER SPEED. PROFILE 5 IS MEASURED IN CORN SYRUP AND a WAS CALCULATED FROM $\bar{\theta}_y$

NO	RADIUS	SIGMA	A	AA	SUM SQ	CORR COEF
1	1.00	22.359	10.411	0.0783	3282.454	0.938
2	3.00	12.139	10.585	0.0783	49.197	0.989
3	4.00	10.140	10.935	0.0783	16.160	0.978
4	2.00	16.516	15.034	0.1443	472.274	0.981
5	2.00	17.497	7.664	0.1443	97.301	0.987
6	4.00	13.418	15.149	0.1443	30.106	0.998
7	3.50	11.825	23.220	0.2643	176.225	0.967

NO	RADIUS	CFM	COS(PHI)	ANGLE	P(4)
1	1.00	1.3485	0.3420	69.9999	0.00110294
2	3.00	9.3016	0.9497	18.2540	0.00785892
3	4.00	14.1817	0.9720	13.5872	0.00143896
4	2.00	5.4788	0.5000	59.9999	0.00325974
5	2.00	2.7134	0.5000	59.9999	-0.00012700
6	4.00	16.4476	0.9014	25.6589	0.00901890
7	3.50	16.0885	0.4226	64.9999	-0.00330399

NO	UHALF	BHALF	BCALC
1	86.37	0.0066	0.0066
2	35.94	0.0363	0.0364
3	25.75	0.0579	0.0488
4	64.81	0.0178	0.0179
5	34.00	0.0168	-0.0172
6	39.51	0.0438	-0.0429
7	44.49	0.0435	0.0365

TABLE G-35

ANALYSIS OF NIELSON'S DATA AT VARYING IMPELLER DIAMETER IMPELLER SPEED. PROFILE 5 IS MEASURED CORN SYRUP, a WAS CALCULATED FROM $\bar{\theta}_y$ AND σ IS CONSTANT

NO	RADIUS	SIGMA	A	AA	SUM SQ	CORR COEF
1	1.00	12.621	10.965	0.0783	9220.676	0.814
2	3.00	12.621	10.556	0.0783	55.338	0.987
3	4.00	12.621	10.500	0.0783	84.190	0.979
4	2.00	12.621	15.089	0.1443	1585.530	0.934
5	2.00	12.621	7.636	0.1443	608.912	0.919
6	4.00	12.621	15.161	0.1443	63.226	0.995
7	3.50	12.621	23.084	0.2643	203.196	0.962

NO	RADIUS	CFM	COS(PHI)	ANGLE	P(4)
1	1.00	1.8902	0.3420	69.9999	0.00095300
2	3.00	9.0968	0.9497	18.2540	0.00776102
3	4.00	12.2064	0.9720	13.5872	0.00128100
4	2.00	6.2901	0.5000	59.9999	0.00342909
5	2.00	3.1834	0.5000	59.9999	0.00015200
6	4.00	16.9717	0.9014	25.6589	0.00908992
7	3.50	15.4822	0.4226	64.9999	-0.00311699

NO	UHALF	BHALF	BCALC
1	68.34	0.0116	-0.0082
2	36.55	0.0349	0.0361
3	27.59	0.0466	0.0486
4	56.86	0.0233	0.0197
5	28.78	0.0233	-0.0187
6	38.35	0.0466	-0.0442
7	45.70	0.0407	-0.0460

TABLE G-36

ANALYSIS OF CUTTER'S DATA WITH A 4.0 INCH DIAMETER IMPELLER AT VARYING RADIAL DISTANCE r. IMPELLER SPEED IS 200 RPM

NO	RADIUS	SIGMA	A	AA	SUM SQ	CORR COEF
1	2.00	9.727	33.651	0.1511	111.991	0.995
2	2.75	18.137	11.995	0.1511	314.775	0.976
3	3.38	13.684	18.465	0.1511	195.787	0.985
4	4.13	6.476	24.057	0.1511	165.588	0.896
5	4.38	23.624	15.267	0.1511	114.262	0.877
6	5.13	7.842	24.800	0.1511	177.289	0.647

NO	RADIUS	CFM	COS(PHI)	ANGLE	P(4)
1	2.00	14.6906	0.4226	64.9999	-0.02394919
2	2.75	7.0338	0.7520	41.2337	0.00062511
3	3.38	16.2317	0.8440	32.4305	-0.00941076
4	4.13	38.7569	0.8985	26.0331	-0.05382648
5	4.38	13.7459	0.9103	24.4462	0.01227761
6	5.13	46.0176	0.9355	20.6915	-0.03418881

NO	UHALF	BHALF	BCALC
1	102.34	0.0302	0.0306
2	48.32	0.0223	0.0204
3	55.70	0.0363	0.0354
4	42.15	0.0937	0.1002
5	48.49	0.0272	0.0694
6	39.28	0.0961	1.6344

TABLE G-37

ANALYSIS OF CUTTER'S DATA WITH A 4.0 INCH DIAMETER IMPELLER AT VARYING RADIAL DISTANCE r. IMPELLER SPEED IS 200 RPM AND σ IS CONSTANT

NO	RADIUS	SIGMA	A	AA	SUM SQ	CORR COEF
1	2.00	12.621	19.901	0.1511	204.598	0.991
2	2.75	12.621	17.205	0.1511	493.321	0.962
3	3.38	12.621	20.490	0.1511	205.075	0.984
4	4.13	12.621	12.888	0.1511	265.910	0.827
5	4.38	12.621	19.714	0.1511	275.356	0.667
6	5.13	12.621	17.753	0.1511	213.444	0.548

NO	RADIUS	CFM	COS(PHI)	ANGLE	P(4)
1	2.00	7.6272	0.4226	64.9999	-0.00761387
2	2.75	12.0942	0.7529	41.2337	-0.01329975
3	3.38	18.7552	0.8440	32.4305	-0.01452986
4	4.13	14.8731	0.8985	26.0331	0.00144298
5	4.38	24.2854	0.9103	24.4462	0.00805079
6	5.13	25.9648	0.9355	20.6915	-0.00550986

NO	UHALF	BHALF	BCALC
1	68.94	0.0233	0.0239
2	57.82	0.0320	0.0338
3	59.36	0.0393	0.0399
4	31.53	0.0481	-0.0659
5	45.77	0.0510	0.0814
6	35.67	0.0597	2.1508

TABLE G-38

ANALYSIS OF CUTTER'S DATA AT 400 RPM, IMPELLER DIAMETER = 4.0 INCH AND VARYING RADIAL DISTANCE r

NO	RADIUS	SIGMA	A	AA	SUM SQ	CORR COEF
1	2.00	17.231	36.750	0.1511	2107.017	0.983
2	2.81	9.802	45.808	0.1511	177.116	0.991
3	2.86	11.110	45.390	0.1511	371.038	0.986
4	3.44	7.395	53.219	0.1511	331.713	0.966
5	3.56	13.260	28.374	0.1511	277.402	0.982
6	4.19	10.095	35.448	0.1511	225.606	0.912
7	4.75	13.346	21.005	0.1511	195.181	0.885
8	5.56	14.151	8.499	0.1511	81.739	0.673

NO	RADIUS	CFM	COS(PHI)	ANGLE	P(4)
1	2.00	12.0543	0.4226	64.9999	0.00560960
2	2.81	37.6362	0.7641	40.1700	-0.01767693
3	2.86	35.8710	0.7735	39.3296	-0.01392590
4	3.44	64.9946	0.8499	31.7978	-0.03736138
5	3.56	26.9499	0.8607	30.6080	-0.00365220
6	4.19	46.4812	0.9016	25.6330	0.00516760
7	4.75	27.4970	0.9243	22.4330	-0.00294100
8	5.56	12.7910	0.9454	19.0268	-0.01379981

NO	UHALF	BHALF	BCALC
1	148.76	0.0171	0.0185
2	133.84	0.0421	0.0454
3	139.57	0.0378	0.0297
4	116.35	0.0683	0.0579
5	80.78	0.0394	0.0150
6	76.57	0.0610	-0.0533
7	46.59	0.0523	0.3481
8	16.77	0.0577	0.0452

TABLE G-39

ANALYSIS OF CUTTER'S DATA AT 400 RPM, 4.0 INCH DIAMETER IMPELLER,

WITH VARYING RADIAL DISTANCE AND σ CONSTANT

NO	RADIUS	SIGMA	A	AA	SUM SQ	CORR COEF
1	2.00	12.621	42.899	0.1511	4489.527	0.963
2	2.81	12.621	35.450	0.1511	313.018	0.984
3	2.86	12.621	39.694	0.1511	396.503	0.985
4	3.44	12.621	31.559	0.1511	626.418	0.934
5	3.56	12.621	29.497	0.1511	281.643	0.982
6	4.19	12.621	31.835	0.1511	272.330	0.892
7	4.75	12.621	21.800	0.1511	194.950	0.885
8	5.56	12.621	9.449	0.1511	81.711	0.673

NO	RADIUS	CFM	COS(PHI)	ANGLE	P(4)
1	2.00	16.4413	0.4226	64.9999	0.00012974
2	2.81	25.6676	0.7641	40.1700	-0.00533983
3	2.86	29.4310	0.7735	39.3296	-0.00777088
4	3.44	29.5016	0.8499	31.7978	-0.00183398
5	3.56	28.7167	0.8607	30.6080	-0.00577998
6	4.19	37.3338	0.9016	25.6330	0.01012972
7	4.75	29.3451	0.9243	22.4330	-0.00531084
8	5.56	15.0565	0.9454	19.0268	-0.02175795

NO	UHALF	BHALF	BCALC
1	148.61	0.0233	0.0240
2	117.53	0.0327	0.0344
3	130.09	0.0333	0.0341
4	90.14	0.0400	0.1555
5	81.93	0.0414	0.0092
6	76.89	0.0488	-0.0569
7	47.03	0.0553	0.3396
8	17.61	0.0647	0.0524

TABLE G-40

ANALYSIS OF CUTTER'S DATA AT 600 RPM, 4.0 INCH DIAMETER

IMPELLER, WITH VARYING RADIAL DISTANCE

NO	RADIUS	SIGMA	A	AA	SUM SQ	CORR COEF
1	2.14	16.023	54.450	0.1511	2157.039	0.995
2	2.75	16.626	45.298	0.1511	1407.293	0.990
3	3.38	7.437	303.429	0.1511	1654.206	0.968
4	4.13	11.180	91.405	0.1511	2343.385	0.959
5	4.38	12.690	61.949	0.1511	1876.343	0.889
6	5.13	19.173	29.998	0.1511	304.292	0.873

NO	RADIUS	CFM	COS(PHI)	ANGLE	P(4)
1	2.14	22.2254	0.5316	57.8885	0.00146885
2	2.75	27.7440	0.7520	41.2337	0.00405681
3	3.38	361.8181	0.8440	32.4305	-0.10265386
4	4.13	112.0712	0.8985	26.0331	-0.03925925
5	4.38	76.1055	0.9103	24.4462	-0.01402729
6	5.13	35.5976	0.9355	20.6915	0.00465751

NO	UHALF	BHALF	BCALC
1	222.77	0.0196	0.0185
2	174.73	0.0243	0.0251
3	674.74	0.0668	-2.0082
4	210.44	0.0543	0.0529
5	144.22	0.0507	0.0789
6	74.30	0.0393	0.1511

TABLE G-41

ANALYSIS OF CUTTER'S DATA AT 600 RPM, 4.0 INCH DIAMETER IMPELLER, WITH VARYING RADIAL DISTANCE AND σ CONSTANT

NO	RADIUS	SIGMA	A	AA	SUM SQ	CORR COEF
1	2.14	12.621	66.180	0.1511	4770.551	0.989
2	2.75	12.621	54.230	0.1511	3145.988	0.978
3	3.38	12.621	59.044	0.1511	2477.665	0.951
4	4.13	12.621	72.044	0.1511	2391.879	0.958
5	4.38	12.621	62.255	0.1511	1876.371	0.889
6	5.13	12.621	37.850	0.1511	360.018	0.848

NO	RADIUS	CFM	COS(PHI)	ANGLE	P(4)
1	2.14	30.4369	0.5316	57.8885	-0.00531002
2	2.75	38.1213	0.7520	41.2337	-0.00372712
3	3.38	54.0455	0.8440	32.4305	-0.01435998
4	4.13	83.1381	0.8985	26.0331	-0.02546079
5	4.38	76.6890	0.9103	24.4462	-0.01434196
6	5.13	55.3585	0.9355	20.6915	-0.00674190

NO	UHALF	BHALF	BCALC
1	240.30	0.0249	0.0258
2	182.26	0.0320	0.0322
3	171.05	0.0393	0.0348
4	176.23	0.0481	0.0443
5	144.53	0.0510	0.0787
6	76.06	0.0597	0.1551

APPENDIX H

DETAILED ANALYSIS OF A VELOCITY PROFILE IN THE NEIGHBORHOOD OF THE IMPELLER

In this Appentix a velocity profile analysis will be presented in detail. The results of this analysis has been treated in section 4.1 and 4.4. The analysis was performed on an IBM 360/65 computer. The program written for this analysis is called FLOWANL and is described in Appendix F. The raw data are punched on cards and these are also given in Appendix F at the end of List F-1. The data is presented in sets; each set is for a constant impeller speed.

In Table H-1 is shown a typical printout of the raw data by the program FLOWANL. The item height of pitot tube off tank bottom given in the list in Table H-1 needs explanation. It is the height of the pressure tap P_1 on the probe when the "VERNIER STAND READING" = 13.95. This serves to locate the position of the pressure tap P_1 in the tank. A simple calculation will show that the vernier stand will read 14.10 when P_1 is in the plane of the impeller centerline. This point is considered as $z = 0$ for analysing the flow profile. Also given in the list is the relative location of $\theta_y = 0$ and is called the zero error for the yaw angle, this corresponds to the reading from the vernier protractor when pressure tap P_1 is aligned with the center of the impeller. It is used to correct the item ANGLE to obtain the true direction of the velocity vector $\vec{q}$,

Table H-1. Raw Data for Run No. 29.
RAW DATA MAR 10, 1969

RUN NUMBER	=29
IMPELLER DIAMETER	= 3.00
IMPELLER HT OF TANK BOTTOM	= 6.00
LEVEL OF WATER IN TANK	=12.00
HEIGHT OF PITOT TUBE OFF TANK BOTTOM	= 3.25
VERNIER STAND READING	=13.95
ZERO ERROR FOR ANGLE	=27.20
DIST PROBE TO AXIS	= 3.00
RPM SETTING	=333.33
FLUID TEMP	=75.00 DEG F
ANGULAR POSITION FROM BAFFLE	= 5.50 DEG

P(1)-P(ATM) LEFT	P(1)-P(ATM) RIGHT	P(1)-P(2) LEFT	P(1)-P(2) RIGHT	P(2)-P(3) LEFT	P(2)-P(3) RIGHT	P(4)-P(5) LEFT	P(4)-P(5) RIGHT	H	ANGLE
3.10	-12.90	-0.40	0.95	0.0	0.0	0.40	1.60	10.50	62.40
3.10	-12.90	-0.40	1.00	0.0	0.0	-1.60	2.85	10.60	60.00
3.15	-12.95	-1.05	1.60	0.0	0.0	-3.30	4.70	10.70	57.20
3.20	-13.00	-1.70	2.70	0.0	0.0	-3.90	5.30	10.80	56.60
3.25	-13.05	-3.70	4.20	0.0	0.0	-4.40	5.80	10.90	55.20
3.30	-13.10	-4.80	5.20	0.0	0.0	-3.10	4.40	11.00	53.80
3.30	-13.15	-5.50	5.90	0.0	0.0	-0.15	1.30	11.10	53.60
3.30	-13.10	-5.55	5.90	0.0	0.0	3.00	-2.20	11.20	53.00
3.25	-13.05	-5.00	5.40	0.0	0.0	5.10	-4.50	11.30	53.80
3.25	-13.05	-4.00	4.40	0.0	0.0	5.80	-5.25	11.40	54.60
3.20	-13.00	-2.45	2.90	0.0	0.0	5.50	-4.90	11.50	57.00
3.12	-12.94	-1.50	2.00	0.0	0.0	4.20	-3.60	11.60	58.80
3.10	-12.96	-0.65	1.05	0.0	0.0	2.50	-1.85	11.70	60.00
3.05	-12.95	-0.60	1.00	0.0	0.0	1.45	-0.60	11.80	60.00

The headings of table H-2 will now be explained. The column headings P(1) - P(ATM), P(1) - P(2) - P(3) and P(4) - P(5) are readings taken on manometers A, B, C, and D of Figure III-7. The subscripts on P refer to the pressure tap of the three dimensional probe. LEFT and RIGHT signifies the left and right arms of the manometer. The heading H refers to the vernier stand reading. Since the vernier stand reading for z = 0 is known, the z coordinate or the location of pressure tap P_1 can thus be calculated. The ANGLE refers to the reading on the vernier protractor and together with the value of the zero error gives the yaw angle θ_y of the velocity vector $\vec{q}$.

The program FLOWANL consists of a MAIN program and several subroutines. A brief description of FLOWANL and its subroutines follow.

FLOWANL: Main program, reads in raw data and other necessary information. It calculates the z coordinates and corresponding values of $\vec{q}$. It calls the various subroutines and prints output in desired format.

PATERN: Subprograms called by FLOWANL. It performs Patters Search and returns to FLOWANL the values of parameters obtained for a least square fit on the data. The theoretical basis of this program is described in Appendix C.

PROC: Subprogram called by PATERN. It calculates the least square criteria which is stored as COST.

BOUNDS: Subprogram called by PATERN. This program checks parameters for violation of constraints.

Table H-2. Analysis of Velocity Profile $\vec{q}$, for Run No. 29.

D = 3.00000

R = 3.00000

Y	Q	ANGLE
0.05833	44.82013	35.20000
0.05000	45.64259	32.80000
0.04167	62.79556	30.00000
0.03333	80.91562	29.39999
0.02500	108.42258	28.00000
0.01667	121.98497	26.59999
0.00833	130.24434	26.39999
-0.00000	130.52959	25.80000
-0.00833	124.40071	26.59999
-0.01667	111.80104	27.39999
-0.02500	89.22432	29.80000
-0.03333	72.16724	31.59999
-0.04167	50.29568	32.80000
-0.05000	48.79399	32.80000

	PARAMETERS
1	11.27798748
2	18.54493713
3	0.11587989
4	0.00274200

AVG ANGLE = 29.65705872
WT AVG ANGLE= 27.61441040 VELOCITY FACTOR= 0.50

Q	QC
44.82012939	36.85945129
45.64259338	50.17221069
62.79556274	66.47894287
80.91561890	85.00456238
108.42257690	103.86741638
121.98497009	120.08189392
130.24433899	130.23974609
130.52958679	131.81726074
124.40071106	124.39604187
111.80104065	109.88250732
89.22431946	91.54614258
72.16723633	72.63247681
50.29568481	55.42958069
48.79399109	41.06221008

SUM OF SQUARES OF (Q-QCALC) 235.63095093

GOODNESS OF FIT 0.99190027

BHALF = 0.03907494 BCALC = 0.03734012

UHALF = 66.16113281

HALF WIDTH OF JET AT XD =3.00, 1.60 INCHES

OMEGA: Subprogram called by FLOWANL. This program performs a three point Lagrange interpolation and is used to obtain the value of z at which $\bar{q} = 1/2\ \bar{q}_{max.}$

YAW: Subporgram called by FLOWANL. This program analyses the readings obtained from manometer D.

AVG: Subporgram called by FLOWANL. It calculates an average value of a data set and also its variance and a confidence limit or deviation based on a "t-test" with a 0.95 confidence level.

In Table H-2 is shown a sample printout of the output obtained from the program FLOWANL. The symbols in Table H-2 are:

D = diameter of impeller, inches

R = distance of prove form impeller axis, inches

z = vertical distance at which velocity $\bar{q}$ is measured, z = 0 is at impeller centerline, ft.

Q = $\vec{q}$, ft./min., calculated from equation

ANGLE = yaw angle θ_y in degrees which $\vec{q}$ makes with the radius vector

QC = $\vec{q}$ calculated from equation II-13, ft./min.

$\vec{q}$ is experimental calculated using equation III-3

PARAMETERS, are the parameters obtained from Pattern Search subroutine and are as follows.

1 = σ

2 = A

3 = a

4 = z_o

Table H-3. Radial Velocity Profile Analysis for Run No. 29.

RADIAL VELOCITY ANALYSIS

Q	QC
36.62449646	32.66082764
38.36560059	44.45713806
54.38250732	58.90635681
70.49476624	75.32167053
95.73139954	92.03572083
109.07333374	106.40310669
116.66134644	115.40379333
117.51817322	116.80154419
111.23338318	110.22555542
99.25863647	97.36524963
77.42572021	81.11764526
61.46673584	64.35850525
42.27684021	49.11526489
41.01455688	36.38455200

SUM OF SQUARES OF (Q-QCALC) 214.25904846

GOODNESS OF FIT 0.99151355

The value of $\bar{q}$ theoretical or sometimes referred to as calculated, is obtained form equation II-10 which is reproduced below

$$\bar{q}_{calc} = \frac{A}{2} \left(\frac{\sigma}{r}\right)^{\frac{1}{2}} \frac{1}{(r^2 - a^2)^{\frac{1}{4}}} \left[1 - \tanh^2 (\eta/2)\right] \qquad \text{II-10}$$

Three of the parameters σ, A and z_o are obtained by a least square fit of the data. The parameter a, is obtained from a weighted average value of θ_y, the yaw angle, as explained in Section 4.1. Both average value of θ_y and the weighted average value of θ_y are next reported in Table H-2. Also given is the velocity factor that modifies the weighted average angle.

QC is the predicated value of $\vec{q}$ and is seen to be close to the experimental value. The goodness of fit is the value of the correlation coefficient R defined by Equation 4-1. The sum of squares (Q - QC) is the value of the sum squares about regressions, given by Equation C-2.

The quantity BHALF in Table H-2 should not be confused with $b_{\frac{1}{2}}$. It is the value of z for which $\bar{q}$ is $1/2\bar{q}_{max}$. From a similar reasoning as that used in Appendix B to obtain the half width of jet, Equation B-33, it can be shown that

$$BHALF = 1.763 \frac{r}{\sigma} \qquad \text{H-1}$$

The factor of 1.763 is the value of $\eta/2$ which makes $\tanh^2 (\eta/2) = 0.5$

UHALF is equal to $1/2\bar{q}_{max}$ and is obtained by calculating $\bar{q}_{max}$ from equation II-10 putting $\eta = 0$. UHALF is used to interpolate $\bar{q}$ experimental to obtain BCALC. The interpolation is done using a three point Lagrange interpolation formula. The interpolated value is corrected for shift in origin by subtracting z_o, and the result reported as BCALC. It is secondary check on the goodness of fit. The closeness between BHALF and BCALC in Table H-2 indicates a very good fit between the experimental and calculated values of $\vec{q}$. BCALC is sometimes reported as a negative value because the interpolation program OMEGA chooses three values of $\vec{q}$ closest to UHALF which in this case corresponds with negative values of z. As the velocity profile is symmetirc about the impeller centerline the sign of z is hence of no significance.

The last item in Table H-2 is the half width of the jet at the point of measurement. It is calculated from Equation B-34 and is the value of z at which the velocity is less than 1% of $\bar{q}_{max}$. Thus at r = 3 the width of the tangential jet is 3.34 inches. These facts are shown in Figure IV-11 which gives both the experimental and theoretical value of $\bar{q}$ versus z for Run Number 29. The theoretical line is obtained from Equation II-10 using the value of the parameters as given in Table H-2. The fit by the model is seen to be very good except at the profile ends where the probe response is poor. This is because for a velocity of 30 ft/min, the ΔH_{21} recorded by a manometer using a fluid of sp. gr. of 0.8 is 0.66 inch (calculated from Equation III-3). At this low value of ΔH_{21} the manometer

response falls tending to take an extremely long time to reach equilibrium. Thus velocity measurements are not feasible below this limiting velocity. Hence with the present probe the profile cannot be checked very far beyond BHALF as shown in Figure IV-11, which shows a plot of the experimental and theoretical velocity profiles.

Also shown in Figure IV-11 is the jet displacement z_o and the half width of the jet $b_{\frac{1}{2}}$. It is seen that for $z = \pm (b_{\frac{1}{2}} + z_o)$ the velocity reaches less than 1% of $\bar{q}_{max}$. Figure IV-11 also demonstrates the goodness of fit as measured by the correlation coefficient. The correlation coefficient for this particular profile from Table H-2 is 0.99 and the agreement between experiment and theory is excellent as shown in Figure IV-11. In general the fit by the model for the velocity profiles is excellent in a majority of cases and can be verified by examining the correlation coefficient in Appendix G.

In Table H-3 is shown the result of the analysis of the radial velocity profile for Run Number 29. Q is the experimentally determined value of $\bar{v}_r$ and is obtained from Equation B-22.. QC is the calculated value of $\bar{v}_r$ obtained from the tangential jet model using Equation B-22 with the parameters σ, A, a and z_o obtained for the least square fit on $\vec{q}$ and given in Table H-2.

The goodness of fit has the same meaning as in Table H-2 and is obtained from Equation IV-1 written for $\bar{v}_r$. Similarly, sum of squares is obtained from Equation C-2 written for $\bar{v}_r$. The correlation coefficient is 0.99 indicating that the prediction for $\bar{v}_r$ is

very good. In Figure IV-17 is plotted the experimental and calculated values of $\bar{v}_r$. This figure also illustrates the relationship between $\bar{v}_r$ and the pumping capacity Q.

In Table H-4 is shown the results obtained from Subroutine YAW. P(1) - P(2) and P(4) - P(5) are the pressure drops recorded by manometers B and D in inches of manometer fluid. DEL U**2 EXP and DEL U**2 CALC are the experimental and calculated values of Δq^2 obtained from Equations IV-28 (b) and IV-31 respectively. Next VZ CALC is $\bar{v}_z$ obtained from Equation B-23. Finally the last column gives the difference between the calculated and experimental values of Δq^2.

Table H-4: Results of Analysing Manometer D for Run No. 29

P(1)-P(2)	P(4)-P(5)	DEL U**2 EXP	DEL U**2 CALC	V? CALC	DIFF OF U**2
0.5315	-0.8661	-0.2309	-0.2475	-0.2002	-0.0165
0.5512	-2.1457	-0.5720	-0.4234	-0.1597	0.1487
1.0433	-3.5433	-0.9447	-0.6617	-0.1172	0.2829
1.7323	-4.0157	-1.0706	-0.9114	-0.0768	0.1592
3.1102	-4.4094	-1.1756	-1.0484	-0.0432	0.1271
3.9370	-3.3465	-0.8922	-0.9140	-0.0197	-0.0218
4.4882	-0.9646	-0.2572	-0.4419	-0.0060	-0.1848
4.5079	1.6535	0.4408	0.2228	0.0028	-0.2180
4.0945	3.3858	0.9027	0.7881	0.0141	-0.1145
3.3071	3.9567	1.0549	1.0399	0.0340	-0.0150
2.1063	3.7008	0.9866	0.9791	0.0644	-0.0076
1.3780	2.6772	0.7137	0.7505	0.1029	0.0368
0.6693	1.3189	0.3516	0.4990	0.1452	0.1474
0.6299	0.4134	0.1102	0.2998	0.1868	0.1896

APPENDIX J

RESULTS OF VELOCITY PROFILES ANALYSIS FROM PROGRAM TANKANL

The analysis of the manometer readings obtained from the pitot tube, in making a horizontal pass through Ports 1, 2, and 3 is present in this appendix. The theoretical basis of this analysis is discussed in Section 4.3.

In Table J-1 is given a list of the abbreviations used as column headings in this appendix. In Table J-2 is given the raw data converted to pressure drops in inches of manometer fluid from manometers B and D for Port 1. The results of the analysis for Ports 1, 2, and 3 are given in Tables J-3, J-4, and J-5 respectively. In Table J-2 it is seen that only fourteen of the readings could be analyzed out of thirty-four reported in Table J-2. This is because twenty of these readings gave a θ_p larger than 40° and thus was outside the range of probe response.

TABLE J-1

LIST OF ABBREVIATIONS USED FOR COLUMN HEADINGS

IN THE TABLES OF APPENDIX J

NO	= Item Number
T-R	= T-r, distance from tank wall, in.
DEL P12	= ΔP_{12}, pressure drop reading from manometer B, inches of manometer fluid
DEL P45	= ΔP_{45}, pressure drop reading from manometer D, onches of manometer fluid
V	= $\vec{V}$, resultant velocity (ft/min)
VR	= $\bar{v}_r$, (ft/min)
VZ	= $\bar{v}_z$, (ft/min)
VTHETA	= $\bar{v}_\theta$, (ft/min)
PITCH ANGLE	= θ_p, (degrees)
YAW ANGLE	= θ_y, (degrees)
CORRECTED DEL P12	= ΔP_{12}, corrected pressure drop from probe manufacturers calibration chart, Figure IV-15

TABLE J-2

RAW DATA CONVERTED TO PRESSURE DROPS
ACROSS MANOMETERS B AND D FOR PORT 1

	T-R	DEL P12	DEL P45
1	0.1000	1.5000	-3.0734
2	0.2000	1.5500	-1.9050
3	0.3000	1.5500	-0.7620
4	0.4000	1.2500	-0.4064
5	0.4500	1.2500	-0.1016
6	0.5000	1.1500	-0.3048
7	0.6000	1.2000	0.4318
8	0.7000	1.2000	0.7112
9	0.8000	1.0000	0.5080
10	0.9000	0.2000	0.5080
11	1.0000	1.0000	0.2540
12	1.1000	1.0000	0.0
13	1.2000	0.9500	-0.5334
14	1.3000	1.0000	-0.8890
15	1.4000	1.0000	-1.1938
16	1.5000	0.8000	-1.6510
17	1.6000	0.7500	-0.4318
18	1.8000	0.2000	-1.5240
19	2.0000	0.2000	-1.6002
20	2.2000	0.5000	-1.7272
21	2.4000	0.6000	-1.8034
22	2.6000	0.6000	-1.9050
23	2.8000	0.5500	-1.9050
24	3.0000	0.5500	-1.9050
25	3.2000	0.5500	-1.8288
26	3.4000	0.5000	-1.9050
27	3.6000	0.7000	-2.1590
28	3.8000	0.7500	-2.1590
29	4.0000	0.9500	-5.8420
30	4.2000	0.8500	-5.3340
31	4.4000	0.2500	-4.8260
32	4.6000	0.9000	-4.7752
33	4.8000	0.8500	-4.8260
34	5.0000	0.8500	-4.8260

TABLE J-3

RESULTS OF VELOCITY PROFILE ANALYSIS FOR PORT 1

	T-R	V	VR	VZ	VTHETA	PITCH ANGLE	YAW ANGLE	CORRECTED DEL P12
2	0.200	52.712	-25.025	38.461	25.942	-28.343	34.000	1.867
3	0.300	52.057	-5.412	42.924	28.952	-5.967	34.000	1.821
4	0.400	46.431	-1.817	43.255	16.778	-2.242	21.200	1.449
5	0.450	45.659	4.228	42.033	17.325	5.313	22.400	1.401
6	0.500	44.402	-0.417	41.050	16.920	-0.538	22.400	1.325
7	0.600	43.788	12.360	36.811	20.237	16.395	28.800	1.289
8	0.700	43.716	15.774	33.068	23.849	21.151	35.800	1.294
9	0.800	39.901	13.310	30.738	21.693	19.485	35.200	1.070
11	1.000	40.171	9.934	26.446	28.559	14.317	47.200	1.085
12	1.100	40.633	5.455	22.516	33.381	7.715	56.000	1.119
13	1.200	40.860	-5.793	11.149	38.880	-8.151	74.000	1.122
14	1.300	42.011	-14.986	10.422	37.838	-20.899	74.600	1.186
15	1.400	42.293	-19.503	5.871	37.066	-27.460	81.000	1.202
17	1.600	36.322	-5.446	-35.909	0.376	-8.623	179.400	0.887

TABLE J-4

RESULTS OF VELOCITY PROFILE ANALYSIS FOR PORT 2

	T-R	V	VR	VZ	VTHETA	PITCH ANGLE	YAW ANGLE	CORRECTED DEL P12
1	0.080	71.755	12.894	66.331	24.142	10.352	20.000	3.461
2	0.180	72.034	15.863	66.028	24.032	12.722	20.000	3.488
3	0.230	70.936	20.157	63.910	23.261	16.509	20.000	3.382
4	0.280	70.251	23.993	61.475	24.092	19.970	21.400	3.317
5	0.330	70.325	27.189	58.780	27.410	22.744	25.000	3.324
6	0.430	71.539	29.155	55.642	34.231	24.050	31.600	3.440
7	0.530	72.579	28.477	54.417	38.672	23.101	35.400	3.541
8	0.630	63.240	26.986	46.620	33.131	25.259	35.400	2.688
9	0.730	65.723	28.075	42.020	42.020	25.288	45.000	2.903
10	0.830	65.095	27.626	37.887	45.152	25.112	50.000	2.848
11	0.930	60.591	23.750	19.976	52.040	23.077	69.000	2.468
12	1.030	60.613	24.141	19.925	51.906	23.470	69.000	2.469
13	1.130	55.457	12.744	-53.448	7.511	13.285	172.000	2.067
14	1.230	55.702	10.264	-54.743	0.764	10.618	179.200	2.085
15	1.330	56.008	7.519	-41.245	37.137	7.715	138.000	2.108
16	1.530	55.266	7.420	-21.750	50.262	7.715	113.400	2.053
17	1.730	56.740	7.617	-18.120	53.227	7.715	108.800	2.164
18	1.930	56.740	7.617	-17.188	53.535	7.715	107.800	2.164
19	2.130	58.021	9.166	-10.539	56.315	9.090	100.600	2.263
20	2.330	57.163	10.396	-6.461	55.837	10.479	96.600	2.196
21	2.530	57.163	10.396	-6.461	55.837	10.479	96.600	2.196
22	2.730	64.103	9.858	-9.472	62.629	8.846	98.600	2.762
23	2.930	59.426	9.324	-8.776	58.031	9.027	98.600	2.374
24	3.130	58.021	9.166	-8.567	56.648	9.090	98.600	2.263
25	3.330	57.306	9.086	-12.536	55.174	9.123	102.800	2.207
26	3.530	57.306	9.086	-15.216	54.496	9.123	105.600	2.207
27	3.830	57.306	9.086	-21.379	52.386	9.123	112.200	2.207
28	4.130	57.306	9.086	-21.379	52.386	9.123	112.200	2.207
29	4.330	62.803	9.708	-22.842	57.690	8.892	111.600	2.651
30	4.530	58.656	9.894	-23.700	52.735	9.711	114.200	2.312
31	4.730	58.728	9.245	-25.424	52.126	9.058	116.000	2.318
32	4.930	65.006	19.628	-27.167	55.700	17.574	116.000	2.840

TABLE J-5

RUSULTS OF VELOCITY PROFILE ANALYSIS FOR PORT 3

	T-R	V	VR	VZ	VTHETA	PITCH ANGLE	YAW ANGLE	CORRECTED DEL P12
1	0.030	76.246	5.113	71.395	26.268	3.845	20.200	3.907
2	0.130	74.045	18.621	67.258	24.746	14.566	20.200	3.685
3	0.230	70.829	22.874	62.152	25.111	18.841	22.000	3.372
4	0.330	67.948	23.634	57.923	26.519	20.355	24.600	3.103
5	0.430	61.299	24.890	50.435	24.381	23.957	25.800	2.526
6	0.530	58.632	23.799	47.487	24.826	23.948	27.600	2.311
7	0.630	56.618	23.855	45.504	23.789	24.919	27.600	2.155
8	0.730	56.556	23.049	43.894	27.216	24.050	31.800	2.150
9	0.830	54.998	18.677	37.833	35.280	19.852	43.000	2.033
10	0.930	55.039	16.733	38.347	35.760	17.699	43.000	2.036
11	1.030	53.368	10.729	2.554	52.216	11.598	87.200	1.914
12	1.230	54.604	6.569	-22.909	49.128	6.910	115.000	2.004
13	1.630	54.699	5.801	-22.986	49.294	6.088	115.000	2.011
14	1.830	55.266	7.420	-23.145	49.635	7.715	115.000	2.053
15	2.230	57.463	7.714	-24.065	51.608	7.715	115.000	2.219
17	2.630	56.309	11.590	-23.288	49.940	11.878	115.000	2.131
18	2.830	56.309	11.590	-23.288	49.940	11.878	115.000	2.131
19	3.030	56.309	11.590	-23.288	49.940	11.878	115.000	2.131
20	3.230	56.309	11.590	-23.288	49.940	11.878	115.000	2.131
21	3.430	56.309	11.590	-23.288	49.940	11.878	115.000	2.131
22	3.630	56.309	11.590	-23.288	49.940	11.878	115.000	2.131
23	3.830	57.753	11.699	-23.902	51.257	11.687	115.000	2.242
24	4.030	57.753	11.699	-16.535	54.084	11.687	107.000	2.242
25	4.230	60.671	16.377	-21.126	54.465	15.660	111.200	2.474
26	4.430	59.284	16.815	-20.558	53.002	16.478	111.200	2.362
27	4.630	59.284	16.815	-20.558	53.002	16.478	111.200	2.362
28	4.830	58.660	15.823	-19.504	53.011	15.649	110.200	2.313

VITA

Abel DeSouza was born on November 1, 1936 in Ratlain, Madhya, Pradesh, India. He completed his secondary education at St. Mary's High School, Bombay. He graduated from the Department of Chemical Technology, University of Bombay, Bombay, in March 1959, obtaining a Bachelor of Chemical Engineering degree. After graduation he was employed by the Government of India, Atomic Energy Establishment, Trombay, Bombay, with their Chemical Engineering Division.

Five years later in September 1964, he joined the Graduate School of the Louisiana State University. In August 1966, he received the Master of Science degree in Chemical Engineering and is presently working towards a Doctor of Philosophy degree in the same curriculum. He has accepted a position with the Shell Development Company, Emeryville, California.

EXAMINATION AND THESIS REPORT

Candidate: Abel DeSouza

Major Field: Chemical Engineering

Title of Thesis: Fluid Dynamics and Flow Patterns in Stirred Tanks With a Turbine Impeller

Approved:

Ralph W. Pike
Major Professor and Chairman

Max Goodrich
Dean of the Graduate School

EXAMINING COMMITTEE:

Paul W Murrill

Johnny R Johnson

Jesse Coates

Clayton D Calhoun

Date of Examination:

July 10, 1969